

INTERNATIONAL COUNCIL FOR BUILDING RESEARCH STUDIES AND DOCUMENTATION

WORKING COMMISSION W18 - TIMBER STRUCTURES

# **CIB - W18**

MEETING TWENTY - FOUR

OXFORD

UNITED KINGDOM

SEPTEMBER 1991



## CONTENTS

- 1 List of Participants
  - 2 Chairman's Introduction
  - 3 Cooperation with other Organisations
  - 4 Reports from Sub-Groups
  - 5 The Role of CIB W18
  - 6 Plywood
  - 7 Timber Beams
  - 8 Laminated Beams
  - 9 Trussed Rafters
  - 10 Fire
  - 11 Stress Grading
  - 12 Duration of Load
  - 13 Stresses for Solid Timber
  - 14 Statistics and Data Analysis
  - 15 Load Sharing
  - 16 Structural Stability
  - 17 Timber Joints and Fasteners
  - 18 Structural Design Codes
  - 19 Any other Business
  - 20 Programme for the next meeting
  - 21 Close
  - 22 List of CIB W18 Papers/Oxford, United Kingdom 1991
  - 23 Current List of CIB W18 Papers
- CIB-W18 Papers 24-4-1 up to 24-102-2







U Korin National Building Research Institute, Haifa

ITALY

A Ceccotti University of Florence  
N de Robertis University of Florence

JAPAN

Y Hirashima University of Shizuoka  
M Yasumura Building Research Institute, Tsukuba

MOROCCO

E Kortbi L.P.E.E., Casablanca

NEW ZEALAND

A Buchanan University of Canterbury, Christchurch  
P J Moss University of Canterbury, Christchurch  
B Walford Forest Research Institute, Rotorua

NETHERLANDS

H J Blass University of Technology, Delft  
A J M Leijten University of Technology, Delft  
J W G van de Kuilen TNO-Building & Construction Research, Delft  
T C van der Put University of Technology, Delft  
G Sebestyen CIB, Rotterdam

NORWAY

E Aasheim Norwegian Institute of Wood Technology, Oslo

POLAND

Z Mielczarek Politechnika Szczecińska, Plastow  
Ms B Szyperska Building Research Institute, Warsaw

PORTUGAL

Ms H Cruz National Laboratory of Civil Engineering,  
Lisbon

SWEDEN

I Czmocho Chalmers University of Technology, Goteborg  
B L O Edlund Chalmers University of Technology, Goteborg  
B Kallsner Swedish Institute for Wood Technology  
Research, Stockholm  
R Kliger Chalmers University of Technology, Goteborg  
J Konig Swedish Institute for Wood Technology  
Research, Stockholm  
M Perstorper Chalmers University of Technology, Goteborg  
S Thelandersson University of Lund



## 2. CHAIRMAN'S INTRODUCTION

In his opening address, DR STIEDA welcomed the participants to Oxford and commented that over the years meetings of CIB W18A had consistently been well supported. This has enabled close ties to be maintained with other organisations with similar interests. In particular the chairman welcomed MR LARSEN who is Chairman of CEN TC124, DR CECCOTTI representing RILEM, MR LEE who has worked closely with CIB W18 over many years, and PROFESSOR SEBASTYEN who is the General Secretary of CIB.

It was with deep regret that DR STIEDA reported the sudden death of MR BURGESS shortly after the last meeting in Lisbon. MR BURGESS had been a good friend to many Members and had worked intensively for CIB W18, both as an active participant and latterly as secretary of CIB W18A. His participation in future meetings will be greatly missed.

DR STIEDA then confirmed that he would be stepping down as Chairman of CIB W18A at the end of this meeting. In Lisbon last year a small search committee was appointed to identify a suitable successor and DR. STIEDA was pleased to report that PROFESSOR BLASS would take over as Chairman from 1992.

In concluding his introduction DR STIEDA asked all Members to inform the Secretary if they are aware of any errors or omissions in previous minutes and reiterated his plea for papers in future to be provided to the Secretary in sufficient time to enable them to be circulated well in advance of the meeting.

## 3. COOPERATION WITH OTHER ORGANISATIONS

### CIB W18A

In his report DR LEICESTER stated that the role of CIB W18B "Tropical and Hardwood Timber Structures" is concerned primarily with the southern hemisphere and has the following main objectives:

- . to enhance standards
- . to protect the interests of hardwood producers
- . to effect technology transfer to developing countries.

The Group has a large membership that has been relatively inactive due to problems encountered by some members in securing funding to attend meetings. A number of regional coordinators have been appointed to expand and develop the role of this group. Projects currently underway include the utilisation of mixed species, plantation timbers in tropical countries, the development of simplified standards etc. DR LEICESTER commented that the group is looking for support from ITTO to assist with its activities.

The second CIB International Conference on Tropical and Hardwood Timber Structures will be held in Kuala Lumpur, Malaysia from 7 to 10 September 1992. The themes of the Conference will be resource and science, technology and engineering, and there will a pre-conference technical tour.

## ISO TC165

MR LARSEN said that it had become increasingly difficult for him to undertake the dual roles of Chairman of CEN TC124 and Chairman of ISO TC165 and that the rules of cooperation between CEN and ISO made it problematical to maintain both activities. As a result he had decided earlier this year to resign as Chairman of TC165 and announced that DR STIEDA will be taking over this Chairmanship. A transfer of the secretariat is in hand.

## RILEM

DR CECCOTTI stated that there are four Rilem Committees with timber engineering interests.

- . TC109 - behaviour of timber structures and seismic action.
- . TC110 - application of fracture mechanics to timber structures.
- . TC111 - behaviour of timber and concrete composite load bearing structures.
- . TC112 - creep in timber structures.

TC109 is chaired by PROFESSOR NIELSEN and met last week at the Building Research Establishment in England. This Committee is charged with two tasks:-

- i) to prepare a state-of-the-art report. This is now nearing completion.
- ii) to define test methods. There are differing views on the Committee regarding this and more time is needed to complete this item.

TC110 has completed its work and a state-of-the-art report has already been published, copies of which are available from the Group Chairman, PROFESSOR RANTA-MAUNUS. It was said that activities relating to fracture mechanics will continue in Committee TC133 "Fracture of Timber" which has two specific aims:

- i) to develop testing standards
- ii) to apply fracture mechanics to the design of timber structures

PROFESSOR RANTA-MAUNUS said that he would like to hear from any members willing to participate in the activities of TC133. It is intended to hold a workshop on fracture mechanics methods in Bordeaux, France, in February 1992.

TC111 is currently preparing a state-of-the-art report covering its activities. It is likely to take one more year before this report is completed.

TC112 will next meet in London in September 1991 under the Chairmanship of PROFESSOR MORLIER. The objectives of this Group are to prepare a state-of-the-art report which is likely to be completed in approximately one year. In response to a comment from MR LARSEN regarding criticism of the state of the art creep report at the last IUFRO meeting in New Brunswick, DR CECCOTTI confirmed that this related to an earlier draft which was now being substantially updated.

Concluding his report DR CECCOTTI added that there are several RILEM Committees e.g. Design by testing, where there were no timber interests represented. He urged anyone interested in participating in the work of RILEM to offer their services.

#### CEN

MR SUNLEY made reference in his report to the presentations at the ITEC Conference earlier in the week at which many CIB W18 members had been present, and said that it was his intention at this meeting only to give a brief overview and to highlight areas of potential problems, many of which relate to a lack of coordination between the various committees. In particular MR SUNLEY made reference to TC38 "Wood Preservation" which is preparing a draft on Hazard Classes and which do not coincide with the service classes currently included in the EC5 draft.

TC103 "Wood Adhesives". This is a small Committee with a Dutch Convenor and a UK secretariat. It is preparing one main standard on the classification of structural adhesives, and four subsidiary standards on test methods. There has also been a recent request to prepare a new standard on casein adhesives. PROFESSOR GLOS said that Germany supports this initiative because casein is regarded as a good adhesive from an environmental point of view. PROFESSOR MADSEN said that casein glues are not now permitted in Canada on the grounds of inadequate performance. MR SUNLEY confirmed that the work of this Committee will cover glues for hardwoods but could not confirm whether it was intended that adhesives for bonding wood to other materials would be included.

TC112 "Wood-based Panel Products". MR SUNLEY said that this is the largest Committee in terms of activity and that it has a programme of work to produce over 80 standards. It has a German secretariat and is largely composed of panel products manufacturers and those with interests in quality control. A large part of the programme of work is concerned with test methods and sampling. TC112 has six sub committees; four dealing with materials (particleboard, plywood, fibreboard and cement bonded particleboard), one with test methods and one with formaldehyde emissions. There is also a joint TC112/124 ad hoc Group currently looking at test methods and means of deriving characteristic values for structural applications. This group is also starting to look at performance standards.

TC124 "Timber Structures". MR LARSEN is the chairman of this committee which comprises four working groups; WG1 "test methods" (Irish convenor); WG2 "Solid Timber" (UK Convenor); WG3 "Glulam" (Danish Convenor); WG4 "Timber Connectors" (German Convenor). WG1 has now prepared a set of tests methods for basic material properties based on ISO standards, drawn heavily from earlier CIB W18 Work. The group is

now moving on to address test methods for components e.g. walls, floors. MR SUNLEY commented that WG2 has the closest interface with the producer industry and also has the greatest problems to get agreement on issues such as timber sizes. MR LEE applauded the work of the ad hoc group on the testing of sheet materials, commented on parallel work which is going on in some of the working groups of TC112 and TC124 and asked if it was possible for the ad hoc group to include these areas of overlap. MR LARSEN replied that the scope of the groups was different and that it had been agreed that TC112 should give up its work and let TC124 continue. DR LEICESTER asked if CEN standards cover quality control procedures and whether CIB W18 should concern itself with quality control matters. MR SUNLEY replied that attestation of conformity is an essential part of CEN standards, but that the requirements may conflict with current producer country procedures. This is now being addressed within CEN.

TC175 "Round and sawn timber for non-structural use". This Committee has a French Convenor and French Secretariat and is heavily dominated by Belgian and French sawmillers. The work of the Committee is slowly progressing and a programme of work has recently been agreed. There are four working groups responsible for a technical language for all timber work ( e.g. definitions, measurements, symbols etc.), general quality standards and specification and utilisation of round timber. PROFESSOR GLOS commented that there was not enough representation on TC175 by timber engineers and that many problems could arise by failing to bridge the gap between timber designers and producers. There is also considerable misunderstanding between what is meant by structural and non structural timber e.g. structural timber has both structural and non structural aspects and often it is the non structural aspects that dictate whether the material can be used or not. MR SUNLEY added that PROFESSOR GLOS's comments serve to illustrate the general lack of coordination between the CEN Committees. In response to a question from MR MARSH regarding the mechanism to effect change within CEN, Mr SUNLEY said that this should be channelled through the various nations' standards bodies.

TC250 "Structural Eurocodes". MR LARSEN said that funding had recently been agreed for Eurocode 5 and that there is a target date of the end of April 1992 for completion of the draft. It was recommended that those in Europe likely to be involved should make contact with their national standards organisations as 14 and 15 November 1992 has been set as the date for discussion of the translated drafts. MR LARSEN added that a major item for the next CIB W18 meeting should be a discussion of the EC5 draft. PROFESSOR GLOS asked why the activities of TC127 (Fire) were not on the Agenda and whether CIB W18 should concern itself with fire matters. MR LARSEN replied that TC127 lacks specialist timber knowledge and that there is nobody at the meeting who could report on the work of this Committee. DR STIEDA suggested that someone from TC127 could be invited to attend future CIB W18 meetings on an ad hoc basis to give a presentation on the work of this committee.

## IUFRO S5.02

The proceedings of the New Brunswick meeting (850 pages; 2 volumes) are now available from the S5.02 Chairman, PROFESSOR HOFFMEYER at a cost of USD 60. The next meeting of S5.02 will be held in Bordeaux, France from 17 - 21 August 1992, and is being organized by PROFESSOR MORLIER. The meeting will have the following themes:-

- Structural panel products
- Creep of structural timber
- Duration of load for joints
- New joints
- System reliability
- Seismic design
- Juvenile structural timber
- Non-destructive testing of timber structures

A Division 5 conference is to be held in Nancy from 23 - 28 August 1992, and a IUFRO centennial meeting will be held in Berlin the following week. It is intended to form a joint working party with S5.01 to address the properties of wood as required by users, and also another working party on non-destructive testing.

## IABSE

In his report, PROFESSOR EDLUND said that IABSE is an important forum to promote timber amongst engineers who specialise in steel and concrete. There is an international bridge conference in Leningrad next week, which will address the interaction between construction and design. Two timber papers and two timber posters have been accepted. The next IABSE congress meeting is in New Delhi in March 1992 and has the theme "Civilization through Civil Engineering"; there are no special timber sessions. From 13 - 17 September 1993 a symposium "Preservation of the Architectural Heritage" will be held in Rome with the theme of structures more than one hundred years old. A symposium on earthquake-resistant structures is planned for September 1995 in San Francisco.

## CIB W85 (Structural Serviceability)

DR LEICESTER said that a state-of-the-art document is being drafted to address human comfort, equipment functioning and the building environment (eg roofs); it is suggested that a session may be held in association with the IABSE meeting in 1993.

## JCSS

This is a coordinating group looking at questions of safety between different materials. DR STIEDA said that there are seven associations currently participating, including CIB, IABSE and RILEM. W18 has not had representation in the past, however, if anyone is interested in taking part, they should contact either DR STIEDA or the secretary to be nominated on behalf of CIB. PROFESSOR SEBASTYEN said that this meeting is not open to all to participate, and that if anyone from CIB wished to attend, W18 should make a nomination to the General Secretary.



NATO WORKSHOP ON RELIABILITY BASED DESIGN - TIMBER STRUCTURES

MR ANTHONY gave a report of this meeting.

This workshop, the first of its kind on the reliability-based design (RBD) of engineered timber structures, focussed on the comparison of basic approaches associated with the major national and multi-national design codes. The technical issues were divided into four topics:

- A: Fundamentals of Reliability Assessment
- B: Reliability Assessment of Multi-Member Structures
- C: Material Resistance Considerations
- D: Formulation of Internationally Harmonized Codes

In addition to a keynote presentation by DR BRUCE ELLINGWOOD of the US, the state-of-the-art for each of the above topics was summarized by a speaker. Four working groups, covering the above four topics, deliberated on the research and development needs to move toward internationally harmonized RBD codes. Table 1 provides a list of the workshop participants and their working group assignments.

Table 1. NATO ARW Group Assignments

**GROUP A: FUNDAMENTALS OF RELIABILITY ASSESSMENT**

Organizing Committee Member	: Hans Larsen (unable to attend)	Denmark
Speaker	: Henrik Madsen	Denmark
Group Leader	: Sven Thelandersson	Sweden
Rapporteur	: Frederic Rouger	France
Participants	: Bruce Ellingwood	U.S.A.
	: Zsolt Kovacs	Hungary
	: John Zahn	U.S.A.
	: Mike Caldwell (unable to attend)	U.S.A.

**GROUP B: RELIABILITY ASSESSMENT OF MULTI-MEMBER STRUCTURES**

Organizing Committee Member	: Peter Glos (unable to attend)	Germany
Speaker	: Rudiger Rackwitz	Germany
Group Leader	: Marita Kerskin-Bradley	Germany
Rapporteur	: Joe Murphy	U.S.A.
Participants	: Marvin Criswell	U.S.A.
	: Lars Ostlund	Sweden
	: David Rosowsky	U.S.A.
	: Erol Varoglu	Canada

**GROUP C: MATERIAL RESISTANCE CONSIDERATIONS**

Organizing Committee Member	: Dave Barrett	Canada
Speaker	: Ricardo Foschi	Canada
Group Leader	: Bob Tichy	U.S.A.
Rapporteur	: Roger Lovegrove	U.K.

Participants	: Jean-Pierre Biger	France
	: Ario Ceccottti	Italy
	: Vijaya Gopu	U.S.A.
	: Cathy Marx	U.S.A.
	: Takashi Nakai	Japan
	: Lauge Nielsen	Denmark
	: Juhani Taipale	Finland

GROUP D: FORMULATION OF INTERNATIONAL HARMONIZED CODES

Organizing Committee Member	: Bob Leicester	Australia
Speaker	: Bob Leicester	Australia
Group Leader	: Geoff Boughton	Australia
Rapporteur	: Bryan Walford	New Zealand

Participants	: Erik Aasheim	Norway
	: Ron Anthony	U.S.A.
	: Ad J M Leijten	Netherlands
	: Tom McLain	U.S.A.
	: Raphael Mutuku	Kenya
	: Tom Williamson	U.S.A.

It was recognized that sufficient fundamental knowledge and analytical tools exist to conduct reliability assessments. However, because of their unique mechanical properties modifications in methodologies are needed to allow assessment of the true reliability of timber structures.

Special focus needs to be given to the long-term reliability of timber structures, especially as this reliability is affected by time-dependent behaviour, cyclic environment, and biological degradation. Both strength limit states and serviceability limit states should be considered.

Timber products are used in a variety of structural configurations. Unified definitions of structural sub-systems are needed so proper mathematical model representations could be assigned to them. It was emphasized that in typical engineered timber structures, components are interacting at several organizational levels. This multi-level interaction makes it difficult to utilize simple reliability assessment methods and, hence, accurate reliability assessments of entire timber structures are not available today.

Material characterisation is a critical component of reliability assessment and reliability-based design. A united approach to the characterisation of strength and elastic parameters of wood products is critical for code harmonization. The harmonization has to begin with the coordination of various mechanical test methods by which numerical values are assigned for material properties. Since sampling procedures, specimen dimensions, test conditions and the test method itself all affect the obtained property values, the development of unified test procedures needs to be harmonized first.

Unfortunately, to date, very few activities have been coordinated at the international level to allow the development of comparable test data. For example, in the EC countries, lumber testing is conducted with the visually defined worst defect placed at the highest stress

location. On the other hand, in North America, lumber pieces are tested in random arrangement. Data obtained in the EC countries cannot be utilized in North America and vice versa. Thus, when a product developed in one region is to be utilized for construction in another region, complete retesting and re-evaluation are required. This duplication of effort greatly increases the cost and unnecessarily complicates the activities of international commerce.

The overall logistics of international code harmonization was the topic of one of the four working groups. Key areas of concern were identified and the priorities established. Development and acceptance of common nomenclature, glossary and data collection format were identified as the most critical issues where harmonization needs to focus. These issues need immediate attention as most countries are in the process of developing or modifying RBD codes. If the current opportunity for harmonization is missed, the process will become more difficult at a later date.

It was unanimously agreed by the participants that the ARW represented a very important first step toward the long and extensive effort needed to harmonize "reliability based timber codes". The participants suggested follow-up workshops, seminars and short courses to begin addressing a number of key issues.

The ARW participants recommended that NATO assume a leading role and continue its support for the efforts of harmonizing RBD codes for engineered timber structures. NATO should designate this topic as a critical area of concern and provide longer-term financial support for further activities. The organizing committee of the ARW would be interested to continue its involvement in this important issue.

#### CIB W18

The next meeting of W18 will take place in Ohus in Southern Sweden from 24 - 27 August 1992. Tentative arrangements for the 1993 meeting have been made for Atlanta, Georgia. The US Forests Products Laboratory has indicated that they are interested in supporting this meeting and MR O'HALLORAN reported that tours of manufacturers' facilities would be possible.

#### 4. REPORTS FROM SUB-GROUPS

##### a) Characteristic Values for Timber

PROFESSOR GLOS reported that this group is now inactive, and that the final draft of the Standard on characteristic values has been prepared. A suggestion was made that this group could establish a new link to try to harmonize European, North American and Australian methods for determining characteristic values.

##### b) Characteristic Values for Panel Products

MR ELIAS reported that this group was formed following a suggestion at Lisbon and that the work should be of interest to the relevant CEN groups. There is a need to coordinate methods between the various panel products; plywood, particleboard, etc. and that methods involving

ranking or statistical distribution have been investigated. It was suggested that CIB members try to provide papers on this subject for next year's meeting. MR RIBERHOLT suggested that the scope be widened to include all manufactured products, eg glulam, finger joints, where procedures for the derivation of characteristic values are needed. MR FEWELL said that the joint CEN 112/124 Ad hoc committee is currently producing a paper on the derivation of the characteristic values for all board materials. In responding to a question on sample size, MR SUNLEY said that the end result would be a compromise between what industry is prepared to pay for and what a statistician would deem necessary. MR FALK reported that the LRFD project in the US has looked at fitting distributions to sample sizes and that CEN could perhaps make use of this work. MR MARSH added that it is the engineer's problem to advise a client of the cost of his building and that he needs to be satisfied that the level of reliability (safety) satisfies the National Building Regulations. He asked if increasing the sample size gives increased reliability and if so, what is the cost implication.

MR LARSEN said that in the EC5 draft, it is stated that characteristic values must be established in a satisfactory way and that it must be unacceptable for producers to say that they cannot afford to test a sufficient number of samples. Code writers have a responsibility too and the goal of a code committee should be to produce a code with a consistent degree of crudity. MR FEWELL said that the CEN approach is to penalise results if simple procedures and smaller samples are used.

MR BUCHANAN was concerned that CIB W18 has not defined what the tasks of the sub-groups are, and MR GLOS added that sub-groups should be identified. MR STIEDA requested that chairmen of all sub-groups should let the secretary know who the members are, and should define the objectives of the sub-groups.

#### c) Stability of Structures

PROFESSORS BRUNNINGHOF and BLASS and MR VAN DER PUT met in August to address inconsistencies in the stability design methods in Eurocode 5. It was concluded that a recommendation be made to disband this sub-group. PROFESSOR BLASS said that no formal report had been prepared. MR LARSEN asked if any problems had been solved in this sub-group and what were their recommendations. MR SUNLEY added that if it were proposed to produce a new CIB Code, this working group could have an important role.

#### d) Punched Metal Truss Plates

In his report, PROFESSOR STERN said that this sub-group had met the previous day. Its original scope was "to 'globalize' the European Union of Agreement (UEAtc) Rule of Assessment of Punched Metal Plate Timber Fasteners, as published in M.O.A.T. No. 16 of 1979; to assess the performance of connections and structural and non-structural components and assemblies fabricated with these connectors; to prepare a glossary of terms covering these connectors and to prepare a listing of publications covering this field." It was pointed out that it is not acceptable to include in a standard alternative test methods, as were incorporated in the incomplete First Draft of July 1991 of the proposed CIB/W18A/TC6 report (prepared by the Coordinator on the basis of

information received). Furthermore, to base a 'global' standard on the M.O.A.T. document was considered undesirable in the light of the subsequently developed, agreed upon, and published ISO Standard 8969 of 1990 on "Timber Structures - Testing of Unilateral Punched Metal Plate Fasteners and Joints". In addition, a European Community (EC) Committee is in the process of writing a CEN Standard, with comments invited to bring it up-to-date as much as feasible. Regrettably, this First Draft of the proposed CEN Standard is available only to the CEN Committee members, excluding any non-members from actively participating in the deliberations. On the other hand, it was agreed that TC6 could assist the CEN Committee in providing expertise (available within TC26). Therefore, the following revised scope of TC6 was suggested and subsequently accepted during the meeting,

"to identify significant problems and establish requirements, including the need for specific information, to serve as a basis for the establishment and promulgation of an appropriate up-to-date ISO Test Standard which leads to reliable test data, making it feasible to evaluate them properly and to design appropriately connections of timber (lumber) components and assemblies fabricated with LIGHTWEIGHT METAL PLATE CONNECTORS (TRUSS PLATES) with or without integral teeth:

"to prepare a glossary of terms covering these connectors; and

"to prepare a listing of publications and related documents covering these connectors".

Thus, the scope of TC6 includes the drafting of a Standard on test methods and on procedures for the evaluation of the test data and the design of the connections.

On the basis of the information to be submitted by the TC6 members to the TC6 Coordinator, a decision can be made whether to continue efforts to prepare a draft for an up-to-date ISO Standard which would be globally applicable, or whether it will be necessary to accept at least two major Standards for global use, that is, the proposed CEN Standard and the ASTM Standard, possibly in addition to other regionally accepted Standards.

Prior to the September 6 meeting of TC6, comments were received from MESSRS. ELHBECK, GUPTA, LHUEDE, PALKA and POUTANEN. These comments covered terminology, testing for combined axial load and eccentric load resistance, multi-stage loading sequence, characteristic loads, and additional publications in the field.

MR STIEDA concluded that this working group should proceed with these objectives and report back to the next meeting.

e) Reliability Based Design

DR LEIJTEN said that this group met on 6 September and that a proposal was put forward to set up an official sub-group of W18 with the aim of addressing the need for reliability methods in the CIB (EC5) Code context. DR LEIJTEN's notes from this meeting are presented below:-

Let me briefly outline how this group came about and what happened. Since the meeting in Lisbon where JAN KUIPERS called a meeting for those interested in reliability, a number of Europeans responded (10) and formed an ad hoc group which met in Delft at the beginning of this year. The members of the ad hoc group expressed the wish to transform the ad hoc group into a working group of CIB W18. The meeting included a discussion on this.

Briefly, the following matters emerged from the discussion:

- . what could be our contribution to RBD with regard to the CIB-W18?
- . is there a need to provide studies which indicate the relations between the various ULSD codes which will be hard or soft calibrated?
- . this could also mean a survey of differences in definitions.
- . could reliability studies of timber structures influence proposals of the committee on Structural Safety so as to prevent them accepting load models and design methods which penalise d timber structures? For instance, the relation between live and dead load is in many cases different for timber structure compared to steel and concrete.
- . To what extent can RBD add to the existing CIB code? Current articles deal with components. Combinations of these form a system with reliability aspects. Could reliability considerations be a useful tool here?

In conclusion, it is recognised that much work has been done outside Europe and that reliability can be a useful tool for design and research. Before asking for a working group status, the group feels it should first prescribe a specific goal. As this appears to be difficult, the existence of the present group is questioned. At the moment within CIB W18 there is room for discussion of reliability subjects and perhaps this should remain the case. It is however felt that a discussion within a small group of interested professional people and amateurs would be more fruitful.

DR LEICESTER commented that theories are already established and that what is needed is for the Code writing committees to take them up. MR LARSEN added that it might be appropriate to await publication of the proceedings of the NATO meeting and then discuss at the next W18A meeting whether or not to form a sub-group. He added that he believed there was no basis for further work on this topic at the moment.

MR THELANDERSSON said that he felt that there was a need for activity to deal with uncertainties in timber. However, he added that this was not a sub-group function but should be a topic for discussion at the next W18 meeting.

## 5. THE ROLE OF CIB W18

Opening this topic of discussion, MR STIEDA said that, in the past, CIB W18 had concerned itself with providing background material for the preparation of timber engineering design Codes and Standards and that in his opinion, this role should continue. PROFESSOR BLASS added that in recent years, W18 has undertaken the important task of condensing

research results for practical use in Codes and Standards. Existing Codes need now to be enhanced to take account of new research results. MR SUNLEY said that he saw three important tasks for W18 in future.

1. to update the CIB Code;
2. to develop state-of-the art documentation on major timber engineering topics;
3. to maintain links with what is happening with other materials.

MR LARSEN added that W18 should spend time on developing/commenting on EC5. DR LEICESTER said that he was reluctant to follow MR SUNLEY's suggestion to prepare state-of-the-art documents as work presented at this meeting is at the frontier of research. He said that W18 should focus on Codes and Standards and related aspects. MR RIBERHOLT said that very little innovation had recently been discussed, eg new types of connectors, materials, etc. MR WALFORD said that the production of state-of-the-art documents would put too much emphasis on Northern Europe activities.

A general discussion then took place as to the format of future W18 meetings. It was agreed that DR STIEDA, PROFESSOR BLASS and MR ABBOTT would get together during the forthcoming meeting and prepare a paper which would be presented for discussion on the final morning. If agreed, this would then be circulated to all members in advance of the minutes. The paper is attached. (See also item 20.)

#### 6. PLYWOOD

Paper 24-4-1 "APA Structural Use Panel Design values, an update to Panel Design Capabilities" by Elias, Kuchar and O'Halloran was presented by DR KUCHAR. DR KLIGER asked how the author had defined the initial elastic deformation. DR KUCHER replied that this was done at a FPL. MR ABBOTT commented that there was no time-to-failure date included in the paper and DR KUCHAR said that this was also part of the FPL study. Referring to Tables 5 and 6, MR RIBERHOLT said that the reduction in the shear capacity ratio suggests that some inherent damage has occurred, and asked why nothing similar was noted for bending. DR KUCHAR said that the moisture content values that relate to the 0.75 wet use adjustment factor are close to fibre saturation point. MR ELIAS added that the panels in the programme fit into the EC5 service classes "1 and 2". MR APLIN asked if there was any evidence in service conditions of the large creep deflections found in the research. DR KUCHAR replied that this was not the case, because in service such high moisture contents and stresses do not occur.

#### 7. TIMBER BEAMS

Paper 24-10-1 "Shear Strength of Continuous Beams" by Leicester and Young was presented by DR LEICESTER. In response to a question from PROFESSOR SMITH, DR LEICESTER said that the reactions were determined by conventional structural analysis. MR SUNLEY asked if the reactions were measured, to which DR LEICESTER replied that they were not. MR LARSEN asked how wide was the load application point. DR LEICESTER replied that it was ensured that it was wide enough to avoid local crushing failure.

## 8. LAMINATED BEAMS

Paper 24-12-1 "Glued Laminated Timber-Contribution to the Determination of the Bending Strength of Glulam Beams" by Colling, Ehlbeck and Gorlacher was presented by DR COLLING. MR FALK asked the author if he could explain ' $K_{VAR}$ ' and also the lateral displacements in testing. DR COLLING added that  $K_{VAR}$  was not now needed, as data is available to replace the effects which it represented. Test work by MR LARSEN has shown the effects of  $K_{ISO}$ . Referring to alternative proposals for the volume effect, DR BUCHANAN said that he would support just having a length effect. He asked how the volume effect equations for beams would be modified for finger joints closer than 5.4 metre spacing. DR COLLING said that this can be done by introducing a factor into the equations for height and length. DR AICHER said that it might be considered desirable to have a minimum requirement for spacing finger joints in Codes. He reported that he had seen finger joints in practice as close as 350mm. MR LARSEN said that the length and depth effects are relative and that finger joint spacing will show up in the strength values of the beams. He added that it would not be possible to give design rules for bilateral bending if the depth effects proposed are adopted. In his view, it would be better to keep a 300mm reference depth.

Commenting on MR LARSEN's remarks regarding finger joint modifications, DR GEHRI suggested that the author should consider higher values due to lateral displacements. MR RIBERHOLT asked which strength values had been assigned to the finger joints in the simulation. DR COLLING replied that he had based his model on good production joints and that the distribution used for finger joint strength excluded improperly glued joints. MR FEWELL said that it was imperative that size effects were included in Codes. MR FALK added that analysis of over 12,000 beams tested in the US (Southern pine and Douglas fir) had shown that there was a definite size effect. DR AICHER added that he had found large size effects in glulam beams tested for quality control purposes. DR COLLING said that sometimes size effects cannot be analysed just by testing and that models are also required.

PROFESSOR GLOS said that the question is not whether size effects exist, but whether it is desirable to include them in Codes. DR BUCHANAN added that proof testing of laminations could eliminate the need for size effects. Concluding the discussion, DR STIEDA said that it was evident that there was a need for a major session at the next meeting to address the various aspects of size effects.

Paper 24-12-2 "Influence of Perpendicular to Grain Stressed Volume on the Load Carrying Capacity of Curved and Tapered Glulam Beams" by Ehlbeck and Kurth was presented by DR KURTH. Commenting on this paper, DR COLLING said that the reference volume should be  $0.2m^3$  and not  $0.02m^3$  as printed. MR RIBERHOLT asked why no measurements were made of tensile strength perpendicular to grain. PROFESSOR EHLBECK replied that there were practical problems in doing this.

If the specimens are cut from tested beams, the material has already been damaged; if they are acquired from others, the specimens would not be matched. PROFESSOR RANTA-MAUNUS asked if the moisture content was kept constant between manufacture and test. MR KURTH said that



this was the case, and therefore there were no moisture influences. PROFESSOR GLOS noted that the test values showed that the volume effect is not as large as is given in the EC5 draft.

#### 9. TRUSSED RAFTERS

MR KEVERINMAKI presented his paper 24-14-4 "Capacity of Support Areas reinforced with Nail Plates in Trussed Rafters". DR GEARY asked if the drying of timber after pressing had been taken into account, and if there was any experience of long-term behaviour. The answer given was "No" in both cases. DR KORIN said that it had not been agreed what deflection can be allowed, ie no values have been defined for compressibility limits. PROFESSOR EHLBECK replied that this is a serviceability issue and would depend on the structure and application. PROFESSOR SMITH asked whether such plates can take other forces, eg from diagonal members, in addition to their reinforcing effect. The author replied that he had not investigated this.

#### 10. FIRE

Paper 24-16-1 "Modelling the effective cross section of timber frame members exposed to Fire" by DR KONIG was presented by the author. DR LEICESTER asked the author why he had not used a residual cross-section with 100 per cent strength, as it would then be much easier to predict the behaviour for other size members. DR KONIG replied that any reduction can be chosen. MR THELANDERSSON pointed out that the approach had to define an empirical fit to test data, and that this should not be extrapolated to other members such as wall studs without further checking. DR BUCHANAN said that the stress distributions in the cross-section are critical to the conclusions and that the choice seems to be between full stress over a reduced area or reduced stress over the full area; for either case, information is needed on the variability.

#### 11. STRESS GRADING

Paper 24-5-1 "Influence of Stress Grading System on Length Effect Factors for Lumber Loaded in Compression" by Campos and Smith was presented by PROFESSOR SMITH. In response to a question from MR PERSTORPER, PROFESSOR SMITH said that the correlation coefficient for the data presented was of the order of 0.6 to 0.7. MR LARSEN asked that even if there was a length effect, what would it be used for, to which PROFESSOR SMITH replied that it would have application in the column formula in the Canadian Code. MR THELANDERSSON asked that, if the whole data group is considered without sorting, what is the length effect factor. PROFESSOR SMITH replied that this is similar to that which would be obtained with flatwise E mean values.

#### 12. DURATION OF LOAD

Paper 24-9-3 "Deformation Modification Factors for Calculating Built-Up Wood-based Structures" by DR KLIGER was presented by the author. MR AICHER suggested that an alternative approach could be to perform a stepwise iterative analysis to give a redistribution of stresses using an MOE versus time relationship. MR LARSEN said that no Code would describe the design of composite steel and wood structures by using modification factors from just the timber Code.

MR THELANDERSSON said that the tests were carried out at constant moisture content and asked the author to consider i) the effect of moisture content changes, and ii) for an asymmetric structure, the deflection due to moisture changes, which may not be insignificant.

MR TORATTI presented his paper 24-9-1 "Long Term Bending Creep of Wood". Referring to Fig. 1, MR PERSTORPER asked the author whether he would expect the same creep line without moisture content changes. MR TORATTI replied that with varying moisture content there would be much less creep. MR LARSEN suggested that the notation relative creep is confusing and that the phrase relative deformation should be used instead. PROFESSOR RANTA-MAUNUS added that this kind of programme could be used to model deformations in structures provided there is accurate information on loading.

Paper 24-9-2 "Collection of Creep Data on Timber" by PROFESSOR RANTA-MAUNUS was presented by the author. Referring to Table 2, PROFESSOR MADSEN asked the significance of the brackets. PROFESSOR RANTA-MAUNUS replied that the number in brackets indicates the number of years of load duration. DR LEICESTER asked the author to explain the similar deflections which had been observed for the I-beams and glulam beams in outdoors exposure. PROFESSOR RANTA-MAUNUS replied that the I-beam might have deflected more. However, the conditions were variable.

### 13. STRESSES FOR SOLID TIMBER

MR VAN DER PUT presented his paper 24-6-1 "Discussion of the Failure Criterion for Combined Bending and Compression". There were no questions.

Paper 24-6-3 "Effects of Within Member Variability on the Bending Strength of Structural Timber" by Czmocho, Thelandersson and Larsen was presented by MR THELANDERSSON. PROFESSOR BLASS commented that in the paper the lengths of the weak zones were taken as zero and asked how the results would differ for realistic weak zone length. MR THELANDERSSON replied that this had not yet been investigated. PROFESSOR SMITH said that weak zones could be in a high shear zone not in a high bending zone and asked how this could be accounted for. MR FEWELL pointed out that the difference between the in-grade and the CEN method was only about 10 - 15 per cent and that the paper had also shown this. It should be possible to use this work to study load configuration factors. MR SUNLEY added that the objectives of the CEN Standard are to find the strength of the weakest section from which to determine the characteristic value. If failures occur outside the loading region then a lower moment should be used.

Paper 24-6-5 "Derivation of the Characteristic Bending Strength of Solid Timber according to CEN Document prEN 384" was presented by the author, DR LEIJTEN. MR LARSEN said that the moisture contents for the service classes of EC5 should be observed, and the results should be adjusted accordingly. It was also not necessary to discard old test results. The Building Regulations will not require individual pieces to have a guaranteed strength; the requirement is that material is evaluated and marked according to a standardised system. MR SUNLEY added that the paper says that the CEN Standard should not permit more than one way of evaluating characteristic strength, however, the

Standard writers have decided that it should. The small clear test route is more conservative. DR BARRATT said that the issue is not only of how to define the defect for test, but how the grade is assigned. Dr LEICESTER said that the recent revision of the Australian Code, downrates species/grades for critical applications (which it defines) if they have been tested only by small clear methods. PROFESSOR GLOS said that the introduction of prEN 384 recognizes the need to retain the use of old data.

#### 14. STATISTICS AND DATA ANALYSIS

Paper 24-17-1 "Use of Small Samples for Ingrade Strength Measurement" by Leicester and Young was presented by DR LEICESTER. PROFESSOR GLOS said that it is important in a Standard to acquire a representative sample and that it is questionable whether what is proposed can be standardised. DR LEICESTER replied that the paper does give a method to check this. MR FALK asked whether random/specific location of defects depends upon the end-use. DR LEICESTER replied that the Code committee has defined the determination characteristic values in a specific way.

Paper 24-17-3 "Effects of Sampling Size on Accuracy of Characteristic Values of Machines Grades" by Chui, Turner and Smith was presented by PROFESSOR SMITH. PROFESSOR GLOS said that non-parametric methods have been selected by CEN for the determination of characteristic values, because results obtained with them and other distributions for large numbers of data sets have shown the non-parametric methods to be more reliable.

Paper 24-17-2 "Equivalence of Characteristic Values" by LEICESTER and Young and Paper 24-17-4 "Harmonization of LSD Codes" by LEICESTER were presented consecutively by DR LEICESTER. MR THELANDERSSON commented on the substantial differences between the test methods A and C in Figure 2, Paper 24-17-2. The author agreed that these were possibly large than the differences reported in MR THELANDERSSON's simulation studies because of the small section depths of the test pieces.

#### 15. LOAD SHARING

Paper 24-8-1 "On the Possibility of Applying Neutral Vibrational Serviceability Criteria to Joisted Wood Floors" by Smith and Chui was presented by PROFESSOR SMITH.

DR CECCOTTI asked the author if he could explain more fully the conclusions given. PROFESSOR SMITH replied that physical observations on human discomfort were not practical and that as a consequence, arbitrary choices were made in the EC5 draft. MR RIBERHOLT said that in EC5, it is assumed that the mass is equally distributed over the floor, and that the impulse due to footfalls has a specific character. PROFESSOR SMITH replied that it is not always possible to predict the critical impulse.

#### 16. STRUCTURAL STABILITY

Paper 24-15-2 "Discussion about the Description of Timber Beam Column Formula" by Huang was not presented.

Paper 24-15-3 "Seismic Behaviour of Wood Framed Shear Walls" by DR YASAMURA was presented by the Author. DR KORIN asked if the author had any experience of using cement-bonded particleboard as structural sheathing. DR YASAMURA replied that he had, but only with monotonic loading and not cyclic loading. MR ABBOTT asked if any tests had been carried out using combined plywood and plasterboard panels. DR YASAMURA said that some tests had been performed but the results had not yet been analysed. DR CECCOTTI said that papers from outside Europe were now recognizing the importance of the Au/Ay ratios and although the definition of these factors differed, nevertheless it was helpful in drafting EC8. PROFESSOR BLASS asked whether the strength reduction in subsequent cycles was as a result of the damage and if there were any signs of this. The author said that he had assumed plastic deformation of nails and embedment in the sheathing. DR GEHRI said that different nails had been used for each board type and therefore was it possible to assess how much of the shear deformation is carried by the board and how much by the connector. DR YASAMURA replied that some 20 - 40 per cent was carried by the plywood; the remainder by the nails. With Gypsum board, most deformation from the nails. MR APLIN asked if there would be different results if dry wall screws had been used to which the author replied that he had tested these, but only in non-domestic situations.

MR BUCHANAN pointed out that the composition of the boards is critical and that boards with incorporated fibre reinforcement are superior.

#### 17. TIMBER JOINTS AND FASTENERS

Paper 24-7-1 "Theoretical and Experimental Tension and Shear Capacity of Nail Plate Connections" by Kallsner and Kangas was presented by DR KANGAS. MR RIBERHOLT pointed out that the assumptions presented in this paper fit better to larger plates and the author agreed with this.

MR AASHEIM commented that in Norway it is hoped that a single angle can be used in the formula for anchorage capacity and that the difference between the two methods was less than is shown in the paper. Discussions have been held, and it has been agreed to start a Scandinavian cooperative project in this area. MR KANGAS replied that Gangnail plates are more amenable to Mr Aasheim's simplification than others used in Finland. MR RIBERHOLT said that there are problems using empirical formulae that cannot take into account factors such as internal equilibrium, etc. Any changes in plate size or configuration will invalidate the results presented. Also the interpretation of EC5 given in the paper in Fig. 1 is not correct.

PROFESSOR EHLBECK commented that it was encouraging that Finland and Norway would be getting together to evaluate the results of all countries' tests in drafting EC proposals. MR RIBERHOLT added that it is important that the test results are compared and not just different evaluations of results.

Paper 24-7-2 "Testing Method and Determination of Basic Working Loads for Timber Joints with Mechanical Fasteners" by Hiroshima and Kamiya was not presented.

## 18. STRUCTURAL DESIGN CODES

Paper 24-102-2 "Timber Footbridges - a Comparison between Static and Dynamic Design Criteria" by Ceccotti and de Robertis was presented by DR DE ROBERTIS.

PROFESSOR SMITH pointed out that the ratio of 1.5 between  $E_{dynamic}$  and  $E_{static}$  seemed high to which the author replied that this was a reference value and that  $E_{dynamic}$  was determined from tests on a reference structure. PROFESSOR SMITH invited the author to comment on the fact that BS and ISO Standards use an acceleration limit, whereas the Eurocode uses a velocity limit. DR CECCOTTI replied that EC5 Part 1 is just for domestic floors and that no other references could be found for bridges. MR METTEM commented that a recent bridge he had investigated was giving rise to human discomfort but was statically acceptable. The problem related to vibration in a sway mode and vertically. He asked whether the EC Bridge Code drafters are considering this aspect. PROFESSOR GEHRI said that it is important to consider sway, torsion and other modes.

## 19. ANY OTHER BUSINESS

As a result of a lively discussion during the meeting, DR STIEDA invited MR FEWELL to introduce the topic of Depth Effects. MR FEWELL made a brief presentation reviewing last year's paper by Barrett and Fewell on size effects, and stating that the conclusions were supported by the paper given this year by MR LEIJTEN. He stated that the size effect was too large to ignore and illustrated this with tables showing the effects of the proposed intentions of the drafters of EC5 and the CEN Standard, on the economy and safety of timber structures. MR FEWELL asked that anyone with relevant data should send it to him for inclusion in an updated analysis.

Considerable discussion followed regarding the need for and different approaches to determining volume and size effects and it was agreed that this should form a major topic for the next meeting.

## 20. PROGRAMME FOR THE NEXT MEETING

Following discussion earlier in the meeting (see Item 5) PROFESSOR BLASS made a brief presentation on the proposed format for the future meetings. This is summarised below:-

"At the 24th Meeting of CIB W18 in Oxford, England earlier this year, considerable discussion took place regarding the future role of CIB W18 and the format and procedures for future meetings. Subsequent to this, a paper was prepared by the immediate past and newly elected Chairmen and this is now circulated to all members (enclosed). Reference to the full discussions during the meeting will be presented in the minutes which will be published with the proceedings.

I would draw your attention to the first two items under the heading "Implementation" which require that all Chairmen of sub-groups inform the Secretariat of the objectives of their groups' activities and that

members intending to present papers at the 1992 Meeting in Sweden submit a brief abstract of their paper to the Secretariat, in both cases by 31 December 1991."

PROFESSOR BLASS suggested the following topics for the next meeting:-

Size effects  
Truss plates  
Sheet Materials  
Mechano-sorptive effects on strength and creep  
Desire for durability  
Innovations (new products etc)  
Mechanical Timber Joints

21. CLOSE

PROFESSOR BLASS thanked DR STIEDA for his hard work as Chairman of CIB W18A in recent years and this was acknowledged by the meeting. In response, DR STIEDA thanked all participants and authors for their contributions without which the meetings would not have been as lively and interesting as they had been. DR STIEDA thanked the staff at Karlsruhe University for their efforts in preparing and printing the proceedings and he also thanked TRADA for undertaking the secretarial duties through Mr ABBOTT and MR BURGESS. DR STIEDA also thanked MR ABBOTT and his colleagues at TRADA for their hard work in organising a successful meeting in Oxford. The Chairman then closed the 24th Meeting of CIB W18A and said he looked forward to seeing members in Ahus, Sweden next year for the 25th meeting to be held from 24 - 27 August.



**22. List of CIB-W18 Papers,  
Oxford, United Kingdom 1991**





**23. Current List of CIB-W18(A) Papers**



### 23. CURRENT LIST OF CIB-W18(A) PAPERS

Technical papers presented to CIB-W18(A) are identified by a code CIB-W18(A)/a-b-c, where:

- a denotes the meeting at which the paper was presented.  
Meetings are classified in chronological order:

- 1 Princes Risborough, England; March 1973
- 2 Copenhagen, Denmark; October 1973
- 3 Delft, Netherlands; June 1974
- 4 Paris, France; February 1975
- 5 Karlsruhe, Federal Republic of Germany; October 1975
- 6 Aalborg, Denmark; June 1976
- 7 Stockholm, Sweden; February/March 1977
- 8 Brussels, Belgium; October 1977
- 9 Perth, Scotland; June 1978
- 10 Vancouver, Canada; August 1978
- 11 Vienna, Austria; March 1979
- 12 Bordeaux, France; October 1979
- 13 Otaniemi, Finland; June 1980
- 14 Warsaw, Poland; May 1981
- 15 Karlsruhe, Federal Republic of Germany; June 1982
- 16 Lillehammer, Norway; May/June 1983
- 17 Rapperswil, Switzerland; May 1984
- 18 Beit Oren, Israel; June 1985
- 19 Florence, Italy; September 1986
- 20 Dublin, Ireland; September 1987
- 21 Parksville, Canada; September 1988
- 22 Berlin, German Democratic Republic; September 1989
- 23 Lisbon, Portugal; September 1990
- 24 Oxford, United Kingdom; September 1991

b denotes the subject:

- 1 Limit State Design
- 2 Timber Columns
- 3 Symbols
- 4 Plywood
- 5 Stress Grading
- 6 Stresses for Solid Timber
- 7 Timber Joints and Fasteners
- 8 Load Sharing
- 9 Duration of Load
- 10 Timber Beams
- 11 Environmental Conditions
- 12 Laminated Members
- 13 Particle and Fibre Building Boards
- 14 Trussed Rafters
- 15 Structural Stability
- 16 Fire
- 17 Statistics and Data Analysis
- 18 Glued Joints
- 19 Fracture Mechanics
- 100 CIB Timber Code
- 101 Loading Codes
- 102 Structural Design Codes
- 103 International Standards Organisation
- 104 Joint Committee on Structural Safety
- 105 CIB Programme, Policy and Meetings
- 106 International Union of Forestry Research Organisations

c is simply a number given to the papers in the order in which they appear:

Example: CIB-W18/4-102-5 refers to paper 5 on subject 102 presented at the fourth meeting of W18.

Listed below, by subjects, are all papers that have to date been presented to W18. When appropriate some papers are listed under more than one subject heading.

## LIMIT STATE DESIGN

- 1-1-1 Limit State Design - H J Larsen
- 1-1-2 The Use of Partial Safety Factors in the New Norwegian Design Code for Timber Structures - O Brynildsen
- 1-1-3 Swedish Code Revision Concerning Timber Structures - B Noren
- 1-1-4 Working Stresses Report to British Standards Institution Committee BLCP/17/2
- 6-1-1 On the Application of the Uncertainty Theoretical Methods for the Definition of the Fundamental Concepts of Structural Safety - K Skov and O Ditlevsen
- 11-1-1 Safety Design of Timber Structures - H J Larsen
- 18-1-1 Notes on the Development of a UK Limit States Design Code for Timber - A R Fewell and C B Pierce
- 18-1-2 Eurocode 5, Timber Structures - H J Larsen
- 19-1-1 Duration of Load Effects and Reliability Based Design (Single Member) - R O Foschi and Z C Yao
- 21-102-1 Research Activities Towards a New GDR Timber Design Code Based on Limit States Design - W Rug and M Badstube
- 22-1-1 Reliability-Theoretical Investigation into Timber Components Proposal for a Supplement of the Design Concept - M Badstube, W Rug and R Plessow
- 23-1-1 Some Remarks about the Safety of Timber Structures - J Kuipers
- 23-1-2 Reliability of Wood Structural Elements: A Probabilistic Method to Eurocode 5 Calibration - F Rouger, N Lheritier, P Racher and M Fogli

## TIMBER COLUMNS

- 2-2-1 The Design of Solid Timber Columns - H J Larsen
- 3-2-1 The Design of Built-Up Timber Columns - H J Larsen
- 4-2-1 Tests with Centrally Loaded Timber Columns - H J Larsen and S S Pedersen
- 4-2-2 Lateral-Torsional Buckling of Eccentrically Loaded Timber Columns - B Johansson
- 5-9-1 Strength of a Wood Column in Combined Compression and Bending with Respect to Creep - B Källsner and B Norén
- 5-100-1 Design of Solid Timber Columns (First Draft) - H J Larsen
- 6-100-1 Comments on Document 5-100-1, Design of Solid Timber Columns - H J Larsen and E Theilgaard
- 6-2-1 Lattice Columns - H J Larsen
- 6-2-2 A Mathematical Basis for Design Aids for Timber Columns - H J Burgess
- 6-2-3 Comparison of Larsen and Perry Formulas for Solid Timber Columns - H J Burgess
- 7-2-1 Lateral Bracing of Timber Struts - J A Simon
- 8-15-1 Laterally Loaded Timber Columns: Tests and Theory - H J Larsen
- 17-2-1 Model for Timber Strength under Axial Load and Moment - T Poutanen
- 18-2-1 Column Design Methods for Timber Engineering - A H Buchanan, K C Johns, B Madsen
- 19-2-1 Creep Buckling Strength of Timber Beams and Columns - R H Leicester
- 19-12-2 Strength Model for Glulam Columns - H J Blaß

- 20-2-1 Lateral Buckling Theory for Rectangular Section Deep Beam-Columns  
- H J Burgess
- 20-2-2 Design of Timber Columns - H J Blaß
- 21-2-1 Format for Buckling Strength - R H Leicester
- 21-2-2 Beam-Column Formulae for Design Codes - R H Leicester
- 21-15-1 Rectangular Section Deep Beam - Columns with Continuous Lateral  
Restraint - H J Burgess
- 21-15-2 Buckling Modes and Permissible Axial Loads for Continuously Braced  
Columns - H J Burgess
- 21-15-3 Simple Approaches for Column Bracing Calculations - H J Burgess
- 21-15-4 Calculations for Discrete Column Restraints - H J Burgess
- 22-2-1 Buckling and Reliability Checking of Timber Columns - S Huang,  
P M Yu and J Y Hong
- 22-2-2 Proposal for the Design of Compressed Timber Members by Adopting  
the Second-Order Stress Theory - P Kaiser

## SYMBOLS

- 3-3-1 Symbols for Structural Timber Design - J Kuipers and B Norén
- 4-3-1 Symbols for Timber Structure Design - J Kuipers and B Norén
- 1 Symbols for Use in Structural Timber Design



## PLYWOOD

- 2-4-1 The Presentation of Structural Design Data for Plywood - L G Booth
- 3-4-1 Standard Methods of Testing for the Determination of Mechanical Properties of Plywood - J Kuipers
- 3-4-2 Bending Strength and Stiffness of Multiple Species Plywood  
- C K A Stieda
- 4-4-4 Standard Methods of Testing for the Determination of Mechanical Properties of Plywood - Council of Forest Industries, B.C.
- 5-4-1 The Determination of Design Stresses for Plywood in the Revision of CP 112 - L G Booth
- 5-4-2 Veneer Plywood for Construction - Quality Specifications  
- ISO/TC 139. Plywood, Working Group 6
- 6-4-1 The Determination of the Mechanical Properties of Plywood Containing Defects - L G Booth
- 6-4-2 Comparison of the Size and Type of Specimen and Type of Test on Plywood Bending Strength and Stiffness - C R Wilson and P Eng
- 6-4-3 Buckling Strength of Plywood: Results of Tests and Recommendations for Calculations - J Kuipers and H Ploos van Amstel
- 7-4-1 Methods of Test for the Determination of Mechanical Properties of Plywood - L G Booth, J Kuipers, B Norén, C R Wilson
- 7-4-2 Comments Received on Paper 7-4-1
- 7-4-3 The Effect of Rate of Testing Speed on the Ultimate Tensile Stress of Plywood - C R Wilson and A V Parasin
- 7-4-4 Comparison of the Effect of Specimen Size on the Flexural Properties of Plywood Using the Pure Moment Test - C R Wilson and A V Parasin
- 8-4-1 Sampling Plywood and the Evaluation of Test Results - B Norén
- 9-4-1 Shear and Torsional Rigidity of Plywood - H J Larsen

- 9-4-2 The Evaluation of Test Data on the Strength Properties of Plywood  
- L G Booth
- 9-4-3 The Sampling of Plywood and the Derivation of Strength Values  
(Second Draft) - B Norén
- 9-4-4 On the Use of the CIB/RILEM Plywood Plate Twisting Test: a  
progress report - L G Booth
- 10-4-1 Buckling Strength of Plywood - J Dekker, J Kuipers and  
H Ploos van Amstel
- 11-4-1 Analysis of Plywood Stressed Skin Panels with Rigid or Semi-Rigid  
Connections - I Smith
- 11-4-2 A Comparison of Plywood Modulus of Rigidity Determined by the  
ASTM and RILEM CIB/3-TT Test Methods - C R Wilson and  
A V Parasin
- 11-4-3 Sampling of Plywood for Testing Strength - B Norén
- 12-4-1 Procedures for Analysis of Plywood Test Data and Determination of  
Characteristic Values Suitable for Code Presentation - C R Wilson
- 14-4-1 An Introduction to Performance Standards for Wood-base Panel  
Products - D H Brown
- 14-4-2 Proposal for Presenting Data on the Properties of Structural Panels  
- T Schmidt
- 16-4-1 Planar Shear Capacity of Plywood in Bending - C K A Stieda
- 17-4-1 Determination of Panel Shear Strength and Panel Shear Modulus of  
Beech-Plywood in Structural Sizes - J Ehlbeck and F Colling
- 17-4-2 Ultimate Strength of Plywood Webs - R H Leicester and L Pham
- 20-4-1 Considerations of Reliability - Based Design for Structural Composite  
Products - M R O'Halloran, J A Johnson, E G Elias and  
T P Cunningham
- 21-4-1 Modelling for Prediction of Strength of Veneer Having Knots  
- Y Hirashima

- 22-4-1 Scientific Research into Plywood and Plywood Building Constructions the Results and Findings of which are Incorporated into Construction Standard Specifications of the USSR - I M Guskov
- 22-4-2 Evaluation of Characteristic values for Wood-Based Sheet Materials - E G Elias
- 24-4-1 APA Structural-Use Design Values: An Update to Panel Design Capacities - A L Kuchar, E G Elias, B Yeh and M R O'Halloran

#### STRESS GRADING

- 1-5-1 Quality Specifications for Sawn Timber and Precision Timber - Norwegian Standard NS 3080
- 1-5-2 Specification for Timber Grades for Structural Use - British Standard BS 4978
- 4-5-1 Draft Proposal for an International Standard for Stress Grading Coniferous Sawn Softwood - ECE Timber Committee
- 16-5-1 Grading Errors in Practice - B Thunell
- 16-5-2 On the Effect of Measurement Errors when Grading Structural Timber - L Nordberg and B Thunell
- 19-5-1 Stress-Grading by ECE Standards of Italian-Grown Douglas-Fir Dimension Lumber from Young Thinnings - L Uzielli
- 19-5-2 Structural Softwood from Afforestation Regions in Western Norway - R Lackner
- 21-5-1 Non-Destructive Test by Frequency of Full Size Timber for Grading - T Nakai
- 22-5-1 Fundamental Vibration Frequency as a Parameter for Grading Sawn Timber - T Nakai, T Tanaka and H Nagao
- 24-5-1 Influence of Stress Grading System on Length Effect Factors for Lumber Loaded in Compression - A Campos and I Smith

## STRESSES FOR SOLID TIMBER

- 4-6-1 Derivation of Grade Stresses for Timber in the UK - W T Curry
- 5-6-1 Standard Methods of Test for Determining some Physical and Mechanical Properties of Timber in Structural Sizes - W T Curry
- 5-6-2 The Description of Timber Strength Data - J R Tory
- 5-6-3 Stresses for EC1 and EC2 Stress Grades - J R Tory
- 6-6-1 Standard Methods of Test for the Determination of some Physical and Mechanical Properties of Timber in Structural Sizes (third draft) - W T Curry
- 7-6-1 Strength and Long-term Behaviour of Lumber and Glued Laminated Timber under Torsion Loads - K Möhler
- 9-6-1 Classification of Structural Timber - H J Larsen
- 9-6-2 Code Rules for Tension Perpendicular to Grain - H J Larsen
- 9-6-3 Tension at an Angle to the Grain - K Möhler
- 9-6-4 Consideration of Combined Stresses for Lumber and Glued Laminated Timber - K Möhler
- 11-6-1 Evaluation of Lumber Properties in the United States - W L Galligan and J H Haskell
- 11-6-2 Stresses Perpendicular to Grain - K Möhler
- 11-6-3 Consideration of Combined Stresses for Lumber and Glued Laminated Timber (addition to Paper CIB-W18/9-6-4) - K Möhler
- 12-6-1 Strength Classifications for Timber Engineering Codes - R H Leicester and W G Keating
- 12-6-2 Strength Classes for British Standard BS 5268 - J R Tory
- 13-6-1 Strength Classes for the CIB Code - J R Tory

- 13-6-2 Consideration of Size Effects and Longitudinal Shear Strength for Uncracked Beams - R O Foschi and J D Barrett
- 13-6-3 Consideration of Shear Strength on End-Cracked Beams - J D Barrett and R O Foschi
- 15-6-1 Characteristic Strength Values for the ECE Standard for Timber - J G Sunley
- 16-6-1 Size Factors for Timber Bending and Tension Stresses - A R Fewell
- 16-6-2 Strength Classes for International Codes - A R Fewell and J G Sunley
- 17-6-1 The Determination of Grade Stresses from Characteristic Stresses for BS 5268: Part 2 - A R Fewell
- 17-6-2 The Determination of Softwood Strength Properties for Grades, Strength Classes and Laminated Timber for BS 5268: Part 2 - A R Fewell
- 18-6-1 Comment on Papers: 18-6-2 and 18-6-3 - R H Leicester
- 18-6-2 Configuration Factors for the Bending Strength of Timber - R H Leicester
- 18-6-3 Notes on Sampling Factors for Characteristic Values - R H Leicester
- 18-6-4 Size Effects in Timber Explained by a Modified Weakest Link Theory - B Madsen and A H Buchanan
- 18-6-5 Placement and Selection of Growth Defects in Test Specimens - H Riberholt
- 18-6-6 Partial Safety-Coefficients for the Load-Carrying Capacity of Timber Structures - B Norén and J-O Nylander
- 19-6-1 Effect of Age and/or Load on Timber Strength - J Kuipers
- 19-6-2 Confidence in Estimates of Characteristic Values - R H Leicester
- 19-6-3 Fracture Toughness of Wood - Mode I - K Wright and M Fonselius
- 19-6-4 Fracture Toughness of Pine - Mode II - K Wright

- 19-6-5 Drying Stresses in Round Timber - A Ranta-Maunus
- 19-6-6 A Dynamic Method for Determining Elastic Properties of Wood  
- R Görlacher
- 20-6-1 A Comparative Investigation of the Engineering Properties of  
"Whitewoods" Imported to Israel from Various Origins - U Korin
- 20-6-2 Effects of Yield Class, Tree Section, Forest and Size on Strength of  
Home Grown Sitka Spruce - V Picardo
- 20-6-3 Determination of Shear Strength and Strength Perpendicular to Grain  
- H J Larsen
- 21-6-1 Draft Australian Standard: Methods for Evaluation of Strength and  
Stiffness of Graded Timber - R H Leicester
- 21-6-2 The Determination of Characteristic Strength Values for Stress  
Grades of Structural Timber. Part 1 - A R Fewell and P Glos
- 21-6-3 Shear Strength in Bending of Timber -U Korin
- 22-6-1 Size Effects and Property Relationships for Canadian 2-inch Dimension  
Lumber - J D Barrett and H Griffin
- 22-6-2 Moisture Content Adjustements for In-Grade Data - J D Barrett and  
W Lau
- 22-6-3 A Discussion of Lumber Property Relationships in Eurocode 5  
- D W Green and D E Kretschmann
- 22-6-4 Effect of Wood Preservatives on the Strength Properties of Wood  
- F Ronai
- 23-6-1 Timber in Compression Perpendicular to Grain - U Korin
- 24-6-1 Discussion of the Failure Criterion for Combined Bending and  
Compression - T A C M van der Put
- 24-6-3 Effect of Within Member Variability on Bending Strength of Structural  
Timber - I Czmocho, S Thelandersson and H J Larsen

- 24-6-4 Protection of Structural Timber Against Fungal Attack Requirements and Testing - K Jaworska, M Rylko and W Nozynski
- 24-6-5 Derivation of the Characteristic Bending Strength of Solid Timber According to CEN-Document prEN 384 - A J M Leijten

#### TIMBER JOINTS AND FASTENERS

- 1-7-1 Mechanical Fasteners and Fastenings in Timber Structures - E G Stern
- 4-7-1 Proposal for a Basic Test Method for the Evaluation of Structural Timber Joints with Mechanical Fasteners and Connectors  
- RILEM 3TT Committee
- 4-7-2 Test Methods for Wood Fasteners - K Möhler
- 5-7-1 Influence of Loading Procedure on Strength and Slip-Behaviour in Testing Timber Joints - K Möhler
- 5-7-2 Recommendations for Testing Methods for Joints with Mechanical Fasteners and Connectors in Load-Bearing Timber Structures  
- RILEM 3 TT Committee
- 5-7-3 CIB-Recommendations for the Evaluation of Results of Tests on Joints with Mechanical Fasteners and Connectors used in Load-Bearing Timber Structures - J Kuipers
- 6-7-1 Recommendations for Testing Methods for Joints with Mechanical Fasteners and Connectors in Load-Bearing Timber Structures (seventh draft) - RILEM 3 TT Committee
- 6-7-2 Proposal for Testing Integral Nail Plates as Timber Joints - K Möhler
- 6-7-3 Rules for Evaluation of Values of Strength and Deformation from Test Results - Mechanical Timber Joints - M Johansen, J Kuipers, B Norén
- 6-7-4 Comments to Rules for Testing Timber Joints and Derivation of Characteristic Values for Rigidity and Strength - B Norén
- 7-7-1 Testing of Integral Nail Plates as Timber Joints - K Möhler

- 7-7-2 Long Duration Tests on Timber Joints - J Kuipers
- 7-7-3 Tests with Mechanically Jointed Beams with a Varying Spacing of Fasteners - K Möhler
- 7-100-1 CIB-Timber Code Chapter 5.3 Mechanical Fasteners;CIB-Timber Standard 06 and 07 - H J Larsen
- 9-7-1 Design of Truss Plate Joints - F J Keenan
- 9-7-2 Staples - K Möhler
- 11-7-1 A Draft Proposal for International Standard: ISO Document ISO/TC 165N 38E
- 12-7-1 Load-Carrying Capacity and Deformation Characteristics of Nailed Joints - J Ehlbeck
- 12-7-2 Design of Bolted Joints - H J Larsen
- 12-7-3 Design of Joints with Nail Plates - B Norén
- 13-7-1 Polish Standard BN-80/7159-04: Parts 00-01-02-03-04-05. "Structures from Wood and Wood-based Materials. Methods of Test and Strength Criteria for Joints with Mechanical Fasteners"
- 13-7-2 Investigation of the Effect of Number of Nails in a Joint on its Load Carrying Ability - W Nozynski
- 13-7-3 International Acceptance of Manufacture, Marking and Control of Finger-jointed Structural Timber - B Norén
- 13-7-4 Design of Joints with Nail Plates - Calculation of Slip - B Norén
- 13-7-5 Design of Joints with Nail Plates - The Heel Joint - B Källsner
- 13-7-6 Nail Deflection Data for Design - H J Burgess
- 13-7-7 Test on Bolted Joints - P Vermeijden
- 13-7-8 Comments to paper CIB-W18/12-7-3 "Design of Joints with Nail Plates" - B Norén



- 13-7-9 Strength of Finger Joints - H J Larsen
- 13-100-4 CIB Structural Timber Design Code. Proposal for Section 6.1.5 Nail Plates - N I Bovim
- 14-7-1 Design of Joints with Nail Plates (second edition) - B Norén
- 14-7-2 Method of Testing Nails in Wood (second draft, August 1980) - B Norén
- 14-7-3 Load-Slip Relationship of Nailed Joints - J Ehlbeck and H J Larsen
- 14-7-4 Wood Failure in Joints with Nail Plates - B Norén
- 14-7-5 The Effect of Support Eccentricity on the Design of W- and WW-Trussed with Nail Plate Connectors - B Källsner
- 14-7-6 Derivation of the Allowable Load in Case of Nail Plate Joints Perpendicular to Grain - K Möhler
- 14-7-7 Comments on CIB-W18/14-7-1 - T A C M van der Put
- 15-7-1 Final Recommendation TT-1A: Testing Methods for Joints with Mechanical Fasteners in Load-Bearing Timber Structures. Annex A Punched Metal Plate Fasteners - Joint Committee RILEM/CIB-3TT
- 16-7-1 Load Carrying Capacity of Dowels - E Gehri
- 16-7-2 Bolted Timber Joints: A Literature Survey - N Harding
- 16-7-3 Bolted Timber Joints: Practical Aspects of Construction and Design; a Survey - N Harding
- 16-7-4 Bolted Timber Joints: Draft Experimental Work Plan - Building Research Association of New Zealand
- 17-7-1 Mechanical Properties of Nails and their Influence on Mechanical Properties of Nailed Timber Joints Subjected to Lateral Loads - I Smith, L R J Whale, C Anderson and L Held
- 17-7-2 Notes on the Effective Number of Dowels and Nails in Timber Joints - G Steck

- 18-7-1 Model Specification for Driven Fasteners for Assembly of Pallets and Related Structures - E G Stern and W B Wallin
- 18-7-2 The Influence of the Orientation of Mechanical Joints on their Mechanical Properties - I Smith and L R J Whale
- 18-7-3 Influence of Number of Rows of Fasteners or Connectors upon the Ultimate Capacity of Axially Loaded Timber Joints - I Smith and G Steck
- 18-7-4 A Detailed Testing Method for Nailplate Joints - J Kangas
- 18-7-5 Principles for Design Values of Nailplates in Finland - J Kangas
- 18-7-6 The Strength of Nailplates - N I Bovim and E Aasheim
- 19-7-1 Behaviour of Nailed and Bolted Joints under Short-Term Lateral Load - Conclusions from Some Recent Research - L R J Whale, I Smith and B O Hilson
- 19-7-2 Glued Bolts in Glulam - H Riberholt
- 19-7-3 Effectiveness of Multiple Fastener Joints According to National Codes and Eurocode 5 (Draft) - G Steck
- 19-7-4 The Prediction of the Long-Term Load Carrying Capacity of Joints in Wood Structures - Y M Ivanov and Y Y Slavic
- 19-7-5 Slip in Joints under Long-Term Loading - T Feldborg and M Johansen
- 19-7-6 The Derivation of Design Clauses for Nailed and Bolted Joints in Eurocode 5 - L R J Whale and I Smith
- 19-7-7 Design of Joints with Nail Plates - Principles - B Norén
- 19-7-8 Shear Tests for Nail Plates - B Norén
- 19-7-9 Advances in Technology of Joints for Laminated Timber - Analyses of the Structural Behaviour - M Piazza and G Turrini
- 19-15-1 Connections Deformability in Timber Structures: A Theoretical Evaluation of its Influence on Seismic Effects - A Ceccotti and A Vignoli

- 20-7-1 Design of Nailed and Bolted Joints-Proposals for the Revision of Existing Formulae in Draft Eurocode 5 and the CIB Code  
- L R J Whale, I Smith and H J Larsen
- 20-7-2 Slip in Joints under Long Term Loading - T Feldborg and M Johansen
- 20-7-3 Ultimate Properties of Bolted Joints in Glued-Laminated Timber  
- M Yasumura, T Murota and H Sakai
- 20-7-4 Modelling the Load-Deformation Behaviour of Connections with Pin-Type Fasteners under Combined Moment, Thrust and Shear Forces  
- I Smith
- 21-7-1 Nails under Long-Term Withdrawal Loading - T Feldborg and M Johansen
- 21-7-2 Glued Bolts in Glulam-Proposals for CIB Code - H Riberholt
- 21-7-3 Nail Plate Joint Behaviour under Shear Loading - T Poutanen
- 21-7-4 Design of Joints with Laterally Loaded Dowels. Proposals for Improving the Design Rules in the CIB Code and the Draft Eurocode 5  
- J Ehlbeck and H Werner
- 21-7-5 Axially Loaded Nails: Proposals for a Supplement to the CIB Code  
- J Ehlbeck and W Siebert
- 22-7-1 End Grain Connections with Laterally Loaded Steel Bolts A draft proposal for design rules in the CIB Code - J Ehlbeck and M Gerold
- 22-7-2 Determination of Perpendicular-to-Grain Tensile Stresses in Joints with Dowel-Type Fasteners - A draft proposal for design rules - J Ehlbeck, R Görlacher and H Werner
- 22-7-3 Design of Double-Shear Joints with Non-Metallic Dowels A proposal for a supplement of the design concept - J Ehlbeck and O Eberhart
- 22-7-4 The Effect of Load on Strength of Timber Joints at high Working Load Level - A J M Leijten
- 22-7-5 Plasticity Requirements for Portal Frame Corners - R Gunnewijk and A J M Leijten

- 22-7-6 Background Information on Design of Glulam Rivet Connections in CSA/CAN3-086.1-M89 - A proposal for a supplement of the design concept - E Karacabeyli and D P Janssens
- 22-7-7 Mechanical Properties of Joints in Glued-Laminated Beams under Reversed Cyclic Loading - M Yasumura
- 22-7-8 Strength of Glued Lap Timber Joints - P Glos and H Horstmann
- 22-7-9 Toothed Rings Type Bistyp 075 at the Joints of Fir Wood - J Kerste
- 22-7-10 Calculation of Joints and Fastenings as Compared with the International State - K Zimmer and K Lissner
- 22-7-11 Joints on Glued-in Steel Bars Present Relatively New and Progressive Solution in Terms of Timber Structure Design - G N Zubarev, F A Boitemirov and V M Golovina
- 22-7-12 The Development of Design Codes for Timber Structures made of Composite Bars with Plate Joints based on Cylindrical Nails - Y V Piskunov
- 22-7-13 Designing of Glued Wood Structures Joints on Glued-in Bars - S B Turkovsky
- 23-7-1 Proposal for a Design Code for Nail Plates - E Aasheim and K H Solli
- 23-7-2 Load Distribution in Nailed Joints - H J Blass
- 24-7-1 Theoretical and Experimental Tension and Shear Capacity of Nail Plate Connections - B Källsner and J Kangas
- 24-7-2 Testing Method and Determination of Basic Working Loads for Timber Joints with Mechanical Fasteners - Y Hirashima and F Kamiya
- 24-7-3 Anchorage Capacity of Nail Plate - J Kangas

## LOAD SHARING

- 3-8-1 Load Sharing - An Investigation on the State of Research and Development of Design Criteria - E Levin
- 4-8-1 A Review of Load-Sharing in Theory and Practice - E Levin
- 4-8-2 Load Sharing - B Norén
- 19-8-1 Predicting the Natural Frequencies of Light-Weight Wooden Floors - I Smith and Y H Chui
- 20-8-1 Proposed Code Requirements for Vibrational Serviceability of Timber Floors - Y H Chui and I Smith
- 21-8-1 An Addendum to Paper 20-8-1 - Proposed Code Requirements for Vibrational Serviceability of Timber Floors - Y H Chui and I Smith
- 21-8-2 Floor Vibrational Serviceability and the CIB Model Code - S Ohlsson
- 22-8-1 Reliability Analysis of Viscoelastic Floors - F Rouger, J D Barrett and R O Foschi
- 24-8-1 On the Possibility of Applying Neutral Vibrational Serviceability Criteria to Joisted Wood Floors - I Smith and Y H Chui

## DURATION OF LOAD

- 3-9-1 Definitions of Long Term Loading for the Code of Practice - B Norén
- 4-9-1 Long Term Loading of Trussed Rafters with Different Connection Systems - T Feldborg and M Johansen
- 5-9-1 Strength of a Wood Column in Combined Compression and Bending with Respect to Creep - B Källsner and B Norén
- 6-9-1 Long Term Loading for the Code of Practice (Part 2) - B Norén
- 6-9-2 Long Term Loading - K Möhler

- 6-9-3 Deflection of Trussed Rafters under Alternating Loading during a Year  
- T Feldborg and M Johansen
- 7-6-1 Strength and Long Term Behaviour of Lumber and Glued-Laminated  
Timber under Torsion Loads - K Möhler
- 7-9-1 Code Rules Concerning Strength and Loading Time - H J Larsen and  
E Theilgaard
- 17-9-1 On the Long-Term Carrying Capacity of Wood Structures - Y M Ivanov  
and Y Y Slavic
- 18-9-1 Prediction of Creep Deformations of Joints - J Kuipers
- 19-9-1 Another Look at Three Duration of Load Models - R O Foschi and  
Z C Yao
- 19-9-2 Duration of Load Effects for Spruce Timber with Special Reference to  
Moisture Influence - A Status Report - P Hoffmeyer
- 19-9-3 A Model of Deformation and Damage Processes Based on the  
Reaction Kinetics of Bond Exchange - T A C M van der Put
- 19-9-4 Non-Linear Creep Superposition - U Korin
- 19-9-5 Determination of Creep Data for the Component Parts of Stressed-Skin  
Panels - R Kliger
- 19-9-6 Creep an Lifetime of Timber Loaded in Tension and Compression  
- P Glos
- 19-1-1 Duration of Load Effects and Reliability Based Design (Single  
Member) - R O Foschi and Z C Yao
- 19-6-1 Effect of Age and/or Load on Timber Strength - J Kuipers
- 19-7-4 The Prediction of the Long-Term Load Carrying Capacity of Joints in  
Wood Structures - Y M Ivanov and Y Y Slavic
- 19-7-5 Slip in Joints under Long-Term Loading - T Feldborg and M Johansen
- 20-7-2 Slip in Joints under Long-Term Loading - T Feldborg and M Johansen

- 22-9-1 Long-Term Tests with Glued Laminated Timber Girders - M Badstube, W Rug and W Schöne
- 22-9-2 Strength of One-Layer solid and Lengthways Glued Elements of Wood Structures and its Alteration from Sustained Load - L M Kovaltchuk, I N Boitemirova and G B Uspenskaya
- 24-9-1 Long Term Bending Creep of Wood - T Toratti
- 24-9-2 Collection of Creep Data of Timber - A Ranta-Maunus
- 24-9-3 Deformation Modification Factors for Calculating Built-up Wood-Based Structures - I R Kliger

#### TIMBER BEAMS

- 4-10-1 The Design of Simple Beams - H J Burgess
- 4-10-2 Calculation of Timber Beams Subjected to Bending and Normal Force - H J Larsen
- 5-10-1 The Design of Timber Beams - H J Larsen
- 9-10-1 The Distribution of Shear Stresses in Timber Beams - F J Keenan
- 9-10-2 Beams Notched at the Ends - K Möhler
- 11-10-1 Tapered Timber Beams - H Riberholt
- 13-6-2 Consideration of Size Effects in Longitudinal Shear Strength for Uncracked Beams - R O Foschi and J D Barrett
- 13-6-3 Consideration of Shear Strength on End-Cracked Beams - J D Barrett and R O Foschi
- 18-10-1 Submission to the CIB-W18 Committee on the Design of Ply Web Beams by Consideration of the Type of Stress in the Flanges - J A Baird
- 18-10-2 Longitudinal Shear Design of Glued Laminated Beams - R O Foschi
- 19-10-1 Possible Code Approaches to Lateral Buckling in Beams - H J Burgess

- 19-2-1 Creep Buckling Strength of Timber Beams and Columns  
- R H Leicester
- 20-2-1 Lateral Buckling Theory for Rectangular Section Deep Beam-Columns  
- H J Burgess
- 20-10-1 Draft Clause for CIB Code for Beams with Initial Imperfections  
- H J Burgess
- 20-10-2 Space Joists in Irish Timber - W J Robinson
- 20-10-3 Composite Structure of Timber Joists and Concrete Slab  
- T Poutanen
- 21-10-1 A Study of Strength of Notched Beams - P J Gustafsson
- 22-10-1 Design of Endnotched Beams - H J Larsen and P J Gustafsson
- 22-10-2 Dimensions of Wooden Flexural Members under Constant Loads  
- A Pozgai
- 22-10-3 Thin-Walled Wood-Based Flanges in Composite Beams - J König
- 22-10-4 The Calculation of Wooden Bars with flexible Joints in Accordance  
with the Polish Standard Code and Strict Theoretical Methods  
- Z Mielczarek
- 23-10-1 Tension Perpendicular to the Grain at Notches and Joints  
- T A C M van der Put
- 23-10-2 Dimensioning of Beams with Cracks, Notches and Holes. An  
Application of Fracture Mechanics - K Riipola
- 23-10-3 Size Factors for the Bending and Tension Strength of Structural Timber  
- J D Barret and A R Fewell
- 23-12-1 Bending Strength of Glulam Beams, a Design Proposal - J Ehlbeck and  
F Colling
- 23-12-3 Glulam Beams, Bending Strength in Relation to the Bending Strength  
of the Finger Joints - H Riberholt
- 24-10-1 Shear Strength of Continuous Beams - R H Leicester and F G Young



## ENVIRONMENTAL CONDITIONS

- 5-11-1 Climate Grading for the Code of Practice - B Norén
- 6-11-1 Climate Grading (2) - B Norén
- 9-11-1 Climate Classes for Timber Design - F J Keenan
- 19-11-1 Experimental Analysis on Ancient Downgraded Timber Structures  
- B Leggeri and L Paolini
- 19-6-5 Drying Stresses in Round Timber - A Ranta-Maunus
- 22-11-1 Corrosion and Adaptation Factors for Chemically Aggressive Media  
with Timber Structures - K Erler

## LAMINATED MEMBERS

- 6-12-1 Directives for the Fabrication of Load-Bearing Structures of Glued  
Timber - A van der Velden and J Kuipers
- 8-12-1 Testing of Big Glulam Timber Beams - H Kolb and P Frech
- 8-12-2 Instruction for the Reinforcement of Apertures in Glulam Beams  
- H Kolb and P Frech
- 8-12-3 Glulam Standard Part 1: Glued Timber Structures; Requirements for  
Timber (Second Draft)
- 9-12-1 Experiments to Provide for Elevated Forces at the Supports of Wooden  
Beams with Particular Regard to Shearing Stresses and Long-Term  
Loadings - F Wassipaul and R Lackner
- 9-12-2 Two Laminated Timber Arch Railway Bridges Built in Perth in 1849  
- L G Booth
- 9-6-4 Consideration of Combined Stresses for Lumber and Glued Laminated  
Timber - K Möhler

- 11-6-3 Consideration of Combined Stresses for Lumber and Glued Laminated Timber (addition to Paper CIB-W18/9-6-4) - K Möhler
- 12-12-1 Glulam Standard Part 2: Glued Timber Structures; Rating (3rd draft)
- 12-12-2 Glulam Standard Part 3: Glued Timber Structures; Performance (3 rd draft)
- 13-12-1 Glulam Standard Part 3: Glued Timber Structures; Performance (4th draft)
- 14-12-1 Proposals for CEI-Bois/CIB-W18 Glulam Standards - H J Larsen
- 14-12-2 Guidelines for the Manufacturing of Glued Load-Bearing Timber Structures - Stevin Laboratory
- 14-12-3 Double Tapered Curved Glulam Beams - H Riberholt
- 14-12-4 Comment on CIB-W18/14-12-3 - E Gehri
- 18-12-1 Report on European Glulam Control and Production Standard - H Riberholt
- 18-10-2 Longitudinal Shear Design of Glued Laminated Beams - R O Foschi
- 19-12-1 Strength of Glued Laminated Timber - J Ehlbeck and F Colling
- 19-12-2 Strength Model for Glulam Columns - H J Blaß
- 19-12-3 Influence of Volume and Stress Distribution on the Shear Strength and Tensile Strength Perpendicular to Grain - F Colling
- 19-12-4 Time-Dependent Behaviour of Glued-Laminated Beams - F Zaupa
- 21-12-1 Modulus of Rupture of Glulam Beam Composed of Arbitrary Laminae - K Komatsu and N Kawamoto
- 21-12-2 An Appraisal of the Young's Modulus Values Specified for Glulam in Eurocode 5 - L R J Whale, B O Hilson and P D Rodd
- 21-12-3 The Strength of Glued Laminated Timber (Glulam): Influence of Lamination Qualities and Strength of Finger Joints - J Ehlbeck and F Colling

- 21-12-4 Comparison of a Shear Strength Design Method in Eurocode 5 and a More Traditional One - H Riberholt
- 22-12-1 The Dependence of the Bending Strength on the Glued Laminated Timber Girder Depth - M Badstube, W Rug and W Schöne
- 22-12-2 Acid Deterioration of Glulam Beams in Buildings from the Early Half of the 1960s - Preliminary summary of the research project; Overhead pictures - B A Hedlund
- 22-12-3 Experimental Investigation of normal Stress Distribution in Glue Laminated Wooden Arches - Z Mielczarek and W Chanaj
- 22-12-4 Ultimate Strength of Wooden Beams with Tension Reinforcement as a Function of Random Material Properties - R Candowicz and T Dziuba
- 23-12-1 Bending Strength of Glulam Beams, a Design Proposal - J Ehlbeck and F Colling
- 23-12-2 Probability Based Design Method for Glued Laminated Timber - M F Stone
- 23-12-3 Glulam Beams, Bending Strength in Relation to the Bending Strength of the Finger Joints - H Riberholt
- 23-12-4 Glued Laminated Timber - Strength Classes and Determination of Characteristic Properties - H Riberholt, J Ehlbeck and A Fewell
- 24-12-1 Contribution to the Determination of the Bending Strength of Glulam Beams - F Colling, J Ehlbeck and R Görlacher
- 24-12-2 Influence of Perpendicular-to-Grain Stressed Volume on the Load-Carrying Capacity of Curved and Tapered Glulam Beams - J Ehlbeck and J Kürth

## PARTICLE AND FIBRE BUILDING BOARDS

- 7-13-1 Fibre Building Boards for CIB Timber Code (First Draft)  
- O Brynildsen
- 9-13-1 Determination of the Bearing Strength and the Load-Deformation  
Characteristics of Particleboard - K Möhler, T Budianto and J Ehlbeck
- 9-13-2 The Structural Use of Tempered Hardboard - W W L Chan
- 11-13-1 Tests on Laminated Beams from Hardboard under Short- and  
Longterm Load - W Nozynski
- 11-13-2 Determination of Deformation of Special Densified Hardboard under  
Long-term Load and Varying Temperature and Humidity Conditions -  
W Halfar
- 11-13-3 Determination of Deformation of Hardboard under Long-term Load in  
Changing Climate - W Halfar
- 14-4-1 An Introduction to Performance Standards for Wood-Base Panel  
Products - D H Brown
- 14-4-2 Proposal for Presenting Data on the Properties of Structural Panels  
- T Schmidt
- 16-13-1 Effect of Test Piece Size on Panel Bending Properties - P W Post
- 20-4-1 Considerations of Reliability - Based Design for Structural Composite  
Products - M R O'Halloran, J A Johnson, E G Elias and  
T P Cunningham
- 20-13-1 Classification Systems for Structural Wood-Based Sheet Materials  
- V C Kearley and A R Abbott
- 21-13-1 Design Values for Nailed Chipboard - Timber Joints - A R Abbott

## TRUSSED RAFTERS

- 4-9-1 Long-term Loading of Trussed Rafters with Different Connection Systems - T Feldborg and M Johansen
- 6-9-3 Deflection of Trussed Rafters under Alternating Loading During a Year - T Feldborg and M Johansen
- 7-2-1 Lateral Bracing of Timber Struts - J A Simon
- 9-14-1 Timber Trusses - Code Related Problems - T F Williams
- 9-7-1 Design of Truss Plate Joints - F J Keenan
- 10-14-1 Design of Roof Bracing - The State of the Art in South Africa - P A V Bryant and J A Simon
- 11-14-1 Design of Metal Plate Connected Wood Trusses - A R Egerup
- 12-14-1 A Simple Design Method for Standard Trusses - A R Egerup
- 13-14-1 Truss Design Method for CIB Timber Code - A R Egerup
- 13-14-2 Trussed Rafters, Static Models - H Riberholt
- 13-14-3 Comparison of 3 Truss Models Designed by Different Assumptions for Slip and E-Modulus - K Möhler
- 14-14-1 Wood Trussed Rafter Design - T Feldborg and M Johansen
- 14-14-2 Truss-Plate Modelling in the Analysis of Trusses - R O Foschi
- 14-14-3 Cantilevered Timber Trusses - A R Egerup
- 14-7-5 The Effect of Support Eccentricity on the Design of W- and WW-Trusses with Nail Plate Connectors - B Källsner
- 15-14-1 Guidelines for Static Models of Trussed Rafters - H Riberholt
- 15-14-2 The Influence of Various Factors on the Accuracy of the Structural Analysis of Timber Roof Trusses - F R P Pienaar

- 15-14-3 Bracing Calculations for Trussed Rafter Roofs - H J Burgess
- 15-14-4 The Design of Continuous Members in Timber Trussed Rafters with Punched Metal Connector Plates - P O Reece
- 15-14-5 A Rafter Design Method Matching U.K. Test Results for Trussed Rafters - H J Burgess
- 16-14-1 Full-Scale Tests on Timber Fink Trusses Made from Irish Grown Sitka Spruce - V Picardo
- 17-14-1 Data from Full Scale Tests on Prefabricated Trussed Rafters - V Picardo
- 17-14-2 Simplified Static Analysis and Dimensioning of Trussed Rafters - H Riberholt
- 17-14-3 Simplified Calculation Method for W-Trusses - B Källsner
- 18-14-1 Simplified Calculation Method for W-Trusses (Part 2) - B Källsner
- 18-14-2 Model for Trussed Rafter Design - T Poutanen
- 19-14-1 Annex on Simplified Design of W-Trusses - H J Larsen
- 19-14-2 Simplified Static Analysis and Dimensioning of Trussed Rafters - Part 2 - H Riberholt
- 19-14-3 Joint Eccentricity in Trussed Rafters - T Poutanen
- 20-14-1 Some Notes about Testing Nail Plates Subjected to Moment Load - T Poutanen
- 20-14-2 Moment Distribution in Trussed Rafters - T Poutanen
- 20-14-3 Practical Design Methods for Trussed Rafters - A R Egerup
- 22-14-1 Guidelines for Design of Timber Trussed Rafters - H Riberholt
- 23-14-1 Analyses of Timber Trussed Rafters of the W-Type - H Riberholt

- 23-14-2 Proposal for Eurocode 5 Text on Timber Trussed Rafters - H Riberholt
- 24-14-1 Capacity of Support Areas Reinforced with Nail Plates in Trussed Rafters - A Kevarinmäki

## STRUCTURAL STABILITY

- 8-15-1 Laterally Loaded Timber Columns: Tests and Theory - H J Larsen
- 13-15-1 Timber and Wood-Based Products Structures. Panels for Roof Coverings. Methods of Testing and Strength Assessment Criteria. Polish Standard BN-78/7159-03
- 16-15-1 Determination of Bracing Structures for Compression Members and Beams - H Brüninghoff
- 17-15-1 Proposal for Chapter 7.4 Bracing - H Brüninghoff
- 17-15-2 Seismic Design of Small Wood Framed Houses - K F Hansen
- 18-15-1 Full-Scale Structures in Glued Laminated Timber, Dynamic Tests: Theoretical and Experimental Studies - A Ceccotti and A Vignoli
- 18-15-2 Stabilizing Bracings - H Brüninghoff
- 19-15-1 Connections Deformability in Timber Structures: a Theoretical Evaluation of its Influence on Seismic Effects - A Ceccotti and A Vignoli
- 19-15-2 The Bracing of Trussed Beams - M H Kessel and J Natterer
- 19-15-3 Racking Resistance of Wooden Frame Walls with Various Openings - M Yasumura
- 19-15-4 Some Experiences of Restoration of Timber Structures for Country Buildings - G Cardinale and P Spinelli
- 19-15-5 Non-Destructive Vibration Tests on Existing Wooden Dwellings - Y Hirashima

- 20-15-1 Behaviour Factor of Timber Structures in Seismic Zones.  
- A Ceccotti and A Vignoli
- 21-15-1 Rectangular Section Deep Beam - Columns with Continuous Lateral Restraint - H J Burgess
- 21-15-2 Buckling Modes and Permissible Axial Loads for Continuously Braced Columns - H J Burgess
- 21-15-3 Simple Approaches for Column Bracing Calculations - H J Burgess
- 21-15-4 Calculations for Discrete Column Restraints - H J Burgess
- 21-15-5 Behaviour Factor of Timber Structures in Seismic Zones (Part Two)  
- A Ceccotti and A Vignoli
- 22-15-1 Suggested Changes in Code Bracing Recommendations for Beams and Columns - H J Burgess
- 22-15-2 Research and Development of Timber Frame Structures for Agriculture in Poland - S Kus and J Kerste
- 22-15-3 Ensuring of Three-Dimensional Stiffness of Buildings with Wood Structures - A K Shenghelia
- 22-15-5 Seismic Behavior of Arched Frames in Timber Construction  
- M Yasumura
- 22-15-6 The Robustness of Timber Structures - C J Mettem and J P Marcroft
- 22-15-7 Influence of Geometrical and Structural Imperfections on the Limit Load of Wood Columns - P Dutko
- 23-15-1 Calculation of Wind Girder Loaded also by Discretely Spaced Braces for Roof Members - H J Burgess
- 23-15-2 Stability Design and Code Rules for Straight Timber Beams  
- T A C M van der Put
- 23-15-3 A Brief Description of Formula of Beam-Columns in China Code  
- S Y Huang



- 23-15-4 Seismic Behavior of Braced Frames in Timber Construction  
- M Yasumura
- 23-15-5 On a Better Evaluation of the Seismic Behavior Factor of Low-Dissipative Timber Structures - A Ceccotti and A Vignoli
- 23-15-6 Disproportionate Collapse of Timber Structures - C J Mettem and J P Marcroft
- 23-15-7 Performance of Timber Frame Structures During the Loma Prieta California Earthquake - M R O'Halloran and E G Elias
- 24-15-2 Discussion About the Description of Timber Beam-Column Formula - S Y Huang
- 24-15-3 Seismic Behavior of Wood-Framed Shear Walls - M Yasumura

## FIRE

- 12-16-1 British Standard BS 5268 the Structural Use of Timber: Part 4 Fire Resistance of Timber Structures
- 13-100-2 CIB Structural Timber Design Code. Chapter 9. Performance in Fire
- 19-16-1 Simulation of Fire in Tests of Axially Loaded Wood Wall Studs  
- J König
- 24-16-1 Modelling the Effective Cross Section of Timber Frame Members Exposed to Fire - J König

## STATISTICS AND DATA ANALYSIS

- 13-17-1 On Testing Whether a Prescribed Exclusion Limit is Attained  
- W G Warren
- 16-17-1 Notes on Sampling and Strength Prediction of Stress Graded Structural Timber - P Glos

- 16-17-2 Sampling to Predict by Testing the Capacity of Joints, Components and Structures - B Norén
- 16-17-3 Discussion of Sampling and Analysis Procedures - P W Post
- 17-17-1 Sampling of Wood for Joint Tests on the Basis of Density - I Smith, L R J Whale
- 17-17-2 Sampling Strategy for Physical and Mechanical Properties of Irish Grown Sitka Spruce - V Picardo
- 18-17-1 Sampling of Timber in Structural Sizes - P Glos
- 18-6-3 Notes on Sampling Factors for Characteristic Values - R H Leicester
- 19-17-1 Load Factors for Proof and Prototype Testing - R H Leicester
- 19-6-2 Confidence in Estimates of Characteristic Values - R H Leicester
- 21-6-1 Draft Australian Standard: Methods for Evaluation of Strength and Stiffness of Graded Timber - R H Leicester
- 21-6-2 The Determination of Characteristic Strength Values for Stress Grades of Structural Timber. Part 1 - A R Fewell and P Glos
- 22-17-1 Comment on the Strength Classes in Eurocode 5 by an Analysis of a Stochastic Model of Grading - A proposal for a supplement of the design concept - M Kiesel
- 24-17-1 Use of Small Samples for In-Service Strength Measurement - R H Leicester and F G Young
- 24-17-2 Equivalence of Characteristic Values - R H Leicester and F G Young
- 24-17-3 Effect of Sampling Size on Accuracy of Characteristic Values of Machine Grades - Y H Chui, R Turner and I Smith
- 24-17-4 Harmonisation of LSD Codes - R H Leicester

## FRACTURE MECHANICS

- 21-10-1 A Study of Strength of Notched Beams - P J Gustafsson
- 22-10-1 Design of Endnotched Beams - H J Larsen and P J Gustafsson
- 23-10-1 Tension Perpendicular to the Grain at Notches and Joints  
- T A C M van der Put
- 23-10-2 Dimensioning of Beams with Cracks, Notches and Holes. An  
Application of Fracture Mechanics - K Riipola
- 23-19-1 Determination of the Fracture Energie of Wood for Tension  
Perpendicular to the Grain - W Rug, M Badstube and W Schöne
- 23-19-2 The Fracture Energy of Wood in Tension Perpendicular to the Grain.  
Results from a Joint Testing Project - H J Larsen and P J Gustafsson
- 23-19-3 Application of Fracture Mechanics to Timber Structures  
- A Ranta-Maunus
- 24-19-1 The Fracture Energy of Wood in Tension Perpendicular to the Grain -  
H J Larsen and P J Gustafsson

## GLUED JOINTS

- 20-18-1 Wood Materials under Combined Mechanical and Hygral Loading  
- A Martensson and S Thelandersson
- 20-18-2 Analysis of Generalized Volkersen - Joints in Terms of Linear Fracture  
Mechanics - P J Gustafsson
- 20-18-3 The Complete Stress-Slip Curve of Wood-Adhesives in Pure Shear  
- H Wernersson and P J Gustafsson
- 22-18-1 Perspective Adhesives and Protective Coatings for Wood Structures  
- A S Freidin

## CIB TIMBER CODE

- 2-100-1 A Framework for the Production of an International Code of Practice for the Structural Use of Timber - W T Curry
- 5-100-1 Design of Solid Timber Columns (First Draft) - H J Larsen
- 5-100-2 A Draft Outline of a Code for Timber Structures - L G Booth
- 6-100-1 Comments on Document 5-100-1; Design of Solid Timber Columns - H J Larsen and E Theilgaard
- 6-100-2 CIB Timber Code: CIB Timber Standards - H J Larsen and E Theilgaard
- 7-100-1 CIB Timber Code Chapter 5.3 Mechanical Fasteners; CIB Timber Standard 06 and 07 - H J Larsen
- 8-100-1 CIB Timber Code - List of Contents (Second Draft) - H J Larsen
- 9-100-1 The CIB Timber Code (Second Draft)
- 11-100-1 CIB Structural Timber Design Code (Third Draft)
- 11-100-2 Comments Received on the CIB Code  
a U Saarelainen  
b Y M Ivanov  
c R H Leicester  
d W Nozynski  
e W R A Meyer  
f P Beckmann; R Marsh  
g W R A Meyer  
h W R A Meyer
- 11-100-3 CIB Structural Timber Design Code; Chapter 3 - H J Larsen
- 12-100-1 Comment on the CIB Code - Sous-Commission Glulam
- 12-100-2 Comment on the CIB Code - R H Leicester
- 12-100-3 CIB Structural Timber Design Code (Fourth Draft)
- 13-100-1 Agreed Changes to CIB Structural Timber Design Code

- 13-100-2 CIB Structural Timber Design Code. Chapter 9: Performance in Fire
- 13-100-3a Comments on CIB Structural Timber Design Code
- 13-100-3b Comments on CIB Structural Timber Design Code - W R A Meyer
- 13-100-3c Comments on CIB Structural Timber Design Code - British Standards Institution
- 13-100-4 CIB Structural Timber Design Code. Proposal for Section 6.1.5 Nail Plates - N I Bovim
- 14-103-2 Comments on the CIB Structural Timber Design Code - R H Leicester
- 15-103-1 Resolutions of TC 165-meeting in Athens 1981-10-12/13
- 21-100-1 CIB Structural Timber Design Code. Proposed Changes of Sections on Lateral Instability, Columns and Nails - H J Larsen
- 22-100-1 Proposal for Including an Updated Design Method for Bearing Stresses in CIB W18 - Structural Timber Design Code - B Madsen
- 22-100-2 Proposal for Including Size Effects in CIB W18A Timber Design Code - B Madsen
- 22-100-3 CIB Structural Timber Design Code - Proposed Changes of Section on Thin-Flanged Beams - J König
- 22-100-4 Modification Factor for "Aggressive Media" - a Proposal for a Supplement to the CIB Model Code - K Erler and W Rug
- 22-100-5 Timber Design Code in Czechoslovakia and Comparison with CIB Model Code - P Dutko and B Kozelouh

#### LOADING CODES

- 4-101-1 Loading Regulations - Nordic Committee for Building Regulations
- 4-101-2 Comments on the Loading Regulations - Nordic Committee for Building Regulations

## STRUCTURAL DESIGN CODES

- 1-102-1 Survey of Status of Building Codes, Specifications etc., in USA  
- E G Stern
- 1-102-2 Australian Codes for Use of Timber in Structures - R H Leicester
- 1-102-3 Contemporary Concepts for Structural Timber Codes - R H Leicester
- 1-102-4 Revision of CP 112 - First Draft, July 1972  
- British Standards Institution
- 4-102-1 Comparison of Codes and Safety Requirements for Timber Structures  
in EEC Countries - Timber Research and Development Association
- 4-102-2 Nordic Proposals for Safety Code for Structures and Loading Code for  
Design of Structures - O A Brynildsen
- 4-102-3 Proposal for Safety Codes for Load-Carrying Structures  
- Nordic Committee for Building Regulations
- 4-102-4 Comments to Proposal for Safety Codes for Load-Carrying Structures -  
Nordic Committee for Building Regulations
- 4-102-5 Extract from Norwegian Standard NS 3470 "Timber Structures"
- 4-102-6 Draft for Revision of CP 112 "The Structural Use of Timber"  
- W T Curry
- 8-102-1 Polish Standard PN-73/B-03150: Timber Structures; Statistical  
Calculations and Designing
- 8-102-2 The Russian Timber Code: Summary of Contents
- 9-102-1 Svensk Byggnorm 1975 (2nd Edition); Chapter 27: Timber Construction
- 11-102-1 Eurocodes - H J Larsen
- 13-102-1 Program of Standardisation Work Involving Timber Structures and  
Wood-Based Products in Poland

- 17-102-1 Safety Principles - H J Larsen and H Riberholt
- 17-102-2 Partial Coefficients Limit States Design Codes for Structural Timberwork - I Smith
- 18-102-1 Antiseismic Rules for Timber Structures: an Italian Proposal - G Augusti and A Ceccotti
- 18-1-2 Eurocode 5, Timber Structures - H J Larsen
- 19-102-1 Eurocode 5 - Requirements to Timber - Drafting Panel Eurocode 5
- 19-102-2 Eurocode 5 and CIB Structural Timber Design Code - H J Larsen
- 19-102-3 Comments on the Format of Eurocode 5 - A R Fewell
- 19-102-4 New Developments of Limit States Design for the New GDR Timber Design Code - W Rug and M Badstube
- 19-7-3 Effectiveness of Multiple Fastener Joints According to National Codes and Eurocode 5 (Draft) - G Steck
- 19-7-6 The Derivation of Design Clauses for Nailed and Bolted Joints in Eurocode 5 - L R J Whale and I Smith
- 19-14-1 Annex on Simplified Design of W-Trusses - H J Larsen
- 20-102-1 Development of a GDR Limit States Design Code for Timber Structures - W Rug and M Badstube
- 21-102-1 Research Activities Towards a New GDR Timber Design Code Based on Limit States Design - W Rug and M Badstube
- 22-102-1 New GDR Timber Design Code, State and Development - W Rug, M Badstube and W Kofent
- 22-102-2 Timber Strength Parameters for the New USSR Design Code and its Comparison with International Code - Y Y Slavik, N D Denesh and E B Ryumina
- 22-102-3 Norwegian Timber Design Code - Extract from a New Version - E Aasheim and K H Solli

- 23-7-1 Proposal for a Design Code for Nail Plates - E Aasheim and K H Solli
- 24-102-2 Timber Footbridges: A Comparison Between Static and Dynamic Design Criteria - A Ceccotti and N de Robertis

#### INTERNATIONAL STANDARDS ORGANISATION

- 3-103-1 Method for the Preparation of Standards Concerning the Safety of Structures (ISO/DIS 3250) - International Standards Organisation ISO/TC98
- 4-103-1 A Proposal for Undertaking the Preparation of an International Standard on Timber Structures - International Standards Organisation
- 5-103-1 Comments on the Report of the Consultation with Member Bodies Concerning ISO/TC/P129 - Timber Structures - Dansk Ingeniorforening
- 7-103-1 ISO Technical Committees and Membership of ISO/TC 165
- 8-103-1 Draft Resolutions of ISO/TC 165
- 12-103-1 ISO/TC 165 Ottawa, September 1979
- 13-103-1 Report from ISO/TC 165 - A Sorensen
- 14-103-1 Comments on ISO/TC 165 N52 "Timber Structures; Solid Timber in Structural Sizes; Determination of Some Physical and Mechanical Properties"
- 14-103-2 Comments on the CIB Structural Timber Design Code - R H Leicester
- 21-103-1 Concept of a Complete Set of Standards - R H Leicester



## JOINT COMMITTEE ON STRUCTURAL SAFETY

- 3-104-1 International System on Unified Standard Codes of Practice for Structures - Comité Européen du Béton (CEB)
- 7-104-1 Volume 1: Common Unified Rules for Different Types of Construction and Material - CEB

## CIB PROGRAMME, POLICY AND MEETINGS

- 1-105-1 A Note on International Organisations Active in the Field of Utilisation of Timber - P Sonnemans
- 5-105-1 The Work and Objectives of CIB-W18-Timber Structures - J G Sunley
- 10-105-1 The Work of CIB-W18 Timber Structures - J G Sunley
- 15-105-1 Terms of Reference for Timber - Framed Housing Sub-Group of CIB-W18
- 19-105-1 Tropical and Hardwood Timbers Structures - R H Leicester
- 21-105-1 First Conference of CIB-W18B, Tropical and Hardwood Timber Structures Singapore, 26 - 28 October 1987 - R H Leicester

## INTERNATIONAL UNION OF FORESTRY RESEARCH ORGANISATIONS

- 7-106-1 Time and Moisture Effects - CIB W18/IUFRO 55.02-03 Working Party

INTERNATIONAL COUNCIL FOR BUILDING RESEARCH STUDIES AND DOCUMENTATION  
WORKING COMMISSION W18 - TIMBER STRUCTURES

APA STRUCTURAL-USE DESIGN VALUES:  
AN UPDATE TO PANEL DESIGN CAPACITIES

by

A L Kuchar  
E G Elias  
B Yeh  
M R O'Halloran  
American Plywood Association  
United States of America

MEETING TWENTY - FOUR

OXFORD

UNITED KINGDOM

SEPTEMBER 1991



## SERVICE MOISTURE ADJUSTMENT

### Background

Two separate studies were conducted to evaluate the effect of moisture on the properties of structural-use panels. One study examined the effects on panel bending stiffness while another examined shear properties. Both studies utilized cyclic moisture conditioning including humidity, one-sided wetting and redrying. In general, specimens were cycled through moisture conditions and tested for bending and shear performance at intervals in the cycling. The intent being to expose panels to the full range of conditions that could be expected in service.

The panels selected for these studies were taken from routine Quality Assurance (QA) samples sent to the APA laboratory. Routine QA panels are randomly selected by an APA Auditor directly from the production line. The panels used in the studies, therefore, were representative of panels entering the marketplace. Table 1 outlines the product type, thickness, species, specimen size and test method used in each study.

### Moisture Effects on Bending Stiffness

**Relative Humidity Exposure.** Two cycles were used to evaluate the moisture effects on bending stiffness. Each cycle used a separate set of specimens. The first cycle involved steady-state conditioning of test specimens at specific relative humidity (RH) conditions prior to bending tests. Specimens were cycled to a high RH and then back down to dry conditions to examine the effect of increasing or decreasing moisture content on panel bending properties. Panels were cycled as follows:

Phase 1: ambient→oven-dry→30%→50%→65%→80%→90% RH

Phase 2: 90%→65%→50%→30%RH→oven-dry

Except for the ambient and oven-dry conditions, the RH cycling was conducted in a room where RH and temperature could be controlled. The temperature for each of the above RH conditions was set at a constant 20° C (68° F). Specimens were considered to reach an equilibrium moisture content (EMC) when the weight change, over a 24-hour period, was less than 0.05% as per ASTM D1037(5). Panels were tested for bending stiffness (non-destructive) capacity following conditioning at each increment in Phases 1 and 2.

**Water Exposure.** The second moisture cycle consisted of wet-one-side conditioning as follows:

oven-dry→3→7→9→24→47→60→83 hours→soak

Where the soak was a vacuum-pressure soak. This exposure represents the type of unsteady-state water exposure that panels can experience in service. One-sided wetting was accomplished in a tank with the specimens held in place within 30° of vertical. Water was sprayed continuously on one side for the durations listed above. The opposite side of the panel was not sprayed with water directly but was free to absorb moisture. As in the RH cycling, bending stiffness capacity was measured following each increment in the one-sided wetting cycle.

**Bending Stiffness.** Bending stiffness tests were accomplished using ASTM D3043 Method C(4). This method is consistent with the bending test outlined in RILEM TT-2(14). Each specimen was non-destructively evaluated for bending stiffness capacity. Care was taken to avoid over-loading the specimen by keeping the applied stress well below the proportioned limit.

**Results.** The average EMC results for the RH cycle are tabulated in Table 2. Since the objective was to establish an adjustment factor for wet use, ratios of wet-to-dry stiffness capacity were calculated for each increment in the moisture cycles. In each case, the ratio is equal to:

$$\text{Wet Ratio} = \frac{\text{Average Stiffness Capacity at Condition}}{\text{Average Stiffness Capacity at Oven-Dry}}$$

These ratios are summarized in Tables 3 and 4 and graphically represented in Figures 1 and 2.

## MOISTURE EFFECTS ON SHEAR

Two types of horizontal shear can occur in structural-use panel applications depending on the orientation of the panel in relation to the induced stresses. A horizontal shear stress that is induced parallel to the plane of the panel is said to be stressing the panel in planar shear. Applications where panels are laid flat across closely spaced supports and subjected to high loads, for example concrete forming, will stress a panel in planar shear. A horizontal shear stress induced perpendicular to the plane of the panel is stressing the panel in shear-through-thickness. Panels used as the webs of I-beams can experience shear-through-thickness stress. The study to determine the effects of moisture on shear properties examined both types of shear.

**Moisture Cycle.** Three moisture conditions were utilized: [1] dry or ambient, [2] 72-hour wet-one-side and [3] redry after wet-one-side. The 72-hour wet-one-side condition was selected as one that would likely simulate water exposure conditions in actual field applications.

One-sided-wetting was conducted in the same manner as the moisture effects on bending stiffness study. Specimens were tested to failure for planar shear and shear-through-thickness following conditioning at one of the three above conditions.

**Shear Strength Capacity.** Shear-through-thickness tests were accomplished using ASTM D2719 Method C(6). This method closely follows the method called for in RILEM TT-2(14). All specimens for shear-through-the-thickness were tested with the stress applied parallel to the original long dimension of the panel.

Normally, planar shear tests are conducted using ASTM D2718(7). This method calls for two steel plates to be glued to the surfaces of the specimen. The entire assembly is then placed in compression such that a shear stress in the plane of the specimen is induced. Due to the need to glue steel plates to the specimens, this is not a convenient method to use when conducting wet shear tests. Therefore, an alternative method was chosen.

A method introduced as five-point bending was used to test panels for planar shear(8). This method places the specimen in a bending mode using three reactions and two load points, all equally spaced. By selecting an appropriate span-to-depth ratio, shear failures occur a majority of the time. All specimens for planar shear were tested with the stress applied parallel to the original long dimension of the panel. The test set-up and shear and moment diagrams appear in Figure 3.

**Results.** A summary of planar shear and shear-through-thickness results appear in Tables 5 and 6. The wet-to-dry and redry-to-dry ratios were calculated based on an estimated lower 5 percent capacity (3-parameter Weibull distribution). This data is graphically displayed in Figure 4.

### **Determination of Wet-Use Factors**

A prerequisite to determination of a wet-use factor is to determine the conditions that constitute wet-use in service. Traditionally, APA has regarded service moisture conditions that correspond to an EMC of 16% or greater to be wet-use. For these cases, APA has recommended the use of design stresses or capacities that have been reduced, compared to dry condition capacities(3). For structural-use panels, an EMC of 16% or greater corresponds to relative humidities above approximately 85%(18).

Most interior use applications correspond with EMC levels below 16% while most exterior uses will have an EMC above this(16). It is, therefore, reasonable to regard an EMC of 16% or greater as constituting wet-use service conditions.

Little data exists that could be used for comparison and guidance in review of the wet bending stiffness and wet shear strength data presented or in determination of wet-use factors. Additionally, the wet bending stiffness and wet shear strength results were to be used as a guide to develop factors for other properties such as bending strength, tension, compression, axial stiffness, etc. Therefore, a conservative approach was used to determine wet-use adjustment factors for structural panel capacities.

Examination of Tables 3 and 4 and Figures 1 and 2 indicate that the average worst case capacity ratio for bending stiffness ranged from approximately 0.80 to 0.90. Most of the worst case stiffness ratios within this range correspond to an EMC above 16% (see Tables 2, 5 and 6). Therefore, a wet-use stiffness reduction factor of 0.85 was established as being conservative and representative of the results.

A similar examination of Tables 5 and 6 and Figure 4 reveal that the worst case cycled-to-dry ratios (based on the estimated lower 5 percent value) are 0.69 and 0.72 for planar shear and shear-through-the-thickness, respectively. These ratios apply to average moisture contents above, or very close to, saturation due to direct exposure to water (see Tables 5 and 6). A strength reduction factor of 0.75 was selected as representative for wet-use conditions.

Wet-use adjustment factors for stiffness and strength appear in Table 7. These factors will be shown in the next revision of APA Technical Note N375.

## **CREEP ADJUSTMENT FACTORS**

### **Background**

Deflection under long-term loading or creep can be a factor in the design of structures utilizing structural-use panels. When APA Technical Note N375 was published, included was an adjustment to account for creep when it is a factor in design. This factor, however, was based on limited data and the need for further information and study was recognized. For that reason, APA participated in a cooperative test program to examine the creep and creep-rupture behavior of structural panels. The study was conducted by the USDA Forest Products Laboratory (FPL), Madison, Wisconsin and developed in cooperation with Forintek Canada Corporation, APA and the Structural Board Association (then known as the Waferboard Association)(12).

## Review of the FPL Study

A complete review of the study is beyond the scope of this paper. A more thorough report on test parameters, procedures, results and analysis was done by McNatt and Laufenberg(12). In addition, this paper will concentrate on the creep deflection information provided by this study.

**Panels Sampled.** Panels from the routine production of sixteen structural panel mills were sampled by APA. Each panel sampled was 16 mm (5/8-inch) nominal thickness. The panels represented on-grade material with an APA Span Rating of 40/20. The sampling attempted to be representative of U.S. structural panel manufacturers, therefore, a range of panel types and species was selected. Represented in the sampling was OSB as well as Western and Southern U.S. plywood. Two common constructions, 4- and 5-ply, were represented in the plywood sampling.

**Testing.** From the sampling, a total of 144 specimens 300x1000 mm were used for the creep deflection phase of the study. In general, specimens were placed in third-point bending and loaded to 15 or 30% of ultimate strength. (Estimates of ultimate strength for the panels sampled were obtained in the creep-rupture phase of testing). Deflection was measured at intervals over the loading period, which was 6 months. Specimens were creep tested under three moisture conditions: [1] 50% RH, [2] 85% RH, and [3] cyclic 50%-85% RH.

**Results.** Average initial (elastic) and final (6 month) deflections were reported for the two load levels and three moisture conditions. From these results, a fractional creep (FC) can be calculated where:

$$FC = \frac{\text{Total 6 month deflection}}{\text{Initial deflection}}$$

Fractional creep results for the 30% load level tests from the FPL study appear in Table 8.

These results compare favorably with several previous studies. Pierce, Dinwoodie and Paxton(13) reported creep of 18 and 19 mm flooring and general purpose grade chipboard loaded for periods ranging from approximately 15 to 42 months. These specimens were loaded to 30 or 60% of ultimate stress under conditions of 20° C, 65% RH. Fractional creep in this study ranged from 1.75 to 2.13 for phenol formaldehyde bonded chipboard at 30% stress level and 2.36 to 2.70 for phenolic bonded chipboard at the 60% stress level.



Alexopoulos(1) examined creep deflection at 90% RH, 20° C for waferboard of 11.1 mm nominal thickness. Specimens were loaded for a total of 59 days to a level representing 78% of the proportional limit for specimens tested in bending. Fractional creep for the 11.1 mm panel under these conditions was found to be 5.26 for a long wafer (nominal 76 mm length) board and 4.58 for a short wafer (nominal 38 mm length) board.

### Determination of a Creep Factor

The FPL study utilized stress levels of 15 and 30% of ultimate stress measured in short term bending tests. In order to develop a meaningful creep recommendation, it was necessary to see how these levels relate to design capacities for APA panels. The initial release of APA Technical Note N375 recommended that creep be a consideration if a permanent load stressed a panel to 50% of its stated bending strength design capacity. For the panel classification corresponding to the panels used in the FPL study (40/20 Span Rating), a stress level was calculated using the following:

$$\text{Stress level} = \frac{(0.50) * \text{stated design capacity}}{5\% \text{ LTL}}$$

Where the 5% LTL is the estimated lower 5th percent level for bending strength capacity (non-parametric estimate). This was calculated for each panel type/construction combination within the 40/20 Span Rating classification. The stress levels ranged from 19 to 24%, all clearly within the 15 to 30% range used in the FPL creep study. Given the above, it was decided to retain the recommendation that creep be considered if the panel is stressed to 50% of design capacity by a permanently applied load.

The results of the FPL study suggest that for cases where creep is a factor in a dry-use, the tabulated stiffness used in bending deflection calculations be multiplied by a factor ranging from 0.65 to 0.78 for both OSB and plywood. Also suggested by the results is that in creep-critical applications where the panels will be wet in-service, a different creep adjustment be used for OSB than for plywood. For OSB, this factor should be approximately 0.22. For plywood, the results show that a factor ranging from 0.55 to 0.46 could be considered appropriate.

In establishing creep adjustments for APA Structural-Use Panels, APA took into consideration the FPL data plus the results of other studies(1, 13). Although these studies provide valuable data, it is recognized that they do not cover all moisture and loading conditions. Therefore, values that are conservative compared to the FPL results were established. These are listed in Table 9.

## **SUMMARY**

This paper reviewed research conducted by APA in regard to the moisture effects on the properties of structural-use panels. It also reviewed a study that APA supported to examine the creep behavior of panels. The results of these studies and cooperative efforts are:

- Design capacity adjustment factors for APA panels used in wet service (16% moisture content and above) applications
- A wet and dry creep adjustment factor for applications where deflection under long-term loading must be considered

**Table 2. Average Moisture Content Results for Humidity Cycle**

RH	MC (%)			
	Plywood		OSB	
	Para.	Perp.	Para.	Perp.
OD 1	0.0	0.0	0.0	0.0
ambient	8.2	6.7	3.5	3.9
30%	2.6	2.4	1.9	2.0
50%	7.5	7.1	5.9	6.1
65%	8.9	8.4	7.4	7.4
80%	12.6	12.3	10.9	11.2
90%	18.6	17.3	17.2	17.5
65%	9.2	9.2	8.2	8.3
50%	10.4	10.2	9.0	9.2
30%	5.7	5.5	4.7	4.8
OD 2 <sup>a</sup>	-0.2	-0.3	-0.6	-0.5

a: The negative MC value at OD 2 conditions indicates a slight weight loss based on oven-dry weight at OD 1 conditions.

**Table 3. Average Wet-To-Dry Bending Stiffness Ratio for Humidity Cycle**

RH	Plywood		OSB	
	Para.	Perp.	Para.	Perp.
OD 1	1.00	1.00	1.00	1.00
ambient	0.94	0.97	0.92	0.94
30%	1.00	0.99	1.02	1.02
50%	1.04	1.23	1.13	1.18
65%	1.04	1.18	1.12	1.11
80%	0.96	1.13	1.01	1.00
90%	0.97	1.01	1.06	1.01
65%	1.01	0.93	1.13	1.12
50%	1.03	0.85	1.10	1.04
30%	1.07	1.10	1.11	1.09
OD 2	0.96	0.97	1.04	0.96

**Table 4. Average Wet-To-Dry Bending Stiffness Ratio for Wet-One-Side Cycle**

Duration (hours)	Plywood		OSB	
	Para.	Perp.	Para.	Perp.
0(OD)	1.00	1.00	1.00	1.00
3	1.02	0.91	0.93	0.89
7	1.02	1.00	0.93	0.91
9	1.01	1.01	0.91	0.89
24	1.05	1.08	0.92	0.89
47	1.02	0.89	0.94	0.90
60	1.01	0.87	0.96	0.94
83	0.97	1.00	0.93	0.84
VPS	0.96	0.85	0.86	0.81

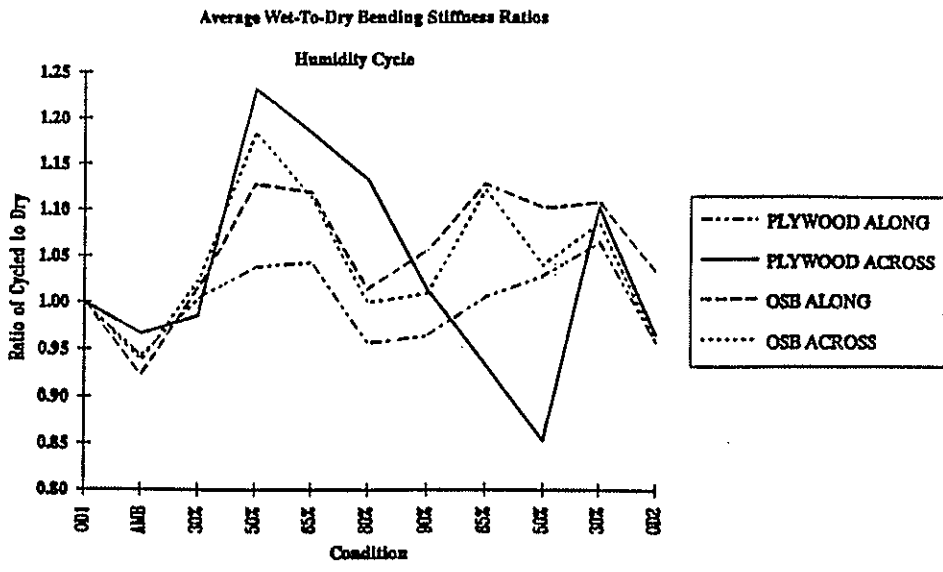


Figure 1. Wet-to-dry bending stiffness ratio for humidity cycle specimens.

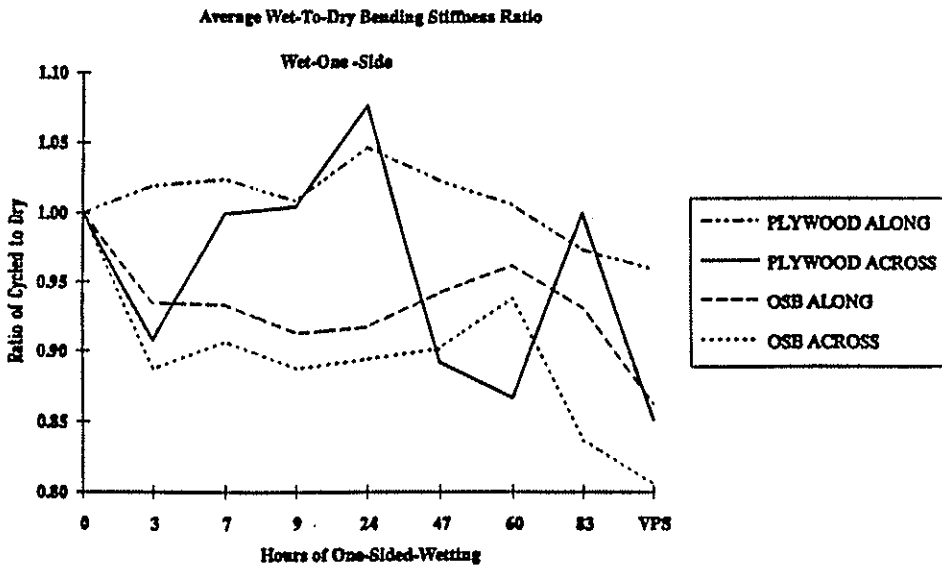


Figure 2. Wet-to-dry bending stiffness ratio for wet-1-side cycle.

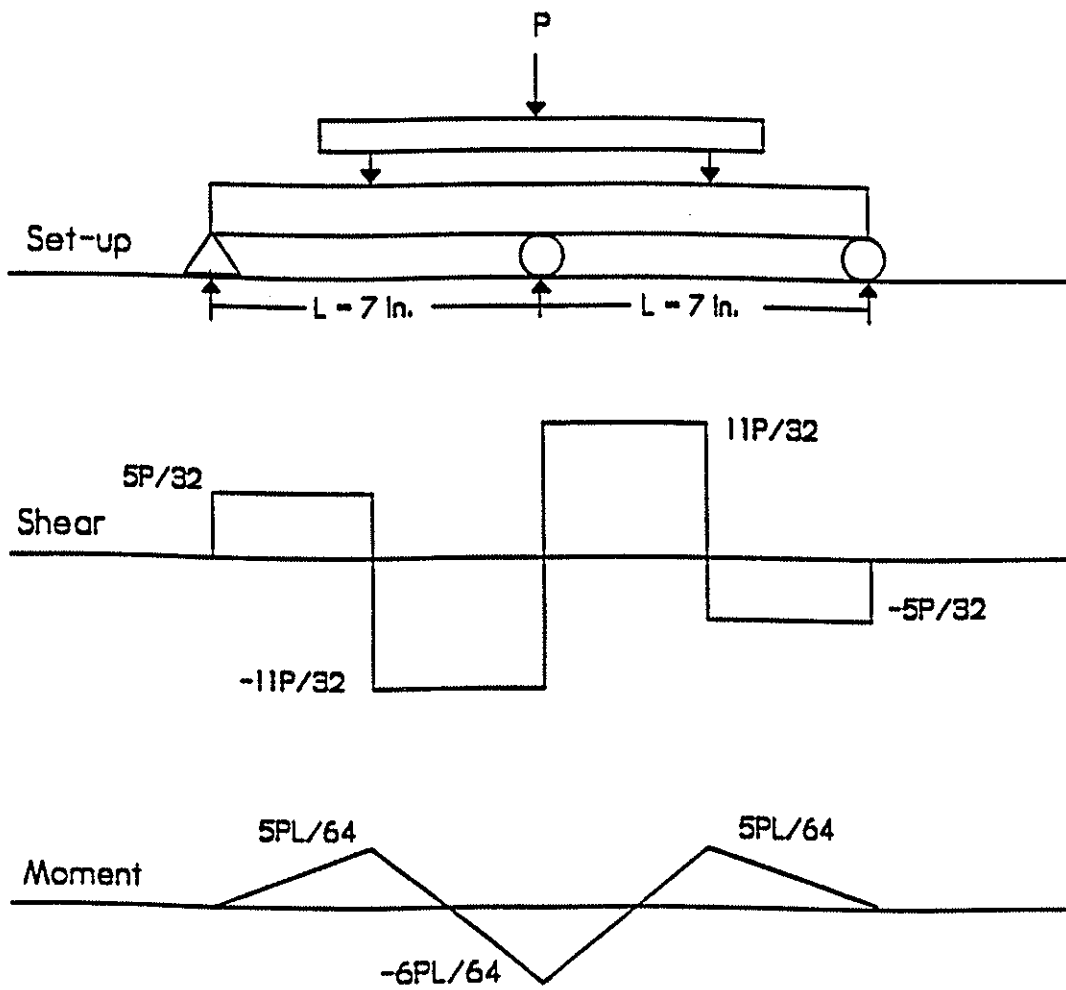


Figure 3. Test set-up for five-point bending tests.

**Table 5. Planar Shear Results**

Condition	Average MC (%)			Shear Capacity Ratio to Dry (5% Est) <sup>b</sup>
	Dry	W1S	Redry	
Dry	7.8 (5.0) <sup>a</sup>	--	--	1.00
W1S	6.8 (13.0)	31.6 (16.2)	--	.69
Redry	7.0 (13.5)	32.6 (22.3)	10.2 (8.7)	.81

a: Numbers in parentheses are coefficient of variation (%).

b: Lower 5% estimate based on 3-parameter Weibull distribution.

**Table 6. Shear-Through-Thickness Results**

Condition	Average MC (%)			Shear Capacity Ratio to Dry (5% Est) <sup>b</sup>
	Dry	W1S	Redry	
Dry	7.9 (7.8) <sup>a</sup>	--	--	1.00
W1S	8.0 (7.9)	27.7 (17.2)	--	.72
Redry	6.6 (16.4)	28.9 (23.4)	11.6 (8.2)	.81

a: Numbers in parentheses are coefficient of variation (%).

b: Lower 5% estimate based on 3-parameter Weibull distribution.

Average Wet-To-Dry Planar and Shear-through-thickness Ratio

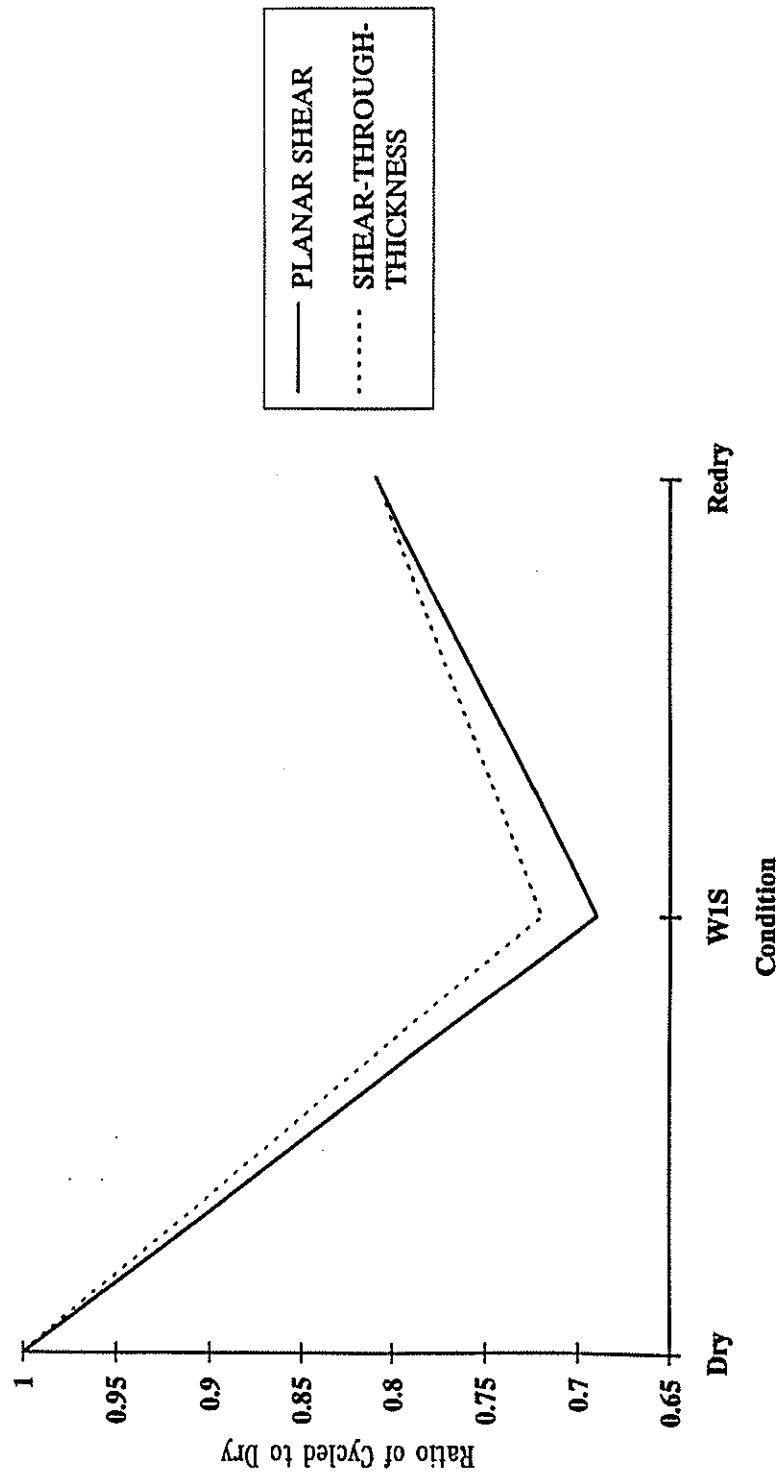


Figure 4. Wet-to-dry shear strength ratios.



**Table 9. Creep Adjustment Factors for APA Structural-Use Panels<sup>a</sup>**

<b><u>Moisture Condition</u></b>	<b><u>Plywood</u></b>	<b><u>Mat-Formed Panel (OSB)</u></b>
Dry	1/2	1/2
16% MC or greater	1/2	1/6

a: Where creep is a factor, the bending stiffness capacity used in deflection calculations is multiplied by the factor listed.



**INTERNATIONAL COUNCIL FOR BUILDING RESEARCH STUDIES AND DOCUMENTATION**  
**WORKING COMMISSION W18 - TIMBER STRUCTURES**

**INFLUENCE OF STRESS GRADING SYSTEM ON LENGTH EFFECT**  
**FACTORS FOR LUMBER LOADED IN COMPRESSION**

by

A Campos  
Instituto Forestal, Santiago  
Chile  
I Smith  
Wood Science and Technology Centre  
University of Brunswick  
Fredericton, N.B.  
Canada

**MEETING TWENTY - FOUR**

**OXFORD**

**UNITED KINGDOM**

**SEPTEMBER 1991**



## ABSTRACT

Severity of the so-called "length effect" is shown to vary according to the method of stress grading used to segregate lumber. For kiln dried 38x89 mm red pine loaded in compression parallel to grain, the length effect was more severe if the lumber was graded using a commercial grading machine rather than on the basis of knot area ratio. The conclusion reached is that length effects result from relationships between length and the probability that the strength controlling feature will not be the "grade" determining feature.

## INTRODUCTION

In the last decade several investigations have been carried out on the so-called "length effect" in strength of stress graded lumber. As can be observed from Table 1, the majority of the work has addressed length effects in tensile strength. Only few studies have addressed length effects in compression and bending strengths. Table 1 summarises the results of various studies in terms of the length effect factor,  $g_L$ , equation (1).

$$g_L = \frac{\log(X_1/X_2)}{\log(L_2/L_1)}$$

where:

$X_1$  and  $X_2$  = strengths at lengths  $L_1$  and  $L_2$  respectively  
 $g_L$  = length effect factor

The present study was undertaken to examine the effects of specimen length and stress grading parameters on the compressive strength of red pine lumber.

Table 1. Summary of  $g_l$  values in the literature

Author	Size (mm)	Grade and Species	Strength Percentile	Length effect factors ( $g_l$ ) <sup>1/</sup>		
				Compression	Tension	Bending
Buchanan (1986)	38x89	No2 and Better S-P-F.	50th	0.07	0.20	---
Madsen and Buchanan (1986)	38x89	No2	50th	---	0.12	---
	38x140	No2 S-P-F.	50th	---	0.33	---
Showalter et al. (1987)	38x89	No2	50th	---	0.25	---
	38x235	No2 South. pine	50th	---	0.10	---
Barrett and Griffin (1989)	Several sizes of 38 mm. thick lumber.	SS, No2 and No3 Douglas fir - Larch and S-P-F.	50th	0.10	0.15	0.22
Lam and Varoglu (1990)	38x89	SS	50th	---	0.09	---
		SS	5th	---	0.11	---
		No2	50th	---	0.09	---
		No2 S-P-F.	5th	---	0.18	---
Madsen (1990)	38x89	No2 and Better	50th	0.09	0.12	0.17
		S-P-F.	5th	0.10	0.23	0.22

<sup>1/</sup> $g_l$  is estimated from the slope of the line resulting from plotting the logarithm of strength vs the logarithm of specimen length.

## MATERIALS AND TEST METHODS

Kiln dried (14 percent M.C.) 38x89 mm red pine lumber was used in this study. Four test lengths were defined; 0.6, 1.2, 2.4 and 3.6 meters, with 50 specimens in each group. Initially 165 pieces with lengths up to 4.8 meters were run through a Techmach SG-AF 100 commercial stress grading machine to obtain the  $E_{flat}$  profiles along pieces. The matching criterion used to select the pieces for the groups was the low point  $E_{flat}$ , Figure 1.

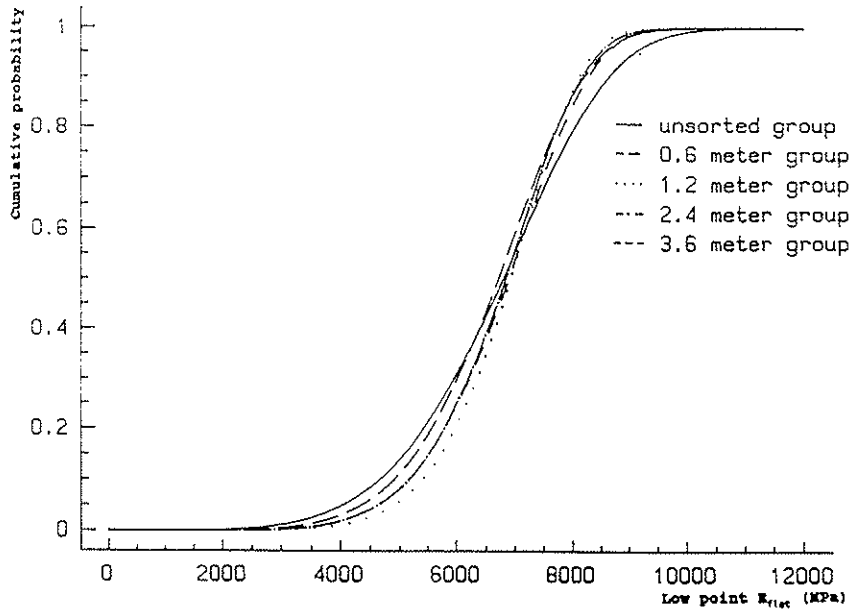


Figure 1. Matching of groups on basis of low point  $E_{flat}$ .

To enable a comparison between mechanical and visual grading systems, the knot area ratio (KAR) was also measured for each specimen, assuming that knots occurring within one section depth of each other lie in the same cross section.

The compression tests were carried out with a test apparatus designed to provide lateral restraint against buckling according to the provisions of clause 23.3: ASTM D 198-84 (ASTM 1990). A load cell was located at each end of the compression frame to enable simultaneous real time monitoring of actuator and reaction forces. Discrepancies between load cell readings were used to detect any errors due to specimens binding in the apparatus.

Load was applied at a constant rate according to clause 25.3: ASTM D 198-84 (ASTM 1990), to achieve the failure load in about 10 minutes, but not less than 5 nor more than 20 minutes.

The compressive strengths of the specimens were calculated from the equation;

$$F_c = \frac{P}{A}$$

where:

$F_c$  = compressive strength (MPa)  
 $P$  = maximum load registered (N)  
 $A$  = cross sectional area ( $\text{mm}^2$ )

## RESULTS

### Mechanical grading criterion

Table 2 shows the compressive strength results for the groups sorted according to the mechanical stress grading parameter, of low point  $E_{flat}$ . As can be observed there is a dependence between the  $g_L$  values and the "quality of the lumber" expressed in terms of low point  $E_{flat}$ . The higher the low point  $E_{flat}$  range considered the more severe is the length effect in strength in compression.

Table 2. Results based on mechanical grading parameter

Low point $E_{flat}$ (MPa)	$g_L$	Crushing Strength (MPa)			
		length = 0.6 m.	length = 1.2 m.	length = 2.4 m.	length = 3.6 m.
4000 - 6000	0.07	18.9 (n=15)	17.9 (n=10)	15.5 (n=11)	17.3 (n=15)
6001 - 8000	0.09	21.2 (n=29)	20.0 (n=35)	17.6 (n=32)	18.6 (n=29)
8001 - 10000	0.11	24.1 (n=6)	23.7 (n=5)	21.0 (n=7)	19.7 (n=6)

$1/g_L$  estimated on basis of least squares linear regression.

Figure 2 shows the length effect factors and regression lines for the results given in Table 2.

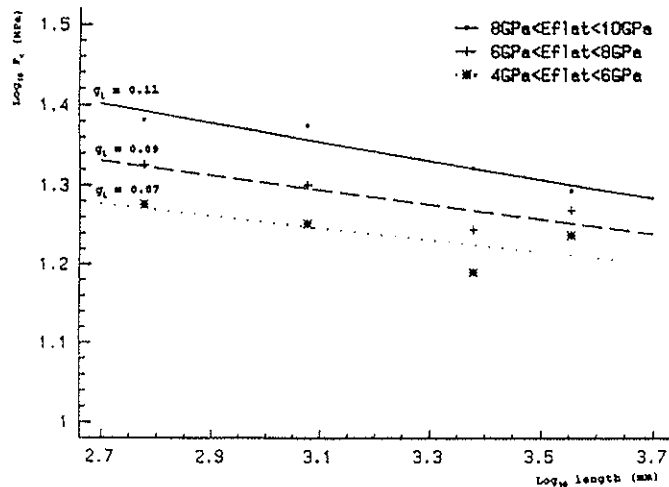


Figure 2. Length effect factor regressions based on a mechanical grading parameter.



Visual grading criterion

Table 3 shows the compressive strength results for the groups sorted according to their KAR values. It can be observed that if the groups are subdivided according to this visual grading parameter the length effect factor presents almost no variation among groups. This observation leads to the belief that the length effect depends not only of the specimen length but also of the grading system used to select the specimens.

Table 3. Results based on visual grading parameter

KAR (%)	$g_L'$	Crushing Strength $F_c$ (MPa)			
		length = 0.6 m.	length = 1.2 m.	length = 2.4 m.	length = 3.6 m.
0.0 - 25.0	0.06	22.2 (n=23)	21.0 (n=26)	20.8 (n=9)	19.4 (n=8)
25.1 - 40.0	0.05	20.1 (n=16)	19.2 (n=14)	18.2 (n=15)	18.4 (n=17)
> 40.0	0.05	19.0 (n=11)	18.3 (n=10)	16.2 (n=26)	17.9 (n=25)

$1/g_L'$  estimated on basis of least squares linear regression.

Figure 3 shows the length effect factors and regression lines for the results given in Table 3.

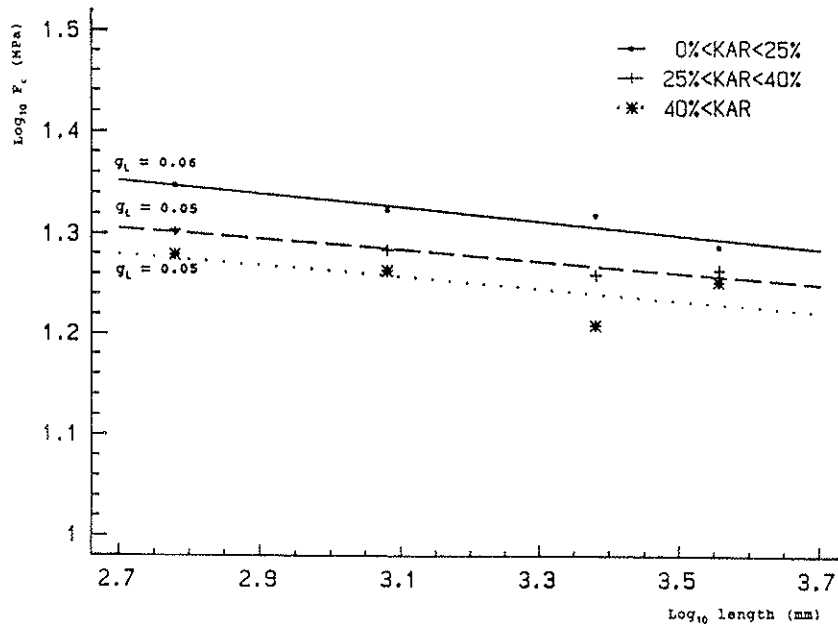


Figure 3. Length effect factor regressions based on a visual grading parameter.

## LITERATURE

- American Society for Testing and Materials (ASTM). 1990. Static tests of timbers in structural sizes. ASTM D198-84 Annual Book of ASTM Standards. Philadelphia, Pa.
- Barrett, J.D. and Griffin, H. 1989. Size effects for Canadian dimension lumber. Proceedings of International Council for Building Research Studies and Documentation: Working Commission W18A-Timber Structures, Berlin. September 1989.
- Buchanan, A. 1986. Combined bending and axial loading in lumber. American Society of Civil Engineering, Journal of Structural Engineering 112(12):2592-2609.
- Campos, A. 1991. The effects of specimen length and stress grading parameters on the compressive strength of red pine lumber. MScFE thesis, University of New Brunswick, Fredericton, N.B.
- Lam, F. and Varoglu, E. 1990. Effect of length on the tensile strength of lumber. Forest Products Journal 40(5):37-42.
- Madsen, B. 1990. Length effect in 38 mm spruce-pine-fir dimension lumber. Canadian Journal of Civil Engineering, 17(2):226-237.
- Madsen, B. and Buchanan, A. 1986. Size effect in timber explained by a modified weakest link theory. Canadian Journal of Civil Engineering, 13(2):218-232.
- Showalter, K.L., Woeste F.E. and Bendtsen B.A. 1987. Effect of length on the tensile strength of lumber. Research paper FPL-RP-482. USDA Forest Service, Forest Products Laboratory, Madison, WI.



**INTERNATIONAL COUNCIL FOR BUILDING RESEARCH STUDIES AND DOCUMENTATION**  
**WORKING COMMISSION W18 - TIMBER STRUCTURES**

**DISCUSSION OF THE FAILURE CRITERION FOR COMBINED BENDING AND COMPRESSION**

by

T A C M van der Put  
Delft University of Technology  
The Netherlands

**MEETING TWENTY - FOUR**  
**OXFORD**  
**UNITED KINGDOM**  
**SEPTEMBER 1991**



## **Summary**

One of the conclusions of the stability group of CIB-W18A was that the Code must allow for analytical solutions for stability design based on quasi linear behaviour and must revert to these methods (p.e. to the Larsen-Theilgaard method for columns).

Although a new parabolic failure criterion for bending with compression is proposed for the Eurocode, based on glulam simulation, the interaction equation for in plane buckling of the code, being applicable for short columns as well, suggests a much less curved failure criterion. It therefore could be seen as a task of the stability group to reconsider the failure criterion.

For that purpose a derivation is given of a consistent simple improved failure criterion for bending with compression, that may account for the influence of quality and moisture content, leads to simple interaction equations for beam-columns and may meet the requirements of the Eurocode.

Together with the proposal of CIB-paper 23-15-2 a possible consistent design method for braced and free beam-columns is proposed for the Eurocode and is used in the new Dutch Code.

In the appendix an explanation is given of the bearing- and shear strength.

## **Introduction**

At the CIB-W18-meeting in Lisbon 1990, a proposal for stability design was given, (paper 23-15-2), based on the quasi linear approach, as is used in timber engineering, and on a lower bound failure criterion for bending and compression as, for instance, can be deduced from the publication in the proceedings of the IUFRO 1982 paper 24. This lower bound criterion was felt to be too conservative for all cases and a differentiation ought to be possible for the different cases as for different moisture contents and grades.

Because pure experimental design methods should not be used and the proposed methods for stability design are based on the second order stress theory, there must be agreement on the failure criterion to be used. Therefore a discussion is given here of this criterion for bending with compression that is suitable for analytical solutions and for the Eurocode and is verified by the experimental research of the above mentioned IUFRO-paper 24.

The criterion should account for the elastic-plastic behaviour of wood, showing a plastic failure in compression with a high deformation capacity (like steel) and brittle-like failure in tension (thus showing a volume effect for tension). Thus after the flow strain at the end of the linear range, it need not be assumed (as for steel) that there is a limiting ultimate strain in compression because there is no indication of such a limit (Pure plastic flow is possible in a compression test if it is managed to keep the system stable at flow). For tension it can be assumed that the flow strain at the end of the elastic stage is also the ultimate strain.

### **Discussion of the basic equations for beam-columns**

The stability equations for beam-columns, proposed in CIB-W18A-paper 23-15-2, are based on the quasi linear approach. In principle if a beam-column is elastic plastic, the sectional properties along the length of the member are not constant. The analysis then can be based on a deflection method assuming the deflected shape of the beam-column by a simple function such as an orthogonal function (depending upon the applied loading and boundary conditions) and establishing equilibrium at least at the end and at the most yielded cross section. For this purpose the equilibrium equations of Chen and Atsuta were chosen and extended for lateral loading. The derivation of these equations is based on the assumption that the warping torsional rigidity and the St. Venant torsional rigidity do not alter during yielding of the cross section. (This applies for lateral buckling by bending for low quality wood where the yielding is small or neglectable). When the influence of the smaller terms are neglected the dominating linear terms remain, leading to the proposed equations for beam-columns of paper 23-15-2 (It is assumed that the initial excentricity for compressional loading alone is chosen to be high enough to be able to neglect these non-linear terms).

The assumption of a quasi constant warping rigidity is in accordance with the method for wood to express the bending strength in an equivalent linear behaviour up to failure with an equivalent bending modulus. So the two opposite bending parts determining the warping rigidity are quasi linear and with that also the warping rigidity. This warping rigidity dominates for profiles (when "buckling" of the compressed flange is determining) and for short columns and the assumption of constant torsional rigidity has a minor influence.

For wood it is also a use to estimate also for torsion and shear the quasi elastic values. Because these shear stresses act only in the elastic part of the section a compensation for the reduced area is given by low ultimate shear strengths and a low torsional shear modulus. This thus has to be applied for high grade timber and for bending with compression.

The elastic-plastic approach doesn't account for the Engesser effect for low grade timber when by bending and compression just both the flow stress in compression and ultimate tensile stress is reached. For this case a correction is possible by assuming earlier flow by increasing the value "s" of the failure criterion (see further).

### **Derivation of the failure criterion for bending with compression**

The derivation can be based on the elastic-plastic behaviour of wood with the usual starting points:

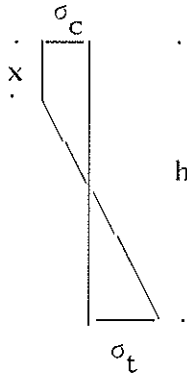
The modulus of elasticity is the same for compression and tension;

Plane sections remain plane (symmetry condition for bending);

In tension the behaviour is elastic until failure at a critical stress or strain. How-

ever this stress may increase according to the volume effect. This effect can be accounted for in the parameter "s" of the failure criterion,  
In compression the behaviour is elastic-plastic, being linear to the flow strain and then showing constant stress at increasing plastic strain.

Equilibrium of a section loaded in bending and compression.



For a beam of width b loaded by a moment M and normal force N is according to the figure:

$$\frac{M}{b} = \frac{\sigma_c + \sigma_t}{2} \cdot (h - x) \cdot \left( \frac{h}{2} - \frac{h - x}{3} \right) \quad (1)$$

$$\frac{N}{b} = \sigma_c \cdot h - \frac{\sigma_t + \sigma_c}{2} \cdot \left( 1 - \frac{x}{h} \right) \cdot h \quad (2)$$

or after elimination of x/h:

$$\frac{6 \cdot M}{\sigma_t \cdot b \cdot h^2} = \frac{\sigma_c}{\sigma_t} \cdot \left( 1 - \frac{N}{b \cdot h \cdot \sigma_c} \right) \cdot \left( \frac{-1 + 3 \cdot \sigma_t / \sigma_c + 4 \cdot N / (b \cdot h \cdot \sigma_c)}{1 + \sigma_t / \sigma_c} \right) \quad (3)$$

For N = 0 is:  $\sigma_c = \frac{\sigma_t + \sigma_c}{2} \cdot \left( 1 - \frac{x}{h} \right)$

or:  $\frac{6 \cdot M}{b \cdot h^2} = \sigma_c \cdot \frac{3 \cdot \sigma_t - \sigma_c}{\sigma_t + \sigma_c} = \sigma_m \quad (4)$

Thus:

$$\frac{6 \cdot M}{\sigma_m \cdot b \cdot h^2} = \left( 1 - \frac{N}{b \cdot h \cdot \sigma_c} \right) \cdot \left( \frac{-1 + 3 \cdot \sigma_t / \sigma_c + 4 \cdot N / (b \cdot h \cdot \sigma_c)}{3 \cdot \sigma_t / \sigma_c - 1} \right) \quad (5)$$

So with:

$$Y = \frac{6 \cdot M}{\sigma_m \cdot b \cdot h^2}; \quad X = \frac{N}{b \cdot h \cdot \sigma_c} \quad \text{and} \quad s = \sigma_t / \sigma_c \quad (= \varepsilon_t / \varepsilon_v),$$

or for the ultimate state:  $\sigma_t = f_t, \sigma_c = f_c$ , then  $\sigma_m = f_m$ , eq.(5) becomes:

$$Y = (1 - X) \cdot \left( 1 + \frac{4 \cdot X}{3 \cdot s - 1} \right) = 1 - X + \frac{4 \cdot X \cdot (1 - X)}{3 \cdot s - 1} \quad (5')$$

It is seen that:  $Y \approx 1 - X$  as lower bound for high values of s and for s = 1.67:  
 $Y \approx 1 - X^2$  as is proposed now in the Code based on glulam.

Eq.(5') provides a simple design criterion that can be further simplified as shown later.



Curvature

The relation for the radius of bending is with  $s = \sigma_t/f_c$ :

$$\kappa = \frac{1}{R} = \frac{\epsilon_v + \epsilon_t}{h - x} = \frac{\epsilon_v(1 + s)}{h - x} = \frac{f_c(1 + s)}{E(h - x)} = \frac{f_c(1 + s)^2}{2Eh} = \frac{2\sigma_m}{Eh} \cdot \frac{(s + 1)^3}{4(3s - 1)} \quad (6)$$

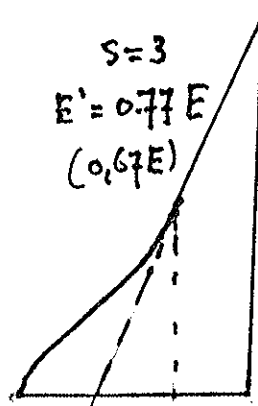
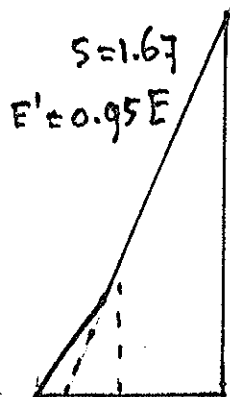
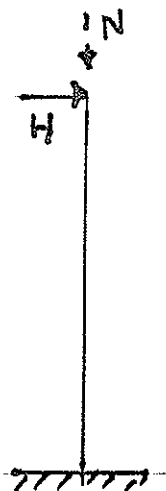
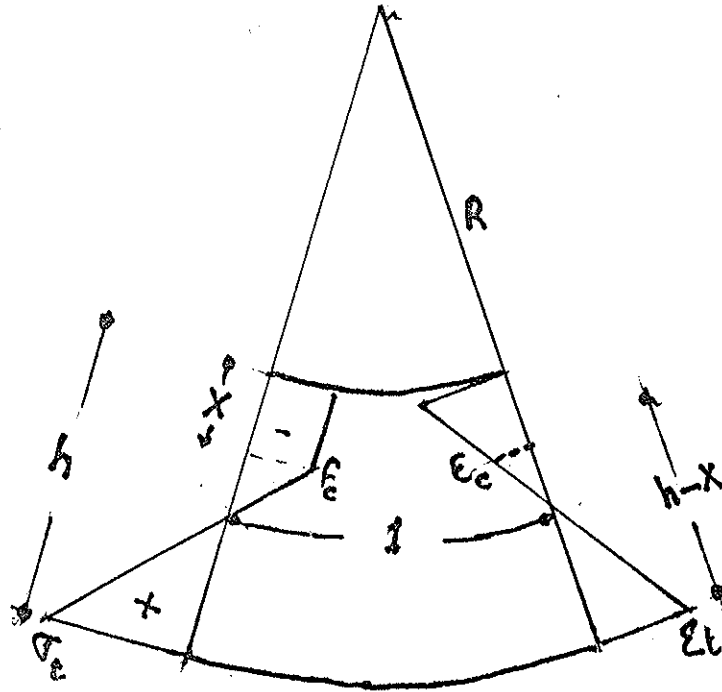
To eliminate the varying values of  $s$  along the beam this can be approximated to:

$$\kappa = \frac{2\sigma_m}{Eh} \cdot \frac{(s + 1)^3}{4(3s - 1)} = \frac{2\sigma_m}{Eh} \cdot \frac{(s + 1)^4}{4(3s - 1)^2} \cdot \frac{\sigma_m}{f_c} \approx \frac{2\sigma_m}{Eh} \cdot \frac{\sigma_m}{f_c} \cdot 0.8 \quad \left(1.25 \leq \frac{\sigma_m}{f_c} \leq \frac{f_m}{f_c}\right) \quad (7)$$

$s$	$\frac{(s + 1)^4}{4(3s - 1)^2}$
1	1
1.25	0.85
1.5	0.8
1.75	0.8
2	0.8
2.25	0.8
2.5	0.9
2.75	0.9
3	1

giving the curvature in the elastic-plastic range. In the elastic part of the column:  $\kappa = 2\sigma_m/(Eh)$  ( $\leq 2f_c/(Eh)$ )

It is seen that a reduced modulus has to be applied as quasi linear modulus for extreme cases ( $s = 3$ ).



$$\frac{M}{EI} = \kappa$$

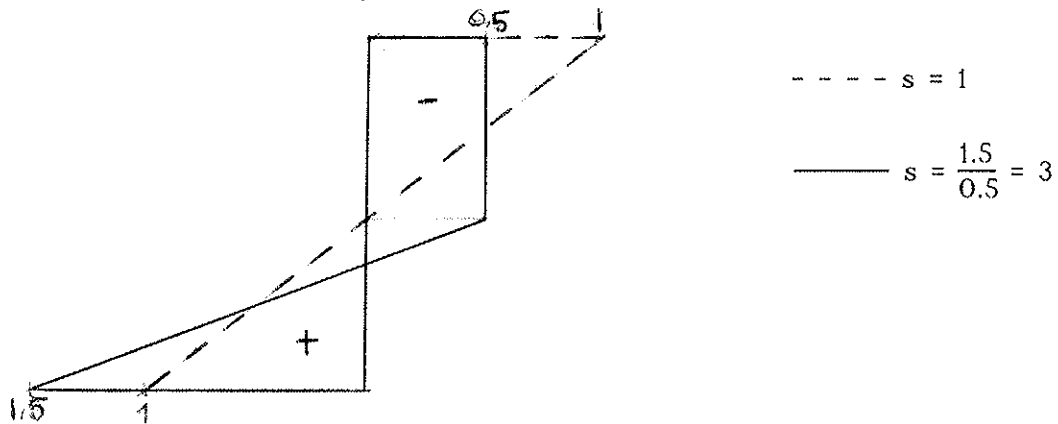
Elimination of  $(h - x)$  from (2) and (6) gives:

$$(s + 1)^2 = 2\alpha h \frac{E}{f_c} \left(1 - \frac{N}{f_c b h}\right) = 2\alpha h \frac{E}{f_c} (1 - X) \quad (8)$$

or for a combination with a normal force N:  $\alpha = \frac{x_{\text{bending}}}{1 - X}$  (9)

Extreme values

For high quality wood is  $f_t/f_c \approx 1.3$  according to the measured values of the tension and compression strength tests of paper 24 of IUFRO 1982. Because there is a strong volume effect ( $k_{\text{dis}}$ ) for tension only, increasing "s", and moisture effects reducing mainly compression and not tension, also increasing "s", the value of "s" may reach values of about 3 to 4 for high quality green wood (especially for small dimensions when the volume effect is the highest and changing moisture content effects are quick). Mechano-sorptive slip is much higher for compression than for tension and may differ nearly one order at working stress level. If it therefore is assumed, as first approximation, that tension is not affected, the slope of the elastic line must be two times steeper for a two times increase of deformation by this slip. This causes the stress distribution according to the figure below, differing an internal equilibrium system with the initial stresses to carry the same moment. Thus "s" may change from 1 to 3 and eq.(11) should be used for these cases. The increase of deformation by a factor 2 may occur within m.c. class 2 by the 6% m.c. change at working stress level. Thus it can be predicted that a long lasting climate change may strongly flatten the failure criterion for high loaded structures and thus flattens the failure criterion of the long term strength.



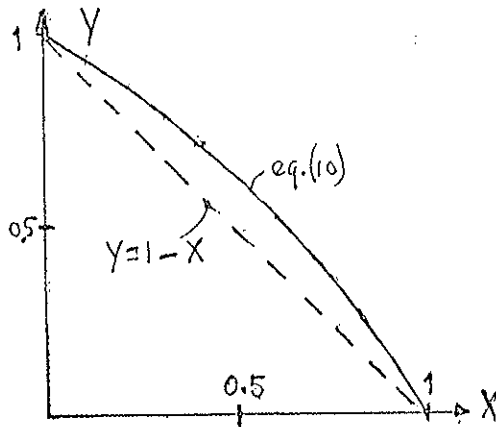
Prediction of stress re-distribution by mechano-sorptive slip

For  $s = 3$ , as for instance applies for wet clear wood or for every grade when a climate change occurs, eq.(5') becomes:

$$Y = 1 - X + 0.5 \cdot X \cdot (1 - X) \quad (10)$$

and the maximum deviation from the line:  $Y = 1 - X$  is obtained for  $X = 0.5$ . Then the third term of the right side of eq.(10) is: 0.13 or:

$Y = 1.13 - X$ . The slopes are about:  $Y'|_{X=0} = -0.5$  and  $Y'|_{X=1} = -1.5$  (see fig. below)



M - N - diagram for high quality wood

This curve will be flattened by the higher volume effect for bending with compression than for bending alone, especially for higher values of  $X$  and by the Engesser effect. So the failure condition for this case will be not far from:

$$Y + X = 1 \tag{11}$$

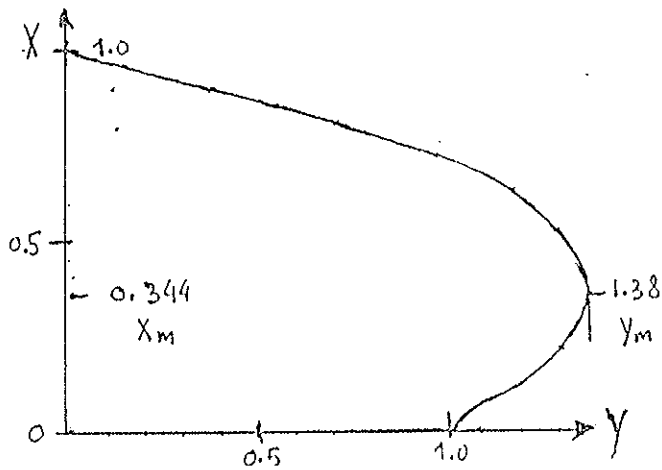
as earlier was proposed in the Eurocode.

For very low quality wood is according to the mentioned paper 24:  $f_t/f_c \approx 3/4$  and for bending failure  $f_t$  is determining and the compression stress will be equal to  $f_t$ . This means that  $s = 1$  at bending and "s" decreases at application of compression. The boundary value, where "s" becomes constant, is reached when in eq.(2),  $x = 0$  or when:  $X = (1 - s)/2$ . Thus for  $s = 3/4$  is  $X = 1/8$ . For  $X \geq 1/8$  is eq.(5'):

$$Y = 1 - X + 3.2 \cdot X \cdot (1 - X) \tag{12}$$

and the slope is:  $Y' = 2.2 - 6.4 \cdot X$ . thus the curve shows a maximum for  $X = 0.34$ , giving  $Y_{\max} = 1.38$ . At  $X = 1/8$  is  $Y = 1.22$  and the slope is  $Y' = 1.4$ . For  $X = 0$  is:  $Y' = 1$  and  $f_m = f_c$  ( $s = 1$ ).

The curve shows that there is quite a reserve with respect to line, eq.(11), and eq.(12) of this curve will be applicable if major defects determ the tensile strength following fracture mechanics thus showing no volume effect. For common cases the curve will be flattened by the volume effect of the tensile strength as will be shown in the following section. Around  $Y_{\max}$ , the point of first flow of the section in this case, a correction for the Engesser effect is necessary. Because this effect acts as an earlier flow of the section this can be done by increasing "s", flattening the curve there.



M - N - diagram for low quality wood

Curves like eq.(12), or based on the 5 % lower percentiles of the combined compression with bending strengths of the lowest grade are not general applicable because accounting for these lower percentiles is advantageous for the failure criterion.

To use a curved failure criterion at constant moisture conditions, there must be a guarantee that the compression strength is high enough in all circumstances. According to the strength class system of the Code the value of  $s$  is close to  $s \approx 1$  for lowest grade (as will be shown later) but the different influence of the moisture content on tension and compression is not introduced in the code. Thus there is a problem that a separate moisture effect on  $s$  has to be introduced in the Code.

When for the lowest strength class a value of  $s \approx 1$  is introduced eq.(5') becomes:

$$Y = 1 - X + 2X(1 - X) \tag{13}$$

and:  $Y' = 1 - 4X$ , showing a maximum at:  $X = 0.25$ , being:  $Y = 9/8$ .  $Y$  is again 1 at  $X = 0.5$ . Thus an approximation of eq.(13) for these calculations can be in the form:

$$Y = 2 \cdot (1 - X) \leq 1 \tag{14}$$

(also in agreement with the Code to use nowhere values above  $Y = 1$ ).

For wet conditions "s" will be a factor 1.6 higher with respect to the value at 10 % m.c. and the lowest value for  $s$  will be about 1.3.

#### Bi-axial bending

For the combination of "double" bending in the two main directions the interaction line will be straight (see CIB paper 18-2-1):

$$Y_y + Y_z = 1 \tag{15}$$

for low grades if there is no volume effect (tensile failure by great defects) and this straight line will be a real lower bound. Due to the volume effect of the maximal tensile stress (acting at one point) the interaction line for combined bending

will be curved and can be represented according to paper 18-2-1 by:

$$Y_y^{1.3} + Y_z^{1.3} = 1 \quad (16)$$

or approximately in a linear form:

$$Y_1 + 0.7 \cdot Y_2 = 1 \quad \text{when } Y_1 > Y_2 \quad (17)$$

$$0.7 \cdot Y_1 + Y_2 = 1 \quad \text{when } Y_1 \leq Y_2 \quad (18)$$

The form of this curve, eq.(16), doesn't change much when bending failure becomes elastic-plastic for high grades and high m.c. (being a reason to maintain a quasi linear approach for bending failure in wood).

Because the interaction line is not far from the straight line eq.(15) there is no coercive reason to replace the usual applied eq.(15) by eq.(17) and (18) as strength criterion.

### Experimental verification

The measurements of IUFRO paper 24 are based on a sample from one mill at one time of all grades of 2x6" lumber, kiln dried to 14 % m.c. There were done 21 different tests on each 100 boards. It was tried to make a quality distinction by visual grading. However this didn't lead to consistent differences of the different quality classes. Thus the measured curve is for all grades and the 5 % lower percentile, showing an advantageous failure criterion for bending with compression, is not representative for structural timber.

It can be derived from the failure criterion that for the top-values, for lower grades, where  $Y^l = 0$  and  $Y$  is maximal equal to  $Y_m$  at  $X = X_m$ , the following applies:

$$Y_m = \frac{(1 - X_m)^2}{1 - 2 \cdot X_m} \quad \text{where: } X_m = \frac{5 - 3 \cdot s}{8} \quad (19)$$

Thus  $Y_m$  may also be expressed in  $s$ , being:

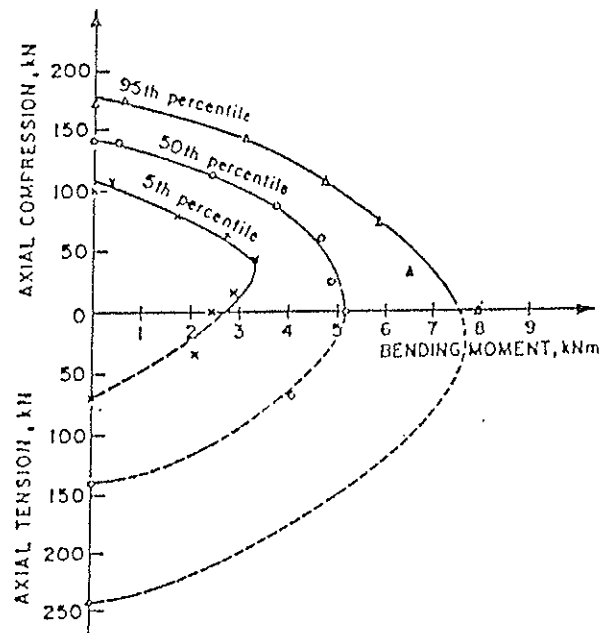
$$Y_m = \frac{9 \cdot (1 + s)^2}{16 \cdot (3 \cdot s - 1)} \quad (20)$$

These relations can be used by constructing the interaction curve for bending failure with compression.

In the figure below the measured values of the interaction curve are given with the 5 % percentiles for the 0.9 m long members. This may be regarded as the failure criterion because of the only small buckling effects (lateral buckling in the weak direction was prevented).

It can be seen that a good fit of the derived curve is possible by:

$s = 2.33$  for the 95 percentile,  
 $s = 1.67$  for the 50 percentile, showing the top-value at  $X_m = 0$  giving  $Y_m = 1$ ,  
 $s = 0.95$  for the 5 percentile, showing the top-value at  $X_m = 0.27$  giving  $Y_m = 1.16$ ,  
This shows that "s" is about 1.7 times higher for the 95 percentile as is to be expected from the tensile test. This can be explained by the volume effect as mentioned in paper 24. At bending already 0.4 times the height of the beam flows in compression for this high percentile and thus the volume factor is higher than for linear bending when compared with pure tension failure of the member. The value of 1.7 is in accordance with the usual applied  $k = 5$  value of the Weibull model. For the 50 percentile this factor is 1.67, where the Weibull value is 1.66 and for the 5 percentile this factor is about 1.5, where the Weibull value for bending without flow of the compression zone predicts 1.64. This difference of 10 % is not astonishing because not the pure tension strengths of the members were measured but combined values with bending and the percentiles were found by transposing the results into polar coordinates, using the found radius for each percentile. The values above show that it is reasonable to account for the volume effect by the stress distribution that is incorporated in the bending strength, replacing  $s = f_t/f_c$  (ratio of tensile/compression strengths) by:  $s = f_m/f_c$  (ratio of bending/compression strengths) or to use safely  $s \approx 1.7 \cdot f_t/f_c$ .



Measurements of proceedings IUFRO Boras 1982, paper 24.

Higher values of "s" are to be expected from the measurements of paper 24 at higher moisture contents. The mentioned measured values of "s" were for a m.c. of 15 %. At 25 % m.c. "s" will be about a factor 1.3 higher than at 15 % m.c.. Thus:

for the 95 percentile at 25 % m.c.,  $s \approx 3.1$ ;  
 for the 50 percentile at 25 % m.c.,  $s \approx 2.2$ , and  
 for the 5 percentile at 25 % m.c.,  $s \approx 1.2$ .

However the Code makes no distinction between compression and tension strengths depending on moisture content and other moisture effects and if that is retained these lower bound values have to be used or a separate moisture effect on "s" has to be introduced.

The results of paper 19-12-2 show that also for gluelam a volume effect has to be assumed.

Strength classes

To use a curved failure criterion for constant moisture conditions, there must be a guarantee that the compression strength is high enough with respect to the tensile strength in all circumstances. the strength classes may contain timber with a compression strength value of a lower class giving values of  $s \approx 1.7 \cdot f_t / f_c$ :

s - values	15% m.c.	25% m.c.
class C <sub>7</sub> to C <sub>10</sub>	1.7	~ 2.2
C <sub>3</sub> to C <sub>6</sub>	1.3	~ 1.7
C <sub>1</sub> and C <sub>2</sub>	~ 1.2	

It can be seen that the now in the Eurocode proposed parabolic criterion wherefore  $s = 1.67$ , applies or is safe at 15% m.c. but is unsafe for the 4 highest classes above 15% and a m.c. correction is necessary and can be:

Class C<sub>7</sub> to C<sub>10</sub>:  $s = 1.7/k_{\text{moist}}$  (21)

C<sub>1</sub> to C<sub>6</sub>:  $s = 1.3/k_{\text{moist}}$  (22)

with:  $k_{\text{moist}} = 1 - 2.5(\omega - 0.15)$  ( $\omega$  is relative moisture content)

Shear strength

Another reduction of the curved form of the failure criterion for bending with compression can be due to shear. This is derived in the appendix. Because this criterion is a straight line, there can always be a cut off of a curved failure criterion and it is necessary to introduce this additional criterion in the Code when a curved criterion for bending with compression is used thus:

$$\tau_d / f_{v,d} \leq 1 - \sigma_{c,d} / f_{c,0,d} \tag{23}$$

**Conclusion**

- It is shown that a simple design failure criterion for bending and compression is possible that can be explained by the elastic-full-plastic approach, with linear elasticity for tension up to failure, determined by the volume effect, and by unlimited flow in compression. This criterion:

$$Y = 1 - X + \frac{4 \cdot X \cdot (1 - X)}{3 \cdot s - 1}$$

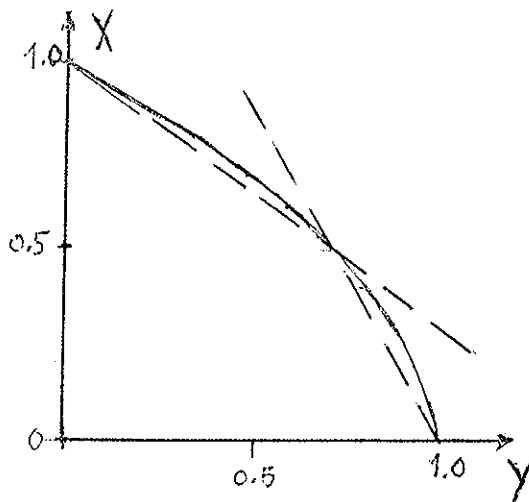
accounts for quality and moisture effects by the value of "s".

- For s = 1.67 this is:

$$Y = 1 - X^2$$

the new criterion of the Eurocode, applicable at constant m.c. except for the highest four grades above 15% m.c. Here s = 2.3 is safe giving:  $Y = 1 - X/3 - 2X^2/3$ .

- Because there will always be a linear cut off of the failure criterion, a simple linear approach of the parabolic failure criterion is appropriate, and lines can be drawn through the Y values of point X = 0 and point X = 0.5 and the Y values of the points X = 1 and X = 0.5 (avoiding too high estimates at  $Y_m$ ).



bi-linear failure criterium for bending with compression and shear

Thus the failure criterion then becomes in general:

$$Y + c_1 X = 1 \quad \text{when } X \leq 0.5 \quad \text{with } c_1 = (s - 1)/(s - 0.33)$$

$$c_2 Y + X = 1 \quad \text{when } X > 0.5 \quad \text{with } c_2 = (s - 0.33)/(s + 0.33)$$

or when smaller:  $c_2 = f_m \tau_d / f_{v,d} \sigma_{m,d}$  (or eq.(23))

where for rectangular cross sections:

$$Y = \frac{6 \cdot M}{f_m \cdot b \cdot h^2} ; \quad X = \frac{N}{b \cdot h \cdot f_{c,0}} \quad \text{and "s" is given by eq.(21) and (22).}$$



Or as proposal for the Code:

$$c_2 Y + c_1 X \leq 1$$

with:  $c_2 = 1$  and  $c_1 = (s - 1)/(s + 0.33)$  when  $X \leq 0.5$ ,

or:  $c_2 = (s - 0.33)/(s + 0.33) \leq f_{m,d}/(f_{v,d} \sigma_{m,d})$  and  $c_1 = 1$ , when  $X \geq 0.5$ .

The advantage of this criterion is that simple consistent interaction equations are possible for twist-bend buckling. The proposed stability equations of CIB paper 23-15-2 can be retained replacing the compression strength  $f_c$  by a higher value:

$$f_c \cdot \frac{s-0.33}{s-1} \quad \text{below the 50\% normal load level or:}$$

replacing the bending strength  $f_m$  by a higher value:

$$f_m \frac{s+0.33}{s-0.33} \quad \text{above the 50\% normal load level.}$$

- As lower bound:

- when a climate change can be expected at high loading;
- at high shear loading;
- for reinforced timber, improved gluelam or veneerwood, wet clear wood, etc.,

$c_1 = c_2 = 1$  in the criterion above and the criterion becomes:

$$Y = 1 - X$$

and this lower bound criterion can better be retained in the Code (as is done for the Dutch Code) because of the possible restrictions on the use of a parabolic criterion.

## Appendix

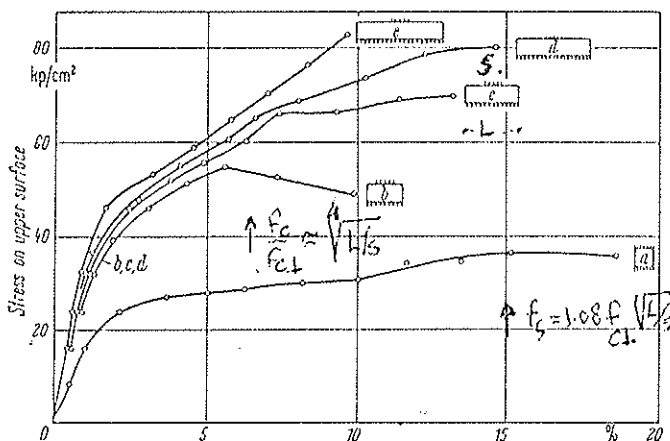
### a. Bearing strength perpendicular to the grain of locally loaded blocks

The compression strength perpendicular to the grain may increase due to confined dilatation perpendicular to the loading direction.

From the figure below it can be seen that the strength increases with the increasing possibility of spreading of the load. Further it is seen that there is a maximal spreading of about  $4 \times h$ . An increase of the strength is then only possible by increasing  $h$ . At plastic flow the increase of strength is about proportional with  $\sqrt{L/s}$  (see figure).

$$f_s = c \cdot f_{C,90} \cdot \sqrt{L/s} = 1.08 \cdot f_{C,90} \cdot \sqrt{L/s} \quad (1)$$

At lower strain this is about proportional to  $\sqrt[4]{L/s}$  when the cube strength is not regarded and it is seen that this empirical relation, proposed for the Eurocode, is not very well to represent the ultimate state.



Bearing strength  $\perp$ , specimen 15x15 cm, lengths: 15, 30, 45, 60, 75 cm, of a to e, [1]

The dependence of the strength upon spreading can be explained by the equilibrium method of the theory of plasticity.

In the plastic region a stress field can be constructed in the specimen that satisfies the equilibrium conditions:

$$\frac{\partial \sigma_x}{\partial x} + \frac{\partial \tau}{\partial y} = 0, \quad \frac{\partial \tau}{\partial x} + \frac{\partial \sigma_y}{\partial y} = 0, \quad (2)$$

and the boundary conditions and nowhere surmounts the failure criterion.

This failure criterion is of the Mohr-type in the radial plane:  $\tau/f_v = \sqrt{1 - \sigma_{c,0}/f_{c,0}}$ , [2], or can be approached by a Coulomb criterion. In the radial plane an inscribed Tresca criterion can be used being a maximum stress criterion:

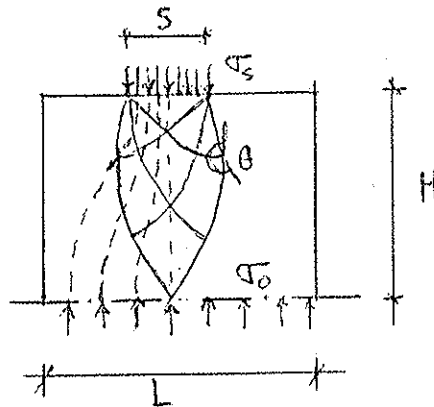
$$(\sigma_1 - \sigma_2)/2 = k = f'_v \tag{3}$$

However the result of the derivation does not depend much on the failure criterion used. The Coulomb or the Mohr criterion gives a higher value of  $c$  of eq.(1) than the Tresca criterion, the strength  $f_{c,90}$  however is related to a prism strength and is lower than the cube strength associated with the Tresca criterion. Both criteria therefore will give comparable values of  $f'_s$ .

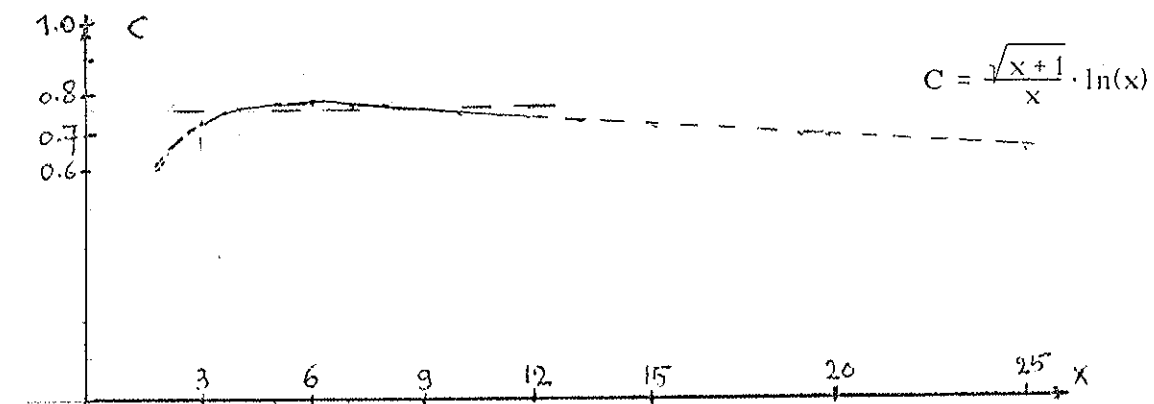
Although "shear-flow" is in the weak direction as in the compression test perpendicular to the grain, the behaviour is similar to a reinforced material (in the strong direction) having the shear strength of the weak direction and confined pressure may build up in all directions when there is friction between bearing plate and specimen in the width direction where the width of the bearing plate is equal to the width of the block. Because failure, according to a shear plane in the weak direction, not affecting the reinforcement, is not determining in this case, the upper stress is determined by the spreading possibility in the strong direction.

Equations (1) to (3) can be written as equations along discontinuity lines (characteristics as for instance Prandtl slip lines) and from the construction of these lines it follows that  $\sigma_s = 4k\vartheta + \sigma_0$  and  $\vartheta \approx 0.62 \cdot \ln(2H/s)$ , see [3], giving:

$$\sigma_s - \sigma_0 = 2.48 \cdot k \cdot \ln(2H/s) \tag{4}$$



"Slip-lines" determining the direction of the main stresses



Function C

and because  $\sigma_s \cdot s = \sigma_0 \cdot L$  (see figure below) is:  $\sigma_s(1 - s/L) = 2.48 \cdot k \cdot \ln(2H/s)$ . Further the construction for a finite block gives the indication that the spreading of the stress is below:  $L \approx 2H + s$  or:  $H \approx (L - s)/2$  when  $H > s$ , thus:  $L/s > 3$  (Below this value the spreading is less strong and finally failure is similar to the cube test).

Substitution of the values for  $\sigma_0$  and  $H$  in eq.(4) gives:

$$\sigma_s = 2.48 \cdot k \cdot \ln\left(\frac{L}{s} - 1\right) \cdot \frac{\sqrt{L/s}}{L/s - 1} \cdot \sqrt{L/s} = 2.48 \cdot k \cdot C \cdot \sqrt{L/s} \quad (5)$$

where  $C$  is a function of  $L/s$  only and can be regarded constant of about 0.78.

Thus:

$$\sigma_s = 0.97 \cdot 2k \cdot \sqrt{L/s} \quad (6)$$

The value of  $k$  follows from the compression test (cube test) with  $\sigma_1 = f_{c,90}$  and  $\sigma_2 = 0$ , or:  $k = f_{c,90}/2$ . Thus eq.(6) becomes:

$$f_s = c \cdot f_{c,90} \cdot \sqrt{L/s} \quad \text{with } c \approx 1 \quad (7)$$

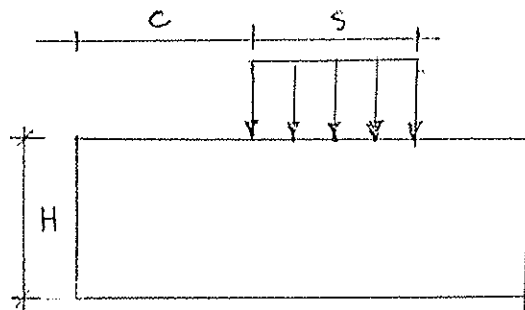
The higher experimental value of  $c$  given in eq.(1) shows the lower bound approach of the chosen method (the real slip-lines must give a higher value). At lower flow strains  $c$  also will be lower in experiments. Thus  $c$  gives the possibility to adapt the model to test results.

Eq.(7) provides a basis for design rules and is able to explain the different results. As mentioned before the rules of the Eurocode based on  $\sqrt[4]{L/s}$  suggest to be based on small deformations (and not the ultimate state) and the dependence on  $H$  is omitted in the Code. However for very small values of  $H$  there is hardly any spreading and the given rules don't apply. Increase in bearing is then only possible after flow at hardening if the structure remains stable in that state. The given rules seem to apply for a special case:  $H \geq (a + l_1)/3 = 250/3 = 84$  mm. This has to be mentioned in the Code.

As discussed in paper CIB-W18/5-10-1, the French rules show the dependence of  $H$  and the results are closer to the the ultimate state (see table):

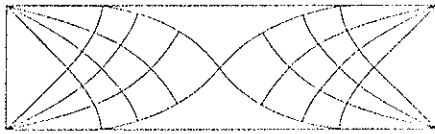
$f_s/f_{c,90}$

s/H	c/H			
	≥ 1.5	1	0.5	0
1	2	1.5	1.25	1
2	1.5	1.25	1.12	1
≥ 3	1	1	1	1



When  $c/H = (L - s)/2H \geq 1.5$ , thus when  $L \geq 3H + s$ , the maximal spreading is reached according to the table and to the first figure above of [1]. (This indicates friction

of the plates in the strong direction because without that:  $L \approx 2H + s$  is expected). For  $s/H \geq 3$ , it is assumed that in the middle the same conditions appear as in the cube test. However this is even too low when friction is ignored here and test values will be higher than the table values. The same applies for  $c = 0$  when  $L > s$ , only without friction (and  $L = s$ ) the situation is comparable with the cube test and test values will be higher than 1. The confined pressure may be build up according to the following figure.



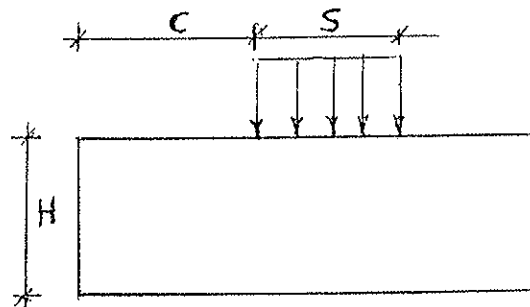
"Failure" between two plates

The influence of no friction along the bearing plate in the strong direction (and thus full friction in the width direction) can be assessed as lower bound by assuming that only symmetrical spreading is possible. Thus  $L = 2c + s$ . Further  $s/H \geq 3$  must comprise  $s/H \gg 3$ .  $c/H \geq 1.5$  must be  $c/H \geq 1$  and the first column has to be omitted when no friction is assumed.  $c = 0$  must comprise  $L = s$  giving a value 1.

According to eq.(7) is then:

$$f_s / f_{c,90}$$

s/H	c/H = (L - s)/2H			
	≥ 1.5	1	0.5	0
1	2	1.7	1.4	1
2	1.6	1.4	1.2	1
≥ 3	1	1	1	1



These values are close to the values of the French rules and are comparable when in eq.(7)  $c \approx 0.9$  is used indicating that a limited flow is regarded as the ultimate state in the French tests or that safe lower bounds where given.

In paper CIB-W18A/23-6-1 test results are given of bearing in the range where H is not limiting for spreading because:  $L < 2H + s$ . The determination of  $f_{c,90}$  is done on a specimen that is long in the strong direction and the results will be higher than those of the compression test. However the strain chosen as failure strain was lower than the ultimate giving compensating lower strength values. The comparison of this compression test with the ASTM-bearing test in the paper shows that the ASTM

values are about  $\sqrt{3}$  times higher according to the theory ( $L/s = 3$  in the ASTM-specimens).

In the following table the test results are compared with eq.(7) and it is seen that also non-symmetrical spreading is possible of end loaded blocks because of the friction between plate and specimen (and the high value of H).

According to the Eurocode a limiting value occurs at  $s/L \leq 0.125$  for central loading. The results here show that for end loaded blocks the limit of  $k_c$  is about  $k_c \approx 2$  for  $s/L \leq 0.25$ . These limits are due to a local mechanism as for instance given in the figure below. It has to be remembered that the lines are not real slip lines here but means to construct a stress field that satisfies equilibrium, boundary conditions and the failure criterion. The theoretical value of the limit of  $k_c$  is higher for central loading and it seems to be possible to obtain higher values by tests.

$$f_s / f_{c,90} = k_c$$

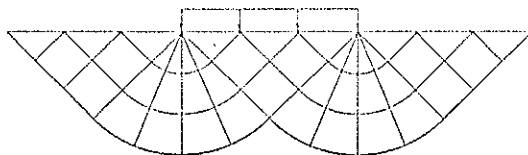
s/L	measurements		$\sqrt{L/s}$	adaption c of eq.(7)	
	central loaded $k_c$	end loaded $k_c$		central loaded $c = k_c / \sqrt{L/s}$	end loaded $k_c / \sqrt{L/s}$
1	1	1	1	1	1
0.875	1.063	1.063	1.069	1	1
0.75	1.188	1.156	1.155	1.03	1
0.625	1.375	1.281	1.265	1.09	1
0.5	1.625	1.438	1.414	1.15	1
0.375	1.969	1.625	1.633	1.2	1
0.25	2.344	1.875	2.0	1.17	0.94 limit
0.125	2.781	2.156	2.83	1 limit	

mean of c:

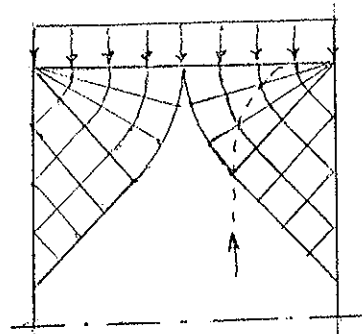
1.08

1

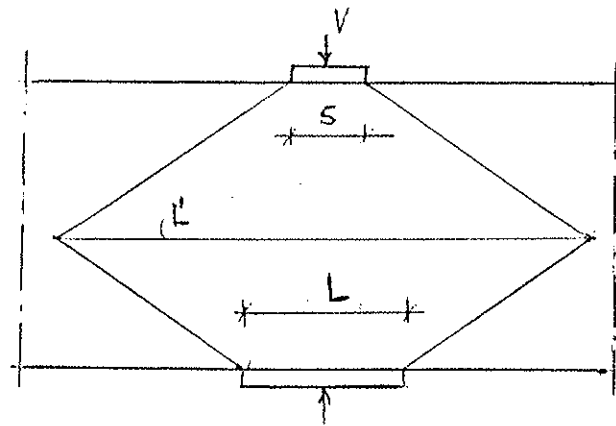
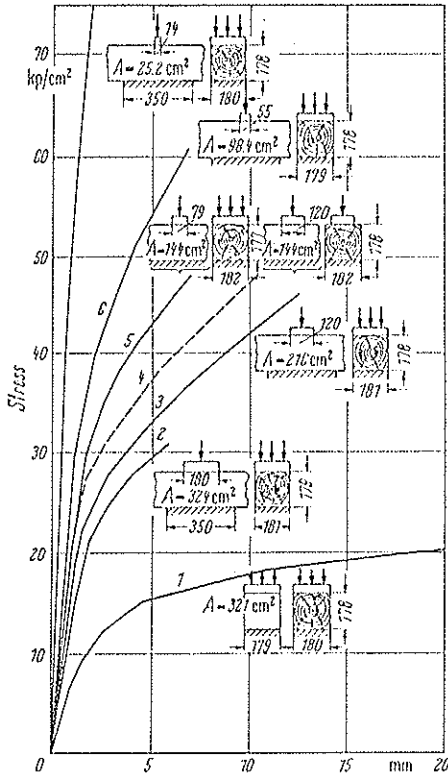
"slip-lines" when the plate transfers the entire shear stress



"Local failures"



For long blocks with respect to the bearing plates the maximal spreading will occur at both plates according to the figures below.



Local loading perp. to the grain [1] Graf

Possible spreading

From the figure it follows that:  $s + 3\alpha H = L + 3 \cdot (1 - \alpha)H$ . Thus:

$$\alpha = 0.5 + \frac{L - s}{6H}$$

and thus the equivalent spreading factor (of the strength determining plate) is:

$$\frac{L'}{s} = \frac{s + 3\alpha H}{s} = 1 + \frac{3H}{s} \left( 0.5 + \frac{L - s}{6H} \right) = 0.5 + \frac{3H + L}{2s}$$

With  $H = 17.9$ ;  $L = 35$ ;  $b = 18.1$  cm according to the measurements of O. Graf is:

$$k_{C,90} = c \cdot \sqrt{0.5 + 800/s \cdot b} = 1.1 \cdot \sqrt{0.5 + 800/s \cdot b}$$

leading to the values of  $f_s$  at 5 mm deformation (see fig.) of the curves:

1: 16 - 2: 30 - 3: 36 - 5: 43 - 6: 52 kgf/cm<sup>2</sup>, about the same as the measurements.

The highest maximum is not shown (at  $f = s \cdot b = 25.2$ , see fig.). Predicted according to the last formula is:  $f_s = 100$  kgf/cm<sup>2</sup>. However this will be cut off by a local mechanism. Because  $f_s \geq 75$  is measured, the maximum value of  $k_{C,90}$  is at least  $75/16 = 4.7$  (close to the theoretical value obtained from a local failure mechanism (giving an upper bound value) of about 5.5 to 6).

The measurements suggest a higher spreading possibility than to:  $s + 3\alpha H$ . However the model applies for high plastic deformation and after splitting softening may

occur similar to the specimen with 30 cm length in the first figure of this appendix. Because complete curves are not given, rules have to be based on the limited deformation (~ 5 mm here).

It can be concluded that the theory is able to explain the, contradictory, test results and design proposals of the Eurocode, the French rules, the measurements of Suen-son, Graf, CIB-W18A/23-6-1 and design rules should be adapted in this way.

As proposal for the Eurocode the following rules are possible for bearing blocks:

$$\sigma_{d,90,d} \leq k_{C,90} \cdot f_{C,90,d}$$

where:

$$k_{C,90} = \sqrt{L/s}$$

with:  $L \leq a + s + l_1/2$ ;  $L \leq 3H + s$  and:

$$k_{C,90} = 2.8 \text{ when } s/L \leq 0.125 \text{ for central loads;}$$

$$k_{C,90} = 2 \text{ when } s/L \leq 0.25 \text{ for end loads.}$$

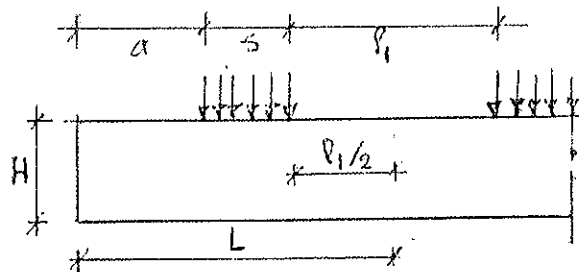
For safe rules (when friction is only in the width direction), the conditions are:

$$L \leq 2a + s; L \leq s + l_1; L \leq 2H + s,$$

$$k_{C,90} = 2.8 \text{ when } s/L \leq 0.125$$

For the bearing strength of a middle section of a beam between two plates of lengths  $L$  and  $s$  is:

$$k_{C,90} = 1.1 \cdot \sqrt{0.5 + \frac{3H + L}{2s}} \leq 5$$



#### Literature

- [1] F. Kollmann, Principles of wood science and technology, vol. I, 1984, Springer-Verlag, Berlin.
- [2] T.A.C.M. van der Put, A general failure criterion for wood, Proc. IUFRO S5.02 paper 23, 1982, Boras, Sweden.
- [3] H. Schwartz, PhD dissert. Stuttgart, 1969.
- [4] P. Vermeijden, P.B.B.J. Kurstjens, Shear strength of close to support loaded beams on 3 supports, report 4-68-13 HE-2, Stevinlab. Delft, 1968 (in Dutch).



These results were discussed in a small groupe after the presentation of paper CIB-W18A/23-6-1. The general opinion was that failure perpendicular to the grain does not really exist and there would always occur enough hardening at the end to make any rule safe. It thus was decided not to present these results. However this hardening is only possible when the structure at failure remains stable p.e. by locking up the failed wood. This is not always achieved in a real structure.

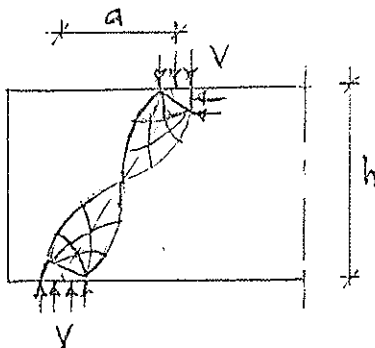
Further understanding of bearing is also necessary to explain the mechanism of shear failure for loading close to the supports. Therefore the proposal for design rules based on the start of the first stable ultimate flow state is given here as annex of this paper and provide better and more consistent rules for the Eurocode.

### b. Shear strength of beams

#### Shoring model:

For shear loading by a load on a beam close to the support, the bearing strength is determining for the strength as given in appendix a. The strength is:  $V_u = f_s bs$  when  $a/h \leq 1$  (see fig. below). Above about  $a/h = 1$  the shear strength (along the grain) can be determining (when  $s$  is long enough) and a similar formula applies as for the bearing strength with  $f'_v$  in stead of  $f_{c,90}$  that also can be given as:  $V_u = 0.67 f'_v bh$ , where  $f'_v$  depends on the volume effect (of the shearing plane along the grain; see test results of [4]). For the lowest grade, that may show early failure by bending-tension showing a linear stress distribution along the height of the beam, the shear strength  $V_u$  according to the beam theory is the same. For higher qualities, flow in compression may occur and the shear strength decreases while the bending strength increases according to the bending theory.

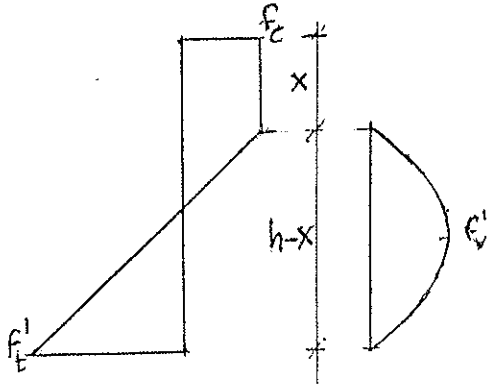
At about  $a/h \geq 1.5$ , depending on the grade, the bending theory may apply (showing the same value of  $V_u$  according to the shoring (or bearing) model for loads close to the supports).



Bearing or shoring mechanism

Beam model:

When there is plastic flow in compression, shear can only be carried in the elastic region. According to the figure below is for bending:



$$V_u = \frac{2}{3} \cdot f'_v \cdot b \cdot h \cdot \left(1 - \frac{x}{h}\right) \quad (1)$$

$$1 - \frac{x}{h} = \frac{2 \cdot f_c}{f'_t + f_c} \quad (2)$$

or from eq.(1) and (2):

$$V_u = \frac{4}{3} \cdot \frac{f'_t \cdot f_c}{f'_t + f_c} \cdot b \cdot h = \frac{2}{3} \cdot f'_v \cdot b \cdot h$$

or:

$$f'_v = \frac{2 \cdot f'_t \cdot f_c}{f'_t + f_c} \quad (3)$$

where  $f'_v$  is the quasi linear shear strength.

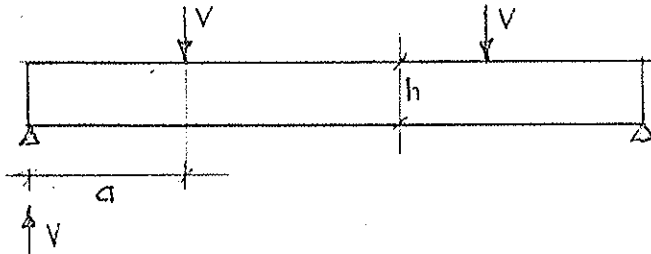
For bending with compression is:

$$V = \frac{2}{3} \cdot f'_v \cdot b \cdot h \cdot \left(1 - \frac{x}{h}\right) = \frac{2}{3} \cdot f'_v \cdot b \cdot h \cdot \left(1 - \frac{N}{f'_c \cdot b \cdot h}\right) \cdot \frac{2 \cdot f_c}{f'_c + f'_t} = \frac{2}{3} \cdot f'_v \cdot b \cdot h \cdot \left(1 - \frac{N}{f'_c \cdot b \cdot h}\right)$$

or:

$$V = V_u \cdot \left(1 - \frac{N}{N_c}\right) = V_u \cdot (1 - X) \quad (4)$$

For failure in bending and in shear there is a critical value of the shear slenderness  $M_u/V_u h$  where the ultimate bending strength is reached ( $\sigma'_t = f'_t$ ) and at the same time the ultimate shear stress ( $\tau = f'_v$ ) is reached. In a four point bending test is:



$$M_u/V_u h = a_c/h = \frac{3f'_t - f_c}{8f'_v} =$$

$$= \frac{f_m}{4f'_v} \approx 3 \quad \text{for most}$$

strength classes (that may contain timber with a bending strength value of one higher class).

Above this critical value shear is not determining and there is bending failure. Below this value rotation and bending strength is reduced by the high shear force reducing the length  $x$  until  $x = 0$ . Then the maximal possible shear strength is reached:

$$V_u = 0.67f'_v bh \text{ at a moment: } M = f'_m bh^2/6 = f'_c bh^2/6 (\leq f'_t bh^2/6).$$

When both terms of eq.(4) are multiplied by  $a_c$ , then this equation becomes:

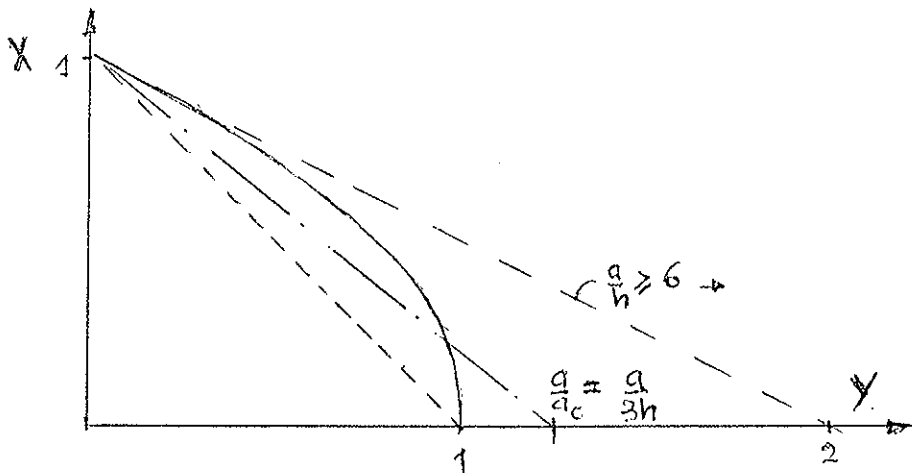
$$V a_c = V_u a_c (1 - X) = M_u (1 - X) = \frac{M}{a} \cdot a_c \quad \text{or:}$$

$$\frac{M}{M_u} \cdot \frac{a_c}{a} = 1 - X \quad \text{or:} \quad Y(a_c/a) = 1 - X$$

being a straight line and giving a cut off of a curved failure criterion. See for instance the figure below where the now proposed parabolic criterion is given. Only for  $a/h \geq \sim 6$ , the situation of the loads in the 4-points bending test, there is no cut off of the failure criterion. For loads closer to the support this reduction has to be accounted for bending with compression.

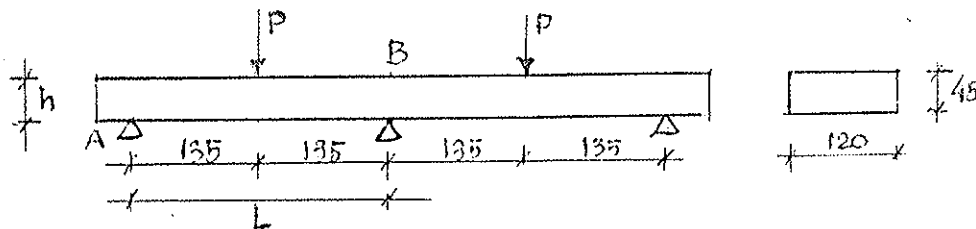
The experimental verification of this model is p.e. given by the test results of paper CIB-W18/24-10-1

Although for an explanation of test results a refined elastic plastic model has to be used, accounting precisely for the volume effects of shear and bending-tension and with adapted compression strengths at reduce rotation according to the work-curve of compressional failure, the method can be applied in its simple form as lower bound and has to be used when a non-linear failure criterion for bending with compression is introduced.



Cut off of the parabolic failure criterion for combined bending and compression by high shear loading

Eplation of the test results of paper CIB- W18/24-10-1



For the beam on 3 supports a cut of the beam at the middle support at point B will give a rotation at B by the loading P of:  $\varphi = PL/16EI$ . The shear strain will give no rotation at B. Because the beam is fixed at point B the moment at the support will

close the gap by  $\varphi' = M_B/3EI$ . However the shear by the reaction  $M_B/L$  of this moment will also close the gap by:  $\gamma = \tau/G \approx M_B/(LAG)$ . Thus:

$$\varphi - \gamma = \frac{PL^2}{16EI} - \frac{M_B}{LAG} = \frac{M_B}{3EI} \quad \text{or:} \quad M_B = \frac{3PL}{16} \cdot \frac{1}{1 + 4h^2/L^2}$$

With:  $h = 45$ ;  $L = 270$  is:  $M_B = 0.9 \cdot 3PL/16$ . Thus  $\sigma_B = 0.9 \cdot 50 = 45$  MPa (see paper).

Now the field- and support moments are equal but bending failures are initiated from the field if there is a volume effect.

The shear slenderness:  $M/Vh$  of the field moment at the side of the free support is:

$M/Vh = L/2h = 3$  is not determining. At the midsupport is  $M_B/V_B h \approx L/4h \approx 1.5$ .

In general is:

$$\frac{M}{Vh} = \frac{3s - 1}{s + 1} \cdot \frac{f_c}{4f_v} \quad \text{or at point B:} \quad 1.5 = \frac{3s - 1}{s + 1} \cdot \frac{45}{4 \cdot 7.6} \quad \text{giving: } s \approx 1$$

showing that there is just no plastic flow and indicating that:  $f_c \approx 45$  MPa and the maximal shear stress is:  $f_v' \approx 7.6$  MPa.

The value of  $f_c$  may be used to explain the strength of the centre-point loading, single span test of the paper where:  $M/Vh = L/2h = 3$  and  $f_v = 5.4$  MPa:

$$3 = \frac{3s - 1}{s + 1} \cdot \frac{45}{4 \cdot 5.4} \quad \text{or} \quad s = 1.56 \quad \text{giving a bending strength of:}$$

$$\sigma_m = 45 \cdot (3 \cdot 1.56 - 1) / (1 + 1.56) = 64.9 \text{ MPa (measured is 64.8 MPa)}$$

The pure bending strength of the 4 point bending test is:  $f_m = 77.8$  MPa. Thus:

$$77.8 = 45 \cdot \frac{3s - 1}{s + 1} \quad \text{or} \quad s = 2.15$$

The maximal shear stress of 7.6 occurs at the neutral line. For shear failure at plastic flow in compression the maximal shear stress is combined with a tension stress and will be about 0.9 times lower. Thus:  $f_v'' = 0.9 \cdot f_v' = 0.9 \cdot 7.6 = 6.8$  MPa.

This means that the shear strength at the maximal bending strength will be:

$$\tau_m = \frac{2f_v''}{s + 1} = 2 \cdot 6.8 / (1 + 2.15) = 4.3 \text{ MPa}$$

and will occur at:  $a/h = (3 \cdot 2.15 - 1) \cdot 45 / (3 \cdot 15 \cdot 4 \cdot 4.3) = 4.5$ .

Thus the 4-point bending test can be repeated with loads at a distance of 203 mm from the support to obtain the shear strength at ultimate bending.

It is assumed that corrections for volume effects, as for clear wood, can be ignored here for LVL (this has to be checked first).

It then can be concluded that the quasi linear shear strength has to be 4.3 MPa in order to predict a correct reduction of the bending strength by ultimate shear control. This of course is a prediction because data are lacking.



**INTERNATIONAL COUNCIL FOR BUILDING RESEARCH STUDIES AND DOCUMENTATION**

**WORKING COMMISSION W18 - TIMBER STRUCTURES**

**EFFECT OF WITHIN MEMBER VARIABILITY ON BENDING  
STRENGTH OF STRUCTURAL TIMBER**

by

I Czmochn

Chalmers University of Technology

Sweden

S Thelandersson

Lund University

Sweden

H J Larsen

Danish Building Research Institute

Denmark

Lund University

Sweden

**MEETING TWENTY - FOUR**

**OXFORD**

**UNITED KINGDOM**

**SEPTEMBER 1991**



# EFFECT OF WITHIN MEMBER VARIABILITY ON BENDING STRENGTH OF STRUCTURAL TIMBER

by

I. CZMOCH, S. THELANDERSSON AND H.J. LARSEN

## 1 INTRODUCTION

In this paper a simple model of the length-wise variation of strength of a piece of timber is used, see FIG 1. The model is similar to that proposed by Riberholt & Madsen [1].

It is assumed that

- \* timber is composed of short weak zones connected by sections of clear wood
- \* the weak zones correspond to knots or groups of knots and are randomly distributed
- \* failure occurs only in the middle of the weak zones
- \* the strengths of the weak zones are random.

Hence the distribution of the strength is modelled by means of composite random point series: Random series of strength are assigned to randomly distributed weak zones.

The basis for this model is the fact that failure almost always occurs in the vicinity of knots because of grain distortions around knots resulting in stresses perpendicular to the grain, stress concentrations caused by knot holes and encased knots, and because of differences between the properties of the knot and the surrounding wood.

The model can be used to evaluate

- \* the influence of length on the strength of timber members
- \* the influence of load configurations deviating from the standard test configuration used for assigning characteristic strength values



- \* the influence of different test procedures e.g. the difference between North American practice (where the length to be tested is chosen randomly) and European practice (where Eurocode 5 prescribes that the tested length shall contain a grade determining defect)
- \* the influence of the test procedure on the reliability parameters (e.g. safety index). Standard test procedures result in extreme value distributions. If they are used instead of the parent distribution (i.e. the distribution of the strength of the weak zones), the reliability of timber structures will be higher than for material like steel and reinforced concrete for the same safety index or partial safety factors.

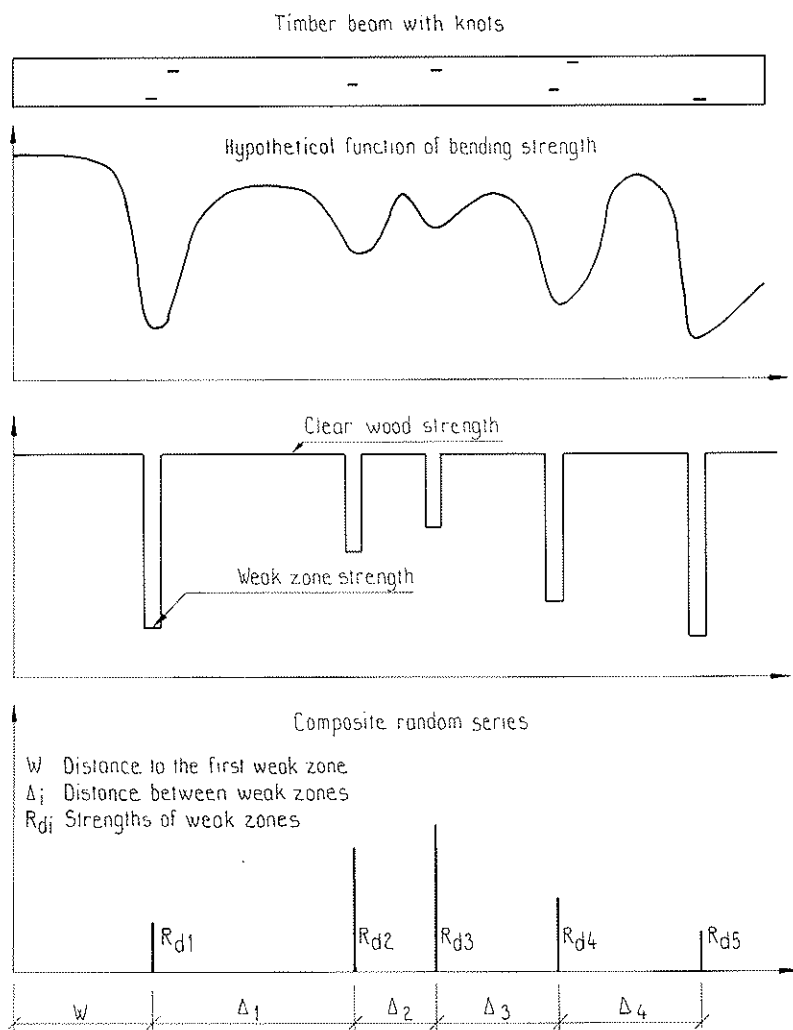


FIG 1 Modelling of length-wise distribution of strength of timber beam.

## 2 SIMULATION OF PROBABILITY DISTRIBUTION FUNCTION OF LOAD BEARING CAPACITY OF TIMBER BEAM

Load effect function  $S(x)$  versus the composite random series describing the bending strength of a timber beam is presented in FIG 2. It is assumed that the function  $S(x)$  and the bending strengths of weak zones  $R_d$  are expressed in the same units.

In the case of one parameter load, the load effect function  $S(x)$  can be expressed as

$$S(x) = Z \sigma(x) \quad (2.1)$$

where  $\sigma(x)$  is a normalized, deterministic function describing the bending moment distribution along the beam for a given load case;  $Z$  is the maximum external load effect expressed in the same units as the bending strength of weak zones  $R_d$ .

In this study the load bearing capacity of a timber beam is defined as

$$Z = \min \left[ \frac{R_{d1}}{\sigma(x_1)}, \dots, \frac{R_{dN}}{\sigma(x_N)} \right] \quad (2.2)$$

where  $R_{di}$  – the bending strength of the  $i$ -th weak zone

$$x_i = W + \sum_{k=1}^{i-1} \Delta_k \text{ – position of the } i\text{-th weak zone (for } i > 1)$$

$W$  – position of the first weak zone

$\Delta_i$  – the distance between the  $i+1$  and  $i$ -th weak zones

$N$  – random number of weak zones within given beam length.

Since all above quantities are random, the load bearing capacity is also a random function. In general, its probability distribution function must be evaluated by means of Monte Carlo simulation.

## 3 DATA NECESSARY FOR SIMULATION

In order to determine the probability distribution function  $Z$  according to the

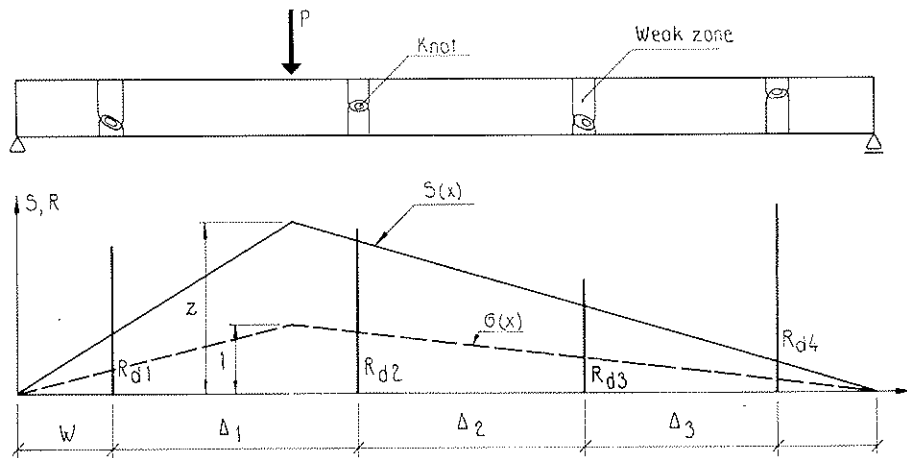


FIG 2 Distribution of bending strength of timber beam modelled by means of composite random series

assumed model the following data should be available:

- \* distribution function of the distance to the first weak zone
- \* distribution function of the distance between weak zones
- \* correlation function for distances between weak zones
- \* distribution function of the strength of weak zones
- \* correlation function for strengths of weak zones.

Data concerning the distances between knots are available in the literature. However, the numbers of weak zones within separate beams are relatively small (6 – 12 weak zones within beam of length 3.5 m). Therefore the confidence intervals for the estimated parameters (e.g. mean value and standard deviation) can be quite large. Furthermore, small sample sizes make it difficult to fit any probability distribution function and to estimate the correlation function. Hence, the maximum available information about the distribution of weak zones seems to be (now and also in the future) the intensity of occurrence of weak zones, i.e. the mean number of weak zones within a unit length (e.g. 1 m).

Very few data on the strength of weak zones (cross-sections with knots) or the length-wise distribution of bending strength of structural timber are available.

Standard test results, see FIG 3, can be approximately interpreted as the lowest strength within the length of maximum moment, i.e. they represent an extreme value distribution. The parent distribution of strength of weak zones is difficult to evaluate since information is lacking on the degree of correlation between strength of consecutive weak zones. The latter may however to some degree be approximated by the degree of correlation for the variation of stiffness.

On the basis of the physical consideration it seems reasonable to assume that both the distances between consecutive weak zones and the bending strength of weak zones constitute stationary random series. This means that the marginal probability distributions of bending strengths are identical for all weak zones. The same applies to the marginal probability distributions of distances between weak zones.

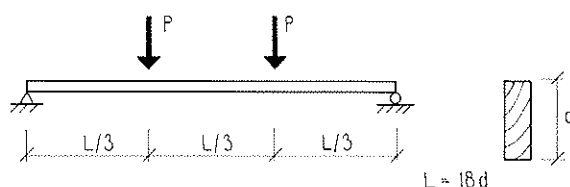


FIG 3 Standard test configuration

#### 4 SENSITIVITY ANALYSIS OF RIBERHOLT–MADSEN MODEL

##### 4.1 Riberholt–Madsen model

The report by Riberholt–Madsen [1] presents a method to derive the cumulative distribution function (CDF) for the strength of weak zones,  $F_d$ , on the basis of the CDF of the strength of the weakest cross section along a tested length,  $F_t$ .

The main assumptions in the Riberholt–Madsen model are:

1. The occurrence of weak zones along a beam is modelled by a Poisson process, i.e. the distances between weak zones follows the Exponential distribution

and they are stochastically independent. The intensity of occurrence of weak zones along the beam is constant and equal to  $\lambda$ .

2. The strengths of weak zones,  $R_d$ , are stochastically independent.

Riberholt & Madsen presents a formula for  $F_d$  in terms of  $F_t$  derived under the assumption that failure can only occur at a cross-section with a defect

$$F_{dRM} = -\frac{1}{N} \ln(1 - F_t + F_t e^{-N}) \quad (4.1)$$

where  $N$  is the mean number of weak zones along the test length  $L$

$$N = \lambda L \quad (4.2)$$

The length  $L$  to be employed in the above formula depends on the test procedure. When the part of structural lumber subjected to standard test (FIG 3) is chosen randomly (In-grade method), Riberholt & Madsen suggested that  $L$  should be equal to the range of maximum bending moment. When the structural lumber is inspected before test and a strength reducing grade determining defect is put within the maximum bending moment (EC-5), then according to [1] the length should be taken equal to the whole test beam span.

#### 4.2 Purpose of the sensitivity analysis

In this section a sensitivity analysis is performed to check if the CDF of strength of weak zones  $F_{dRM}$ , estimated from Eq. (1) under the assumption of stochastic independence, can be applied even when one would expect some degree of correlation between the strengths of weak zones or the distances between weak zones.

A very high degree of correlation for strengths of weak zones would result in disappearance of length and load configuration effects, which is in contradiction with the outcome of many experiments, see e.g. [2] and [3]. Furthermore, if there is any degree of correlation between strengths of weak zones, it is likely that only the strengths of the neighbouring weak zones are correlated. Tests in tension by

Lam & Varoglu [4], indicate a non-negligible strength correlation within zones 0.5 – 1.0 m apart. The influence of correlation between the strength  $R_d$  for consecutive weak zones on the estimated CDF  $F_{dRM}$  is studied in the sensitivity analysis.

The intensity of occurrence of weak zones can be recorded during experimental tests of timber beams. Colling & Dinort [5] report a mean distance of 0.5 m between major knot or knot groups. The intensity of occurrence was about the same for high grade and low grade timber. Similar results were found from analysis of other data [6, 7].

A reliable estimation of the correlation of distances demands a great number of long sequences of distances between weak zones  $\{\Delta_1, \dots, \Delta_N\}$ . Before such laborious experimental tests are started, it seems worth to know the answer to the basic question: How much does the distribution  $F_t$  actually depend on the degree of correlation between components of the sequence  $\{\Delta_1, \dots, \Delta_N\}$ ?

### 4.3 Correlation function used in the simulation

A Gaussian type correlation function is assumed both for the stationary random series of strength of weak zones and the stationary random series of distances between weak zones

$$\text{for } NZ > 0 \quad \rho(i-k) = \exp \left[ - \left[ \frac{i - k}{NZ + 1} \right]^2 \right] \quad (4.3)$$

$$\text{for } NZ = 0 \quad \rho(i-k) = \begin{cases} 1 & \text{if } i = k \\ 0 & \text{if } i \neq k \end{cases} \quad (4.4)$$

where  $NZ$  is the scale of fluctuation. For both random series it was assumed that the correlation function depends on the difference of indices  $(i-k)$ , where  $i, k$  denote  $i$ -th and  $k$ -th weak zones' strengths in the sequence  $\{R_{d1}, \dots, R_{dN}\}$ , or  $i$ -th and  $k$ -th distances in the sequence  $\{\Delta_1, \dots, \Delta_{N-1}\}$

By changing NZ different correlation functions can be obtained. Some examples of the correlation functions are given in FIG 4 for various values of NZ. If  $NZ = 0$  there is no correlation.

Two kinds of scale of fluctuations NZ are used in further calculations:

NZDLT : scale of fluctuation for distances between weak zones

NZSTR : scale of fluctuation for strengths of weak zones.

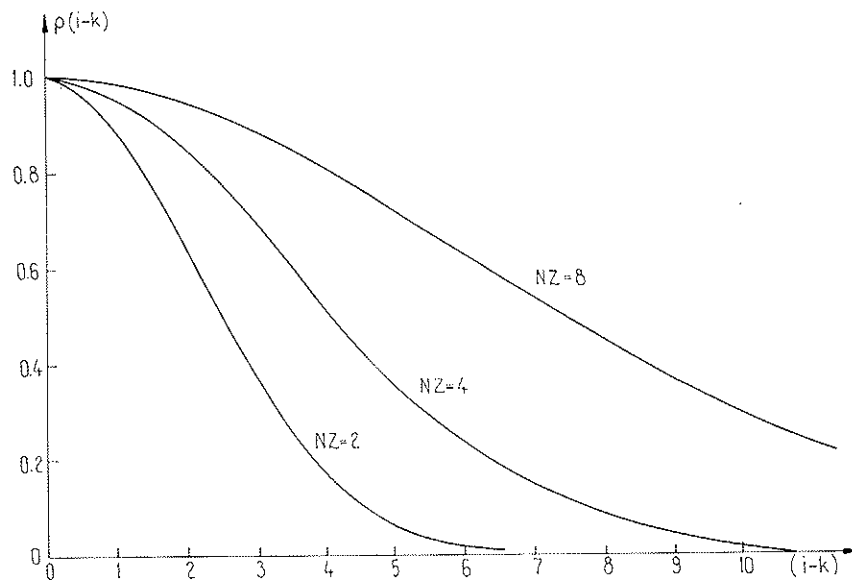


FIG 4 Gaussian type correlation function

#### 4.4 Simulation

##### Phase I

The idea is to start with an assumed "reality", described by the following statistical timber properties

- \* cumulative distribution function of distance to the first weak zone  $F_w$
- \* cumulative distribution function of distance between weak zones  $F_{\Delta}$

- \* scale of fluctuation  $NZDLT \geq 0$
- \* cumulative distribution function of weak zones  $F_d$
- \* scale of fluctuation  $NZSTR \geq 0$

Given these properties, the "real" load-bearing capacities  $R_t$  and  $R_u$  for the two load cases shown in FIG 5 are directly obtained by Monte-Carlo simulation. The corresponding CDF:s are denoted  $F_t$  and  $F_u$ , respectively.

### Phase II

In practice we have no direct information about strength of weak zones, and limited information about the degree of correlation. Therefore, in phase II it is assumed that the only information available is the CDF  $F_t$  and the intensity of occurrence of weak zones  $\lambda$ .

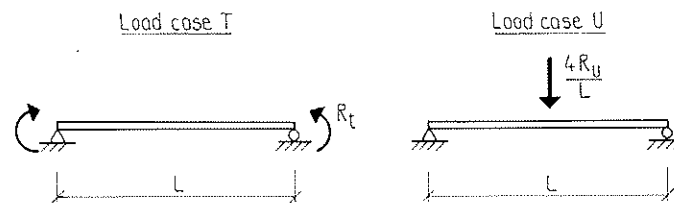


FIG 5 Load cases considered in sensitivity analysis

Both  $F_t$  and  $\lambda$  are taken from phase I, i.e. from the assumed reality. In practice  $F_t$  and  $\lambda$  can be estimated from standard testing of timber samples.

Under these assumptions an approximative CDF for strength of weak zones  $F_{dRM}$  is derived from Eq. (4.1). Using this approximate distribution the load cases in FIG 5 were again simulated under the further assumptions:

- \* the distance between weak zones follow a Poisson process with the intensity of weak zones  $\lambda$  according to phase I of the simulation



- \* stochastic independence of both random series ( $NZDLT = NZSTR = 0$ )

The result from phase II is the estimated cumulative distribution functions  $F_{dRM}$ ,  $F_{tRM}$  and  $F_{uRM}$ , which can be compared with their "real" counterparts  $F_d$ ,  $F_t$  and  $F_u$ .

#### 4.5 Data for calculations

Calculations were carried out for three Data Sets described in Table 1. In all cases the beam length was 3 m and 2000 beams were simulated in each calculation.

#### 4.6 Results from sensitivity analysis

In FIG 6 distribution functions based on estimates from the Riberholt–Madsen model and the corresponding "reality" are compared. It is assumed from the outset that no correlation is present ( $NZDLT = NZSTR = 0$ ). The estimate is obviously quite accurate in this case.

Another case is shown in FIG 7, where it is assumed that a correlation corresponding to  $NZDLT = NZSTR = 2$  is present and that data set No. 3 (see Table 1) represents the assumed "reality". As seen in FIG 7a and 7b the estimated distribution for weak zones strength and load case U differs considerably from the "correct" one, but the error is smallest at the lower tail. The error is mainly due to the presence of correlation, which is not taken into account in the Riberholt–Madsen formula. For load case T the estimate is correct, because in this case the "correct" CDF is used as a basis for the estimate.

Some results from the simulations of the lower 5th percentile are summarized in Table 2. For reasonable degrees of correlation ( $NZ \leq 2$ ) the error of the Riberholt–Madsen estimation for load case U is less than 10 % for all three data sets. Results for unrealistically high assumed correlation ( $NZDLT = NZSTR = 8$ ) are also given. In that case the error is of the order 15 – 20 %.

It is interesting to compare load case T and U, as two extreme cases illustrating the stochastic load configuration effect, which is of similar nature as the stochastic

Table 1 Data sets used in sensitivity analysis

	DATA SET		
	1	2	3
Distance to first weak zone			
	EXP(0.5, 0)	EXP(0.5, 0.15)	EXP(0.5, 0)
E(x), m	0.5	0.65	0.5
D(x), m	0.5	0.50	0.5
Distance between weak zones			
	EXP(0.5, 0)	EXP(0.5, 0.15)	LN (-1.25, 1.25)
E(x), m	0.5	0.65	0.63
D(x), m	0.5	0.50	1.22
Bending strength of weak zones:			
	W 2	W 2	LN (3.91, 0.35)
E(x), [MPa]	63.0	63.0	53
D(x), [MPa]	11.0	11.0	19

**Notation:**

EXP (m,  $x_0$ ) = exponential distribution (m = scale parameter,  $x_0$  = location parameter)

W 2 = 2 parameter Weibull distribution

LN (m,  $\sigma$ ) = lognormal distribution (m = mean value,  $\sigma$  = standard deviation of corresponding normal distribution)

E(x) = expectation value (mean value)

D(x) = standard deviation.

length effect [2]. It is seen from Table 2 that the capacity for load case U is about 30 % higher than for load case T. This is valid for all three data sets. If very high correlation levels are assumed the difference becomes smaller.

#### 4.7 Applicability of Riberholt–Madsen model

This primary analysis suggest that the Riberholt–Madsen model can be used to obtain the distribution function of strength of weak zones on the basis of the following information

- \* cumulative distribution function  $F_t$  of load bearing capacity of timber beam under test load configuration with well–defined methods of selection of tested length
- \* intensity of occurrence  $\lambda$  of weak zones along tested beams.

This approach makes it possible to improve the information from standard test programs by recording the number of weak zones (according to some appropriate definition) along with the strength.

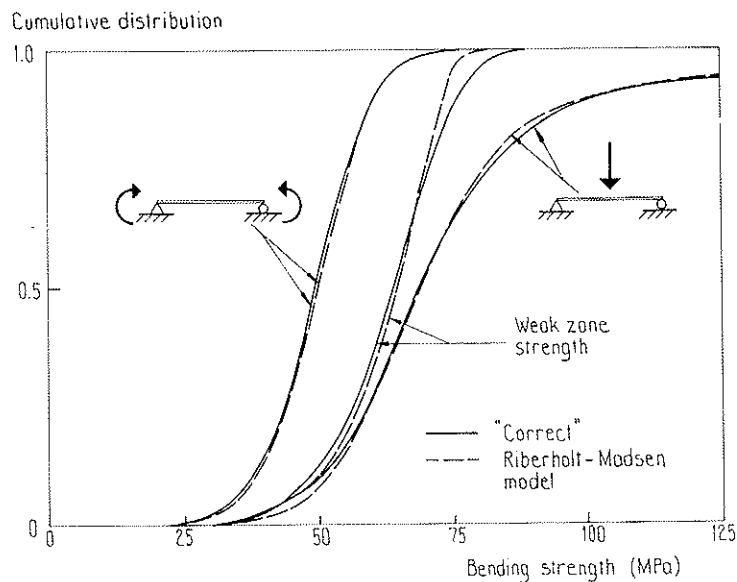


FIG 6 Simulation for data set No 1 with NZDLT = NZSTR = 0

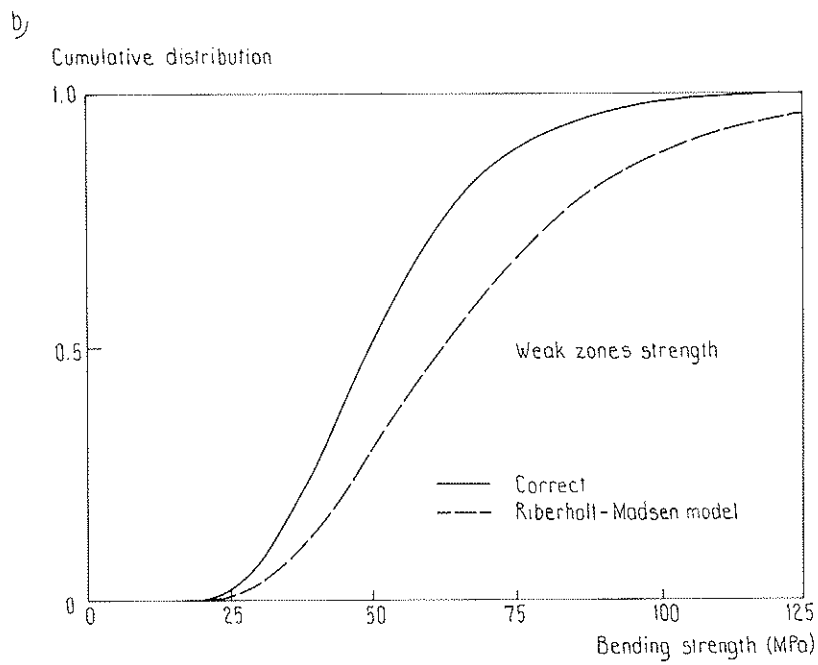
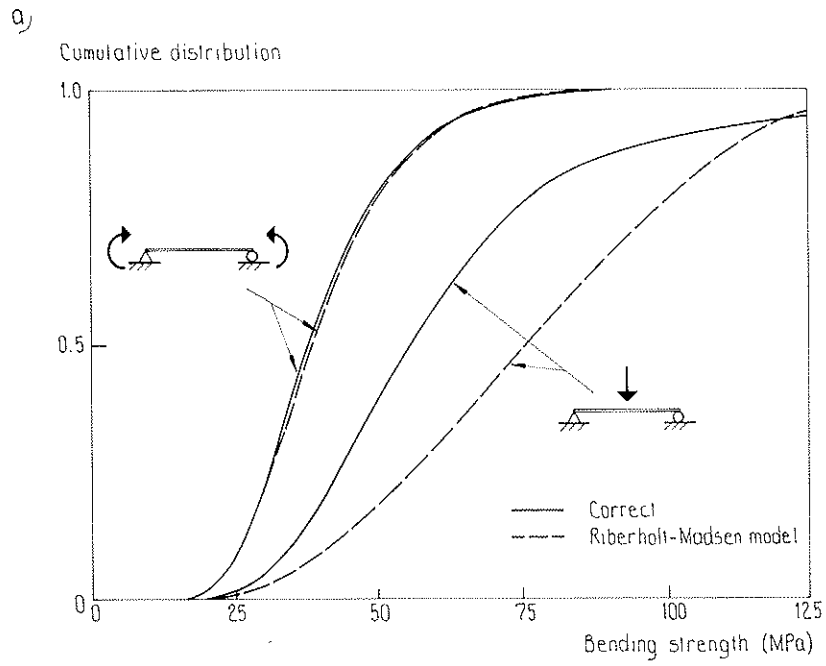


FIG 7 Simulation for data set No 3 with  $NZSTR = NZDLT = 2$

TABLE 2 Characteristic values (5 % quantiles) from simulations

DEGREE OF CORRELATION		WEAK ZONES STRENGTH		LOAD CASE T		LOAD CASE U			
NZ STR	NZ DLT	$R_d$	$R_{dRM}$	$R_t$	$R_{tRM}$	$R_u$	$R_{uRM}$	$\frac{R_{uRM}}{R_u}$	$\frac{R_u}{R_t}$
DATA SET NO. 1									
0	0	43.0	43.3	33.2	34.9	43.4	46.6	1.07	1.31
0	2	43.0	44.1	32.0	32.6	42.5	44.3	1.04	1.33
2	0	43.0	49.1	36.3	37.3	47.7	52.2	1.09	1.31
2	2	43.0	50.2	35.5	35.8	46.4	49.6	1.07	1.31
8	8	43.0	55.2	38.6	38.3	45.7	53.5	1.17	1.18
DATA SET NO. 2									
0	0	43.0	42.6	34.8	34.1	46.7	46.7	1.00	1.34
0	2	43.0	43.7	33.4	33.7	44.8	45.4	1.01	1.34
2	0	43.0	47.5	37.9	36.9	48.6	51.6	1.06	1.28
2	2	43.0	49.0	36.4	36.8	47.2	50.3	1.07	1.30
8	8	43.0	52.6	39.7	40.6	47.1	56.1	1.19	1.19
DATA SET NO. 3									
0	0	27.9	26.5	21.9	21.3	28.9	29.9	1.03	1.32
0	2	27.9	26.8	21.1	20.2	27.7	27.7	1.00	1.31
2	0	27.9	30.2	23.6	23.4	31.7	34.1	1.08	1.34
2	2	27.9	30.8	22.7	22.3	29.8	31.8	1.07	1.31
8	8	27.9	39.8	24.9	24.8	29.8	34.9	1.17	1.20

## 5 PARAMETRIC ANALYSIS OF PRACTICAL PROBLEMS BY SIMULATION WITH WEAK-ZONES TIMBER MODEL

### 5.1 General idea of analysis

The data necessary for simulation of load bearing capacity of timber beams are generally not available for different timber grades and species. In this situation a solution is to carry out calculations for extensive data sets covering the possible ranges of parameter values and types of distribution functions. In fact, a distribution function belonging to some set of admissible statistical models is always considered as a possible description of experimental data.

Parametric analysis can help to check if there is any relation between, e.g. degree of correlation and the property of interest.

### 5.2 Comparison between EC-5 test method and IN-GRADE test method for timber

The EC-5 method to determine timber beam strength [8] is based on a subjective choice of a strength reducing grade determining defect. Therefore the EC-5 method cannot be exactly represented by means of simulation. What is possible to compare is the load bearing capacity related to random choice of tested part of lumber (IN-GRADE method) with the load bearing capacity when the part containing the minimum value of bending strength have been chosen (EC-5 method).

In order to compare IN-GRADE method with EC-5 method it was assumed that the length of structural lumber  $L$  is greater than the test beam span  $S$ . Standard four-point load configuration according to FIG 3 was assumed. First the distribution of weak zones and their strengths are simulated. The timber beam strength is then calculated in two ways:

IN-GRADE method:

Part of the simulated lumber close to the left end is subjected to test load configuration.

EC-5 method:

The weak zone with the lowest value of bending strength is identified and then trial is undertaken to impose the load in such a way that the weakest weak zone is in the constant bending moment range. The finite length  $L$  of the lumber makes that sometimes impossible and then the weakest weak zone is placed as close as possible to the maximum bending moment zone.

Simulations were made for a wide range of data given in Table 3. The distance between weak zones was modelled by an exponential distribution controlled by the scale parameter  $\sigma_{\Delta}$ , which was varied between 0.25 and 0.75 m. (For the exponential distribution the mean value is equal to the scale parameter  $\sigma_{\Delta}$ ). The bending strength of weak zones is described by a three parameter Weibull distribution. By varying the scale and shape parameters  $\sigma_{Rd}$  and  $\lambda_{Rd}$  a wide range of distributions with different means, variances and shapes can be represented, see FIG 8. The original length  $L$  of the boards was taken to 7.2 m and the test span  $S$  was 3.6 m in all simulations.

As an example, results from simulations with data set E3 (see Table 2) are represented in FIG 9. There is a significant difference between the two test methods; the ratio  $\gamma$  between the lower 5th percentiles is 1.20 when correlation is disregarded (FIG 9 a). With a correlation corresponding to  $NZDTL = NZSTR = 4$  (FIG 9b) the ratio  $\gamma$  is changed to 1.17, i.e.  $\gamma$  is not very sensitive to correlation.

The ratio  $\gamma$  between the characteristic values determined by the IN-GRADE and the EC-5 testing methods for all data sets in Table 3 is represented in FIG 10. The  $\gamma$ -values are plotted against c.o.v. of timber beam strength according to the EC-5 simulation.

As expected the IN-GRADE method always gives higher strength than the EC-5 method. The value of  $\gamma$  is mainly in the interval 1.10 – 1.25 for a very wide range of input data assumptions. It is also somewhat surprising that there is a very weak influence of the coefficient of variation.

TABLE 3 Data sets for parametric analysis

Data set	$\sigma_{\Delta}$	$\mu_{Rd}$	$\sigma_{Rd}$	$\lambda_{Rd}$	$m_{Rd}$	$s_{Rd}$	$\text{cov}_{Rd}$	$R_{dk}$
A1	0.25	10.	30.	1.5	37.1	18.4	0.50	14.0
A2	0.25	10.	30.	3.0	36.8	09.7	0.26	20.9
A3	0.25	10.	30.	4.5	37.4	06.9	0.18	25.3
A4	0.25	10.	30.	6.0	37.8	05.4	0.14	28.1
B1	0.25	10.	60.	1.5	63.5	35.7	0.56	17.9
B2	0.25	10.	60.	3.0	63.3	19.2	0.30	31.8
B3	0.25	10.	60.	4.5	64.6	13.7	0.21	40.6
B4	0.25	10.	60.	6.0	65.5	10.7	0.16	46.2
C1	0.25	10.	90.	1.5	91.3	55.2	0.60	21.9
C2	0.25	10.	90.	3.0	90.4	29.2	0.32	42.7
C3	0.25	10.	90.	4.5	92.1	20.7	0.22	55.8
C4	0.25	10.	90.	6.0	93.5	16.2	0.17	64.3
D1	0.50	10.	30.	1.5	37.1	18.4	0.50	14.0
D2	0.50	10.	30.	3.0	36.8	09.7	0.26	20.9
D3	0.50	10.	30.	4.5	37.4	06.9	0.18	25.3
D4	0.50	10.	30.	6.0	37.8	05.4	0.14	28.1
E1	0.50	10.	60.	1.5	63.5	35.7	0.56	17.9
E2	0.50	10.	60.	3.0	63.3	19.2	0.30	31.8
E3	0.50	10.	60.	4.5	64.6	13.7	0.21	40.6
E4	0.50	10.	60.	6.0	65.5	10.7	0.16	46.2
F1	0.50	10.	90.	1.5	91.3	55.2	0.60	21.9
F2	0.50	10.	90.	3.0	90.4	29.2	0.32	42.7
F3	0.50	10.	90.	4.5	92.1	20.7	0.22	55.8
F4	0.50	10.	90.	6.0	93.5	16.2	0.17	64.3
G1	0.75	10.	30.	1.5	37.1	18.4	0.50	14.0
G2	0.75	10.	30.	3.0	36.8	09.7	0.26	20.9
G3	0.75	10.	30.	4.5	37.4	06.9	0.18	25.3
G4	0.75	10.	30.	6.0	37.8	05.4	0.14	28.1
H1	0.75	10.	60.	1.5	63.5	35.7	0.56	17.9
H2	0.75	10.	60.	3.0	63.3	19.2	0.30	31.8
H3	0.75	10.	60.	4.5	64.6	13.7	0.21	40.6
H4	0.75	10.	60.	6.0	65.5	10.7	0.16	46.2
J1	0.75	10.	90.	1.5	91.3	55.2	0.60	21.9
J2	0.75	10.	90.	3.0	90.4	29.2	0.32	42.7
J3	0.75	10.	90.	4.5	92.1	20.7	0.22	55.8
J4	0.75	10.	90.	6.0	93.5	16.2	0.17	64.3

Notation:

$\sigma_{\Delta}$	scale parameter of the Exponential distribution for distance to the first weak zone and distances between weak zones
$\mu_{Rd}, \sigma_{Rd}, \lambda_{Rd}$	location, scale and shape parameters of the Weibull distribution for bending strength of weak zones.
$m_{Rd}, s_{Rd}, \text{cov}_{Rd}$	mean value, standard deviation and coefficient of variation of bending strength of weak zones
$R_{dk}$	characteristic value (0.05-quantile) of bending strength of weak zone.



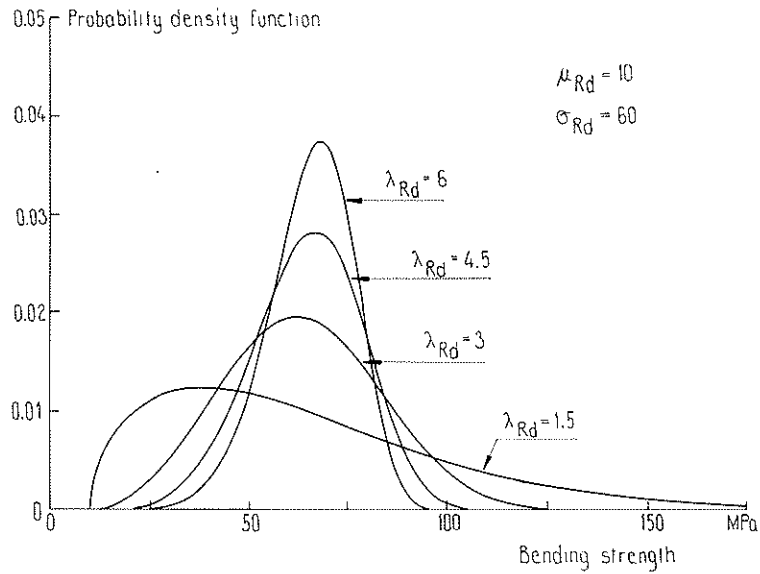


FIG 8 Density functions for three parameter Weibull distribution with different shape parameters

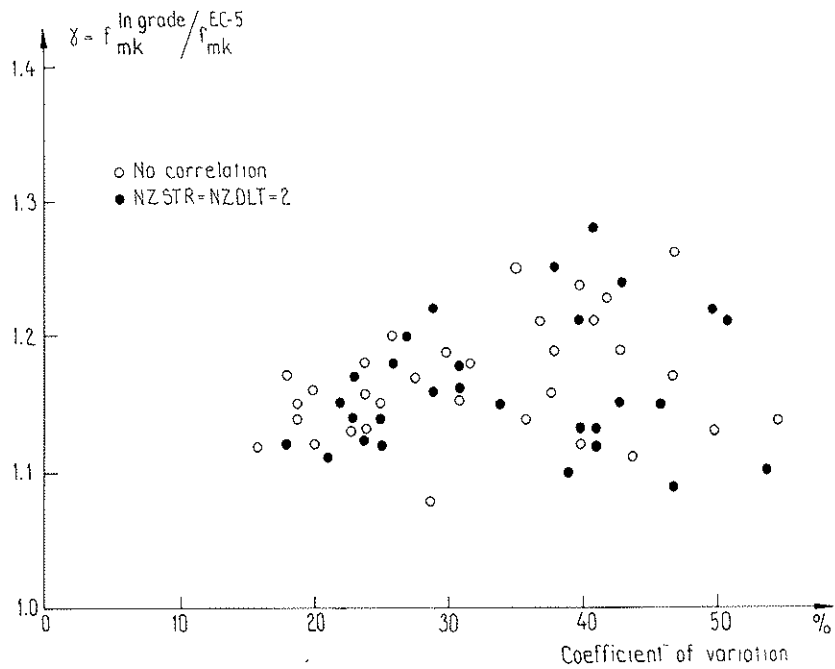


FIG 10 Ratio  $\gamma$  between characteristic values simulated according to IN-GRADE and EC-5 testing methods versus c.o.v. of EC-5 test beam strength

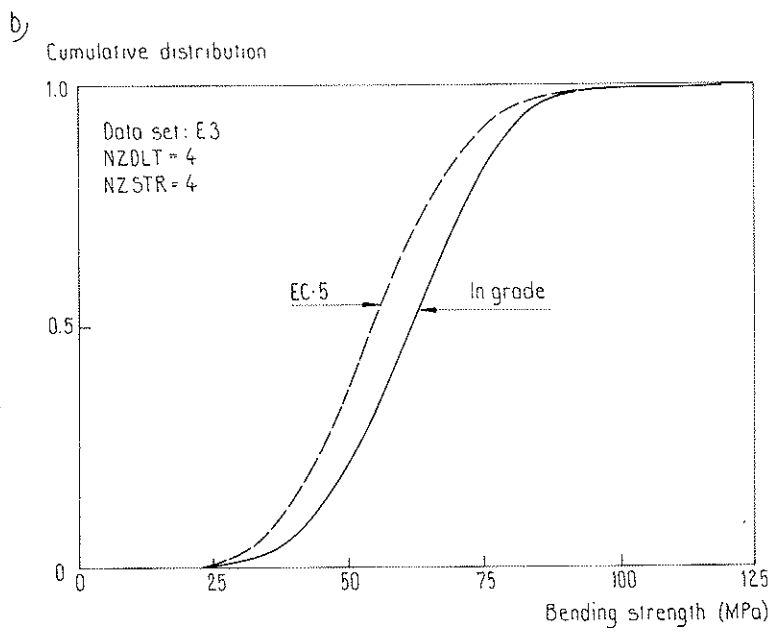
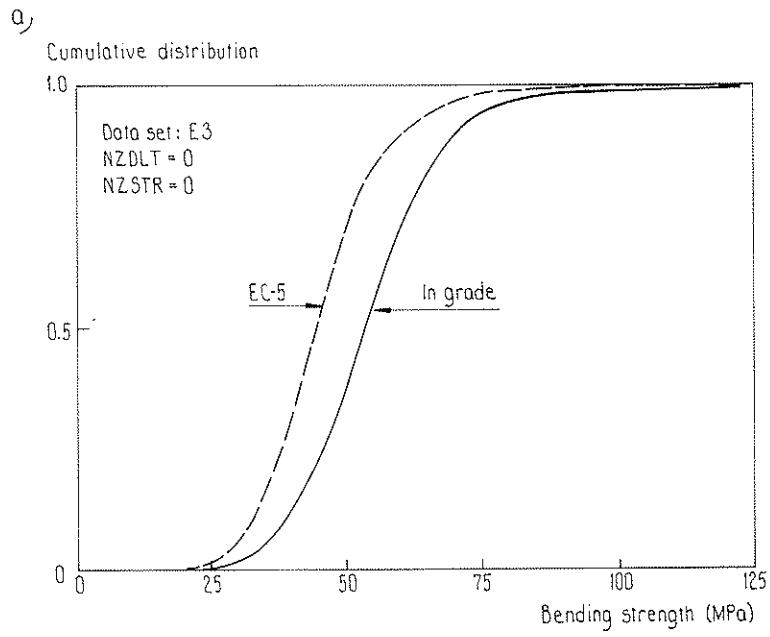


FIG 9 Simulated timber beam strengths according to IN-GRADE and EC-5 testing methods

Since the actual EC-5 test method is non-conservative in relation to the simulated one, the  $\gamma$ -values presented in FIG 10 may be too high. The error is probably rather small at the lower tail of the distribution, but nevertheless there is a need to be more precise in the EC-5 testing method as regards the biased procedure to place a grade-determining defect within the region of maximum moment. A modification of the method should be considered, aiming at a mathematically defined procedure, enabling a more stringent interpretation of the test results for practical use.

### 5.3 Amplification factor for continuous timber beams

Chords of trussed rafters can be considered as continuous timber beams. The maximum moment in such beams is found at the supports, with distinct moment peaks within a small region. Since the probability is small that a sharp moment peak coincides with a very weak zone, the effective moment capacity can be considerably higher than the capacity determined in a standard bending test.

In the following analysis failure is defined on a weakest link basis, i.e. once the moment in any (weak) section exceeds the capacity, failure is assumed to occur. Semibrittle or plastic type moment redistribution may also to some extent improve the load-bearing capacity of statically indeterminate timber beams, but is not considered here.

Three types of beams subjected to uniform loading were considered (see FIG 11):

- A) 2-span continuous beam simply supported
- B) 2-span continuous beam simply supported with right end clamped
- C) 3-span continuous beam simply supported

The beam lengths considered: 3.6, 5.4 and 7.2 m.

The moment capacity amplification factor  $\beta$  due to purely stochastic influences is defined as

$$\beta = \frac{\text{characteristic moment capacity of continuous beam}}{\text{characteristic timber beam strength according to EC-5}}$$

The test span in the simulated EC-5 test was taken to 3.6 m. The minimum value of the ratio  $\beta$  was always obtained for case A in FIG 11 with  $L = 7.2$  m. The values of  $\beta$  for this case are plotted in FIG 12 against the coefficient of variation of timber beam strength according to EC-5 test method. The results presented in FIG 12 are based on data sets D, E and F in Table 3 with mean distance 0.5 m between weak zones. The simulations showed that the ratio  $\beta$  increases somewhat with increasing mean distance but the effect is not very strong.

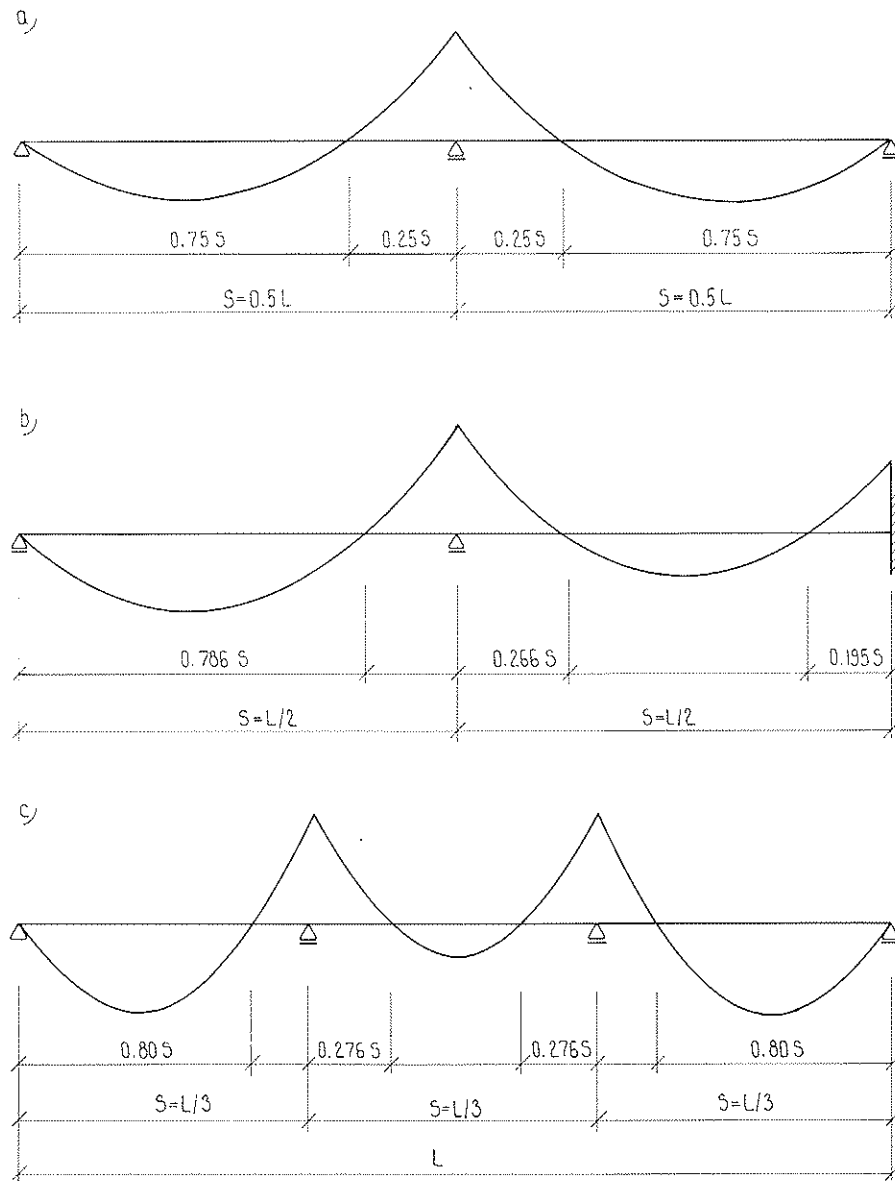


FIG 11 Continuous timber beams considered in parametric study

The arrows in FIG 12 shows how the ratio  $\beta$  changes with increased value of the degree of correlation (at the base of the arrow the correlation is zero and at the end NZSTR = NZDLT = 2). The single points in the diagram represent a high degree of correlation: NZSTR = NZDLT = 8. Increased degree of correlation leads to higher coefficient of variation for the simulated EC-5 test. For moderate degree of correlation the ratio  $\beta$  is only slightly changed, but if the correlation is high  $\beta$  is reduced significantly, as expected. The simulated ratios are compared with the proposal for magnification factor given in [9]. The results indicate that the proposal is conservative.

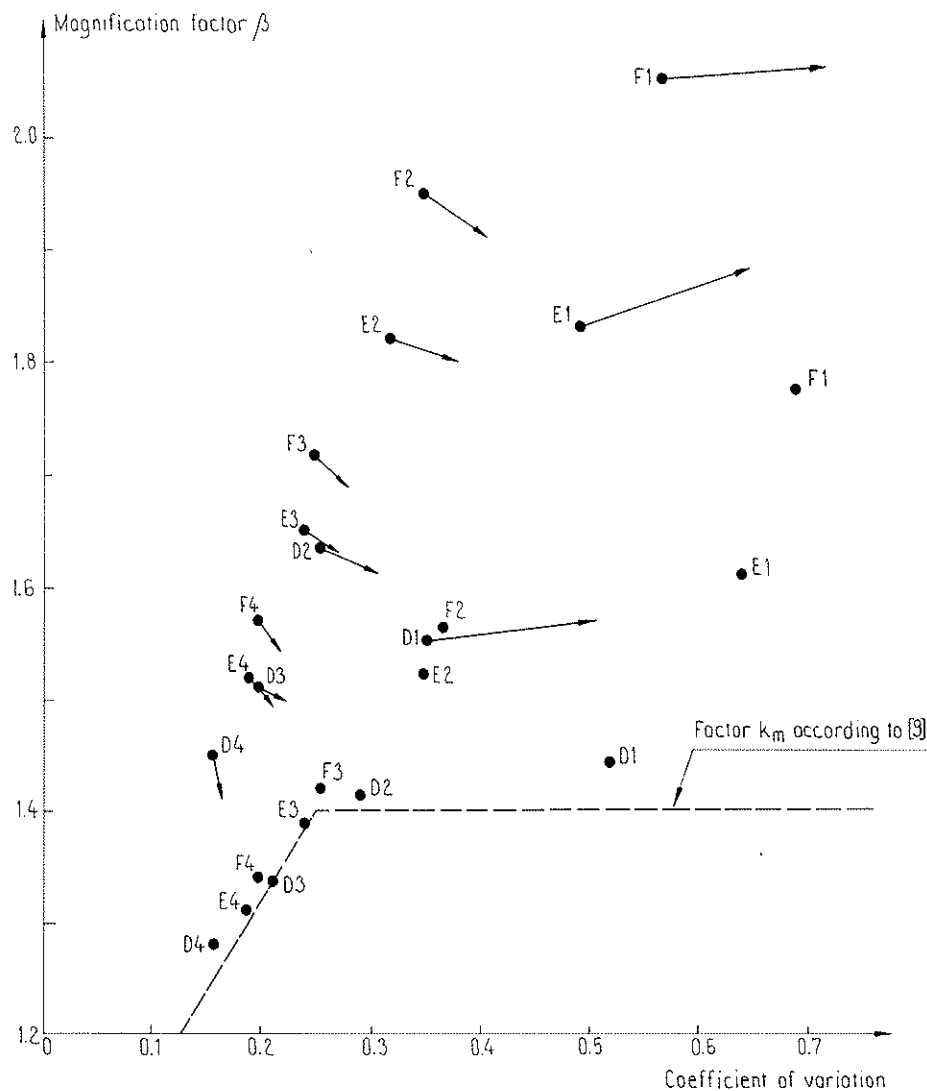


FIG 12 Magnification factor for strength of continuous timber beams versus c.o.v. of EC-5 test beam strength

## 6 CONCLUSIONS

The stochastic/mechanical weak zone model of timber proved to be a useful tool for analysis of effects of within member variability in timber.

It was found that the basic information needed in the model can be indirectly estimated with reasonable accuracy by the procedure proposed by Riberholt & Madsen [1], provided that the correlation between strengths of weak zones is reasonably small.

The relation between the EC-5 method and the IN-GRADE method of testing timber was analysed. It was found that the characteristic value obtained from the EC-5 method is significantly smaller. The EC-5 characteristic value should be multiplied by a factor 1.10 – 1.25 to make it correspond to the characteristic value from IN-GRADE testing.

The moment capacity in regions with sharp peaks in the moment diagram can be increased by a factor 1.3 – 2.0 due to purely stochastic effects. The proposal by Riberholt [9] for such magnification factors for trusses seems to be conservative.

It is obvious from the studies in this paper that effects of within-member variability are very significant from the practical point of view. Further studies of these effects and in particular experimental programs to improve the knowledge about variability and correlation of strength within timber elements are of great interest. In experimental investigations of strength, the intensity of occurrence of weak zones should be recorded. This can be done either by machine grading readings or by visual observations of knots (knot area ratios).

The method presently proposed in EC-5 to determine characteristic strength is difficult to relate to situations characteristic for practical use of timber. The method is not unambiguously defined from a statistical point of view as is the case for IN-GRADE testing where the tested length is chosen randomly. However, a method based on biased choice of tested segment has great advantages, since the sample size can be reduced significantly. For the purpose of discussion, a modified version of the EC-5 test method is proposed below.

## Proposed modification of EC-5 method of testing

- \* The timber boards in full length from a sample are run through a stress grading machine and the flatwise bending stiffness is recorded along the length.
- \* The section with minimum stiffness is defined as the weakest section.
- \* Other sections within the board with flatwise stiffness not more than (say) 5 % higher than the minimum stiffness, can qualify as a weakest section.
- \* The test specimen shall be cut from the board so that a weakest section is placed within the length of maximum moment. If this is not possible, the board shall be omitted from the sample.
- \* The specimens qualifying for the test are tested according to ISO 8375. The characteristic value is evaluated on the basis of the reduced sample.

## Comments

The suggested procedure will give a result which is very close to the minimum strength over a length equal to the original length of the boards. The result will depend on this length, and an adjustment with respect to this length might be considered in the evaluation of the characteristic value.

A statistical analysis of the sample size necessary to get a sufficiently reliable estimate of the characteristic value should also be performed.

## REFERENCES

- 1 Riberholt, H., Madsen, P.H.; Strength distribution of timber structures, measured variation of the cross sectional strength of structural lumber, Struct. Research Lab., Technical University of Denmark, Report No. R 114, 1979.





**INTERNATIONAL COUNCIL FOR BUILDING RESEARCH STUDIES AND DOCUMENTATION**  
**WORKING COMMISSION W18 - TIMBER STRUCTURES**

**PROTECTION OF STRUCTURAL TIMBER AGAINST FUNGAL ATTACK**  
**REQUIREMENTS AND TESTING**

by

K Jaworska

M Rylko

W Nozynski

Institute of Building Technics Wood & Biocorrosion Establishment, Warsaw  
Poland

**MEETING TWENTY - FOUR**

**OXFORD**

**UNITED KINGDOM**

**SEPTEMBER 1991**



M.Sc. Krystyna Jaworska  
Dr. Maria Ryłko  
Asst.Prof.Dr.Eng. Władysław Nożyński

Institute of Building Technics  
Wood and Biocorrosion Establishment  
ul. Kasawerów 21  
02-656 Warszawa, Poland

Protection of Structural Timber against Fungal Attack  
Requirements and Testing

F o r e w o r d

In Poland the obligation of structural timber protection /timber used for erection of buildings, especially elements and structures of building/ against fungal attack is being established by the rules of the Building Code /Sejm Act/. Those rules obliging to the application of wood preservatives lay down the appropriate requirements; but there are no rules for the quality of wood preservatives used nor for the preservative treatment itself and finishing quality obtained. For evaluation of wood preservatives quality some standards are being used /with standard test methods their content being in accordance with the respective western european standards. Nevertheless for the final quality of treatment neither test methods nor building rules have been developed. We are lacking requirements for the preservative treatment of wooden elements and structures used in the building.

Considering such state of affairs a research work has been carried out by the Wood and Biocorrosion Establishment of the Building Technics Institute in order to fill in the gap in the Building Code. The results of that research work are described below.

1. Bioisotopic test method for determination of protection effectiveness of structural timber against fungal attack

1.1. Principle

The principle of this method is as follows:

/a/ The test and control samples are submitted to the attack of the test fungus cultivated on an artificial biological substrate containing radio-active phosphorous isotope  $^{32}\text{P}$  in form of  $\text{Na}_2\text{HPO}_4$  during specified period and under specified conditions;

/b/ measurement of radio-active radiation pulses emitted by the samples as a result of labelled mycelium penetration into them;

/c/ determination of protection effectiveness factor "Z" as a relation between the radio-active radiation pulses of the test samples and those of the control ones.

The test samples can be cut out of any place of the preservative treated elements /or segments of such elements/ from different depth; the control samples shall be taken from any specified control material.

For this a pine-wood having high content of sapwood and specified quality has been taken. The details of this method are described below.

## 1.2. Materials

1.2.1. Substrate for fungi /nutrient maltose agar/ - to 40g of maltose extract placed in an Erlenmeyer flask 1000 ml of distilled water is added and then the content is heated up to 50°C and 30g of powdered agar is added while stirring all the time with a glass rod until all components are dissolved. The flask corked with a cotton wool is sterilized in an autoclave under steam pressure at 120±2°C for 25 minutes.

1.2.2. Test fungus. Pure cultures of *Coniophora puteana*/Fr./, Karst = *Coniophora cerebella* Pers., Ehw.15 strain stored at 6° to 10°C on the agar-maltose substrate prepared acc. to the clause 1.2.1 with addition of 1% of sawdust. The mycelium shall be grafted on a fresh substrate once for 6 months at least. Every 2 years the mycelium shall be grafted and cultivated on a wooden disc saturated with 5 to 8 ml of maltose extract solution.

1.2.3. The radionuclide <sup>32</sup>P shall be used in form of Na<sub>2</sub>HPO<sub>4</sub>.

## 1.3. Apparatus

/a/ set of instruments for radio-activity measurement /fig.1/ integrated by:

- universal sounder, sample and protective shields
- radiometric pulse counter,

/b/ radiochemical extract,

/c/ radionuclide sample injector,

/d/ magnetic agitator,

/e/ sterilizer,

- /f/ electric thermostat with temperature and relative humidity control,
- /g/ 15 cc glass measuring cell having diameter of 30 mm with glass separators /fig.2/,
- /h/ measuring needle,
- /i/ 2000 ml Erlenmeyer flask.

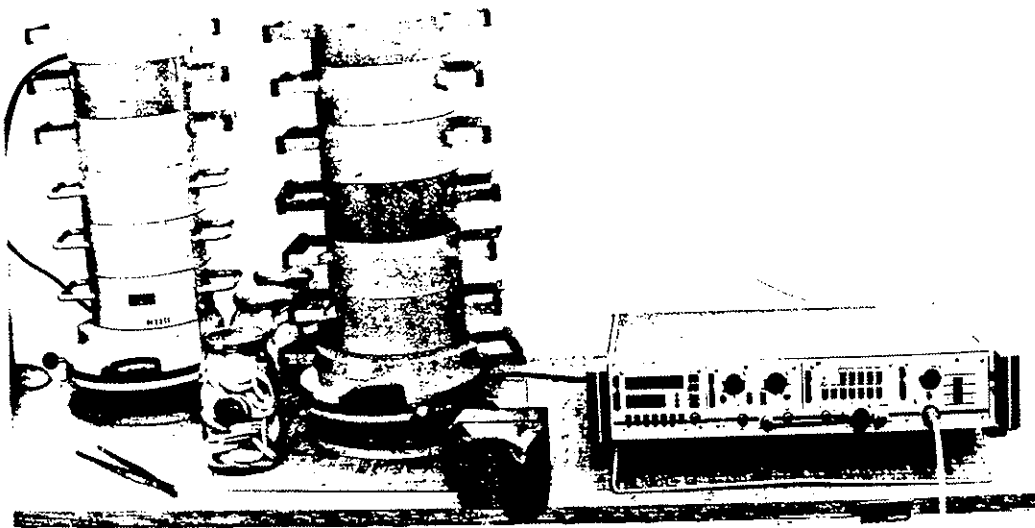


Fig. 1 Apparatus for measuring of samples radioactivity  
/made by "Polon" Warszawa - Poland/

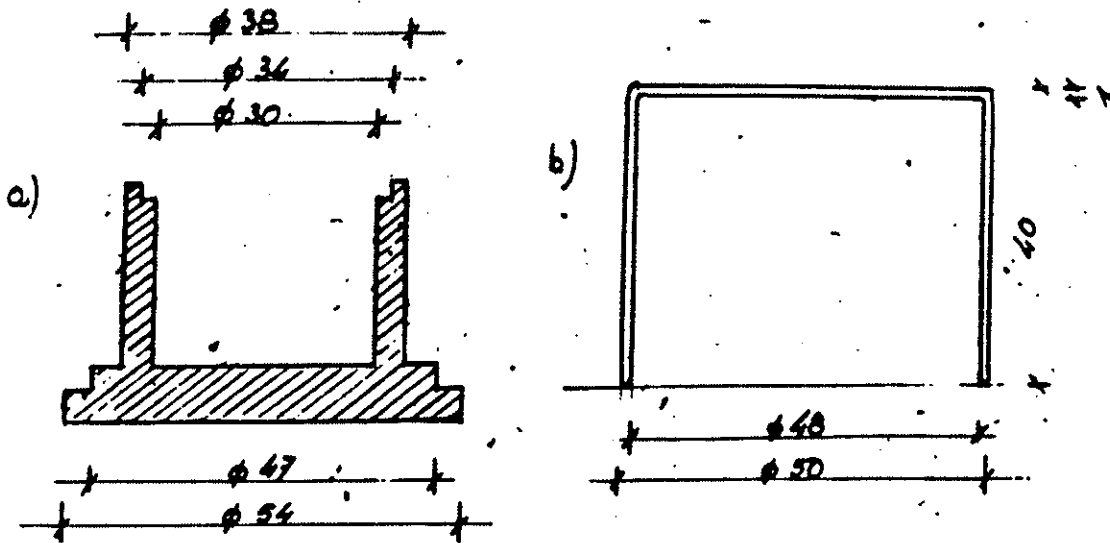


Fig. 2 /a/ Cell for bioisotopic tests and /b/ separator

#### 1.4. Preparation of test samples

1.4.1. Aspect and material of samples. The sample has a form of 30 mm thick disk having a diameter of 40 mm, cut out of a segment of an element from a specified depth. The sample shall have two test faces: a right one - from the surface of the element and the left one - from the interior of the element. Those faces of the samples shall be marked in order to determine their depth in relation with the surface of the element which is zero depth. The edges of the sample shall be flat and smooth.

1.4.2. Number of samples. For one test for one specified depth at least 10 samples shall be taken. One sample shall be used for one test only.

1.4.3. Sampling. The samples shall be taken as follows:

- The segment shall be cut into layers 3.0 mm thick parallel to its surface and disks having 40 mm of diameter cut out from the specified depth,
- rollers having 40 mm of diameter shall be cut out of the segment perpendicular to its surface and then the rollers shall be cut into disks while the kerf shall be of 2 mm. It makes possible to evaluate the effectiveness of protection on the following depths:
  - 0 and 3 mm - the right and the left side of the samples from the first layer,
  - 5 and 8 mm - the right and the left side of the samples from the second layer
  - 10 and 13 mm - the right and the left side of the sample from the third layer, etc.

1.4.4. Conditioning. Before the test the samples shall be conditioned in the air having the relative humidity of 80-85% at  $20 \pm 2^{\circ}\text{C}$  for 7 days.

1.4.5. Preparation of control samples

1.5.1. Aspect and material of control samples. The sample shall have a form of no treated disk 3mm thick having a diameter of 40 mm with a grain paralel to the tested face cutted out of a sapwood of pinewood /*Pinus silvestris* L./, which shall be sound, without defects, taken from the central part of the log, 2m down the tree top, having the density of 0,43-0.53 g/cc, with 5-8 annual rings per cm. The number of control samples shall be more than 10.

1.5.2. Sampling and conditioning - acc. to the clause 1.4.3 and 1.4.4.

1.6. Preparation for tests

1.6.1 Preparation of radioactive substrate

To the sterilized hot substrate prepared acc. to the clause 1.6.1 the radioactive solution of  $\text{Na}_2\text{HPO}_4$  shall be added using the dosimeter in order to obtain radioactive substrate concentration of 0.2  $\mu\text{Cu/ml}$ . Then the substrate containing radionuclide shall be thoroughly stirred with the magnetic agitator using the sterilized mixer and distributed into sterilized measuring cells in which the meniscus shall be 2mm down the upper edge of the cell /each cell having the capacity of approx. 15 ml/. The substrate in the measuring cells shall be covered with sterilized separators and left for setting. All those operation shall be done in an isolated sterilized room.

1.6.2. Preparation of fungus culture

The radioactive substrate congealed in the measuring cells shall be grafted with a measuring needle under sterilized conditions with a pieces of mycelium of 2 sq.mm from the fresh pure /approx. of 3-4 weeks/ culture of the test fungus acc. to the clause 1.2.2 placing them in the centre of the substrate. The pieces of mycelium used for grafting shall be of the same size in order to evitate non uniform growth of the fungus on the substrate surfaces in each cell. The cells covered with the separators containing the substrate with the fungus shall be placed in the thermostat at  $22 \pm 1^{\circ}\text{C}$  and 85-90% of relative humidity for 6 days.

After this time is over the cells shall be taken out and submitted to a selection in order to eliminate the cells contaminated with bacteria or moulds and showing poor growth.

### 1.7. Procedure

1.7.1. Submission of samples to the fungal attack. Each test sample together with the control one shall be placed on the edge of the cell with fully grown mycelium its test surface facing the interior of the cell. The samples placed in such manner shall be covered with separators and placed in the thermostat at  $22 \pm 1^{\circ}\text{C}$  and 85-90% r.h. for 7 days.

1.7.2. Measurement of radioactivity. After the 7 days attack of the test fungus the samples shall be taken from the cells under the radiochemical ventilation hood and the mycelium growing removed with a metal spatula. The samples cleaned off mycelium shall be placed freely on the metal or glass tray with their test face up and conditioned at  $20 \pm 2^{\circ}\text{C}$  and  $65 \pm 2\%$  r.h. for 18-20 hours. After this time is over the surface of all of them shall be cleaned off the remainders of mycelium using a hair brush under the radiochemical ventilation hood. The cleaned samples shall be placed one by one into the sample changer using forceps with their test surfaces facing the sounder and the emitted radioactive pulses registered at least for 1 minute. The registration time shall be equal for the test and control samples.

### 1.8. Determination of protection effectiveness index "Z"

On the basis of number of radioactive pulses emitted by the /at least/ 10 samples the following values shall be calculated:

$N_{mb}$  - medium number of radioactive pulses counted for /at least/ 10 test samples of the same kind /from the same depth/,

$N_{mk}$  - medium number of radioactive pulses counted for /min. 10/ control samples

$$Z = \frac{N_{mb}}{N_{mk}} - \text{value of protection effectiveness factor for the samples from specified depth}$$

## 2. Evaluation of structural timber protection effectiveness

The value of protection effectiveness index for structural timber samples is from 0 to 1 and the higher is that value the protection results worse. To use the index "Z" in practice for evaluation of structural timber protection effectiveness 4 categories of protection have been established as given in the table 1.



Table 1 Protection categories for structural timber

Index "Z"	Protection category
$\leq 0.30$	1 - good
0.31 - 0.50	2 - medium
0.51 - 0.75	3 - insufficient
$> 0.75$	4 - no protection

On the basis of the table 1 the protection quality for structural timber tested layer shall be evaluated comparing the test results with the values given in the table and determining the protection category.

For information: the value  $Z=0.30$  corresponds to the protection quality of the timber treated with the preservative dose expressed as a fungicidal value equal to 100%; for  $Z= 0.50$  the corresponding fungicidal value is of 75% and for  $Z=0.75$  the fungicidal value is of 50%.

### 3. Classification of structural timber considering the risk of fungal attack

The elements of buildings or building structures in dependence of their location or incorporation are exposed to different climate and environment conditions. Considering such conditions and climatic zones the following categories of fungal attack risk have been established:

/a/ 2 zones of environment influence have been introduced:

- zone A - exposure of structural timber in the closed space
- zone B - exposure of structural timber in the open air

The elements of exterior walls of buildings are classified to the zone A.

/b/ In dependence of the intensity of climatic factors favorable for the fungal attack in the specified zones of environment effect 3 degrees of risk of fungal attack for structural for both zones have been introduced as given in the table 2.

Table 2. Exposure conditions and degree of fungal attack risk for structural timber

Degree of fungal attack risk	Conditions of exposure for structural timber in the zone	
	A	B
I minimum	in the air having up to 75% r.h. possibility of condensation water A1	isolated from the direct effect of precipitations; no possibility of condensation water B1
II medium	in the air having above 75% r.h.; possibility of periodic short-term wetting and easy drying; short-term condensation water A2	possibility of periodic wetting with condensation water; direct effect of precipitations B2
III serious	possibility of long-term penetration wetting with lack of drying or difficult drying; penetration of moisture A3	direct contact with ground or water B3

4. Requirements for resistance of structural timber to fungal attack

In order to facilitate to the designer the determination of requirements for structural timber preservative treatment in technical documentation while designing a building and to the contractor of a building or structure, the following have been introduced:

- /a/ classification of structural timber resistance to fungal attack, and
- /b/ requirements for quality of preservative treatment for structural timber.

4.1. Classification of structural timber resistance to fungal attack

In dependence of the degree of fungal attack risk and climatic zone 6 categories of required resistance of structural timber to fungal attack have been established as given in the table 2:

- for zone A: required categories of resistance to fungal attack  
A1, A2, A3
- for zone B: required categories of resistance to fungal attack  
B1, B2, B3

4.2. Requirements for quality of structural timber preservative treatment

In dependence of required category of structural timber resistance to fungal attack the requirements for protection category acc. to the table 1 on specified penetration depth acc. to the table 3.

Table 3, Requirement for quality of structural timber preservative treatment

Required category of resistance to fungal attack	Required depth of penetration and protection category		Required category of resistance to fungal attack	Required depth of penetration and protection category	
	depth of penetration mm	protection category		depth of penetration mm	protection category
A1	0	2	B1	0	1
	3	2		3	2
A2	0	1	B2	0	1
	3	2		3	1
				8	2
A3	0	1	B3	≤ 8	1
	3	1		> 8	2
	5	2			
	8	3			

5. Conclusions

The proposed bioisotopic test method and method of evaluation of preservative treatment quality for structural timber as protection against fungal attack makes possible:

- rapid accomplishment of tests;
- evaluation of preservative treatment effectiveness irrespective of the wood preservative used;
- determination of resistance to fungal attack of different wood species in relation with the specified one/the suggested is *Pinus silvestris*/ or resistance of wood of unknown treatment /whether it was treated or not and what preservative have been used/;

- possibility of application of different test fungi /instead of *Coniophora puteana*/ considering its occurrence in any region or activity in relation with the determined timber species;
- stipulation of requirements for preservative treatment of designed elements in technical designs of timber structures and wooden buildings with marking on the drawings the required categories of resistance to fungal attack establishing in such way the depth of preservative penetration and protection categories;
- application of appropriate technologies and wood preservatives in the manufacturing process in order to achieve a good quality preservative treatment for specified building members,
- quality control of preservative treatment and possibility of arbitrary decisions in case of divergences.

The requirements for protection quality of structural timber shall be stipulated by the designer or contractor of the building.

The examples of requirements according to our opinion:

- category A1 of required resistance to fungal attack:- elements of internal floors over dry rooms; elements of exterior walls not adjacent to the wet rooms /kitchens, bathrooms/ etc.
- category A2 of required resistance to fungal attack: floors of attics and internal floors above the wet rooms; exterior walls above the ground floor, interior walls adjacent to the wet rooms; rafter framing, etc.
- category A3 of required resistance to fungal attack: elements of ground beams; parts of exterior walls of the ground floor; parts of basement floors, etc.
- category B1 of required resistance to fungal attack: - elements of certain forms of balconies and loggias /protected against direct rainfall/;
- category B2 of required resistance to fungal attack - elements like those mentioned in B1 but exposed to the rainfall whose structure facilitates formation of condensation water, balusters, etc.
- category B3 of required resistance to fungal attack - balusters in direct contact with the ground, etc.

## Literature

1. F.F. Mazur - Wliwanié rozlicznych faktorow na riezultaty bioispytanji antisepticzeskoj driewiesiny. /Influence of different factors on results of bioisotopic testing of preserveted wood/. Trudy Instytutu Lesa XXIII Ryga 1961
2. F.F. Mazur - Biologiczeskije ispytanija antisiepkrowanoj driewiesiny s primienieniem radioaktywnych izotopow. /Preservated wood biological testing with application of radioactive isotopes/. Moskwa 1959
3. J. Michalak, J. Wojczyński - Metoda bioizotopowa okrešlania granicznej wartości grzybobójczej impregnatów. /Bioisotopic method for testing of fungicidal value of preservatives/. PCO COBR PSB rok I Zeszyt 1. Wołomin 1974
4. W. Nożyński, M. Ryłko - Poprawa jakości ochrony drewna budowlanego przed zagrzybieniem. Część I. Opracowanie wymagań w zakresie impregnacji drewnianych elementów i konstrukcji budowlanych przed zagrzybieniem. /Improvement of quality of Timber. Part.1. Requirements for resistance protection of elements of buildings and building structures against fungal attack/. Praca ITB nr 2840/ND-40. Maszynopis 1990.
5. W. Nożyński, M. Ryłko, K. Jaworska - Ochrona drewna budowlanego przed zagrzybieniem. Wymagania i badania. /Protection of timber against fungal attack. Requirements and testing/. Przegląd budowlany 3/91
6. W. Nożyński, M. Ryłko, K. Jaworska - Skuteczność ochrony drewna budowlanego przed zagrzybieniem. /Timber protection effectiveness against fungal attack/. Biuletyn COIB 3/91



**INTERNATIONAL COUNCIL FOR BUILDING RESEARCH STUDIES AND DOCUMENTATION**  
**WORKING COMMISSION W18 - TIMBER STRUCTURES**

**DERIVATION OF THE CHARACTERISTIC BENDING STRENGTH OF SOLID TIMBER**  
**ACCORDING TO CEN-DOCUMENT pr EN384**

by

A J M Leijten  
Delft University of Technology  
The Netherlands

**MEETING TWENTY - FOUR**

**OXFORD**

**UNITED KINGDOM**

**SEPTEMBER 1991**





## **Summary**

In the near future european standards about the derivation of characteristic strength and stiffness values for structural timber will overrule the national standards of the EC-countries. An important standard is prEN384 about the derivation of the characteristic bending strength and stiffness which incorporate elements of recent research. The current characteristic bending strength is based in many cases on former structural size tests performed sometimes decades ago. Will the new EN-standard make all previous research invalid because of the prescribed test conditions ? The effect of the proposed modification factors of prEN384 is shown. On the bases of prEN384, Dutch research is re-analysed and the effect of the modification factors monitored. It can be concluded that for the old test data considered, the prEN384 as well as the old derivation method give approximatly the same characteristic bending strength.

## **Introduction**

Parcels of structural timber have attached a set of characteristic properties belonging to a specified grade. This paper focus the attention on the characteristic bending strength derivation method used traditionally and the one being proposed in a CEN-standard-prEN384. The proposal and background for this CEN-standard has been presented in paper 21-6-2 by Fewell and Glos (1988). Some implication have been mentioned in paper 22-6-2 by Barrett and Lau as well as in paper 22-6-3 by Green and Kretchmann Both methods were applied on test data available in the Netherlands to notice any deviations.

## **Strength determination**

At present there is no agreement on a european visual grading standard with specified requirements. So it appears that for the "ease" of the design engineer all national grades will be maintained in the EC- countries. As borders between the EC-countries disappear unfamiliar grades and species can be introduced. There could sometimes be serious doubt about the stated characteristic bending strength or strength class of a particular grade whether this is due to mistrust or real doubt. Attestation of conformity test according to final version of prEN384 will have to reveal the "real" properties in these cases. The present prEN384 offers three different methods to find the characteristic bending strength value.

## **Three characteristic bending strength values**

The three determination methods in prEN384 will of course lead to three different values given one population. The authors have included these methods to use as much existing data as possible. The three methods are:

- a) - straight forward structural size destructive bending tests
- b) - data from small clear specimens
- c) - data from other grades and species

The question is whether method b) and c) give the same reliable result.

For both no prescribed sampling technique is given in the prEN. To prevent unfair competition one method should be the standard method.

Method a)

Undoubtedly this method will be used for the determination of strength and stiffness properties. Let us assume that this determination method gives you an answer closest to reality.

Verification of stated characteristic bending strength

For attestation of conformity purposes, to check a stated characteristic value, also this EN-standard will be used in the near future by all EC-countries. The same modification factors are used as method a).

Method b)

The second method is the one which make use of an relation between the mean bending strength of small clear specimens and the characteristic bending strength of structural size specimens. This relation should be established for at least three species (not a mixture of softwoods and hardwoods). The procedure for a different grade of another species will than be, that one performs small clear specimen tests and determines the mean value and use the above established relations for the determination of the characteristic bending strength. As this method is probably the cheapest it will gain popularity at first ? When however the results are not always so reliable, as attestation of conformity tests will indicate, this method should perhaps beter be moved to an annex of the EN-standard. Moreover this method uses relations between properties from small clear tests where no rules have been given about the sample size, test method, etc. The authors have tried not encouraged this approach by introducing a reduction coefficient of 0.9 for the characteristic bending strength found in this way.

Method c)

Furthermore the third method of prEN384 is the method called "mechanical properties for other grades". The grade under consideration is not tested at all. One takes the structural size test data of two or more other grades of that species and also the structural size data of at least three other species (nothing is mentioned about the grade). The mean of the ratios of the characteristic bending strength may be used as a factor which can be applied to another species where only one of the grade values is known. As there is no european grading rule grades will differ considerable. Does this method provides reliable values with regard to method a). Again attestation of conformity test(method a) will reveal the mistake made.

**Other implications, validity of old test data.**

The strength of a particular grade is fixed on the bases of former research sometimes decades ago and with other data analyses methods than currently used. When the CEN-standard is completed and accepeted unchanged some questions may arize which are:

- a) - Are all former test data still valid ?
- b) - Does the new characteristic bending strength derivation method lead to different values when old data is re-analysed - application of a depth factor ?

ad a)

As mentioned previously many present grades have fixed characteristic bending strength values based on former tests (method a). When the test data are re-analysed on the bases of prEN384, considerable deviations could perhaps appear. This procedure

can only be justified when all conditions now set out by the prEN are satisfied. There are two test conditions which in former days were not always so restrictive. The first one is the moisture content and secondly the location of the strength determining section. As for the bending strength no modification for moisture content is made this item is to overcome. This second one invalidates much research. Does all the research has to be done again where this condition is not satisfied ? Leicester shows in paper 24-17-2 the implication of this requirement for Radiata Pine. An EC-sponsored research project, carried out by France and Ireland which tried to find the differences between the national grades of 8 EC-countries for one given population of Spruce, has shown that this restriction leads to smaller differences than expected.

When in the final version of the draft prEN this condition is maintained one should clearly define what is to be regarded as a strength determining defect. Specially when we have high grade material with small knots or hardwoods without knots. When is the slope of grain a strength determining defect ?

ad b)

The writers of prEN384 have provided background information for there choise of modification factors. However amoung european experts the depth effect is still a major discussion item specially whether or not the results presented in paper 23-10-3 of Barrett and Fewell are valid for european spruce. Some are in favour for a exponential factor of 0 while Barrett and Fewell support a value of 0.4. For this reason an attempt was made to re-analyse Dutch test data from former research.

**The prEN384 procedure .**

From a given population samples are selected. A sample contains timber of one size. In short the procedure is: test the beams of a number of samples of different cross-section size, calculate the lower fifth percentile for each sample, adjust to a reference size, span to height ratios and then take the weighted mean of the fifth percentiles as the characteristic value. All timber should be conditioned to the standard climate of 20°C and 65 r.h. which results in a moisture content of about 12%.

The modification factors for bending strength are :

	factor	paper 21-6-2	prEN384
for sample size	$k_s$	figure 1	figure 1
moisture content $10\% \leq \omega \leq 18\%$	-	no adjustment	no adjustment
depth	$k_h$	$(200/h)^{0.3}$ $60 < h < 400$	$(200/h)^{0.2}$ $38 < h < 250$ *
test depth/length ratios	$k_t$	$\left( \frac{L_{et} + 3.5 a}{L_{es} + 3.5 a} \right)^{0.3}$ $L_{es}$ standard span $L_{et}$ actual span $a$ = distance inner load points	$\left( \frac{L_{et} + 3.5 a}{L_{es} + 3.5 a} \right)^{0.3}$
garding method	$k_v$	1.0 visual 1.2 machine grade	1.0 visual 1.2 machine
for verification purposes	$k_q$	figure 2	figure 2

\* : these limitations have been agreed at the last meeting of the CEN/TC124/WG2 with  $k_h \leq 1.25$

The characteristic bending strength is calculated following:

$$f_{m;o;k} = \frac{\sum_{j=1}^m ( f_{m;j;k} k_h k_t n_j ) k_s k_v}{\sum_{j=1}^m n_j}$$

were:

$f_{m;j;k}$  characteristic bending strength of sample  $j$

$m$  number of samples

$n_j$  number of specimens in sample  $j$

### **Analysis of old Dutch test data**

In the Netherlands, grading rules have emerged from a big research program in the fifties performed by TNO. This research was focused on european Spruce (*Picea Abies*). The grading rules make no distinction between Spruce from the North- or Middle of Europe. The tests comprised a total amount of 1143 beams (four sizes) and within one size descended from 10 to at least 3 different sawmills. After a first rough selection 2 grades were indentified on the bases of visual defects. This made the population fall apart into two major sub-populations. Because in later years each grade was divided again into 2; there now exists 4 grades A,B,C and D. For construction purposes however grades A and B are taken together. Further on we only speak about grade B (actually A and B) and C as the two grades under consideration. The working stresses were found by taking the lower 1.5 % value as reduction for duration of load was still a dark area.

The test data comprises 4 cross-sectional sizes ranging from 51x152mm (2"x6") to 76x229mm (3"x9"). Table 1 show the sizes and the number of the specimens involved. These were choisen because they are the most in practice used sizes.

### **Values of the modification factors and validity of conditions**

#### *Sample size:*

As shown in Table 1 the samples size is large enough to justify a  $k_s$ -factor of 1.0 for grade C and  $k_s = 0.95$  for Grade B. Regarding the amount of tests for the other samples in Grade B this factor is penalizing (to much).

#### *Moisture content and location of weakest section:*

- the beams were not conditioned: moisture content ranging from 10 to 28%
- there is no clear statment that the weakest section was located between the inner loading points.

When we disregard the problem of the climatic conditioning because no adjustment factors are given we may proceed. The high grade material is penalized by this rule as indicated by paper 22-62 and 22-6-3. The question of the weakest section can only be solved after thorough investigation of all test reports. For the time being we disregard this matter also knowing that it could have a major influence, see paper 24-17-2.

#### *Depth effect:*

In the old investigation no depth effect was considered. As this item is of interest especially the value of the exponential factor, some efforts have been made to show the influence of an exponential factor of 0.2, 0.4 and also 0.6.

#### *Depth/span ratios*

Four point bending test were performed with mostly a span to depth ratios of 16 only for the 51x152mm sample this was 12. The modification factor  $k_t$  is almost equal to 1 as indicated in Table 2.

#### *Grading method:*

The grading was performed visually so  $k_v = 1.0$

#### **Reference depth**

There are some tendencies in WG2 of CEN/TC124 to decrease the reference depth of 200 mm to 150 mm but is this wise. When strength is referred to a depth of 200 mm, Eurocode5 may use the inverse factor in the design equation for strength. Of course the design engineer will find this depth factor troublesome as it has minor effects for many practical applications of solid timber. When we assume the reference depth of 200 mm is maintained in the final version of prEN384 and the inverse in the Eurocode5, he may neglect this depth factor for sizes smaller than about 200 mm; he will be on the safe side. Is the design engineer in desperate need for all strength capacity he should be allowed to use this depth factor. To change the reference depth to 150 mm has the reversal effect.

Regarding the range of sizes where the depth factor should be applied, it is strange that despite of previous papers by Fewell, Gloss and Barrett this range has been extended from  $60 < h < 400$  mm to  $38 < h < 250$  mm. This is combined with a restricted maximum value of 1.25 for  $k_h$  (which is found for  $h = 65$  mm). This means strictly speaking that also the strength of thick laminations is governed by this depth effect. What about the other thinner laminations?

#### **Results**

Comparing the characteristic bending strength of each grade and each size derived with the old lower 5% value approach (standard normal) and the non-parametric method of prEN384 leads to the conclusion that there is no difference, see Table 2. In Table 3 the final characteristic bending strength of the whole population is calculated with Table 2 data which is modified with appropriate modification factors. For the depth factor the exponential value have been varied from 0.2 to 0.6 to show its effect. It appears that the final characteristic bending strength is relatively insensitive for any depth factor in this case. Is this a reason to neglect the depth factor? When the graphs (at the end) are taken into consideration it will be clear that it has a influence in reducing the scatter at the 5% level. The separate samples come near each other as the exponential factor grows. In some cases data of samples coincide almost completely. Probably the weighted mean is not affected due to the choice of sizes, above and below the reference depth, see last column Table 3. When a choice has to be made between an exponential factor of 0.4 or 0.2 the graphs tend to be in favour of 0.4. When only sizes are tested with depth smaller than the reference depth the application of a depth factor should be encouraged. To show that the modification factors for moisture content has a minor effect, some results of the earlier mentioned EC-project are added in Table 2; indicated with subscript characters.

#### **Conclusion**

The conditions set out in prEN384 can invalidate former research and should be given good thought. The determination method for the characteristic bending strength should be limited to method a) (destructive tests on structural sizes). On the bases of the research presented for the species Spruce (*Picea Abies*) there is a preference to apply exponential value of 0.4 in the depth factor.

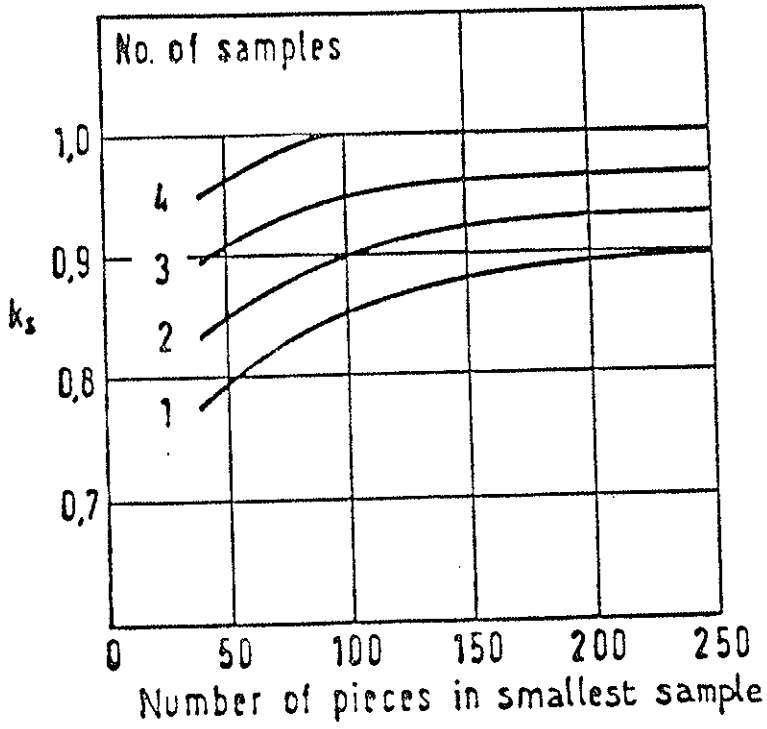


Figure 1: adjustment factor  $k_s$  for sample size.

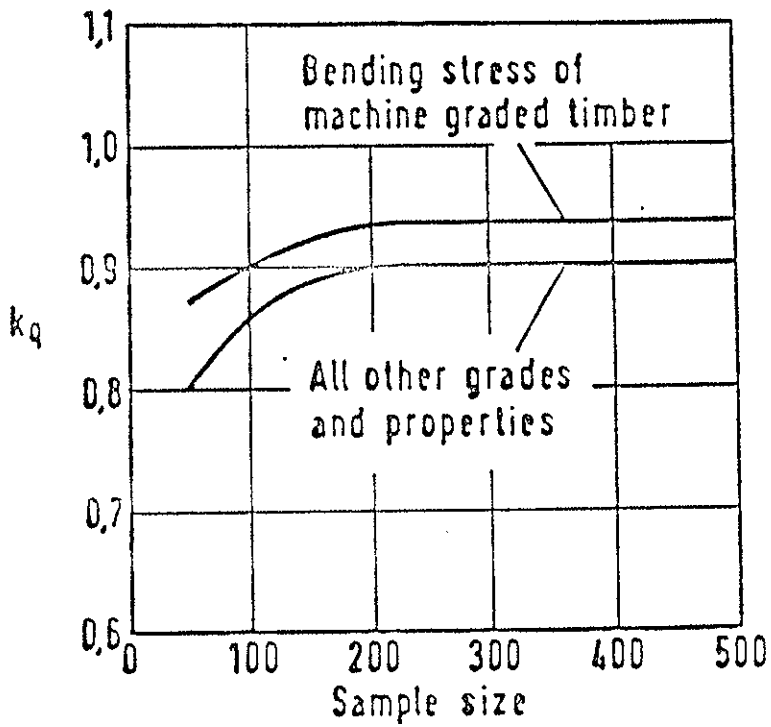


Figure 2: modification factor in cases of verification procedures (attestation of conformity)

Table 1 : Sizes and number of specimens involved for each grade.

sizes [mm] (inch)		number of specimens (beams)	
		grade B	Grade C
51x152	(2x6)	183	263
64x165	(2.5x6.5)	93	119
76x203	(3x8)	154	106
76x229	(3x9)	42	183
total		472	671

Table 2: Characteristic bending strength of samples; no modification factor applied

Grade B sizes [mm]	n	character. strength		k <sub>h</sub> with expon.			span/height ratio			
		non-para	st.n.5%	0.2	0.4	0.6	* L <sub>et</sub>	* L <sub>es</sub>	a	k <sub>t</sub>
38x105**	79	35.4	34.7							
51x152	183	32.9	32.6	0.95	0.89	0.85	12h	18h	5.3h	0.94
64x165	93	20.4	20.9	0.96	0.93	0.89	16h	18h	5.3h	0.98
44x175**	88	29.7	29.1							
76x203	154	25.8	25.6	1.00	1.01	1.01	16h	18h	5.3h	0.98
76x229	42	21.4	21.4	1.03	1.06	1.09	16h	18h	5.3h	0.98
<b>Grade C</b>										
38x105**	80	24.9	25.8							
51x152	263	22.7	22.6	0.95	0.89	0.85	12h	18h	5.3h	0.94
64x165	119	19.6	19.5	0.96	0.93	0.89	16h	18h	5.3h	0.98
38x175**	106	17.6	18.5							
76x203	106	16.9	16.7	1.00	1.01	1.01	16h	18h	5.3h	0.98
76x229	183	13.9	13.7	1.03	1.06	1.09	16h	18h	5.3h	0.98

\*in mm \*\* values taken from Irisch and France EC-Project, disregarded in Table 3

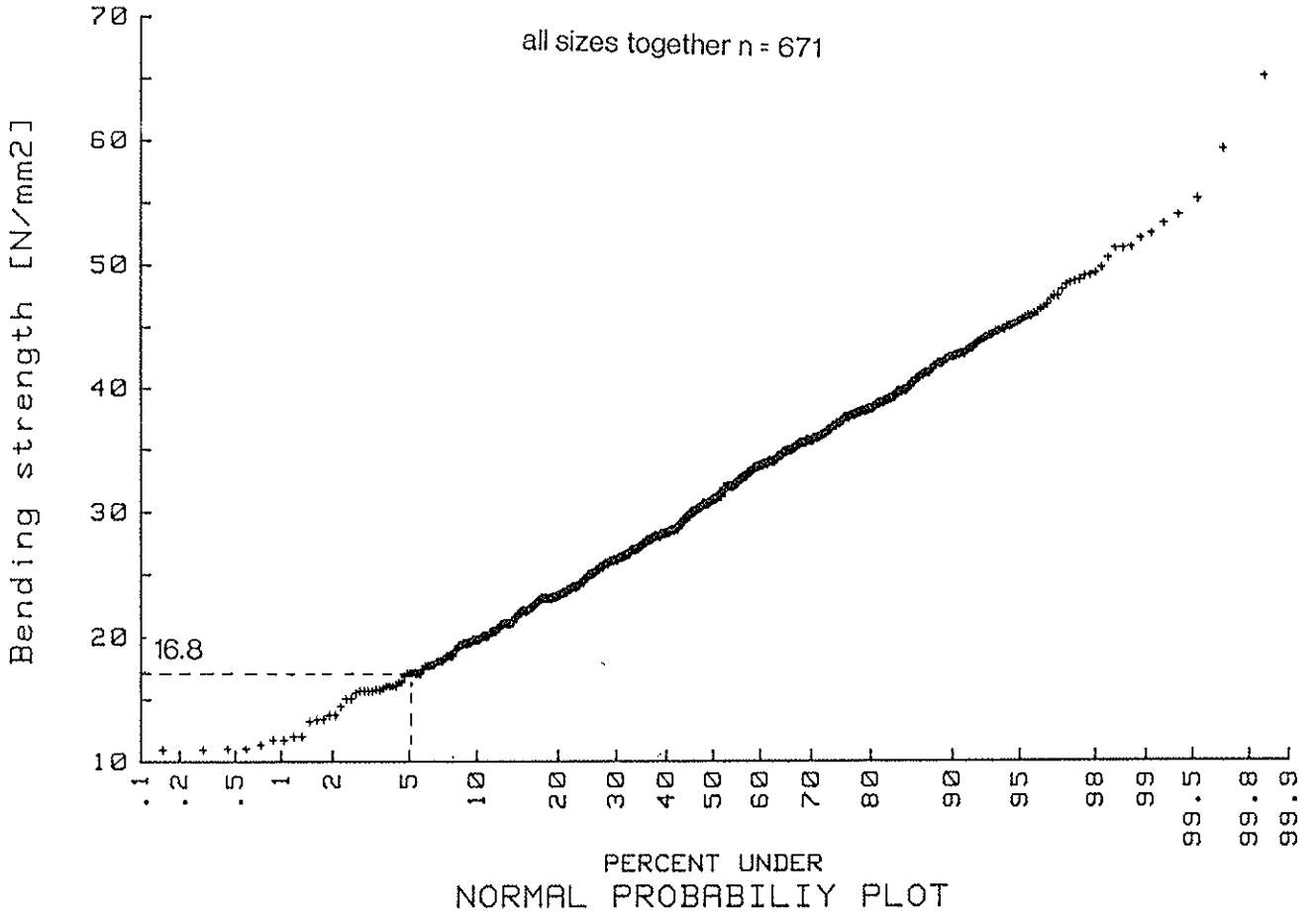
Table 3: Review of characteristic values

			$f_{m;o;k} = \frac{\sum_{j=1}^m (f_{m;j;k} k_h k_t n_j) k_s k_v}{\sum_{j=1}^m n_j}$
Grade B	depth factor k <sub>h</sub> exponent	k <sub>s</sub>	characteristic strength [N/mm <sup>2</sup> ]
traditional* prEN384	0	1.0	<b>25.8</b>
	0.2	0.95	<b>25.5</b> × 0.95 = 24.2
	0.4	0.95	<b>24.7</b> × 0.95 = 23.5
	0.6	0.95	<b>24.1</b> × 0.95 = 22.9
Grade C traditional* prEN384	0	1.0	<b>16.8</b>
	0.2	1.0	<b>17.7</b>
	0.4	1.0	<b>17.2</b>
	0.6	1.0	<b>16.9</b>

\*: lower 5% of total population st.normal distribution

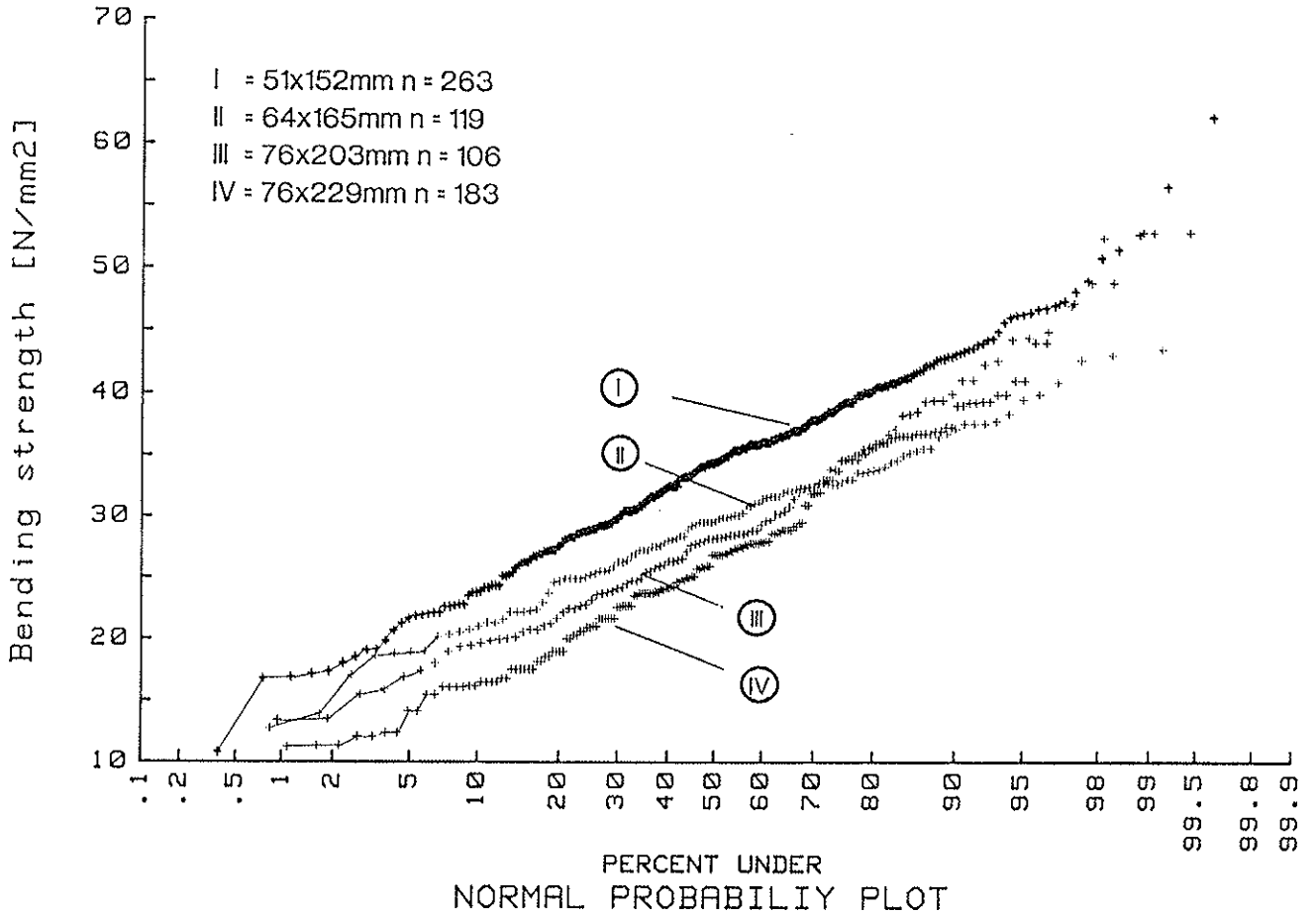
Grade C: mod.for depth exp.= 0

all sizes together n = 671



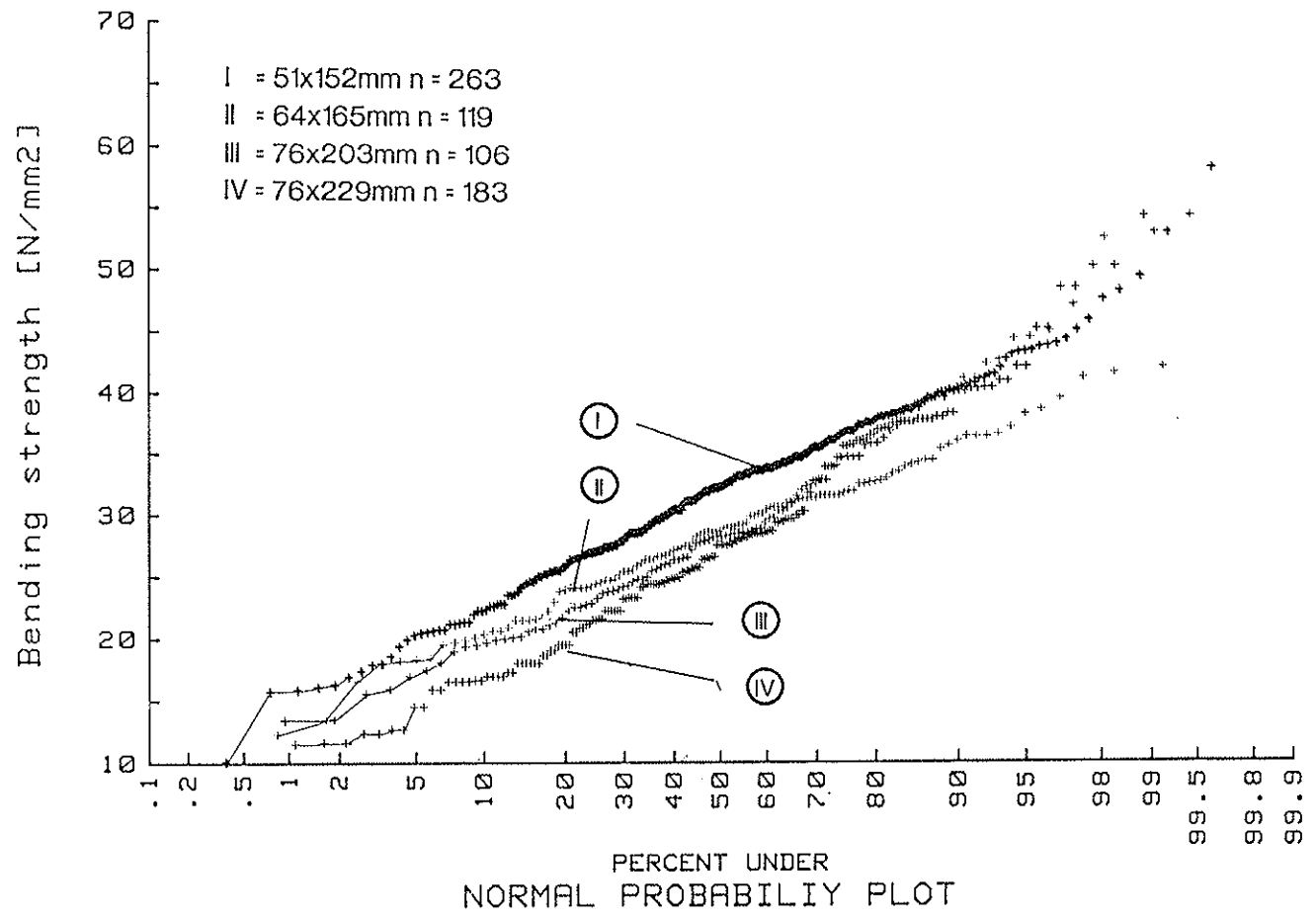
Grade C: mod.for depth exp.= 0.2

- I = 51x152mm n = 263
- II = 64x165mm n = 119
- III = 76x203mm n = 106
- IV = 76x229mm n = 183

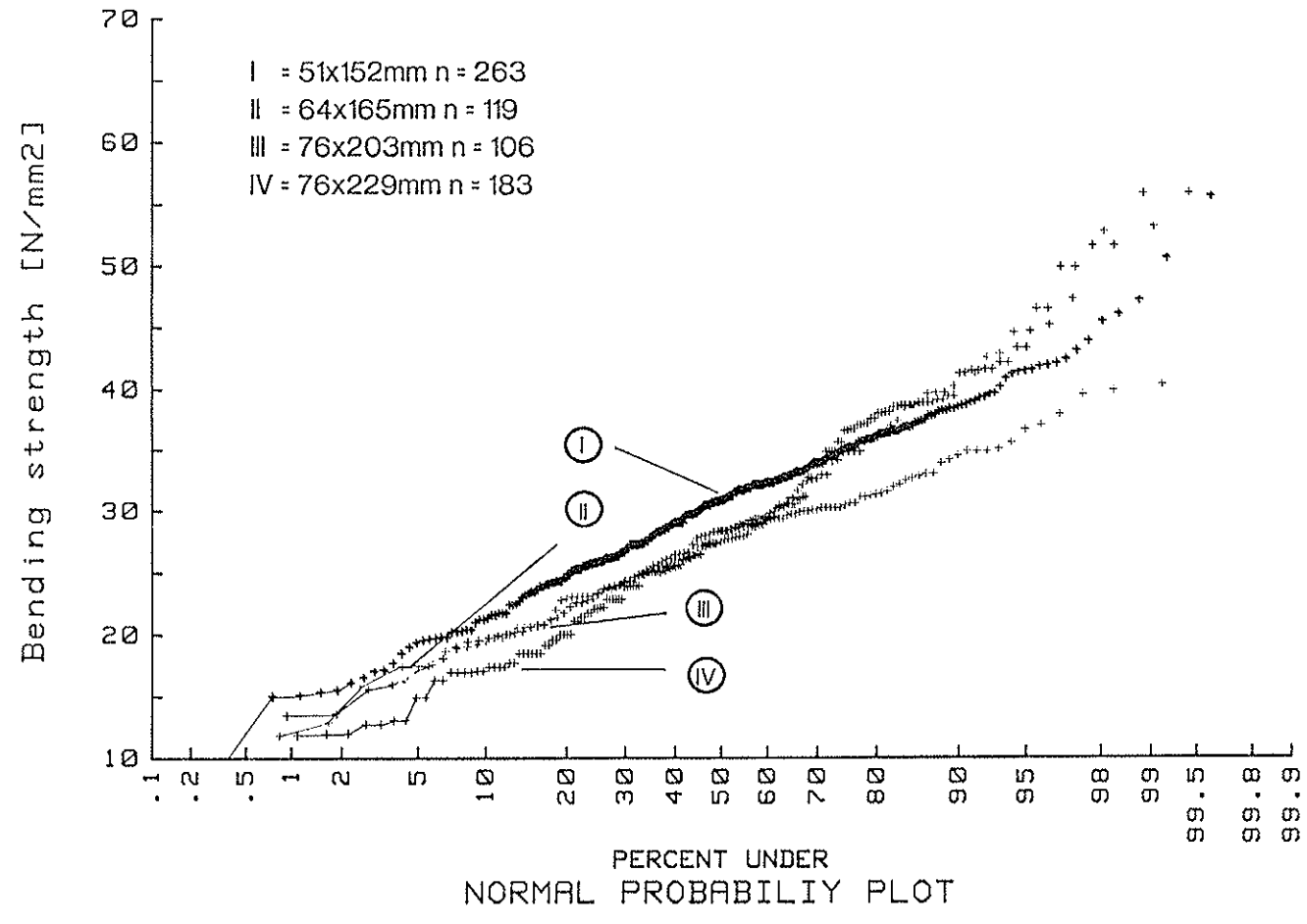




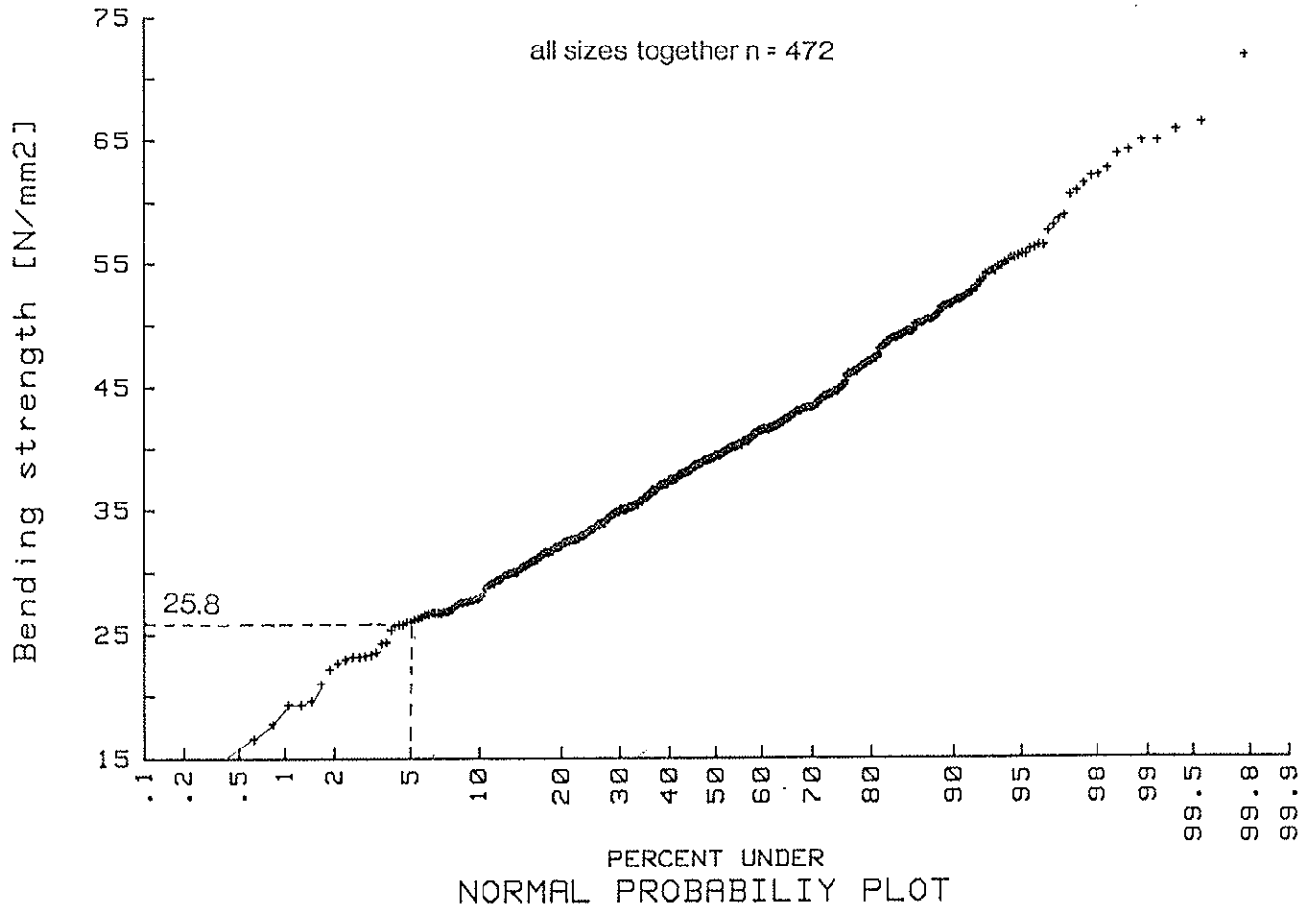
Grade C: mod.for depth exp. = 0.4



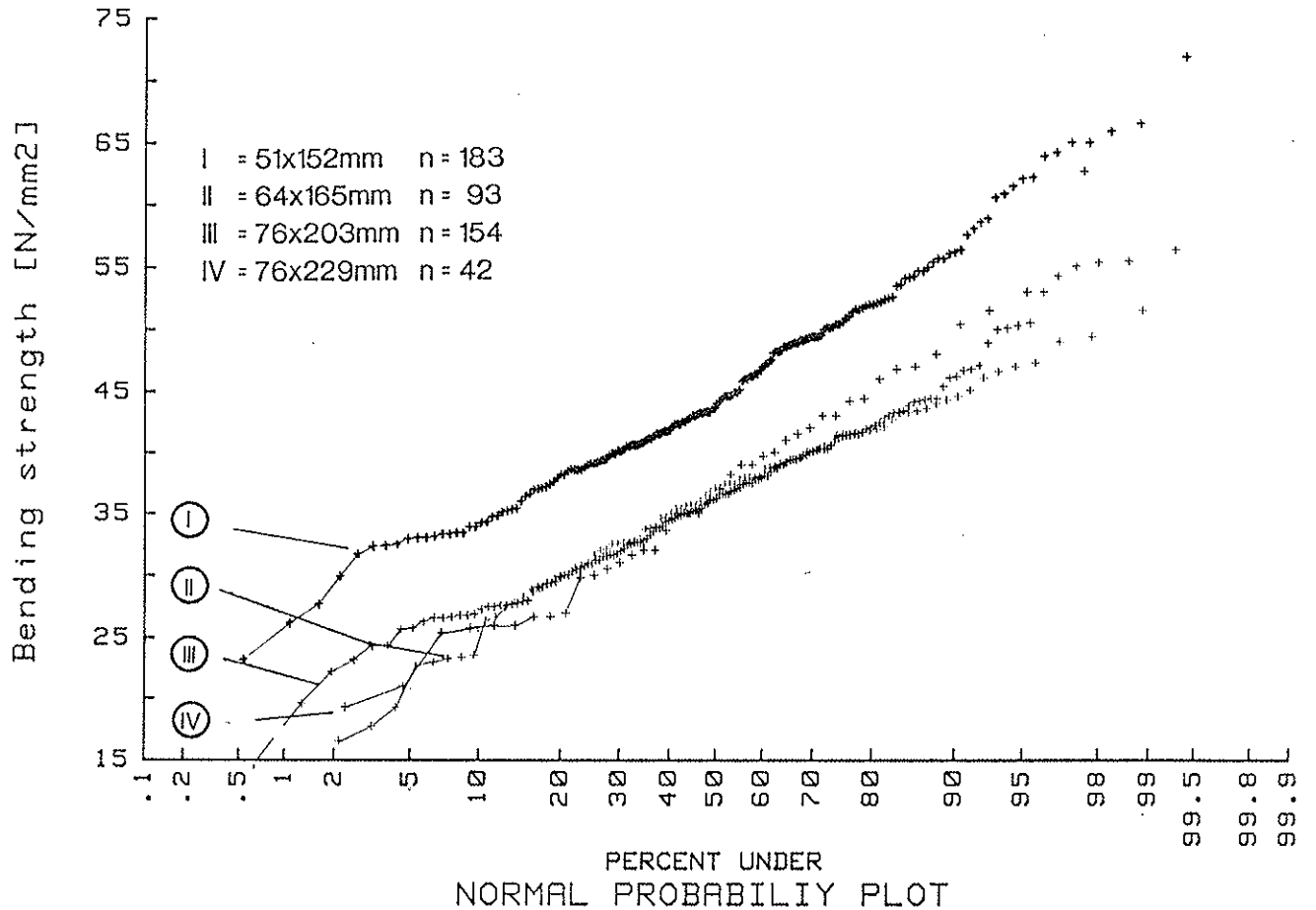
Grade C: mod.for depth exp. = 0.6



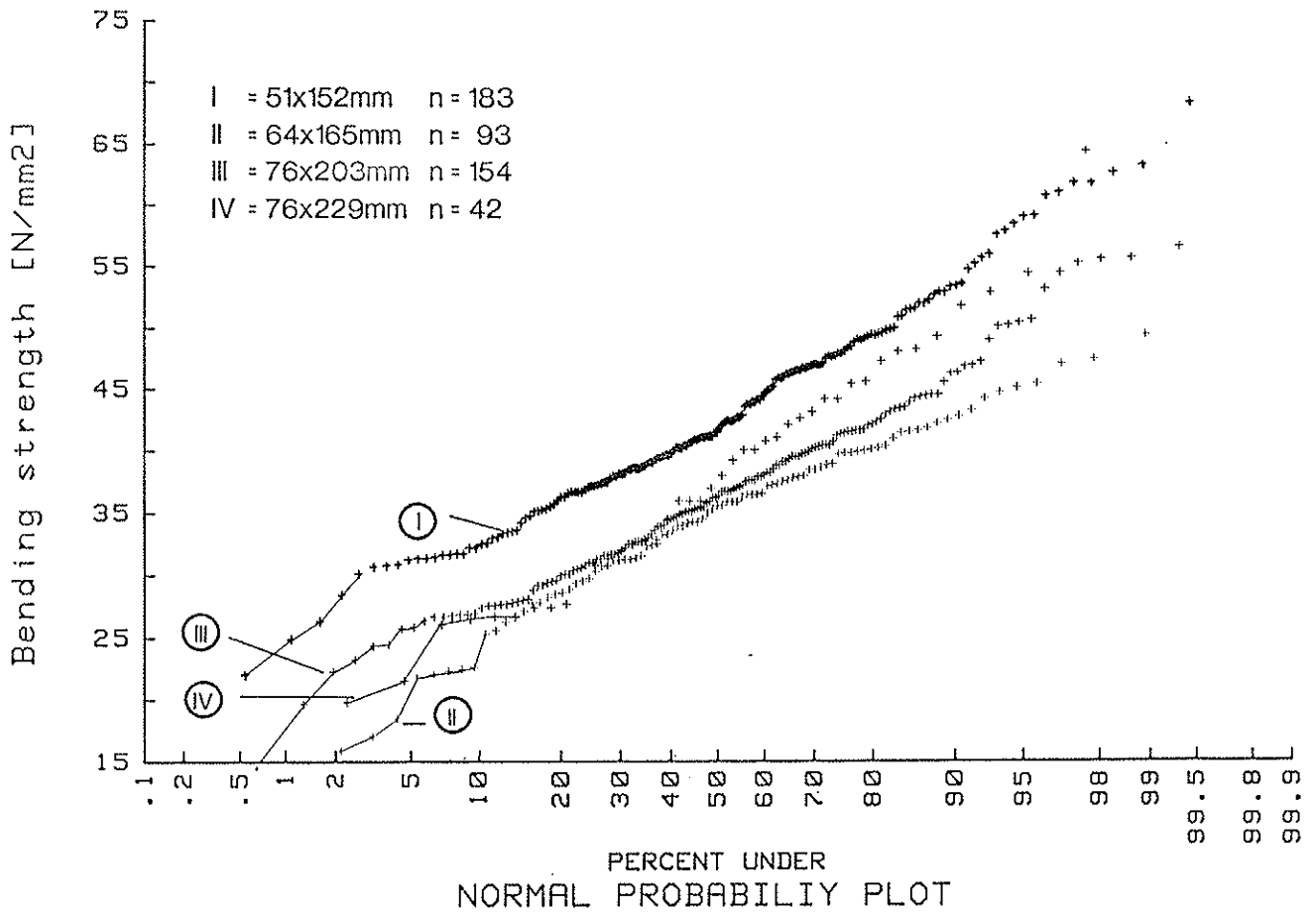
Grade B: (depth effect exp. = 0)



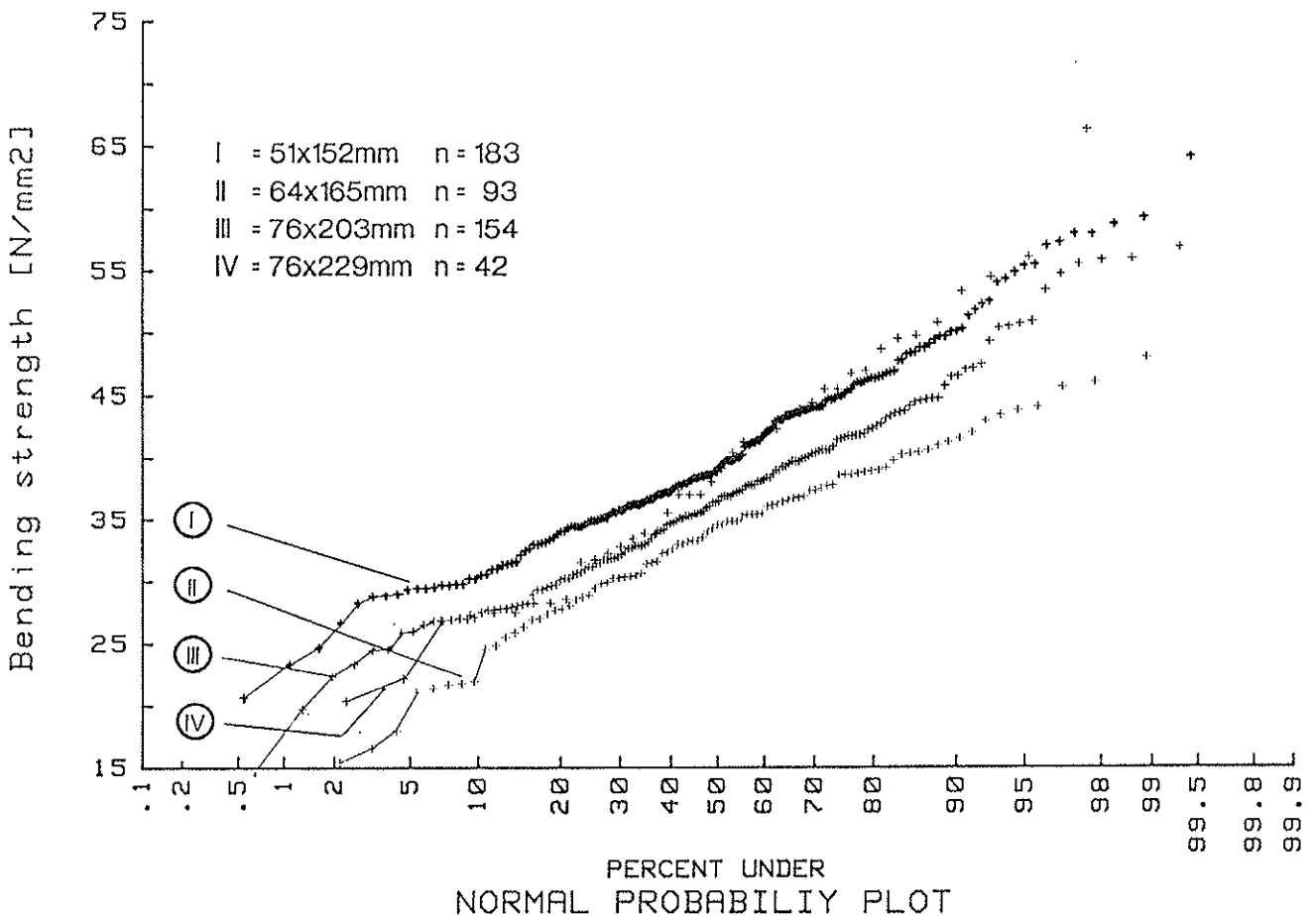
Grade B: (depth effect exp. = 0)



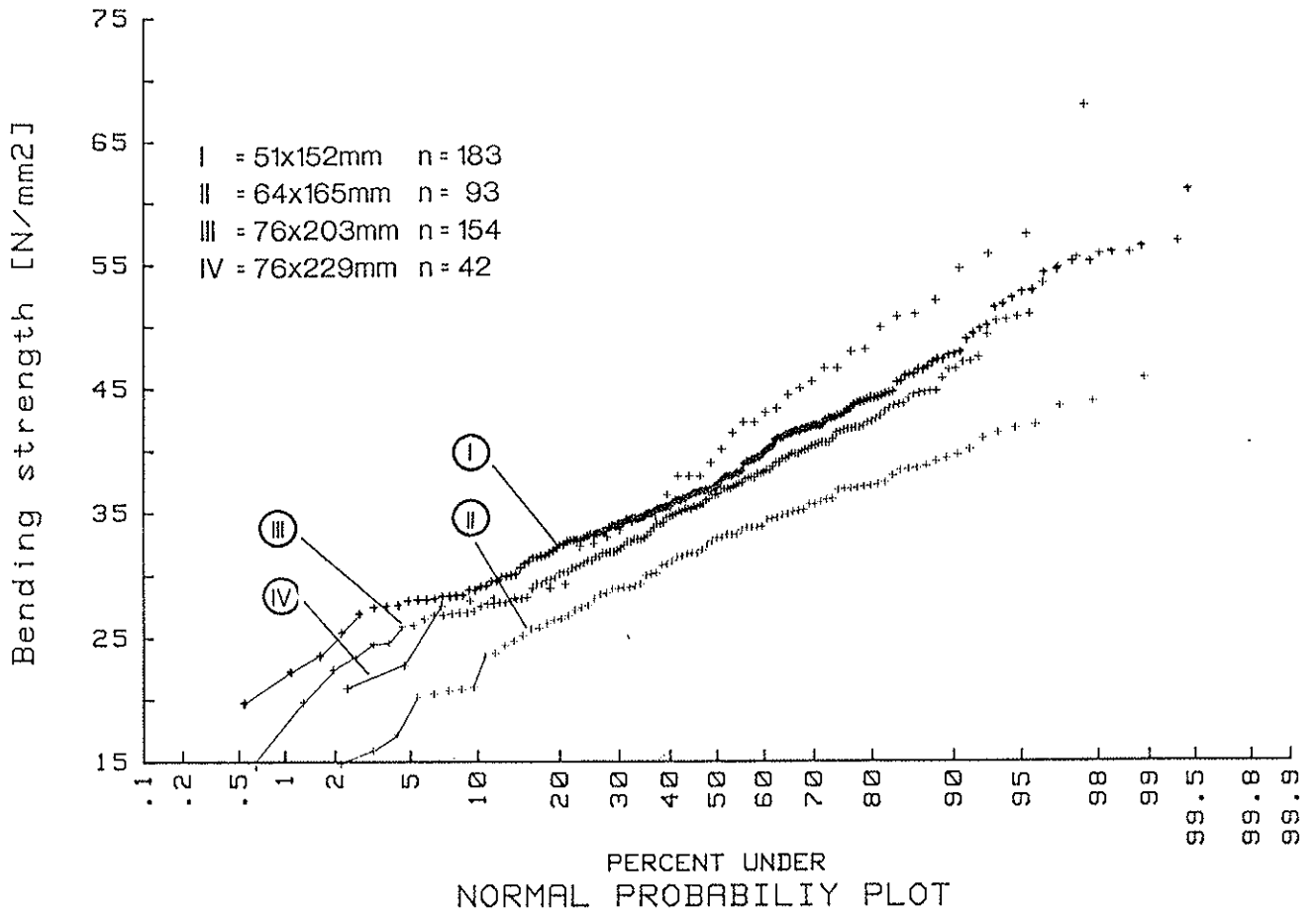
Grade B: mod. for depth exp. = 0.2



Grade B: mod. for depth exp. = 0.4



Grade B: mod. for depth exp. = 0.6



INTERNATIONAL COUNCIL FOR BUILDING RESEARCH STUDIES AND DOCUMENTATION

WORKING COMMISSION W18 - TIMBER STRUCTURES

THEORETICAL AND EXPERIMENTAL TENSION AND  
SHEAR CAPACITY OF NAIL PLATE CONNECTIONS

by

B Källsner

Swedish Institute for Wood Technology Research

Sweden

J Kangas

Technical Research Centre of Finland (VTT)

Laboratory of Structural Engineering

Finland

MEETING TWENTY - FOUR

OXFORD

UNITED KINGDOM

SEPTEMBER 1991



## BACKGROUND

The strength of nail plates with respect to the plate material has been studied at the Norwegian Institute of Wood Technology. This work served as a basis for a Nordic proposal for a design method and was presented by Norén 1981 in reference /1/.

In 1985 Bovim and Aasheim presented a paper /2/ where they made comparisons between measured and calculated values of plate strength. For all the tests a Gang Nail 18 plate was used. Their conclusion was that the design method presented gave a good prediction of the plate strength of nail plates.

During 1980-81 the Technical Research Centre of Finland (VTT) made an extensive investigation of one type of nail plate to achieve an approval using different shapes and sizes of the nail plate. The tests were carried out mainly by following the testing rules M.O.A.T. No 16:1979 of UEAtc. On the basis of the experience from these tests and the recommendations from RILEM/CIB 3TT published in 1982 and ISO 6891-1983 (E) a draft to a detailed testing method for nail plate joints was worked out in Finland. The method was presented 1985 in a paper /3/ by Kangas. In connection with this work a method to calculate design values /4/ was also presented. 15 complete series of different nail plates have so far been tested in Finland using this detailed testing method.

In 1990 Aasheim and Solli presented a translated version of the Norwegian design rules for nail plates /5/. It is expected that these rules will be included in the truss annexes in Eurocode no.5.

## PURPOSE AND SCOPE

At the Swedish Institute for Wood Technology Research the design method given in /1/ has been used for several years in connection with the evaluation of results from testing of nail plate connections. Since it is possible to derive rather simple expressions for the tension and the shear capacity one purpose with this paper is to present these expressions and to explain where they are valid.

It has often been questioned if the proposed design method can be used for any nail plate. In order to elucidate this, the results from testing of 6 different nail plates are compared with the theory. All the tests have been carried out at the Technical Research Centre of Finland.

## THEORY

Consider the nail plate connection given in Figure 1 where the nail plate is subjected to a force  $F_p$ . The axes a and b denote the main directions of the plate. Normally the a-axis is chosen as the direction where the plate has its maximum tensile strength. The b-axis is perpendicular to the a-axis. The a-axis is positive pointing outwards from the cut line. The x-axis is parallel to the cut line.

The angle between the x-axis and the a-axis is denoted by  $\alpha_{xa}$  and is in the range  $0 \leq \alpha_{xa} \leq \pi$ . The angle between the a-axis and the length direction of the plate force  $F_p$  is denoted by  $\alpha_{aF}$  and is in the range  $0 \leq \alpha_{aF} \leq 2\pi$ .

By denoting the length of the cut line in the nail plate by  $f$ , expressions for the widths  $a_n$  and  $b_n$  can be obtained to

$$a_n = \begin{cases} f \cos \alpha_{xa} & \text{for } 0 \leq \alpha_{xa} \leq \pi/2 \\ f \cos (\pi - \alpha_{xa}) & \text{for } \pi/2 \leq \alpha_{xa} \leq \pi \end{cases} \quad (1)$$

$$b_n = \begin{cases} f \sin \alpha_{xa} & \text{for } 0 \leq \alpha_{xa} \leq \pi/2 \\ f \sin (\pi - \alpha_{xa}) & \text{for } \pi/2 \leq \alpha_{xa} \leq \pi \end{cases} \quad (2)$$

The plate force  $F_p$  can be divided into the components  $F_a$  and  $F_b$  along the a- and the b-axes giving

$$F_a = F_p \cos \alpha_{aF} \quad (3)$$

$$F_b = F_p \sin \alpha_{aF} \quad (4)$$

In the design method it is assumed that the strength of the nail plate is based on capacity values obtained from 6 different tests. In Figure 2 the different test specimens for determination of the capacity values are shown. All tests should be carried out without contact between the timber members. The following capacity values of the nail plate have to be determined

$p_{at}$  = tension capacity per unit width in the a-direction

$p_{ac}$  = compression capacity per unit width in the a-direction

$s_a$  = shear capacity per unit width in the a-direction

$p_{bt}$  = tension capacity per unit width in the b-direction

$p_{bc}$  = compression capacity per unit width in the b-direction

$s_b$  = shear capacity per unit width in the b-direction

The strength of the nail plate should be verified by the condition

$$\left( \frac{F_a}{R_a} \right)^2 + \left( \frac{F_b}{R_b} \right)^2 = 1 \quad (5)$$

where  $R_a$  and  $R_b$  are the capacities of the nail plate in the a- and b-direction. The capacity values  $R_a$  and  $R_b$  are determined as maximum values according to the following expressions



$$R_a = \max \begin{cases} p_{at} b_n & \text{for } -\pi/2 \leq \alpha_{aF} \leq \pi/2 \\ s_a a_n & \text{(i.e. } F_a \text{ tensile force)} \end{cases} \quad (6)$$

$$R_a = \max \begin{cases} p_{ac} b_n & \text{for } \pi/2 \leq \alpha_{aF} \leq 3\pi/2 \\ s_a a_n & \text{(i.e. } F_a \text{ compression force)} \end{cases} \quad (7)$$

$$R_b = \max \begin{cases} p_{bt} a_n & \text{for } 0 \leq \alpha_{aF} \leq \pi \\ s_b b_n & \text{(i.e. } F_b \text{ tensile force)} \end{cases} \quad (8)$$

$$R_b = \max \begin{cases} p_{bc} a_n & \text{for } \pi \leq \alpha_{aF} \leq 2\pi \\ s_b a_n & \text{(i.e. } F_b \text{ compression force)} \end{cases} \quad (9)$$

### Nail plate connection subjected to tensile force

First we will study the load case when a nail plate connection is subjected to a tensile force perpendicular to the cut line between the timber members. See Figure 3. The plate force  $F_p$  is in this case equal to the external force  $F$  acting on the connection. By denoting the angle between the a-axis and the length direction of the force  $F$  by  $\alpha$  we obtain the following relations between the angles  $\alpha$ ,  $\alpha_{aF}$  and  $\alpha_{xa}$

$$\alpha_{aF} = \alpha \quad (10)$$

$$\alpha_{xa} = \pi/2 - \alpha \quad (11)$$

To be able to give analytical expressions for the capacities  $R_a$  and  $R_b$  we need to determine the angles for which the capacities change their equations. If we start with the capacity  $R_b$  we find the critical angle  $\alpha$  from Equation (8) by putting the expressions equal to each other.

$$p_{bt} a_n = s_b b_n \quad (12)$$

By inserting the Equations (1) and (2) into Equation (12) and replacing  $\alpha_{xa}$  with  $\alpha$  according to Equation (11) we find

$$\alpha = \alpha_{p1} = \arctan \frac{s_b}{p_{bt}} \quad (13)$$

In the same way it is possible to derive an expression for the critical angle for the capacity  $R_a$  from Equation (6). We obtain

$$\alpha_{p2} = \arctan \frac{P_{at}}{s_a} \quad (14)$$

Now we can calculate the tension capacity per unit width perpendicular to the cut line

$$p = \frac{F}{f} \quad (15)$$

By inserting the Equations (1)-(6), (8), (10) and (11) into Equation (15) we will obtain three different curves for the tension capacity when  $\alpha$  is within the interval  $0 \leq \alpha \leq \pi/2$ .

$$p = \frac{1}{\sqrt{\left(\frac{1}{P_{at}}\right)^2 + \left(\frac{\tan \alpha}{s_b}\right)^2}} \quad \text{for } 0 \leq \alpha \leq \alpha_{p1} \quad (16)$$

$$p = \frac{1}{\sqrt{\left(\frac{1}{P_{at}}\right)^2 + \left(\frac{1}{P_{bt}}\right)^2}} \quad \text{for } \alpha_{p1} \leq \alpha \leq \alpha_{p2} \quad (17)$$

$$p = \frac{1}{\sqrt{\left(\frac{1}{s_a \tan \alpha}\right)^2 + \left(\frac{1}{P_{bt}}\right)^2}} \quad \text{for } \alpha_{p2} \leq \alpha \leq \pi/2 \quad (18)$$

The equations are graphically presented in Figure 4 for a Hydro Nail E nail plate. The equations are shown for all  $\alpha$ -values between 0 and  $\pi/2$  even if they are only valid between certain limits. Equation (16) corresponds to the failure criterion that the tension capacity in the a-direction  $p_{at}$  and the shear capacity in the b-direction  $s_b$  is utilized. This failure criterion is valid for  $0 \leq \alpha \leq \alpha_1$ . The theoretical failure criteria for the different curves can be seen from the top of Figure 4 where the capacities  $R_a$  and  $R_b$  are given for different  $\alpha$ -values.

#### Nail plate connection subjected to shear force. No contact between timber members.

We are now going to study the load case in Figure 5 where a nail plate connection subjected to a shear force along the cut line is shown. It is assumed that there is no contact between the timber members. This means that the entire shear force has to be transmitted merely by the nail plate i.e.  $F_p$  is equal to  $F$ . Depending on the value of the angle  $\alpha$  we obtain two cases. The first case is usually called tension shear and occurs when  $0 \leq \alpha_{xa} \leq \pi/2$ . With notations according to Figure 5 we obtain

$$\alpha_{aF} = 2\pi - \alpha \quad (19)$$

$$\alpha_{xa} = \alpha \quad (20)$$

We want now to determine analytically the angles  $\alpha$  for which the capacities  $R_a$  and  $R_b$  obtain changed equations. For the capacity  $R_a$  the critical angle  $\alpha$  is obtained from Equation (6) by the relation

$$P_{at} b_n = s_a a_n \quad (21)$$

By inserting the Equations (1), (2) and (19) into Equation (21) we find

$$\alpha_{s1} = \arctan \frac{s_a}{P_{at}} \quad (22)$$

A corresponding calculation, for the capacity  $R_b$ , based on Equation (9) will give

$$\alpha_{s2} = \arctan \frac{P_{bc}}{s_b} \quad (23)$$

It is now possible to calculate the shear capacity per unit width along the cut line.

$$s = \frac{F}{f} \quad (24)$$

By inserting the Equations (1)-(6), (9), (19) and (20) into Equation (24) we will get the following expressions for the shear capacity of the plate when  $0 \leq \alpha \leq \pi/2$ .

$$s = \frac{1}{\sqrt{\left(\frac{1}{s_a}\right)^2 + \left(\frac{\tan\alpha}{P_{bc}}\right)^2}} \quad \text{for } 0 \leq \alpha \leq \alpha_{s1} \quad (25)$$

$$s = \frac{1}{\sqrt{\left(\frac{1}{P_{at}\tan\alpha}\right)^2 + \left(\frac{\tan\alpha}{P_{bc}}\right)^2}} \quad \text{for } \alpha_{s1} \leq \alpha \leq \alpha_{s2} \quad (26)$$

$$s = \frac{1}{\sqrt{\left(\frac{1}{P_{at}\tan\alpha}\right)^2 + \left(\frac{1}{s_b}\right)^2}} \quad \text{for } \alpha_{s2} \leq \alpha \leq \pi/2 \quad (27)$$

So far we have only dealt with the load case tension shear. If the angle  $\alpha$  is within the interval  $\pi/2 \leq \alpha \leq \pi$  the nail plate is said to be in compression shear. By using the same fundamental equations as in the case of tension shear we obtain

$$s = \frac{1}{\sqrt{\left(\frac{1}{p_{ac}\tan(180-\alpha)}\right)^2 + \left(\frac{1}{s_b}\right)^2}} \quad \text{for } \pi/2 \leq \alpha \leq \alpha_{s3} \quad (28)$$

$$s = \frac{1}{\sqrt{\left(\frac{1}{p_{ac}\tan(180-\alpha)}\right)^2 + \left(\frac{\tan(180-\alpha)}{p_{bt}}\right)^2}} \quad \text{for } \alpha_{s3} \leq \alpha \leq \alpha_{s4} \quad (29)$$

$$s = \frac{1}{\sqrt{\left(\frac{1}{s_a}\right)^2 + \left(\frac{\tan(180-\alpha)}{p_{bt}}\right)^2}} \quad \text{for } \alpha_{s4} \leq \alpha \leq \pi \quad (30)$$

where the angles  $\alpha_{s3}$  and  $\alpha_{s4}$  are given by

$$\alpha_{s3} = \pi - \arctan \frac{p_{bt}}{s_b} \quad (31)$$

$$\alpha_{s4} = \pi - \arctan \frac{s_a}{p_{ac}} \quad (32)$$

The Equations (25)-(27) and (28)-(30) are graphically presented in Figure 6 for the same nail plate as was previously mentioned. The different failure criteria can be seen in the top of Figure 6 where the capacities  $R_a$  and  $R_b$  are given as functions of the angle  $\alpha$ .

Nail plate connection subjected to shear force. Contact between timber members. No friction.

So far we have only dealt with nail plate connections assuming that the entire shear force is transmitted merely by the nail plates. We are now going to consider the case when there is contact between the timber members but no friction between them. To use contact between the timber members in the calculation model is advantageous when the nail plates are subjected to tension shear. The principle is shown for the nail plate connection in Figure 7. It is assumed that the shear force  $F$  can be divided into one plate component  $F_p$  parallel to the length direction of the plate and one component perpendicular to the cut line. It is possible to find more advantageous directions for the plate component  $F_p$  but that will necessitate much more complicated equations. For ordinary nail plates it seems reasonable to use the

proposed assumption. To calculate the shear capacity of the nail plate connection we shall use the following values for the angles  $\alpha_{aF}$  and  $\alpha_{xa}$ .

$$\alpha_{aF} = 0 \quad (33)$$

$$\alpha_{xa} = \alpha \quad (34)$$

The relation between the nail plate force  $F_p$  and the shear force  $F$  is

$$F = F_p \cos \alpha \quad (35)$$

By using the Equations (1)-(6) and (33)-(35) we can calculate the shear capacity per unit width of the nail plate connection to

$$s = \frac{F}{f} = p_{at} \sin \alpha \cos \alpha \quad (36)$$

The shear capacity  $s$  as a function of the angle  $\alpha$  is shown in Figure 8. As a comparison the curves assuming no contact between the timber members are shown with thin lines in the figure. Obviously there is a lot to gain by assuming contact in the connection.

#### Nail plate connection subjected to shear force. Contact between timber members. Friction included.

We now want to study the influence of friction forces between the timber members. In this case we assume that the shear force  $F$  in Figure 9 is built up of three components namely one plate force  $F_p$  parallel to length direction of the plate, one contact force  $F_t$  perpendicular to the cut line and one friction force  $\mu F_t$  parallel to the cut line. With one exception the same equations as in the case of no friction can be used. Thus Equation (35) has to be replaced by

$$F = F_p \cos \alpha + \mu F_t \quad (37)$$

where

$$F_t = F_p \sin \alpha \quad (38)$$

After deduction the shear capacity per unit width of the nail plate connection is obtained to

$$s = p_{at} \sin \alpha (\cos \alpha + \mu \sin \alpha) \quad (39)$$

The shear capacity  $s$  is shown in Figure 10 as a function of the angle  $\alpha$ . The coefficient of friction  $\mu$  has been given the value of 0.3. It should be pointed out that Equation (39) is also valid for angles  $\alpha \geq \pi/2$  i.e. in compression shear. For  $\alpha = \pi/2$  we obtain that the shear capacity per unit width of the nail plate connection is  $\mu p_{at}$  which should be compared with the shear capacity per unit width  $s_0$  of the nail plate.

#### TEST RESULTS. COMPARISON WITH THEORY.

The tests reported in this paper have all been carried out at the Technical Research Centre of Finland. The selection of the material and the performance of the tests are in agreement with the procedure described in /3/. The specimens used in the tension and the shear tests are shown in Figure 11. The test specimen in shear deviates from what is specified in ISO 8969 but is preferred in Finland because it is simple to manufacture and easy to test. The experience in Finland is that the specimen seems to give reliable test values which are in good agreement with values determined according to the ISO standard. The load arrangement in shear is shown in Figure 11.

The results from testing 6 different nail plates are presented. The plates have been chosen for practical rather than scientific reasons. Some nail plate producers have kindly given us permission to publish their test results.

The punching patterns of the tested nail plates are shown in Annex A. The nominal values of the tooth length and the plate thickness are given in Table 1. For the nail plates Hydro Nail M and Hydro Nail PTN, Swedish structural steel of grade SIS 2122 was used. For the rest of the plates a Finnish structural steel Z36 was used. In Table 1 the required minimum values of the yield point and the tensile strength are presented. In connection with the manufacturing of the nail plates, strips of unpunched plate material were taken out and tested in tension. These tests showed that for the nail plates Hydro Nail M and Hydro Nail PTN the yield point was between 357 and 390 N/mm<sup>2</sup> and the tensile strength between 452 and 530 N/mm<sup>2</sup>. For the other plates the yield point was between 395 and 445 N/mm<sup>2</sup> and the tensile strength between 530 and 575 N/mm<sup>2</sup>. This means that the strength of all the tested plate material was rather high.

In Annex B the tension capacity  $p$  and the shear capacity  $s$  of all the tested nail plate connections are shown as functions of the angle  $\alpha$ . The test values in the annex represent mean values. The number of test specimens of each type have in most cases been 3 but in some cases 5. The nail plate dimensions are given as width times length. In connection with the shear tests four different shear capacities  $s$  have been evaluated from the load-slip curves namely:

$s_{con}$  shear capacity when the initial gap of 2 mm is closed and contact between the timber members is obtained. This value is only given if there is a distinct change of slope in the load-slip curve (denoted + in Annex B)

$s_{ex}$	extrapolated shear capacity up to a slip limit of 7.5 mm obtained from the initial curvature of the load-slip curve i.e. assuming no contact between the timber members (denoted $\Delta$ in Annex B)
$s_{7.5}$	the maximum shear capacity up to a slip limit of 7.5 mm (denoted $\square$ in Annex B)
$s_{max}$	the maximum shear capacity up to a slip limit of 15 mm (denoted $\circ$ in Annex B)

All these s-values are shown in Annex B. In most cases however  $s_{7.5}$  is the only one present. As different shapes of each type of nail plate were tested, the shear capacity values had to be presented in two figures. The first figure contains shear capacities for plates of normal size and shape. The second figure contains results from testing of plates with low and high length-to-width ratios. Thus for the angle of 0 degrees the plate shape has been chosen in order to obtain anchorage failure. For  $\alpha=30, 45, 60$  and 150 degrees the behaviour of long and narrow plates have been studied. For  $\alpha=45$  and 150 degrees the capacity of very short and wide plates have been determined. The latter have been chosen mainly for theoretical reasons.

**Table 1** Nominal tooth length and plate thickness. Minimum yield point and tensile strength of the plate material.

Nail plate	Nominal tooth length mm	Nominal plate thickness mm	Minimum yield point N/mm <sup>2</sup>	Minimum tensile strength N/mm <sup>2</sup>
Hydro Nail E	14	1.25	360	480
Hydro Nail M	14	1.5	350	430
Hydro Nail PTN	8.5	1.0	350	430
FIX (PEIKKO)	13	1.3	360	480
TOP-83R	7 & 12	1.3	360	480
TOP-91	14	1.3	360	480

The failure modes of all the tested nail plate connections are shown with capital letters in Annex B. The following notations are used:

- A = Anchorage failure, bending of the nails.
- B = Local buckling of the plate edge in shear test.
- D = Exceeding of the slip limit 15 mm. The increase of the load beyond the slip limit is not considered (D from deformation)
- S = Shear failure in the plate.
- T = Tension failure in the plate.

Calculations of the tension capacity  $p$  and the shear capacity  $s$  of the tested nail plate connections have been carried out applying the theory described in this paper. Thus to determine the tension capacity  $p$  per unit width the Equations (16)-(17) have been used. The shear capacity  $s$  per unit width has been calculated under the

three different assumptions:

- \* No contact between timber members.
- \* Contact between timber members. No friction.
- \* Contact between timber members. Friction included ( $\mu=0.3$ ).

In this case the Equations (25)-(30), (36) and (39) have been used. To be able to perform the calculations, values on the 6 fundamental plate capacities  $p_{at}$ ,  $p_{ac}$ ,  $s_a$ ,  $p_{bt}$ ,  $p_{bc}$  and  $s_b$  are needed. These values are given in Table 2 for each of the plates. The values represent mean values and comprise only the proper failure modes. Thus in the case of shear we have only accepted capacity values where there is no contact between the timber members. It must be pointed out that the capacity values in Table 2 are dependent on the steel quality and the thickness of the plate material used in the test specimens. No adjustment of the capacity values with respect to the nominal strength of the plate material and the nominal thickness of the plate has been undertaken. The values in Table 2 should therefore not be regarded as values which can be used for approving or comparing different plates.

Table 2 Plate capacity values obtained in the tests.

Nail plate	$p_{at}$	$p_{ac}$	$s_a$	$p_{bt}$	$p_{bc}$	$s_b$
	N/mm	N/mm	N/mm	N/mm	N/mm	N/mm
Hydro Nail E	394	185	109	120	75	98
Hydro Nail M	409	266	135	157	146	120
Hydro Nail PTN	262	112	115	155	122	81
FIX (PEIKKO)	414	194	140	228	141	107
TOP-83R	459	180	139	236	158	114
TOP-91	372	187	119	228	147	72

A comparison of the measured and the theoretical tension capacities  $p$  in Annex B shows that the agreement is somewhat varying but mostly rather good for the investigated nail plates. There seems to be a tendency for the theory to underestimate the plate capacity when the angle  $\alpha$  is 30 degrees. For the angle of 60 degrees the theory overestimates the plate capacity in four cases and underestimates it in one case.

It is more difficult to make an evaluation of the agreement between the measured and the theoretical capacities in shear than in the case of tension. That is a consequence of the more complicated conditions in shear, where it often is contact between the timber members. It must be pointed out that it is very important to make a distinction between the capacity of the nail plate and the capacity of the nail plate connection. Thus it is only when we talk about the capacity of the nail plate connection that contact and friction forces can occur.

If we compare the measured shear capacities with those obtained by the theory assuming no contact between the timber members (the



lower curve) we find that the test values mostly are above the theoretical curve. Due to local buckling of the plate edge (failure mode B) the test values sometimes are below the curve. This is often the case when  $\alpha$  is equal to 30, 45, 135 and 150 degrees. In a few cases, anchorage failure (failure mode A) is the reason why the test values are below the theoretical curve. For those plate types where the local buckling mode occurs it might be possible in design to use reduced effective widths for some angles  $\alpha$ .

In the case of tension shear ( $0 \leq \alpha \leq 90$  degrees) we find that the test values often are much higher than what may be expected from the theoretical capacity of merely the nail plate. In the shear-failure mode (S) the test values almost always are above the upper curve i.e. the theoretical capacity assuming contact and friction. An other conclusion which can be drawn is that the shear capacity increases when the length-to-width ratio is increased and  $\alpha$  is between 30 and 60 degrees. The capacity values for the plates with high length-to-width ratios are mostly higher than given by the theoretical curve assuming contact but no friction.

It is the authors' intention to extend the investigation to some other nail plate types which already have been tested. In particular plates with different punching patterns will be analysed.

#### CONCLUSIONS.

The proposed design code in /5/ is presented in a format easily applicable to results from standard tests. An evaluation of 6 different types of nail plates is made. The agreement between the measured and the theoretical capacity values in tension is somewhat varying but mostly rather good. The capacity values from the shear tests are often higher than the results from a theoretical calculation assuming no contact between the timber members. Special attention should be payed to the local buckling mode of the nail plate edge in the shear test. In the case of tension shear it might be possible to use a theory based on the assumption that there is contact but no friction between the timber members if the length-to-width ratio of the plate is high enough.

Even if only a limited number of nail plate connections have been investigated in this paper it can be stated that the theory is very useful for making reliable evaluations of test results.

#### REFERENCES

1. Norén B. 1981: Design of Joints with Nail Plates. Paper 14-7-1, Proceedings, CIB-W18 Meeting, Warsaw, Poland.
2. Bovim N.I. & Aasheim E. 1985: The Strength of Nail Plates. Paper 18-7-6, Proceedings, CIB-W18 Meeting, Beit Oren, Israel.

3. Kangas J. 1985: A Detailed Testing Method for Nail Plate Joints. Paper 18-7-4, Proceedings, CIB-W18 Meeting, Beit Oren, Israel.
4. Kangas J. 1985: Principles for Design Values of Nail Plates in Finland. Paper 18-7-5, Proceedings, CIB-W18 Meeting, Beit Oren, Israel.
5. Aasheim E. & Solli K.H. 1990: Proposal for Design Code for Nail Plates. Paper 23-7-1, Proceedings, CIB-W18 Meeting, Lisbon, Portugal.

#### ACKNOWLEDGEMENTS

The authors thank the following nail plate producers for their contribution of test results:

FIXRON OY, Norokatu 5, 15170 Lahti, Finland

Top-Levy OY, Sepänkatu 9, 11710 Riihimäki, Finland

Nordisk Kartro AB, Box 124, 123 22 Farsta, Sweden

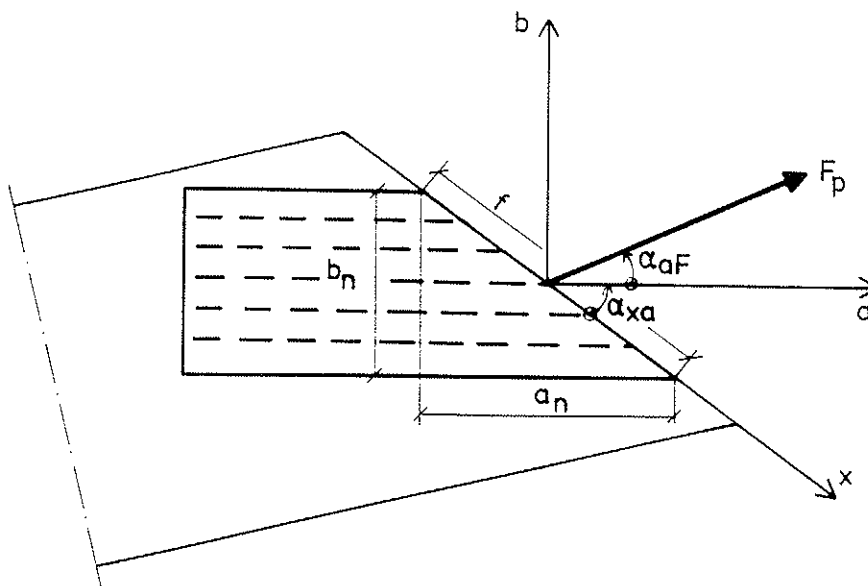


Figure 1 Nail plate subjected to a force  $F_p$ . Definition of angles and geometry.

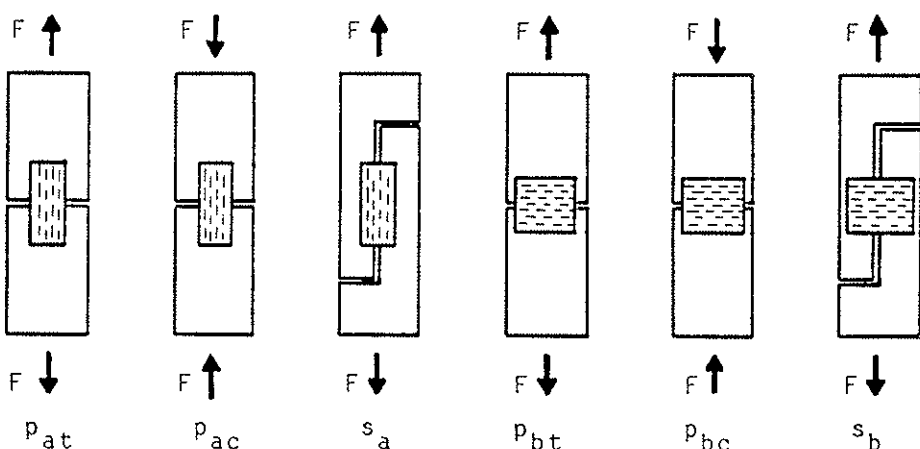


Figure 2 Test specimens used for determination of capacity values.

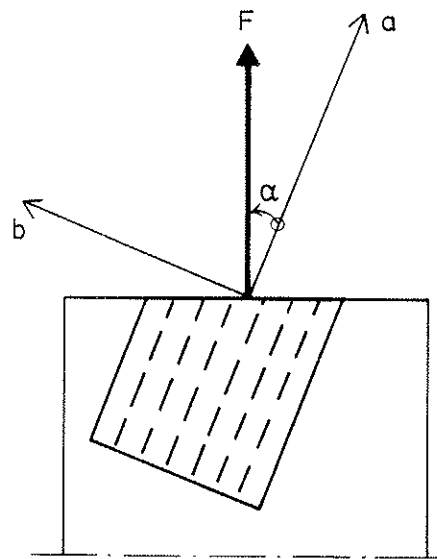


Figure 3 Nail plate connection subjected to a tensile force F.

$$R_a = \begin{array}{|c|c|} \hline p_{at} b_n & s_a a_n \\ \hline \end{array}$$

$$R_b = \begin{array}{|c|c|} \hline s_b b_n & p_{bt} a_n \\ \hline \end{array}$$

Tension capacity p

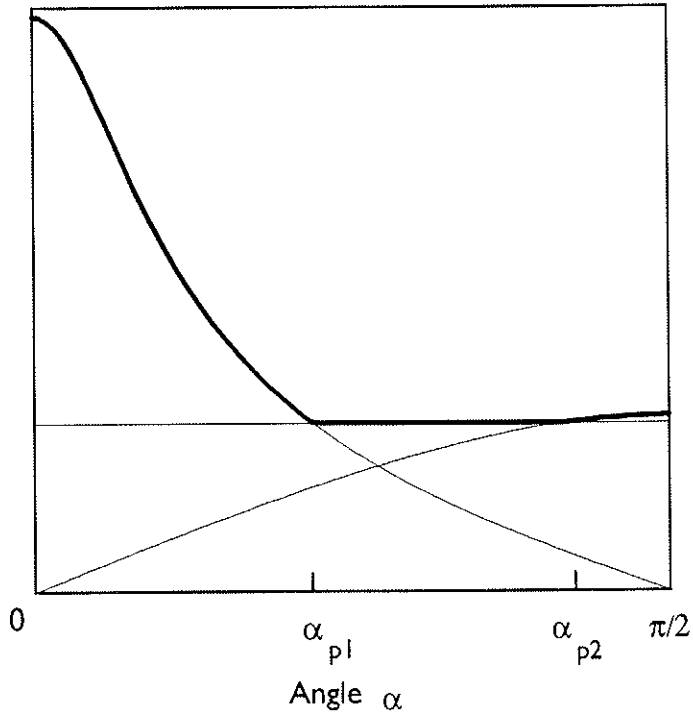


Figure 4 Theoretical tension capacity p as a function of the angle alpha for a nail plate connection.

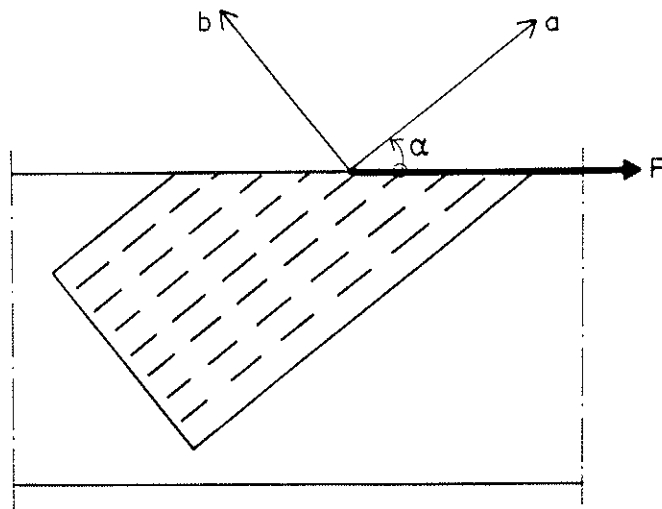


Figure 5 Nail plate connection subjected to a shear force F. No contact between timber members.

$$R_a = \begin{array}{|c|c|c|c|} \hline s_a a_n & p_{at} b_n & p_{ac} b_n & s_a a_n \\ \hline p_{bc} a_n & s_b b_n & p_{bt} a_n & \\ \hline \end{array}$$

Shear capacity s

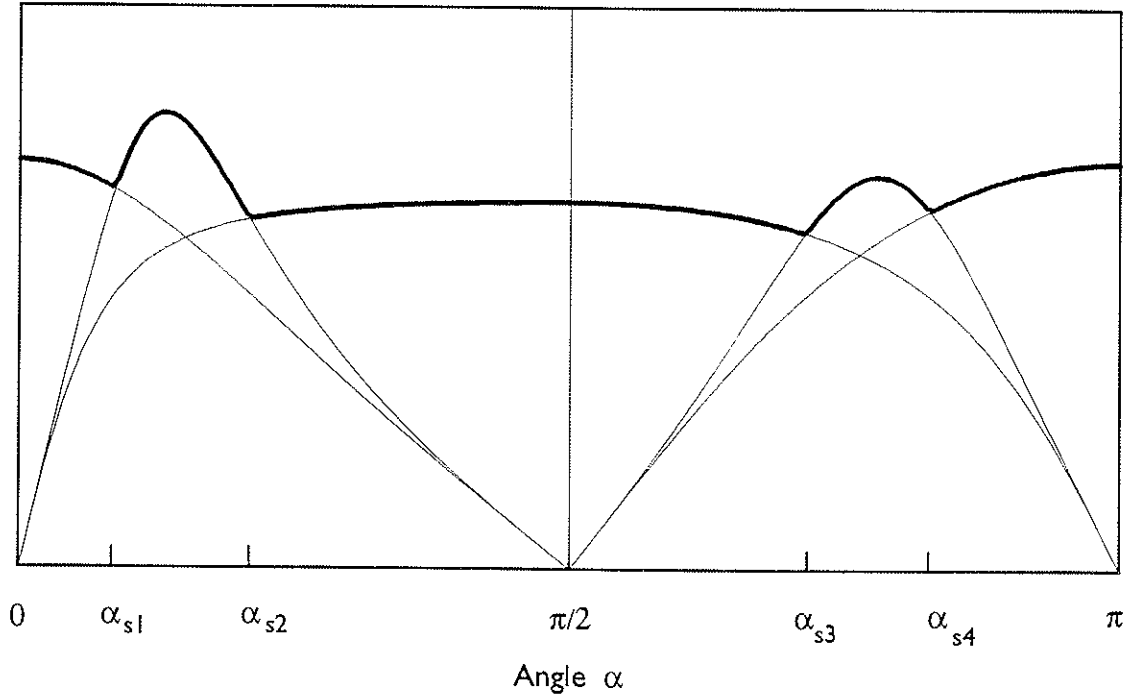


Figure 6 Theoretical shear capacity s as a function of the angle  $\alpha$  for a nail plate connection. No contact between timber members.

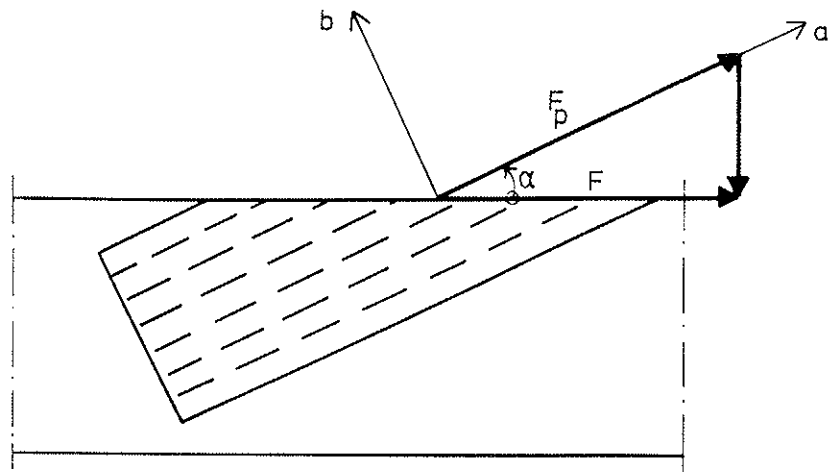


Figure 7 Nail plate connection subjected to a shear force  $F$ . Contact between timber members. No friction.

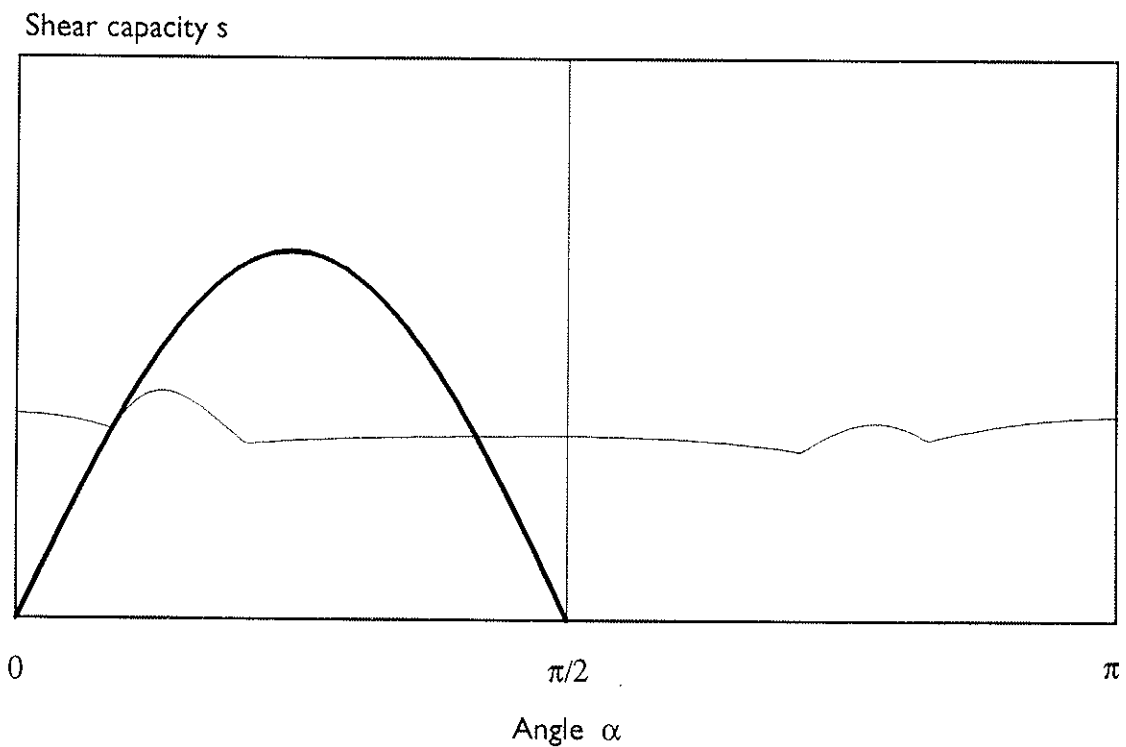


Figure 8 Theoretical shear capacity  $s$  as a function of the angle  $\alpha$  for a nail plate connection. Contact between timber members. No friction.

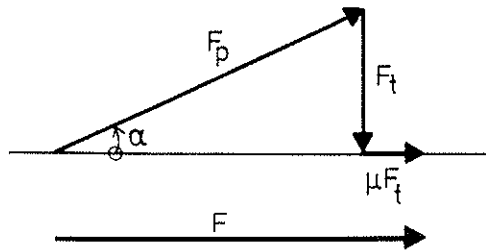


Figure 9 Internal and external forces in a nail plate connection subjected to shear. Contact between timber members. Friction included.

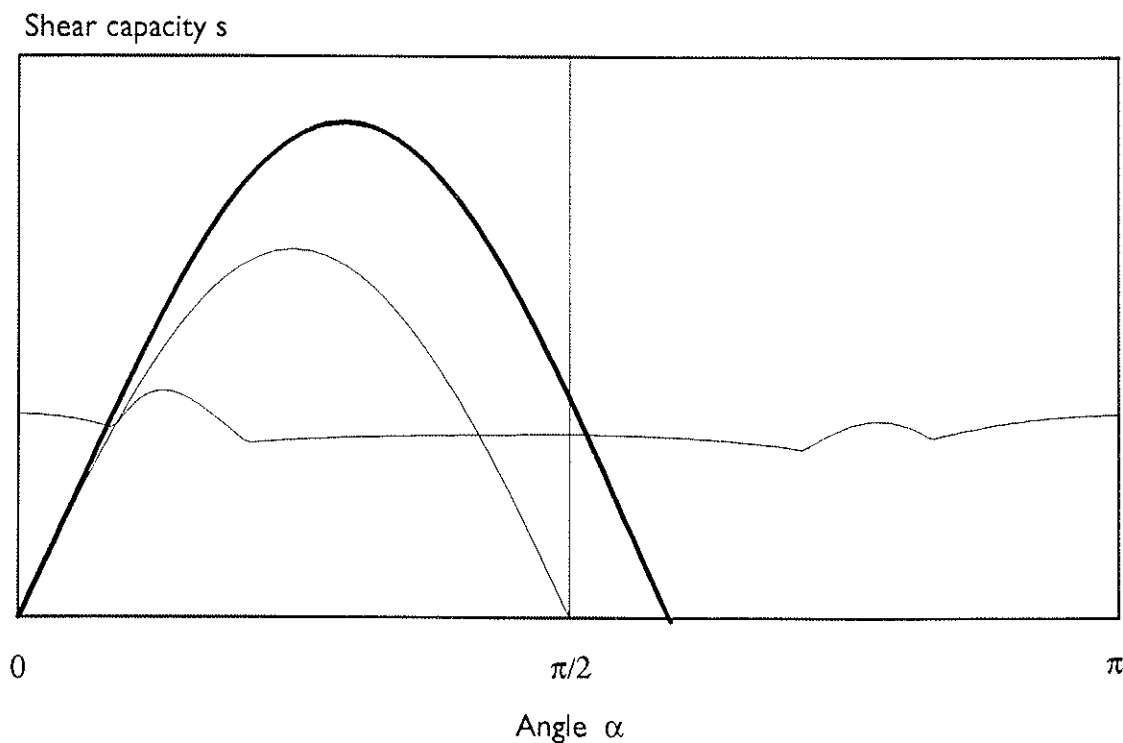


Figure 10 Theoretical shear capacity  $s$  as a function of the angle  $\alpha$  for a nail plate connection. Contact between timber members. Friction included.

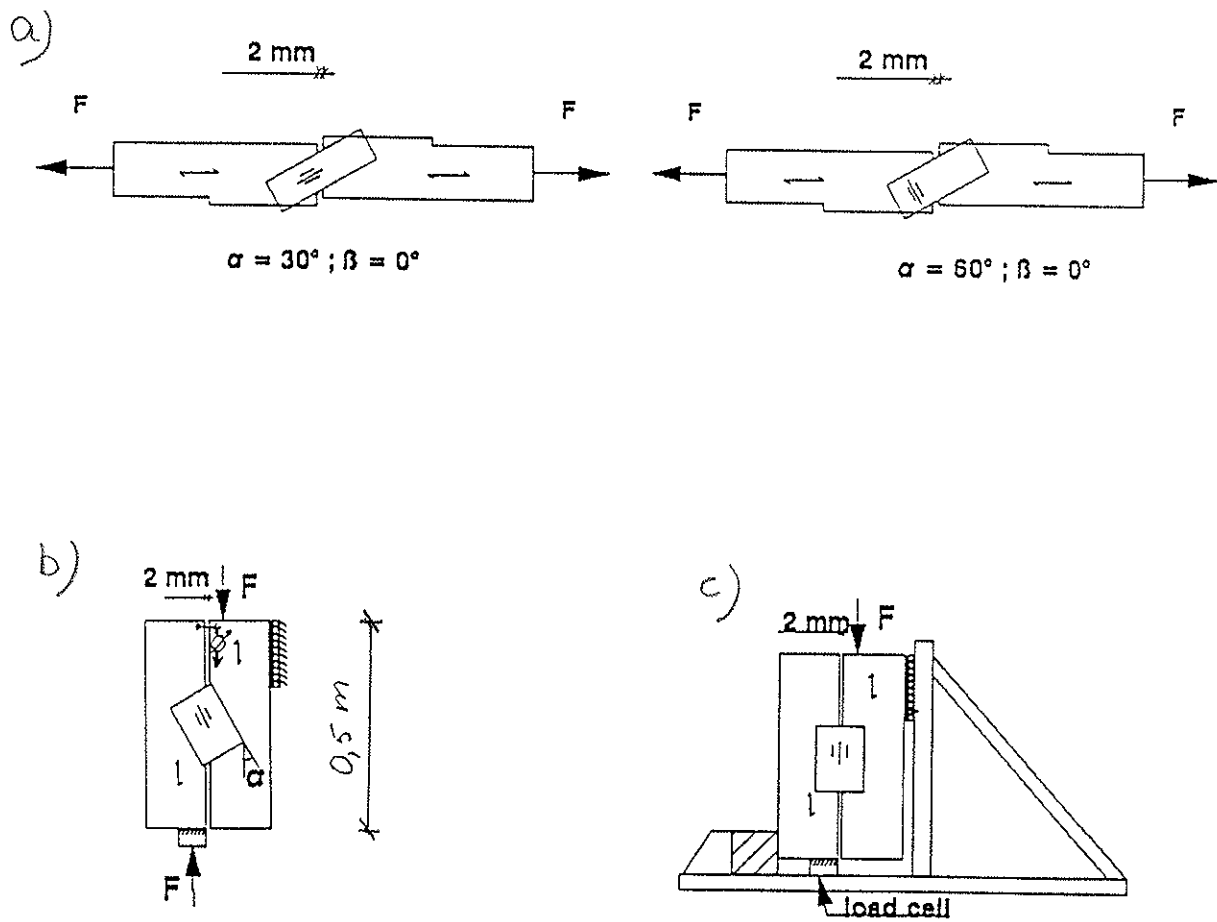


Figure 11 a) Test specimen used in tension test.  
 b) Test specimen used in shear test.  
 c) Load arrangement in shear.



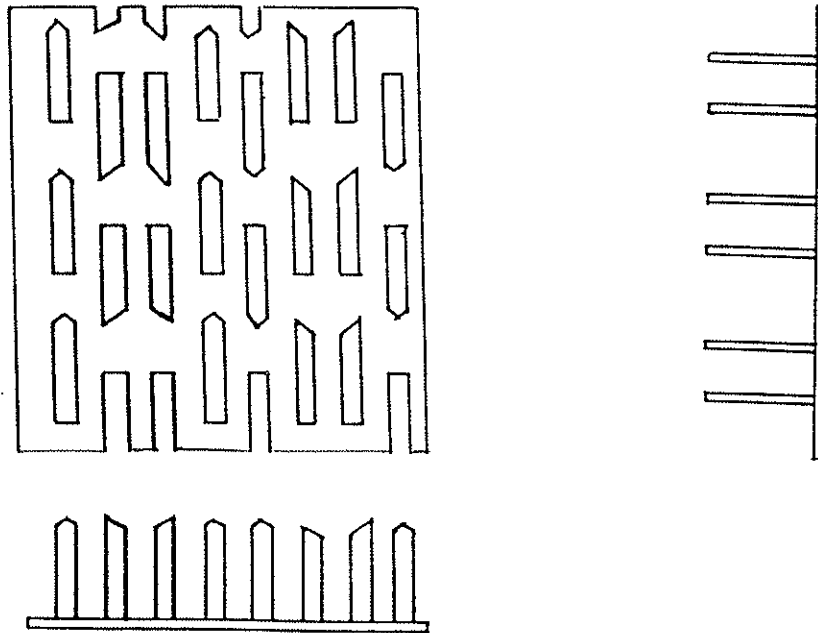


Figure A1 Hydro Nail E

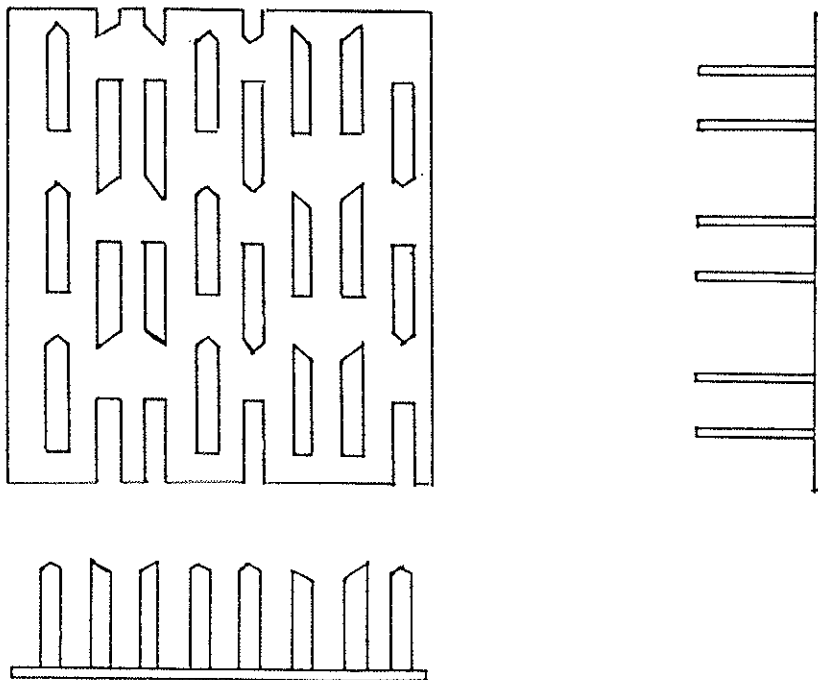


Figure A2 Hydro Nail M

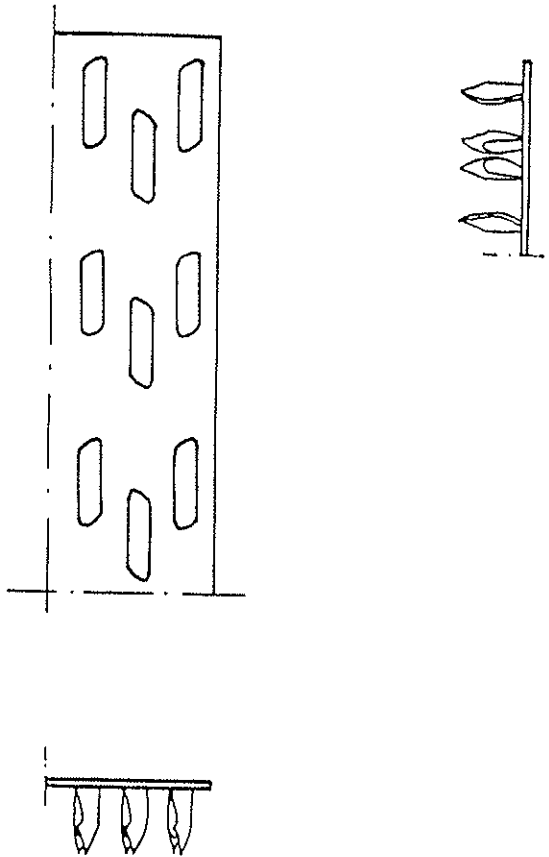


Figure A3 Hydro Nail PTN

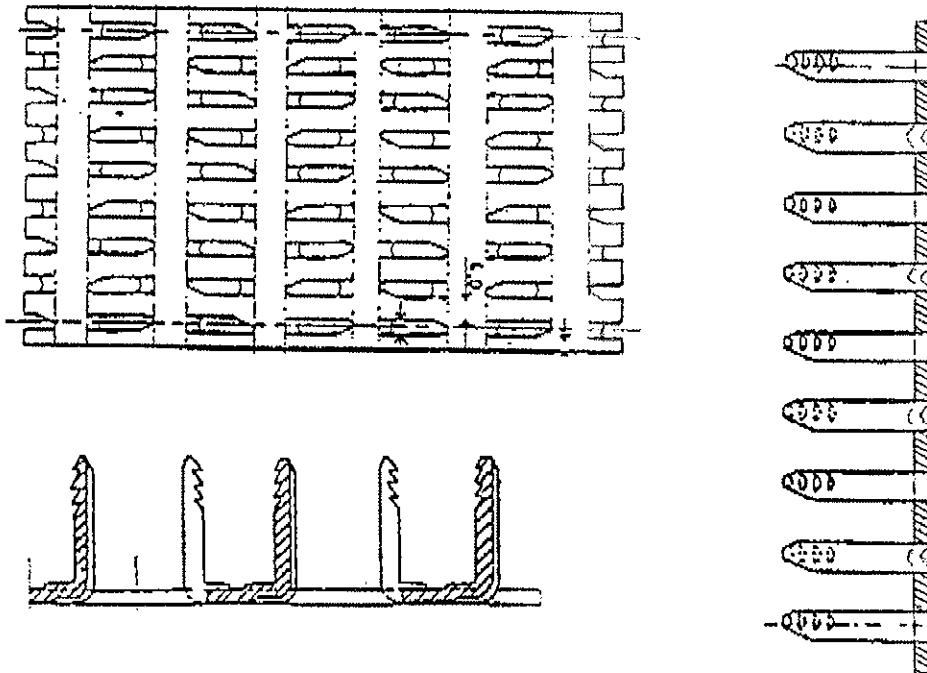


Figure A4 FIX (PEIKKO)

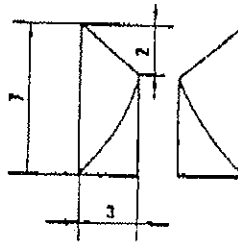
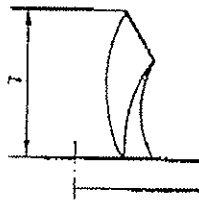
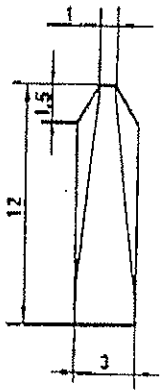
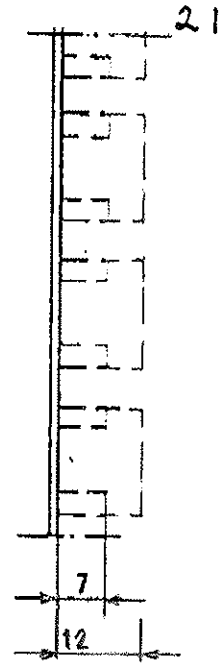
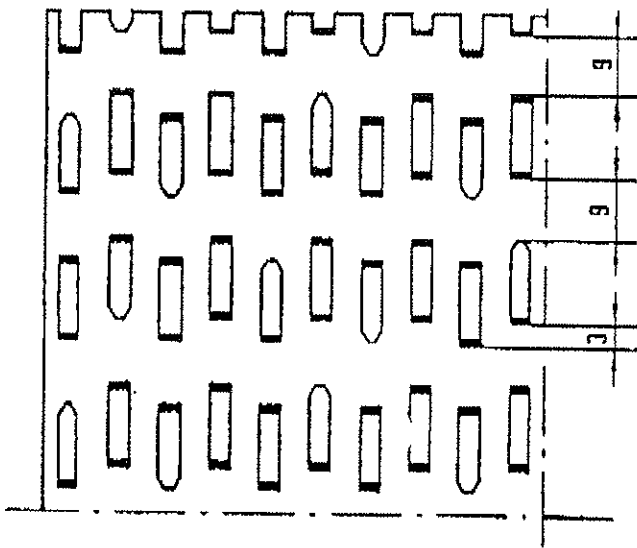


Figure A5 TOP-83 R

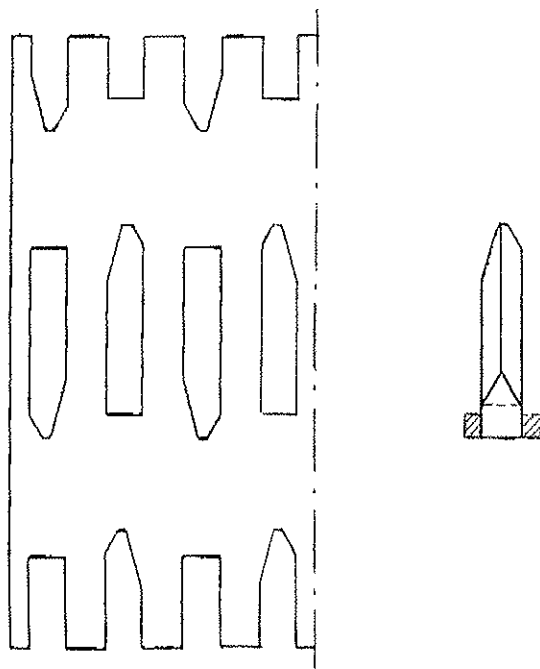


Figure A6 TOP-91

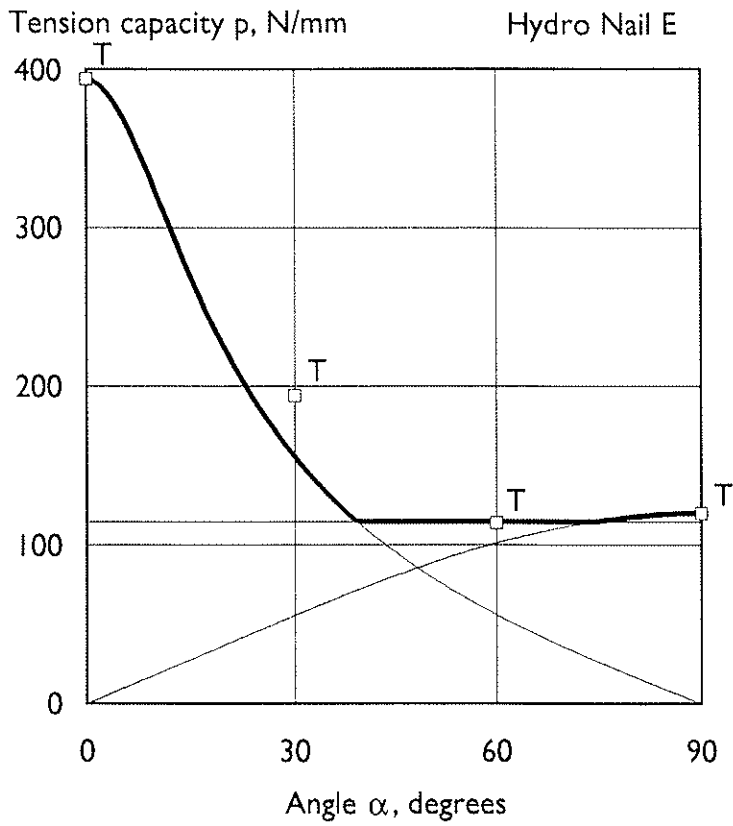


Figure B1

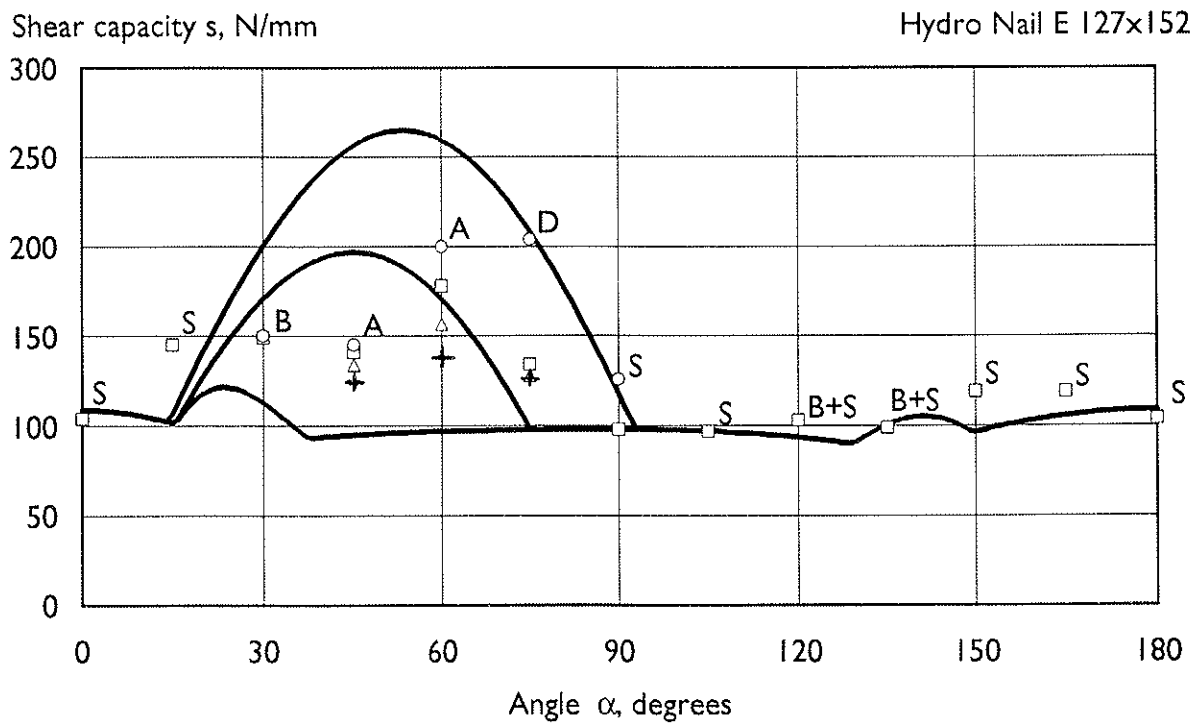


Figure B2

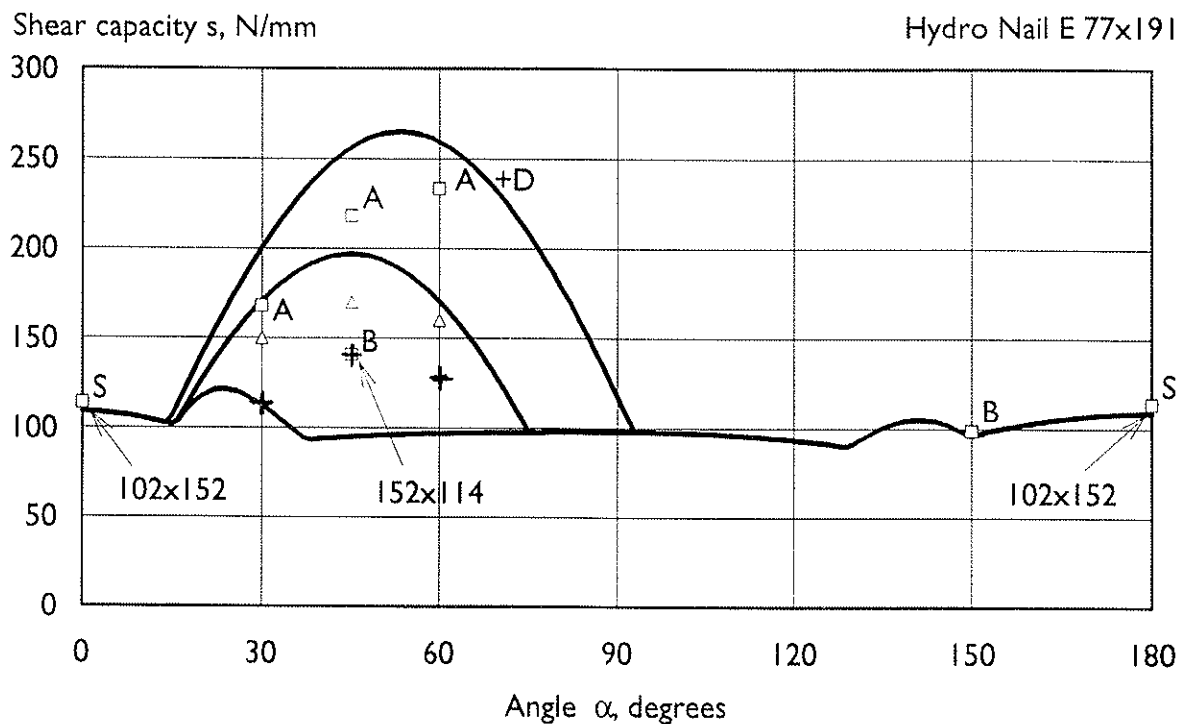


Figure B3

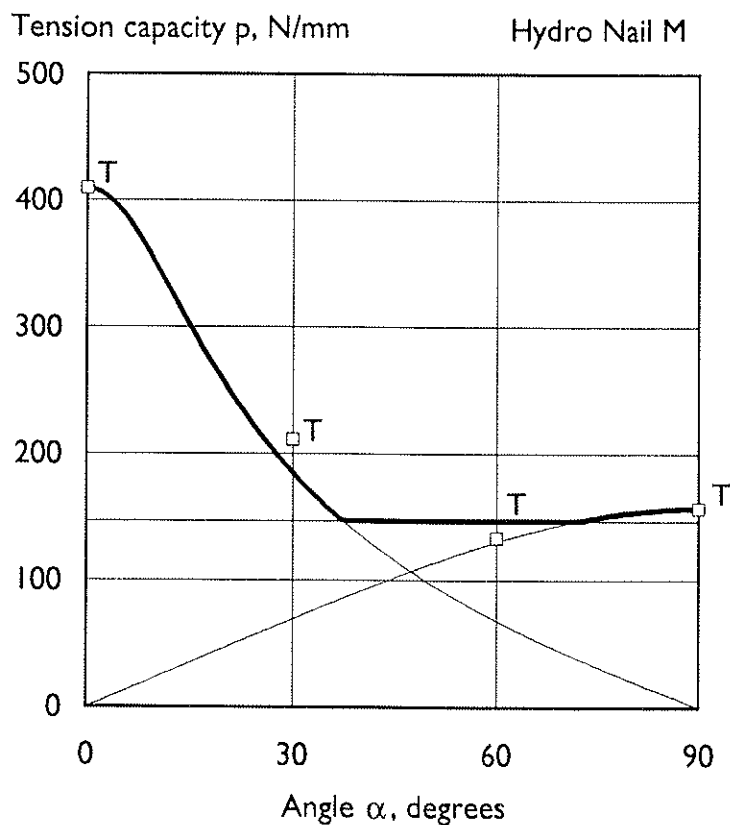


Figure B4

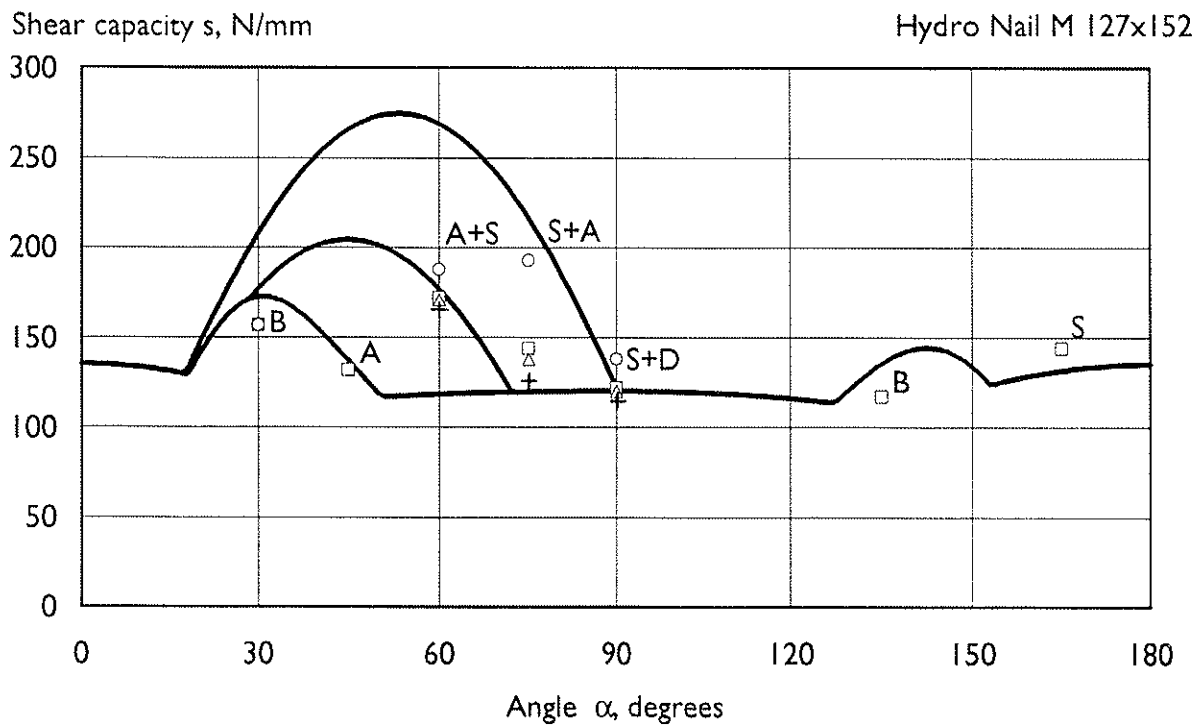


Figure B5

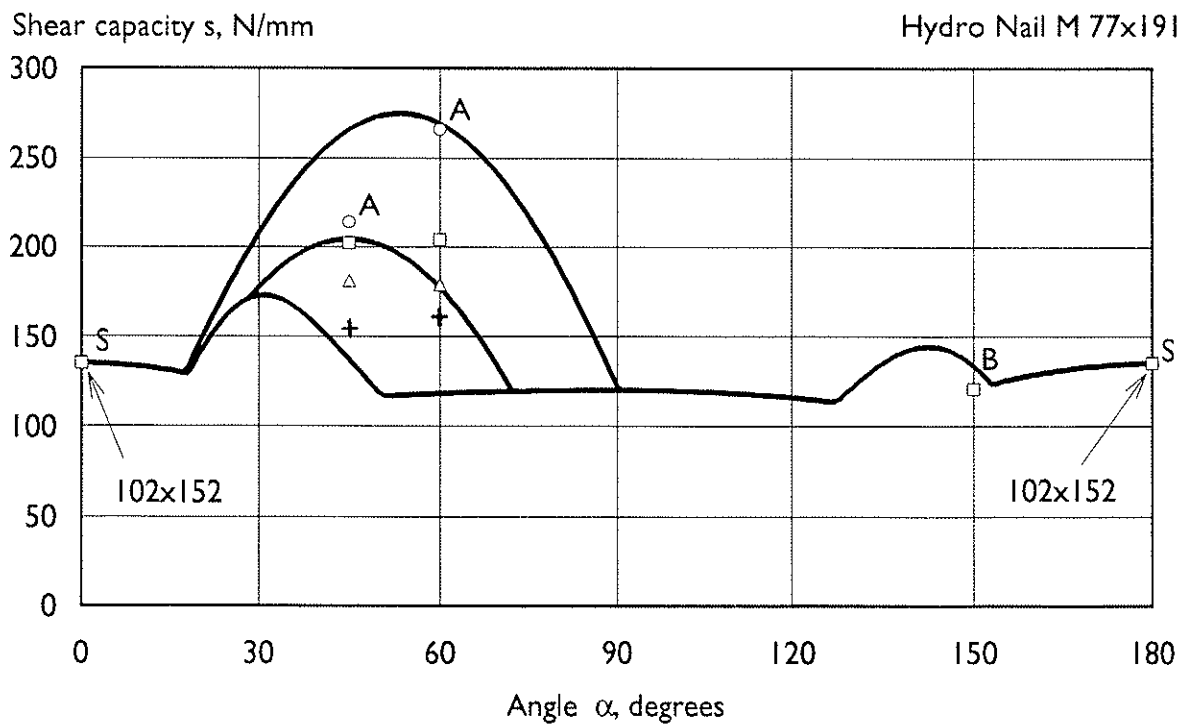


Figure B6

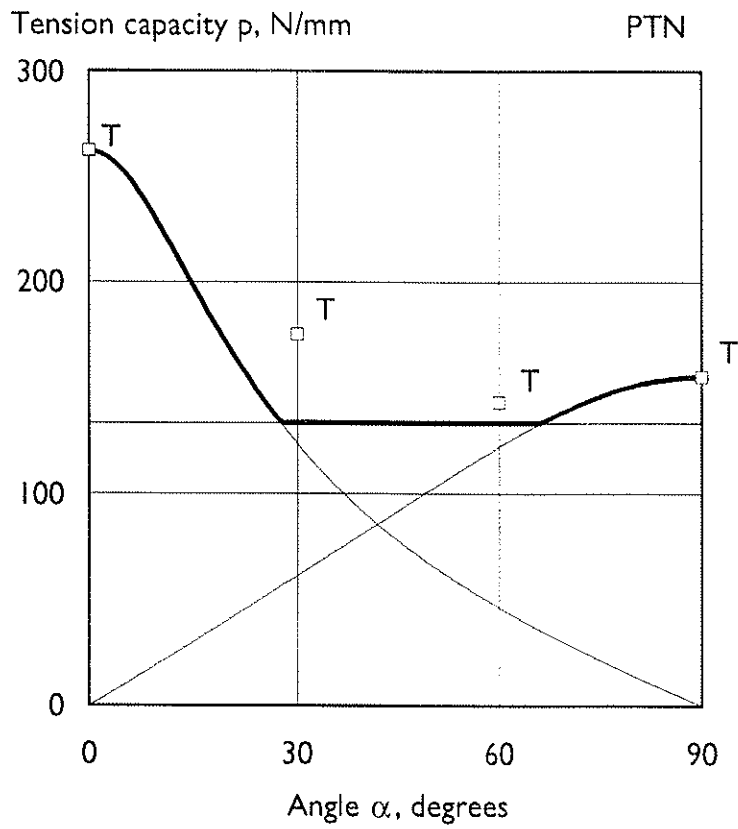


Figure B7

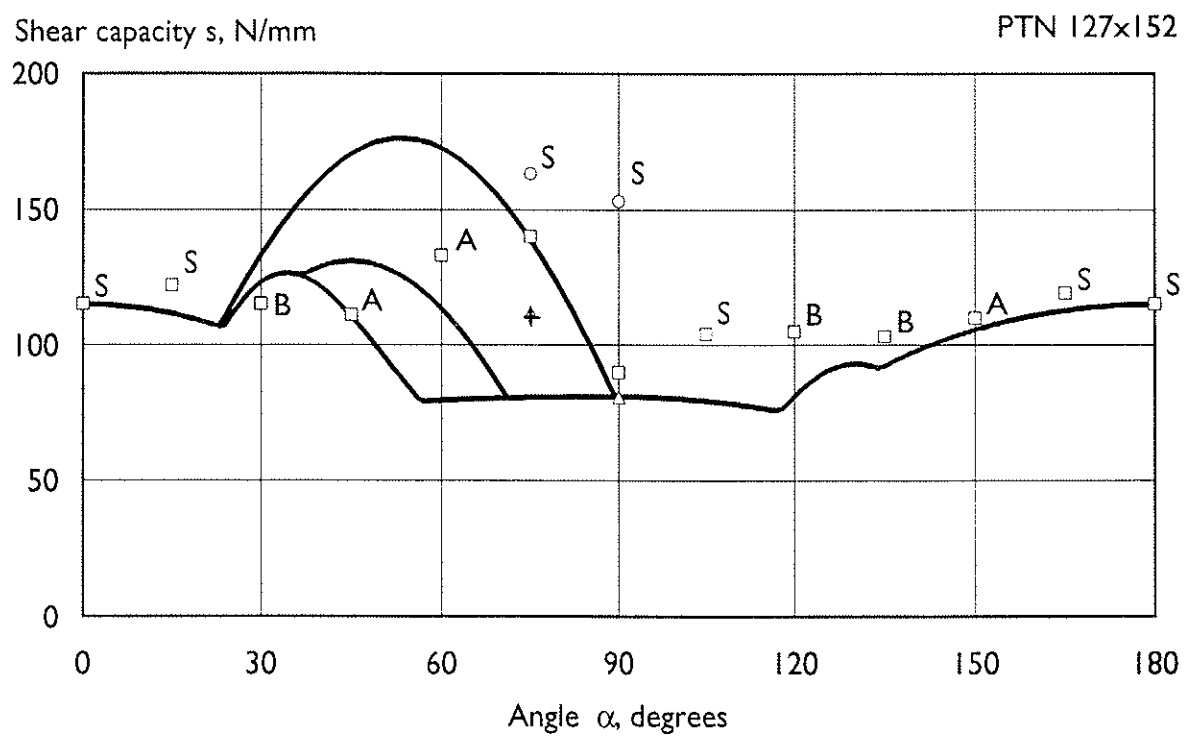


Figure B8

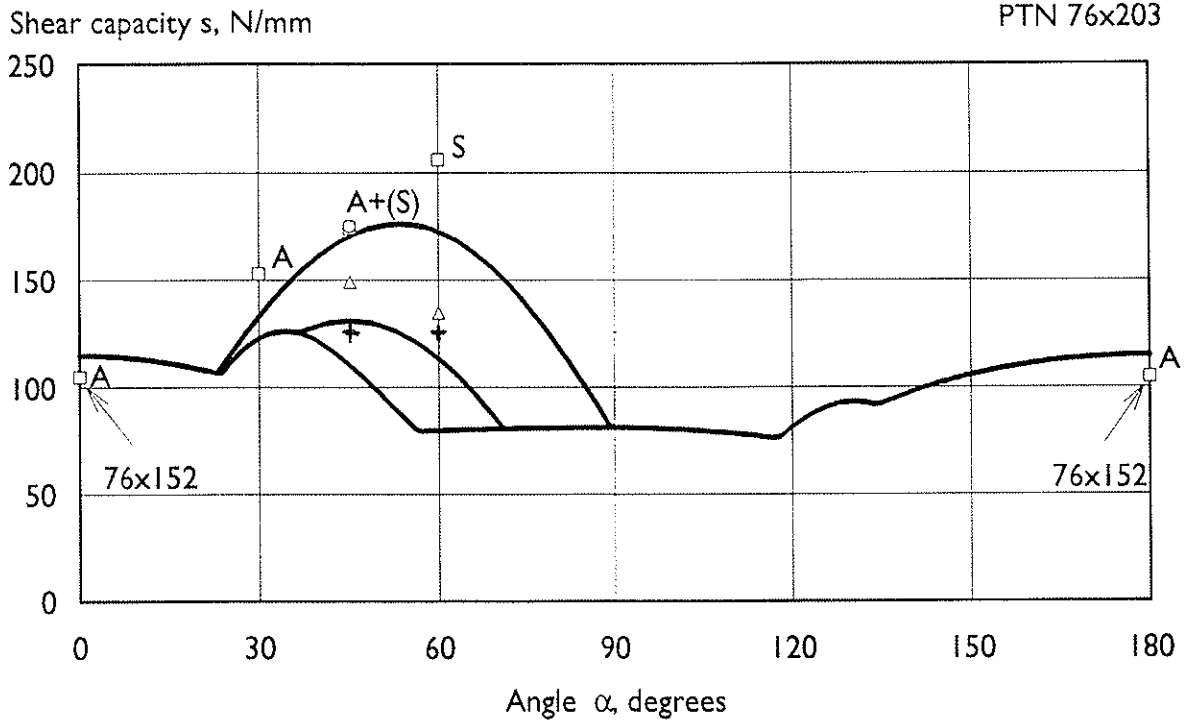


Figure B9

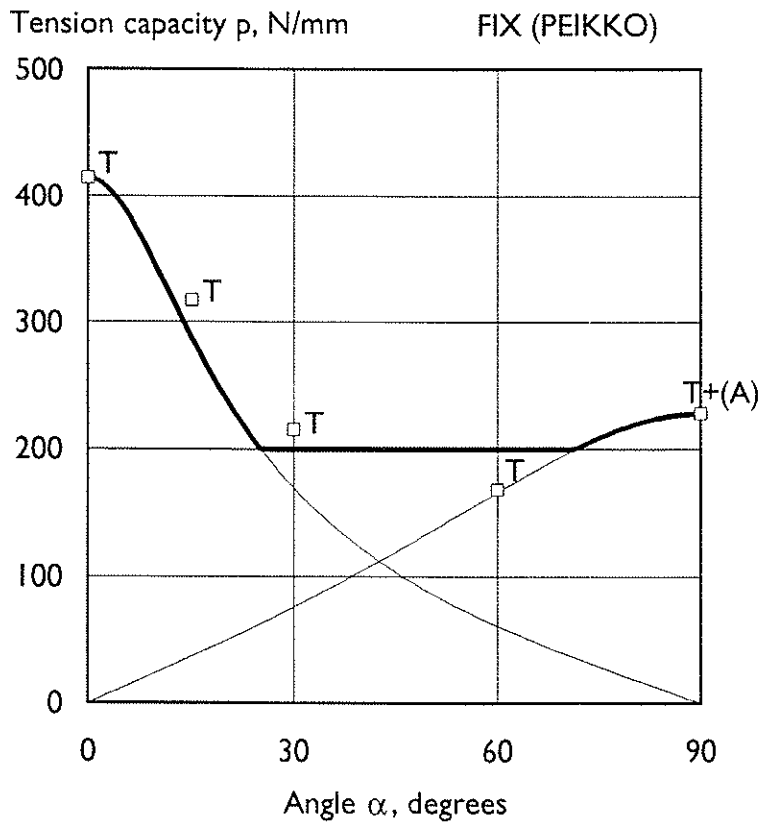


Figure B10



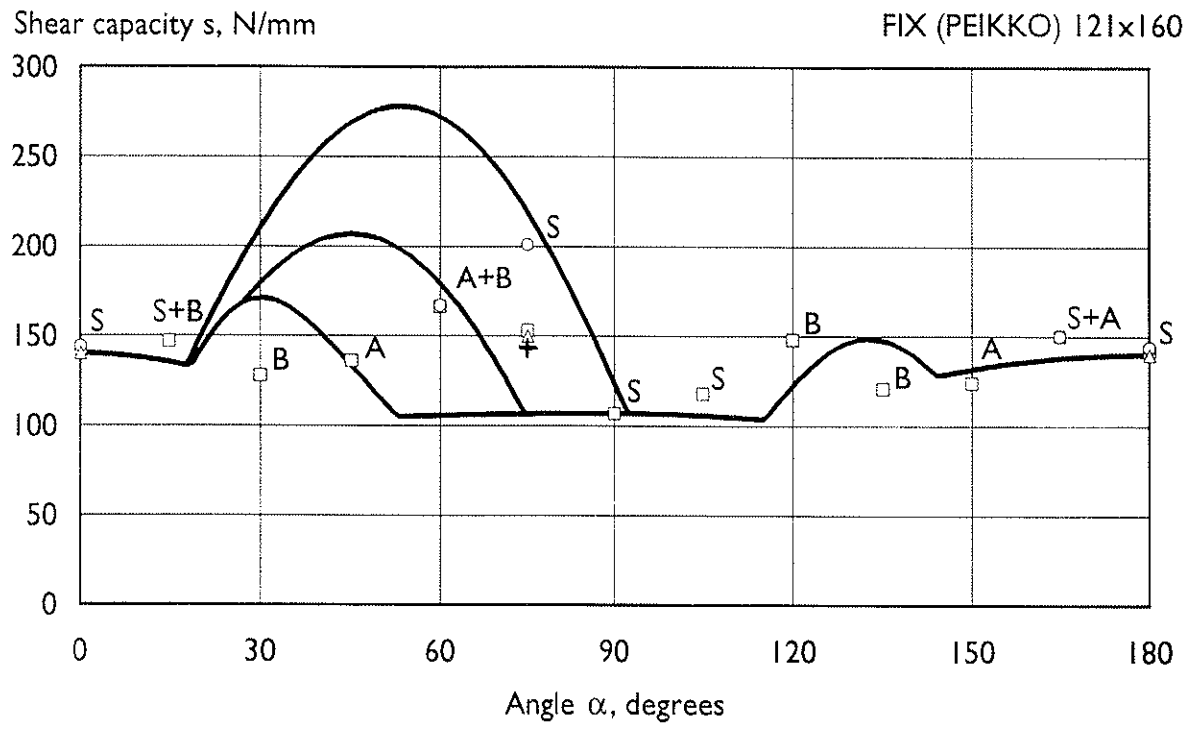


Figure B11

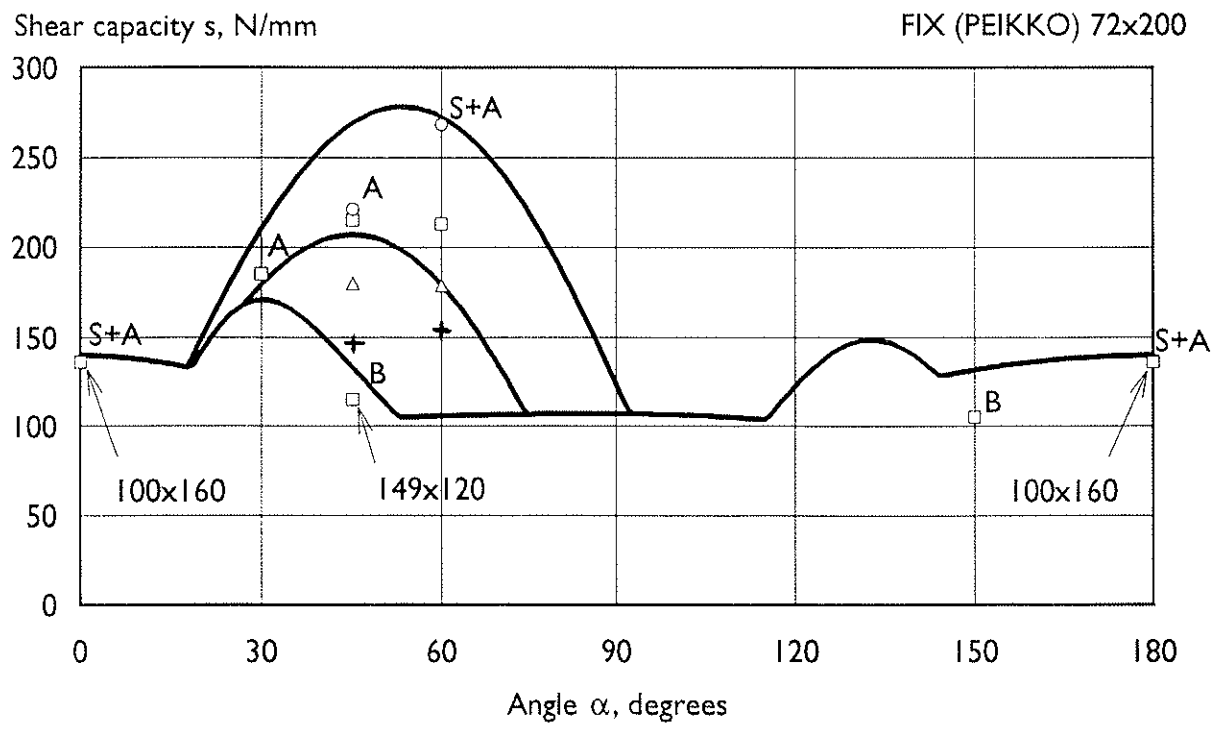


Figure B12

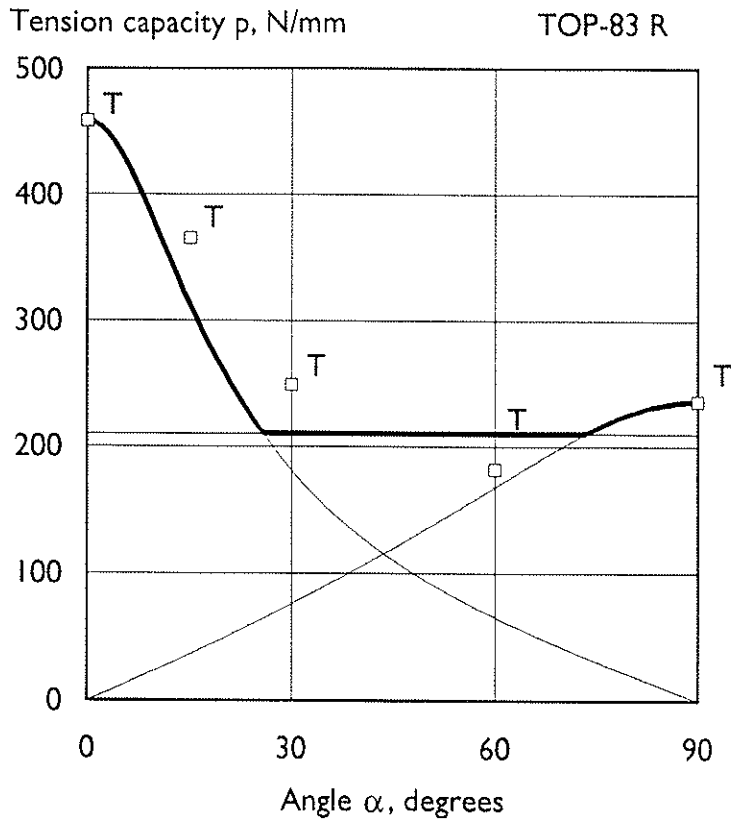


Figure B13

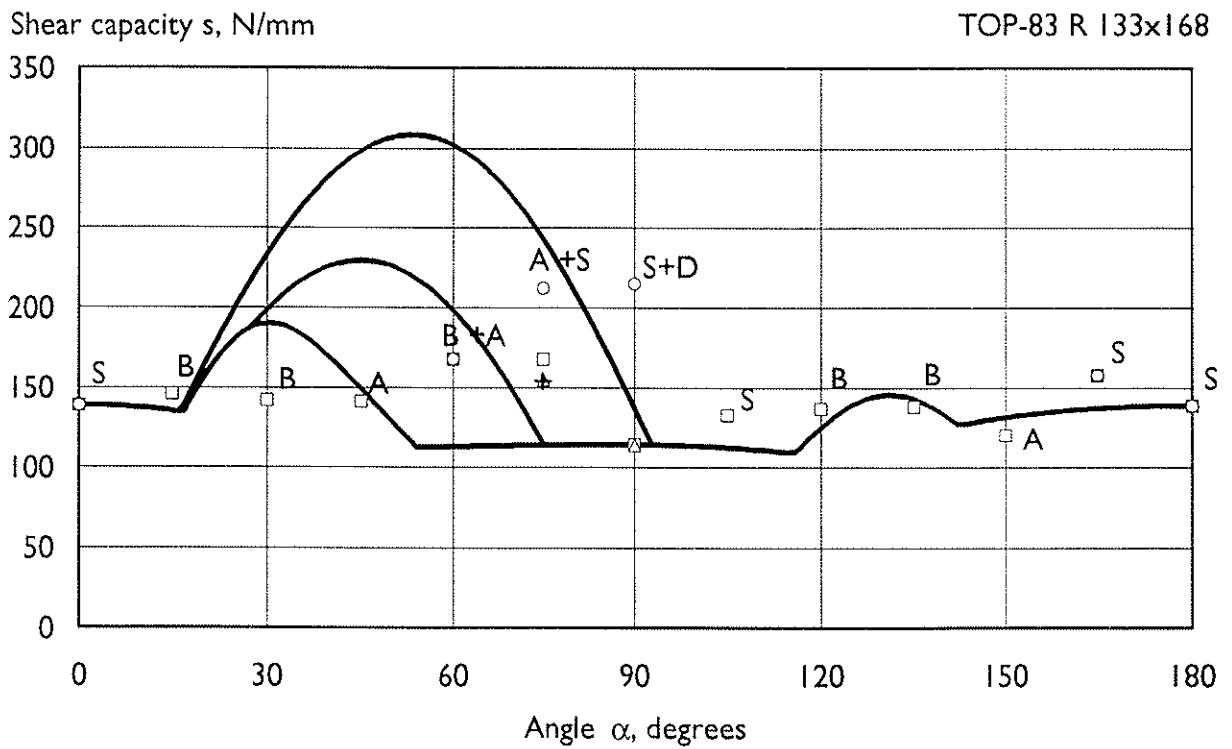


Figure B14

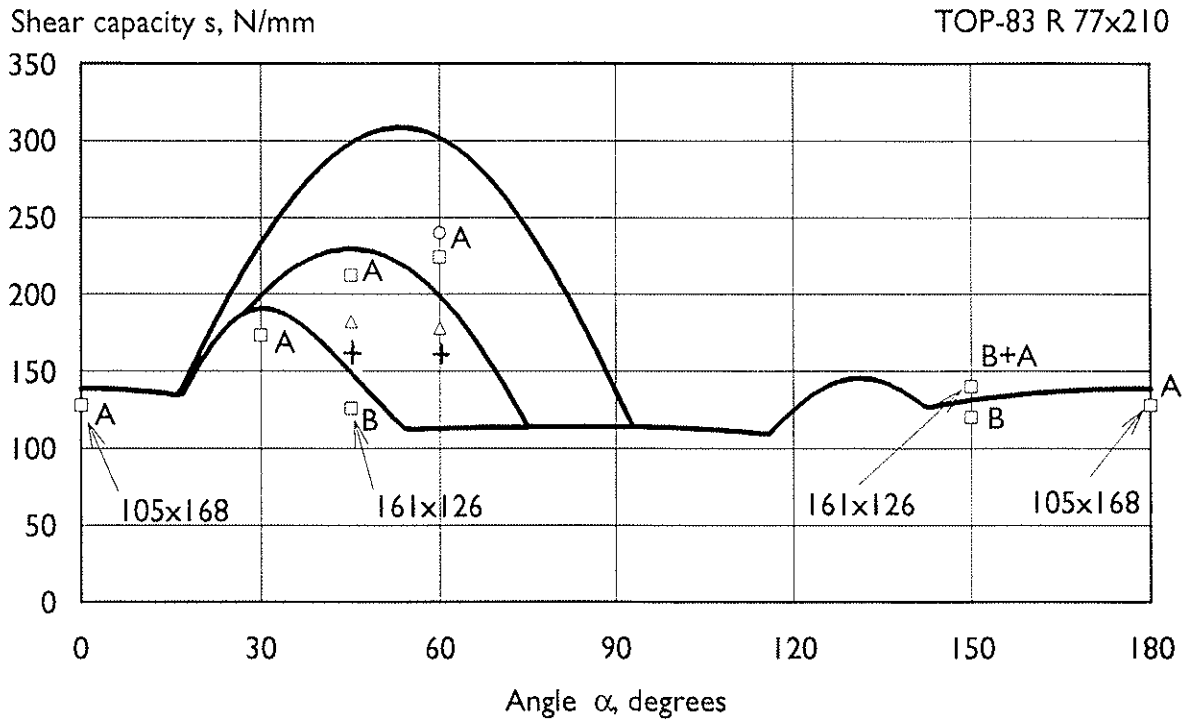


Figure B15

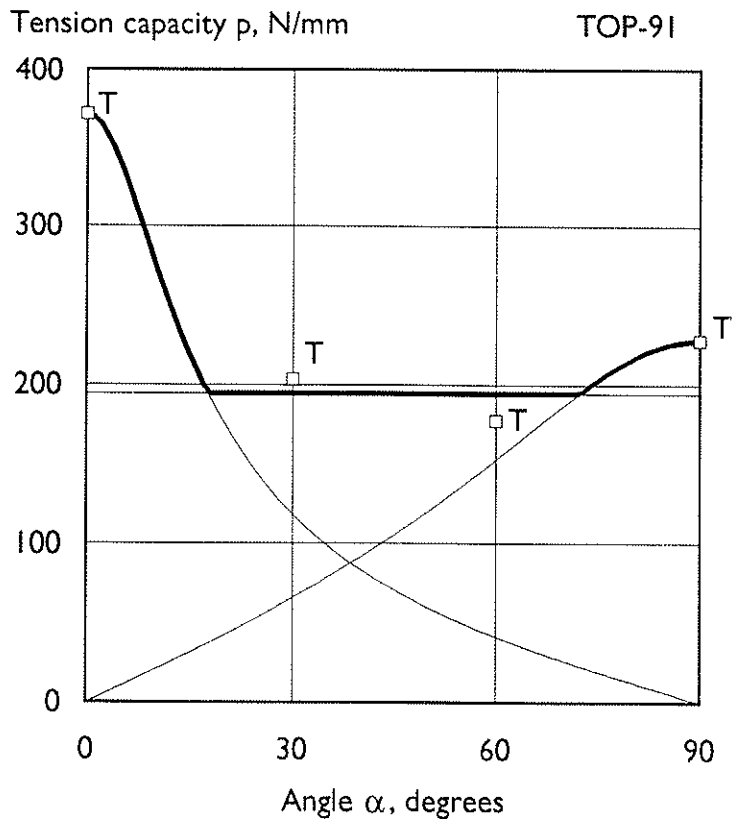


Figure B16

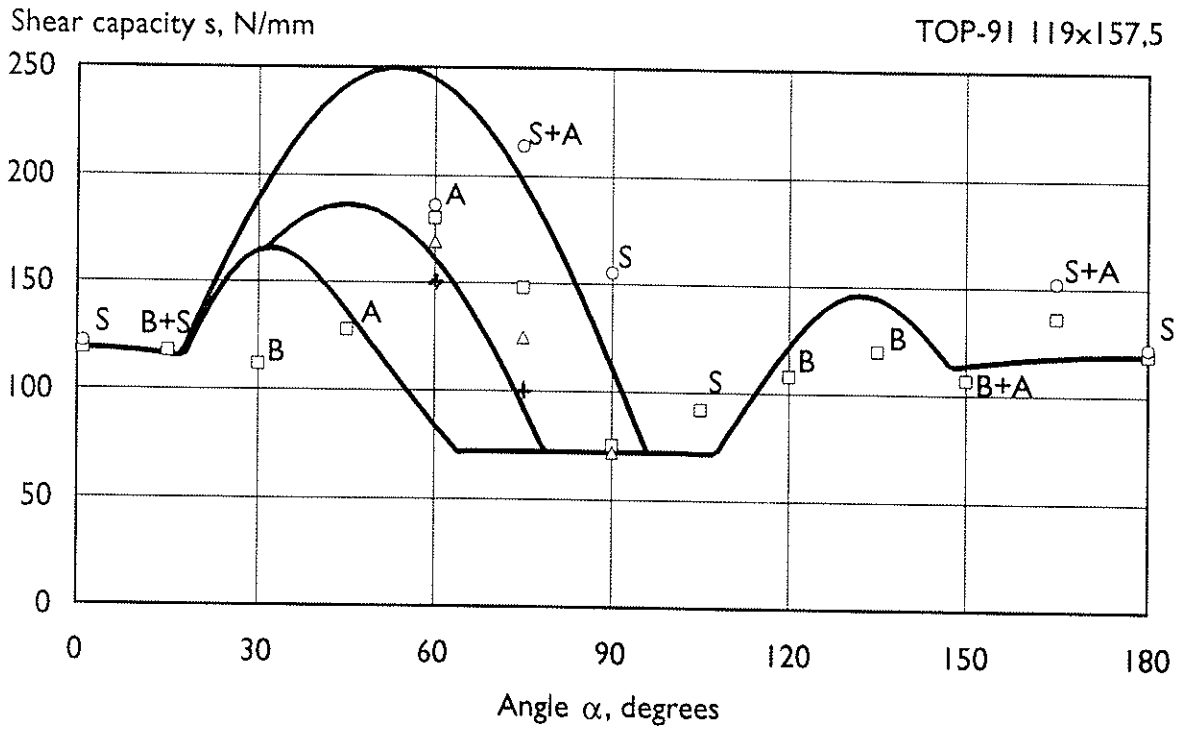


Figure B17

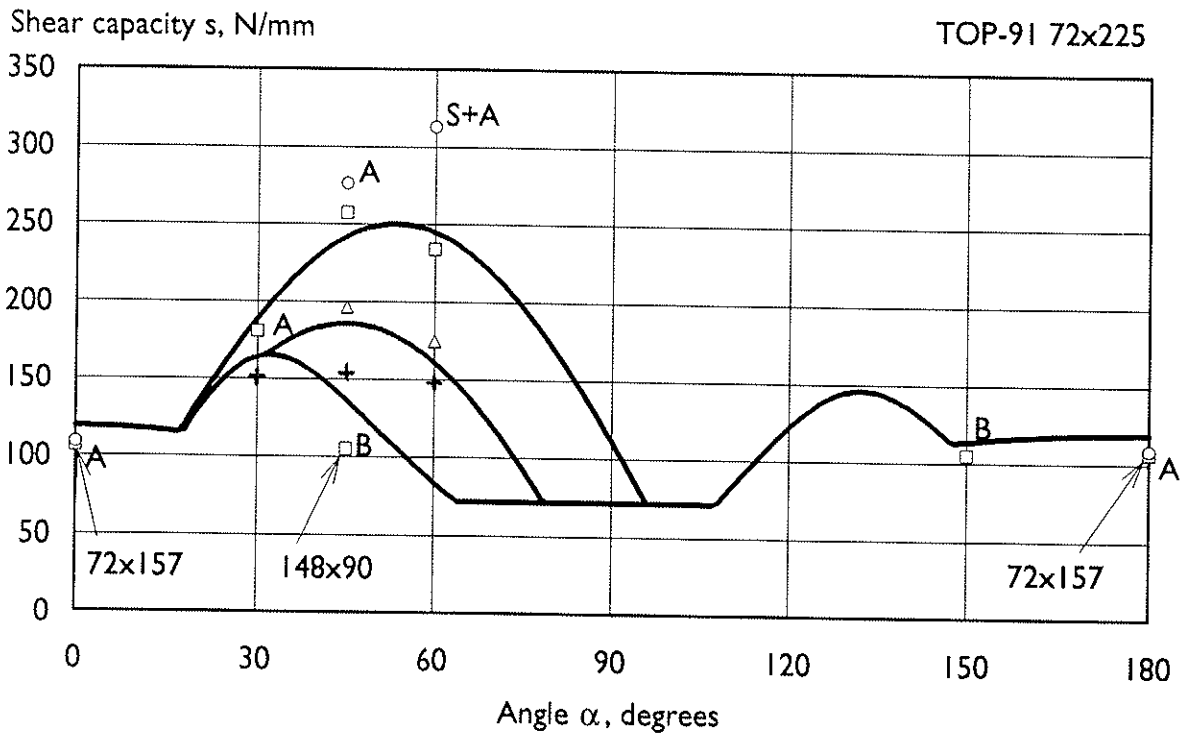


Figure B18

**INTERNATIONAL COUNCIL FOR BUILDING RESEARCH STUDIES AND DOCUMENTATION**  
**WORKING COMMISSION W18 - TIMBER STRUCTURES**

**TESTING METHOD AND DETERMINATION OF BASIC WORKING LOADS**  
**FOR TIMBER JOINTS WITH MECHANICAL FASTENERS**

by

Y Hirashima  
Shizuoka University  
F Kamiya  
Forestry and Forest Products Research Institute  
Japan

**MEETING TWENTY - FOUR**

**OXFORD**

**UNITED KINGDOM**

**SEPTEMBER 1991**



## CONTENTS:

### Preface

#### 1 General

- 1-1 Scope
- 1-2 Categories of joints
- 1-3 Scope of testing
- 1-4 Sampling of fasteners and timber
- 1-5 Configuration and dimensions of test specimen
- 1-6 Number of test specimen
- 1-7 Loading method
- 1-8 Measuring method of load and displacement
- 1-9 Recording of load and displacement

#### 2 Testing method for lateral resistance

- 2-1 Category A joints
- 2-2 Category B joints
- 2-3 Category C joints(Nail plates or nail-on-plates)

#### 3 Testing method for withdrawal

- 3-1 Test specimen
- 3-2 Testing method

#### 4 Derivation of basic working loads

- 4-1 Purpose A testing
- 4-2 Purpose B testing
- 4-3 Nail plates

Appendix 1 Species group and its specific gravity assigned

Appendix 2 Determination of number of test specimen by non-parametric method

Appendix 3 Method of recording

Appendix 4 K value when calculating 95% lower tolerance limit with 75% confidence

Appendix 5 Determination of lower tolerance limit by non-parametric method

## Preface

This paper is intended to introduce the methods for testing and derivation of working loads of timber joints with mechanical fasteners prepared by the authors and discussed by the Committee on Timber Structures of Architectural Institute of Japan. This standard has already been reviewed by the Committee and has been published as a part of 'Standard for Structural Calculation of Timber Structures(1988)'.

Its purpose is to provide standard procedures for testing timber joints with particular mechanical fasteners. It also provides standard methods for determination of basic design information for use in the application of mechanical fasteners in timber structures.

### 1 General

#### 1-1 Scope

This standard defines categories of mechanical fasteners, specifies methods of testing joints incorporating mechanical fasteners, and describes general procedures for the determination of basic working loads for timber joints using the test results. The alternative methods other than ones specified by this standard may be employed if the use and required performance of the relevant fasteners are specifically determined and the methods for testing and determination of basic values for joints are already established and available.

#### 1-2 Categories of joints

For the convenience of testing joints are classified into the following three categories:

Category A Joints- joints with fasteners such as nails, staples and screws in which the fasteners may be subjected either lateral or axial loading or both(Fig.1).

Category B Joints- joints with fasteners other than nails, staples or screw, acting as dowels or the like capable of transferring load from the face of one joint member to the face



of another(Fig.2). These fasteners usually require to be set in predrilled holes or in precut grooves or, if toothed, to be placed between the members which are subsequently pressed together to effect the joint.

Category C Joints- joints with fasteners acting as gusset or splice plates capable of transferring load from the face of one member to the face of another, the two faces involved lying in the same plane(Fig.3). Such fasteners usually of flat steel plate either predrilled to allow nails to be driven through them into the timber members, or with attached teeth formed from the parent metal, the toothed plates being pressed into the timber members to form the required joint.

### 1-3 Scope of testing

Scope of testing shall be determined according to the purpose of testing as follows:

Purpose A testing- to determine design loads for particular or limit number of species of timber.

Purpose B testing- to determine design loads for general species of timber, or to know the influence of the factors on joint performance.

### 1-4 Sampling of fasteners and timber

(i) Fasteners- Fasteners selected for test purpose shall be unbiased representative of commercial production, i.e. fasteners shall be a random selection of the particular type, make and size of fastener.

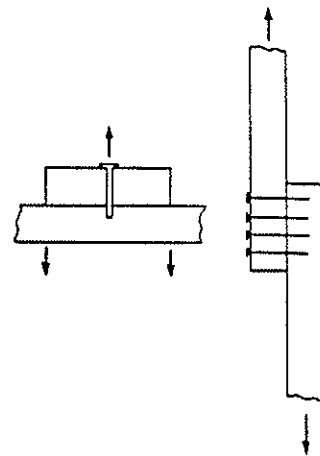


Fig.1 Category A joints

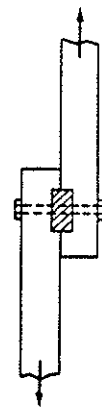


Fig.2 Category B joints

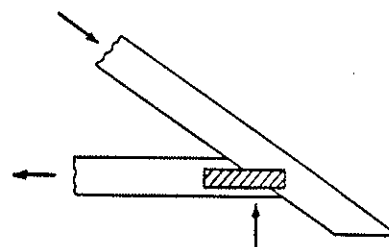


Fig.3 Category C joints

(ii) Timber- Timber for test shall be selected according to the purpose of testing.

Purpose A testing- Material for testing shall be selected in such a manner that the mean value of specific gravity of main member and side member are equal or less than that generally assigned or specified for the relevant species.\*

Purpose B testing- Species for test purpose shall be selected from the species group J1, J2 and J3 to have a wide range of specific gravity for testing materials.\*\*

Mean value of specific gravity of each species for testing materials shall be as close as possible to the assigned one. Main and side member (except other materials than timber) of joint shall be same species, and where possible, should be cut from the same sawn timber.

Difference of specific gravity between main and side member shall be equal or less than 5%.

Moisture content of timber shall be adjusted according to the test purpose.\*\*\*

#### 1-5 Configuration and dimensions of test specimen

Configuration of test specimen shall be determined considering the practical use of fasteners, purpose of testing, method of testing and failure mode of the joint. Dimensions of test specimen shall be determined in such a manner that the end or edge distance and spacing of fasteners are minimum in practical use.

-----  
\* The mean value for species may be referred from some publications e.g. 'Handbook of Wood Industries(1982)'.  
-----

\*\* It is recommended that one or more species is selected from each species group J1, J2 and J3. Specific gravity for testing materials shall not be biased to get unbiased correlation with specific gravity.

\*\*\* Moisture content shall be 10 to 15% for testing in the dry condition, and equal or more than 30% for testing in green condition.

1-6 Number of test specimen

A minimum of twelve withdrawal test shall be made under any one of set of conditions. For lateral resistance test, number of testing shall not be less than ten for purpose A testing, and shall not be less than six under any set of conditions for purpose B testing.\*

1-7 Loading method

Loading device shall have enough capacity so that load is applied continuously up to the maximum of the joint strength. Adequate self-alignment shall be prepared in loading devices where required.\*\*

Test specimen, at least one specimen under any one of set of conditions, shall be loaded repeatedly. Loading level of repetition shall be of  $1/2P$  ( $P$  is working load predicted),  $P$  and  $3/2P$ , in addition to those,  $-1/2P$ ,  $-P$  and  $-3/2P$  for fully reversed cyclic loading. Repetition of each loading level shall be at least two (see Fig.4).\*\*\*

-----  
\* Number of test specimen shall be determined in accordance with adequate lower tolerance limit with appropriate confidence level when the characteristic value is estimated using order statistics where the distribution form of population of joint strength might not be determined (See Appendix 2).

\*\* Loading method which can accurately determined the ultimate strength of joint shall be employed considering the failure mode of the joint. Self-alignment should be prepared at both loading sides of the test specimen for tension loading, and at one loading side for compression loading.

\*\*\*

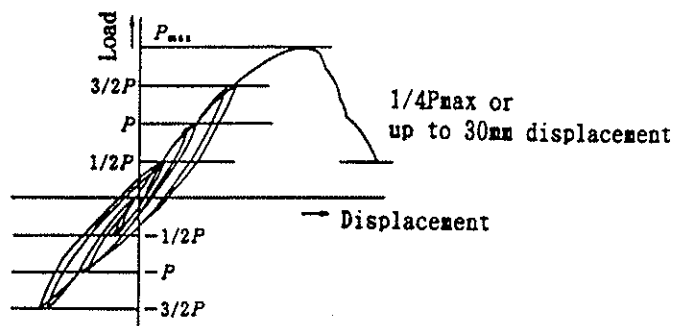


Fig.4 Schedule for loading and finishing point of testing

Load shall be applied continuously to the reducing load level of 1/4 of maximum load. If the load does not reduce to such load level load shall be applied up to the relative displacement 30 mm between main and side member.

1-8 Measuring method of load and displacement

Load and displacement shall be measured by using the adequate instruments calibrated.

Relative displacement shall be measured between main and side member.

1-9 Recording of load and displacement

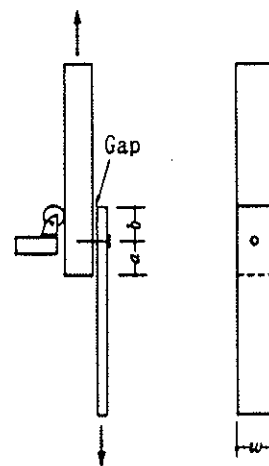
Load and displacement shall be recorded using the method which has high accuracy and enough information(See Appendix 3).

2 Testing method for lateral resistance

2-1 Category A joints

(i) Generally, testing shall be made in both cases of parallel to grain direction(Type A test) and perpendicular to grain direction(Type B test).\*

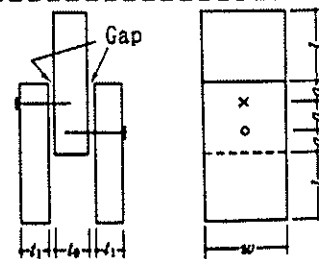
(ii) The side member should be cut from the same sawn timber as main member, where the member of joint is comprised by timber only.



a, b=Minimum allowable end distance  
 $w=14D$ (D:Diameter of fastener)  
 For loading perpendicular to grain direction of side member, the width of side member shall be enough to prevent splitting itself.

Fig. 5 Type A test  
 (Loading parallel to grain)

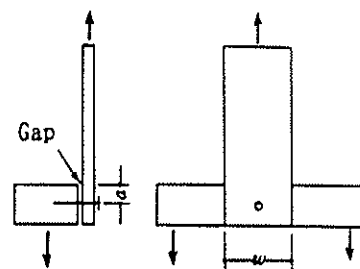
\* Compression type loading may be employed where the load reaches to maximum value with the failure mode of withdrawal or punching-out before any split of timber occurs(Fig.6).



$l_0 + l_1 = L$   
 $w = 14D$   
 $l \geq 25\text{mm}$   
 $a = 20D$   
 (L:Length of fastener)  
 (D:Diameter of fastener)

Fig. 6 Compression type loading

(iii) Fasteners shall be driven normal to the surface of the side member.  
 (iv) Gap of less than 0.8mm shall be prepared between main and side member to eliminate the friction.\*  
 (v) The load shall be applied continuously throughout the test at a rate of cross-head movement of 1.5mm±25% per minute.



a=Minimum allowable edge distance  
 $w=14D$

Fig.7 Type B test (Loading perpendicular to grain)

(vi) The moisture contents and specific gravity of the members comprising each joint shall be determined just before or immediately after the testing.  
 (vii) The test report shall include the following:

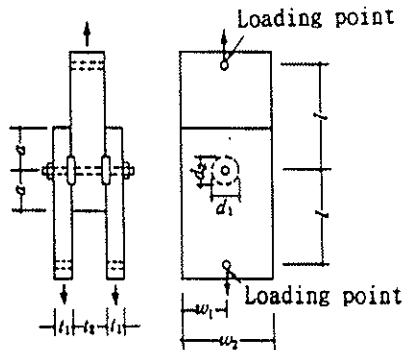
- a. Sampling method for testing materials.
- b. Dimensions and quality of fasteners.
- c. Specific gravity and moisture content of timber.
- d. Ultimate strength of the joint.
- e. Load-displacement curve of each test joint.
- f. A description of dimensions of the test specimens, and that relating to the testing method such as loading, measuring and recording method.
- g. Time required for testing and/or loading head speed.
- h. Any special features that may have had some bearing on the results, particularly any departures from the standard test procedure.

#### 2-2 Category B joints

(i) Generally, testing shall be made in both cases of parallel to grain direction (Type A test) and perpendicular to grain direction (Type B test).

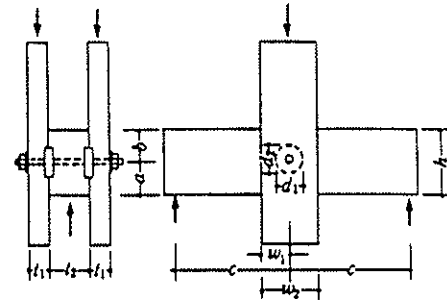
-----

\* Since the friction occurring between members diminishes over time in practice, the influence of friction shall be eliminated at test.



$l > w_2$   
 a=Minimum allowable end distance  
 $w_1$ =Minimum allowable edge distance  
 $d_1, d_2$ =Dimensions of fastener  
 $t_1, t_2$ =Minimum thickness in practical use  
 For steel side plates minimum allowable thickness for joint strength predicted.

Fig. 8 Type A test (Loading parallel to grain)



a=Minimum allowable loaded edge distance  
 $w_1$ =Minimum allowable unloaded edge distance  
 $d_1, d_2$ =Dimensions of fastener  
 $t_1, t_2$ =Same as type A test  
 $c \geq 1.5w_2$  and  $c \geq a + 1.2d$  ( $d: \max(d_1, d_2)$ )  
 Shear stress of joint member shall not exceed the allowable stress.

Fig. 9 Type B test (Loading perpendicular to grain)\*

(ii) Washers, diameter of bolt, diameter of predrilled hole, precut grooves etc. shall be conformed to the description specified by fastener makers.

(iii) Load shall be applied at a rate of cross-head movement of  $1.5\text{mm} \pm 25\%$ .

-----  
 \* Shear stress of joint member calculated from the following formula shall not exceed the allowable stress for short duration of load:

$$= k \frac{3Q}{2 t_2 h_e}$$

where Q : Shear force

k : for  $c/h \geq 5$   $k=2/3$

for  $c/h < 5$   $k=h/h_e$

$h_e = a$  (for bolts)

$= a + d_2/2$  (for connectors)

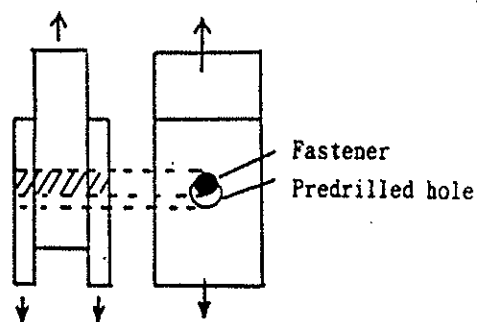
- (iv) Friction between main and side member shall be eliminated.\*
- (v) For one-way loading adequate adjustment for joint shall be made where clearance between fasteners and predrilled holes or precut grooves may be recognized.\*\*
- (vi) The moisture contents and specific gravity of the members comprising each joint shall be determined just before or immediately after the testing.
- (vii) The test report shall include the following:
  - a. Sampling method for testing materials.
  - b. Dimensions and quality of fasteners.
  - c. Specific gravity and moisture content of timber.
  - d. Ultimate strength of the joint.
  - e. Load-displacement curve of each test joint.
  - f. A description of dimensions of the test specimens, and that relating to the testing method such as loading, measuring and recording method.
  - g. Time required for testing and/or loading head speed.
  - h. Any special features that may have had some bearing on the results, particularly any departures from the standard test procedure.

2-3 Category C joints(Nail plates or nail-on-plates)

Further description is omitted.

-----

\* Relaxation of stress occurred in main and side member caused by tightened bolt takes place over time. Influence of friction between members, therefore, shall be eliminated by using adequate method such as using antifriction material, preparation of gap between members, tightening bolt by hand etc.



\*\* Fig. 10 Adjustment of clearance

### 3 Testing method for withdrawal

This procedure provides for direct withdrawal tests for fasteners used in category A or B joints.

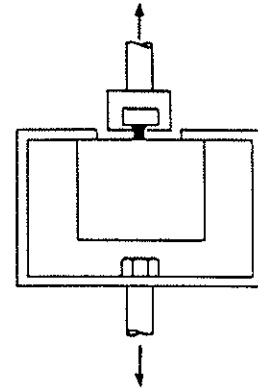


Fig. 11 Withdrawal test

#### 3-1 Test specimen

Dimensions of test specimen shall be such that the end and edge distance are enough to prevent splitting at driving fasteners.

Fasteners shall be driven into the timber to a penetration of 70% of fastener length. For thin wood based materials fasteners shall be entirely driven remaining the grip length for test device of 15mm.

#### 3-2 Testing method

(i) Test shall be done within one hour after driving fasteners.

(ii) Load shall be applied continuously at a rate of cross-head movement of  $2.5\text{mm} \pm 25\%$  per minute.

(iii) The moisture contents and specific gravity of the members comprising each joint shall be determined just before or immediately after the testing.

(iv) The test report shall include the following:

- a. Sampling method for testing materials.
- b. Dimensions and quality of fasteners.
- c. Specific gravity and moisture content of timber or wood based materials.
- d. Load at failure occurred or observed.
- e. Ultimate strength.
- f. Load-displacement curve of each test fastener.
- g. A description of dimensions of the test specimens, and that relating to the testing method such as loading, measuring and recording method.
- h. Time required for testing and/or loading head speed.

### 4 Derivation of basic working loads



The methods to be adopted in deriving basic working loads for fasteners of various categories from the test data based on the ultimate strength of joint are given in Clauses 4-1, 4-2 and 4-3 below.\*

#### 4-1 Purpose A testing

Basic working load shall be calculated as-

$$F_a = \frac{T_L}{a b}$$

where  $F_a$  : Basic working load for permanent duration of load

$T_L$  : Five percentil value of the joint strength.\*\*

a : Safety factor

b : Adjustment factor for permanent duration of load

-----  
\* Methods described here are general standards. Alternative methods may be employed if the use and required performance of the relevant fasteners are specifically determined and standards of estimation are already established like nail plates.

\*\* 5%-ile vale of joint strength shall be determined generally as a estimate of 95% lower tolerance limit with confidence of 75% assuming strength distribution of population as log-normal.

$$T_L = \bar{x} - K \cdot s$$

where  $T_L$  : Tolerance limit

$\bar{x}$  : Mean value of ultimate strength of the joint obtained from the test

s : Standard deviation of test data

K : Constant depending on number of test(See Appendix 4)

Safety factor should be 1.5 to 2.0.

Adjustment factor for permanent duration of load usually should be 2.0.

Considerable distribution form other than log-normal may be used where determined to calculate the 5%-ile value. If it is impossible to determine the distribution form the 5%-ile value shall be calculated by using order statistics as a estimate of 95% lower tolerance limit with 75% confidence( See Appendix 5).

4-2 Purpose B testing

Basic working loads shall be calculated from the following formula for each species or each species group:

$$F_a = \frac{T_p}{a b}$$

where  $T_p$  : 5%-ile value of ultimate strength of joint determined by considering the variability of parameter influencing strength like specific gravity of timber in species or in species group.  $T_p$  should be obtained as follows:

In this clause specific gravity of timber is used as a parameter. At first regression line is calculated for specific gravity vs ultimate strength of joint.

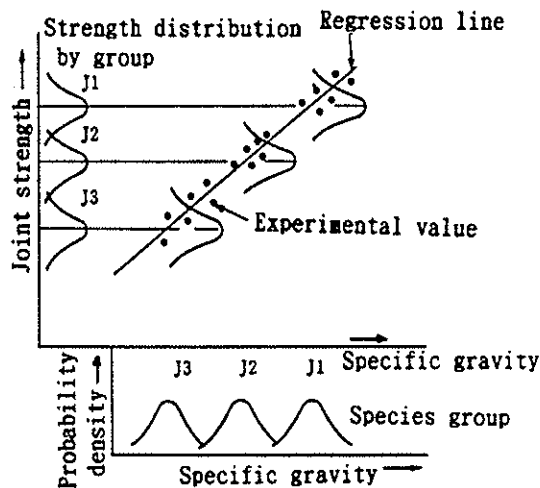


Fig.11 Simulation for obtaining distribution of strength

Then simulation calculation is done\*, or the coefficient of

-----  
 \* Coefficient of variation of 10 % may be used if data of variation for specific gravity is not available.

Monte Carlo simulation may be used for simulation calculation.

variation is calculated for the distribution of strength\*, to obtain 5%-ile value for each distribution.

4-3 Nail plates

Further description is omitted.

-----  
\* Coefficient of variation should be calculated in accordance with ASTM D2555.

Appendix 1 Species group and its specific gravity assigned.

-----

Species group	Species	Specific gravity*
J1	Douglas-fir, Larch, Kuromatsu, Akamatsu, Tsuga	0.50
J2	P.O.Cedar, Western hemlock, Hiba, Hinoki, Momi	0.44
J3	Todomatsu, Ezomatsu, Benimatsu, Spruce, Cedar, Western red cedar	0.37

-----

\* Mean value of specific gravity of the lowest species. Specific gravity is based on airdry weight and airdry volume at moisture content 15%.

Appendix 2 Determination of number of test specimen by non-parametric method.

If it is impossible to determine the distribution form the lower tolerance limit shall be calculated by using order statistics.

Number of test specimen shall be conformed to the following table when calculating 95% lower tolerance limit with 75% confidence.

Table Minimum number of test specimen n when determining the data of r-th order from minimum value as a tolerance limit.

r	1	2	3
n	27	53	78

Appendix 3 Method of recording.  
Further description is omitted.

Appendix 4 K value when calculating 95% lower tolerance limit with 75% confidence.

Number of test	K
6	2.336
7	2.250
8	2.190
9	2.141
10	2.103
11	2.073
12	2.048
15	1.991
20	1.933
25	1.895

Appendix 5 Determination of lower tolerance limit by non-parametric method.

The first, second or third lowest value shall be determined as the 5%-ile value using the test results satisfying the number of test specimen specified in Appendix 2.

INTERNATIONAL COUNCIL FOR BUILDING RESEARCH STUDIES AND DOCUMENTATION  
WORKING COMMISSION W18 - TIMBER STRUCTURES

ANCHORAGE CAPACITY OF NAIL PLATE

by

J Kangas  
Technical Research Centre of Finland (VTT)  
Laboratory of Structural Engineering  
Finland

MEETING TWENTY - FOUR

OXFORD

UNITED KINGDOM

SEPTEMBER 1991



## INTRODUCTION

In CIB-W18A meeting in Lisbon a proposal was introduced for design code for nail plates, which is based on the Norwegian practice [1] and [2]. In Finland we have another practice, which is based directly on the test results and which we want to introduce with its history.

In the 1960's and 70's, in nailplate approvals the design values for anchorage strength were given by one curve like in the proposal mentioned above. In the beginning of 80's, a complete test series for one Finnish nailplate were carried out in VTT using the new test method of UEAtc [3]. Later many other nailplates were tested because of renewing all approvals using a detailed testing method based on the experiences got by the preceding tests [4].

Test results indicated the need for more exact ways to give design values for anchorage stresses. That was introduced in Beit Oren in 1985 [5]. Since then the approvals for nailplates of different types (16 in all) have been given by the same method.

## TESTING OF ANCHORAGE STRENGTH

Tests for anchorage strength  $f_{a\alpha}$  have been made in angles of  $\alpha = 0^\circ, 30^\circ, 60^\circ$  and  $90^\circ$ , when the load is in the grain direction ( $\beta = 0^\circ$ ).

Tests for anchorage strength  $f_{a\alpha\beta}$  (T-joint) have been made in angles

- a)  $\alpha = 0^\circ; \beta = 45^\circ$  and  $90^\circ$
- b)  $\alpha = \beta = 90^\circ$

$f_a$  is anchorage strength pr. area  
 $f_{a\alpha\beta}$  is anchorage strength in different angles of  $\alpha$  and  $\beta$   
 $\alpha$  is the angle between the force and main direction of nailplate  
 $\beta$  is the angle between the force and grain direction

The same angles  $\alpha$  and  $\beta$  are used to calculate anchorage capacity of nailplate.

Anchorage strength of different types of nailplates are depending on the directional angles  $\alpha$  and  $\beta$  in many ways. The following properties have effect on the strength properties are

- shape, number and size of protrusions (nails) punched from one hole
- their mutual situation
- stepwise situation of nails in lines
- threading of nails
- material of nailplate

#### ANCHORAGE DESIGN STRESSES

In Finland the design values of anchorage stress  $f_{\alpha\beta d}$  for different combinations of angles  $\alpha$  and  $\beta$  have been given in two groups of lines (equations) based on test results. One is for maximum (1) and the other for minimum values (2), when force is across the grain. Other values will be obtained by linear interpolation.

As an example the allowable anchorage stresses  $f_{ad}$  in MPa for the most commonly used nailplate in Finland are given as follows.

$$f_{\alpha} = 1,25 - 0,002 * \alpha, \text{ when } \beta = 0^{\circ} \text{ and } \alpha \leq 60^{\circ} \quad (1 \text{ a})$$

$$f_{\alpha} = 1,85 - 0,012 * \alpha, \text{ when } \beta = 0^{\circ} \text{ and } \alpha > 60^{\circ} \quad (1 \text{ b})$$

$$f_{\beta} = 1,25 - 0,008 * \beta, \text{ when } \beta \leq 45^{\circ} \text{ and } \alpha = 0^{\circ} \quad (2 \text{ a})$$

$$f_{\beta} = 0,89, \text{ when } \beta \geq 45^{\circ} \text{ and } \alpha = 0^{\circ} \quad (2 \text{ b})$$

$$f_{\alpha\beta} = 0,89 - \alpha/300, \text{ when } \beta > 45^{\circ} \text{ and } \alpha \leq 45^{\circ} \quad (2 \text{ c})$$

$$f_{\alpha\beta} = 0,74, \text{ when } \beta > 45^{\circ} \text{ and } \alpha > 45^{\circ} \quad (2 \text{ d})$$

In addition, the values of equations above are given in **table 1** and **figure 1**.



**Table 1.** Allowable anchorage stresses  $f_{a\alpha\beta}$  (MPa). Intermediate values will be got by linear interpolation .

$\alpha$	$\beta$	0°	15°	30°	45°-90°
0°		1,25	1,13	1,01	0,89
45°		1,16	1,02	0,88	0,74
60°		1,13	1,00	0,87	0,74
90°		0,77	0,76	0,75	0,74
		$f_{a\alpha}$	$f_{a\alpha 15}$	$f_{a\alpha 30}$	$f_{a\alpha 45}$

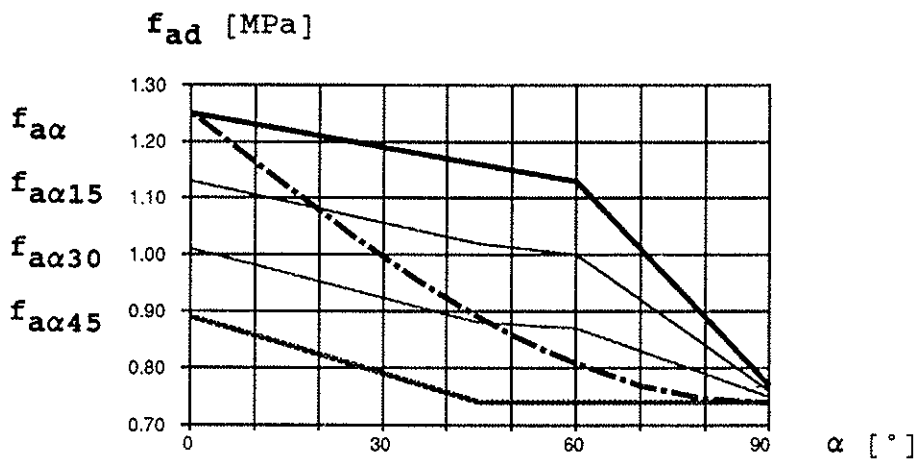


Figure 1. Maximum values of anchorage design stresses  $f_{a\alpha}$  in equations (1) when  $\beta = 0^\circ$  (force in grain direction), minimum values of anchorage design stresses  $f_{a\alpha 45}$  from equations (2 c) and (2 d) (angle between force and grain direction  $\beta \geq 45^\circ$ ) and in the intervals of  $\beta = 15^\circ$  interpolated values. The dotted dash line is according to the proposal for Eurocode 5 in [2].

The designers who have made the computer programs for nailplate structures and used them in designing say that the system is easy to use.

The pattern of anchorage strength in variable combinations of angles  $\alpha$  and  $\beta$  differs in many cases much from the one curve expression in the proposal for Eurocode 5 [2], which can be seen in **figure 2**. The same situation may be in the case of plate capacity.

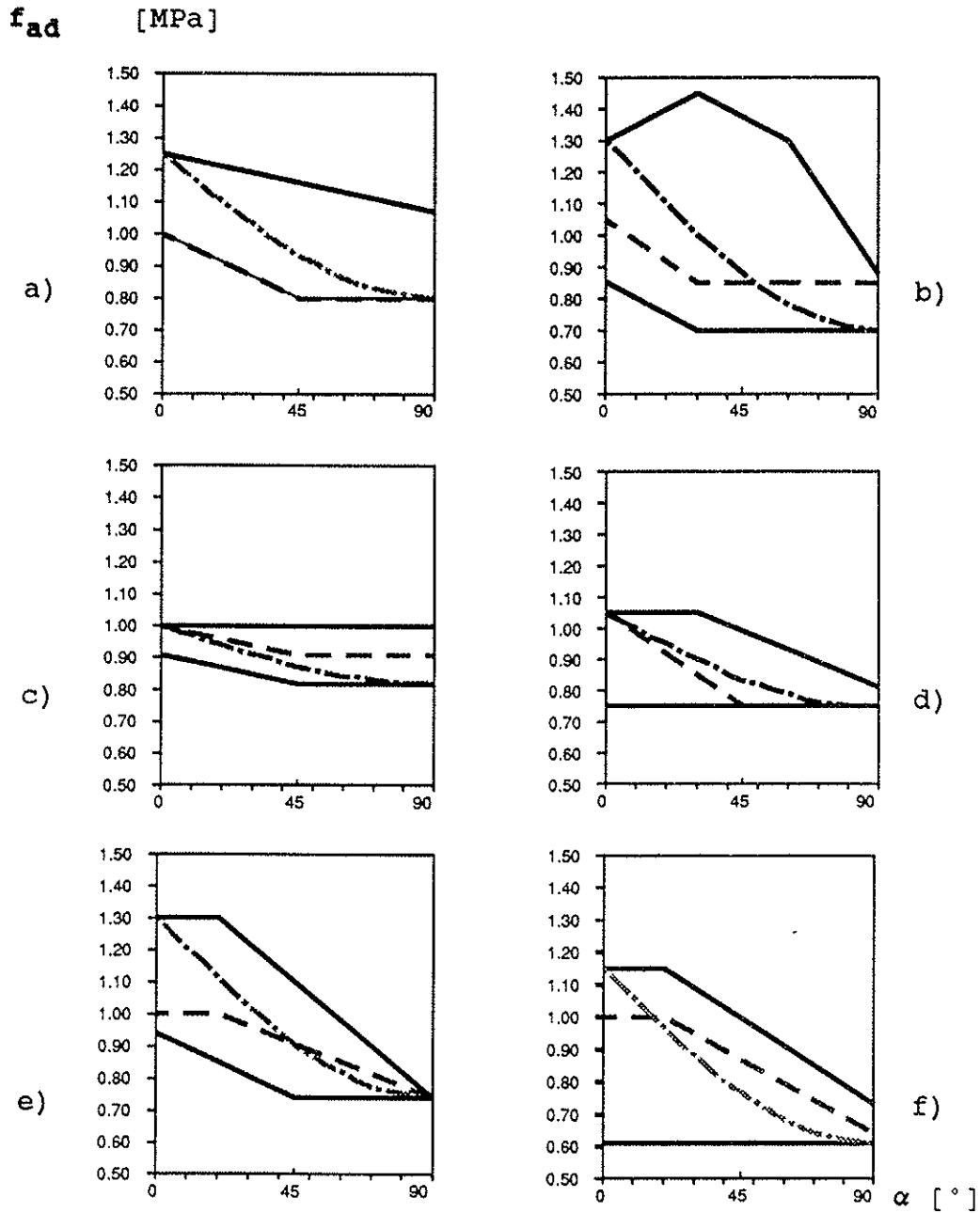


Fig. 2. Maximum and minimum curves of anchorage design stresses  $f_{ad}$  according to the test results and Nordic curve (dotted dash line) proposed for Eurocode 5 in the case of different types of nailplates. Broken line is the maximum curve of anchorage design stresses  $f_{avd}$  in the case of pure shear.

- a) "Common" nailplate with threaded nails
- b) Nailplate with 3 threaded nails punched from the same hole.
- c) Nailplate with double short and normal long nails
- d) Nailplate with 2 short nails punched from the same hole.
- e) "Common" nonhomogeneous nailplate
- f) "Common" thick nailplate

## JOINTS LOADED IN SHEAR

Based on test results separate lower design values  $f_{avd}$  have been given for calculating anchorage capacity in joints where nailplate is loaded in shear. The eccentricity moment is not needed to be taken into account in calculating anchorage capacity.

Lines of maximum anchorage design stresses  $f_{avd}$  are to be seen in figure 2. The effect of buckling of the nailplate on the strength of joint has been considered already in the arrangements of shear tests.

## RESULTS OF QUALITY CONTROL

Nailplate trusses chosen from production are loaded to the failure in the Finnish quality control system of nailplate structures. When the cause of the failure in about 500 loaded trusses has been the loss of anchorage strength or plate strength, the calculated stresses have been in good accordance with the test results obtained in testing for approvals.

On the basis of large number of test results and practical experience in the use of our approvals we propose, that the method used in Finland for the design values for anchorage stresses should be accepted in Eurocode 5.

## PROPOSAL FOR EUROCODE 5

Anchorage stresses  $\tau_F$  from the force in equation (3.1 c) of [2] in different combination of angles  $\alpha$  and  $\beta$  can be chosen from the pattern of two empirical curves of  $f_{a\alpha\beta d}$  for cases where  $\beta = 0^\circ$  and  $\beta \geq 45^\circ$ . Intermediate values will be taken by linear interpolation.

$f_{a\alpha\beta d}$  is the anchorage design capacity pr. area in different combination of angles  $\alpha$  and  $\beta$   
 $\alpha$  is the angle between the force and main direction of nailplate  
 $\beta$  is the angle between the force and grain direction

## REFERENCES

- [1] Aasheim, E. & Solli, K. H., 1990, Proposal for a design code for nail plates, CIB-W18A meeting in Lisbon, paper 23-7-1.
  
- [2] Riberholt, H., 1990, Proposal for Eurocode 5 text on timber trussed rafters, Annex X.4, Strength verification of nail plate connections in timber trussed rafters, CIB-W18A meeting in Lisbon, paper 23-14-2.
  
- [3] UEAtc Testing Rule M.O.A.T. No. 16:1979: Rule for the ., Assessment of Punched Metal Plate Timber Fasteners
  
- [4] Kangas, J., 1985, A detailed testing method for nailplate joints, CIB-W18A meeting in Beit Oren, paper 18-7-4.
  
- [5] Kangas, J., 1985, Principles for design values of nailplates in Finland, CIB-W18A meeting in Beit Oren, paper 1

**INTERNATIONAL COUNCIL FOR BUILDING RESEARCH STUDIES AND DOCUMENTATION**  
**WORKING COMMISSION W18 - TIMBER STRUCTURES**

**ON THE POSSIBILITY OF APPLYING NEUTRAL VIBRATIONAL SERVICEABILITY  
CRITERIA TO JOISTED WOOD FLOORS**

by

I Smith

Y H Chui

Wood Science and Technology Centre

University of New Brunswick

Fredericton, N.B.

Canada

**MEETING TWENTY - FOUR**

**OXFORD**

**UNITED KINGDOM**

**SEPTEMBER 1991**



## ABSTRACT

Prior discussion in CIB-W18A has not clarified whether it is possible to apply vibrational serviceability criteria that are neutral with regard to construction material and structural configuration for floors. By means of examples, it is demonstrated that responses of joisted wood floors are too complex for correct quantification, at the design stage, of parameters that indicate acceptability. Applying arbitrary conditions for imposed mass, excitation and response limits, designers have a means of assessing relative suitabilities of candidate solutions. Candidates would satisfy other (static) design criteria. "Neutral" vibrational serviceability limits in design of joisted wood floors is an ideal that is not presently attainable.

## INTRODUCTION

The authors have discussed in CIB-W18A using the dual criteria of frequency-weighted root-mean-square acceleration,  $A_r$ , and fundamental natural frequency,  $f_0$ , as means of designing against annoying levels of vibration (Chui and Smith, 1987;1988). Specifically, they considered responses of joisted wood floors subjected to excitation by human footfalls. By contrast, Ohlsson (1988) expressed the opinion that a design method for floor vibration should be neutral with regard to construction material and structural configuration. Recently the authors published a study on the sensitivity of vibration response predictions for domestic floors with lumber joists to factors such as variability in stiffnesses and masses of joists, and dispositions of imposed masses (Chui and Smith, 1990). Conclusions from that study were:

1. The influence of random variability in joist stiffness and masses diminishes with any increase in the number of joists in a floor.
2. It is advantageous to use joists of lower grade but bigger cross section, when dynamic response governs suitability of a floor. This is because the increase in self weight helps to reduce response levels through inertia effects.
3. The presence of between-joists bridging and edge support results in lower and more uniform rms accelerations because of the relatively high degree of load-sharing occurring in the across joists direction.

The first conclusion demonstrates that for most practical cases mean joist properties can be used in floor analyses. The latter conclusions demonstrate that qualitative deductions can be made regarding best choice of materials and structural configuration, irrespective of whether absolute limits are placed on variables such as modal frequencies, peak velocity or acceleration.

This paper addresses the influence of modelling assumptions on parameters that indicate the acceptability of vibrational performances of floors. The objective is to establish feasibility of applying a set of "neutral" vibration serviceability criteria in the context of joisted wood floors.

## METHODS

The four sizes of wood I joists listed in Table 1 are used in sensitivity studies, because of their high stiffness-to-mass ratios which facilitates demonstration of special features of joisted wood floors. Properties and allowable spans are based on manufacturer's literature (Trus Joist Canada Ltd., 1989). Allowable spans reflect application of static strength and deflection checks, with the latter giving a degree of indirect control on annoying vibrations. Current practice recommended by the manufacturer is to use I joists without any between joists bridging in the interior of the span, so bridging is not included in situations considered.

Floor performance is characterised in terms of the fundamental natural frequency, and frequency-weighted rms acceleration following an impact. Both  $f_0$  and  $A_r$  predictions are based on a Rayleigh Ritz model developed and verified by Chui (1988). The weighting procedure used with the model is that specified in ISO 2631 (ISO, 1978). Rms acceleration refers to response at the centre of a floor due to an impact at that location. Accelerations are averaged over one second (Chui and Smith, 1987).

## RESULTS AND DISCUSSION

Table 2 shows how fundamental natural frequency and frequency-weighted rms acceleration vary between sizes of joists. The joists are used at spans deemed appropriate on the basis of static design criteria. It can be seen that the highest sensitivity in response parameters,  $f_0$  and  $A_r$ , is to the disposition of imposed mass. These results demonstrate that a balanced loading (uniformly imposed mass) tends towards a conservative estimate of  $A_r$  and an unconservative estimate of  $f_0$  for the range of floors covered in the table. If absolute quantities are used in design checks as limits on parameters such as frequency, velocity and acceleration it is necessary to model the various dispositions of imposed masses that may occur in service.

Results in Table 3 demonstrate that the fundamental natural frequency is relatively insensitive to the plan "shape" of the floor, if other variables are constant. However, rms acceleration is sensitive to changes in floor shape. This demonstrates the need to apply a frequency check and a peak velocity or acceleration check within vibrational response design criteria. The authors have previously shown that this conclusion is true for smaller span floors with lumber joists (Chui and Smith, 1988). Also demonstrated by Table 3 is that floor response is most sensitive to unbalanced arrangements of loads occurring in the across joists direction. Considering floor shape as a variable, it is clear that either balanced or unbalanced loading can lead to the upper bound estimate of  $A_r$ . Both span and width of a floor must be considered in design.

In situations discussed so far the magnitude of the total imposed mass was arbitrarily fixed at 50kg x floor area. Table 4 illustrates sensitivity of  $f_0$  and  $A_r$  to the amount



of imposed mass expressed as the ratio of imposed mass to self mass. Self mass refers to mass of the bare floor. It can be seen that both the response indicating parameters considered are very sensitive to the amount of loading applied to a floor. Thus if absolute limits are to be adopted within vibration response checks loadings must be known accurately. Using upper limit estimates of loads, as in ultimate limit states calculations, would not be an appropriate means of predicting the serviceability of a design solution. The objective is to be representative not conservative.

Table 5 shows how rms acceleration varies according to the shape and duration of the load function (impulse) causing a transient vibration in a floor. Sensitivity to the shape of the load function depends upon the duration of the loading. Individual footfall impulses that result from human activities such as walking and running have durations in the order of 0.05 to 0.10 seconds (Chui and Smith, 1987). Design against annoying vibrations caused by human footfalls requires definition of the duration of the load function used to calculate  $A_r$  or an alternative parameter such as peak velocity.

Although not dealt with directly here, it can be demonstrated that floors having higher degrees of isotropy (with respect to "plate" properties in the span and width directions) tend to produce greater separation between modal frequencies than is observed in most joisted wood floors. Floors built with materials such as concrete have relatively high modal self masses than wood floors. Therefore, had floors of other materials been considered different sensitivities to parameters varied in Tables 2 to 5 would have been observed. The discussion is thus specific to wooden floors with a joist and sheathing arrangement.

The above has neglected factors such as variation in amplitude of the load function, the averaging period and system damping assumed when predicting responses such as rms accelerations. The factors discussed above all seem to have a greater bearing on predicted solutions than other factors such as contributions from higher modes to  $A_r$ . If fundamental natural frequency is highly sensitive to disposition of masses, it is unlikely that the frequencies of higher modes can be estimated with an acceptable degree of accuracy. Overall, there are many factors to which vibrational serviceability predictions are sensitive. It is not practical to adopt envelope type predictions analogous to those utilised for estimating maximum moments, maximum shear forces etc., even with the aid of computers. If the physical parameters that constitute annoying effects on humans were to be agreed upon and absolute limits set on, for example, modal frequencies and peak velocity reliable methods could not be prescribed for quantitative estimation of parameters that indicate floor response characteristics.

## CONCLUSIONS

It is beyond a designer's ability to make quantitative vibration response predictions for joisted wood floors. Arbitrary choices must be made regarding variables such as the

amount of imposed mass, its distribution, and the excitation assumed in design. Arbitrary choices must also be made regarding limits on response. Armed with this approach sensible choices can be made on the basis of relative behaviours of a range of candidate design solutions. The candidates would satisfy static design criteria for both strength and serviceability.

Although a worthy goal to which to aspire, material and structural configuration neutral vibrational response criteria for joisted floors are not valid for contemporary engineering design codes.

## REFERENCES

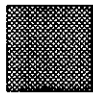
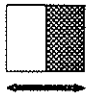
- CHUI, Y.H. 1988. A rational method of evaluating the dynamic response of timber floors. *Structural Engineering Review*, 1, 151-164.
- CHUI, Y.H. and SMITH, I. 1987. Proposed code requirements for vibrational serviceability of timber floors. CIB-W18A Paper No. 20-8-1, Dublin, Ireland
- CHUI, Y.H. and SMITH, I. 1988. An addendum to paper 20-8-1 - Proposed code requirements for vibrational serviceability of timber floors. CIB-W18A Paper No. 21-8-1, Parksville, Vancouver Island.
- CHUI, Y.H. and SMITH, I. 1990. Influence of random variations in material properties and imposed masses on dynamic responses of joisted wood floors. *Proceedings of the International Conference on Vibration Problems in Engineering*, Vol. 1, 480-485. International Academic Press, Beijing, PRC.
- INTERNATIONAL STANDARDS ORGANIZATION. 1978. Guide for the evaluation of human exposure to whole body vibration. Standard 2631, ISO, Geneva, Switzerland.
- OHLSSON, S.V. 1988. Floor vibration serviceability and the CIB model code. CIB-W18A Paper No. 21-8-2, Parksville, Vancouver Island.
- TRUS JOIST CANADA LTD. 1989. Residential products guide. Trus Joist Canada Ltd., Claresholm, Alberta.

**Table 1 Properties of wood I joists assumed in studies**

Depth (mm)	241	302	356	406
Mass per unit length (kg/m)	4.76	5.21	5.50	5.95
EI (*10 <sup>6</sup> Nm <sup>2</sup> )	0.976	1.644	2.400	3.246
Recommended span (m) <sup>1</sup>	4.74	5.37	6.26	6.74

<sup>1</sup> Based on manufacturers literature, assuming joists spaced at 600mm and a total dead plus live load of 2.4 kN/m<sup>2</sup>. This incorporates static deflection limitations of span/360 to 4.5m and span/480 for longer spans; maximum 12.7mm.

**TABLE 2 Influence of section depth and span on fundamental natural frequency and rms acceleration\***

Joist depth (mm)		241	302	356	406
Span(m)		4.74	5.37	6.26	6.74
Disposition of imposed mass <sup>3</sup>		11.4 <sup>1</sup> (1.55) <sup>2</sup>	11.6 (1.33)	10.2 (1.66)	10.1 (1.54)
	 Width	8.9 (1.33)	9.0 (1.16)	7.9 (1.38)	6.8 (1.65)

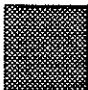
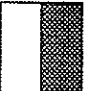
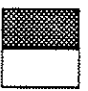
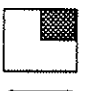
\* Construction data: width 7.2m, all edges simply supported; joist spacing = 600mm; sheathing 18.5mm OSB; load-slip modulus per unit sheathing-to-joist connection  $2 \times 10^6$  N/m<sup>2</sup>. Imposed mass = 50kg/m<sup>2</sup> x floor area.

<sup>1</sup> Fundamental natural frequency (Hz).

<sup>2</sup> Frequency-weighted rms acceleration (m/s<sup>2</sup>), for a sinusoidal impulse of 50Ns and duration 0.10s.

<sup>3</sup> Total imposed mass remains constant for a given span and the associated floor area.

**TABLE 3 Influence of floor "shape" on fundamental natural frequency and rms acceleration\***

Disposition of imposed mass	Width (m)			
	3.6	4.8	7.2	8.4
	12.2 <sup>1</sup> (1.35) <sup>2</sup>	11.8 (1.48)	11.4 (1.55)	11.4 (1.57)
	9.6 (1.10)	9.2 (1.18)	8.9 (1.33)	8.7 (1.85)
	12.0 (1.36)	11.7 (1.49)	11.3 (1.55)	11.2 (1.59)
 Width	9.5 (1.13)	9.1 (1.16)	8.7 (1.38)	8.6 (1.83)

\* Construction data: span = 4.74m, all edges simply supported; joist spacing = 600mm, depth = 241mm; sheathing 18.5mm OSB; load-slip modulus per unit sheathing-to-joist connection  $2 \times 10^6 \text{N/m}^2$ . Imposed mass = 50kg/m.

<sup>1</sup> Fundamental natural frequency (Hz).

<sup>2</sup> Frequency weighted rms acceleration ( $\text{m/s}^2$ ), for a sinusoidal impulse of 50Ns and duration 0.10s.

**TABLE 4 Influence of ratio of imposed mass to self mass on fundamental natural frequency and rms acceleration\***

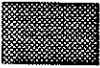


Imposed mass (kg/m <sup>2</sup> )	0	20	40	80	160
Ratio imposed to self mass	0	1	2	4	8
f <sub>o</sub> (Hz)	20.9	15.0	12.3	9.6	7.2
A <sub>r</sub> (m/s <sup>2</sup> ) <sup>+</sup>	1.01	0.708	1.31	1.92	1.91

\* Construction data: span 4.74m, width = 7.20m, all edges simply supported; joist spacing = 600mm, depth = 241mm, sheathing 18.5mm OSB; load-slip modulus per unit sheathing-to-joist connection  $2 \times 10^6$  N/m<sup>2</sup>.

Self mass of system 19.96 kg/m<sup>2</sup>

+ Sinusoidal impulse of 50 Ns, duration 0.10s.

**TABLE 5 Influence of shape and duration of impulse ( $I = 50\text{Ns}$ ) on rms acceleration ( $\text{m/s}^2$ )\***

Shape	Duration (s)			
	0.05	0.10	0.15	0.20
 Rectangular	4.23	0.985	1.18	0.758
 Sinusoidal	5.12	1.55	0.487	0.270
 Triangular	5.98	2.85	2.42	2.03

\* Construction data: span=4.74m, width=7.20m, all edges simply supported; joist spacing=600mm, depth=241mm; sheathing 18.5mm OSB; load-slip modulus per unit sheathing-to-joist connection  $2 \times 10^6 \text{ N/m}^2$ . Imposed distributed mass  $50 \text{ kg/m}^2$ .

Fundamental natural frequency 11.4 Hz.





**INTERNATIONAL COUNCIL FOR BUILDING RESEARCH STUDIES AND DOCUMENTATION  
WORKING COMMISSION W18 - TIMBER STRUCTURES**

**LONG TERM BENDING CREEP OF WOOD**

by

T Toratti  
Helsinki University of Technology  
Finland

**MEETING TWENTY - FOUR**

**OXFORD**

**UNITED KINGDOM**

**SEPTEMBER 1991**



## Summary

Long term creep and recovery test results of wood in a bending load of 10 MPa stress and subjected to relative humidity cycling are analysed. A mechano-sorptive model that fits the test results is proposed. Simulated values of creep at ten years of loading is presented using the model. According to the model, the elastic bending deflection can be about doubled to account for the creep of ten years loading with a cyclic load of 10 - 3 MPa and subjected to a natural outdoor relative humidity.

## Introduction

This paper is focused on the long term mechano-sorptive behaviour of wood under variable loading and its significance on the performance of wood structures. Most creep experiments have been carried out under relatively short duration of loading and the applicability of determined creep models are thus also restricted to a limited load duration.

The test results used here were carried out in The Royale Institute of Technology, Stockholm Sweden by Sepehr Mohager. These tests were carried out for an exceptionally long load duration of up to 1200 days during which up to 60 relative humidity cycles had occurred.

## Test results

The tests were done in four point bending and the bending stress during loading was 10 MPa. Specimens matched by density of small size defect-free and of structural size pine wood, *Pinus Silvestris*, are studied. The tests were done to two different size specimens. The small specimens were of cross section  $10 \times 10 \text{ mm}^2$ , the span was 300 mm. The larger specimens were of cross section  $44 \times 94 \text{ mm}^2$  and these were loaded edgewise. The span was 3900 mm. The specimens were initially conditioned to RH 65 % and during the test the relative humidity was cycled between RH 15 % and 90 % with a cycle length of 20 days. The temperature was held constant at 20°C.

Test results of the small specimens ( $10 \times 10 \text{ mm}^2$ ) are graphed in figures 1. where the creep curves of five specimens are presented. Four of these were loaded for a period of 580 days and then unloaded. One of the specimens was loaded for 1365 days when it was unloaded and the recovery was measured for an additional 250 days.

Test results of the larger specimens ( $44 \times 94 \text{ mm}^2$ ) are graphed in fig.2 . One of the specimens was loaded for 1200 days. The other three specimens were unloaded after 593 days of loading and one of these was re-loaded after 357 days of being unloaded.

## Creep analysis

Using the cross section creep analysis described in ref. Toratti 1991, computed results are compared to these test results. The main principle in the computation is that only a single cross section of the beam is analysed. The procedure is time marching and in every time step the crosswise moisture distribution in the cross section is computed using the finite difference method. This moisture distribution data is used to calculate the creep cumulated during this time step using a trapezoidal scheme. The axial strain of the cross section is computed iteratively until internal stress is in equilibrium with the loads and the compatibility requirement of linear strain distribution is satisfied.

The constitutive equation of wood is assumed linear with respect to stress and the Boltzman superposition principle is used. The strain of wood when subjected to loading and moisture content variation is assumed to consist of the following additive parts: elastic, normal creep, mechano-sorptive creep and free shrinkage strains. The details are described in references Mohager & Toratti 1991 and Toratti 1991.

## Mechano-sorptive creep model

A mechano-sorptive model is introduced that describes these test results better than the previous models. It was found that mechano-sorptive models derived from tests of shorter duration did not give good agreement when extrapolated to these test results.

It is assumed that for tension stress the mechano-sorptive creep approaches a limit value and the creep limit model is used. For compression stress the creep limit model is added with a term which is linearly dependant on the absolute value of moisture change. This added part could be caused from losses of stability of the microfibrils under compression resulting in the formation of slip planes.

In addition it is assumed that this additional strain in compression is of plastic nature (irrecoverable) as all other mechano-sorptive and normal creep strain is fully recoverable under changing humidity conditions when unloaded.

The above mechano-sorptive model was derived from the following observations of the test results:

1. No tendency to approach a mechano-sorptive creep limit is observed during this range of load duration and humidity cycling.
2. When a significant amount of mechano-sorptive deformation is produced, recovery is not complete on unloading even when the relative humidity is cycled. This irrecoverable deformation increases in magnitude as the load duration is increased and seems to be proportional to the mechano-sorptive creep accumulated.

The mechano-sorptive model in constant stress and in discrete moisture content

steps is as follows:

For tension stress:

$$\epsilon_{ms} = \sigma J^{\infty} \{1 - \exp(-c \Sigma |\Delta u|)\} \quad (1)$$

For compression stress:

$$\epsilon_{ms} = \sigma J^{\infty} \{1 - \exp(-c \Sigma |\Delta u|)\} + \sigma J_0 e \Sigma |\Delta u| \quad (2)$$

where

$J^{\infty}$	=	$0.7 J_0$
$J_0$	:	Elastic compliance
$c$	=	$2.5 [-]$
$e$	=	$0.1 [-]$

The mechano-sorptive model is formed to a convolution integral form and the boltzman superposition principle is applied. A trapezoidal rule to integrate the mechano-sorptive deformation is used, details in ref. Mohager & Toratti 1991.

### Simulation of creep

To check how the presented mechano-sorptive model performs for full size timber structures in natural humidity conditions, the creep analysis was used to simulate the creep of two different size beams: a glulam beam of size 190x1460 mm<sup>2</sup> and a timber beam of size 44x94 mm<sup>2</sup>. The cross section was modelled with 15 nodes in the width and 23 nodes in the height direction for the glulam beam and for the timber beam 7 and 11 nodes respectively. The environment relative humidity was taken from the database of the monthly average relative humidity values outdoors in Helsinki area, Finland. The relative humidity varied between RH 55 - 90 %.

The creep was simulated for a period of ten years. The mechano-sorptive model explained above was used with the material parameters defined here. Two different computations were performed: one computation with a constant bending load of 10 MPa and a second computation with cyclic loading between 10 - 3 MPa having a cycle length 182 days.

The ten year simulation of creep gives relative creep values of about 2.4 for the glulam beam and about 2.7 for the timber beam when a constant load resulting in a bending stress of 10 MPa is applied. When the cyclic load is applied the relative creep value after ten years of loading is between 1.0 - 2.0 for the glulam beam and 1.2 - 2.2 for the timber beam.

In this case the variability in loading considerably lowers the magnitude of creep, as the cycling of 10 - 3 MPa compared to a constant 10 MPa load results in 0.5 times the elastic deformation lower creep. Considering that the stress level in most load bearing wood structures probably varies below the allowable stress level with a high amplitude, due to snow loads, the model results that the

beam deflection can be about doubled to account for the ten year creep in a variable relative humidity. This magnitude of creep is in fact quite close to the creep factor given in most design codes for timber structures.

## Conclusions

Creep test results of very long load duration and subjected to a high number of relative humidity cycles are analysed. The results do not seem to support the existence of a mechano-sorptive creep limit. Recovery of deformation does not seem to be complete but is to a certain extent of plastic nature. The irrecoverable deformation increases as mechano-sorptive creep increases. A mechano-sorptive model is presented based on the above observations.

The simulation of the bending creep of wood in natural outdoor environment conditions, using the model presented, results in the following relative creep and  $k_{\text{creep}}$  values:

Table 1. Simulated results at load duration of 10 years.

Definitions:  $\epsilon(t) = (1 + k_{\text{creep}}) \sigma / E$   
 Relative creep: Total deformation per elastic deformation.

	Loading	Relative Creep	$k_{\text{creep}}$
Solid wood 44 x 94 mm <sup>2</sup>	Constant 10 MPa	2.75	1.75
	Cyclic 10 - 3 MPa	2.20	1.20
Glulam 190 x 1460 mm <sup>2</sup>	Constant 10 MPa	2.40	1.40
	Cyclic 10 - 3 MPa	2.00	1.00

## References

Mohager S. 1987: Studier av krypning hos trä (Studies of creep of wood, in Swedish). Doctoral dissertation. Kungliga Tekniska Högskolan, Stockholm Sweden. 139 p.

Mohager S., Toratti T. 1991: Long term bending creep of wood in cyclic relative humidity. To be published in the Wood Science and Technology journal.

Ranta-Maunus A. 1975: The viscoelasticity of wood at varying moisture content. Wood Sci. Technol. 9:189-205.

Toratti T. 1991: Creep of wood in varying environment humidity. Part I Simulation of creep. Report 19. Laboratory of Structural Engineering and building Physics, Helsinki University of Technology. 61 p.

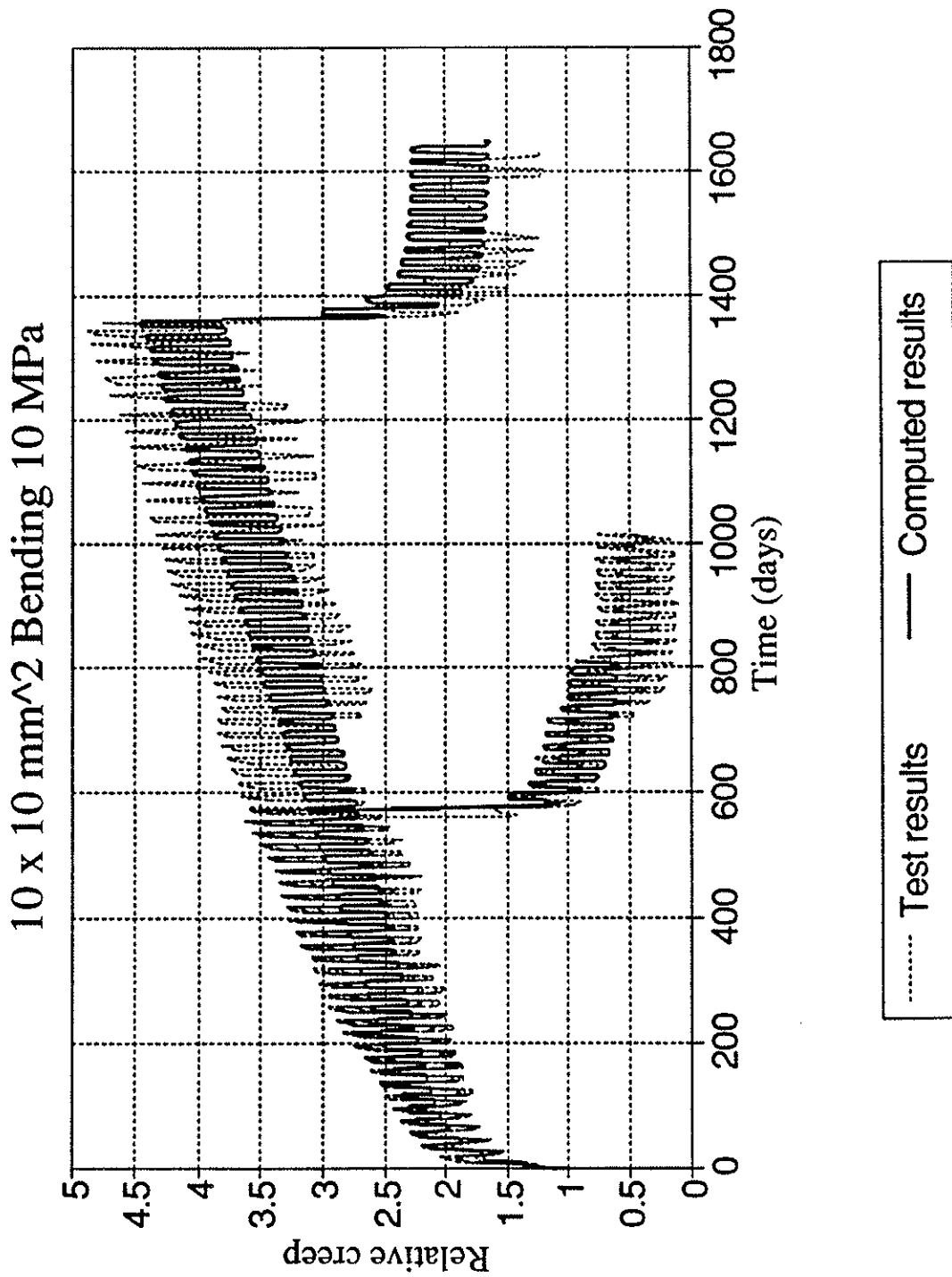


Figure 1. Comparison of computed results to test results of five 10x10 mm<sup>2</sup> specimens in bending, stress 10 MPa. Cyclic relative humidity RH 15 - 90 %, cycle length 20 days.

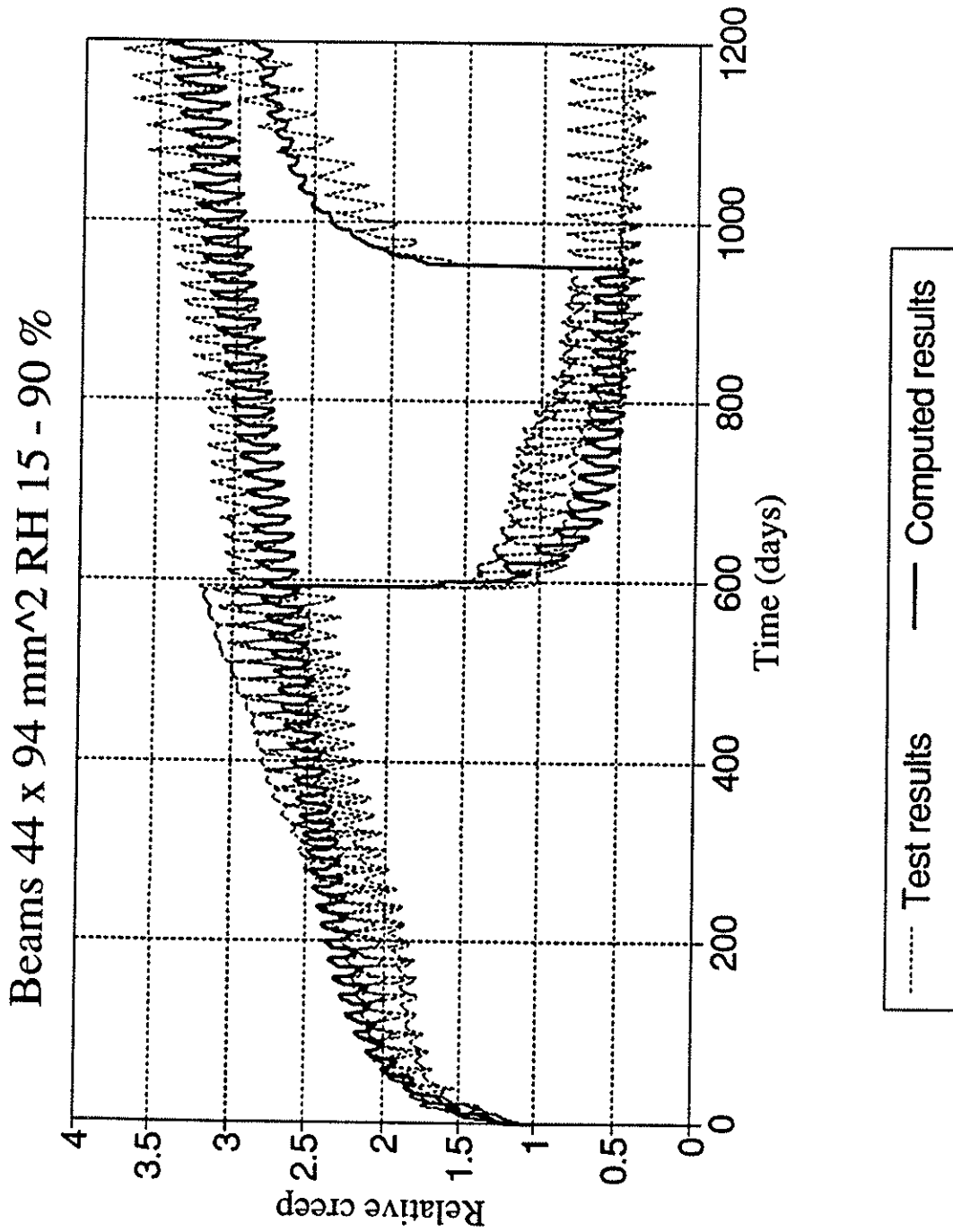
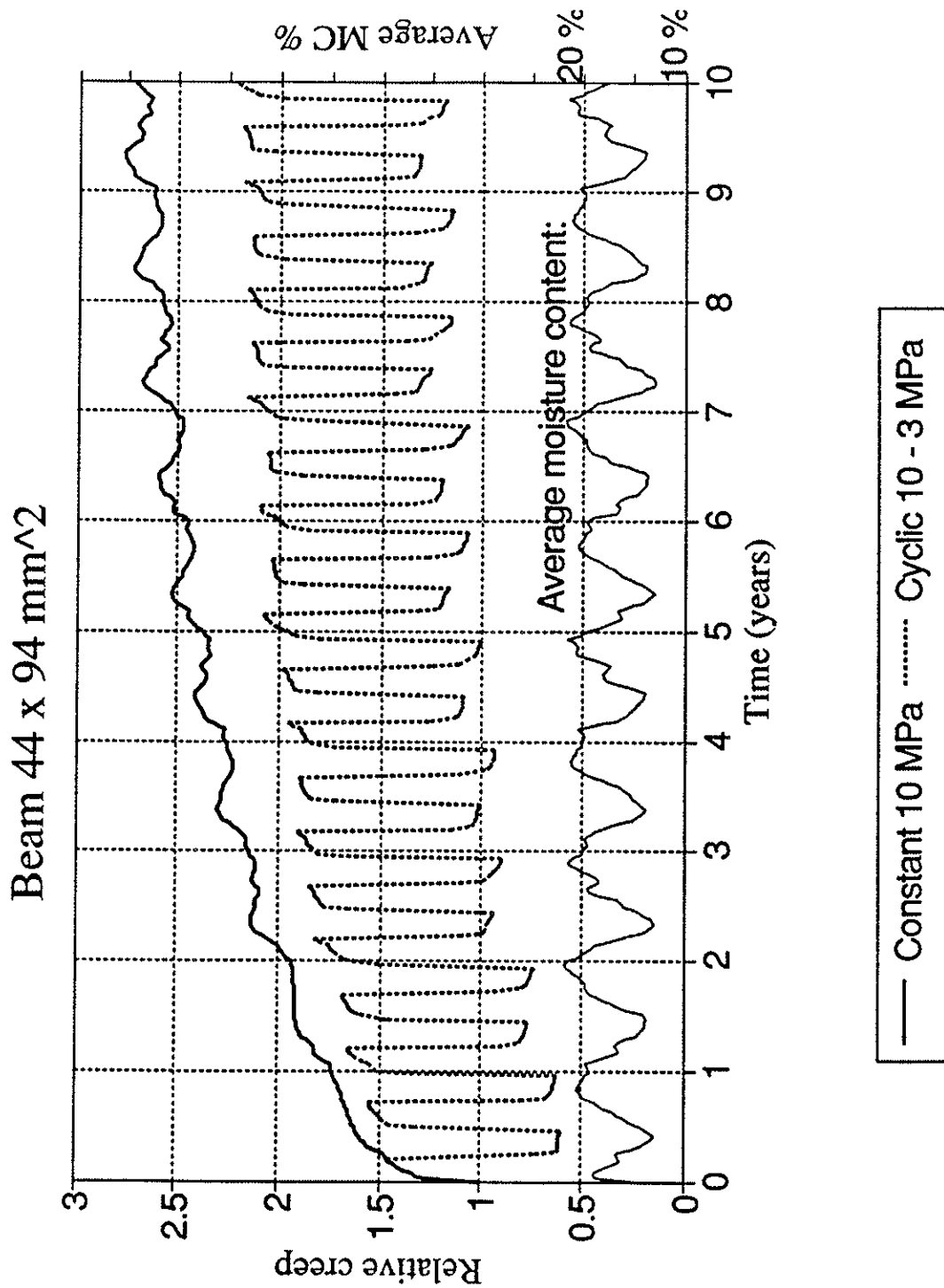
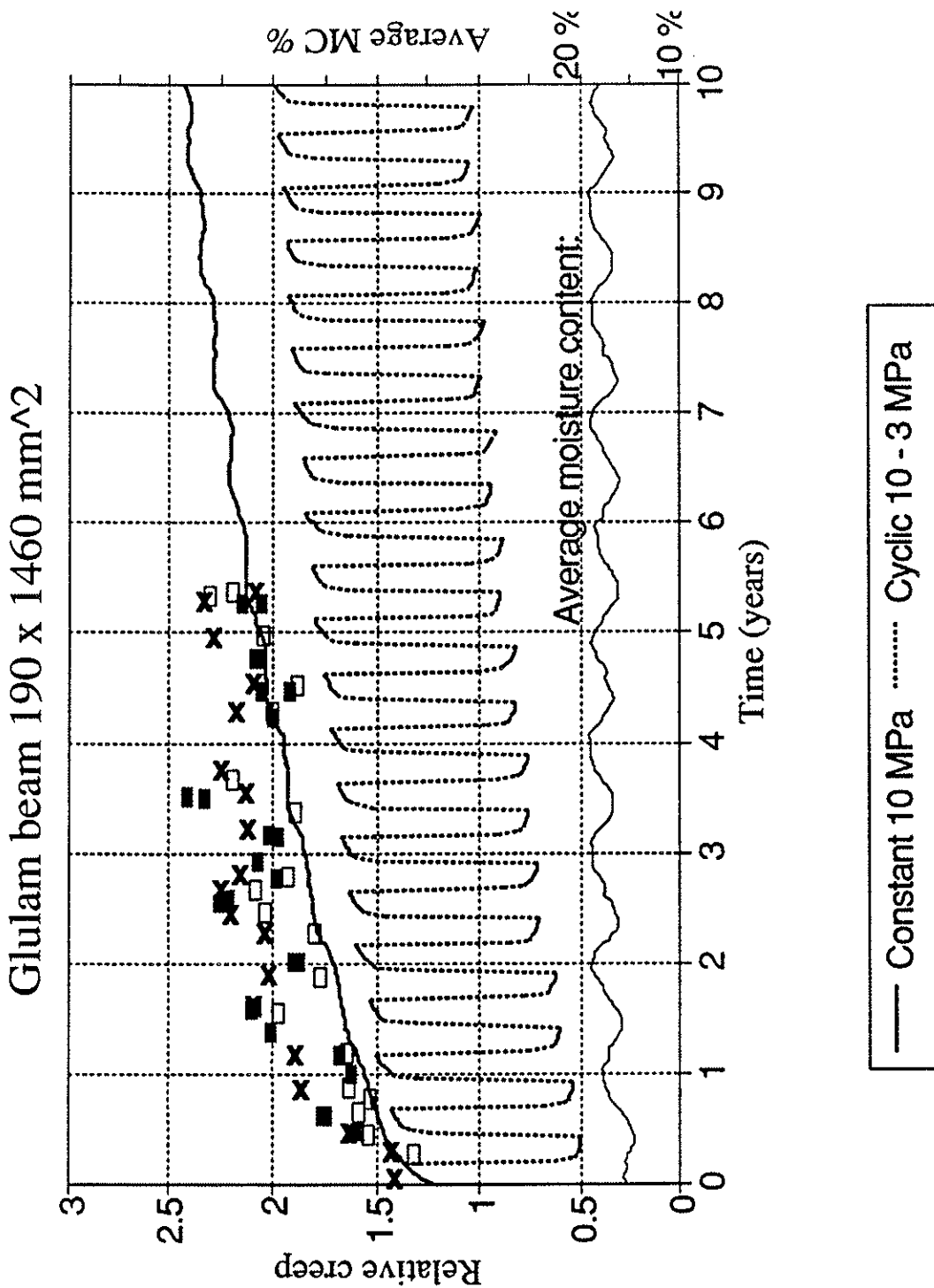


Figure 2. Comparison of computed results to test results of four 44x94 mm<sup>2</sup> specimens in bending, stress 10 MPa. Cyclic relative humidity RH 15 - 90 %, cycle length 20 days.





**Figure 3.** A ten year simulation of creep for a timber beam of cross section 44x94 mm<sup>2</sup> subjected to relative humidity variation of monthly average outdoor value encountered in Helsinki, Finland (between RH 55 - 90 %). One computation with a constant bending load of 10 MPa and a second computation with cyclic loading between 10 - 3 MPa, cycle length 182 days.



**Figure 4.** A ten year simulation of creep for a glulam beam of cross section 190x1460 mm<sup>2</sup> subjected to relative humidity variation of monthly average outdoor value encountered in Helsinki, Finland (between RH 55 - 90 %). One computation with a constant bending load of 10 MPa and a second computation with cyclic loading between 10 - 3 MPa, cycle length 182 days. The markers show existing test results of bending creep (glulam size 95 x 176 mm<sup>2</sup>) subjected to outdoor sheltered environment, ref. Ranta-Maunus 1975.

**INTERNATIONAL COUNCIL FOR BUILDING RESEARCH STUDIES AND DOCUMENTATION**

**WORKING COMMISSION W18 - TIMBER STRUCTURES**

**COLLECTION OF CREEP DATA OF TIMBER**

by

**A Ranta-Maunus**

**VTT Laboratory of Structural Engineering**

**Finland**

**MEETING TWENTY - FOUR**

**OXFORD**

**UNITED KINGDOM**

**SEPTEMBER 1991**



## CREEP DATA

A collection of existing creep data of timber is made in order to assist code writers. Only experiments with direct relevance to structures are included: structural size, allowable stress level and minimum duration of load 6 months.

Data is given in tables, and the values are expressed in terms of  $k_{\text{creep}}$  defined by

$$\varepsilon = (1 + k_{\text{creep}}) \sigma / E$$

Data is divided into 3 climatic groups:

- artificially controlled in order to keep constant humidity
- naturally changing humidity
- artificially controlled to have strong cyclic variation

In some cases values for 50 years are calculated by the models given in the articles. For joints only data concerning nail-plate connections is collected.

Unfortunately, very little creep data related to service class 3 (Eurocode 5) has been available.

## DISCUSSION

In general, the experimental creep data gives high values for creep factors. In naturally varying environment  $k_{\text{creep}}$  exceeds 1 often after a few years of constant loading, and under extreme conditions much sooner. In changing climate creep factor obtains high values, especially with joints.

There are some differences between practical situation in structures and test conditions. Most tests are made at constant temperature and loaded by constant load causing the maximum bending stress 5 to 20 MPa. Experiments with varying load have had a short duration, and are not included in this summary.

It is worth noticing that **permanent** loads of structures are usually low causing bending stress 1 to 3 MPa. Consequently, the total displacement caused by permanent loads is

reasonable even if  $k_{\text{creep}}$  would be 4. Secondly, no creep results are published at stress levels under 5 MPa which leaves the question about the creep at low stress levels open. On the other hand, it is obvious that wood is not a suitable material for structures with high permanent bending loads.

The creep deformation caused by **variable** loads can not be easily estimated from this data. Design loads are normally much higher than average actions on structures. Therefore one could even argue that no additional creep factor is needed. Besides low loads, another factor diminishing creep is the recovery of creep deformation during less loaded periods.

Recovery of creep deformation depends on moisture cycling in a complicated way. A model for calculation of creep with varying moisture content and load is presented in this meeting /14/. A simple way of estimating the effect of variable loads is needed in building codes. The method could be based on the estimation the total duration when loads exceed a limit, say 90 % of design (characteristic) load.

## REFERENCES

1. Bohannon B., Time-dependent characteristics of prestressed wood beams. Research Paper 226. USDA Forest Services, Forest Products Laboratory, Madison 1974. 9 p.
2. Feldborg T., Timber joints in tension and nails in withdrawal under long term loading and alternating humidity. For. Prod. J. 39(1989)11/12, 8 - 12.
3. Hoyle R.J., Hani R.Y., Eckard J.J., Creep of Douglas-fir beams due to cyclic humidity fluctuations. Wood and Fiber Science 18(1986)3, 468 - 477.
4. Leivo, M., On the stiffness changes in nail plate trusses. VTT Publications 80, Espoo, Finland 1991. 192 p. + app. 46 p.
5. Littleford T.W., Performance of glued-laminated beams under prolonged loading. Report VP-X-15, Forest Products Laboratory, Vancouver 1966. 21 p.

6. Mc Nutt D., Superfesky M.J., Long-term load performance of hardboard I-beams. Research paper FPL 441. USDA Forest Service, Forest Products Laboratory, Madison 1983. 10 p.
7. Meierhofer U., Sell J., Physikalische Vorgänge in wetterbeanspruchten Holzbauteilen. Holz als Roh- und Werkstoff 37(1979) 227 - 234.
8. Mohager S., Studier av krypning hos trä. KTH Stockholm 1987. 139 p.
9. Nielsen A., Rheology of Building Materials. National Swedish Building Research. Document D6:1972. 213 p.
10. Ranta-Maunus A., The viscoelasticity of wood at varying moisture content. Wood Sci. Technol. 9 (1975) 189 - 205.
11. Ranta-Maunus A., A Study of the Creep of Plywood. VTT Structural Mechanics Laboratory, Report 5, Espoo 1976. 85 p. + app.
12. Rouger F., Le Govic C., Crubile P., Soubret R., Paquet J., Creep behaviour of French woods. Proceedings of the 1990 International timber engineering conference, p. 330 - 336.
13. Srpčić J., Houska M., Creep factors for wood and glulam structures. Proceedings of the 1990 International timber engineering conference, p. 416 - 423.
14. Toratti T., Long term bending creep of wood. CIB W18A, Oxford 1991. 9 p.
15. Wilkinson T.L., Log-time performance of trussed rafters with different connection systems. Forest Products Laboratory. Madison 1984. 19 p.

**TABLE 1. kcreep values under artificially constant conditions.**

Humidity	Duration			Notes
	week	year	50 years (extrapol)	
35 % or 90 %	0.07	0.30	0.40	Leivo, spruce 45x100, painted
35 % or 90 %	0.14	0.42	0.62	Leivo, spruce 45 x 100
65 %		0.30	0.70	Mohager, 44 x 94 pine
55 % or 85 %	0.12	0.40	1.20	Rouger, spruce 40 x 100 & glulam
65 %/17 C	0.10	0.42		Srpcic, glulam
65 % or 85 %		0.6 2)		Feldborg nail-plate joint
35 %		0.3	1	Leivo, bending nail-plate joint
90 %		0.45	1.4	Leivo, bending nail-plate joint

2) value of 2 years experiment

**TABLE 2. kcreep values under naturally varying conditions. Duration of test in parenthesis (years).**

Humidity				Notes
natural under roof		0.3 (1)		Meierhofer, glulam flatwise bending
natural under roof ?		0.6 (1)	1.2 (5)	Ranta-Maunus 1975 glulam
natural exposed to rain		1.0 (1)	2.0 (5)	Ranta-Maunus 1975 glulam
natural under roof		0.6 (1)		Leivo, truss nail plate connect
natural under roof		0.9 (1)		Wilkinson, truss
natural different cases		1.3 (1)	4 (50)	Nielsen, mean estim old buildings
natural indoors		1.2 (1)	1.6 (5)	Ranta-Maunus 1976 plywood plate
natural indoors		0.3 (1)		Littleford, glulam 80 x 250 Douglas-fir
natural ? indoors		0.4 (1)	0.6 (8)	Bohannan, glulam 80 x 130 Douglas-fir
natural indoors		0.5 (1)	0.9 (5)	McNutt, I-beam plywood, hardboard
natural under roof		0.6 (1)	1.3 (5)	McNutt, I-beam plywood, hardboard



**TABLE 3. kcreep values after a years loading under artificially varying conditions**

Humidity cycle		Notes
40 % <-> 90 % daily or weekly	1.3	Hoyle, 90x90 extrapolation
15 % <-> 94 % 18 x 20 days cycles	1.2	Mohager, 44 x 94
15 % <-> 94 % 18 x 20 days cycles	0.5	Mohager, 44 x 94 old wood
35 % <-> 90 % 10 x 5 weeks cycles	5	Leivo, bending nail-plate joint
50 % <-> 85 % 19 x 6 weeks cycles	6 2)	Feldborg nail-plate joint
20 % <-> 80 % 4 days cycles	2 - 3	McNutt, I-beam plywood, hardboard

2) value of 2 years experiment



**INTERNATIONAL COUNCIL FOR BUILDING RESEARCH STUDIES AND DOCUMENTATION**  
**WORKING COMMISSION W18 - TIMBER STRUCTURES**

**DEFORMATION MODIFICATION FACTORS FOR CALCULATING**  
**BUILT-UP WOOD-BASED STRUCTURES**

by

I R Kliger  
Chalmers University of Technology  
Steel and Timber Structures  
Göteborg, Sweden

**MEETING TWENTY - FOUR**

**OXFORD**

**UNITED KINGDOM**

**SEPTEMBER 1991**



## Deformation modification factors for calculating built-up wood-based structures

by  
I. Robert Kliger

The main purpose of this paper is to discuss the use of modification factors  $k_{\text{mod}}$  (the notation used in the CIB code) or creep factors  $k_{\text{creep}}$  (the notation used in Eurocode No 5) when calculating deflection in built-up structures.

### 1. INTRODUCTION

Structural built-up elements comprising thin-walled components of wood-based board material have been used for several years. A typical example of these elements is a stressed-skin panel section comprising webs of solid structural timber or timber-based I-beams and flanges of various board materials. The joints between webs and flanges can be made using mechanical fasteners such as nails or adhesives which determine the level of composite interaction in the panel. When adhesives are used, the panel is often assumed to be fully restrained. When only mechanical fasteners are used, the degree of restraint is very uncertain. If the values for the slip modulus for both joints due to interface deformation (between webs and compression flange and webs and tension flange) are known, a magnification factor  $\psi$  for the mid-span deflections of stressed-skin panels or built-up structures can be calculated.

The derivation of the magnification factor for deflection is based on classical assumptions. For example in the case of the simply-supported built-up beam (span =  $L$ ) with slipping member interfaces and loaded with a uniformly-distributed load  $q$ , the deflection at midspan  $w$  (Eq. 1) is as follows:

$$w = \psi \frac{5 q L^4}{384 EI_{\text{tot}}} \quad (1)$$

and the magnification factor  $\psi$  (Eq. 2) is:

$$\psi = 1 + \frac{12}{5} \left( \frac{1 - \beta^2}{(\beta\omega)^2} \right) \left[ \frac{2}{\omega^2} \left( \frac{1}{\cosh\omega} - 1 \right) + 1 \right] \quad (2)$$

where

$\beta^2 = \sum E_i I_i / EI_{\text{tot}}$  is the ratio between the sum of the "weighted" moment of inertia of individual members and the moment of inertia of the total built-up cross-section.

$$\omega = KL/2\beta$$

and  $K^2 = S/EA_f$  for a built-up beam with three members and two joints, where  $S$  is the slip modulus in both joints.

$A_f$  is the "fictitious" or "weighted" area of the flange, see [1], [2].

$E$  is the modulus of elasticity.

The slip modulus  $S$  depends on the type of joint and on the displacement modulus in nailed joints or the shear modulus in glued joints.

Those readers who are interested in the derivation of the magnification factor which was produced by many researchers in the past are referred to [2], [3], [4], for example.

The CIB Structural Timber Code [5], Annex 71, gives a simpler method for determining stresses and deflections for built-up members, where the slip modulus between members is taken into account. In this method, the effective moment of inertia is determined using the effectiveness factor  $\gamma$ , which reduces the total value of the moment of inertia calculated around the geometric axis, see Eq. (3):

$$I_{ef} = I_0 + \gamma (I_{tot} - I_0) \quad (3)$$

where

$$\gamma = \frac{1}{1 + \frac{\pi^2 A_f E}{L^2 S}} \quad (4)$$

The notations used in Eq. (4) are the same as those mentioned above.

In what way should these methods be used when calculating deflections in Serviceability Limit State Design? According to the Eurocode No 5 [6], the "deflections shall be determined as the instantaneous elastic deflection calculated with  $E_{0, mean}$  multiplied by the creep factor  $k_{creep}$  given in Table 4.1".

The creep factor  $k_{creep}$  depends on the load-duration class and moisture class. The slip modulus with values given in Eurocode No 5, (Table 5.2.4 a) can also be used with the creep factor  $k_{creep}$  from Table 5.2.4.b for mechanically-jointed members. In the CIB Structural Timber Code [5] and in the Swedish Building Code (Nybyggnadsregler NR) [7] the modification factors are used to reduce the characteristic mean values of the modulus of elasticity due to load-duration class and moisture class. Both these methods are approximatively correct when calculating deflections for flexural members with an even stress distribution in the

cross-section. Some principal questions now arise. Should the values of modulus of elasticity in the code with their corresponding creep factors be used when calculating the deflections of built-up members? How much does the use of members with very different moduli of elasticity, the various stress distributions in the whole cross-section and different degrees of restraint affect the creep in those members? The possible answers to these questions will follow in the next section.

Problems such as the load-bearing capacity of thin, wood-based flanges and the stress distribution in built-up beams (stressed-skin panels) due to well-known phenomena such as shear lag, buckling and flange curling are not the subject of this paper.

## 2. STRESS DISTRIBUTION IN VARIOUS CROSS-SECTIONS

### 2.1 Symmetrical cross-section

A built-up beam or a stressed-skin panel can be composed of materials with different properties. In the symmetrical built-up beam or section of a stressed-skin panel with the same modulus of elasticity in all members or at least the same modulus of elasticity in both flanges, the stress distribution can be like that shown in Figure 1. The variation in stress distribution due to creep was reported before, see Kliger [8]. If the load is constant, the strain increases in the flanges and in the webs due to creep (viscoelastic materials). As the flanges and webs are connected and as  $E_f \leq E_w$ , the strains and the stresses increase in the webs and decrease in the flanges. A reliability analysis of floor structures performed by Rouger et al [9] reported similar stress distribution and changes caused by creep.

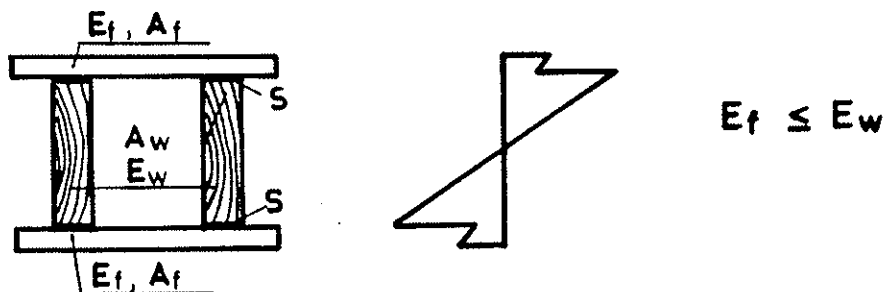


**Figure 1.** Stress distribution in a symmetrical cross-section.

The elastic solution with the mean modulus of elasticity in each member reduced by the  $k_{mod}$  factor for creep is a reasonable approximation for calculating all stresses and the deflection. However, different types of material in the joints produce different slip moduli.

In the case of structures with mechanical fasteners, the slip modulus can be

obtained as recommended in Eurocode No 5, Tables 5.2.4a and b, the second of which includes the modification factor  $k_{creep}$ . The magnification factor  $\psi$  in the first method or the effectiveness factor  $\gamma$  in the CIB method is then adjusted due to the load-duration and the moisture class of the joints.

In the case of adhesive joints where no slip theoretically occurs between the members, we apply only the  $k_{creep}$  factors to all the members in the structure.

Do these  $k_{creep}$  factors for all the members still apply, for example to beam webs which are restrained by the flanges which have either a higher or a lower modulus of elasticity than the webs?.

Obviously, timber beams loaded in bending without any restraint will produce more creep than would be the case if they were built into a stressed-skin element with adhesive joints. However, most adhesive joints produce some slip between the members and even the slip modulus for adhesive joints should probably be adjusted using  $k_{creep}$  factors in a similar manner to the mechanical joints. These two considerations, i.e. too low a modulus of elasticity in the web and too high a slip modulus in the adhesive joints, probably even one another out.

## 2.2 Non-symmetrical cross-section

The problem becomes more complicated when the stress distribution in the cross-section is not symmetrical or if one of the moduli of elasticity in one of the flanges is much higher than that in the web. For example, if the stressed-skin panel comprises timber beams as webs, timber-based panel as the compression flange and thin steel sheet as the tension flange, the stress distribution will be as shown in Figure 2.

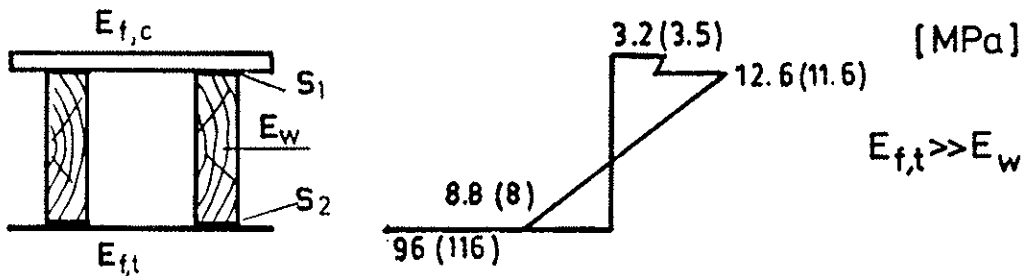


**Figure 2.** Calculated stress distribution in a non-symmetrical cross-section with semi-rigid connections (in brackets with rigid connections).

The value of the slip modulus between the web and compression flange and the web and the tension flange can be very different. In the case of the magnification factor  $\psi$  for the mid-span deflections, this difference can be taken into account by calculating the magnification factor for the first two layers (inverted T-beams) and modifying the bending stiffness of these layers. The calculation can then be



repeated by regarding the first two built-up layers as one unit (rigidly connected) when adding the third layer.

So how can the  $k_{\text{creep}}$  factors be applied to reduce the modulus of elasticity of the timber built into the panel due to moisture and load duration?

Steel sheet on the tension side does not creep and especially not as a result of moisture changes. Creep and relaxation occur in the web, compression flange and both joints. If the joint between the steel sheet and web is very rigid, the stresses (in brackets, Figure 2) will be lower in the web and higher in steel sheet than in the case of a less rigid connection. The stress distribution can change slightly due to creep, i.e. the stresses on the compression side, both in the flange and in the web, can increase and they can also decrease in the web on the tension side. Obviously, the stress will increase in the steel sheet in this case.

How will timber beams which are built into this type of element behave due to creep? Is it reasonable to apply the same  $k_{\text{creep}}$  factors in this case and not to take any account of the characteristics of the joints as was done in the case of the simply-supported beams loaded in bending upon which the code was probably based? There is no definite answer to these questions. In this particular case with the timber beams in the webs and the steel sheet in the tension flange, the creep in the entire element is due to the creep in the compression flange and the creep in the beams is due to the stresses in compression. It is reasonable to assume that the  $k_{\text{creep}}$  in the code for deflection in these beams used as webs are too high.

If the connection between the webs and the steel sheet is not rigid enough or if there is too much creep in this connection, the stresses will increase in the web on the tension side and decrease in the steel sheet. In this case it should be reasonable to calculate using  $k_{\text{creep}}$  factors as suggested by the code.

### 3. COMPARISON BETWEEN MEASURED AND CALCULATED DEFLECTION

A limited test conducted on stressed-skin elements at the Chalmers University of Technology [8] in the mid-80s indicates that the values of measured deflection in constant climate conditions were smaller than those calculated in moisture class I using Eurocode No 5 and the Swedish Building Code, see Table 1. A chipboard ( $E_0 = 3,850$  MPa) was used in the compression flange, timber beams ( $E_0 = 13,700$  MPa) were used in the web and steel sheet ( $E_0 = 200,000$  MPa) were used in the tension flange (measured  $E_0$  values).

The results of this comparison are based on one stressed-skin element and the measured deflection values are smaller than those obtained using calculations

based on the method suggested in the Eurocode and Swedish Building Code. The initial deflection is calculated using the magnification factor  $\psi$  together with the measured initial modulus of elasticity for the component parts of the stressed-skin panel. The deflection according to Eurocode No 5 and corresponding to various time periods was obtained by multiplying the initial deflection values by the creep factor  $k_{\text{creep}}$  given in Table 4.1 [6]. The agreement with measured values was quite good.

**Table 1.** Comparison between mid-span deflection (in mm) for a stressed-skin panel with a non-symmetrical cross-section and rigid connections loaded in climate class I.

<u>Time duration</u>	<u>Eurocode No 5</u>	<u>Swedish Code NR</u>	<u>Measured values</u>
Initial	2.80	2.80	2.74
1 week	3.10	3.73	2.97
1 month	3.35	4.40	3.07
1 year	3.77	4.91	3.45 (9 months)
10 years	5.03	5.97	-

The deflection according to the Swedish Building Code (NR) was obtained by reducing each modulus of elasticity for each component part (secant modulus) using the corresponding  $\kappa_{\text{creep}}$  (the notation used in NR) and calculating the elastic mid-span deflection loaded with a constant uniformly-distributed load  $q$  and the magnification factor  $\psi$ . The results were more conservative than those obtained by the Eurocode No 5.

#### 4. CONCLUSION

It is obviously very difficult for the code writers to have general rules and recommendations and to cover all the possible and "impossible" design cases at the same time. However, most timber members are built into a structure in one way or another. Most structural elements with various material and joint combinations can be designed with high accuracy at the initial stage. In this case, the differences in the calculated and actual initial deflection caused by high scatter in the modulus of elasticity in timber and timber-based materials are not the subject of this paper. When the effects of moisture and creep are added, a normal design procedure for structures with a long life expectancy, more expensive material combinations or connections will probably make the design much too conservative.

When a steel sheet for example is rigidly connected with timber beams, it would perhaps be reasonable to use smaller reduction values of the modulus of elasticity ( $k_{creep}$ ) due to creep for these beams than the values obtained from the codes. Another solution could be to use some sort of reduction factor for the calculated deflection of built-up structures in Serviceability Limit State Design which takes account of various material combinations and durable connections.

In order to promote the use of built-up or composite wood-based structures with more rigid and durable connections (which are often more expensive) in future, we should find a way of producing designs on the conservative side and of taking account of various material combinations and various connections at the same time.

## REFERENCES

- [1] **Larsen, H-J. - Ribberholt, H.:** "Trækonstruktioner - Beregning". (in Danish) Statens Byggeforskningsinstitut. Hörsholm 1983.
- [2] **Norén, B.:** "Nailed Joints - Their Strength and Rigidity under Short-Term and Long-Term Loading". Rapport från Byggeforskningen 22:1968. Stockholm.
- [3] **Smith, J.:** "Plywood stressed skin panels with rigid or semi-rigid connections". Proc. CIB-W18, Vienna, Austria 1979. Paper 11-4-1
- [4] **Kuenzi, E.W. - Wilkinson, T.E.:** "Composite beams - effect of adhesive or fastener rigidity". Forest Prod. Lab., USDA, Res. Paper. FPL 152, 1972.
- [5] CIB Structural Timber Design Code. CIB Report, Publication 66. 1983
- [6] Eurocode No.5: Common unified rules for timber structures. Commission of the European Communities. Report EUR 9887. 1987.
- [7] The Swedish Building Code. (Nybyggnadsregler - in Swedish) Boverket, Stockholm BFS 1988:18 .
- [8] **Kliger, I.R.:** "Experimental study of stressed-skin panels under long-term loading". Proc. IUFRO S 5.02, Turku, Finland 1988.
- [9] **Rouger, F. - Barrett, J.D.- Foschi, R.O.:** "Reliability analysis of viscoelastic floors". Proc. CIB - W18, East Berlin, 1989. Paper 22-8-1.



INTERNATIONAL COUNCIL FOR BUILDING RESEARCH STUDIES AND DOCUMENTATION  
WORKING COMMISSION W18 - TIMBER STRUCTURES

SHEAR STRENGTH OF CONTINUOUS BEAMS

by

R H Leicester  
F G Young  
CSIRO  
Australia

MEETING TWENTY - FOUR

OXFORD

UNITED KINGDOM

SEPTEMBER 1991



# SHEAR STRENGTH OF CONTINUOUS BEAMS

R.H. Leicester and F.G. Young  
(CSIRO, Australia)

## INTRODUCTION

Shear strength tends to be more important in the design of continuous rather than single span beams. For example, in the case of centre-point-loaded beams having a span to depth ratio of 6:1, the ratio of nominal (applied) shear stress  $f_s$  to nominal (applied) bending stress  $f_b$  is given as follows

$$\text{single span: } f_s/f_b = 0.083$$

$$\text{double span: } f_s/f_b = 0.152$$

Because of this, there has been a proposal in Australia, that double span test specimens should be used for in-grade shear strength measurements. However, in some recent studies using LVL (laminated veneer lumber), some anomalies were noted in short-span shear tests, including the fact that shear failures appeared to be inhibited in double-span tests. Some aspects of these tests are reported herein.

## TEST MATERIAL

The test material comprised 120 mm wide strips of 45 mm thick LVL manufactured from *Pinus Elliotii* (slash pine). The outer most laminates comprised nominal 1.6 mm scarf jointed veneers, the next laminates comprised end lapped nominal 3.2 mm veneers, and the remainder of the internal joints comprised nominal 3.2 mm butt jointed veneers. The occurrence of butt joints provided a potential weakness in shear. All test specimens were selected from random locations within LVL sheets.

## TEST PROCEDURES

The three following tests were made:

- third-point loading on 810 mm span, single-span beams
- centre-point loading on 270 mm span, single-span beams
- centre-point loading on 270 mm span, double-span

The three tests are illustrated in Figure 1. The test on the 810 mm span beam is intended to provide a measurement of bending strength, while the other two are intended to provide a measurement of shear strength.

## TEST RESULTS

The test results obtained are given in Table 1. From the observed failure modes it is concluded that the single-span tests provide a good measurement of mean bending strength  $F_b = 77.8$  MPa and shear strength  $F_s = 5.4$  MPa. However, the tests on the double span specimen provided the two following puzzling features:

- (i) Although at ultimate load the nominal shear stress at the mid support on average exceeded the shear strength value of 5.4 MPa, failure in shear did not occur.
- (ii) The bending stress  $F_b = 50.0$  MPa at failure was lower than the value of 77.8 MPa observed in the third point loading test. Because of the shorter test specimen and the more limited area of high stress in the case of the double span test, the reverse would have been expected to be true.

## DISCUSSION

Two possible causes for the observed anomalies are as follows:

- (i) Because of the short span/depth ratio used in the double span test specimen, the true values of peak shear and bending stresses could be significantly different from the nominal values.
- (ii) Failure in shear at the mid-support of the double span beam cannot (because of symmetry considerations) develop as a longitudinal split as is normally observed for single span specimens, Figure 2.

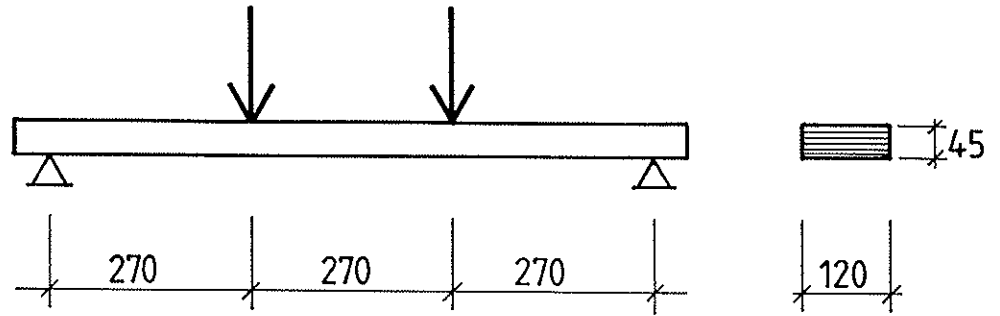
At the time of writing, a finite element analysis is in progress to examine the above matters. However, it is already obvious from the test results, that some modification to conventional structural theory needs to be made in the case of design for the shear strength of continuous beams.



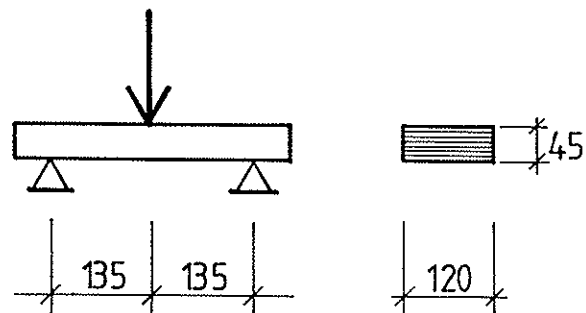
Table 1.  
Summary of Test Results

Type of test	Sample size	No. of shear failures	Nominal stress at failure (MPa)		Coeff. of variation of strength
			Bending	Shear	
Third point loading	50	0	77.8*	3.2	0.10
Centre-point loading, single span	70	70	64.8	5.4*	0.08
Centre-point loading, double span	14	2	50.0*	7.6	0.06

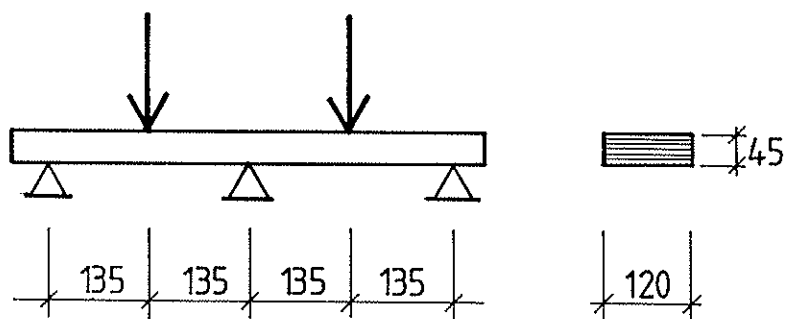
\* Stress corresponding to dominant failure mode.



(a) third point loading, single span



(b) centre-point loading, single span



(c) centre-point loading, double span

Figure 1. Loading configurations.

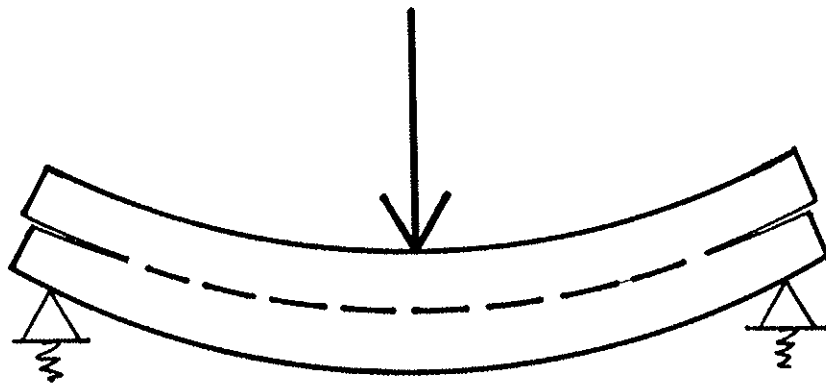


Figure 2. Potential shear failure mechanism for single span specimens.



**INTERNATIONAL COUNCIL FOR BUILDING RESEARCH STUDIES AND DOCUMENTATION**  
**WORKING COMMISSION W18 - TIMBER STRUCTURES**

**CAPACITY OF SUPPORT AREAS REINFORCED WITH NAIL PLATES IN TRUSSED RAFTERS**

by

A Kevarinmäki  
Helsinki University of Technology  
Finland

**MEETING TWENTY - FOUR**

**OXFORD**

**UNITED KINGDOM**

**SEPTEMBER 1991**



## Summary

A low-cost and easy way to reinforce the chord is to use nail plates at the support areas of the trussed rafter. The test results of load-carrying capacity in compression perpendicular to the grain of the support areas reinforced with nail plates are shown in this paper. Although the supporting block is wooden, the bearing capacity will increase at least 30 % with nail plate reinforcement of the chord at an end support because the bearing pressure is rail type in the supporting structure. If the supporting block is steel, concrete or wood in compression parallel to the grain, the nail plate reinforcement will improve the bearing capacity of the end or intermediate support even 2 times higher.

## Introduction

Trussed rafters are structures where small support areas are loaded by quite high forces. Usually the truss loads are carried from chords so that compression stresses are perpendicular to the grain. Because the stiffness and the compression strength of wood are rather low in this loading direction the required length of the support area is quite long, sometimes even longer than the width of the supporting structure. This paper is focused on the reinforcement effect of nail plates in the support areas.

## Testing procedure

A test series of 133 specimens were carried out to test the bearing strength of nail plate structures with nail plate reinforcement at the end and intermediate supports. A reference series of 42 specimens were tested for capacity of support areas without reinforcement. The characteristic strength of each case was calculated from at least 5 parallel specimens.

The main part of tests were done with normal structural size Finnish spruce (*Picea Abies*) of densities 360..400 kg/m<sup>3</sup>. Width of the specimens were 45 mm and height 95..220 mm. Some reference tests were done also with the width of 70 mm spruce, with spruce glulam 45 x 225 mm<sup>2</sup> and with Kerto-LVL 39 x 200 mm<sup>2</sup>. The specimens were initially conditioned to RH 65 %.

Three different types of nailplates were tested as the reinforcement of the chord: 1) Common nailplate with threaded nails, 2) Common homogeneous nailplate and 3) Nailplate with 3 threaded nails punched from the same hole. The thickness of plates was 1.25..1.30 mm, the length of nails was 13..14 mm, the characteristic strength of steel was 360 MPa or 400 MPa and the punched area of plates was from 26.2 % to 27.4 %. The location of nails was in straight lines in all the tested plates so that unbroken steel lines were in the loading directions. The length of nailplates was 140 mm and they were placed to the chords 45 mm inwards of the support edge. The vertical gap between the nailplates and the bearing surface was on the average 7.5 mm. The test were done with the multipurpose nailplates, which function as joints as well as reinforcement nailplates, and with distinct reinforcement nailplates. The distinct reinforcement nailplates were placed with either 10 or 45 mm vertical gap from the joint nailplates. Examples of the tests are illustrated in Figure 1.

The length of the support area was at the end supports 100 mm and at the intermediate supports 50 mm. The material of the supporting block was steel in the main test series. In reference series also the influence of parallel and perpendicular to the grain compression wooden supporting blocks was studied. The main part of specimens were loaded perpendicular to the bearing surface. Six reference specimens were tested with 3° angle between the chord and the bearing surface. The specimens were loaded to failure or to at least 10 % compression with strain controlled loading speed of 2 mm/min. Initial loading to about 50 % from 'design' value of applied load and down to zero was included in the beginning of the test. The deformation was measured in continuous-motion from the bearing surface to the 90 mm level of the chord.

## Test results

### Support areas without reinforcement

Typical test results of the specimens at the end and intermediate support areas without reinforcement are graphed in fig.2. No failure loads in compression perpendicular to the grain are obtained. But the characteristic strengths were calculated from the compression strain of elastic deformation plus 1 %. Thus the characteristic value of the deformation of the whole chord is 1.5..3.0 mm depending of height of the chord.

According to the Finnish Codes the strength value of Finnish softwoods in compression perpendicular to the grain is 6.5 MPa in short-term loading in all strength-classes. The tests at the end support showed that this value is clearly too high for the rather light density spruce. On the stress level of 6.5 MPa the deformation was generally over 10 %. According to the test a suitable characteristic strength of spruces density of 320 kg/m<sup>3</sup> would be 3.3 MPa in compression perpendicular to the grain. Value 6.5 MPa seems to fit to the density of 450 kg/m<sup>3</sup>.

The tests at the intermediate support showed that Codes underestimate the capacity of rail type loading in compression perpendicular to the grain (same increase-coefficient  $k_{c,90}$  is also in the working draft of Eurocode 5). With the Codes coefficient  $k_{c,90} = 1.316$  and compression strength value of 6.5 MPa the calculated capacity of the chord at the intermediate support correspond with the test results of light specimens (380 kg/m<sup>3</sup>). By comparing the tests at the intermediate supports to the tests at the end supports it may be concluded that the coefficient  $k_{c,90}$  could be about 35 % higher than the value of Codes (for example  $k_{c,90} = 1.78$  with 45 mm chord width).

Test results of the support areas with Kerto-LVL chords showed that compression strength and modulus of elasticity are clearly higher than those of light softwoods. The short-term strength in compression perpendicular to the grain was with the Kerto-LVL (density 470 kg/m<sup>3</sup>) 1.9 times higher than the test results of spruce (average density 390 kg/m<sup>3</sup>).

Variation of chord height from 95 mm to 220 mm had no effect to the load-strain dependence of the chord. Glulam spruce (45\*225 mm<sup>2</sup>) had equal behaviour with the same density timber chord. Reference test series with parallel or perpendicular to the grain loaded wooden supporting blocks had no significant effect to the mechanical behaviour of the chords. In the test series where the angle of 3° between the bearing and the chord surface the load strain dependence results at the middle of the supporting area were similar to the cases of the perpendicular supported chords.

### Support areas reinforced with nail plates

Some tests results of the reinforced specimens are graphed in fig.3. where the load-deformation curves of two test series are presented. The nail plate reinforcement improved clearly the modulus of elasticity of the support area: modulus of elasticity was at both the end and the intermediate support at least 2 times higher than it was on the chords without the nail plate reinforcement. Maximal load of the linear elasticity region was also higher (10..20 %) than in case of the ordinary chords. After the strength in compression perpendicular to the grain of wood has been exceeded the stiffness of the support area decreases and the wood compresses at the gap between the nail plates and the bearing surface to about half of its original height. When the pressure is so high that the wood cell structure has collapsed in the gap region, the nail plates carry the loads together with timber and the stiffness of support area increases again. Load carrying capacity is achieved when the nail plates are buckling. That requires about 3 % vertical strains in the nailplate area of the chord.



Test result of the nail plate reinforced chords are analyzed by subtraction of the load carrying capacity of wood and the buckling load of nailplates in the tests. The short-term characteristic strengths of the nail plate reinforcement were calculated from the 5 % fractile. The long-term strengths are obtained by dividing the short-term strengths by a factor 1.3. According to the test results the load-carrying capacity of the support area with the nail plate reinforcement may be calculated as a sum of the wood strength in compression and the reinforcement strength of the nail plates. Fundamental properties of all the tested nailplate types were so similar that there were no significant difference between the test result of the studied nailplates.

The best reinforcement capacity of the nail plates was achieved when the nail plates had been placed in their main direction  $\alpha = 0^\circ$ , because then the loaded steel area is maximal. The buckling occurred in this direction in one line between consecutive nails of plate and the buckling force was about same than in nail plates of a joint with a gap between timber parts. The characteristic strength of nail plate reinforcement is so high in this plate direction that the load carrying capacity of the support area will increase 96 % in the width of 45 mm chord with nail plates placed on both sides of chords in direction  $\alpha = 0^\circ$  to the whole length of the support area.

The plate buckling has a different mechanism in the support area with 'horizontal' ( $\alpha = 90^\circ$ ) placed nail plates than with 'vertical' ( $\alpha = 0^\circ$ ) placed nail plates. Because the distance between the nails is shorter in the plates 'horizontal' loading direction the buckling area is large and almost the whole plates are curling in buckling. The average normal stress of the unbroken steel areas of the nail plates was 220 MPa in buckling of 'horizontal' reinforcement plates. According to the test results the load-carrying capacity of the support area increases 60 % with 'horizontal' placed nail plates reinforcement in the width of 45 mm chord. This additional capacity is obtained with a rather heavy spruce (about 450 kg/m<sup>3</sup>), but with light spruce the relative additional capacity is much higher.

Using the distinct reinforcement nail plates the deformation of the chords are bigger than in the chords with 'multipurpose' nail plates because wood compresses in the gap between nailplates before nailplates are actually carrying loads. According to the test results the gap between the reinforcement and the joint nailplates should be less than 10 mm. At the end support the buckling strength of the distinct reinforcement plates is about 40 % lower than the buckling strength of the multipurpose nailplates because wood is expanding horizontally in the gap between nailplates. This causes earlier buckling. At the intermediate support the spreading of wood is lower and the capacity of the distinct nail plates is almost same than the capacity of the multipurpose nailplates if the height of the distinct plates is sufficient (at least about half of the chord height).

If the length of the reinforcement nail plates is longer than the length of the support area, the load-carrying capacity is clearly higher than the buckling strength calculated according to the support length. According to the test at the intermediate support where nailplates are placed 45 mm over both of the support borders the effective reinforcement length of nailplates was the support length plus 60 mm. If the length of nailplates is sufficiently long the capacity of the support area is rather high at the intermediate support; for example with the support length of 50 mm the capacity of the chord (45 mm) will increase 160 % ( $\alpha = 0^\circ$ ) or 100 % ( $\alpha = 90^\circ$ ) by using correctly placed nailplates in the reinforcement of the support area.

The wood gap between the nailplates and the bearing surface has a high influence on the deformation of the support area. However the influence to the loading capacity is almost insignificant. The gap should be as small as possible to minimize the deformation at serviceability limit state. If the gap is zero the load-deformation curve is linear also after compression failure strength of wood has been exceeded. That will occur when the total compression strain of the chord is about 3 %.

According to the test results the height of the chord has no dependence on the mechanical behaviour of the support areas. The width of the chord however has a great effect to the reinforcement capacity of the nailplates because buckling occurs much earlier in the wide chord where the value of horizontal spearing of the chord is bigger. In reference test series of 70 mm chord width the strength of reinforcement by average was only 61 % from the strength of the reinforcement of the chord width 45 mm. All strengths of the nail plate reinforcements shown in this paper may be applied only with the chord widths below 50 mm.

The capacity of the nail plates reinforcement with the Kerto-LVL chords was almost zero in the tests. In compression perpendicular to the grain the Kerto-LVL has a brittle fracture mode where the ultimate strain is so small that the nail plates don't yet carry the loads. The support areas may be reinforced with nail plates only when the strain ability of the chord is so large that the compression strain may increase to 3 % in the nail plates. For example the nail plate reinforcement of timber is not possible in compression parallel to the grain.

## **A proposal design method for capacity of support areas reinforced with nail plates**

### Requirements of properties and geometry of the nail plates

The strength value of the reinforcements are given in this paper for nail plates that fulfill the following:

- Characteristic strength of the steel is 360..400 MPa
- The thickness of nail plate is at least 1.20 mm
- The length of the nails is 12..15 mm
- The punched area of the plate is 25..30 %
- The punching direction of the nails is parallel to the main direction of the plate
- The location of nails is so that there are unbroken steel lines in directions  $\alpha = 0^\circ$  and  $\alpha = 90^\circ$ .

### Location requirements of the reinforcement nailplates

- The nailplates are placed symmetrically on both sides of the chord
- The loading direction of the nail plates is  $\alpha = 0^\circ$  ('vertical' plate orientation) or  $\alpha = 90^\circ$  ('horizontal' plate orientation).
- The distance between the chord soffit and the underedge of the nailplate is at most 10 mm (maximal tolerance).
- Using distinct reinforcement nailplates the gap between upper and under nailplates should be at most 10 mm and the height of distinct nailplate should be at least 40 % from the height of chord.

### Requirement of the chord

- The chord is strength classed softwood (density over 320 kg/m<sup>3</sup>) sawn timber or glulam.
- The angle between load direction and the grain of chord should be 70°..90°.
- The width of chord should be at most 50 mm.

### Load-carrying capacity of support area reinforced with nail plates

The capacity of the support area is calculated as a sum of strength of wood in compression and the strength of the nail plate reinforcement:

$$F_d = A_t \sigma_{c,90,d} + 2 l_{\text{eff}} p_{c,a,d}$$

Where:  $A_t$  is the area of support surface,  
 $\sigma_{c,90,d}$  is the design strength of wood in compression perpendicular to the grain (includes a possible strength increasing in rail type loading),  
 $l_{\text{eff}}$  is the effective length of reinforcement (see fig.4.) and  
 $p_{c,a,d}$  is the design value of nail plate reinforcement (given in table 1.).

At an intermediate support where the nail plates are placed at least 45 mm over both support edges, as the effective length ( $l_{\text{eff}}$ ) may be used value  $t + 60$  mm, where  $t$  is the support length. In other cases the effective length should not exceed the support length.

If the full reinforcement strength is utilized, the capacity of the supporting block must be high enough. If the supporting structure is wood in loading direction perpendicular to grain, the bearing strength of the supporting block will be a critical factor at the end support with all presented reinforcements cases of the chords.

### Strength values of nail plate reinforcements

The characteristic strengths of nail plate reinforcements are given in table 1. These values are for long-term loading. Strengths for short-term loading may be calculated by multiplying these values by a factor 1.3. The design values of the ultimate limit state are calculated with a partial safety factor  $\gamma_m$ .

Table 1. The characteristic strength of nail plate reinforcements for long-term loading in service class 1 and 2.

Direction of plates	At end support		At intermediate support	
	$\alpha = 0^\circ$ $p_{c,0,k}$ [N/mm]	$\alpha = 90^\circ$ $p_{c,90,k}$ [N/mm]	$\alpha = 0^\circ$ $p_{c,0,k}$ [N/mm]	$\alpha = 90^\circ$ $p_{c,90,k}$ [N/mm]
Multipurpose	<b>108</b>	<b>67</b>	<b>108</b>	<b>67</b>
Distinct	<b>65</b>	<b>40</b>	<b>108</b>	<b>67</b>

The distinct reinforcement may not be utilized if the loading direction of the joint plates are not parallel to the main direction  $\alpha = 0^\circ$  or  $\alpha = 90^\circ$ . If the distinct reinforcement plate is placed in other direction than the upper joint nailplate, the value  $p_{c,90,k}$  is used as the strength of reinforcement.

### The deformation of support area reinforced with nail plates

The strain of a reinforced chord may be estimated according to the figure 5. The mean value of deformation is calculated from the graph by applying the maximal load without any safety factors in the serviceability limit state.

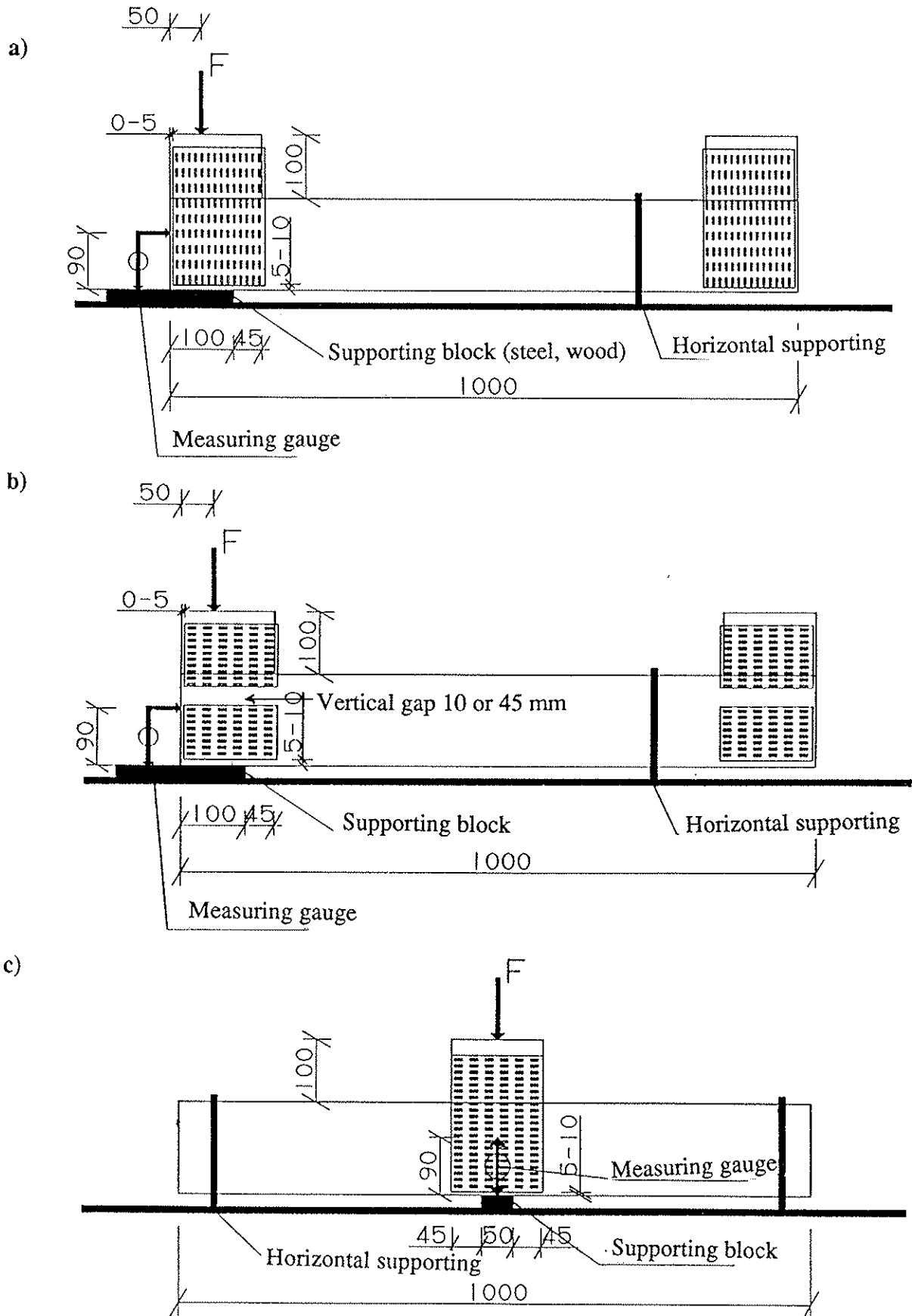
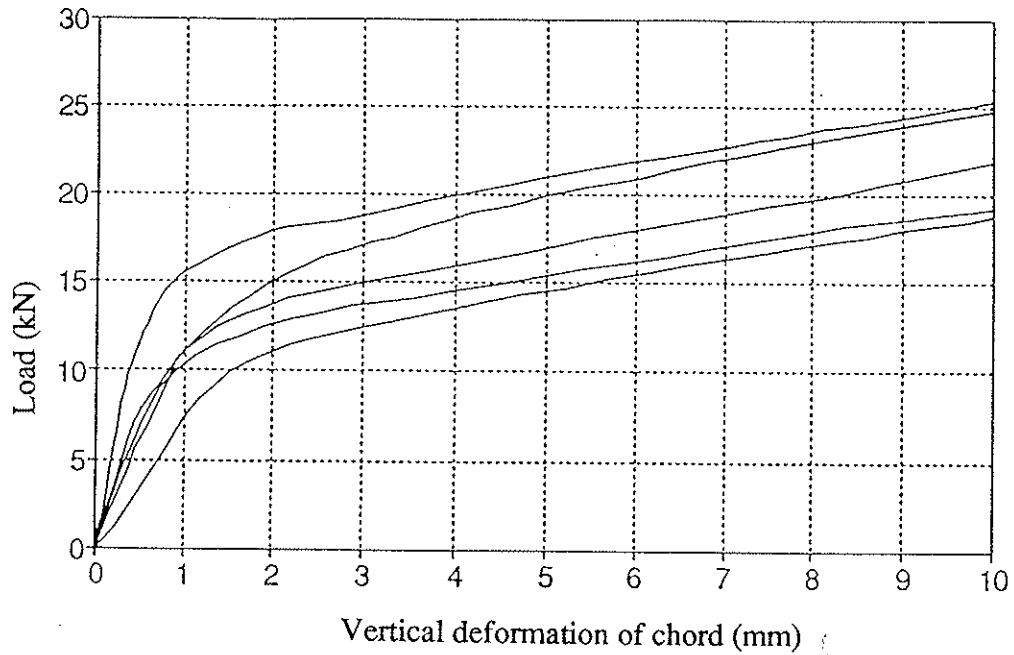


**Figure 1.** Loading and measuring configurations of three test series. a) A support area reinforced with 'vertical' multipurpose nail plates at an end support. b) A support area reinforced with 'horizontal' distinct nail plates at an end support. c) A support area reinforced with 'horizontal' multipurpose nail plates at an intermediate support.

a)

**AT END SUPPORT**  
**without reinforcement**



b)

**AT INTERMEDIATE SUPPORT**  
**without reinforcement**

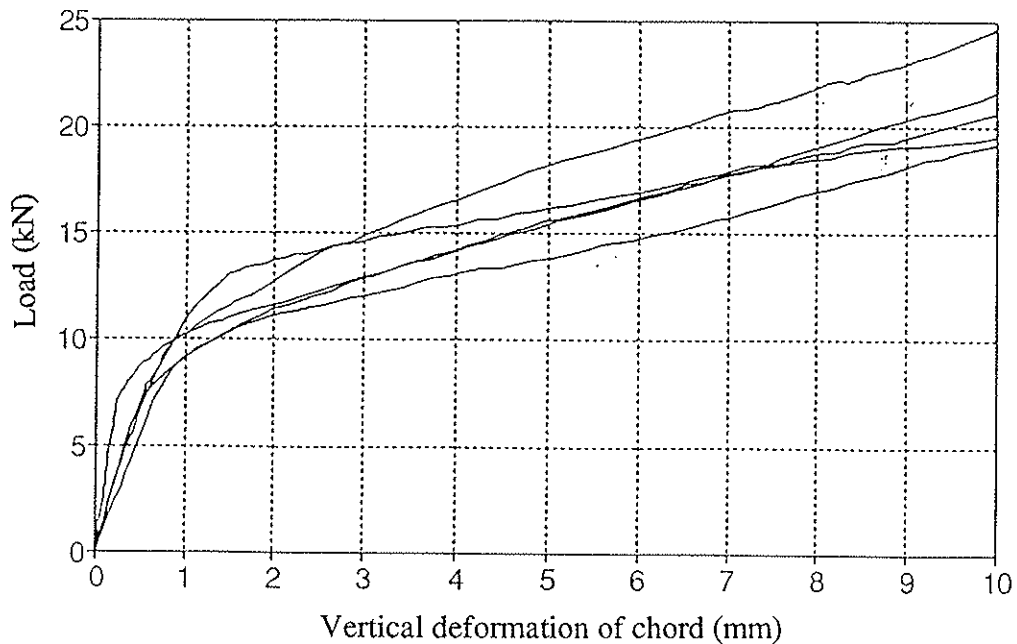
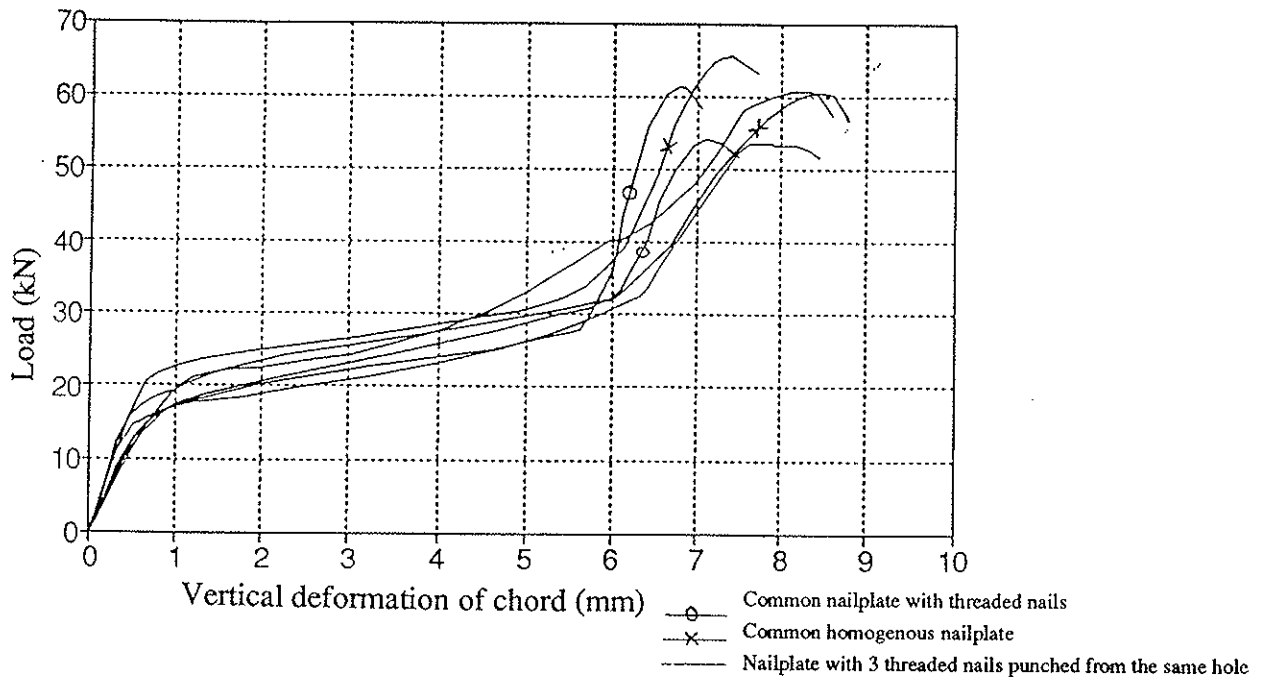


**Figure 2.** Measured load-deformation curves of support areas without reinforcement in two test series. a) Chord  $45 \times 95 \text{ mm}^2$  at an end support. b) Chord  $45 \times 95 \text{ mm}^2$  at an intermediate support.

a) **AT END SUPPORT**  
with nail plate reinforcement



b) **AT INTERMEDIATE SUPPORT**  
with nail plate reinforcement

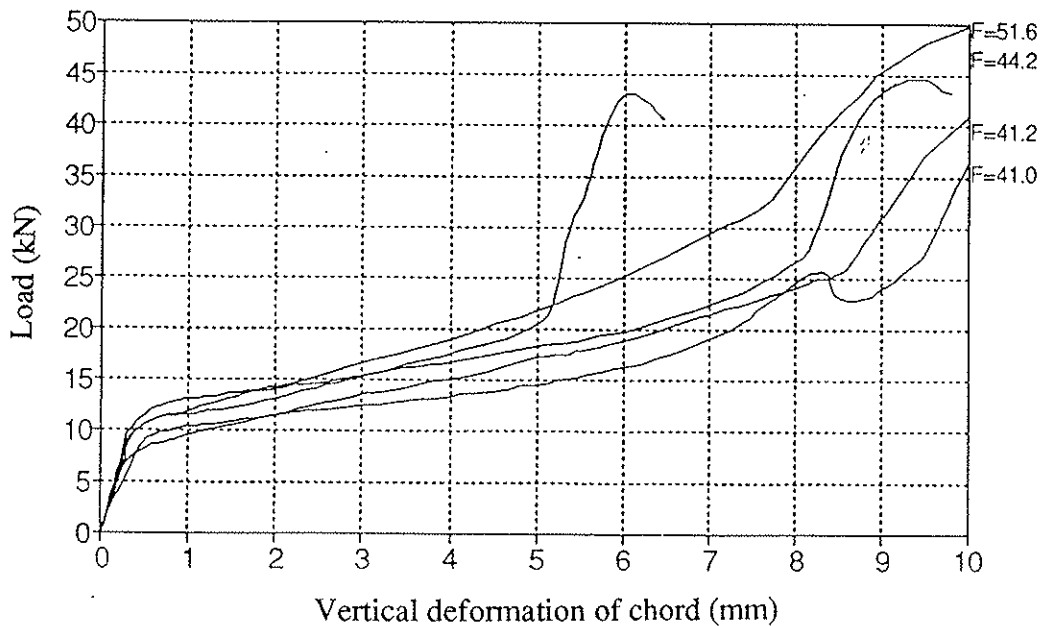


**Figure 3.** Measured load-deformation curves of support areas with nail plate reinforcements in two test series. a) Chord  $45 \times 95 \text{ mm}^2$  reinforced with 'vertical' multipurpose nail plates at an end support. b) Chord  $45 \times 95 \text{ mm}^2$  reinforced with 'horizontal' multipurpose nail plates at an intermediate support.

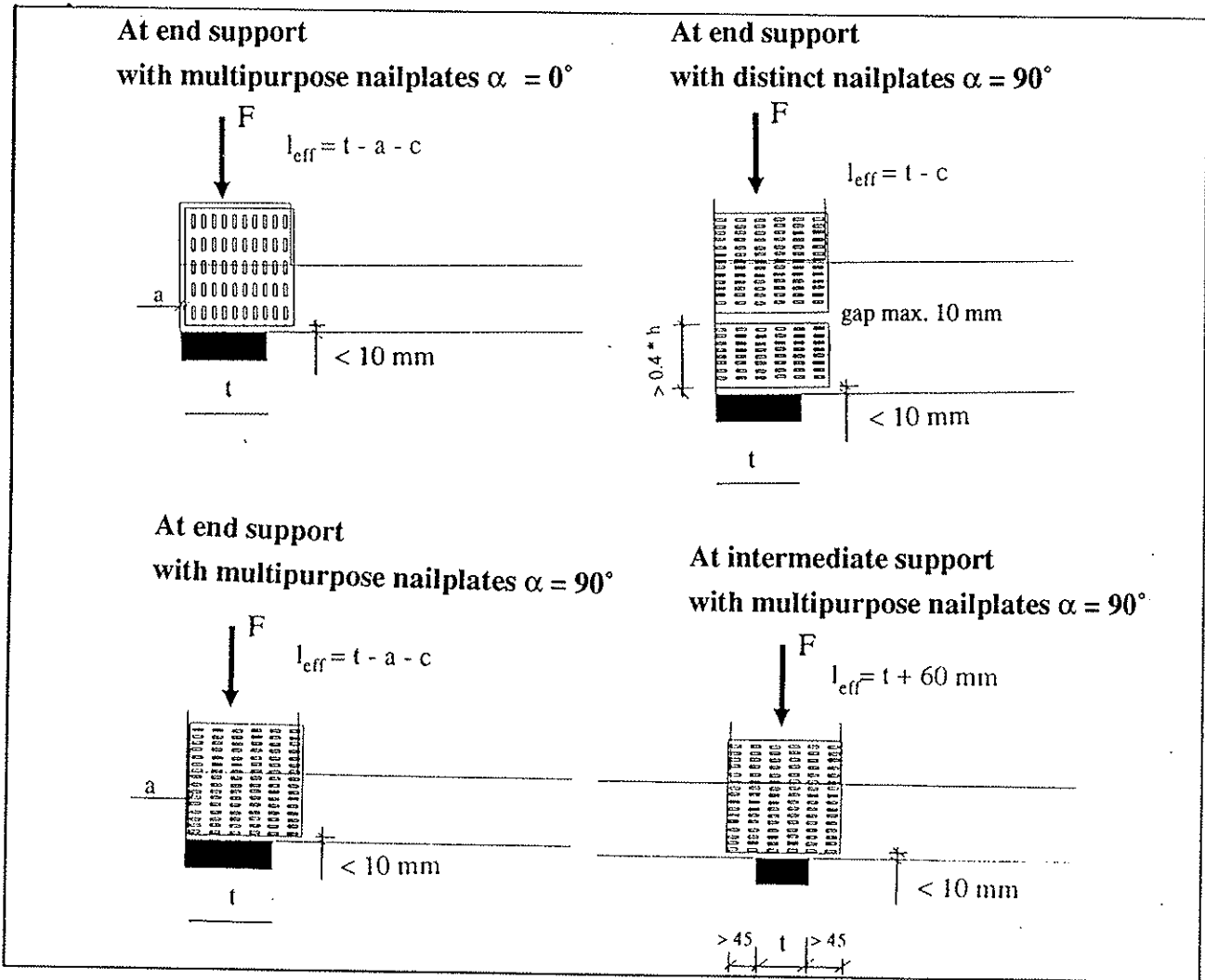


**Figure 4.** Different kinds of nail plate reinforcements and the effective lengths ( $l_{eff}$ ) of reinforcements. Value  $c$  is tolerance.

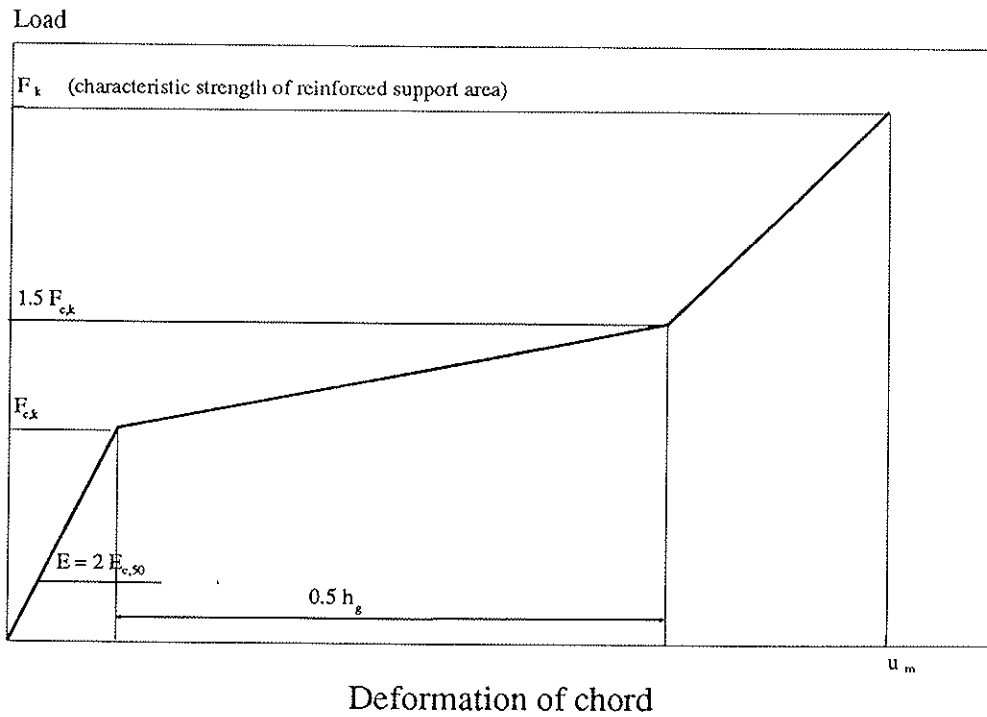


**Figure 5.** The simplification load-deformation curve of reinforced support area. Force  $F_{c,k}$  is characteristic capacity of wood in compression perpendicular to the grain.  $E_{c,50}$  is the appropriate modulus of elasticity of wood. Value  $h_g$  is the height of unreinforced wood gap. Failure deformation  $u_m = 0.5 h_g + 0.03 h$ , where  $h$  is the height of chord.



**INTERNATIONAL COUNCIL FOR BUILDING RESEARCH STUDIES AND DOCUMENTATION**  
**WORKING COMMISSION W18 - TIMBER STRUCTURES**

DISCUSSION ABOUT THE DESCRIPTION OF TIMBER BEAM-COLUMN FORMULA

by

S Y Huang  
Chongqing Institute of Architecture & Engineering  
China

**MEETING TWENTY - FOUR**

**OXFORD**

**UNITED KINGDOM**

**SEPTEMBER 1991**



# DISCUSSION ABOUT THE DESCRIPTION OF TIMBER BEAM-COLUMN FORMULA

S. Y. Huang

Chongqing Institute of Architecture and Engineering  
Department of Civil Engineering, Chongqing, Sichuan, CHINA

## INTRODUCTION

A paper entitled "A Brief Description of Formula of Beam-Columns in China Code" [1] was discussed at the meeting of CIB-W18A at Lisbon in 1990. However some questions from the session were not answered due to the absence of the author. Among the questions the most important ones are:

Why a reduced moment of inertia,  $I$ , corresponding to  $a$  in Figure 3 does not be used, but a fictitious modulus of elasticity?

What is the basis for using the stress-strain relationship shown in Figure 2, when it is not supported by the tests leading to curves B and C in Figure 5?

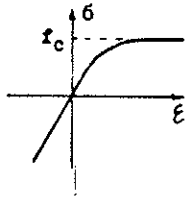


Figure 2

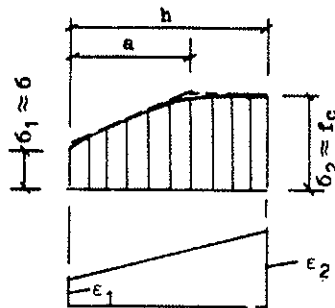


Figure 3

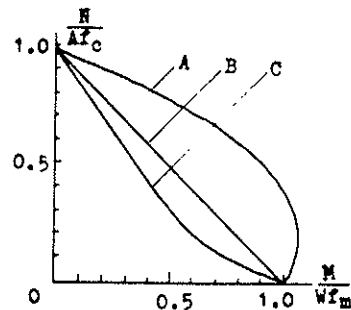


Figure 5

Now, the author wishes to make some explanation of the above questions and expresses sincerely very much thanks to the discussers of the paper, and especially to Mr. Hans Jorgen Larsen who presented the paper on behalf of the author at the meeting and informed the author of the comment from the session.

## ABOUT REDUCED MOMENT OF INERTIA I

Both a fictitious modulus of elasticity  $E_k$  and a reduced moment of inertia I are assumed. The former is used for considering the elastic property of materials, and the latter for the geometric parameter.

Based on these assumptions of  $E_k$  in Equation (9) and a corresponding reduced I in figure 3, the Equation (10) can be obtained from Equation (8):

$$N = \frac{\pi^2 E_k I}{l^2} (1 - K)^2 (1 - K_o) \quad (10)$$

It is easily visible that when  $P=0$  leading to  $M=0$  in Equation (11), then Equation (10) becomes :

$$N = \frac{\pi^2 E_k I}{l^2} (1 - K_o)^3 \quad (10-a)$$

From Eqs. (30) and (25), Equation (10-a) can be rewritten as:

$$N = \frac{\pi^2 E_k I}{l^2} \varphi_m = \frac{\pi^2 E_k I_e}{l^2} \quad (10-a-1)$$

$$\varphi_m = \left[ 1 - \frac{N e_o}{W f_m (1 + \sqrt{6} / f_c)} \right]^3 = [1 - K_o]^3 \quad (10-a-2)$$

$$I_e = \varphi_m I = \frac{b}{12} [(1 - K_o) h]^3 = \frac{b h_e^3}{12} \quad (10-a-3)$$

Where  $I_e$  is the reduced moment of inertia,  $\varphi_m$  is the reduced coefficient of I and  $h_e = (1 - K_o)h$  is the reduced depth of cross-section of column corresponding to a in Figure 3. Of course, it is apparent that there is a difference in definition between a and  $h_e$ , because a in Figure 3 is a variable varying with distance x from origin of the coordinate, but  $h_e$  in Equation (10-a-3) is an equivalent, constant depth along the length of the column.

Therefore  $\varphi_m$  involved in Equation (27) or (10-a-1) in the course of nature means that the concept of the reduced moment of inertia is implicitly involved.

In China Code (GBJ5-88), the concept of reduced moment of inertia,  $I_e = \varphi_m I$ , was not directly used, but  $\varphi_m$  in Equation (27), the reduced coefficient of  $\pi^2 E_k I / l^2$  for approximate simplification in practice. Where  $\pi^2 E_k I / l^2$  is criterion force for axially loaded columns.

At last, Equation (10) then becomes :

$$N = \frac{\pi^2 E_k I}{l^2} \varphi_m \quad (10-1)$$

$$\varphi_m = (1 - K)^2 (1 - K_0) = \left[ 1 - \frac{M + Ne_0}{W f_m \left( 1 + \sqrt{\frac{N}{A f_c}} \right)} \right]^2 \left[ 1 - \frac{Ne_0}{W f_m \left( 1 + \sqrt{\frac{N}{A f_c}} \right)} \right] \quad (28)$$

## ABOUT FICTITIOUS ELASTICITY MODULUS

$E_k$  is used as an equivalent modulus of elasticity representing the elastic property of zone a in Figure 3. For the assumptions the  $E_k$  seems to be a fictitious parameter. However when Equation (10) has been developed we can be aware that Equation (10) shows a relationship between column and beam-column, and that  $E_k$  is in practice a reduced modulus of elasticity of axially loaded column at  $K=K_0=0$ , and is a function of failure stress approximately corresponding to  $E_t$  in Figure 2-1.

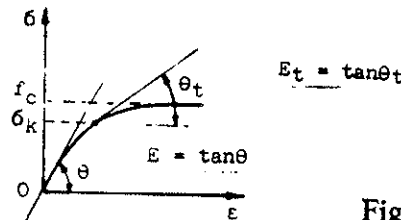


Figure 2-1

When the stress-strain relationship is given,  $E_k$  may be obtained from :

$$-E_k = E_t = \frac{d\sigma}{d\varepsilon} \quad (10-2)$$

such a stress-strain relationship as offered by reference [4] is:

$$\varepsilon = \frac{1}{E} \left[ C \sigma - (1 - C) f_c \ln \left( 1 - \frac{\sigma}{f_c} \right) \right] \quad (10-3)$$

Then the  $E_k$  is obtained as :

$$-E_k = E_t = \frac{d\sigma}{d\varepsilon} = \frac{f_c - \sigma_k}{f_c - C \sigma_k} E \quad (10-3-1)$$

substitute  $E_k$  into the following equation :

$$\sigma_k = \frac{\pi^2 E_k}{\lambda^2} \quad (10-3-2)$$

The column buckling coefficient can be given as:

$$\varphi = \frac{\pi^2 E + f_c \lambda^2 - \sqrt{(\pi^2 E + f_c \lambda^2)^2 - 4 C \lambda^2 \pi^2 E f_c}}{2 C \lambda^2 f_c} \quad (10-3-3)$$

Where  $E = \tan \theta$  is the modulus of elasticity.

When the stress-strain relationship is not given the  $E_k$  can be found by means of that proposed in reference [2], namely:  
Put the test data of axially loaded columns with a series of different slenderness ratios into the  $E_k/E - \sigma_k/f_c$  diagram, and substitute the expression of  $E_k$  obtained from statistics of test data into Equation (10-3-2), the the column buckling coefficient can also be given. Each point in  $E_k/E - \sigma_k/f_c$  relation diagram depends on:

$$\sigma_k = N_k / A \quad (10-4-1)$$

$$E_k = \sigma_k \lambda^2 / \pi^2 \quad (10-4-2)$$

Where  $N_k$  is axial failure load of column,  $A$  and  $\lambda$  are the area of cross section and slenderness ratio of column respectively.

For example the tests on columns made of Yunnan Pine, Sichuan Fir, Mumahuang, Longyuanan and Poplar in China.

For simplification the expression of  $E_k$  obtained from tests of axially loaded columns can be represented in a simple form of straight line, as shown in Figure 7.

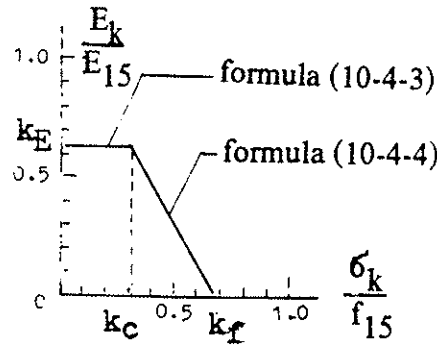


Figure 7

$$E_k = k_E E_{15} = E \quad \left( \frac{\sigma_k}{f_c} \leq \frac{k_c}{k_f} \right) \quad (10-4-3)$$

$$E_k = B E (1 - \sigma_k / f_c) \quad \left( \frac{\sigma_k}{f_c} > \frac{k_c}{k_f} \right) \quad (10-4-4)$$

$$E = k_E E_{15}; \quad f_c = k_f f_{15}; \quad B = \frac{k_f}{k_f - k_c} \quad (10-4-5)$$

Where  $E_{15}$  and  $f_{15}$  are respectively the elasticity modulus and compression strength parallel to the grain of standard test piece with moisture content of 15%;  $k_E$  and  $k_f$  are respectively the reduced coefficient of  $E_{15}$  and  $f_{15}$  caused by timber defects.

Then from Equations (10-4-3), (10-4-4), (10-4-5) and (10-3-2) the column buckling coefficient can be given  $\varphi = \sigma_k / f_c$  as :

$$\varphi = \frac{1}{1 + \left( \frac{\lambda}{\pi} \sqrt{\frac{f_c}{BE}} \right)^2} \quad \lambda \leq \pi \sqrt{\frac{E k_f}{f_c k_c}} \quad (10-4-6)$$

$$\varphi = \frac{\pi^2 E}{\lambda^2 f_c} \quad \lambda > \pi \sqrt{\frac{E k_f}{f_c k_c}} \quad (10-4-7)$$

According to assumption of tangent modulus, Equations (10-4-3) and (10-4-4) can yield a stress-strain relationship corresponding to  $E_k$  :

$$\sigma = E \varepsilon \quad \frac{\sigma}{f_c} < \frac{k_c}{k_f} \quad (10-4-8)$$

$$\frac{\sigma}{f_c} = 1 - e^{-(\frac{Bk_c}{k_f} - \ln B - \frac{BE}{f_c} \varepsilon)} \quad \frac{\sigma}{f_c} > \frac{k_c}{k_f} \quad (10-4-9)$$

In addition, the column buckling coefficient used in Equations (19) and (27) can also be obtained by the means proposed in reference [3], that is:

$$\varphi = k_{v_0} \cdot \sqrt{k_{v_0}^2 - k_{E_x}} \quad (10-5-1)$$

$$k_{E_x} = \frac{\pi^2 E}{\lambda^2 f_c} \quad (10-5-2)$$

$$k_{v_0} = 0.5 \left[ 1 + \left( 1 + \frac{f_c A v_0}{f_m W_x} \right) k_{E_x} \right] \quad (10-5-3)$$

Where  $v_0$  is the initial deviation.

This formula has been used in CIB Code 1983.

## ABOUT THE USE OF STRESS-STRAIN RELATIONSHIP AND CURVES B,C

When the stress-strain relationship shown in Figure 2 is used it is not the case that the stress-strain relationship is not supported by the tests leading to curves B and C in Figure 5, because there is no direct link between them.

The stress-strain relationship is obtained by means of measuring the deformation property of timber specimens loaded axially, as shown in Figure 2-2.

Curve C is found by tests for determination of strength of short columns loaded eccentrically, as shown in Figure 6. As described by the author the strength of short members without column effect corresponding to curve B or C mainly depends on test condition, and its strain certainly does not exceed the limit strain in the stress-strain relation diagram.



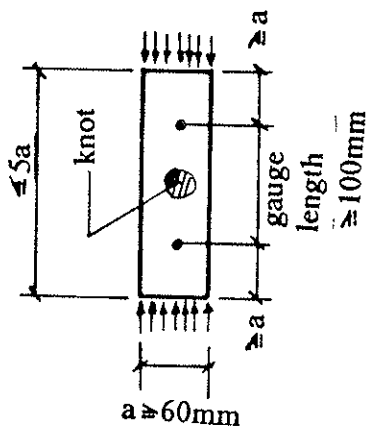


Figure 2-2

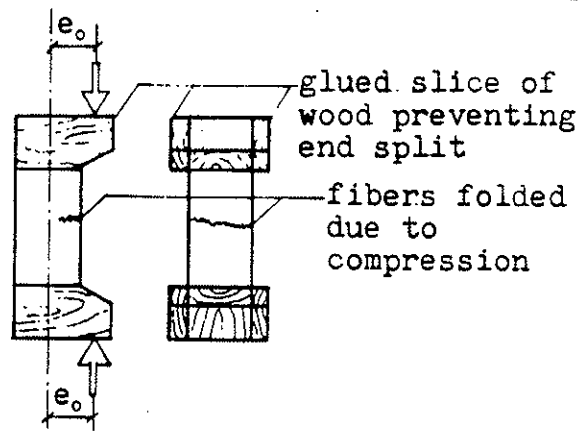


Figure 6

The stress-strain relationship is used for solution of buckling problem of longer columns, in which only the reduced modulus of elasticity  $E_k = E_t$  and compression strength  $f_c$  are used in Equations (8) and (9) in this simplified theoretical analysis method.

Curve B or C is used for the solution of strength problem of short members without column effect, and also certainly used for control of initial moment of other length members through adapting parameter  $\eta$ , as described by the author [1].

Therefore Equation (27) involved (28) is a constant condition of controlling both buckling and strength of the eccentrically loaded columns, beam-columns and other columns with combined eccentric and lateral loads.

## REFERENCES

- [1] S.Y. Huang, "A brief Description of Formula of Beam-Columns in China Code", CIB-W18A/23-15-3, Lisbon, 1990.
- [2] S.Y. Huang, P.M. Yu, J.Y. Hong, "Buckling and Reliability Checking of Timber Columns", CIB-W18A/22-2-1, East Berlin, 1989.
- [3] H.J. Larsen, "Instability of Columns and Beams", the first Pacific Timber Engineering Conference, PAPER No. 159B.
- [4] S.K. Malhotra, "Analysis and Design of Solid and Built-up Timber Compression Members", The first Pacific Timber Engineering conference, PAPER No. 219B.



**INTERNATIONAL COUNCIL FOR BUILDING RESEARCH STUDIES AND DOCUMENTATION**

**WORKING COMMISSION W18 - TIMBER STRUCTURES**

**SEISMIC BEHAVIOR OF WOOD-FRAMED SHEAR WALLS**

by

M Yasumura  
Building Research Institute  
Ministry of Construction  
Japan

**MEETING TWENTY - FOUR**

**OXFORD**

**UNITED KINGDOM**

**SEPTEMBER 1991**



# SEISMIC BEHAVIOR OF WOOD-FRAMED SHEAR WALLS

by Motoi YASUMURA

Building Research Institute, Japan

## Abstract

Wood-framed shear walls sheathed with the plywoods and gypsum boards were subjected to the reversed cyclic lateral loading, and it was found that the reversed cyclic loading affects more on the shear strength of gypsum-sheathed panels than that of plywood-sheathed panels. From the results of time-history earthquake response analysis of these panels, the behavior factor "q" of 2.5 to 3.0 is proposed for the wood-framed shear walls.

## INTRODUCTION

It is recognized that the Wood-framed shear walls such as the plywood-sheathed panels behave well during the severe earthquake motions as they generally show high dissipation of the seismic energy with their good ductile properties[1]. However it is also reported that the load carrying capacity of gypsum-sheathed panels can be affected by the reversed cyclic loading[2], and the influence of the cyclic loads should be considered in aseismic design if the gypsum-sheathed panels are used for the lateral load-carrying shear walls. The purpose of this study is to investigate the influence of the reversed cyclic loading on the mechanical properties of shear walls sheathed with the plywoods and gypsum boards and to evaluate the seismic behavior of Wood-framed shear walls by means of the time-history earthquake response analysis.

## TESTED WALLS

Tested walls were the wood-framed shear walls of 1.82 meters in length and 2.44 meters in height consisting of the nominal 2-by-4 inches studs and plates of Spruce-Pine-Fir sheathed with 9.5 millimeters thick Douglas-fir plywood and 12 millimeters thick gypsum board. Plywoods and gypsum boards were sheathed on the one side of wooden frame with CN 50 and GN40 wire nails respectively. Nail spacings were 10 centimeters in the perimeters of a sheathing and 20 centimeters on the central support. Four specimens for each sheathing were prepared, that is, two for the monotonic loading and two for the reversed cyclic loading.

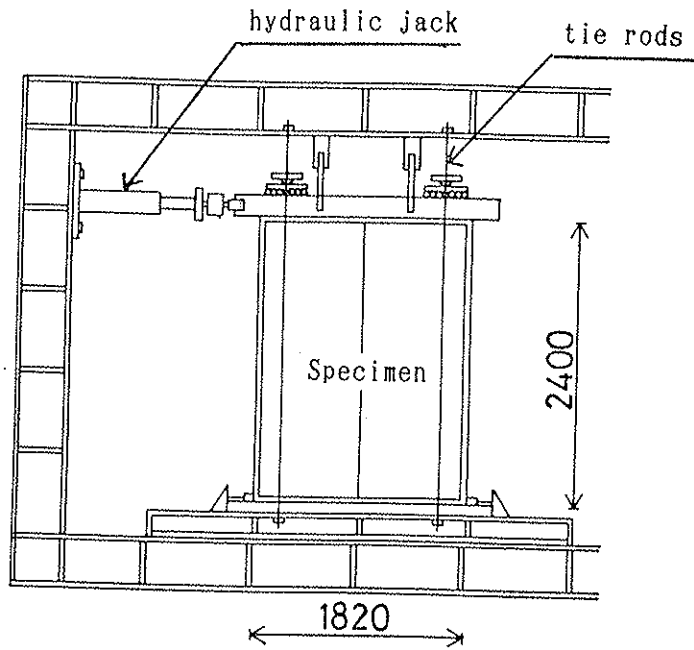


Fig.1 Test method

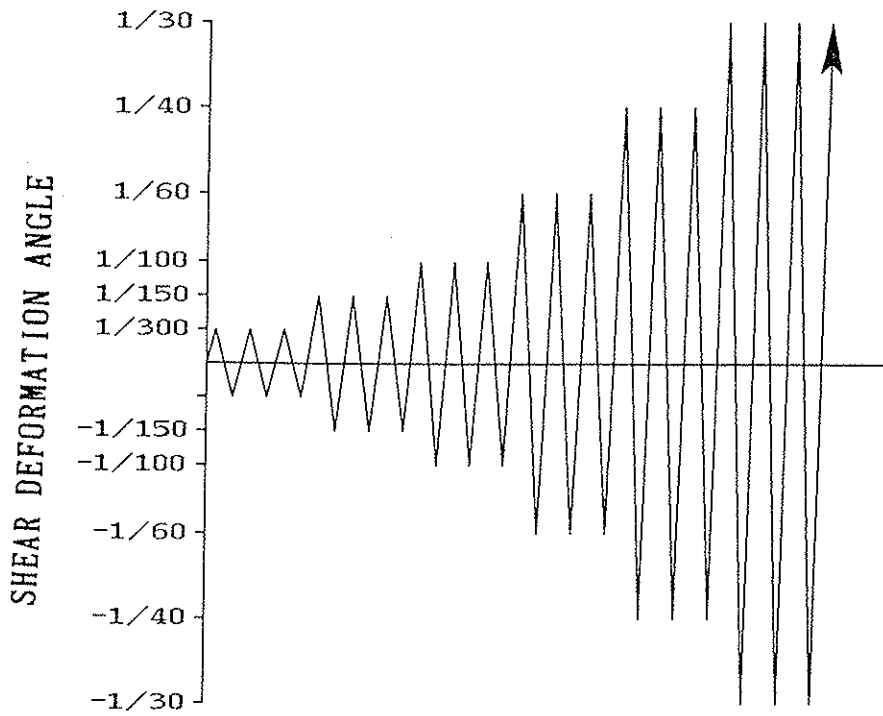


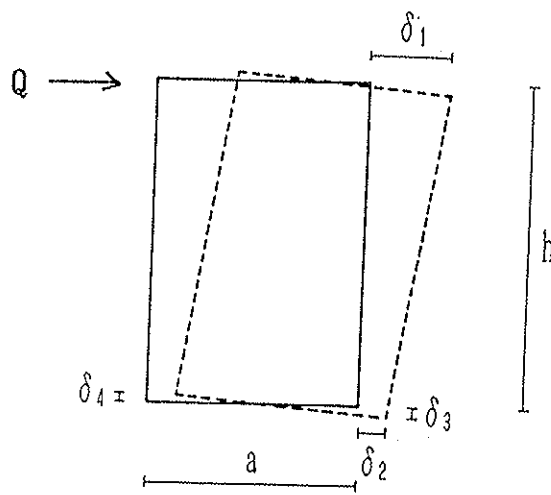
Fig.2 Loading history

## TEST METHOD

Racking test due to ASTM E72 using the tie rods as shown in Fig.1 was applied to the monotonic and reversed cyclic loading test. Although this test method dose not reflect exactly the up-lift of shear walls of full-scale structure, this simple method is widely used to evaluate the shear strength of panel walls. Two specimens for each sheathing were subjected to the monotonic loading, and two others subjected to the reversed cyclic loading as shown in Fig.2.

## DEFINITION OF SHEAR DEFORMATION

In the racking test using the tie rods, the up-lift and embedding of studs appear at the tension and compression side of wall panel. These up-lift and embedding do not necessarily correspond to those in full-scale structure because the up-lift of studs depends on the vertical loads caused by the dead loads and live loads and the connection of studs. Thus the shear deformation angle was defined as shown in Fig.3 by subtracting the rotation from the drift of panel.



## SHEAR DEFORMATION ANGLE

$$\gamma = \frac{\delta_1 - \delta_2}{h} - \frac{\delta_3 + \delta_4}{a}$$

Fig.3 Definition of shear deformation angle

## TEST RESULTS

### Influence of cyclic loading

Fig.4 demonstrates the skeleton curves of the relationship between the lateral loads and the shear deformation angle in plywood-sheathed panels and gypsum-sheathed panels.

In the plywood-sheathed panel, the skeleton curves of the first cycle of each cyclic loading level agreed with the results of the monotonic loading test. The lateral load increased approximately linearly up to 1/300 of the shear deformation angle, and the decrease of the strength at the second and third cycle of 1/300 was very small. These results show that the reversed cyclic load dose not affect on the ultimate properties of the plywood-sheathed shear walls, and the elastic limit of the plywood-sheathed shear walls shall be defined by the shear deformation angle of 1/300 which corresponds to 50 to 60% of the ultimate load.

In the monotonic loading test of the gypsum-sheathed panel, the shear load continued to increase up to 1/40 of shear deformation angle. In the reversed cyclic loading test, the shear load began to decrease at the shear deformation angle of 1/100, and the maximum load in the reversed cyclic loading test was approximately 73% of that in the monotonic loading test. This results agree with the results of full-scale test of wood-framed building[3]. The shear load at the second and third cycles of 1/300 decreased to 87 and 83% respectively comparing to the first cycle. These results show that the reversed cyclic loading makes a serious influence on the shear strength of gypsum-sheathed shear walls and the maximum strength shall be decreased approximately 30% from that obtained by the monotonic loading test, and the elastic limit is much smaller than 1/300 of shear deformation angle as is reported in [2].

### Equivalent viscous damping

The equivalent viscous damping was obtained from the hysteresis curves of each panel, where the equivalent viscous damping is defined as follows;

$$h_{eq} = \frac{\Delta E}{2\pi (E_1 + E_2)} \quad (1)$$

where,  $h_{eq}$  : equivalent viscous damping  
 $\Delta E$  : absorbed energy in a cycle  
 $E_1, E_2$  : external work in a half cycle



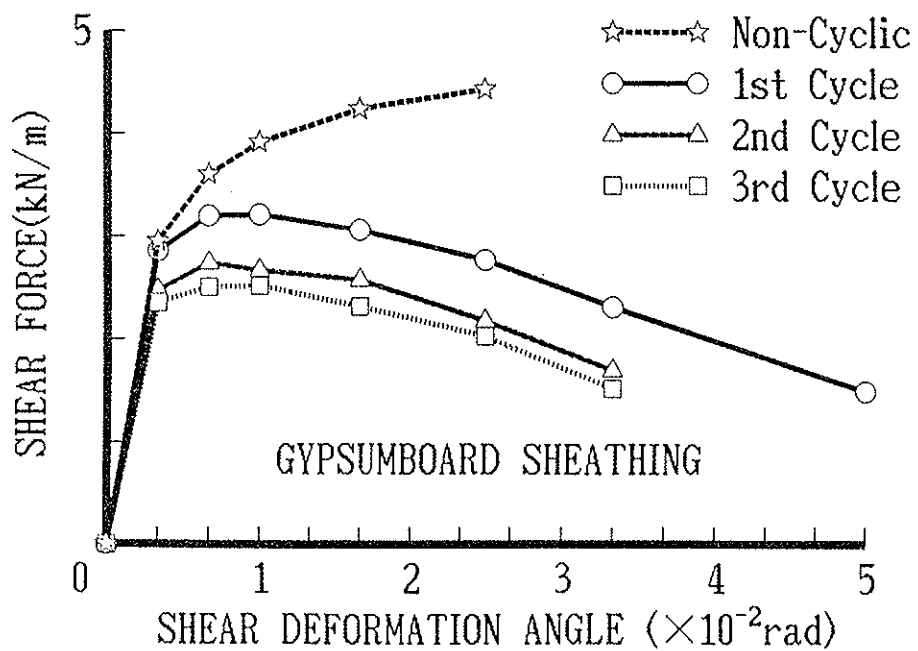
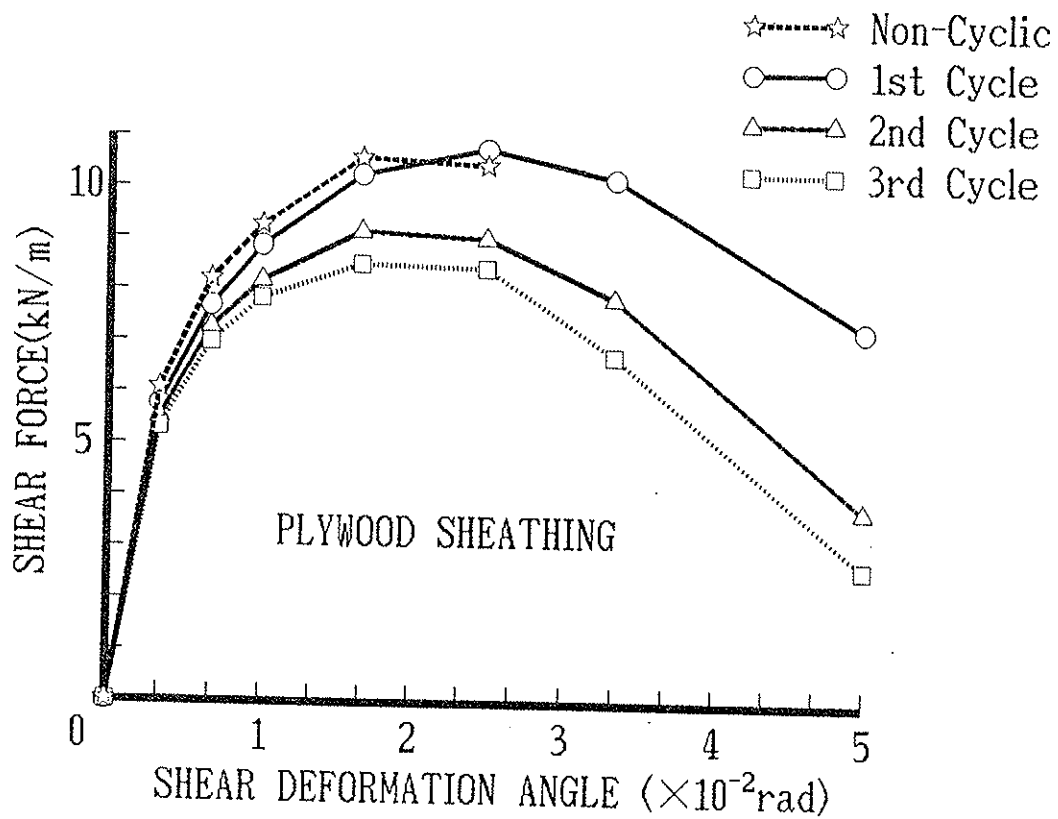


Fig.4 Load-deformation relationship of plywood-sheathed and gypsum-sheathed panels (average of two specimens and of the positive and negative half cycles).

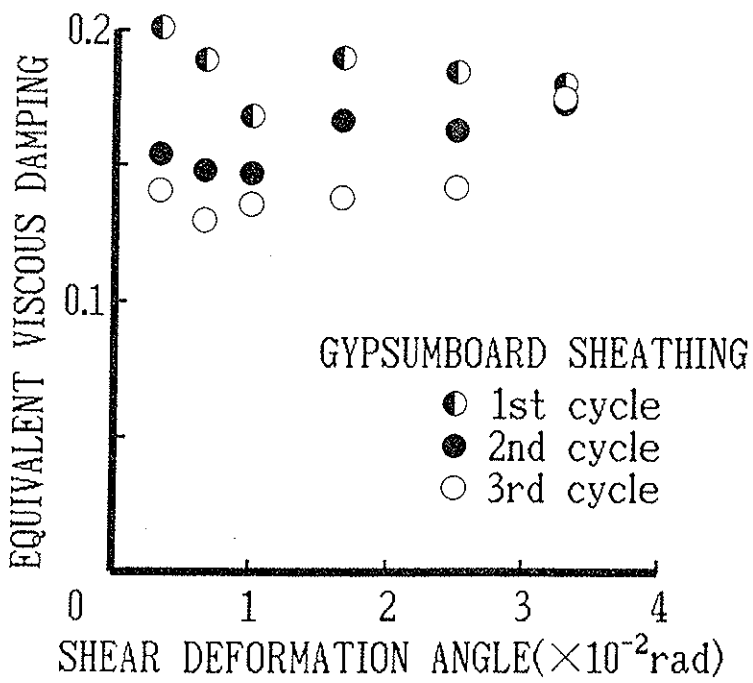
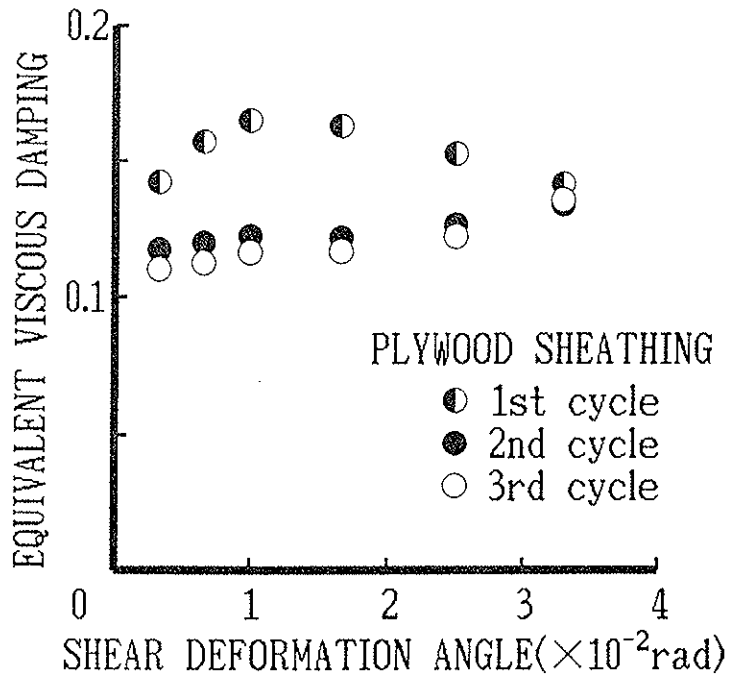


Fig.5 Equivalent viscous damping obtained from the hysteresis curves

Fig.5 shows that the equivalent viscous damping of plywood-sheathed panel was in average 15% at the first cycle and 12% at the second and third cycle, and showed similar values to those of the braced frames[4]. That of gypsum-sheathed panel was in average 18.5% at the first cycle and 15% at the second and third cycles, and showed higher values than those of the plywood-sheathed panel.

## TIME-HISTORY EARTHQUAKE RESPONSE ANALYSIS

### Analytical procedure

Time-history earthquake response analysis was conducted on the plywood-sheathed shear walls and gypsum-sheathed shear walls. Single-degree-of-freedom lumped mass model was applied, and the load-displacement relationship was modeled with the bi-linear slip model as shown in Fig.6. This model includes;

- (1) loading on the primary curve before yielding
- (2) loading on the post yielding primary curve
- (3) unloading from peak on the primary curve
- (4) reloading with soft spring
- (5) loading with hard spring toward previous peak
- (6) unloading from inner peak
- (7) reloading toward peak without pinching effect

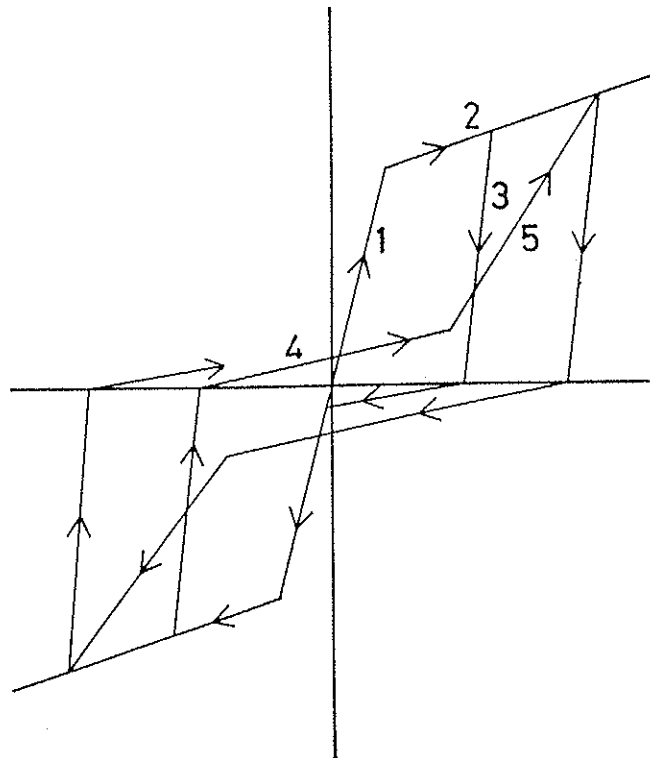


Fig.6 Hysteresis model for shear walls

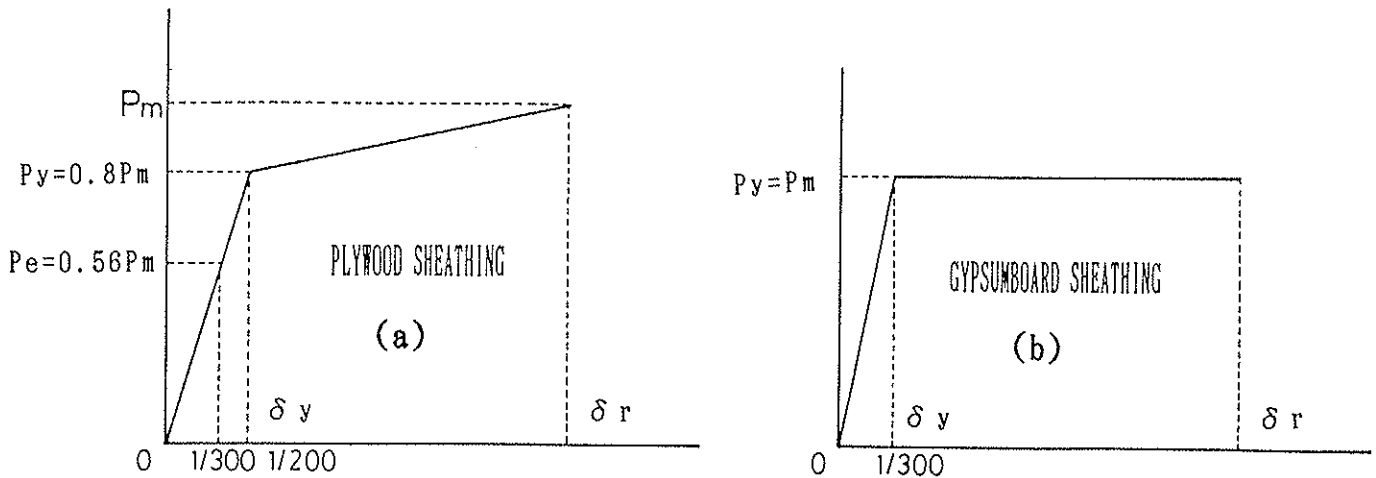


Fig.7 Modeling of load-deflection relationship

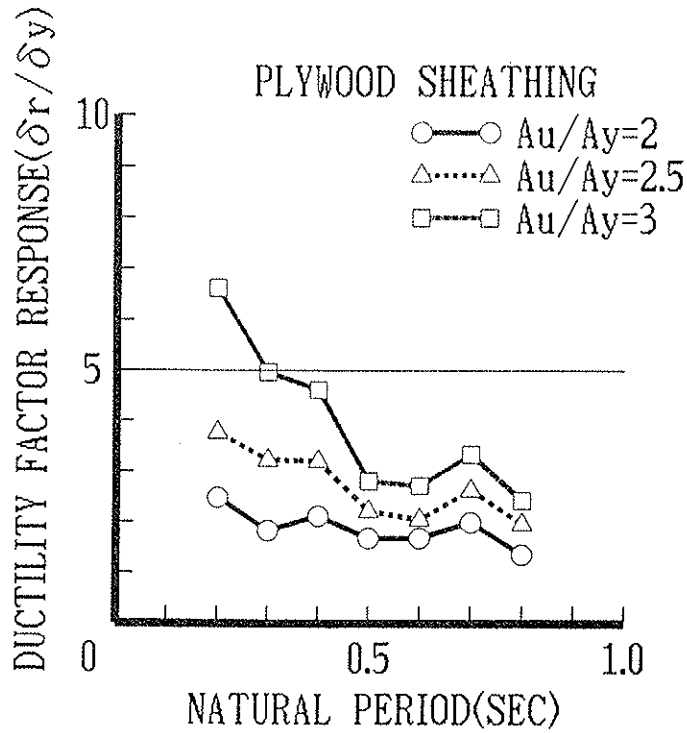
In the plywood-sheathed shear wall, the initial stiffness before yielding was obtained from the load at the shear deformation angle of  $1/300$ , and the yield load was assumed to be 80% of the ultimate load as shown in Fig.7(a). In the gypsum-sheathed shear wall, the initial stiffness and yield load were obtained from the load at the shear deformation angle of  $1/300$  as shown in Fig.7(b). The damping was assumed to be 2%.

Input earthquake ground motions were based on the records of N-S component of the 1940 El Centro, E-W component of the 1952 Taft and E-W component of the 1968 Hachinohe[4]. Following procedures were made;

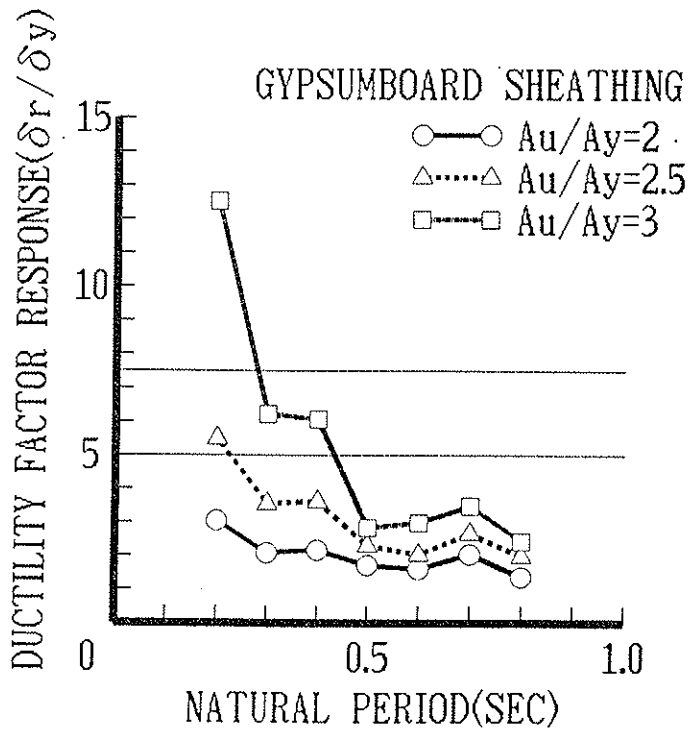
- (1) The accelerogram was linearly scaled at every natural period so that the maximum linear acceleration response became  $1g$ .
- (2) The accelerogram was linearly scaled to have the maximum acceleration of  $300\text{cm}/\text{sec}^2$ .

#### Analytical results

Fig.8(a) shows the average ductility factor response spectrum of three accelerograms in plywood-sheathed shear walls. This figure shows that  $A_u/A_d$  of 3.0 shall be taken if the response at the natural period of 0.2sec which seems rather short for the natural period of wood-framed construction is neglected and the ductility factor of 5.0 which corresponds to the shear deformation angle of  $1/40$  is taken.



(a) Plywood-sheathed shear wall

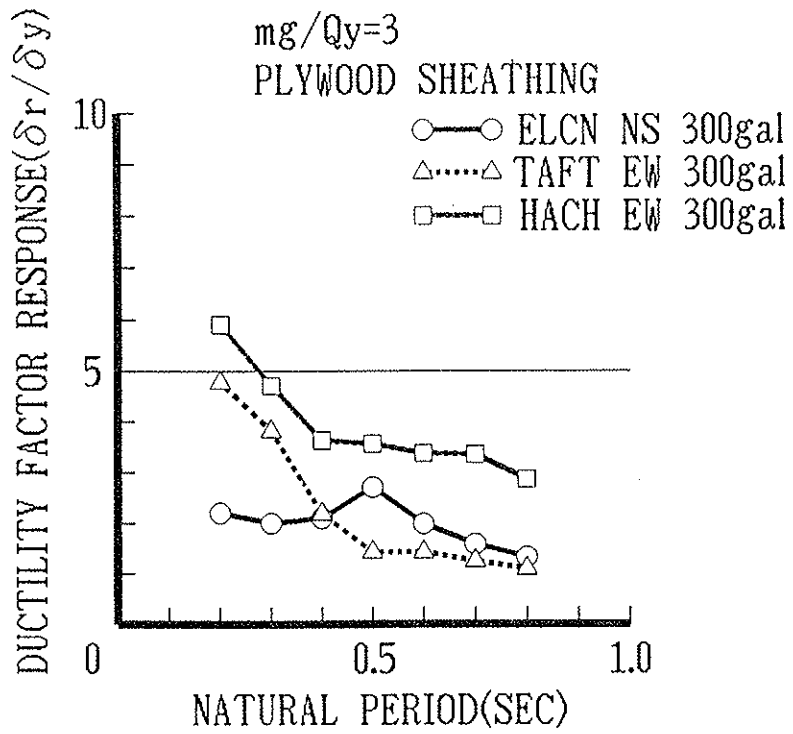


(b) Gypsum sheathed shear wall

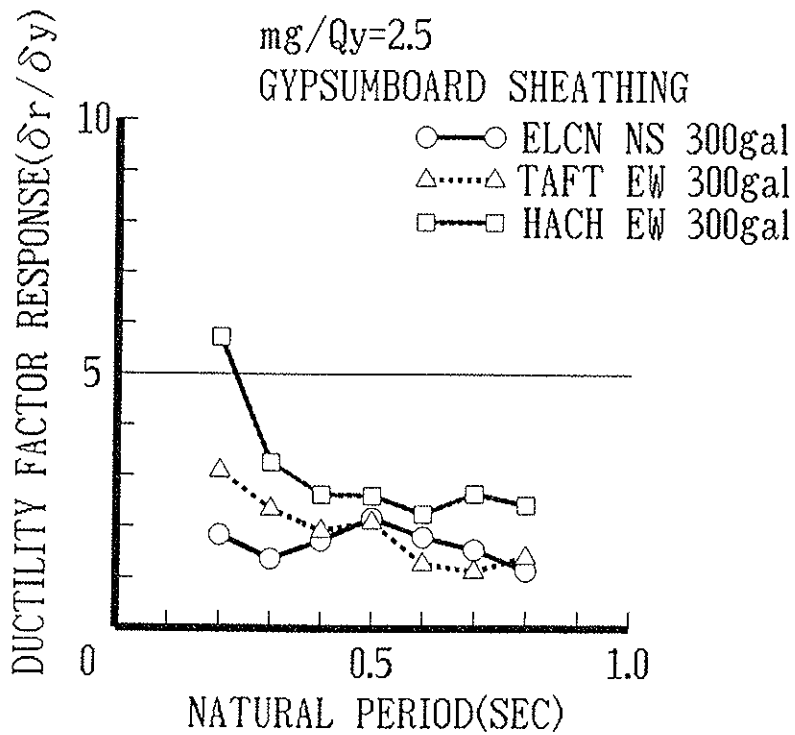
Fig.8 Ductility factor response spectrum  
(average of three accelerograms)

Au: Maximum ground motion acceleration which gives maximum acceleration of 1g in linear response

Ay: Maximum ground motion acceleration which gives yield force in linear response



(a) Plywood-sheathed shear wall



(b) Gypsum sheathed shear wall

Fig.9 Ductility factor response spectrum

Fig.8(b) shows the average ductility factor response spectrum of three accelerograms in gypsum-sheathed shear walls. This figure shows that  $A_u/A_y$  of 2.5 shall be taken if the response at the natural periode of 0.2sec is neglected and the ductility factor of 5.0 which corresponds to the shear deformation angle of  $1/60$  is taken, and  $A_u/A_y$  of 3.0 shall be taken if the ductility factor of 7.5 which corresponds to the shear deformation angle of  $1/40$  is taken.

Fig.9(a) shows the ductility factor response spectrum of plywood-sheathed shear walls when  $m_g/Q_y=3.0$ . It shows that the response due to the 1968 Hachinohe showed higher response than other accelerograms, and the ductility factor response of plywood-sheathed shear walls varied from 1.1 to 5.9 which corresponded to the shear deformation angle of  $1/180$  to  $1/34$  according to the natural period and the generated accerelogram.

Fig.9(b) shows the ductility factor response spectrum of gypsum-sheathed shear walls when  $m_g/Q_y=2.5$ . The ductility factor response varied from 1.1 to 5.7 which corresponded to the shear deformation angle of  $1/270$  to  $1/53$ .

#### CONCLUSION

Summarizing the results of this study, the following conclusions are lead.

- (1) The reversed cyclic loading affected very little on the ultimate properties of plywood-sheathed shear walls, and there were no decrease of ultimate load by the cyclic loading of lower load level.
- (2) The reversed cyclic loading made a serious influence on the shear strength of gypsum-sheathed shear walls, and the ultimate load was decreased 27% comparing to that in monotonic loading test.
- (3) The elastic limit of plywood-sheathed shear walls may be defined by the shear deformation angle of  $1/300$  which corresponds to 50 to 60% of the ultimate load, and the yield load may be defined by multiplying 1.5 by the elastic limit which correspond to 80% of the ultimate load.
- (4) In the gypsum-sheathed panel, the shear load at the second and third cycles of  $1/300$  decreased to 87 and 83% respectively comparing to the first cycle, and it was shown that the elastic limit of gypsum-sheathed panel might be smaller than  $1/300$  of shear deformation angle. The yield load of gypsum-sheathed shear walls may be defined by the shear deformation angle of  $1/300$  considering the effect of cyclic loading.

(5) The equivalent viscous damping of plywood-sheathed panel was in average 15% at the first cycle and 12% at the second and third cycle. That of gypsum-sheathed panel was in average 18.5% at the first cycle and 15% at the second and third cycles, and showed higher values than those of the plywood-sheathed panel.

(6) The ductility factor of 5.0 which corresponds to the shear deformation angle of 1/40 gives the  $A_u/A_y$  value of 3.0 for the plywood-sheathed shear walls.

(7) The ductility factor of 5.0 which corresponds to the shear deformation angle of 1/60 gives the  $A_u/A_y$  value of 2.5, and the ductility factor of 7.5 which corresponds to the shear deformation angle of 1/40 gives the  $A_u/A_y$  value of 3.0 for the gypsum-sheathed shear walls.

(8) The ductility factor response of plywood-sheathed shear walls varied from 1.1 to 5.9 which corresponded to the shear deformation angle of 1/180 to 1/34 when the accelerograms were linearly scaled for  $300\text{cm/sec}^2$  and  $mg/A_y=3.0$ .

(8) The ductility factor response of gypsum-sheathed shear walls varied from 1.1 to 5.7 which corresponded to the shear deformation angle of 1/270 to 1/53 when the accelerograms were linearly scaled for  $300\text{cm/sec}^2$  and  $mg/A_y=2.5$ .

#### ACKNOWLEDGMENTS

The author is grateful to Mr.H.Suzuki of B.R.I and Mr.I.Fukuda of Japan Two-by-four Home Builders Association for their assistance of conducting the racking test.

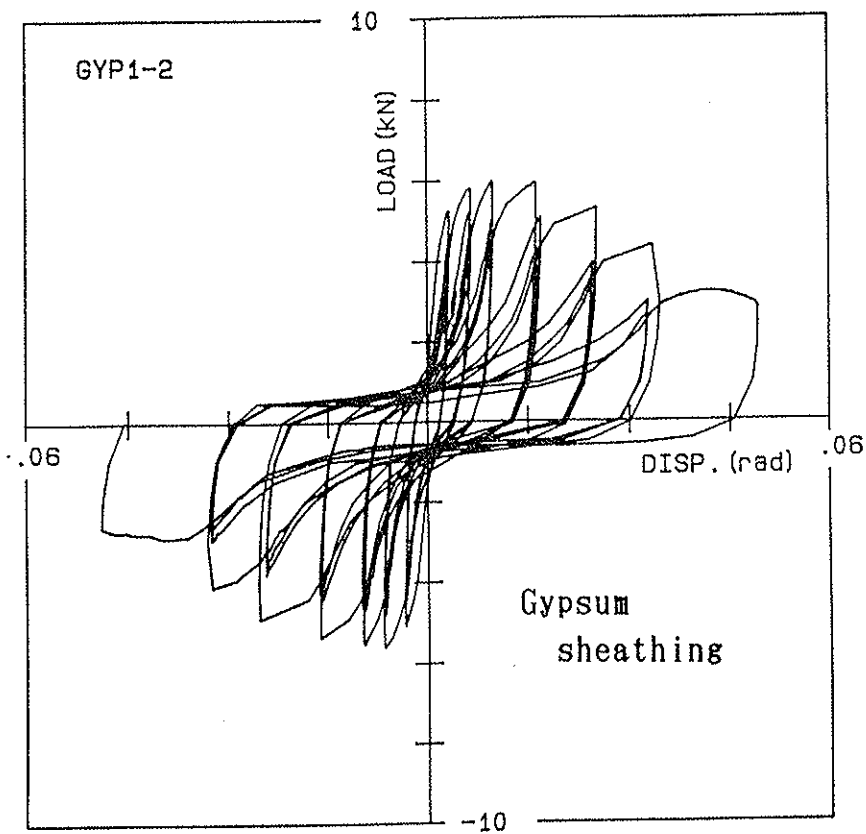
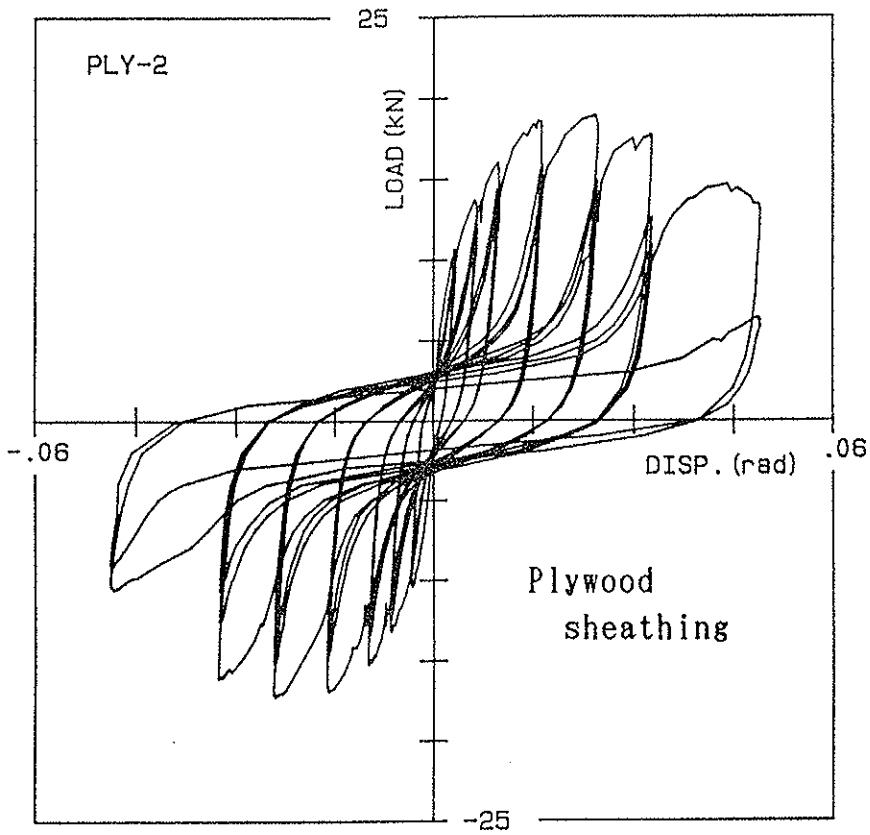
#### LITERATURE

1. Stewart,W.,J.Dean and A.Car,"THE EARTHQUAKE BEHAVIOR OF PLYWOOD SHEATHED SHEAR WALLS", Proceedings of the 1988 International Conference on Timber Engineering, Vol.2, Forest Products Research Society, September 1988
2. Oliva,M.,"RACKING BEHAVIOR OF WOOD-FRAMED GYPSUM PANELS UNDER DYNAMIC LOAD", National Technical Information Service PB90-262643, April 1990
3. Yasumura,M,T.Murota,H.Nishiyama and N.Yamaguchi,"EXPERIMENTS ON A THREE-STORIED WOODEN FRAME BUILDING SUBJECTED TO HORIZONTAL LOAD", Proceedings of the 1988 International Conference on Timber Engineering, Vol.2, Forest Products Research Society, September 1988
4. Yasumura,M.,"SEISMIC BEHAVIOR OF BRACED FRAMES IN TIMBER CONSTRUCTION", Proceedings of CIB-W18A Meeting twenty-three(Lisbon), September 1990



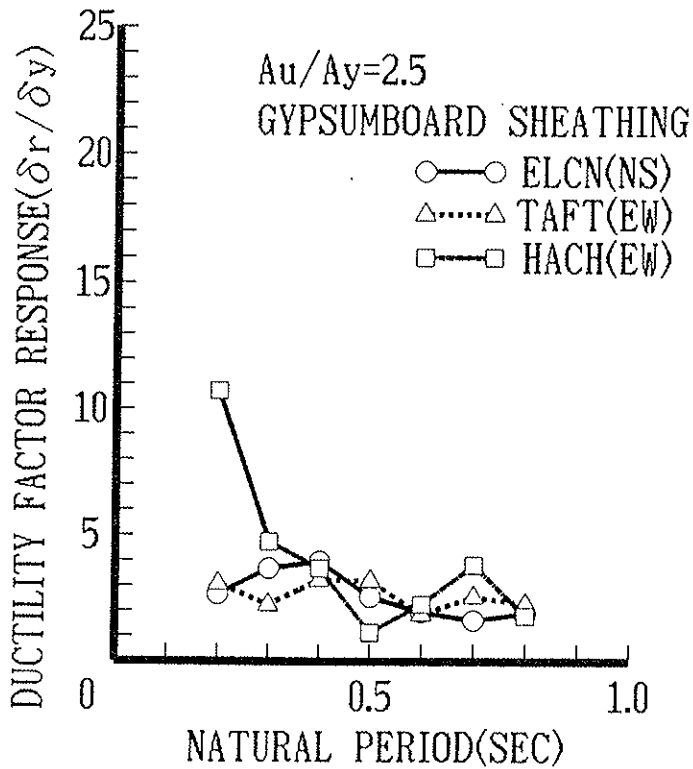
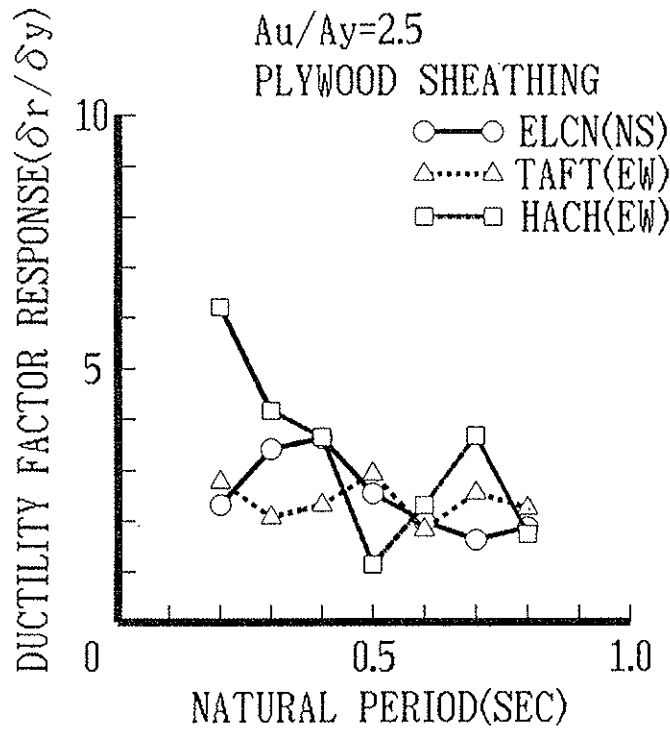
APPENDIX I

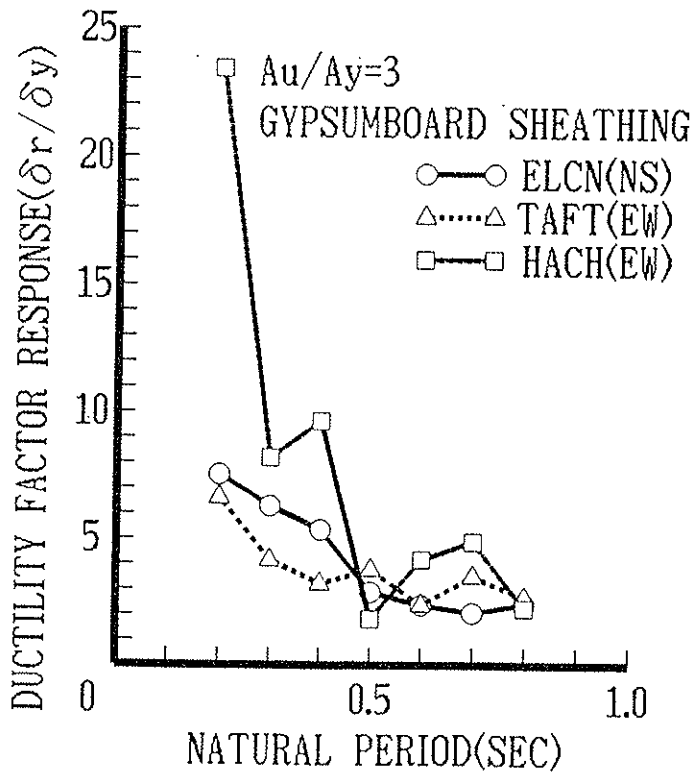
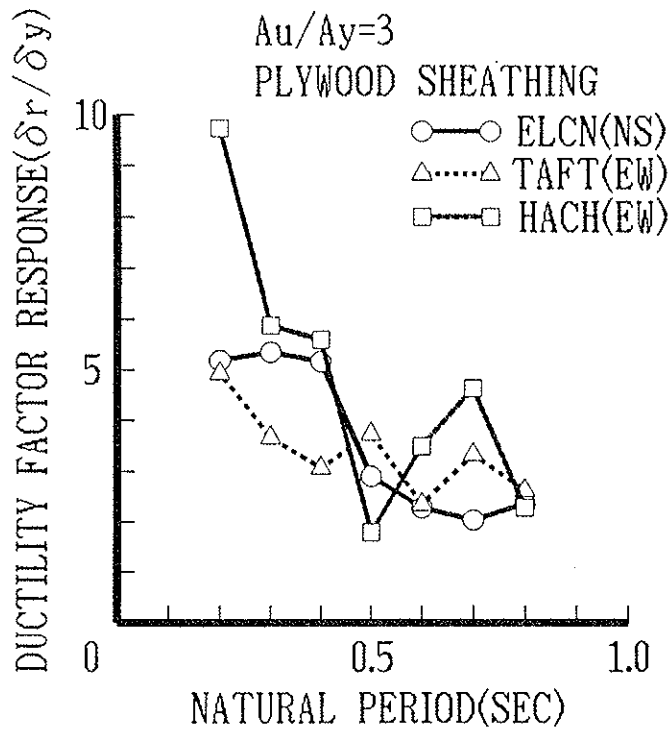
Example of load-displacement curves



APPENDIX II

Examples of ductility factor response spectrum







**INTERNATIONAL COUNCIL FOR BUILDING RESEARCH STUDIES AND DOCUMENTATION**  
**WORKING COMMISSION W18 - TIMBER STRUCTURES**

**MODELLING THE EFFECTIVE CROSS SECTION OF TIMBER**  
**FRAME MEMBERS EXPOSED TO FIRE**

by

J König  
Swedish Institute for Wood Technology Research  
Sweden

**MEETING TWENTY - FOUR**

**OXFORD**

**UNITED KINGDOM**

**SEPTEMBER 1991**



# MODELLING THE EFFECTIVE CROSS SECTION OF TIMBER FRAME MEMBERS EXPOSED TO FIRE.

by J. König

Swedish Institute for Wood Technology Research

## ABSTRACT

The results from fire tests on light, partly protected timber frame members under pure bending are used in order to model the effective cross section of this type of structural members. Since the test results made it possible to regard the influence of some parameters as the influence of the load level in relation to load capacity at normal temperature, the state of stresses, the loading rate and density, the modelling of structural timber in fire is discussed in a wider perspective and some of the consequences for the requirements of an analytical model are described.

## INTRODUCTION

Structural timber exposed to fire performs in a predictable manner. The charring layer increases in depth at an approximately constant rate and the residual section of the member is able to maintain a considerable load-bearing capacity under long time. Due to this behaviour heavy timber is a well-reputed structural material with respect to fire loading. Heavy timber structures do not normally need to be protected as is in the case of steel structures.

Most of the research into the load-bearing capacity of timber members in fire has been done in the field of heavy timber structures, i.e. normally glued laminated timber /1/, /2/. In the tests specimens were chosen fulfilling the requirements of a special quality class according to the national building code and the load was put equal to the "allowable load" according to the code or a part thereof. Since the real load-bearing capacity of the specimen was unknown - at the time of the tests there existed no reliable non-destructive method of predicting strength of heavy timber members - the resultant fire resistance ratings obtained from the fire tests, were related to the design load given in the code and not in relation to the load-bearing capacity at normal temperature.

Charring rates which are applied in different building codes, vary considerably. In most cases they are in the range between 0,5 and 1,0 mm/min. There are various reasons for this. Since the material close to the char-layer is strongly affected by elevated temperature, the decrease of strength and modulus of elasticity is regarded either by applying a notional charring rate which is higher than the real one, or by assuming that strength and modulus of elasticity of the uncharred residual section is reduced. Another reason should be that the charring rates are calibrated to a, rather arbitrary, load level whose relation to load capacity at normal temperature is not known. The introduction of strength classes in codes for timber structures, i.e. the material is characterized by its characteristic strength, makes it necessary to determine charring rates which are related to the real decrease of load-bearing capacities of the members.

In the work on Eurocode 5 - Timber Structures - structural fire design is an essential part. A first draft on structural fire design of timber structures has been presented in 1990 /3/. Within CEN TC250/SC 5 a project team has been appointed with the task of redrafting the first version, taking into account the national comments which have been made.

One of the tasks is to agree on charring rates to be adopted in the code. It has to be decided whether strength and stiffness of the residual section has to be regarded as reduced or unreduced in relation to its values at normal temperature. The aim of this paper is to contribute to the discussion on modelling the effective section of timber members and on determining the relevant parameters.

### FIRE TESTS

Some of the problems in modelling can be elucidated by referring to the results from an experimental investigation which is in progress at the Swedish Institute for Wood Technology Research. Some of the results are presented in /4/. Even though the thermal conditions differ from the general case of unprotected heavy rectangular cross-sections, these results contribute to a better understanding of the mechanical behaviour caused by elevated temperature and the modelling of it. This is partly due to the use of light members where the influence of some parameters is more evident, partly due to the partial protection of the members which allows one to separate the influence of certain parameters.

The aim of the investigation was to study the strength and stiffness properties of protected light timber frame members as they are used in walls and floors. The flat sides of the members with the dimensions 45 x 145 mm<sup>2</sup> were protected by rockwool insulation. The members were exposed to standard fire according to ISO 834 on one narrow side and were in pure edgewise bending in the region inside the furnace. Two different load directions occurred. In test series No. 1 the fire-exposed side was in compression and in series No. 3 in tension. The applied loads were in the range between 10 and 77 % of the predicted ultimate load at normal temperature. In test series No. 2 the fire-exposed side of the members was in compression and, initially, protected by gypsum plasterboard.

### Summary of results.

The results presented in /4/ can be summarized as follows:

- a) The relationship between relative load and failure time can be expressed by exponential functions, which are dependent on whether the fire-exposed side is in compression or tension.
- b) The loss of flexural stiffness is considerably larger when the fire-exposed side is in compression. This is more pronounced when the load level is high, but is negligible at load levels below about 35 % of predicted ultimate load at normal temperature. When the fire-exposed side is in tension flexural stiffness is independent of load level.
- c) The position of the neutral axis is dependent of whether the fire-exposed side is in compression or tension. In the case of



compressive stresses a large portion of the residual section on the fire-exposed side is statically ineffective due to plastic deformations while this ineffective portion is smaller in the case of tensile stresses.

- d) The influence of the gypsum plasterboard lining is purely additive. It can be expressed by a displacement of the exponential function mentioned above in (a) in direction of the time-axis.

#### Additional results.

Temperature and charring line. Some additional results are given below. A typical temperature profile along the centre line of the cross section and the corresponding residual uncharred core after fire-exposure of 30 minutes is shown in Figure 1. The thermocouples were attached on the centre line of the cross section at different sections at equal distances of 100 mm. The location of the charring line at the centre line of the cross section is plotted in the diagram with a dotted line. It is widely accepted

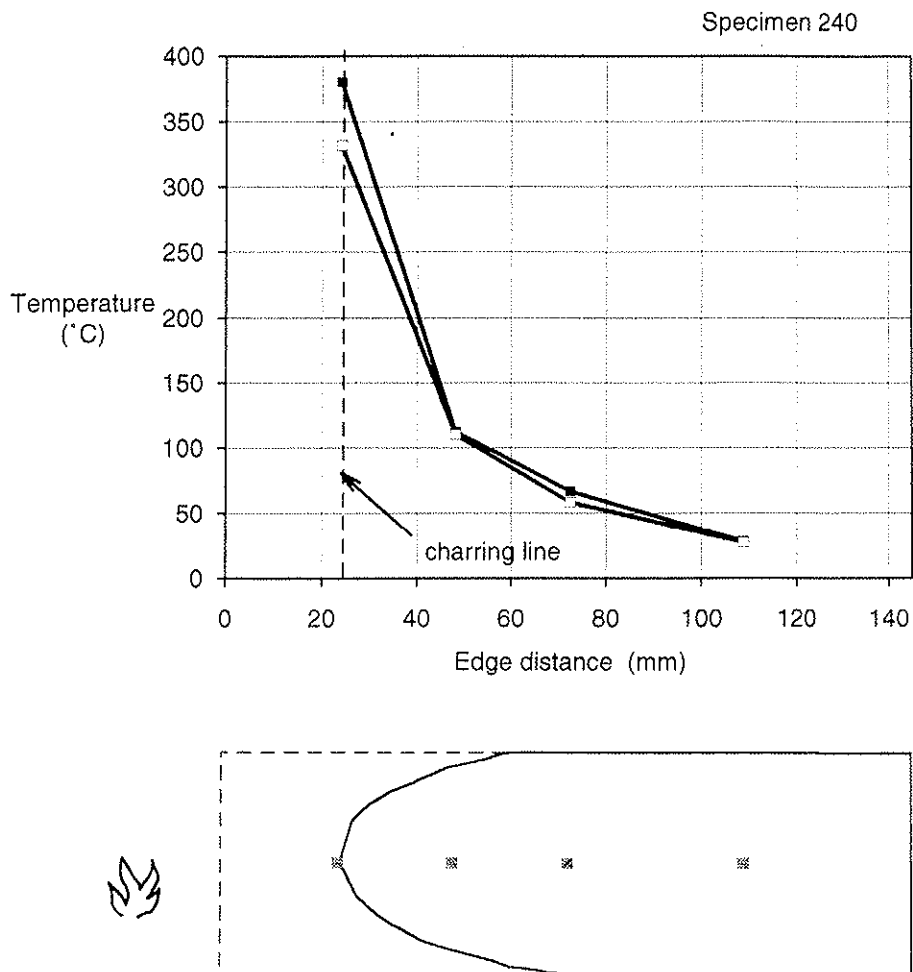


Figure 1 Example of temperature profile along the centre line of the cross section at failure.

that charring occurs at a temperature of about 280 °C. The diagram coincides fairly well with this. The plotted charring line is the mean value of the recorded values from five different sections, which were different from the positions of the thermo-couples.

The propagation of temperature with time can be seen from Figure 2. This diagram shows the two recorded temperature profiles at ultimate state of all specimens in Series No. 3 (fire-exposed side under tensile stresses). The failure times were in the range from 10 to 50 minutes. The vertical axis of the diagram is cut at 300 °C. The intersection of the temperature curves with this level indicates the approximate location of the charring line at the centre line of the cross section. From the diagram it can be seen that the temperature gradient is very steep close to the charring line. In the main part of the uncharred core temperature is considerably below 100 °C.

Three additional tests with unloaded specimens were made in order to measure temperature profiles perpendicular to the centre line, since it could be expected that the thermal flow would be greater in the mineral wool than in the wood. Some typical results can be seen in Figure 3.

The experimental charring depths at the centre line of the cross section are shown in Figure 4. In series No. 2 charring is delayed due to the attached gypsum plasterboard lining on the fire-exposed side of the member. Considering charring depths greater than about 20 mm the delay of charring coincides well with the delay of the loss of load capacity and stiffness. See Figure 6 in /4/.

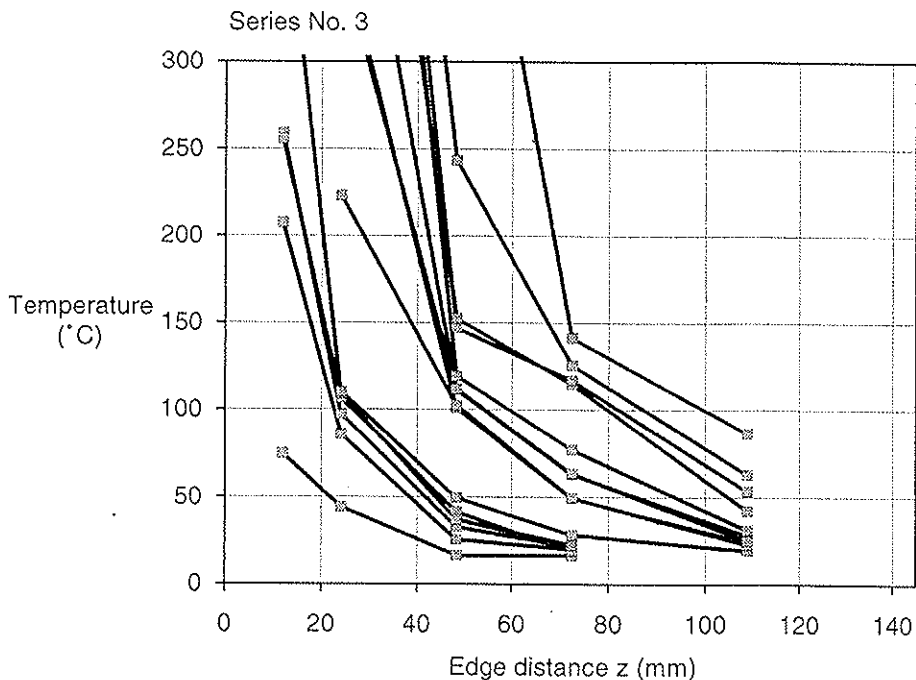
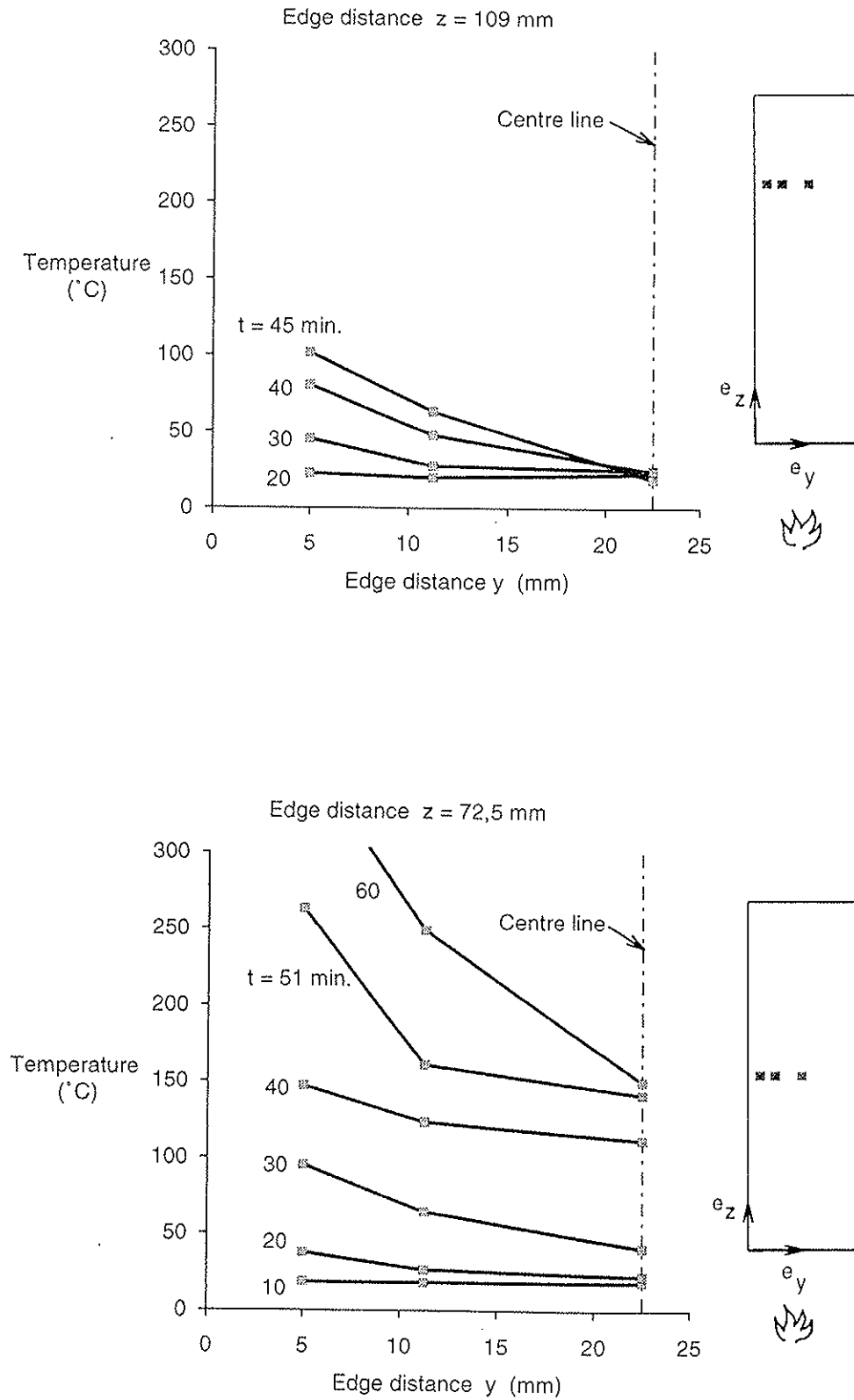


Figure 2 Temperature distributions of test specimens of Series No. 3 at failure.



**Figure 3** Temperature profiles perpendicular to the centre line of the cross section at different times.

Experimental charring rates valid for the centre line of the cross section were determined. See Figure 5. The charring rates were calculated using the minimum edge distance which was normally not exactly on the centre line of the cross section. The squares refer to measured values while the triangles refer to standardized time values with respect to density, see /4/. Both regression lines are almost identical.

The experimental charring rates are in the range between about 0,5 and 1 mm per minute, which is the range mentioned in the introduction of this paper. In contrast to recorded charring rates in heavy timber, the charring rate increases with time. This is due to the fact that the heat flow in the beginning is one-dimensional, while it becomes increasingly more and more two-dimensional, c.f. Figure 3. This effect is increased since the mineral wool insulation is destroyed close to its surface. C.f. the shape of the uncharred core in Figure 3 in /4/.

The influence of density. In /4/ exponential regression curves were calculated, describing the relationship between relative load capacity and failure time. In order to investigate the influence of density on the loss of load capacity, the specimens of series No. 3 were divided into two groups, the first one containing specimens with densities below mean density, and the second one

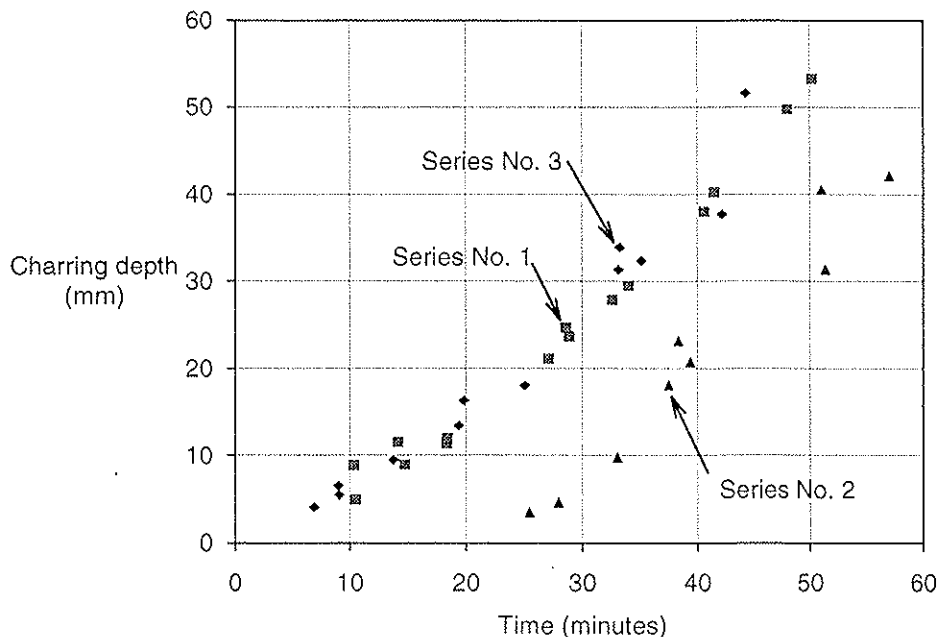


Figure 4 Experimental charring depths at the centre line of the cross section. In series No. 2 a gypsum plasterboard lining is attached to the member.

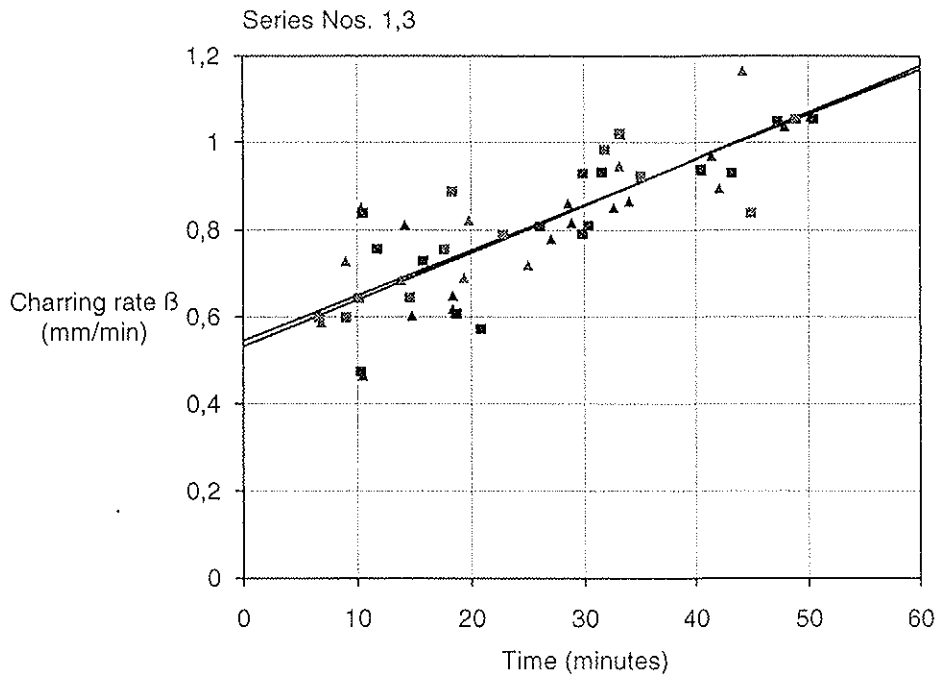


Figure 5 Experimental charring rates in series Nos 1 and 3 at the centre line of the cross section. Squares refer to real time and triangles refer to standardized time with respect to density.

containing specimens with densities above mean density. The ratios of  $\rho/\rho_{mean}$  were 0,939 and 1,053 respectively. For each of these groups exponential regression curves were determined by using real time values. The statistical difference of these two curves is significant at the level of 5 %. The same procedure was followed using standardized time values with respect to density, assuming that

failure time is inversely proportional to density. In this case no significant difference of the corresponding curves was obtained. Thus the influence of density can be taken into account by standardizing failure time with respect to density as described.

The influence of loading rate. In fire tests the applied load is normally held constant until failure. Since the effective cross section is decreasing during the test, strains and stresses increase initially at a very slow and approximately constant rate. Only in the stage close to failure do these rates accelerate more and more. This can be seen from the relationships between deflection and time. See Figures 4b and 5b in /4/. In design by testing it would facilitate the determination of load capacity for a specific fire resistance by increasing the applied loading during the fire test.

In order to investigate the influence of the loading rate, additionally to the tests in series Nos 1 and 3 a number of tests were performed in which the applied load was increased before failure. In these tests different, initially constant loads were applied, at relative load levels between 0 and 25 %. Near the end of the tests the load was increased at a rate of approximately 25 % of the load capacity at normal temperature per minute. The time-

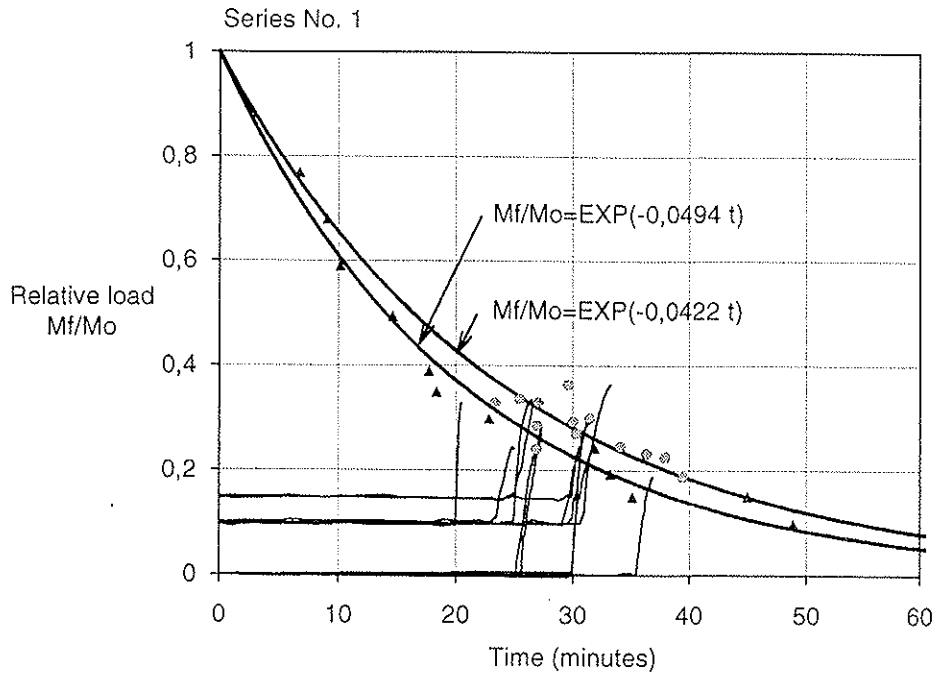


Figure 6 The influence of loading rate on load capacity in series No 1 (fire-exposed side in compression). For specimens with load increasing the whole load-path is plotted.

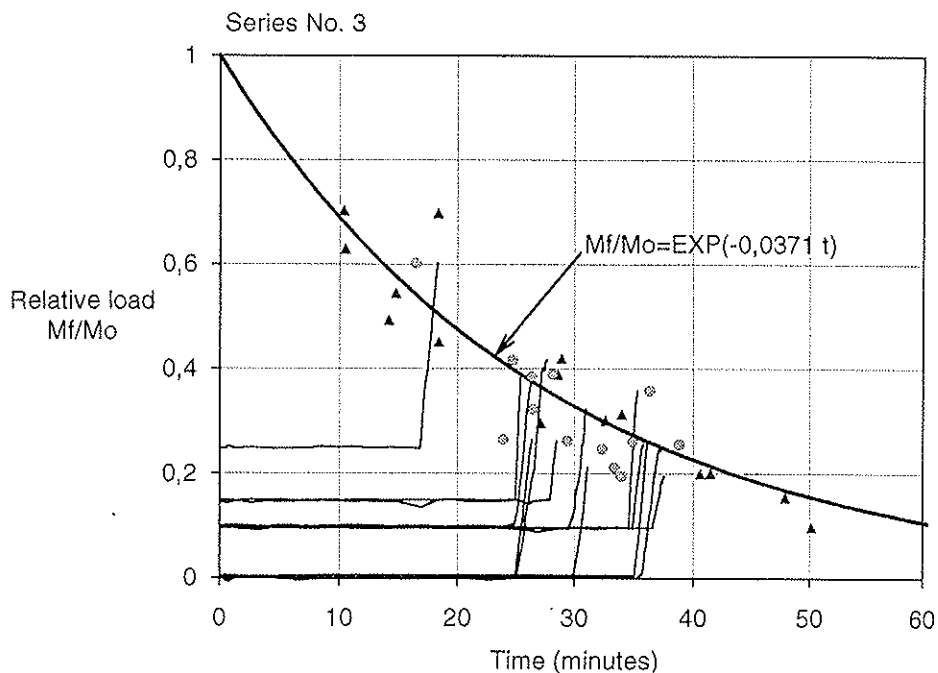


Figure 7 The influence of loading rate on load capacity in series No 3 (fire-exposed side in tension). For specimens with load increasing the whole load-path is plotted.

paths during the tests are shown in Figures 6 and 7. The end-points of these curves are also shown for standardized time values with respect to density as circles, together with corresponding exponential regression curves. These figures correspond to Figures 4a and 5a in /4/. In order to improve legibility of the figures only standardized time values are shown (triangles) with reference to specimens with constant load.

These test results show that the loading rate only exerts an influence in the case of compressive stresses on the fire-exposed side (Series No.1, Figure 6). The difference of the two curves in Figure 6 is statistically significant at the level of 0,2 %, while it is not significant in Figure 7. Thus, determining the ratio of the two regression curves of Figure 6 we get the loading rate coefficient

$$\kappa_l = e^{0,0072 t}$$

which the load capacity is multiplied by when the fire-exposed side is in compression.

An explanation of this different behaviour is that wood is more sensitive to creep when it is in compression. This phenomenon is more accentuated at elevated temperature.

## MODELLING

### "Exact" approach

In principal there are two alternative methods of determining the load bearing capacity and stiffness properties of a wood member in fire. The most exact way would be to determine the real charring line and the temperature and moisture content field in the residual core. With corresponding strength and stiffness data for the material it would then be possible to calculate the properties of the uncharred cross section, even though the procedure would be tedious.

For the time being there is insufficient data on the influence of elevated temperature on the strength and the modulus of elasticity of wood. Recently short-term tests have been performed in order to determine the strength and modulus of elasticity of timber in tension, compression and bending at elevated temperature /5/. The test results referred to above show that there exists an influence of time due to excessive creep in the compressed part of the cross section when the temperature is elevated. In order to use an "exact" approach it would be necessary to introduce modification and creep factors which allow the accentuated influence of time at elevated temperature to be taken into account.

An "exact" method would be most adequate when applied to homogeneous or quasi-homogeneous materials such as LVL (laminated veneer lumber) or glulam timber. In solid timber strength is actually, due to the importance of defects, a reference value, calculated in order to fit test results, assuming that the material is homogeneous and stress varies linearly across the depth. As long as this engineering approach is used in "cold design" of solid timber there should be no advantage in using a more exact method in "hot design". It should have its main application for research purposes.

### Engineering approach

General. The other alternative is an engineering approach which is much easier for the designer to apply. In "cold design" such an approach is applied by replacing the complex behaviour of timber. Thus in bending, fitted reference values of flexural strength and modulus of elasticity are used in order that timber can be regarded as a homogeneous and purely elastic material. An engineering approach in "hot design" should give rules on how the effective cross section of a member should be determined in order that the same design rules which are common in "cold design" can be used. Such a model should fulfil the following requirements:

- a) The model should be easily usable by the designer.
- b) It should be able to give values of relevant effective cross section data, e.g. with respect to strength, stiffness and the position of the centre of gravity.
- c) The model should not pretend an accuracy which does not exist.
- d) Limits of validity should be given.
- e) The formulation of the model should be sufficiently general in order to be able to fit future applications beyond its present limits.
- f) It should be compatible with design by testing, i.e. it should be possible to determine parameters in the model from test results.

In such a model the real charring rate is replaced by a notional or effective one which is a calibrated value in order to fit test results, taking into account effects of charring, elevated temperature, moisture content and creep. Since there are, apart from charring, several other parameters which influence the loss of load capacity and stiffness, the term charring rate should be replaced by another term which takes account of this.

The test results referred to above describe the behaviour of light structural members which are different from those the rules in the present codes generally apply to. In fire tests of heavy members normally three or four sides were exposed to fire. It was therefore difficult to see that the effective charring rate is influenced by the type of loading. In practical applications with the same type of fire-exposure this different behaviour can be disregarded since the applied charring rate represents some kind of mean value.

Shape of effective section. As a consequence of requirement (a) the simplest shape of the effective section should be rectangular with reduced depth and unreduced width, i.e. due to the protection of the flat sides of the member it is assumed that only the depth of the section is affected by charring, even though this assumption differs considerably from the shape of the real uncharred core. See Figure 1. As a consequence of requirement (b) notional charring rates were determined in order to fit section modulus, flexural stiffness and the position of the centre of gravity.



Load bearing capacity at failure time. Notional charring rates were calculated in order to fit the failure times obtained in the tests. See Figures 8 and 9. These calculations were made assuming full and reduced strength respectively. In the case of a loss of strength it was reduced to 75 %, 55 % and 40 % when the fire-exposed side was in compression, and to 90 % and 75 % when the fire-exposed side was in tension. In the present EC5 draft /3/ reduced strength and stiffness values are given, based on /5/. When the bending strength was unreduced ( $f=f_m$ ) - the single values are marked by squares in the figures - linear regression curves were calculated, for each load direction. When reduced strength was assumed the notional charring rate values at the beginning of the tests were disregarded in calculating regression lines.

The results show that the notional charring rates  $\beta_n$  are more or less time-dependent. When the expressions obtained for unreduced strength, i.e.

$$\beta_n = 3,266 - 0,0237 t$$

and

$$\beta_n = 2,571 - 0,0157 t$$

respectively were used in calculating load capacity-time relationships, the curves obtained were almost identical to the experimental regression curves. In order to simplify the model a constant notional charring rate should be chosen which gives the best fit in the region of working load. For some assumed notional charring rates  $\beta_n$  relationships of relative load capacity and failure-time were calculated. See Figures 10 and 11. It is obvious that a constant charring rate does not agree very well with the experimental regression curve when unreduced strength is assumed.

The best agreement between the model and the experimental regression curves at relative loads below about 30 % is obtained by assuming a notional charring rate of 1,7 mm/min and a strength reduction of 55 and 75 % respectively. The best agreement for all load levels should be obtained by assuming an increasing reduction of strength with time. This would describe the real behaviour best but make the model overly complicated.

Flexural stiffness. When the flexural stiffness is used in calculating the buckling load of a member in axial compression, it is necessary to describe its effective cross section during the whole time period of fire-exposure. From Figures 3 and 4 it can be seen that considerable temperature variations exist both at different points of the uncharred cross section and over time. This makes it more complicated to model stiffness. The easiest way to take into account the softening of the material is to choose a larger notional charring rate. Therefore calculations of the relative flexural stiffness were made only for the case of unreduced modulus of elasticity.

Assuming the expression of notional charring rate which fits the load capacity best during the whole time period of the tests, the curves (1) in Figures 12 and 13 were obtained. The dotted experimental curves are identical with those shown in Figures 4c and 5c in /4/. The curves (2) refer to constant average notional charring rates. The difference between the curves (1) and (2) is not very large. The curves (3) were obtained by choosing constant

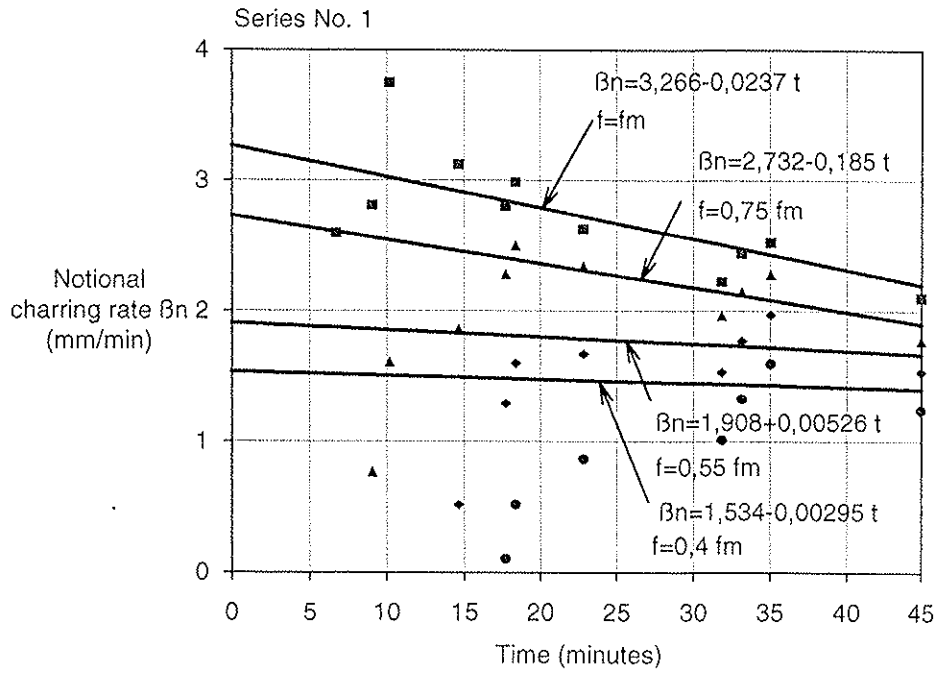


Figure 8 Experimental notional charring rates in series No.1 (fire-exposed side in compression) for ultimate load capacity at failure time.

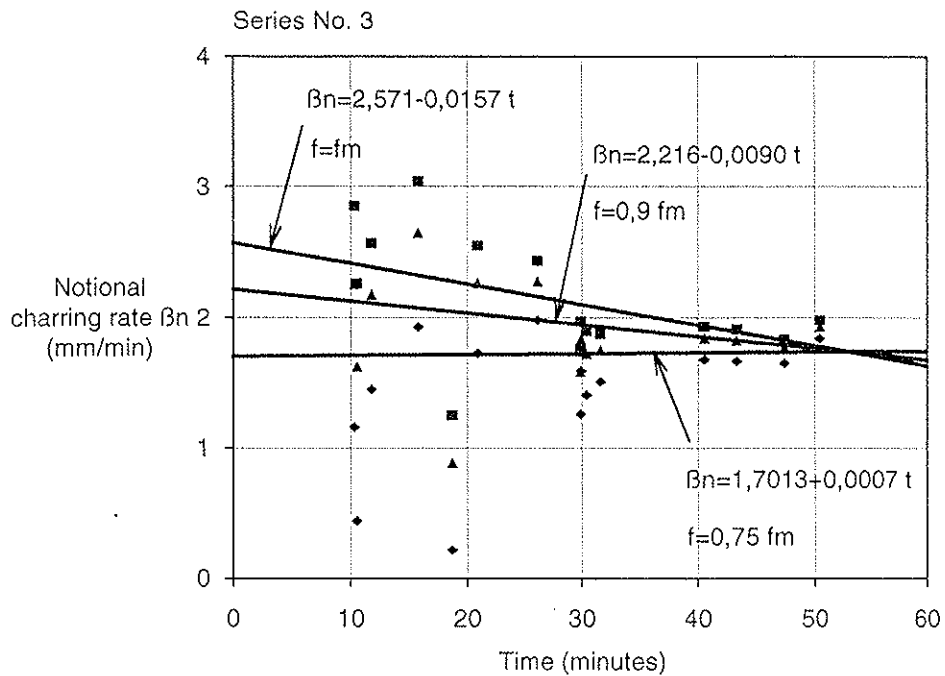


Figure 9 Experimental notional charring rates in series No.3 (fire-exposed side in tension) for ultimate load capacity at failure time.

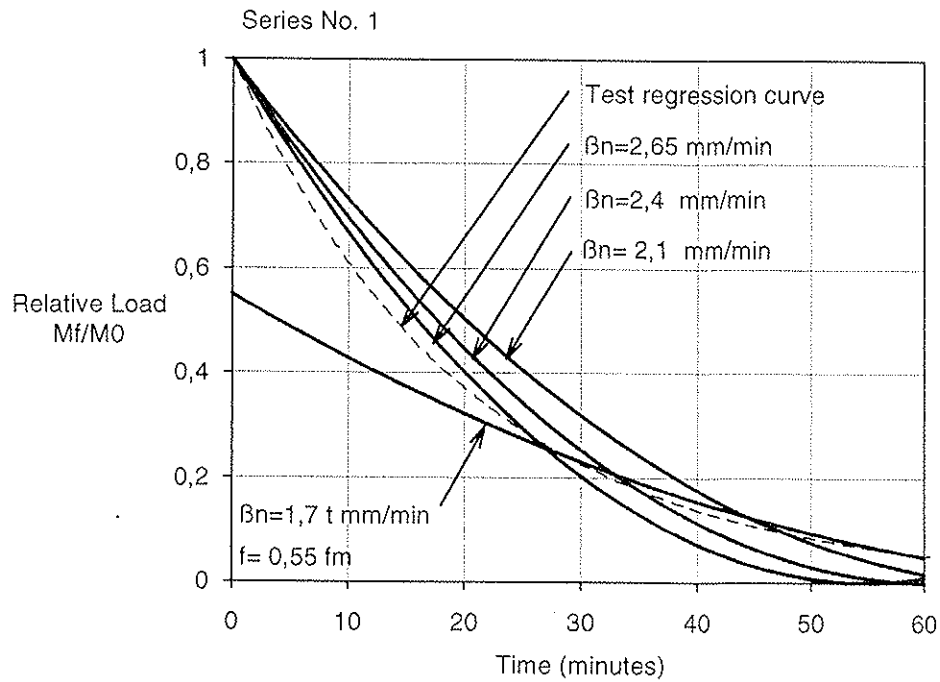


Figure 10 Calculated curves of relative load capacity versus failure time in series No. 1 (fire-exposed side in compression).

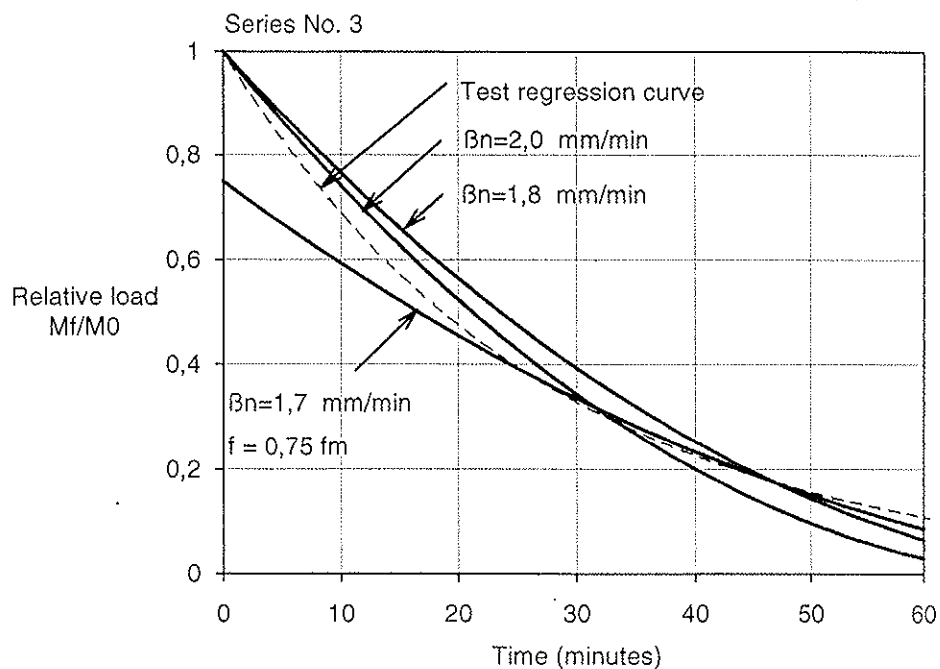


Figure 11 Calculated curves of relative load capacity versus failure time in series No. 3 (fire-exposed side in tension).

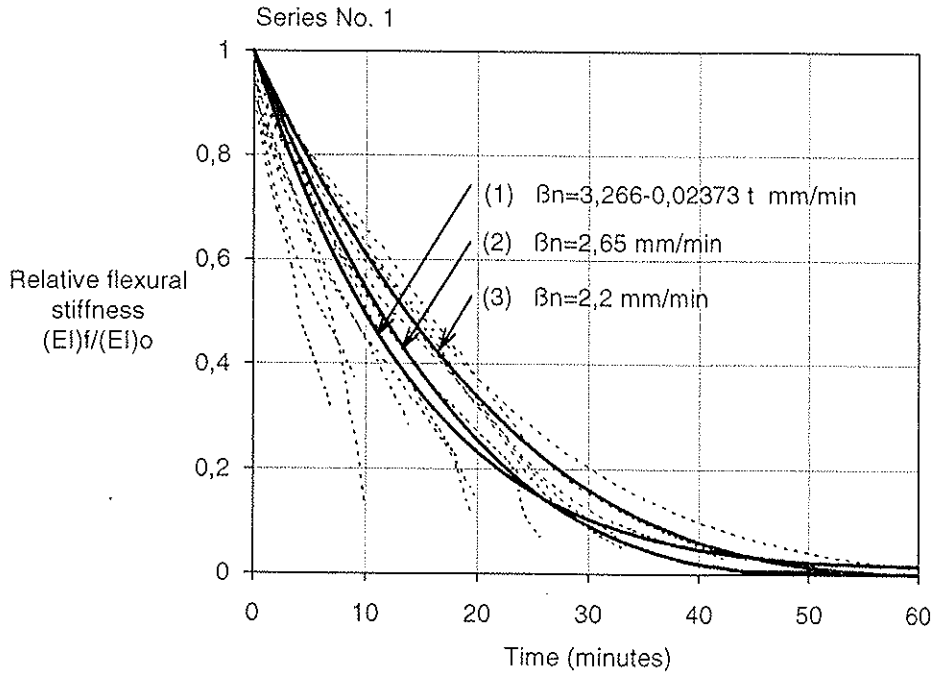


Figure 12 Comparison of calculated and experimental curves of relative flexural stiffness versus time in series No. 1 (fire-exposed side in compression).

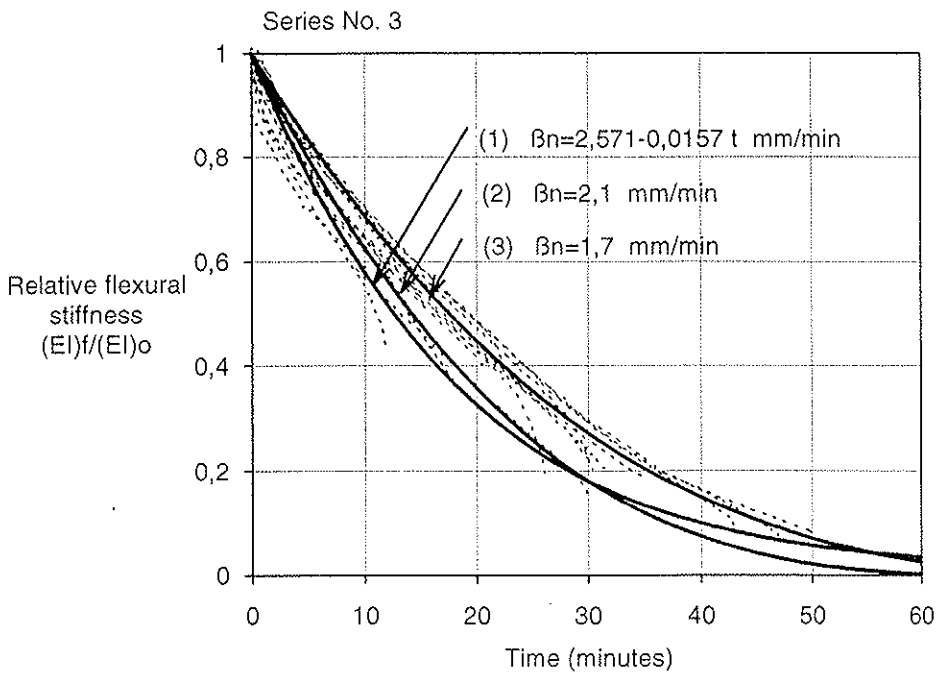


Figure 13 Comparison of calculated and experimental curves of relative flexural stiffness versus time in series No. 3 (fire-exposed side in tension).

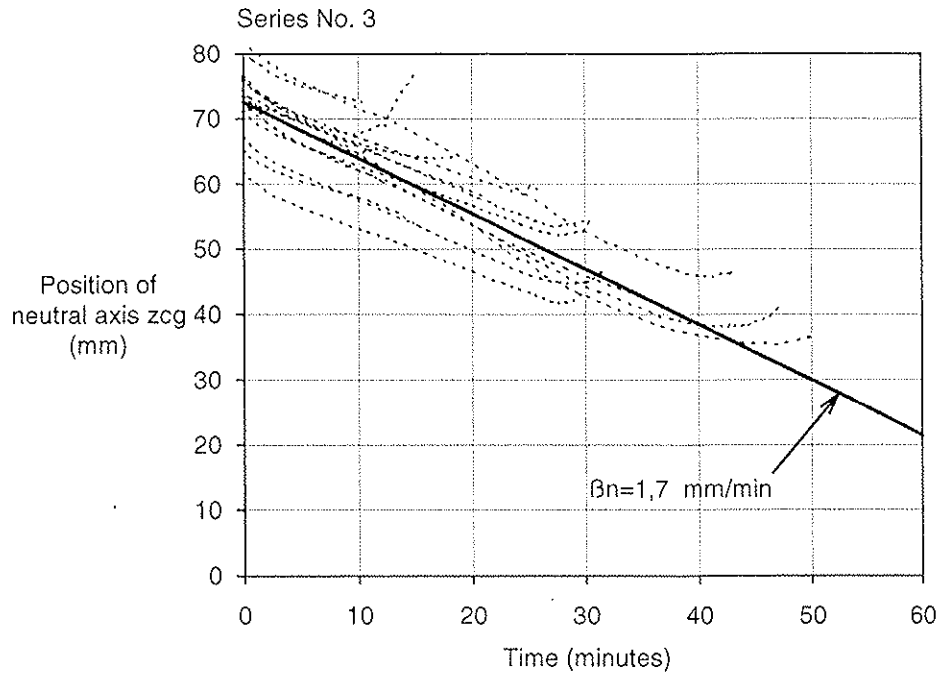


Figure 15 Comparison of calculated and experimental curves of the distance of the neutral axis from the uncharred side versus time in series No. 3 (fire-exposed side in tension).

of load capacity and flexural stiffness, see Figure 6 in /4/. Thus it is easy to consider the effect of claddings by using the delay which is specific for the lining either with the concept of notional or real charring rates.

Conclusions. It is obvious that, in general, different notional charring rates should be used for modelling the effective section, not only with respect to load capacity and stiffness but also with respect to the state of stresses. In many applications this distinction is not necessary as in the case of fire-exposure on four sides or of very large sections. While in calculations of bending load capacity a loss of strength should be taken into account, it is not necessary to regard the loss of the modulus of elasticity when the flexural stiffness of the member is determined. Therefore in design rules notional charring rates should be linked together with rules about, whether, or how much the strength and the modulus of elasticity has to be reduced. In the case of the specimens of the investigation referred to here, it was possible to use only two different charring rates in connection with different reductions of strength and modulus of elasticity. See Figure 16. In other applications this may be different.

Assuming a simple effective cross section of rectangular shape it is possible to achieve good agreement between calculated and test results. It is therefore unnecessary to introduce rounded edges in the model. In most cases the increase in accuracy of the model should be illusory whilst its use would be more complicated.

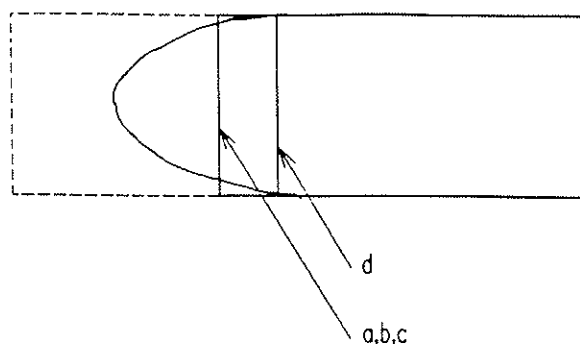


Figure 16 Effective cross sections for uncharred core shown in Figure 1 linked to the following assumptions:

- a) Ultimate load - fire-exposed side in tension -  
 $f=0,75 f_m$
- b) Ultimate load - fire-exposed side in compression -  
 $f=0,55 f_m$
- c) Flexural stiffness - fire-exposed side in tension -  
 $E$  not reduced
- d) Flexural stiffness - fire-exposed side in  
compression -  $E$  not reduced

By using the notional charring concept it is possible to specify expressions which are specific to different applications. Thus the concept is sufficiently general and should be useful in future applications.

#### REFERENCES

- /1/ Meyer-Ottens, C., Feuerwiderstandsdauer unbekleideter hoher Rechteckbalken aus Brettschichtholz. Published in Forschungsbeiträge für die Baupraxis, Karl Kordina zum 60. Geburtstag gewidmet. Wilhelm Ernst & Sohn, Berlin, 1979.
- /2/ Hall, G.S., Fire resistance tests of laminated timber beams. Trada Research Report WT/RR/1, High Wycombe, 1968
- /3/ Eurocode No.5, Part 10: Structural Fire Design. Draft April 1990. Commission of the European Communities.
- /4/ König, J. & Norén, J., Fire tests on timber frame members under pure bending. 1991 International Timber Engineering Conference, London.
- /5/ Glos, P. & Henrici, D., Festigkeit von Bauholz bei hohen Temperaturen. Institut für Holzforschung der Universität München, 1990



**INTERNATIONAL COUNCIL FOR BUILDING RESEARCH STUDIES AND DOCUMENTATION**  
**WORKING COMMISSION W18 - TIMBER STRUCTURES**

**USE OF SMALL SAMPLES FOR IN-SERVICE STRENGTH MEASUREMENT**

by

R H Leicester  
F G Young  
CSIRO  
Australia

**MEETING TWENTY - FOUR**

**OXFORD**

**UNITED KINGDOM**

**SEPTEMBER 1991**





# USE OF SMALL SAMPLES FOR IN-SERVICE STRENGTH MEASUREMENT

by

R.H. Leicester and F.G. Young  
(CSIRO, Australia)

## INTRODUCTION

In-grade test measurements intended to assess in-service strengths are used to define reliable structural strength. For this reason the availability of these in-grade measurements are an important component of effective timber engineering design. Unfortunately however, these in-grade measurements can be prohibitively expensive to undertake. For strength measurements large samples are often needed because the aim is to evaluate the five percentile in-service strength with a certain degree of confidence, usually a 75 per cent confidence. Even within a single species there are many grades and sizes to evaluate for each property; particularly in the case of large timber sizes, the cost of both the material and laboratory tests can be very costly.

For these reasons, it can often be desirable to attempt a compromise in which the testing of limited samples is used to provide a conservative but useful estimate of the in-service characteristic values. The following describes a method for this which is particularly suitable for use with softwood timbers; here it is assumed that these timbers can be modelled as a set of defects, randomly distributed within a matrix of clear wood, Figure 1. Two procedures will be discussed; one is related to the evaluation of in-service bending strength and the other is for use in quality control operations.

## DEFINITIONS OF BENDING STRENGTH

In the following, four definitions of bending strength will be used; in each case third point loading and a span/depth ratio of 18:1 will be assumed. The four definitions of strength are as follows,

- (a) *In-service strength  $R_1$* . For this case, sticks of timber are selected at random from the parent population, and test specimens are cut from random locations within each stick as illustrated in Figure 2a. The edge placed in tension is chosen at random. The in-grade strength is intended to simulate the inservice strength of structural timber.
- (b) *Defect biased strength  $R_2$* . For this case, illustrated in Figure 2b, the test specimen is selected so that the worst apparent defect within each stick is located within the middle third of the specimen; the edge placed in tension is chosen at

random. In making these measurements the number of defects per stick  $N_d$  and the average spacing of defects  $S_d$  are recorded.

- (c) *Defect-edge biased strength  $R_3$ .* For this case, illustrated in Figure 2c, the measurement is made similar to the defect biased strength, except that the worst defect is deliberately placed on the tension edge during the test.
- (d) *Defect-edge-stick biased test  $R_4$ .* For this case, a sub-sample of  $N_s$  sticks is first selected at random, and then a single defect-edge biased specimen is cut from the stick deemed to have the weakest defect in the sub-sample. (The rest of the sub-sample is then returned to the mill, untested.)

The cumulative distribution function for these four types of bending strength measurement are illustrated schematically in Figure 3. An example of test data measured for F5 grade radiata pine is given in Figure 4 and Table 1. In Figures 3 and 4, the notation  $F_1, F_2, F_3$  and  $F_4$  are used to indicate the cumulative frequency values of  $R_1, R_2, R_3$  and  $R_4$  that corresponds to  $R_{0.05}$ , the five percentile value of in-service strength.

## STRENGTH EVALUATION

For a strength evaluation, the defect biased strength  $R_2$  is first measured. This statistical information is then used to derive the in-grade strength through use of mathematical models of strength such as the model developed in an earlier paper (Leicester and Breitingner, 1991).

One procedure would be to use the measured values of  $R_2$  to develop the statistics for single defects. The cumulative distribution function of single defects is similar to that of  $R_2$  except that all strength values are increased by a factor  $\lambda$  obtained from

$$\lambda = \bar{N}_d^\alpha \quad (1)$$

$$\alpha = V_2^{1.085} \quad (2)$$

where  $V_2$  denotes the coefficient of variation of  $R_2$ .

Using this derived statistical population for the strength of defects and assuming the defects have an experimental spacing with mean value  $S_d$ , Monte Carlo techniques can be used to generate strength models for numerous sticks of timber. From each model stick a test specimen for measuring the in-service strength  $R_1$  can be selected. From these computed values  $R_1$  the characteristic value  $R_{0.05}$  can be derived.

To assess the efficiency of this procedure, use will be made of a formula for assessing a characteristic value  $R_k$  which is the F-percentile with 75-percentile confidence (Leicester, 1986). For a sample of size  $N$  this is given by

$$R_k = R_F [1 - 0.6 V_R / \sqrt{NF}] \quad (3)$$

where  $V_R$  denotes the coefficient of variation of in-grade strength.

From equation (3) it is apparent that the required sample size  $N$  is inversely proportional to the value of the targeted frequency  $F$ , for a fixed penalty factor  $[1 - 0.6 V_R / \sqrt{NF}]$ .

To illustrate this concept with an example, the data for F5 radiata pine, shown in Figure 3, will be used. For this case  $F_2 = 0.14$  and hence the required sample size may be reduced by a factor of  $0.14/0.05 \approx 3$ , i.e. for a given target accuracy, the sample size required for obtaining the characteristic strength  $R_{0.05}$  is three times less for an assessment on defect-biased strength  $R_2$  as compared with direct measurement of in-service strength  $R_1$ .

## QUALITY CONTROL

In quality control it is assumed that there is some prior knowledge about the strength distributions  $R_1 - R_4$ .

One method of control is to make direct use of the appropriate percentile  $F_3$  of the defect-edge-biased specimens. For the data on F5 radiata pine given in Table 3, the appropriate target percentile is  $F_3 = 0.19$ . Thus the reduction in sample size for a given accuracy is  $0.19/0.05 \approx 4$ .

An even better efficiency can be obtained if use is made of  $R_4$ , the defect-edge-stick biased strength. To do this, the most appropriate sub-sample size is to use that which leads to  $F_4 = 0.5$  as the target value, i.e. the mean value of  $R_4$ . For this case, the sub-sample size  $N_s$  is obtained from

$$0.5 = (1 - F_3)^{N_s} \quad (4)$$

As an example, for the data of F5 radiata pine shown in Figure 3, the measured value of  $F_3 = 0.19$  leads to  $N_s = 3.3$ . However, since visual selection of the worst defect is not perfect, some value larger than 3.3 would be appropriate; probably a value of  $N_s = 5$  would be about right. (As noted earlier, only one test specimen is cut from each sub-sample.)

It should be noted that since the mean value of  $R_4$  is targeted, then any of the quality control techniques (such as the cusum method) which have been applied to control mean values can be used.

To obtain some idea of the efficiency of this procedure use is made of the following equation for deriving a characteristic strength  $R_k$  that is a mean value assessed with 75 per cent confidence,

$$R_k = \bar{R}_4 (1 - 0.7 V_R / \sqrt{N}) \quad (5)$$

A comparison between equations (3) and (5) indicates that for a given accuracy, the use of defect-edge-stick biased strength leads to a reduction in the required sample size by a factor of  $(0.6/0.7)^2/0.05 \approx 15$ .

## CONCLUSION

Exact evaluation of in-situ structural properties can be assessed only by simulated in-service measurements. However, such evaluations are expensive, and it is proposed that for practical purposes many of these evaluations can be replaced by good estimates based on making use of secondary parameters such as the visual appearance of a defect and the magnitudes of the spacings between the defects.

Some rough analyses were used to estimate the efficiency of applying the proposed procedures to the bending strength of F5 radiata pine. In the case of in-service strength evaluations with a specified accuracy, the use of defect biased strength measurements led to a reduction in the required sample size by a factor of about 3. In the case of quality control operations, the number of test specimens required could be reduced by a factor of about 4 through the use of defect-edge biased specimens and a factor of about 15 through the use of defect-edge-stick biased specimens.

It should be noted that the use of biased specimens is often recommended in existing testing standards, but usually the rules of such standards do not correctly take into account or take useful advantage of such bias.

## REFERENCES

1. Leicester, R.H. (1986). Confidence in estimates of characteristic values. Meeting of CIB-W18A, Firenze, Italy.
2. Leicester, R.H. and Breiting, H.O. (1991). A discrete co-relationship with Weibull. International Timber Engineering Conference, London, UK, September 1991.

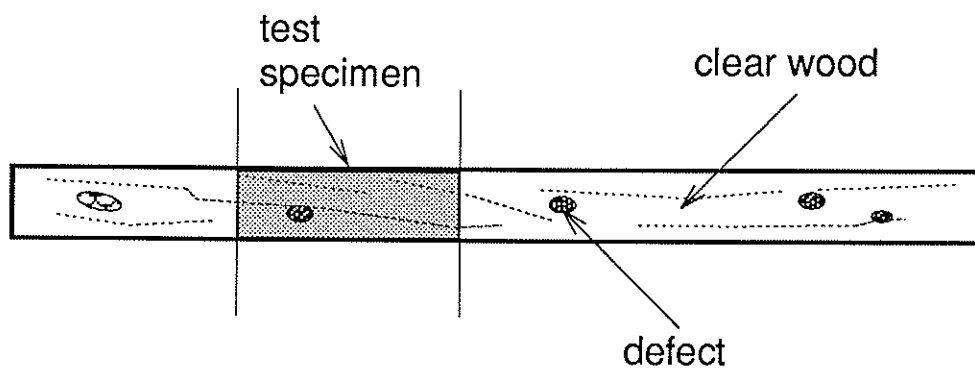
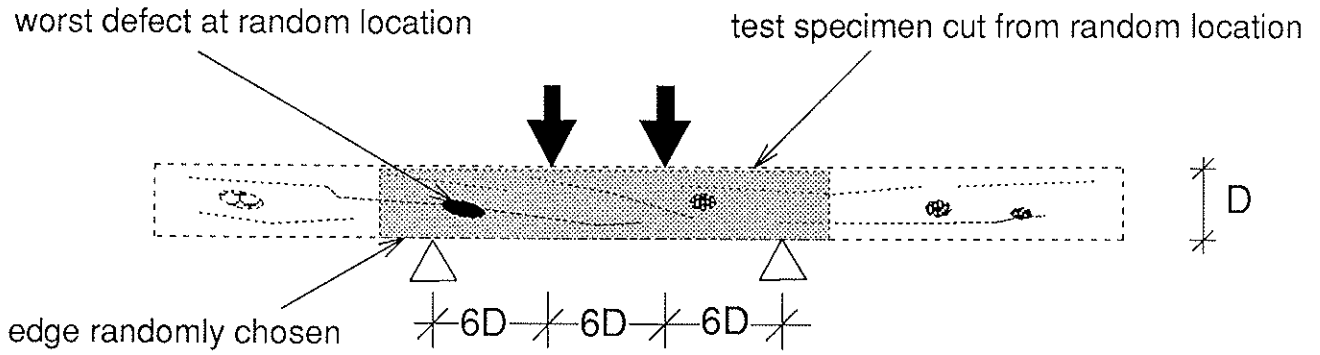
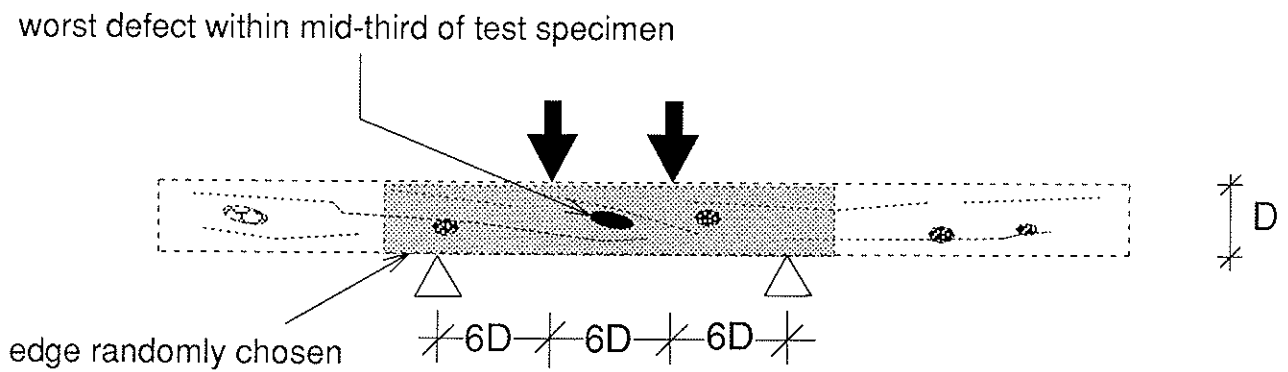


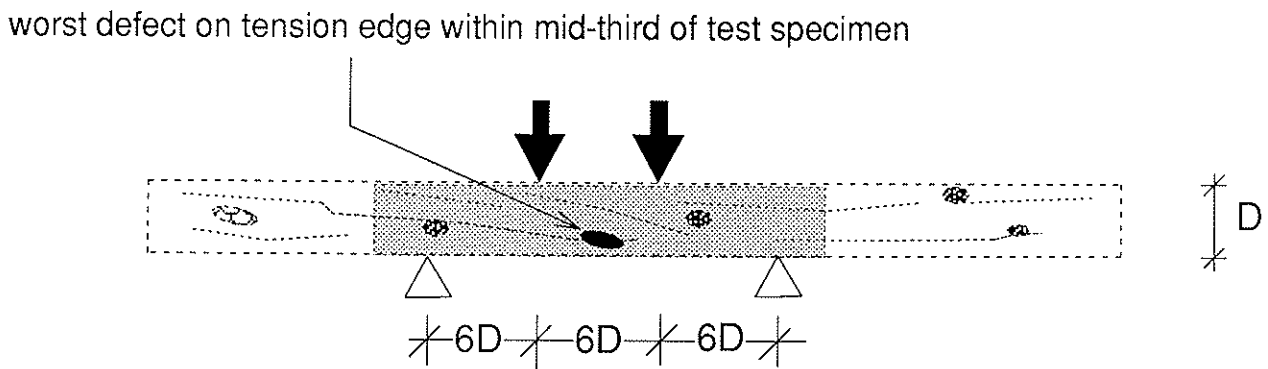
Figure 1. Model for softwood structural lumber



(a) In-service strength



(b) Defect-biased strength



(c) Defect-edge-biased strength

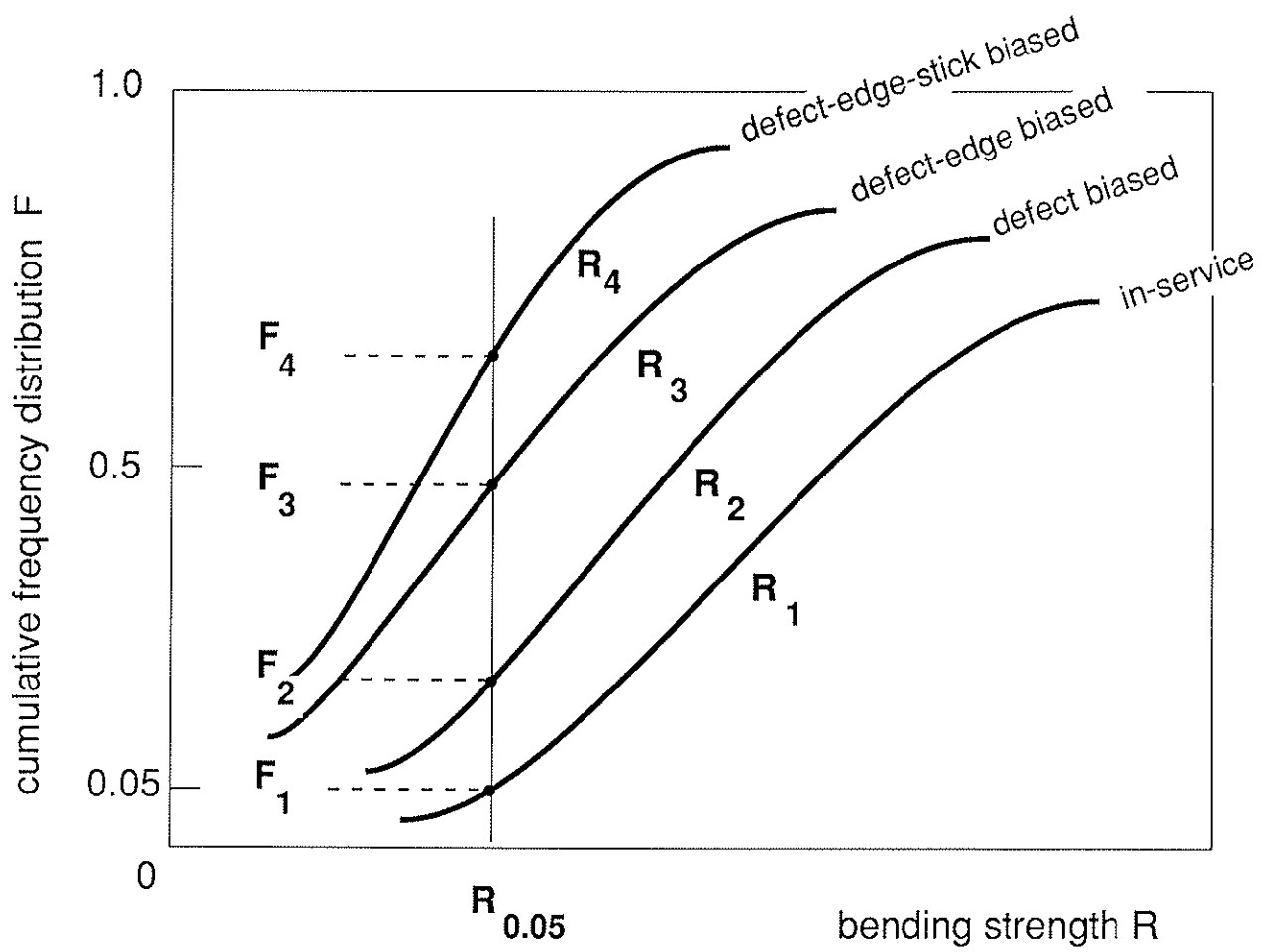


Figure 3. Schematic representation of strength distributions



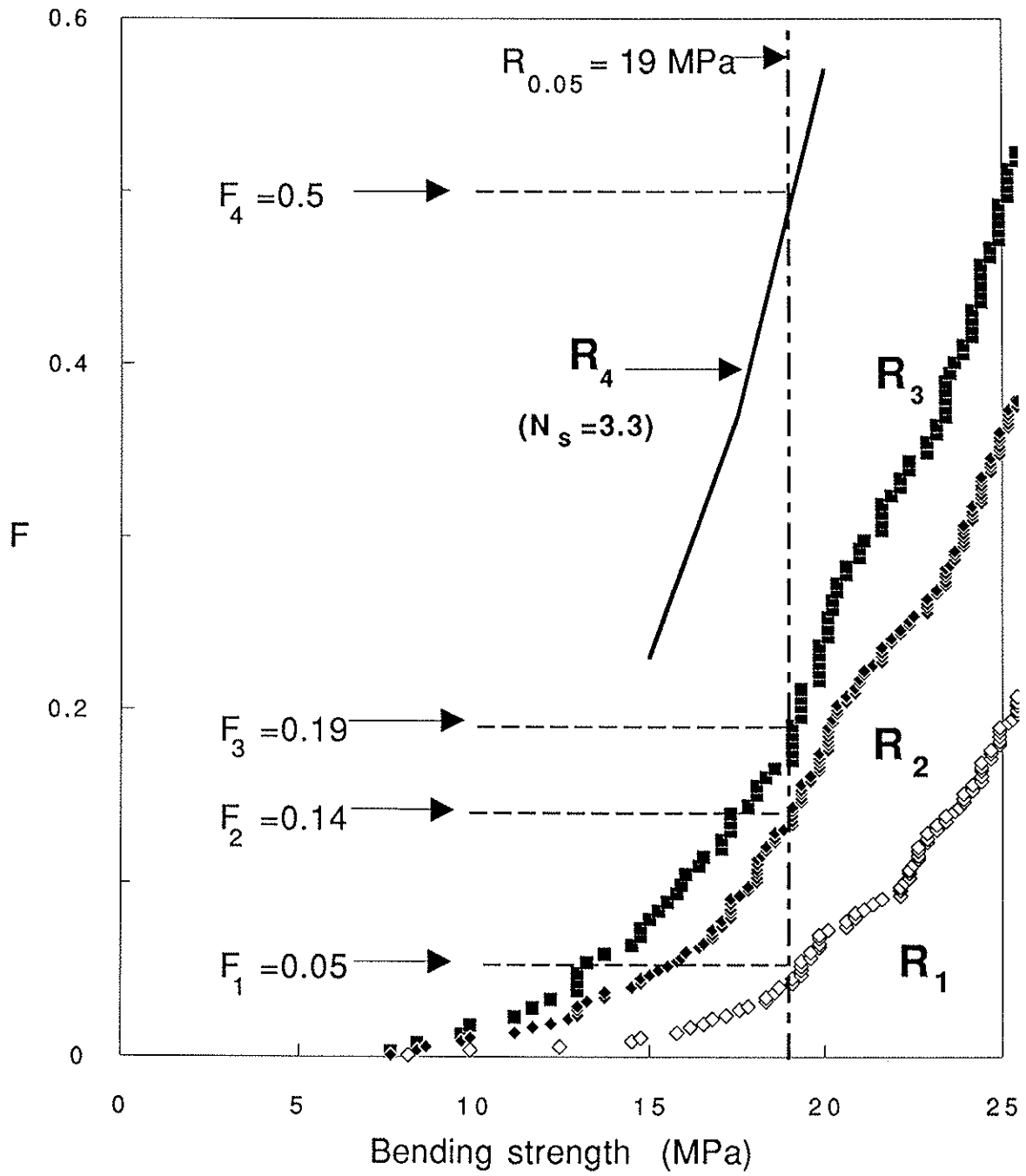


Figure 4. Strength distributions for F5 radiata pine.

**INTERNATIONAL COUNCIL FOR BUILDING RESEARCH STUDIES AND DOCUMENTATION**  
**WORKING COMMISSION W18 - TIMBER STRUCTURES**

**EQUIVALENCE OF CHARACTERISTIC VALUES**

by

R H Leicester  
F G Young  
CSIRO  
Australia

**MEETING TWENTY - FOUR**

**OXFORD**

**UNITED KINGDOM**

**SEPTEMBER 1991**



# EQUIVALENCE OF CHARACTERISTIC VALUES

R.H. Leicester and F.G. Young  
(CSIRO, Australia)

## INTRODUCTION

Methods used for defining characteristic values often differ from country to country. For purposes of trading in structural timber products, it is obviously important to be able to establish the equivalence between these various definitions of characteristic values.

However, there is another equally important reason for being able to establish equivalences. This is because it is essential to do this to be able to transfer technology between countries. Many of the parameters affecting the structural performance of timber components are stated in terms of their effect on characteristic values; typical examples are the influence of load-duration, moisture and size effects. Thus, a change in the definition of the characteristic value will usually require a change in the predicted effects of these parameters.

There are at least two major types of differences in the way in which characteristic values are defined. These are as follows;

- (a) the structural properties are measured in different ways, and
- (b) the test data is processed in different ways.

The processing of the data differs with respect to choice of percentile, statistical confidence limits, and factors related to the design code format. Examples of factors related to the design code format include the partial factors  $\phi_m$  or  $\gamma_m$  for material resistance and the modification factors for size which are specified in timber engineering design codes that use the characteristic values; in data processing due account must be taken of these factors, even though they are not intrinsic properties of the timber material.

To some extent, the differences in characteristic values arising from differences between methods of data processing are an irritant rather than a barrier, because methods for evaluating these differences can be easily developed or the data can be reprocessed. However, differences in characteristic values that arise because of differences in test methods are usually either difficult or impossible to evaluate. For example, in recent times the USA (Green and Evans 1987) and Canada have spent well over US\$10 million for in-grade measurements on their structural timbers; yet because of the test procedures used, to date no satisfactory method has been found to process this data to evaluate characteristic values of structural properties that are acceptable to the EC countries.

The following gives a discussion on the influence of test methods used for evaluating the structural properties of sawn timber in bending, followed by some brief comments on the evaluation of characteristic properties for joint systems.

## **BENDING STRENGTH AND STIFFNESS OF TIMBER**

A summary of the essential specifications in standards for measuring the bending strength and stiffness of timber is given in Figure 1 and Tables 1, 2 and 3; the standards covered include those of ISO, Eurocodes, UK, USA, Canada and Australia.

The test beams are loaded symmetrically as indicated in Figure 1, and the dimensions of the loading configuration are given in Table 1 and 2. Table 1 lists standards for evaluating characteristic values to be used in design. Table 2 lists standards for evaluating 'indicative' characteristic values to be used for quality control purposes in machine stress-grading.

An important aspect of bending tests is the procedure used for the selection of the test specimen from a stick of timber, i.e. the location of the test specimen relative to that of the assessed weakest part of the timber. This has an impact on both the measured bending strength and stiffness. The various ways specified for choosing the location of the test specimen are given in Table 3; the four methods are ranked so that selection according to Procedure 'A' gives the highest strength while that according to Procedure 'D' gives the lowest strength. An example of the bending strength measured by three of these procedures for F5 grade radiata pine is given in Figure 2. Although the strength is considerably influenced by the procedure used for specimen selection, this particular aspect is not included in some standards (e.g. ISO 8375 and BS 5820, see Table 1).

Procedure 'A' is of special interest in that it represents an attempt to simulate the in-situ situation. However, it should be apparent that it will produce results that vary with the length of stick that is graded, the longer sticks giving higher strengths. Some reference to a standard grading length is given in the draft Australian Standard DR 83205. If the stick length which is graded is made equal to the test span, then Procedure 'A' and Procedure 'B' become identical.

Figure 3 gives an example of stiffness measured according to different standards.

The variety of loading configurations and specimen selection procedures used means that it is essential to develop and obtain acceptance of some simple method of establishing equivalences between the various types of characteristic values if expensive retesting is to be avoided whenever structural timber is traded between countries. Unfortunately, no such methods are currently available. With respect to establishing an equivalence between the characteristic strengths of softwood timbers measured by different tests, the theory given in a recent paper (Leicester and Breitingner 1991) could be useful. To apply this theory would require information on the following:

- (a) defect spacing,
- (b) within-stick correlation between defect strengths, and
- (c) correlation between the true and assessed ranking of within-stick defect strengths.

## JOINT SYSTEMS

With respect to establishing characteristic values, a joint may be considered in a manner similar to that of a defect in structural timber. Thus, to obtain the same degree of reliability as in structural timber evaluation, a joint system will have to be tested in similar modes, i.e. in bending, tension, compression, shear, torsion, etc... However, the problem is more complex than this, because for each type of connector an infinite variety of joint systems can be made; for example there can be variations in the number of connectors used within a joint, the edge distances, the number and dimensions of timber connected, the size of connector or plate dimensions, the joint configuration, the direction of load relative to the connector orientation, the direction of load relative to the timber wood grain etc... This great range of variety in connector types is further confounded by the great range of failure modes that occurs; this makes it difficult to interpolate from one configuration to another. For example, failure may be due to either tension or compression forces, either of the connector itself or of the wood, parallel or perpendicular to the grain, and at various locations. Apart from its importance for interpolation purposes, the failure mode is important because (as is the case for solid timber) the influence of design parameters (such as duration-of-load) would be expected to vary with the type of failure mode.

Currently, two methods are used to cope with the great complexity involved in evaluating joint systems. One approach (such as in ISO 8969, 1990) is to specify tests for a set of standard joint and loading configurations; another approach (such as ISO draft N 140, 1990) is to measure the basic parameters of the components of a joint system and then to apply these within a general theory of connector behaviour, such as the European yield theory for nailed and bolted joints.

In view of the above, it would appear to be extremely difficult to establish equivalences between various methods used to evaluate the characteristic strengths and stiffnesses of joint systems. It is an urgent matter to obtain some sort of international harmonisation on either (a) a limited set of standard geometry and load configurations to be used for connector evaluation or (b) the development of internationally accepted theories for predicting the structural performance of generic connector types.

Current progress in building technology is such that the development of new and improved connectors is occurring with ever increasing frequency. Hence, for purposes of effective technology transfer between countries, it is a matter of some urgency to work towards obtaining at least a limited harmonisation in the specification of the characteristic properties for joint systems.

## CONCLUSIONS

For solid timber, the methods used for establishing the characteristic values of structural properties differs from country to country. This creates a barrier both to the trade of structural timber and a barrier to the transfer of technology from one country to another. There is some potential for developing an acceptable procedure for establishing equivalences between the various methods used for establishing characteristic values in particular grades and species.

For the case of connectors, the complexity of jointing systems used would appear to inhibit the development of methods for evaluating the equivalences between characteristic values. This could be a major barrier to technology transfer, particularly with respect to new connector systems. An effective short term action would be to endeavour to obtain limited international harmonisation on standardised joint configurations and on theories of connector actions.

## REFERENCES

- American Society for Testing and Materials. ASTM D. Standard test methods for mechanical properties of lumber and wood-based structural material. (Draft Standard).
- British Standards Institution (1979). Methods of test for determination of certain physical and mechanical properties of timber in structural sizes. BS 5820:1979, London.
- European Committee for Standardisation (1989). 'Structural timber: the determination of characteristic values of mechanical properties and density of timber' (Draft CEN N82 E), Brussels, Belgium.
- Green, D.W. and Evans, J.W. (1987). 'Mechanical properties of visually graded timber'. Vol. 1. A summary. US Dept. of Agriculture, Forest Service, Forest Products Laboratory, Madison, Wisconsin, 75 pages.
- International Organisation for Standardisation (1985). Solid timber in structural sizes: Determination of some physical and mechanical properties. ISO 8375:1985(E), First Edition, Switzerland.
- International Standards Organisation (1990a). 'Nails and other dowel type fasteners; determination of bending strength', (Draft ISO N 140), 10 pages.
- International Standards Organisation (1990b). 'Timber structures – testing of unilateral punched metal plate fasteners and joints', ISO 8969:1990, Geneva, Switzerland, December, 9 pages.
- Leicester, R.H. and Breiting, H.O. (1991). 'A discrete co-relationship with Weibull'. Proc. 1991 International Timber Engineering Conference, London.

Standards Association of Australia (1978). AS 1748 and AS 1749. 'Mechanically stress-graded timber and rules for mechanical stress grading of timber'. Sydney, Australia, 19 pages.

Standards Association of Australia (1986). DR 83205 'Draft Australian standard for the evaluation of strength and stiffness of graded timber', Sydney, Australia.



**TABLE 1**  
**Test specifications for establishing characteristic values of**  
**bending strength and stiffness**

Standard	L/H	b	c	Procedure for selection of specimen location
ISO 8375 and BS 5820				
MOR	18	L/3	–	not specified
true MOE	18	L/3	5H	not specified
apparent MOE	5	0	L	not specified
CEN N82 E				
MOR	18	L/3	–	Procedure 'C'
true MOE	18	L/3	5H	Procedure 'C'
CSA-S442.1 and draft ASTM				
MOR	17	L/3	–	Procedure 'B'
MOE	17	L/3	L	Procedure 'B'
Draft AS DR 83205				
MOR	18	L/3	–	Procedure 'A'
MOE	18	L/3	L	Procedure 'A'

MOR = bending strength.  
MOE = bending stiffness.  
L, H, b, c = notation defined in Figure 1.  
Procedures 'A', 'B', 'C' and 'D' = defined in Table 3.

TABLE 2  
Test specifications for bending strength and stiffness in  
quality control of machine stress grading

Standard	L/H	b	c	Procedure for selection of specimen location
BS 5820 indicative MOE	6H + 1000	1000	900	Procedure 'C'
AS 1749 indicative MOR	13	4H	–	Procedure 'D'
indicative MOE	13	0	L	Procedure 'D'

MOR = bending strength.  
 MOE = bending stiffness.  
 L, H, b, c = notation defined in Figure 1.  
 Procedures 'A', 'B', 'C' and 'D' = defined in Table 3.

Note: All units are in mm.

TABLE 3  
Procedure for selection of specimen location

Procedure type	Method for selection of specimen location
Procedure 'A'	Specimen is selected from random location with a graded stick; tension edge of test specimen chosen at random
Procedure 'B'	Specimen is selected so that the assessed weakest point in a graded stick is located at a random location within the test span; tension edge of the test specimen is chosen at random
Procedure 'C'	Specimen is selected so that the assessed weakest point in a graded stick is located near the centre of the test span; tension edge of the test specimen is chosen at random
Type 'D'	Specimen is selected so that the assessed weakest point in a graded stick is located near the centre of the test span; the assessed weakest edge of the test specimen is placed in tension

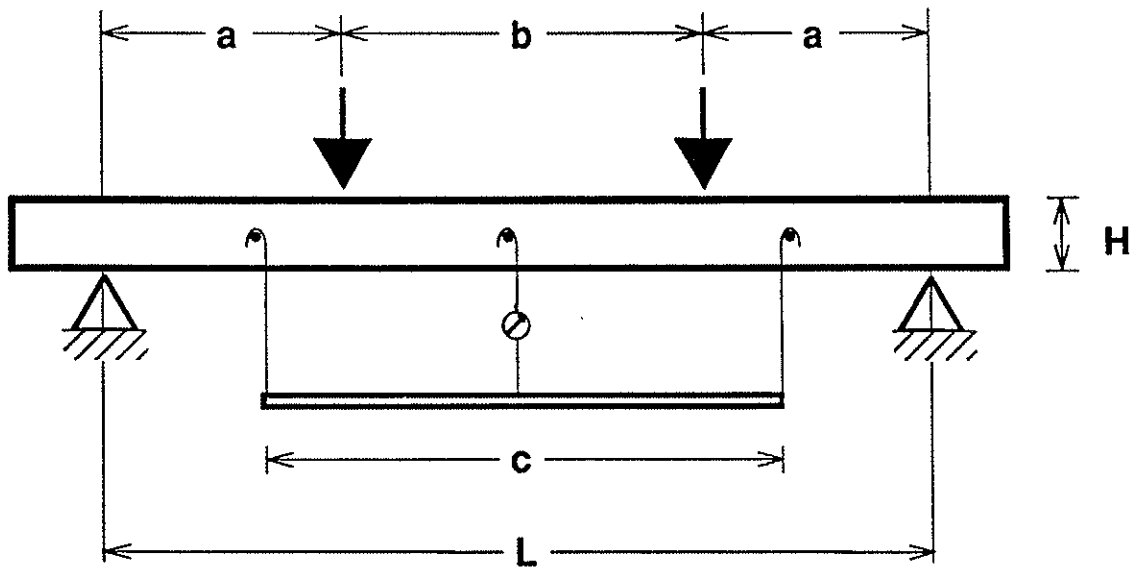


Figure 1. Notation for load and gauge configuration.

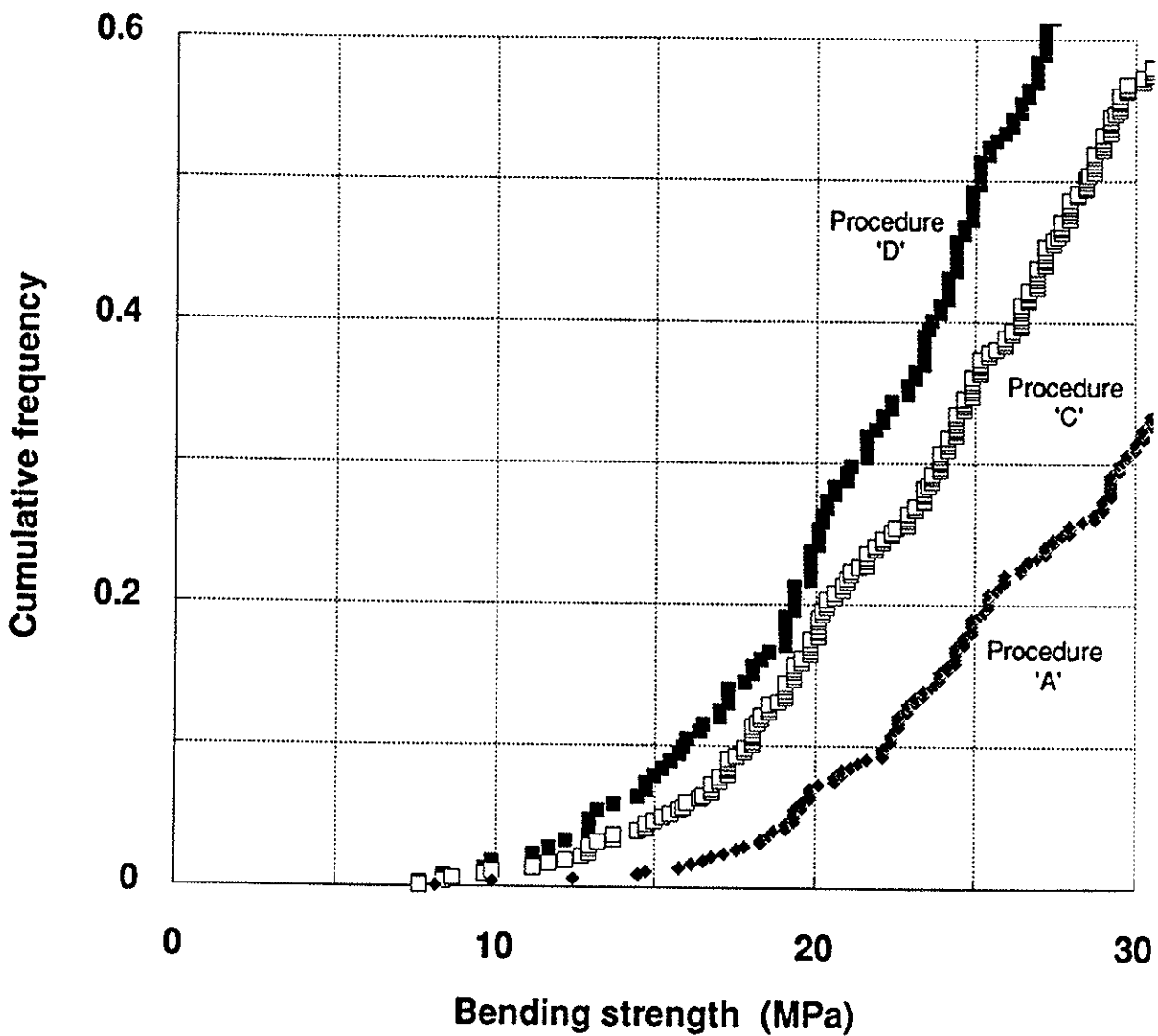


Figure 2. Bending strength of machine stress-graded F5 grade radiata pine (timber size 90 x 35 mm, test span 1620 mm, third point loading, graded stick length 4800 mm).

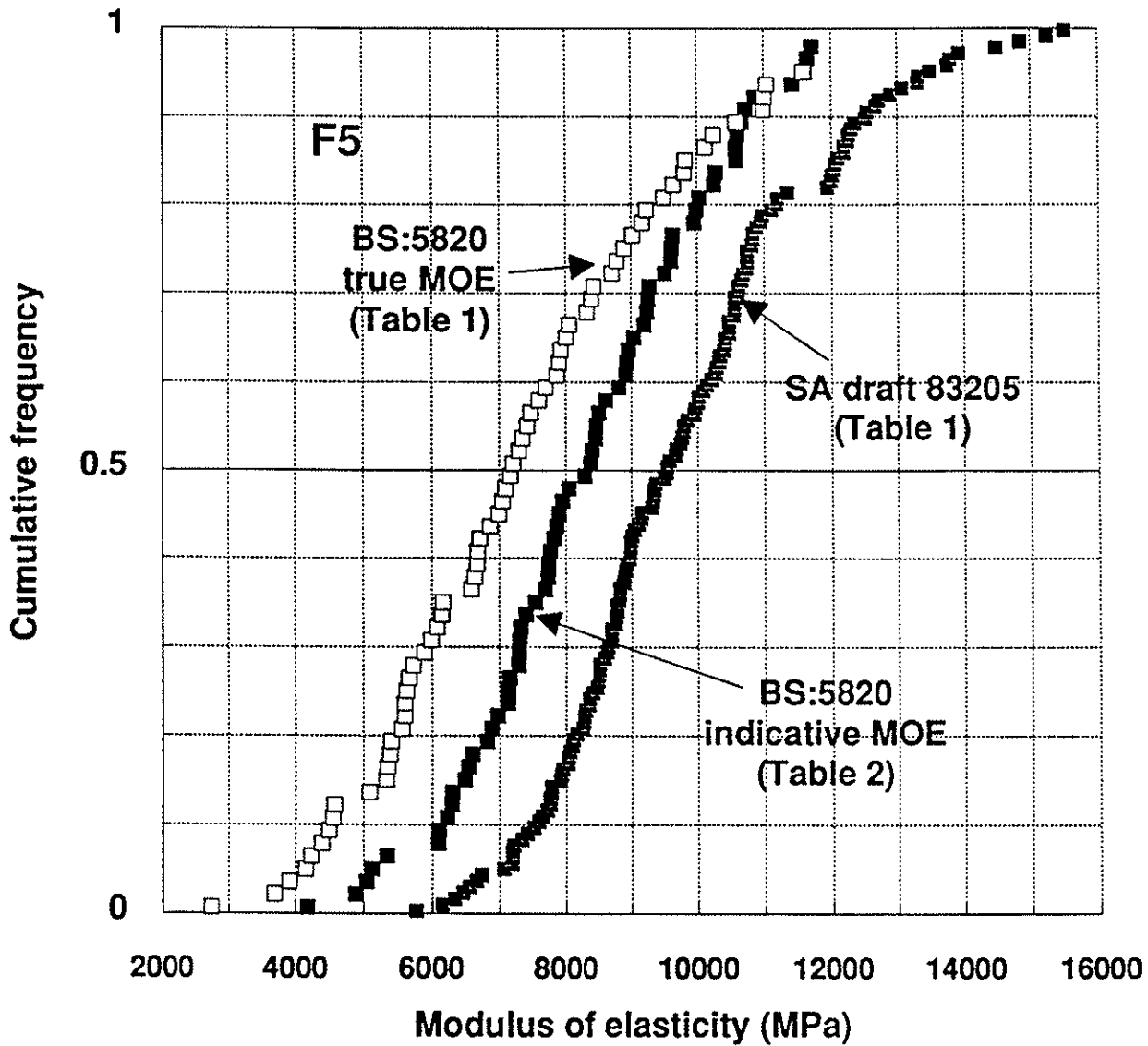


Figure 3. Bending stiffness of machine stress-graded F5 radiata pine (test span 1620 mm; graded length of stick 4800 mm for AS draft 83205 tests and 4000 mm for BS 5820 tests. Timber for AS draft 83205 was 90 x 35 mm; timber for BS 5820 tests was 90 x 45 mm from another source).

INTERNATIONAL COUNCIL FOR BUILDING RESEARCH STUDIES AND DOCUMENTATION

WORKING COMMISSION W18 - TIMBER STRUCTURES

EFFECT OF SAMPLING SIZE ON ACCURACY OF  
CHARACTERISTIC VALUES OF MACHINE GRADES

by

Y H Chui

R Turner

I Smith

University of New Brunswick

Fredericton, N.B.

Canada

MEETING TWENTY - FOUR

OXFORD

UNITED KINGDOM

SEPTEMBER 1991



## INTRODUCTION

Machine stress grading of lumber was first suggested over three decades ago. To facilitate commercial production of machine stress graded lumber, two quality control systems have evolved: output and machine control systems. Output control was first developed in North America and it is currently the only approved quality control system in the USA and Canada. Commercial production of machine stress graded lumber in Europe is confined to a few countries: the UK and the Nordic countries. In those countries machine control system is used exclusively, although both systems are listed in British Standard BS4978 (BSI, 1988) and in the draft European standard on machine stress grading of timber (CEN, 1991).

Under the North American output control system, machine grades with a broad range of primary design properties (bending stress, bending modulus and tensile stress) can be produced as long as quality control data show the material to be "on grade". Individual sawmills are required to have on-line equipment and qualified personnel to conduct tests on selected samples of the graded material. The so-called CUSUM charts are provided by the grading authorities to assist with determining whether properties of the graded material agree with the target design specifications ie "in control" (NLGA, 1987). If the process is "out of control", machine settings are re-adjusted and further quality control samples are taken and tested. This process is repeated until the process is "in control". Adjustment of settings to maximize yields is also permissible.

The machine control system places more emphasis on the characteristics of the grading machines and a pre-determined relationship between strength and flatwise  $E_{min}$  measured by a machine. In contrast to the output control system only those grades listed in design standards are produced. Machine settings ( $E_{min}$  boundaries) for sorting material into these stress grades are given by the grading authorities for each combination of species, size of lumber and type of machine. These settings are derived from strength/ $E_{min}$  relationships which have been established by testing representative samples of lumber prior to the actual production of the machine graded material. In general no in-house quality control tests are required under this quality control system as the process assumes that the sampled material adequately represents those subsequently graded and all machines of the same type have essentially identical performance at the time of manufacture. Periodic verification by the grading authorities ensures that machines perform consistently.

The above outlines the main differences between the two quality control systems for production of machine graded lumber. As mentioned earlier, the establishment of the strength/ $E_{min}$  relationship, and thus sampling of material for the calibration exercises, is central to the reliability of the machine control system. This paper examines how the characteristic values of samples drawn randomly from a typical "parent" population deviate from the target values when sample size changes.



## METHOD

A semi-empirical method of determining  $E_{min}$  boundaries from strength/ $E_{min}$  data has been presented by Fewell (1986). More recently Smith (1989) demonstrated a direct integration approach for deriving these boundaries. In his method both the strength and  $E_{min}$  data are represented by Johnson  $S_B$  distributions. The representation of the data by  $S_B$  distributions enables the relationship to be described by a bivariate normal distribution since  $S_B$  distributions can be transformed into normal distributions (Hahn and Shapiro, 1967). The advantage of Smith's method is that smoothing of data can be achieved using a bivariate normal distribution. The direct integration of the function leads to reduced errors in estimating the  $E_{min}$  boundaries.

A computer program based on the Smith approach has been developed for estimating the  $E_{min}$  boundaries that produce machine grades of lumber with prescribed characteristic values. In this investigation the program was used to estimate the  $E_{min}$  boundaries of machine grades. A separate computer program was developed to conduct a simulation study to assess the effect of sample size on the accuracy of the fifth percentile characteristic value of each grade. The simulations were performed in a transformed x-y space.

## SIMULATIONS

To gain an initial insight into the effect of sample size on characteristic values a data set containing 972 pieces of dry (12% m.c.) softwood lumber tested in bending was used as the "parent" population. A plot of the population is shown in Figure 1. The Johnson  $S_B$  distribution parameters, and the mean and coefficient of variation are given in Table 1 for both the dry bending strength (or MOR) and  $E_{min}$ .

Table 1 - Johnson  $S_B$  parameters of parent (ungraded) population.

Property	Johnson $S_B$				Mean (MPa)	COV (%)
	Location $\epsilon$ (MPa)	Range $\lambda$ (MPa)	Shape $\gamma$	Shape $\eta$		
Bending strength	3.449	128.88	2.205	1.457	29.28	47.0
$E_{min}$	1413.4	23655.6	2.472	1.846	6620	33.5

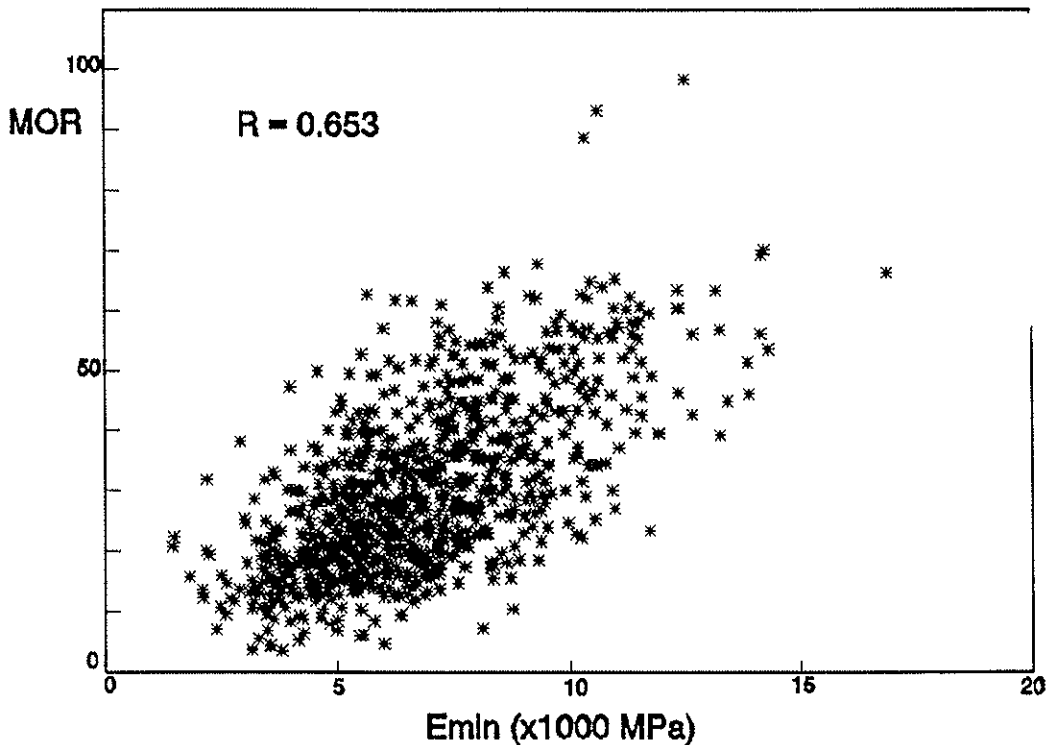


**Figure 1** - "Parent" population.

The machine settings corresponding to the following two combinations of machine grades were determined based on the Smith approach described above:

Combination 1 : F8 (30.8%) and F6 (31.7%)

Combination 2 : F7 (53.1%) and F5 (33.4%)

where the 5th percentile characteristic dry bending strength of each is F8 = 16.8 MPa, F7 = 14.7 MPa, F6 = 12.6 MPa, F5 = 10.5 MPa. The values in parentheses are the yields of the machine grades.

The machine settings were then used in the simulation study to "sort" randomly selected "pieces" into the desired machine grades. Two approaches of determining the 5th percentile values of sub-samples representing each grade were assessed. The first one was by a non-parametric approach in which the data were ranked in order and the 5th percentile value was determined from the raw data. The second approach was by a direct integration of the fitted bivariate normal distribution of the sample. For each sample size 100 sub-samples were simulated. Figure 2 illustrates the simulation procedure.

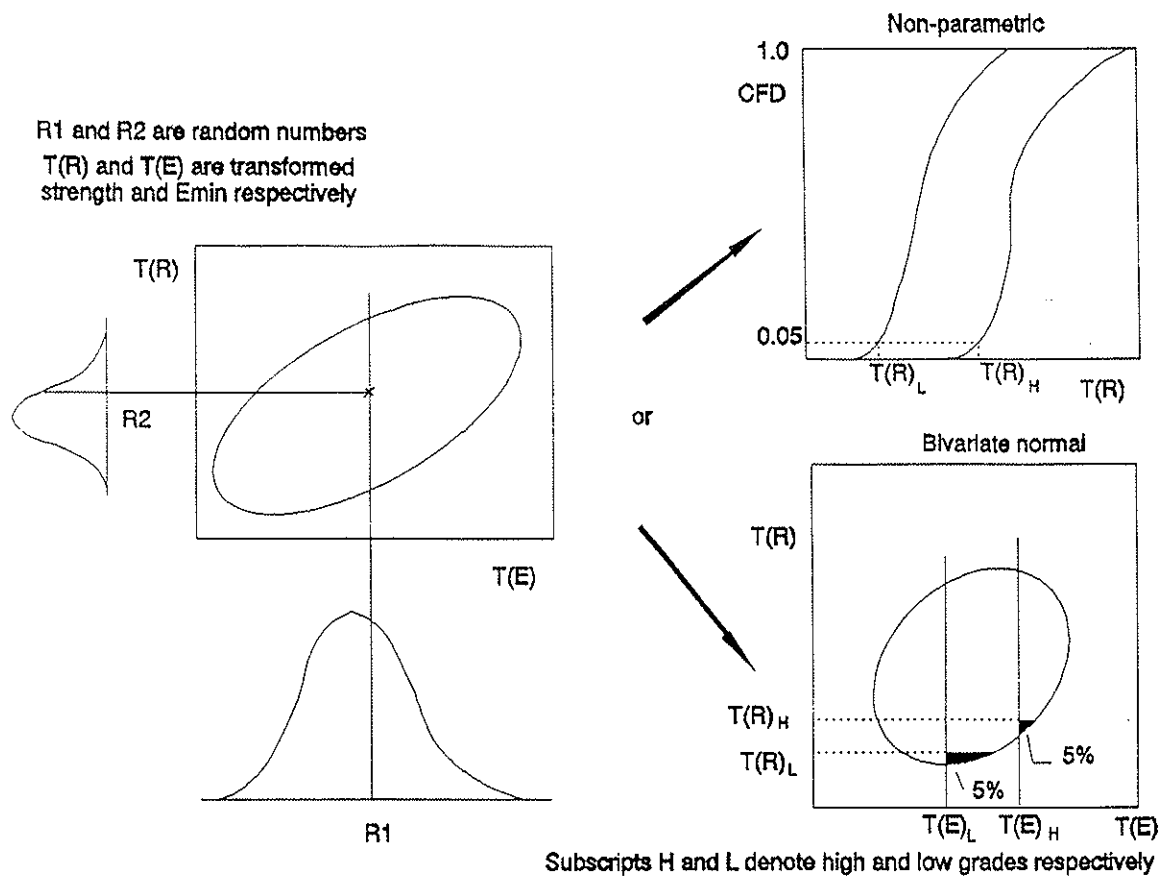


Figure 2 - Illustration of simulation procedures.

## RESULTS AND DISCUSSION

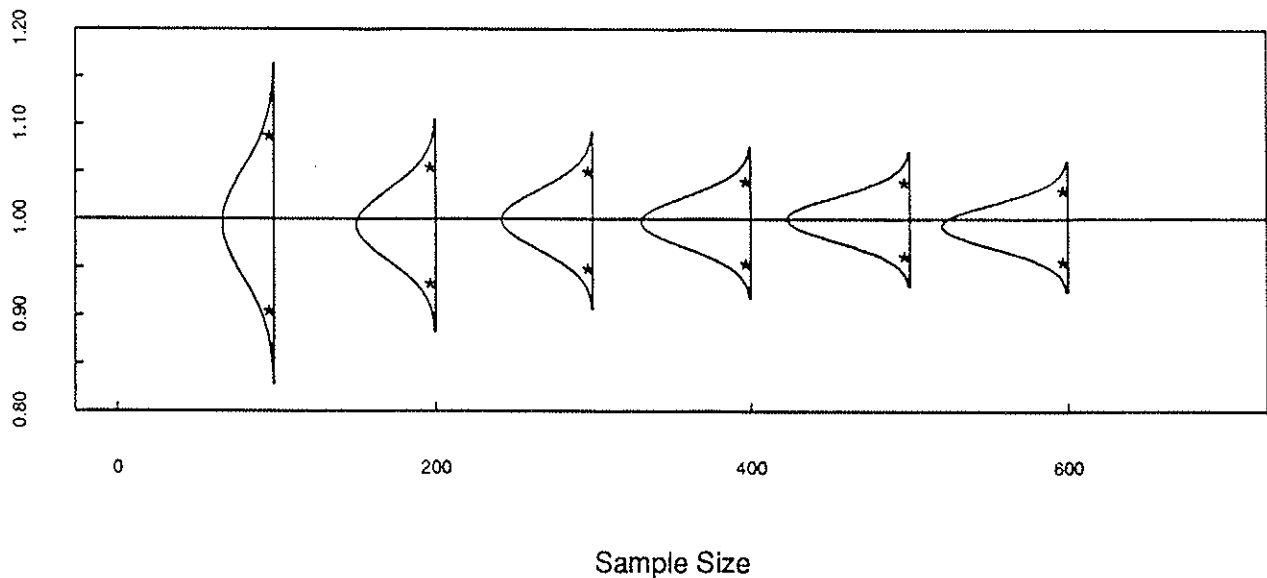
Similar results have been presented by Fewell and Glos (1988) primarily for visually graded lumber. For machine graded material the procedure is a little more complicated, as two grades are involved in each operation. The sample size effects on each grade are influenced by the characteristics of the other grade selected in the same operation.

Figure 3 shows the spread in 5th percentile characteristic values of the sub-samples that is observed in a machine grade as a function of sample size. The results are normalised

relative to the target characteristic value of the machine grade. The example illustrated is the higher grade in the F8/F6 grade combination. A normal distribution is plotted at sample size of 100, 200, 300, 400, 500 and 600. The dots correspond to the upper and lower 5th percentile exclusion limits for the fitted normal distributions. Thus the 90% confidence interval is contained within the group of dots. As expected the upper and lower confidence limits converge to a ratio of 1 when sample size tends to infinity.

Curves were fitted to the upper and lower exclusion limits associated with the grade combinations studied here. The results are presented in Figures 4 to 7. Figures 4 and 5 present the results when the 5th percentile characteristic value of each sample is determined by direct integration of a bivariate normal distribution as described above while Figures 6 and 7 present the results when a non-parametric approach is used to determine the characteristic values. Figures 4 and 6 relate to grade combination 1 (F8/F6) and Figures 5 and 7 correspond to grade combination 2 (F7/F5).

Normalised Characteristic Value



**Figure 3** - Variation of characteristic value ratio with sample size for grade F8 of the F8/F6 combination.

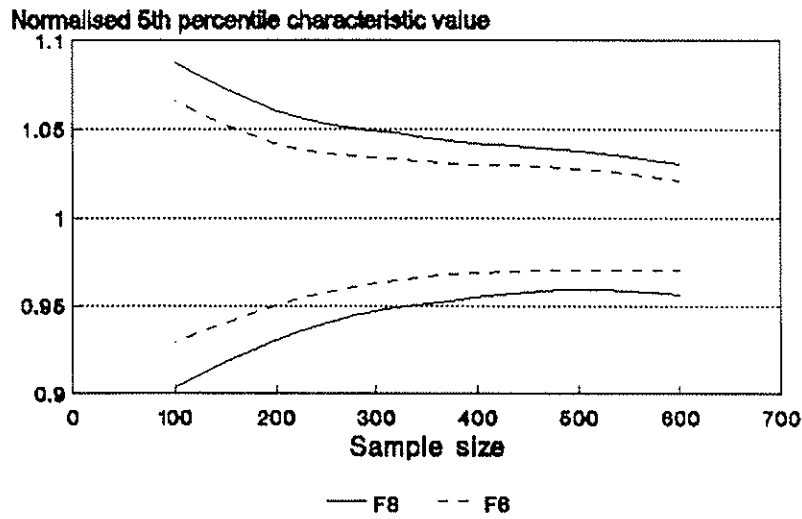


**Figure 4** - Variation of normalised characteristic value with sample size for grade combination 1, based on a parametric approach.

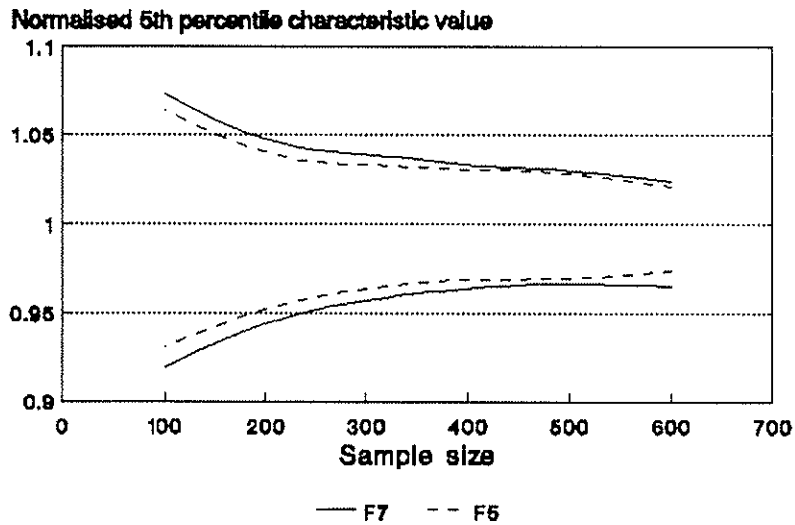


**Figure 5** - Variation of normalised characteristic value with sample size for grade combination 2, based on a parametric approach.

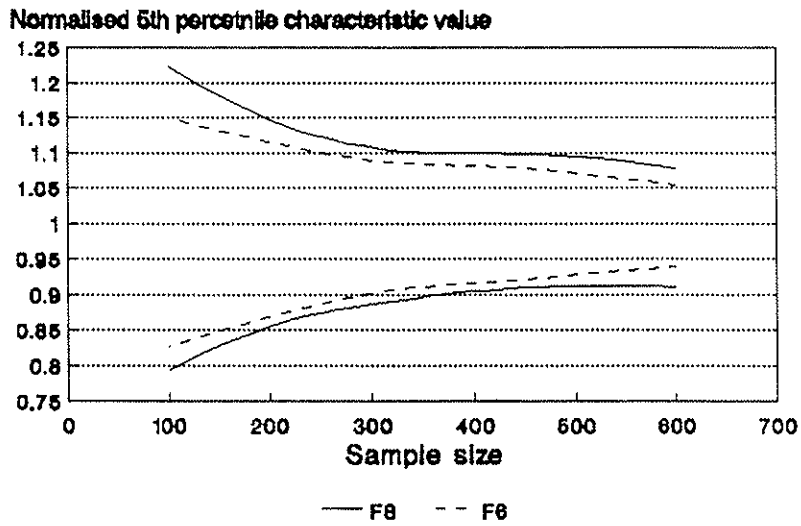


**Figure 6** - Variation of normalised characteristic value with sample size for grade combination 1, based on a non-parametric approach.

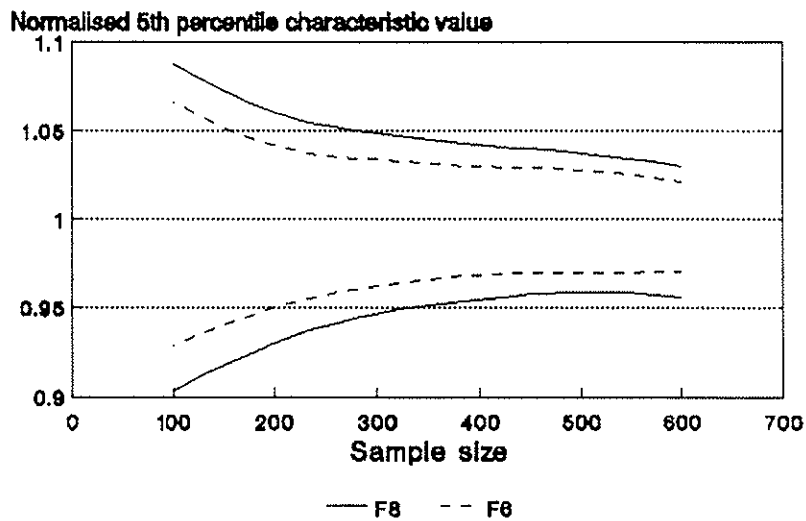


**Figure 7** - Variation of normalised characteristic value with sample size for grade combination 2, based on a non-parametric method.

It can be noticed from the figures that the confidence interval for the high grade is generally wider than for the low grade selected in a grading operation. This implies that the high grade will likely govern the choice of sample size to attain a given tolerance level for the sub-sample characteristic values. If a tolerance level for the normalised characteristic values is set to be 0.95 and for a 95% confidence interval, the following sample sizes are required based on the bivariate approach:

<u>Grade combination</u>	<u>Grades</u>	<u>Sample size</u>
Combination 1	F8/F6	330 (330 F8; 200, F6)
Combination 2	F7/F5	230 (230, F7; 185, F5)

As evident from Figures 6 and 7, the non-parametric approach requires considerably larger sample sizes (greater than 600) for the same tolerance level. This result demonstrates the advantage of utilizing a direct integration approach based on a normal-transformable statistical function for establishing machine stress grading settings. Implications for structural reliability are not assessed here but are also expected to favour use of a direct integration approach based on a normal-transformable statistical function.

## **CONCLUSIONS**

1. Sample sizes to meet certain tolerance and confidence interval requirements for characteristic values of machine grades vary depending on the methods of determining the characteristic values. Required sample sizes estimated using non-parametric approaches are considerably higher than a parametric method based on a distribution functions transformable into bivariate normal distributions.
2. Based on the use of a typical data set of 972 pieces of softwood lumber as the "parent population" and a parametric approach, it was shown that suitable sample sizes for determining machine settings are in the order of a few hundred. The likely range is between 200 and 350 pieces depending on lumber species and the combination of grades to be sorted simultaneously.

## **REFERENCES**

BRITISH STANDARDS INSTITUTION. 1988. British Standard Specification for Softwood grades for structural use. BS 4978, London, BSI.

EUROPEAN COMMITTEE FOR STANDARDIZATION. 1991. Structural timber grading

requirements for machine strength graded timber and grading machines. Draft prEN 519. Brussels, CEN.

FEWELL, A. R. 1986. Derivation of settings for stress grading machines. BRE report. BRE, Garston.

FEWELL, A. R. and GLOS, P. 1988. The determination of characteristic strength values for stress grades of structural timber. Part 1. Proceedings of Meeting Twenty-One of CIB Working Commission W18A, University of Karlsruhe, Germany.

HAHN, G. J. and SHAPIRO, S. S. 1967. Statistical models in engineering. John Wiley & Sons, New York, N. Y.

NATIONAL LUMBER GRADES AUTHORITY. 1987. Special Products Standard for machine stress rated lumber SPS 2. NLGA, Vancouver, B. C.

SMITH, I. 1989. A direct derivation of machine settings in machine controlled stress grading of softwood lumber. Proceedings of the Seventh International Symposium on Non-destructive Testing of Wood. Washington States University, Pullman, WA.



## **ABSTRACT**

Using an appropriate mathematical function, this paper examines the effects of sample size on the deviation of characteristic values of samples from the target grade value of machine graded lumber. For operations involving two machine grades at a time, it is shown that the higher grade will likely govern the sample size required to meet a certain tolerance level. If an error of 5% is allowed in the estimate of the 5th percentile characteristic value at the 95% confidence limit, the required sample size is between 200 and 350 based on a typical population of softwood lumber.

INTERNATIONAL COUNCIL FOR BUILDING RESEARCH STUDIES AND DOCUMENTATION  
WORKING COMMISSION W18 - TIMBER STRUCTURES

HARMONISATION OF LSD CODES

by

R H Leicester  
CSIRO  
Australia

MEETING TWENTY - FOUR

OXFORD

UNITED KINGDOM

SEPTEMBER 1991



# HARMONISATION OF LSD CODES

**R.H. Leicester**  
(CSIRO, Australia)

## 1. INTRODUCTION

During the recent NATO 'Advanced Research Workshop' on 'Reliability Based Design of Engineered Wood Structures' (Florence, Italy, 3–5 June, 1991), it was generally agreed that, while the global trend towards use of the LSD format was encouraging, the lack of harmonisation between the various countries was a disturbing feature. In the short term, lack of harmonisation would be detrimental to technology transfer between countries (thereby necessitating the involvement of unnecessary costs and delays) and it would also act as a barrier to trade in structural products. In the longer term, the lack of harmonisation could reduce timber to the status of a regional or local commodity rather than a global one, thereby leading to a reduction or perhaps even a total loss in the use of timber as a primary structural material.

In the following, examples of the current lack of harmonisation will be discussed. Some of these are critical while others can be circumvented, although usually at the cost of adding unnecessary complexity and delays to implementing efficient timber utilisation. However, it should be emphasised that in this context harmonisation is not meant to imply uniformity; it does however imply compatibility in the sense that the equivalence between various codes may be easily established. Codes of differing complexity can be tolerated provided there is harmony of intent and compatibility of format between them. This is particularly relevant when codes of developing and developed countries are being compared.

## 2. CHARACTERISTIC PROPERTIES OF TIMBER

This is undoubtedly the most disastrous example of lack of harmonisation. Important differences between countries can be placed into two groups, as follows:

- (a) differences due to the test methods used for measuring characteristic values, and
- (b) differences due to the methods used for processing the test data.

Currently the use of different test methods for measuring strength and stiffness tends to form an insurmountable barrier to establishing the equivalences between the characteristic values of various standards. This matter is discussed in some detail in an accompanying paper (Leicester and Young 1991).

Because different methods are used for selecting the test specimens from sticks of lumber, there is (currently) no method for predicting the relationship between strengths and stiffnesses measured according to the standards of one country with that of another. Differences in the values of strengths and stiffnesses also arise because of differences in the specified test spans, loading configuration and gauge length for measuring deformations.

To date there is no accepted procedure for finding the equivalence between the five-percentile values of strengths obtained by these two test methods. It is conceivable that in the future, timber strength models that take into account the frequency of defects may provide a way out of this difficulty (Leicester and Breitingner 1991).

Differences in characteristic values that arise due to differences in the methods used for processing the data are not as critical as those due to differences in test methods. At least (in theory) equivalences can be established if the original raw data can be retrieved. Most of the differences that occur in data processing relate to the choice of confidence level with which the characteristic value is estimated.

It should be emphasised that these differences in the definitions of characteristic values is a critical problem. An example of its impact on trade is the fact that because of such differences, the \$15 million and 10 years worth of in-grade testing undertaken in North American is worthless when it comes to exporting structural timber to Europe. Less obvious, but equally disastrous, is the impact on technology transfer. In the format of design codes, modification factors for moisture content, load duration, size effects, etc., are all related to the characteristic value, and implicitly therefore to the way in which it

is defined. Without establishing the relevant equivalences between characteristic values, the transfer of modification factors from one country to another is fraught with potential errors. For this reason alone it is an urgent matter to establish methods that are accepted for obtaining the equivalence between characteristic values.

### **3. CHARACTERISTIC PROPERTIES FOR CONNECTOR SYSTEMS**

The difficulties associated with establishing harmonisation between standards for the characteristic properties of solid timber are increased many times when it comes to connector systems.

If the reliability of connector systems is to be comparable with that of solid timber, then for each joint a set of characteristic strengths must be evaluated for each basic type of load, as shown in Figure 1(a). However, even this would not be adequate. Each type of connector can be for joints in all manner of complex configurations, such as shown in Figure 1(b). Furthermore, there is a tremendous variety of failure modes that can occur within connector systems. Observed failure modes of connector systems have included tension and compression failures of wood, both parallel and perpendicular to the grain, shear failure in wood, and failure in the connector metal either in tension, bearing, buckling or bending; some times a change in failure mode can occur simply by changing the dimensions used within a given joint configuration.

Because there are numerous types of systems for which each single type of connector can be used, it is unlikely that any country will undertake a comprehensive set of tests. This will create obvious difficulties in obtaining harmonisation of design rules for connectors.

One solution may be that for every connector, a set of standard tests be chosen for which the species, joint system and load configurations are specified. The difficulty will be to choose a set that comprehensively covers all important failure modes and system configurations. Other factors on which agreement needs to be reached is whether the wood should be clear or should contain representative grade defects ( and if so, which types of defects), whether the wood is of average density, the five-percentile density, or

a representative range of densities (including both juvenile and mature wood) and finally whether the joint strength is taken to be the mean value of some agreed percentile such as the five-percentile.

#### **4. MODIFICATION FACTORS**

Within the format of current LSD codes, the modification factors for load duration, moisture content, size effects, etc., are all applied to the characteristic values. Hence, unless there is harmonisation between characteristic values, then there will be a corresponding difficulty in obtaining compatibility between the modification factors used in various countries. For example, the measured size effect will vary depending on whether bending strength relates to the worst defect within a stick, or to randomly selected beams.

There are also difficulties in harmonisation due to differences in test procedures and the methodology used for processing the data. This is particularly true for the studies of load duration effects, where different predictions may be obtained from the one data source; in addition, it often happens that important parameters, such as humidity fluctuations (Fridley *et al.* 1990) and environment air velocity are not taken into consideration in the conceptual theory or recorded during the testing program.

#### **5. SYSTEM EFFECTS**

One modification factor that requires careful attention is the modification factor for system effects. Two quite independent factors can contribute to this factor. One component relates to material characteristics, particularly its variability; the second component relates to the assumed idealisations that a designer will apply in undertaking a structural analysis. For example, both these factors are included in the system effect derived by Foschi (1989), while only the former is covered by the Australian Code AS 1720.1. To illustrate this, comparative values of system factors for a floor joint system are given in Table 1; it should be noted that not only are the two sets of values different, but that they change in opposite directions in response to an increase in the number of floor joists involved.

## 6. STRENGTH GROUPING

There are numerous strength grouping systems used around the world (e.g. Leicester and Keating 1982). These are usually specific to a particular country or a particular region. Some systems, such as the ISO system (Table 2), are intended to have a universal and timeless application; to achieve this, the steps in property values between adjacent strength classes are arranged in an unbiased geometric progression. Other systems, such as that in Eurocode 5, are targeted at making the best use of the timber currently available in the region or country (Table 3).

A temporary solution for harmonising these numerous strength group systems would be to establish each particular strength group in terms of an equivalent ISO strength group. In this way, a rough equivalence between various countries will be achieved.

## 7. PARTIAL SAFETY FACTORS

In comparing the design strengths of various codes, the partial safety factor ( $\gamma_m$ ) or equivalent resistance factor ( $\phi$ ) should be considered. Unfortunately, these are not always taken to be functions of the same parameters. For example, the following have been used (Leicester 1990; Standards Association of New Zealand 1991, Goodman 1990, Gromala *et al.* 1990, Canadian Standards Association 1989; European Committee for Standardisation 1990a; Danish Standards Institute 1982):

- function of material (Australia and New Zealand)
- function of design property (USA, Canada)
- function of importance and quality control (Eurocode, Denmark)

In theory, the equivalence between Australia/New Zealand and the Canada/USA codes can be derived; for both these cases, whole families of theoretically derived resistance factors  $\phi$  that vary with design properties and material type have been grouped into a set of single factors and compensated by modifying the characteristic values specified in design codes; the procedures used for these modifications can be found in relevant standards that are currently being drafted. However, this large number of effective



resistance factors would appear to be replaced by a single partial safety factor in the case of Eurocode 5; the equivalence between Eurocode 5 on the one hand and the Australian, New Zealand, USA and Canadian codes on the other is difficult to determine.

## 8. NEW TECHNOLOGY

In the development of new technology related to formulating design procedures for structural timber engineering, the ultimate aim of obtaining global harmonisation should be borne in mind, and the design format arranged accordingly. Some areas in which this applies are the formulation of design rules for durability, fire resistance and serviceability.

## 9. RELIABILITY

Reliability methods are being increasingly used as a basis for developing code design rules (Foschi *et al.* 1989; Leicester 1991) and is an important consideration in technology transfer between countries. However, to do this usefully, equivalences between the methods used by various countries must be established. Apart from differences in the mathematics used to compute the probability of failure, the following are factors that must be identified in the assessment of equivalence.

- (a) The probability of failure must be related to a specific reference period (e.g. 50 years). Extrapolations from one reference period to another are difficult because time sequential correlations differ for the various structural parameters (e.g. dead load *v.* wind load).
- (b) The definition of failure must be considered. Failure is usually related to single elements, but may be related to structural systems. If structural system effects are considered, then both parallel system effects (e.g. for floor joists) and series system effects (e.g. for truss members) should be taken into account.
- (c) It should also be determined whether computed failure rates are intended to be nominal values (based on the analysis of idealised structures) or real failure rates as would be expected to occur in real building practice due to extreme load and strength values.

- (d) Target failure rates should be identified in terms of their variation with types of loads, materials, stresses and importance factors.
- (e) The intended design procedure to be used with each code should be identified in terms of assumptions to be used in the structural analysis for checking ultimate limit states (e.g. system effects, joint analysis, P- $\Delta$  effects in beam-columns) and in terms of procedures to be used for checking serviceability limit states.

## 10. CONCLUDING COMMENT

Global harmonisation in the sense of establishing the equivalences between various design codes is a critical matter in terms of trade, technology transfer and the acceptance of timber as a structural material. Currently there is a lack of harmonisation between the design codes of various countries. For some important matters, such as characteristic properties, it would appear that harmonisation may not be achievable unless concerted international effort is made to do so.

## 11. REFERENCES

- British Standards Institute (1979) BS 5820 'Methods of test for determination of certain physical and mechanical properties of timber in structural sizes', London, UK, 8 pp.
- Canadian Standards Association (1989) CAN/CSA-086.1-M89 'Engineering design in wood (limit state design)', Toronto, Canada, December, 234 pp.
- Danish Standards Institute (1982) DS 413 'Structural use of timber' (English translation), Copenhagen, Denmark.
- Ellingwood, B., Galambos, T.V., McGregor, J.G. and Cornell, C.A. (1980) 'Development of a probability based load criterion for American National Standard A58, Building code requirements for minimum design loads in buildings and other structures', NBS Special Publication No. 577, National Bureau of Standards, US Dept of Commerce, Washington DC, USA, June, 222 pp.
- European Committee for Standardisation (1989) EN TC 124.202 'Structural timber: the determination of characteristic values of mechanical properties and density of timber' (Draft), Brussels, Belgium.

- European Committee for Standardisation (1990a) CEN TC 250/505.12 Eurocode 5 'Design of timber structures: Part 1. General rules and rules for buildings' (Draft), Brussels, Belgium.
- European Committee for Standardisation (1990b) EN TC 124.202 'Structural timber – strength classes' (Draft), Brussels, Belgium, 6 pp.
- Foschi, R.O., Folz, B.R. and Yao, F.Z. (1989) 'Reliability-based design of wood structures', Report No. 34, Structural Research Series, Dept of Civil Engineering, University of British Columbia, Vancouver, Canada.
- Fridley, K.J., Tang, R.C. and Soltis, L.A. (1990) 'Effect of cyclic relative humidity on the load duration behaviour of structural lumber', Proc. 1990 International Timber Engineering Conference, Tokyo, Japan, October, Vol. 2, 407–415.
- Goodman, J.R. (1990) 'Reliability-based design for engineered wood construction: update and status of US progress', Proc. 1990 International Timber Engineering Conference, Tokyo, Japan, October, Vol. 1, 6–11.
- Gromala, D.S., Sharp, D.J., Pollock, D.G. and Goodman, J.R. (1990) 'Load and resistance factor design for wood: the new US wood design specification', Proc. 1990 International Timber Engineering Conference, Tokyo, Japan, October, Vol. 1, 311–318.
- International Standards Organisation (1988) ISO/DIS 8972 'Solid timber-strength grouping', 3 pp.
- Leicester, R.H. (1990) 'On developing an Australian limit states codes', Proc. 1990 International Timber Engineering Conference, Tokyo, Japan, October, Vol. 1, 12–20.
- Leicester, R.H. and Keting, W.G. (1982) 'Use of strength classifications for timber engineering standards'. Division of Building Research Technical Paper (Second Series) No. 43, CSIRO, Australia.
- Leicester, R.H. and Young, F.G. (1991). 'Equivalence of characteristic values' Proc. CIB-W18A Meeting, Oxford, UK.
- Standards Association of Australia (1986) DR 83205 'Draft Australian standard for the evaluation of strength and stiffness of graded timber', Sydney, Australia.
- Standards Association of Australia (1988) AS 1720.1 'SAA timber structures code. Part 1: Design methods', Sydney, Australia, 85 pp.
- Standards Australia (1989a) AS 1170.1 'SAA loading code. Part 1: Dead and live loads and load combinations', Sydney, Australia, 29 pp.

Standards Australia (1989b) AS 1170.2 'SAA loading code. Part 2: Wind loads',  
Sydney, Australia, 96 pp.

Standards Association of New Zealand (1991) NZS 3603.1 'Code of practice for timber  
design' (Draft), Wellington, New Zealand, 63 pp.

Table 1. A comparison of system factors for a floor

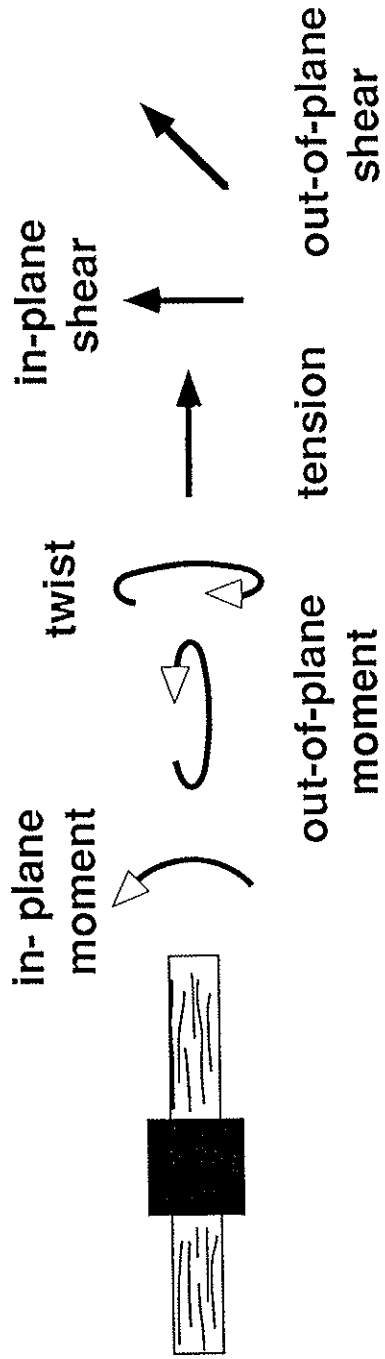
Number of floor joists	System factor	
	Foschi <i>et al.</i> (1989)	AS 1720.1 (SAA 1988)
2	–	1.11
5	1.58	1.20
10	1.44	1.25
20	1.37	–

Table 2. Proposed strength grouped properties for stress-graded timber in ISO/DIS 8972 (International Standards Organisation 1988)

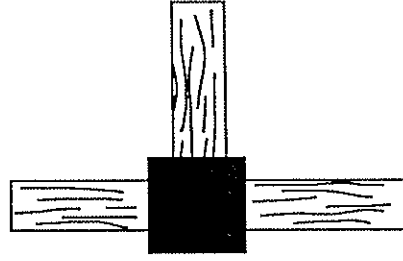
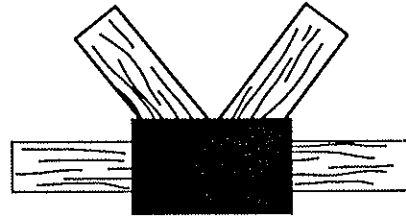
Strength class	Bending strength	Tension strength	Modulus of elasticity (GPa)
	(MPa)	(MPa)	
T75	75	48	19.0
T60	60	38	15.0
T48	48	30	12.0
T38	38	24	9.5
T30	30	19	8.5
T24	24	15	7.5
T19	19	12	6.0
T15	15	9.5	5.4
T12	12	7.6	4.8
T10	9.5	4.8	4.2
T8	7.5	3.8	3.4
T6	6.0	3.0	3.0
T5	4.8	2.4	2.4

TABLE 3. Strength grouped properties for stress-graded timber for Eurocode 5  
(European Committee for Standardisation 1990a)

Strength class	Bending strength (MPa)	Tension strength (MPa)	Modulus of elasticity (GPa)
C60-22E	60	36	22
C48-20E	48	29	20
C37-14E	37	22	14
C30-15E	30	18	15
C30-12E	30	18	12
C24-11E	24	14	11
C21-13E	21	13	13
C21-10E	21	13	10
C18-9E	18	11	9
C15-11E	15	9	11
C15-8E	15	9	8
C13-7E	13	8	7



(a) Typical loads



(b) Joint configurations

Figure 1. Examples of loads and joint configurations of connector systems

**INTERNATIONAL COUNCIL FOR BUILDING RESEARCH STUDIES AND DOCUMENTATION  
WORKING COMMISSION W18 - TIMBER STRUCTURES**

**THE FRACTURE ENERGY OF WOOD IN TENSION PERPENDICULAR TO THE GRAIN**

by

H J Larsen  
P J Gustafsson  
Division of Structural Mechanics  
Lund Institute of Technology  
Sweden

**MEETING TWENTY - FOUR  
OXFORD  
UNITED KINGDOM  
SEPTEMBER 1991**





## ERRATA

Annex A4

Replace the table by the following

Series		41	42	43
No. of spec.		10	9	8
– unstable		3	0	2
$\omega$	%	13.1(2)	13.5(4)	–
$\rho_{\omega,\omega}$	kg/m <sup>3</sup>	481(2)	729(5) <sup>1)</sup>	369(1)
$\alpha$		15°–70°	25°–45°	45°–60°
$G_{I,C}$	Nm/m <sup>2</sup>	418(19)	643(9)	291(12)

- 1) If the results for series 42 are corrected to a density of 481 (see Fig. 5) a fracture energy of 385 Nm/m<sup>2</sup> is found.

Annex A6

The moisture content was about 13 percent.

Annex A7

The only deviation from the draft standard was that in series 2  $a=h=40$  mm instead of 80 mm.

Replace the table with the following.

		Series 1		Series 2	
		rejected <sup>1</sup>	accepted	rejected <sup>1</sup>	accepted
b	mm	35		20	
h	mm	80		40	
No. of spec.		13(7) <sup>1</sup>	9	10(10) <sup>1</sup>	29
$\omega$	%	12.1(9)	11.9(9)	11.0(11)	11.8(10)
$\rho_{0,\omega^2}$		533(12)	550(12)	560(9)	540(10)
$\rho_{\omega,\omega}$		597(12)	615(12)	622(9)	603(10)
$\alpha$		$\sim 0^0$		$\sim 30^0$	
$G_{I,C}$		553(49)	706(45)	651(16)	671(23)

**ANNEX A12**

Chongqing Institute of Architecture and Engineering, Sichuan, China

---

Contact person

Huang Shao-Yin

References

Shao-Yin Huang: Determination of the Fracture Energy of Wood in Splitting Along the Grain, Chongqing Institute of Architecture and Engineering, China 1991

Deviation from draft standard

The tested volume was 60x60x30 mm and the depth of the saw cut was 30 mm.

Wood

Sichuan Fir. The width of the specimens was about 30 mm.

Results

The results are shown in the table below.

Mean value with coefficient of variation (in percent)

---

No. of spec.		20	6	14+6
$\alpha$		~0°–25°	~25°–70°	
$\rho_{\omega,\omega}$	kg/m <sup>3</sup>	438(2)	478(7)	450(6)
$G_{I,C}$	Nm/m <sup>2</sup>	375(16)	410(6)	385(14)

---

The results are shown in Fig. 1. Using the relationship for European softwoods of Fig. 6 of paper CIB W18A–23–19–2 a mean value of 347 Nm/m<sup>2</sup> would be expected.

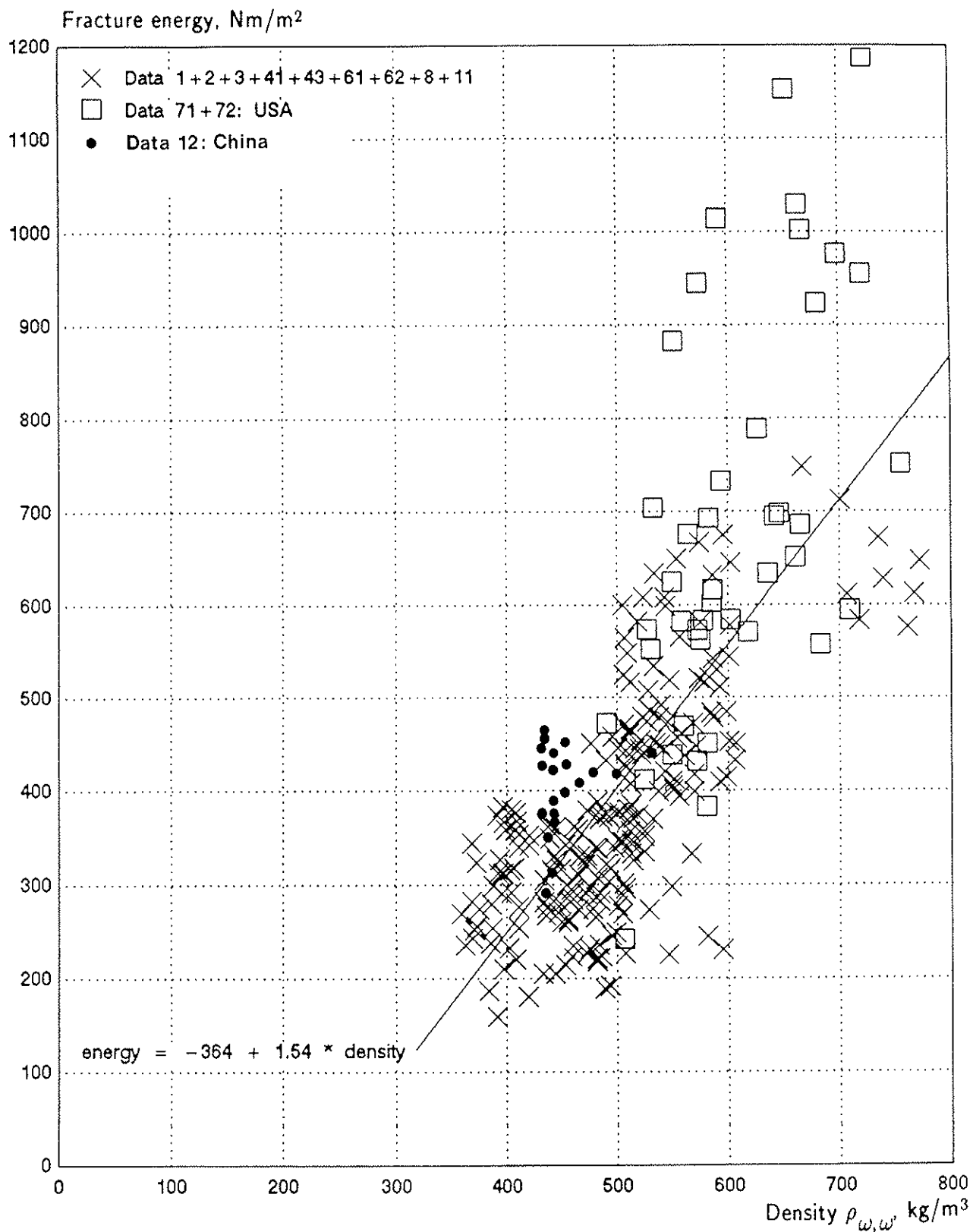


Fig. 1

Results from Annex A12 plotted in Fig. 6 of CIB paper W18A-24-19

## ANNEX A13

Lund Inst. of Techn., Div. of Struct. Mech., Sweden (1991)

---

### Contact persons

Per Johan Gustafsson and Bertil Enquist

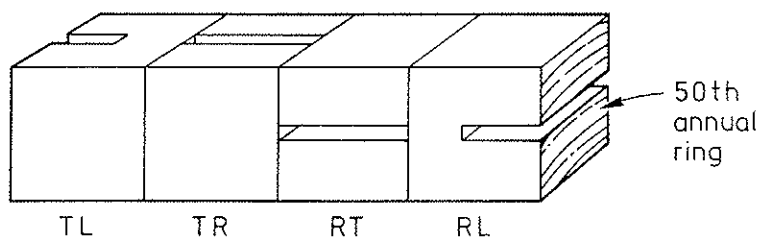
### Supplementary purpose

To study whether the direction of crack growth affects the fracture energy.

### Wood

Redwood (*Pinus Silvestris*) with a moisture content of 11.5 percent. Specimen width  $b = 40$  mm.

Four series of specimens were cut from two planks. Each serie comprises four specimens with different orientation of the notch and cut from adjoining parts of the plank according to the figure below. For all specimens, the fracture plane is within the heart wood and the 50th annual ring is located at the centre of the specimen.



### Deviations from draft standard

$h = h_c/0.4 = a = 60$  mm instead of 80 mm.

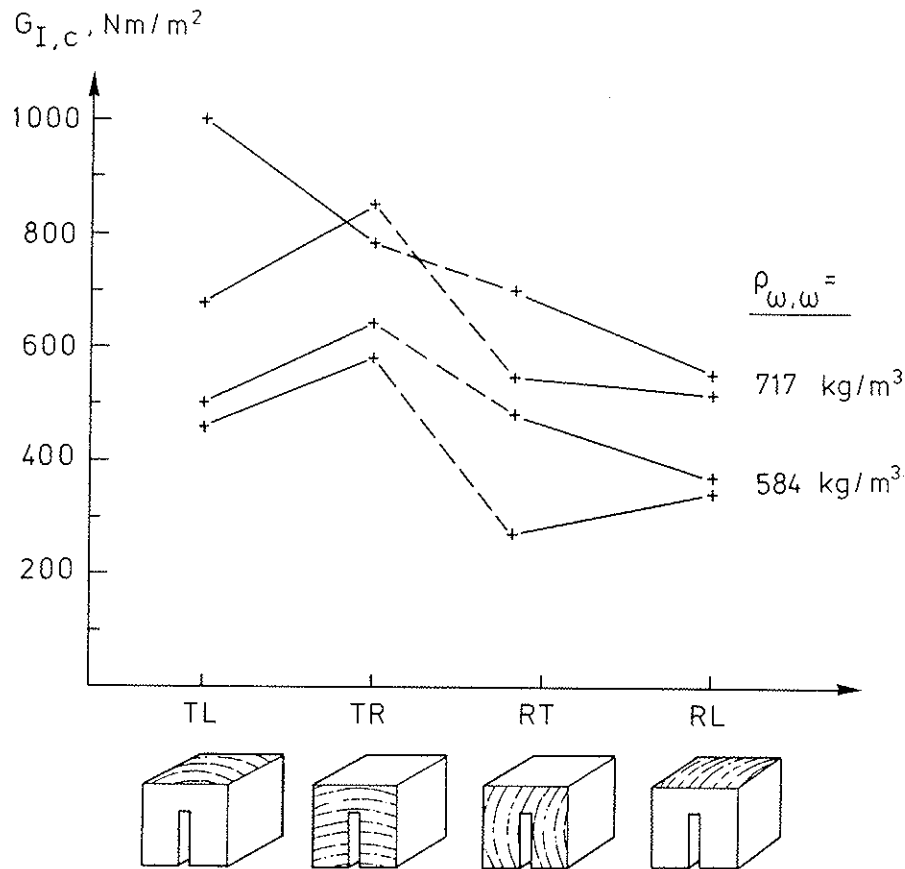
For orientations TR and RT the perpendicular to grain tensile fracture does not develop along grain but instead the crack grows in the direction in between grain.

### Results

All specimens with TL and RL orientation performed in a stable manner. For the TR and RT orientations the load displacement performance was partly unstable.

For the TR orientation complete separation of the fracture plane would require abnormally large beam deflection. To overcome this, in the evaluation of the test results beam weight,  $mg$ , was increased by a fictitious weight (40 N) and the zero level of the external load correspondingly changed (20 N), compare figure 3 in draft standard.

The fracture energy values obtained are shown in diagram below. If the energy required to create a fracture plane with any certain orientation within the material is independent of the direction of crack growth, then  $G_{I,C}$  should be equal for TL and TR, and equal for RT and RL.



### Conclusions

The tests do not indicate any statistically significant influence of crack growth direction.

The orientation of the fracture plane, on the other hand, has a significant effect. A plane orientated with its normal in the T-direction has in mean a 47 percent higher  $G_{I,C}$  than a plane orientated with its normal in the R-direction.





**TIMBER FOOTBRIDGES:  
A COMPARISON BETWEEN STATIC AND DYNAMIC DESIGN CRITERIA**

by Ario Ceccotti and Niccolò De Robertis  
University of Florence, Italy

**1. INTRODUCTION**

This communication reports some results of a study whose purpose is to compare the static and the dynamic serviceability limit states design criteria.

While in the static field the design criteria are turned to the limitation of maximum deflection (usually under live-load only), in the dynamic one such criteria are based on the necessity to limit the vibrations that can cause discomfort to the user.

It is to be emphasized that besides objective factors, such as the natural frequencies of the bridge, psychological and individual factors, such as the age and the habit of the user to walk on footbridges or to use public transport, contribute to define the vibration threshold able to ensure comfort to the user himself.

In the present work reference is made to the vibration serviceability requirements proposed by British Standards 5400 [1], whose background was given by Blanchard, Davies and Smith [2]. The maximum vertical acceleration of any part of the structure shall be limited to the following value:

$$a_{\text{adm}} = 0.5 \cdot \sqrt{f_1} \quad (\text{m/s}^2) \quad (1)$$

where  $f_1$  is the first natural frequency (or fundamental frequency) in Hertz of the unloaded bridge.

On the static side, reference is made to Eurocode 5 – Part II [3], where the allowable maximum deflection, under live load only, is defined as follows:

$$\eta_{\text{adm}} = \frac{\ell}{300} \quad (2)$$

being  $\ell$  the main span length of the footbridge.

## 2. ANALYSIS OF THE DYNAMIC EFFECTS INDUCED BY A MOVING PEDESTRIAN

In the following the background to the design criteria developed by B., D., & S. is reported. Note that the BS do not give any static deflection criteria for serviceability limit state.

### 2.1 General Numerical Model

- It is considered a pedestrian, with static weight of 0.7 kN and a stride length of 0.9 m, walking in resonance with the fundamental frequency of the footbridge.
- It is assumed that it is possible to excite the footbridge in such a way only when the fundamental frequency doesn't exceed 4 Hz, being the latter value a reasonable upper limit of the applied pacing frequency (frequencies above 3 Hz representing running).
- The foot impulse force-time function for each pace is represented in Fig. 2. The pedestrian forcing function is simulated by combining consecutive single foot force-time functions applied at successive intervals equal to the period of vibration  $T_1$ , as shown in Fig. 3.

The structure has been simulated by finite beam elements, each nodal point representing the position consecutively assumed by the foot of the man walking on the footbridge. The equations of motion of the system are:

$$[M]\{\ddot{q}\} + [D]\{\dot{q}\} + [K]\{q\} = \{F\} \quad (3)$$

where:  $\{\ddot{q}\}$ ,  $\{\dot{q}\}$ ,  $\{q\}$  = Acceleration, velocity and displacement vectors of the system

$[M]$ ,  $[D]$ ,  $[K]$  = Structure mass, damping and stiffness matrices

$\{F\}$  = Forces acting on the structure

A sensitivity analysis has shown that the acceleration of the footbridge is slightly sensitive to the second and third modes of vibration. Besides, being the tolerance threshold related to a simple harmonic motion, the first mode of vibration only is taken into account for the evaluation of the response. Assuming the damping matrix as a linear combination of the mass and stiffness matrices – proportional damping – the coupled equations of motion represented by system (3) can be rewritten as a new system of uncoupled equations each one representing one of the modes of vibration of the system. Representing the pedestrian forcing function by a series of point loads, as shown in Fig. 4, with the force-time variation shown in Fig. 3, the equation of motion becomes:

$$p_1 + \frac{\delta}{\pi} \cdot \omega_1 \cdot p_1 + \omega_1^2 \cdot p_1 = \frac{1}{M_1} \cdot \sum_{j=1}^N \phi_1(x_j) \cdot f(t-j \cdot T_1) \quad (4)$$

where:  $p_1, \dot{p}_1, p_1$  = First mode acceleration, velocity and displacement in principal coordinates  
 $\delta$  = Logarithmic decrement  
 $\omega_1$  = First undamped natural frequency  
 $M_1$  = First modal generalized mass  
 $\{\phi_1(x)\}$  = First normalized mode shape  
 $x_j$  = position of the pedestrian at the j-th pace  
 $N$  = number of paces to cross the footbridge  
 $f(t)$  = force-time function for standard foot impulse

Equation (4) was solved numerically using a Fortran program.

### 2.2 Simplified Method

For a single span, or two- or three-span continuous and simply supported symmetric bridges of constant cross section over the entire length as shown in Fig. 5, B., D., & S. have proposed a simplified formula to calculate the maximum vertical acceleration (in  $m/s^2$ ):

$$a_{\max} = 4 \cdot \pi^2 \cdot f_1^2 \cdot y_s \cdot K \cdot \psi \tag{5}$$

where:  $y_s$  = Static deflection at midspan due to pedestrian placed at that point (m)  
 $K$  = Configuration factor  
 $\psi$  = Dynamic response factor

Configuration Factor K: dependent upon the number and lengths of the spans. It can be obtained from Eq. (5) by substituting the peak acceleration determined from a full numerical solution of Eq. (4). Besides, numerical studies have shown that this factor is a simple constant, independent of span. The following table gives the K values for the configurations shown in Fig. 5.

Static Scheme	One Span	Two Span	Three-Span		
			$l_1/l = 1.0$	$l_1/l = 0.8$	$l_1/l \leq 0.6$
K	1	0.7	0.6	0.8	0.9

Dynamic response factor  $\psi$ : dependent upon the main span length and the damping characteristics of the bridge, as shown in Fig. 6 where the damping is expressed in terms of the logarithmic decrement.

In order to evaluate the maximum acceleration response to a pedestrian walking (or

running) on a bridge with a fundamental frequency higher than 4 Hz (upper limit of the applied pacing frequency), a further factor, called attenuation factor,  $\alpha$ , is introduced. In this case, being impossible to the pedestrian to walk in resonance with the fundamental frequency of the bridge (non-resonant vibrations), the maximum acceleration determined from Eq. (5), that corresponds to the situation of resonance, must be reduced by a factor defined as:

$$\alpha = \frac{\text{Maximum acceleration when walking below resonant frequency}}{\text{Maximum acceleration when walking at resonant frequency}}$$

Fig. 7 shows the measured and the proposed  $\alpha$  values for different values of the ratio between the natural frequency of the bridge and the actual walking frequency. B., D., & S. have suggested an attenuation factor decreasing linearly from 1 to 0.3 for bridges with fundamental frequencies between 4 and 5 Hz. For fundamental frequencies above 5 Hz, being too difficult to excite the bridge, the induced vibrations may be ignored. Equation (5) then becomes:

$$a_{\max} = 4 \cdot \pi^2 \cdot f_1^2 \cdot y_s \cdot K \cdot \psi \cdot \alpha \quad \alpha = \begin{cases} 1 & \text{when } f_1 \leq 4 \text{ Hz} \\ -0.7 \cdot f_1 + 3.8 & \text{when } 4 \text{ Hz} < f_1 < 5 \text{ Hz} \\ 0 & \text{when } f_1 \geq 5 \text{ Hz} \end{cases} \quad (6)$$

### 3. PURPOSE OF THE STUDY

In the present study comparisons between the vibration serviceability requirements and the criteria for the limitation of the static deflection due to variable actions have been achieved for glue-laminated timber footbridges. It has been evaluated the possibility to define some cases in which the recurrence to the simple static criterion only allows the designer to avoid the dynamic verifications being sure that such verifications are in any case satisfied. In particular, some values of the maximum deflection (under a reference value of the live load) have been found for simple structural configurations.

The assumptions and the procedures are summarized in the following.

#### 3.1 Assumptions

##### a) Structural configurations

- One-span simply-supported footbridge (Fig.5(a))
- Two-span continuous symmetric footbridge (Fig.5(a))
- Three-span continuous symmetric footbridge (Fig.5(a)). The following side/central span ratio values have been considered:

$$\ell_1/\ell = 0.6-0.8-1.0$$

b) Cross-section type

- Section made up of various rectangular sections placed parallel each other with total width  $b$  and height  $h$ , as shown in Fig. 8.

c) Mechanical and geometrical characteristics

- Main span length:  $\ell = 10 \div 40$  m
- Cross-section height:  $h = 60 \div 200$  cm
- Total cross-section width:  $b = 20 \div 200$  cm
- Width:  $s = 320$  cm
- Static Elastic Modulus of Elasticity of timber:  $E_s = 11$  kN/mm<sup>2</sup>
- Dynamic Elastic Modulus of Elasticity of timber:  $E_d = E_s$ ;  $E_d = 1.5 \cdot E_s$
- Logarithmic decrement:  $\delta = 0.05$
- Mass density of timber:  $\rho = 500$  kg/m<sup>3</sup>
- Unit mass of non-structural elements:  $\mu = 200 \div 500$  kg/m

Width: that value has been chosen being commonly assumed in the practice [4].

Dynamic modulus of elasticity: two different  $E_d$  values have been considered. In fact, the application of dynamic identification techniques to full-scale structures containing a low number of mechanical connections has shown that the actual dynamic behaviour can be satisfactory simulated (in a global way) by introducing an increased dynamic modulus equal to 1.5 times the static one [5]. Anyway such a value has then been chosen (besides a value equal to the static one) as a limit reference value only, in order to allow an evaluation of the main differences occurring in the structural dynamic response when the modulus of elasticity is varying.

Logarithmic decrement: for the logarithmic decrement too, the choice of such a value is supposed to be considered as a reference value (according to BS 5400) to be taken into account in absence of more precise data. Nevertheless the value chosen seems to be in the safety side, since experimental tests performed by Bruninghoff on some glue-laminated timber footbridges, have shown that the measured values of logarithmic decrement vary from 0.15 to 0.20, depending on the kind of induced vibrations and the connectors.

d) Live load

As suggested in several current European codes the live load taken into account in the deflection verifications was assumed to be dependent on the loaded span length, as follows:

$$\begin{array}{llll}
 \ell \leq 10 \text{ m}; & q = 5.00 & \text{kN/m}^2 & \\
 10 \leq \ell \leq 30 \text{ m}; & q = 5.00 \div 4.00 & \text{kN/m}^2 & \text{(linearly decreasing)} \\
 \ell \geq 30 \text{ m}; & q = 4.00 & \text{kN/m}^2 & 
 \end{array}$$

### 3.2 Calculation Formulas

The formulas for the calculation of the parameters necessary to the comparison between the static and the dynamic criterion are summarized in the following:

#### a) Acceleration

- Fundamental Frequency  $f_1$ :

$$f_1 = \frac{(\alpha\ell)_1^2}{2 \cdot \pi \cdot \ell^2} \cdot \sqrt{\frac{E_d \cdot J}{A \cdot \rho + \mu}} \quad (7)$$

where: A = Cross-section area

J = Cross-section Inertial moment

$(\alpha\ell)_1$  = Coefficient depending on the static scheme. In the following tables the values for the static scheme investigated in the present work are reported.

Static Scheme	One Span	Two Span	Three Span			
			$\ell_1/\ell=1.0$	$\ell_1/\ell=0.8$	$\ell_1/\ell=0.6$	$\ell_1/\ell=0.4$
$(\alpha \cdot \ell)_1$	$\pi$	$\pi$	$\pi$	3.534	3.816	3.534

- Midspan static deflection due to the pedestrian

Letting the midspan static deflection induced by the single pedestrian in terms of a unique expression the following equation is obtained:

$$y_s = \frac{P \cdot \ell^3}{E_s \cdot J} \cdot \epsilon \quad (8)$$

where  $\epsilon$  is a coefficient depending on the static scheme only:

Simply supported single span beam:  $\epsilon = \frac{1}{48}$

$$\begin{aligned} \text{Two-span continuous symmetric beam:} \quad \epsilon &= \frac{23}{1536} \\ \text{Three-span continuous symmetric beam:} \quad \epsilon &= \frac{23}{1536} \cdot \left( \frac{1}{3} + \frac{2 \cdot \frac{\ell_1}{\ell}}{2 \cdot \frac{\ell_1}{\ell} + 3} \right) \end{aligned}$$

For each static scheme, once the main span  $\ell$ , the unit mass of non-structural elements  $\mu$  and the dynamic modulus of elasticity  $E_d$  are defined, the variability of the cross-section dimensions,  $b$  and  $h$ , within their own ranges, leads to a lack of univocity between the inertial characteristics of the cross section and the natural frequencies of the footbridge. In fact, regarding the parameters taking part in the calculation of the first natural frequency (see Eq. (7)), it can be seen that a same value of the inertial moment can correspond to different width/height combinations and than to different values of the area  $A$  (et vice-versa). In the following it shall be indicated with  $\Delta a$  the ratio:

$$\Delta a = \frac{\text{maximum acceleration}}{\text{allowable acceleration}} = \frac{4 \cdot \pi^2 \cdot f_1^2 \cdot y_s \cdot K \cdot \psi \cdot \alpha}{0.5 \cdot \sqrt{f_1}} = 8 \cdot \pi \cdot \sqrt{f_1^3} \cdot K \cdot \alpha \cdot y_s \quad (9)$$

#### b) Midspan static deflection due to live load

The midspan maximum deflection calculation was performed taking into account the live load,  $q$ , only. Letting the midspan static deflection induced by live load in terms of a unique expression, the following equation is obtained:

$$\eta_{\max} = \frac{q \cdot s \cdot \ell^4}{E_s \cdot J} \cdot \beta \quad (10)$$

where  $\beta$  is a coefficient depending on the static scheme only:

$$\begin{aligned} \text{Simply supported single span beam:} \quad \beta &= \frac{5}{384} \\ \text{Two-span continuous symmetric beam:} \quad \beta &= \frac{73}{768} \\ \text{Three-span continuous symmetric beam:} \quad \beta &= \frac{1}{96} \cdot \left( \frac{1}{3} + \frac{2 \cdot \frac{\ell_1}{\ell}}{2 \cdot \frac{\ell_1}{\ell} + 3} \right) \end{aligned}$$

As already said, the allowable midspan maximum deflection was calculated at first as

proposed EC 5 – Part II:

$$\eta_{\text{adm}} = \frac{\ell}{300}$$

Unlike what happens in the evaluation of the maximum acceleration, the calculation of midspan deflection, being performed accounting for the live load only, leads to a univocal relationship between the bridge inertial characteristics and the midspan deflection.

In the following it shall be indicated with  $\Delta\eta$  the ratio:

$$\Delta\eta = \frac{\text{maximum midspan deflection}}{\text{allowable midspan deflection}} = \frac{300 \cdot q \cdot s \cdot \ell^3}{E_s \cdot J} \cdot \beta \quad (11)$$

### 3.3 Numerical Procedure

The maximum and allowable accelerations and midspan static deflections have been calculated by means of an automatic procedure for every static scheme and for every value that each geometrical and mechanical parameter (defined at par. 3.1) can assume within its own range of variation. The single procedure consists of the following steps:

#### 1) Input Data

- Static scheme (and  $\ell_1/\ell$  ratio if necessary).
- Main span length,  $l$ .
- Dynamic modulus of elasticity,  $E_d$ .
- Unit mass of non-structural elements,  $\mu$ .

#### 2) Static and dynamic data calculation

- Maximum and allowable midspan deflection induced by live load.
  - Maximum and allowable vertical acceleration.
- by means of a step by step technique using each value of cross-section height and width.

#### 3) Comparison between static and dynamic criteria

The comparison has been performed by comparing the  $\Delta a$  and  $\Delta\eta$  ratios.

This procedure has been repeated till all the possible combinations of input data have been exhausted.



#### 4. STATIC AND DYNAMIC CRITERIA COMPARISON

In the following tables the analysis results are summarized.

- In each table are reported the maximum values of allowable deflection,  $\ell/r$  (or minimum values of denominator  $r$ ) that, in correspondance of the minimum values of inertial moment  $J$  that ensure the static verification ( $\Delta\eta \leq 1$ ), are able to satisfy the dynamic requirements too ( $\Delta a \leq 1$ ). Such minimum values of denominator  $r$  will be noted with  $r_{\min}$ .
- The  $r_{\min}$  value reported in each table is 300, being it the value proposed by EC5 – Part 11.
- Each table is characterized by the following values of dynamic modulus of elasticity  $E_d$  and non-structural mass  $\mu$ :

1) Table 1:  $E_d = E_s = 11.0 \text{ kN/mm}^2$ ;  $200 \leq \mu < 350 \text{ kg/m}$

2) Table 2:  $E_d = 1.5 \cdot E_s = 16.5 \text{ kN/mm}^2$ ;  $200 \leq \mu < 350 \text{ kg/m}$

3) Table 3:  $E_d = E_s = 11.0 \text{ kN/mm}^2$ ;  $\mu \geq 350 \text{ kg/m}$

4) Table 4:  $E_d = 1.5 \cdot E_s = 16.5 \text{ kN/mm}^2$ ;  $\mu \geq 350 \text{ kg/m}$

TABLE 1: $r_{\min}$ values $E_d = E_s = 11 \text{ kN/mm}^2$ ; $\mu < 3.5 \text{ kN/m}$					
Lenght $\ell$ (m)	One Span	Two Span	Three Span		
			$\ell_1/\ell=1.0$	$\ell_1/\ell=0.8$	$\ell_1/\ell=0.6$
20	350	350	300	300	300
25	425	425	300	300	425
30	400	350	300	300	500
35	300	300	300	300	450
40	300	300	300	300	325

TABLE 2: $r_{\min}$ values $E_d = 1.5 \cdot E_s = 16.5 \text{ kN/mm}^2$ ; $\mu < 3.5 \text{ kN/m}$					
Lenght $\ell$ (m)	One Span	Two Span	Three Span		
			$\ell_1/\ell=1.0$	$\ell_1/\ell=0.8$	$\ell_1/\ell=0.6$
20	350	375	300	300	300
25	425	425	300	375	400
30	525	525	300	450	500
35	400	400	300	425	525
40	325	300	300	300	525

**TABLE 3:  $r_{\min}$  values**  $E_d = E_s = 11 \text{ kN/mm}^2$ ;  $\mu \geq 3.5 \text{ kN/m}$

Lenght $\ell$ (m)	One Span	Two Span	Three Span		
			$\ell_1/\ell=1.0$	$\ell_1/\ell=0.8$	$\ell_1/\ell=0.6$
20	350	350	300	300	350
25	325	300	300	300	350
30	300	300	300	300	325
35	300	300	300	300	300
40	300	300	300	300	300

**TABLE 4:  $r_{\min}$  values**  $E_d = 1.5 \cdot E_s = 16.5 \text{ kN/mm}^2$ ;  $\mu \geq 3.5 \text{ kN/m}$

Lenght $\ell$ (m)	One Span	Two Span	Three Span		
			$\ell_1/\ell=1.0$	$\ell_1/\ell=0.8$	$\ell_1/\ell=0.6$
20	350	375	300	300	300
25	425	425	300	350	425
30	475	375	300	350	500
35	350	300	300	300	500
40	300	300	300	300	400

All the features reported in the tables can also be emphasized looking at the figures 9 & 10 where the main numerical results are plotted.

In these figures the  $\Delta a$  and  $\Delta \eta$  ratios are plotted against the ratio between the inertial moment and the cubic value of the main span length,  $J/\ell^3$  being in such a way the  $\Delta \eta$  ratio independent from the main span length  $\ell$  (see Eq. (11)) for a defined value of  $q$ . This was done for each static configuration, each  $E_d$  value and for values of the non-structural mass,  $\mu$ , equal to 200 and 350  $\text{kg/m}^2$ .

Besides, for clarity, in each figure the  $\Delta \eta$  ratio is represented with reference to a constant live load value, equal to 4.50  $\text{kN/m}^2$  (correspondent to the mean value proposed by codes), and to a reference value of the main span ratio, equal to  $\ell/400$  (representing a reasonable mean value among those ones reported in the tables), being possible, in this case, for each assumed static scheme, to use a unique curve to represent the  $\Delta \eta$  values for each main span length,  $\ell$ . This choice has allowed to emphasize the main qualitative differences stood up from the comparison between the dynamic and the static criteria.

With reference to the  $\Delta a$  ratios, it can be seen the “range of variability” caused by the already mentioned lack of univocity between the inertial characteristics and the natural frequencies of the footbridge. It is to be pointed out that, the large amount of data plotted in the figures in order to represent the  $\Delta a$  values, does not allow to single out each “range of variabilities” characteristic of each main span length.

From the analysis both of the tables and the figures the following informations can be deduced:

- For each static scheme, for a same value of unit mass of non-structural elements, when the dynamic modulus of elasticity increases, the values of the ratio  $\Delta a$  between the maximum and the allowable acceleration increases too (even though the differences are often slight). Being the static deformability verifications independent from the  $E_d$  value, an increasing of this value will imply in general an decreasing of the maximum main span ratio  $\ell/r$  (or an increasing of the  $r_{\min}$  value) able to ensure the dynamic verifications too. Looking at the figures where the  $\Delta a$  and  $\Delta \eta$  ratios become less than the unit, this means that, once the live load is defined, when the  $E_d$  value increases, the safety coefficient towards the maximum acceleration acceptable to the pedestrian decreases.
- For each static scheme, for a same value of the dynamic modulus of elasticity, when the non-structural mass increases the  $\Delta a$  ratios decrease (and then decreases the maximum main span ratio  $\ell/r_{\min}$ ).

Both these circumstances are due to the fact that in the calculation of the ratio  $\Delta a$  (see Equations (9) & (7)), the dynamic modulus of elasticity and the non-structural unit mass are in the numerator and in the denominator respectively, while the calculation of the ratio  $\Delta \eta$  is independent from these features.

## 5. CONCLUSIONS

This communication reports some results of a study whose purpose was to evaluate in which cases it is possible to bypass the vibration serviceability requirements by adopting the maximum static deflection verifications only.

The analyses have shown that the main features influencing the results are the dynamic modulus of elasticity  $E_d$ , the non-structural mass  $\mu$ .

The results have shown that in several cases it is possible to adopt the static deformability criterion only: for example, in the case that a dynamic modulus of elasticity equal to the static

one could be assumed, for three-span beam with values of the ratio  $\ell_1/\ell \geq 0.8$  and values of unit mass  $\mu$  superior to 350 kg/m, the analyses have shown that the choice of cross section dimensions able to ensure the static deflection verifications according to EC5 – Part II allow to avoid the vibration verifications. This implies that, if the vibration limit were a little more stringent (i.e.  $\ell/400$ ) more cases could be satisfied by means of the static criterion only.

In conclusion it is to be outlined that, apart from the single numerical result achieved by the analysis, the amount of acquired informations can give a good basis for a useful guidelines in order to choose the simplest designing rules for timber footbridges.

#### ACKNOWLEDGEMENTS

The authors are grateful to Prof. H. Bruninghoff of the University of Wuppertal for his precious technical support.

#### REFERENCES

- [1] British Standards Institution, BS 5400 – PART 2 – 1978: “*Steel, Concrete and Composite Bridge. Part 2: Specification for Loads*”. United Kingdom, 1978.
- [2] Blanchard, J., Davies, B. L. and Smith, J.W., “*Design Criteria and Analysis for Dynamic Loading of Footbridges*”. Proceedings of a Symposium on Dynamic Loading Behaviour of Bridges, Transport and Road Research Laboratory Supplementary Report 275, pp. 90-100, United Kingdom, 1977.
- [3] Eurocode 5 PART II: “*Special Rules for Timber Components and Bridges*”, 1989.
- [4] AA.VV., “*Fussgängerbrücke Hilden*”. BAB n. 46, Beghische Universität Gesamthochschule, Wuppertal, Düsseldorf, Germany, 1989. (in German)
- [5] Ceccotti, A. and Vignoli, A., “*Full-Scale Structures of Glue-Laminated Timber Dynamic Tests: Theoretical and Experimental Studies*”. CIB-W18, Meeting 18, Paper N° 18-5-1, Israel, 1985.
- [6] AA.VV., “*Sovrappassi Pedonali: Progettazione Statica e Progettazione dinamica*”. ILVA Publication, pp. 70-79, Italy, 1989. (in Italian)
- [7] British Standards Institution, BS 5400 – PART 3 – 1982: “*Steel, Concrete and Composite Bridge. Part 3: Code of Practice for Design of Steel Bridges*”. United Kingdom, 1982.
- [8] DIN 1072: “*Straßen- und Wegbrücken; Lastannahmen*”

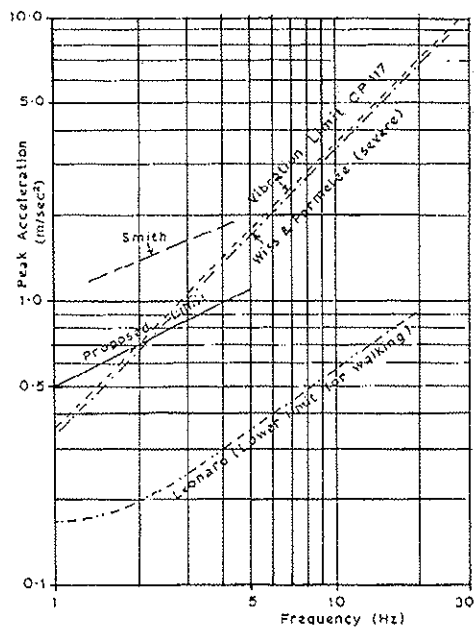


Fig. 1: Tolerance Thresholds & Vibration Limits [2]

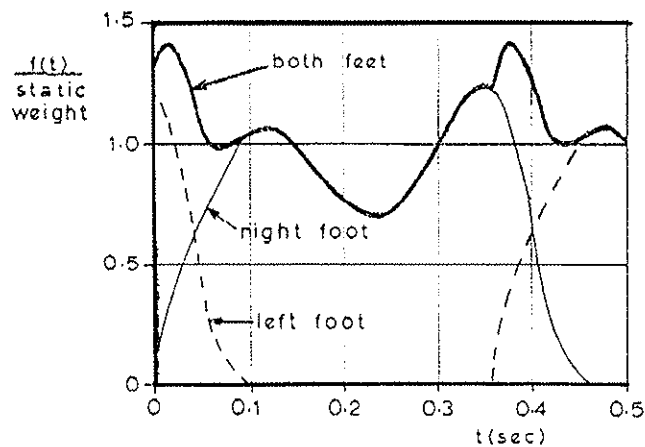
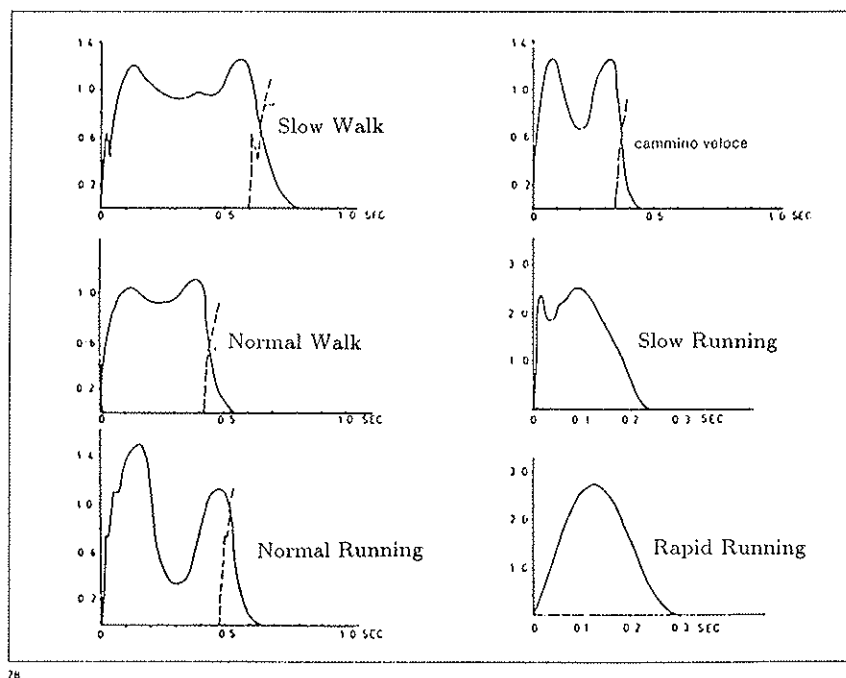


Fig. 3: Foot Impulse Curve: Total Vertical Force [2]



78

Fig. 2: Foot Impulse Force-Time Curves

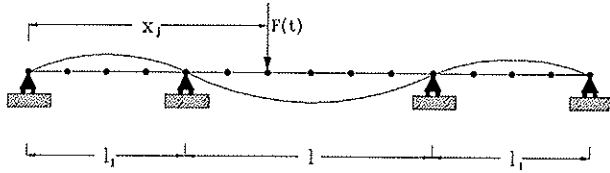


Fig. 4: Modelling the Footbridge and the Pedestrian Loading

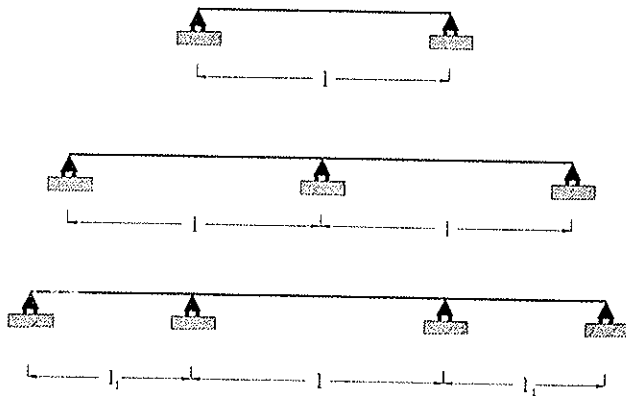


Fig.5: Static Configurations for Simplified Method

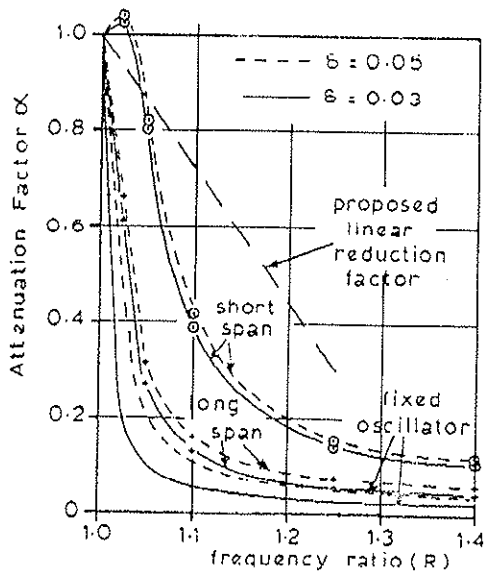
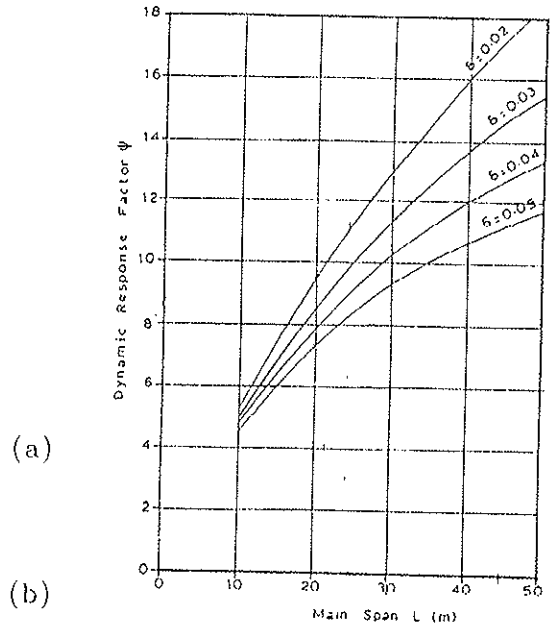


Fig. 7: Attenuation Factor [2]



(a)

(b)

(c)

Fig. 6: Dynamic Response Factor [2]

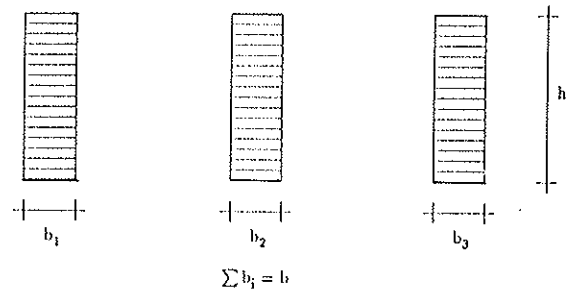


Fig. 8: Cross-Section Type

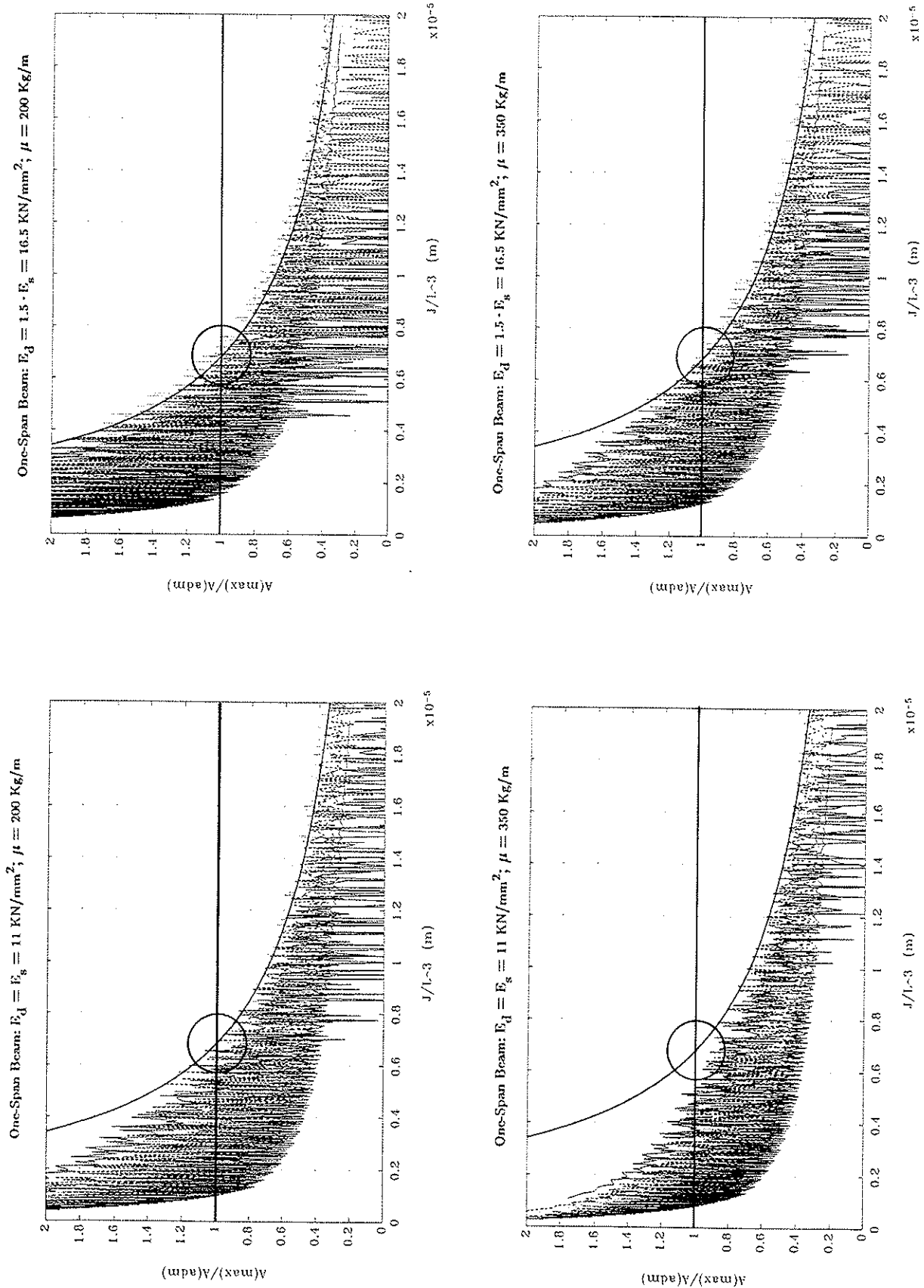


Fig. 9: One-span footbridge: comparison between static and dynamic design criteria

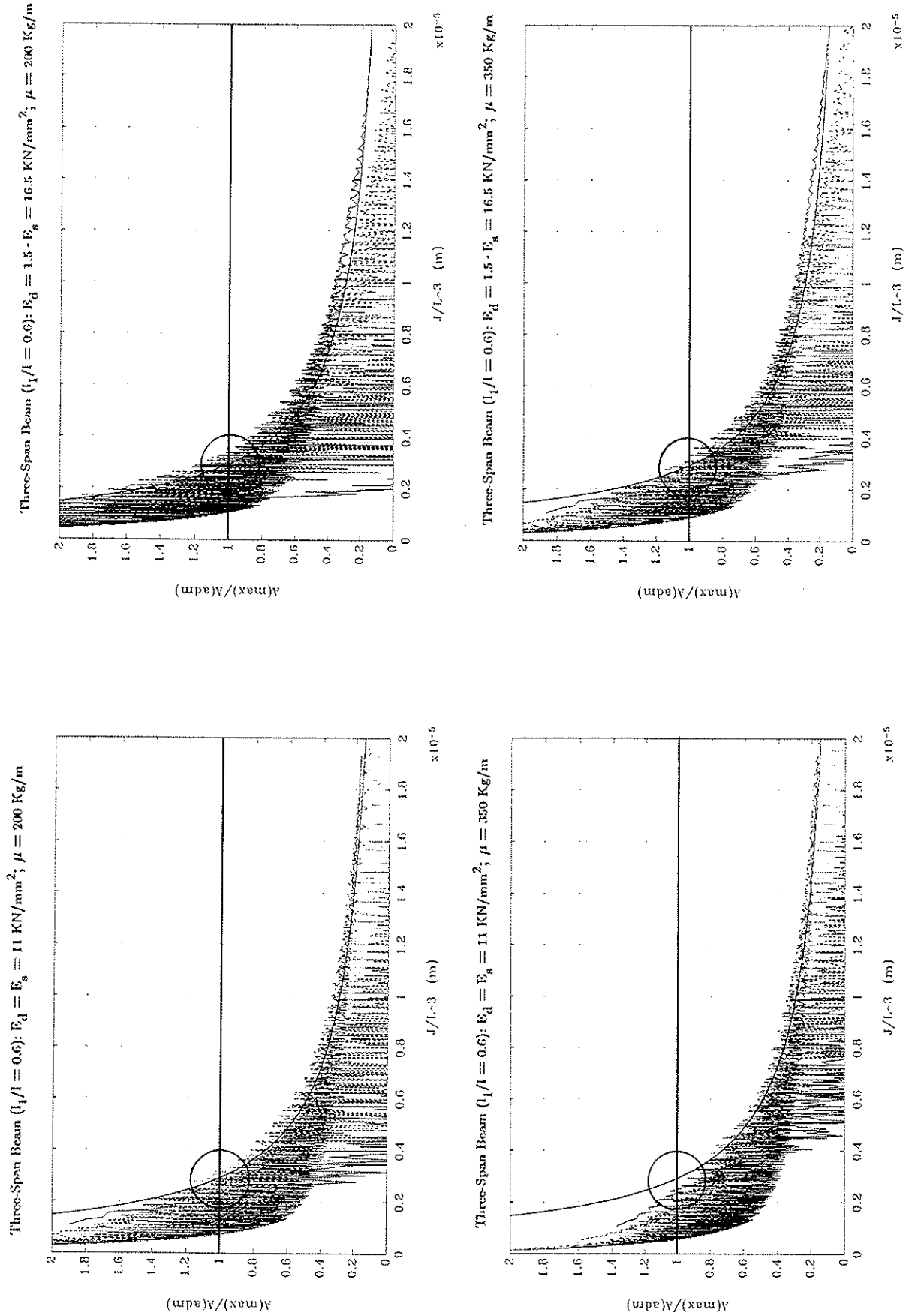


Fig. 10: Three-span symmetric footbridge ( $l_1/l = 0.6$ ): comparison between static and dynamic design criteria



**INTERNATIONAL COUNCIL FOR BUILDING RESEARCH STUDIES AND DOCUMENTATION  
WORKING COMMISSION W18 - TIMBER STRUCTURES**

**GLUED LAMINATED TIMBER  
CONTRIBUTION TO THE DETERMINATION OF THE BENDING STRENGTH OF GLULAM BEAMS**

by

F Colling  
Entwicklungsgemeinschaft Holzbau, Munich  
J Ehlbeck  
R Görlacher  
University of Karlsruhe  
Federal Republic of Germany

**MEETING TWENTY - FOUR**

**OXFORD**

**UNITED KINGDOM**

**SEPTEMBER 1991**



## GLUED LAMINATED TIMBER

-Contribution to the determination of the bending strength of glulam beams-

### 1 Introduction

This paper intends to summarize the results of the extensive research work done in Karlsruhe (Germany) on the bending strength of glulam beams. Above all it is the aim of this essay to develop design rules for glulam beams under bending.

The bending strength of glulam beams is primarily governed by two properties:

- the quality of the lamellations used;
- the strength of the finger joints

This is repeatedly demonstrated and proved by numerous tests in different countries. In order to make the problem easier to understand how the bending strength of glulam beams is influenced by mixing these two properties, it seems useful to consider first of all both effects separately.

### 2 Glulam beams with timber failure

#### 2.1 Influence of lamellation quality

In the first instance the bending strength of a glulam beam is described as dependent on the knot-area ratio (KAR), the density and the modulus of elasticity (MOE) of the lamellations. These parameters are usually also used for grading of the boards and assigning them to different strength classes.

The characteristic values of the tensile strength  $f_{t,o,k}$  of solid structural timber, as given in prEN 338 "Structural timber-strength classes" have been derived from characteristic values of the bending strength  $f_{m,k}$ . The ratio  $f_{t,o,k} / f_{m,k}$  is assumed to be 0,6 . Furthermore, the characteristic tensile

strength of solid timber, as given in prEN 338, is only under certain conditions applicable for determining the glulam bending strength, because when testing the tensile strength according to ISO 8375, the test specimen may deform in such a way that bending moments due to inevitable lateral displacements will reduce the calculated tensile strength. Such lateral deformations of the board are excluded when the board is part of a glulam beam and rigidly glued to the adjacent lamellations. Thus, a board being a lamellation in a glulam beam apparently has a higher tensile strength compared to the strength which is determined in line with ISO 8375. Let us call this phenomenon the "ISO-effect". In addition to this, areas of the board with a low MOE (e.g. due to knots) are relieved of high stresses when glued to another board with a higher tensile stiffness. This leads to a kind of local reinforcement and a fictive increase of the strength. Let us call this the "lamination effect".

Starting with the characteristic tensile strength  $f_{t,o,k}$  of the boards, as given in prEN 338, the characteristic bending strength  $f_{m,k,gl}^0$  of a glulam beam of 300 mm depth (we call this the "standard beam", and its values are denoted with a "0") can be determined using the following relationship [1]:

$$f_{m,k,gl}^0 = k_{iso} \cdot k_{lam} \cdot k_{var} \cdot f_{t,o,k,lam} \quad (1)$$

$k_{iso}$	factor to describe the ISO-effect;
$k_{lam}$	factor to describe the lamination effect
$k_{var}$	taking into account the different variabilities (coefficient of variation) of the glulam bending strength and the board tensile strength.

$k_{iso}$  is not sufficiently exact known and can only be estimated by numerous comparable tests. Based on tests made by H.J. Larsen, a value of

$$k_{iso} = 1,4$$

may be assumed. For the product of  $k_{lam} \cdot k_{var}$  there was also a lack of reliable values. Riberholt/Ehlbeck/Fewell [2] proposed to use the following equation:

$$k_{iso} \cdot k_{lam} \cdot k_{var} = 2,7 - 0,04 \cdot f_{t,o,k,lam} \quad (2)$$

From this, with  $k_{iso} = 1,4$ , we get

$$k_{lam} \cdot k_{var} \approx 1,9 - 0,03 \cdot f_{t,o,k,lam} \quad (3)$$

This value contains only the lamination effect and the effect of variability; but, this value is the basis (or the "key") to determine the characteristic bending strength of glulam beams using the characteristic tensile strength of "restrained"-lamellations. But even this "restrained" tensile strength may only be estimated, but this can be done on the basis of some hundred tension tests with 150 mm long elements taken from boards which has been performed by P. Glos in Munich. These findings can be used for simulation calculations. With various combinations of KAR, density and MOE of the lamellations the restrained tensile strength of 20000 boards of 4,50 m length was simulated according to [3]. With the same quality requirements for the lamellations the glulam bending strength was determined using a computer programme especially developed for this task [4]. This was done for the standard beam of 300 mm depth under the supposition that no failure in the finger joints can occur. Based on the simulations, a regression analysis showed the following relationship for  $k_{lam} \cdot k_{var}$

$$k_{lam} \cdot k_{var} = 1 + \frac{10}{k_{iso} \cdot f_{t,o,k,lam}} \quad (4)$$

and with eq. (1)

$$f_{m,k,gl}^0 = 10 + k_{iso} \cdot f_{t,o,k,lam} \quad (5)$$

Assuming a value of  $k_{iso} = 1,4$ , the calculation results and eq. (5) are shown in Fig. 1. It becomes obvious, that the proposal made by Riberholt/Ehlbeck/Fewell (cf. eq. (2) and (3) resp.) is a good approximation in the central range; but it deviates for low and high lamination quality.

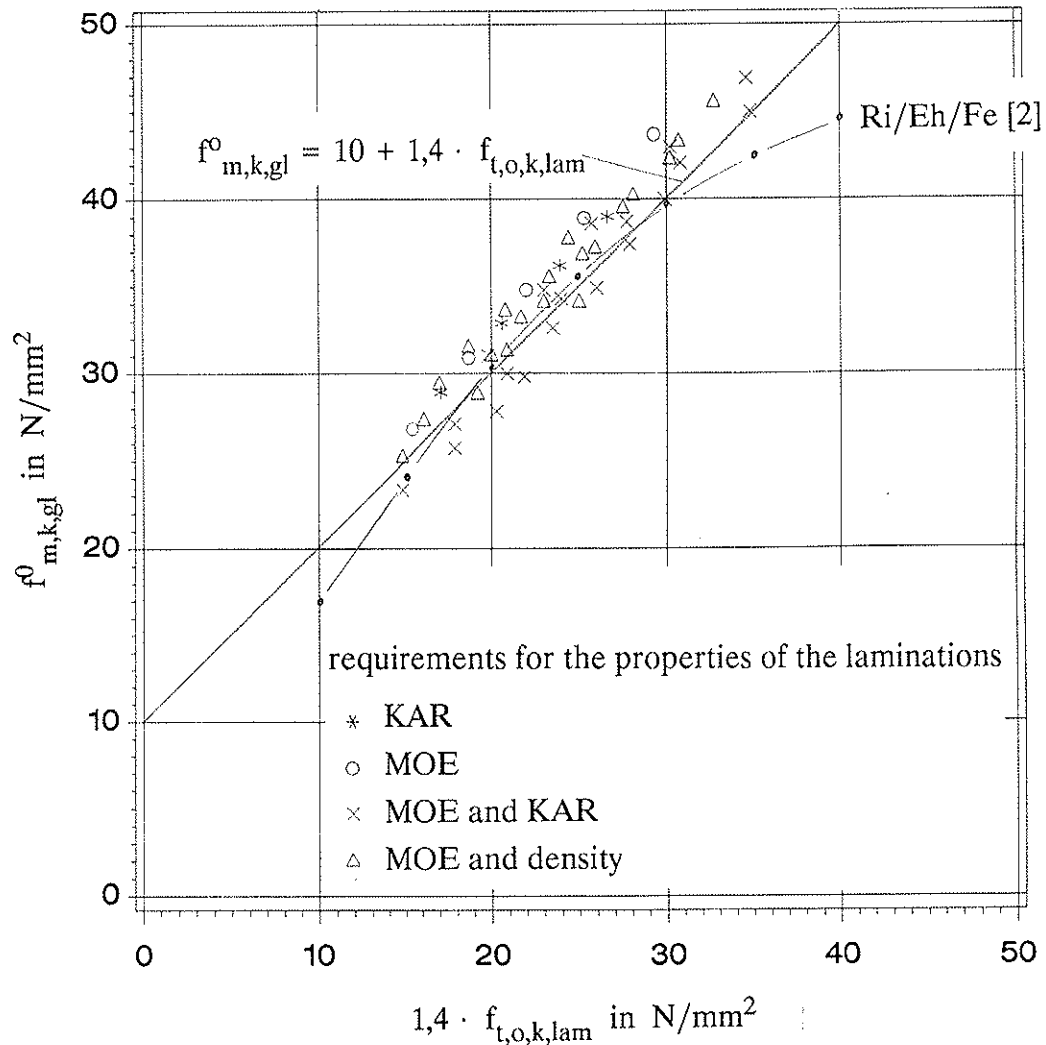


Figure 1: Characteristic bending strength  $f_{m,k,gl}^0$  of standard glulam beams depending on the characteristic tensile strength  $f_{t,o,k,lam}$  of the laminations

For practical application, eq. (5) can be used as a basis to determine the characteristic glulam bending strength from the characteristic strength of the boards used as lamellations.

## 2.2 Minimum values of timber properties to fulfil a strength class of prEN 338

Dividing the simulated restrained tensile strength by  $k_{iso}$  ( $\approx 1,4$ ) we get the "free" tensile strength as given in prEN 338. Taking into consideration that these values have been derived from bending strength values multiplied by the factor of 0,6 as well as the fact that for a solid timber bending member we need other requirements than for a lamellation which is mainly stressed in tension, it was studied which limit values for KAR, MOE and density are necessary to comply with the requirements of the tensile strength of a certain strength class in prEN 338. This was done independent of any existing or agreed grading systems or grading rules. Examples for limit values are given in [Table 1](#). In addition, the percentage of yield is specified on the basis of an extensive study at several German glulam manufacturers [5]. The advantage of machine stress grading becomes obvious.

**Table 1:** Examples of limit values for timber properties to comply with solid timber strength classes in prEN 338

	C18		C24		C30		C37	
	limit value	yield	limit value	yield	limit value	yield	limit value	yield
KAR <	0,67	13%	0,4	59%	0,2	28%		-
MOE >	7000	16%	10500	40%	13500	29%	16500	15%
KAR <	0,67	10%	0,50	32%	0,35	26%	0,35	32%
MOE >	-		9500		11500		14000	
KAR <	0,67	21%	0,50	36%	0,35	40%	0,35	3%
$\rho$ >	-		420		460		560	

KAR = greatest KAR-value within one board

MOE = mean lengthwise MOE in N/mm<sup>2</sup> of a board

$\rho$  = mean density in kg/m<sup>3</sup> of a board (moisture content u = 12%)

### 2.3 Volume effect

Based on simulation calculations [6] the following relationship between bending strength, beam depth and beam length can be assumed for glulam beams with timber failure only:

$$f_{m,k,gl} = \left(\frac{L}{5400}\right)^{-0,07} \cdot \left(\frac{H}{300}\right)^{-0,09} \cdot f_{m,k,gl}^0 \quad (6)$$

with  $L$  = length, in mm

$H$  = depth, in mm

$f_{m,k,gl}^0$  = characteristic glulam bending strength of the 300 mm deep standard beam.

$L$  is assumed to be  $18 \cdot H$ . This relationship turned out to be almost independent of the properties of the boards.

## 3 Glulam beams with failure of finger-joints

### 3.1 General

This chapter deals only with glulam beams the failure of which are only due to failure in the finger-joints.

It was found by simulation calculations that the characteristic bending strength of standard glulam beams (beam depth  $H = 300$  mm; ratio  $L/H = 18$ ) is approximately 20 % higher than the characteristic "restrained" tensile strength of the finger-joints [6]:

$$f_{m,k,gl}^0 = 1,20 \cdot f_{t,o,k,fj} \quad (7)$$

Consequently, in order to guarantee a certain characteristic glulam bending strength, it is necessary to require a defined minimum strength of the finger-



joints. As it is, however, expensive to control the tensile strength during the routine quality control in the production plant, the quality control is supposed to be performed by bending tests of the finger-joints. Hence, the ratio of tensile strength to bending strength of finger joints has to be well known.

### 3.2 Ratio of tensile to bending strength of finger-joints

In a former study tests with 239 tension specimens and 900 bending specimens of finger-joints were performed independently from each other. The characteristic "restrained" tensile strength of randomly taken test pieces was 23,4 N/mm<sup>2</sup>. The characteristic bending strength came to 36,3 N/mm<sup>2</sup>. According to that the ratio is

$$f_{t,o,k,fj} / f_{m,k,fj} = 0,64$$

To underline this ratio, a total 700 finger-jointed lamellations were collected from four German glulam manufacturers; the one half of them was tested in tension, the other half in bending. To make sure that the test pieces are matched and comparable, the test specimens were produced following the system shown in Fig. 2.

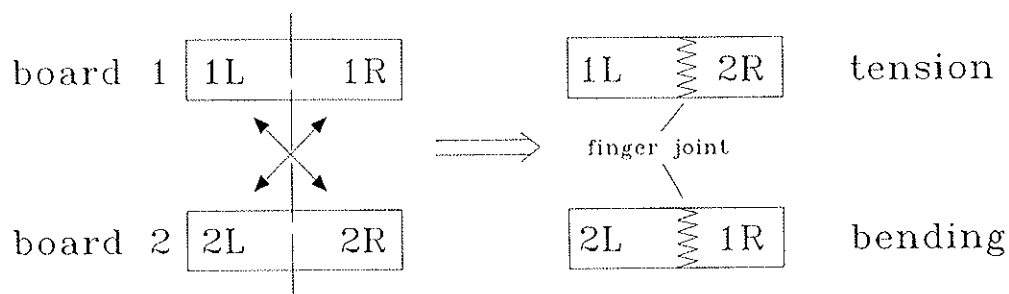


Figure 2: Matching of the test specimen

Two different finger-joint profiles, as used most frequently in Germany, were tested:

- length of the fingers 15 mm
- length of the fingers 20 mm.

Furthermore, three different series were carried out, as shown in Table 2, in order to clear up if the ratio of tensile to bending strength is dependent on the timber properties. In each test series and from each glulam plant 30 test specimens were made.

Table 2: Requirements for timber properties; tests with finger joints

series I	no requirements; random boards
series II	$11500 < \text{MOE} < 13500 \text{ N/mm}^2$
series III	$15000 < \text{MOE}$

Table 3 and 4 contain the results. The following tendencies can be recognized:

- the mean strength values of series 1 and 2 do not differ significantly;
- the variability (coefficient of variation) of the strength values from series 2 is significantly lower due to the lower variability of the timber properties;
- the mean strength values of series 3 are approximately 20 % higher than those of series 1 and 2.

Table 3: Test results; tension tests with finger joints

	plant 1 15 mm	plant 2 15 mm	plant 3 20 mm	plant 4 20 mm	15 mm	20 mm	all
<u>series I:</u>							
mean (MPa)	37,1	33,5	35,3	29,7	35,4	32,5	33,9
coeff. var.	0,27	0,23	0,16	0,19	0,26	0,20	0,23
N	30	27	30	29	57	59	116
<u>series II:</u>							
mean (MPa)	38,8	36,0	35,1	33,1	37,3	34,3	35,7
coeff. var.	0,15	0,16	0,22	0,15	0,16	0,19	0,18
N	27	29	30	28	56	58	114
<u>series III:</u>							
mean (MPa)	48,8	42,9	42,7	34,6	45,9	38,9	42,5
coeff. var.	0,17	0,14	0,16	0,11	0,17	0,18	0,19
N	28	28	29	25	56	54	100

Table 4: Test results; bending tests with finger joints

	plant 1 15 mm	plant 2 15 mm	plant 3 20 mm	plant 4 20 mm	15 mm	20 mm	all
<u>series I:</u>							
mean (MPa)	51,1	48,2	51,6	45,2	49,6	48,7	49,2
coeff. var.	0,17	0,14	0,16	0,15	0,16	0,17	0,16
N	28	30	30	25	58	55	113
<u>series II:</u>							
mean (MPa)	54,7	48,4	54,2	47,0	52,1	50,7	51,3
coeff. var.	0,09	0,09	0,12	0,10	0,11	0,13	0,12
N	29	21	30	29	50	59	109
<u>series III:</u>							
mean (MPa)	66,3	58,9	63,1	54,0	62,6	59,0	60,8
coeff. var.	0,09	0,10	0,13	0,07	0,11	0,13	0,13
N	28	28	30	25	56	55	111

Table 5 shows the ratios  $f_{t,o,k,fj} / f_{m,k,fj}$  assuming a normal Gauss distribution<sup>1</sup>. The individual values range from 0,50 to 0,68 with a mean of 0,60.

Table 5: Ratio  $f_{t,o,k,fj} / f_{m,k,fj}$  , assuming a Gauss-distribution

	plant 1 15 mm	plant 2 15 mm	plant 3 20 mm	plant 4 20 mm	15 mm	20 mm	all
series I	0,55	0,57	0,68	0,60	0,55	0,63	0,58
series II	0,63	0,64	0,50	0,64	0,64	0,59	0,61
series III	0,62	0,65	0,63	0,59	0,65	0,60	0,60

A number of test specimens failed - at least partly - outside the finger joint area. Especially in the tension tests, knots near the grips showed a great influence. Therefore the tests were reevaluated, excluding those test specimen with unsuitable failure mode. This leads to higher tensile strength values of the different series, whereas the bending strengths did not change greatly. Table 6 shows the ratios  $f_{t,o,k,fj} / f_{m,k,fj}$  for test specimen with a failure of at least 80% in the area of finger joints.

Table 6: Ratio  $f_{t,o,k,fj} / f_{m,k,fj}$  for test specimen with at least 80% failure in the area of finger joints

	plant 1 15 mm	plant 2 15 mm	plant 3 20 mm	plant 4 20 mm	15 mm	20 mm	all
series I	0,61	0,58	0,73	0,69	0,59	0,73	0,65
series II	0,68	0,70	0,52	0,67	0,72	0,61	0,63
series III	0,61	0,70	0,70	0,59	0,65	0,62	0,61

<sup>1</sup> A determination of characteristic strength values on the basis of a Student-t- or Weibull-distribution as well as by "counting" showed no significant influence on the ratios  $f_{t,o,k,fj} / f_{m,k,fj}$

On the basis of this, a ratio of

$$f_{t,o,k,fj} / f_{m,k,fj} \approx 0,65$$

may be assumed.

Deviating from the tests made by P. Glos ("restrained" tensile strength), for simplicity the tension tests reported here were carried out by using the test set-up as shown in Fig. 3.

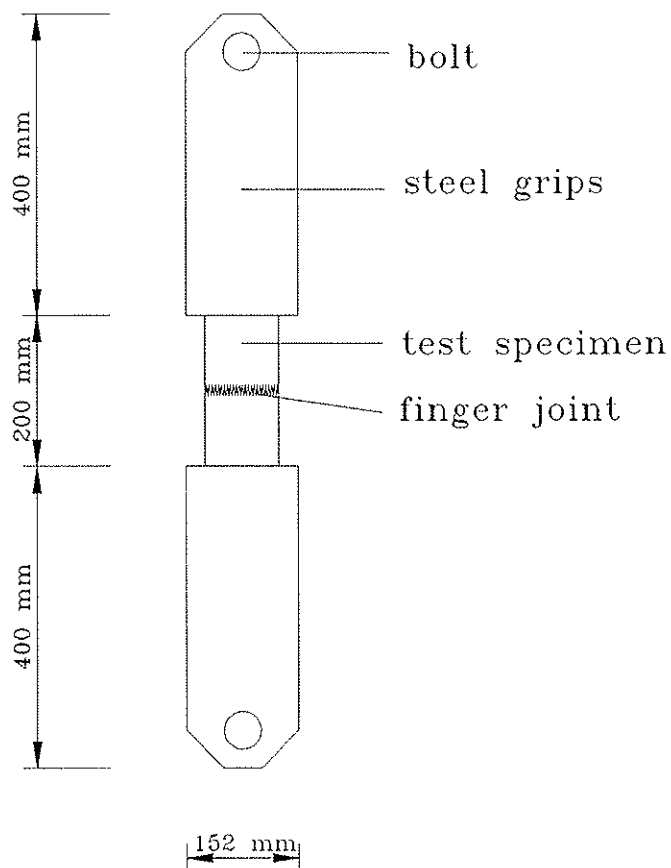


Figure 3: Test set-up for tension tests

Due to that, lateral deformations reducing the tensile strength (compare with ISO-effect!) can not completely be excluded. Therefore, it seems to be justified to use an all-over ratio of

$$f_{t,o,k,fj} / f_{m,k,fj} \approx 0,7 \quad (8)$$

(see also [7]).

From eq. (7) now results:

$$f_{m,k,gl}^o = 0,84 \cdot f_{m,k,fj} \quad (9)$$

This value of 0,84 may be increased if the type of loading is taken into account. A value of 1,04 may be used for uniformly distributed loads instead of 1,00 for two single loads applied at a distance of  $L/3$  from the beam supports ([7]). Then:

$$f_{m,k,gl}^o = 0,87 \cdot f_{m,k,fj} \quad (10)$$

From this the requirement can be derived that

$$f_{m,k,fj} \geq 1,15 \cdot f_{m,k,gl}^o \quad (11)$$

i.e., the characteristic bending strength of the finger-joints shall be at least 15% higher than the characteristic bending strength of the standard glulam beam.

### 3.3 Minimum values of timber properties to fulfil the requirements

In an extensive study on the bending strength of finger-joints [8] the following regression equations were found to describe the bending strength of finger-joints as depending on the MOE and on density of the laminations:

$$f_{m,fj} = 27,58 + 0,0019 \cdot E_{\min} \quad (12)$$

$$f_{m,fj} = 4,26 + 0,11 \cdot \rho_{12,\min} \quad (13)$$

The density  $\rho_{12,\min}$  in  $\text{kg/m}^3$  and the modulus of elasticity  $E_{\min}$  in MPa, respectively, are the lower value of the two adjacent (jointed) boards. Taking into consideration the results of a study on the board material used in German glulam factories [5], examples of limit values for timber properties to comply with finger joint requirements of some glulam strength classes are given in Table 7. This table contains also data on the percentage of yield to be expected.

Table 7: Examples of limit values for timber properties to comply with finger joint requirements of some glulam strength classes

glulam strength class	LH 25		LH 30		LH 35		LH 40	
$f_{m,k,fj} >$	27,5		34,5		40		46	
	limit value	yield	limit value	yield	limit value	yield	limit value	yield
$\rho >$	none	6 %	390	23 %	440	50 %	510	22%
MOE >	none	5 %	9000	31 %	12000	37 %	15000	27 %

$\rho$  = mean density in  $\text{kg/m}^3$  (moisture content  $u = 12\%$ )

MOE = mean lengthwise MOE in  $\text{N/mm}^2$

### 3.4 Volume effect

Fig. 4 contains the characteristic glulam bending strength related to the strength value of the standard beam with failure at the finger-joints over the beam length based on calculations in [6].

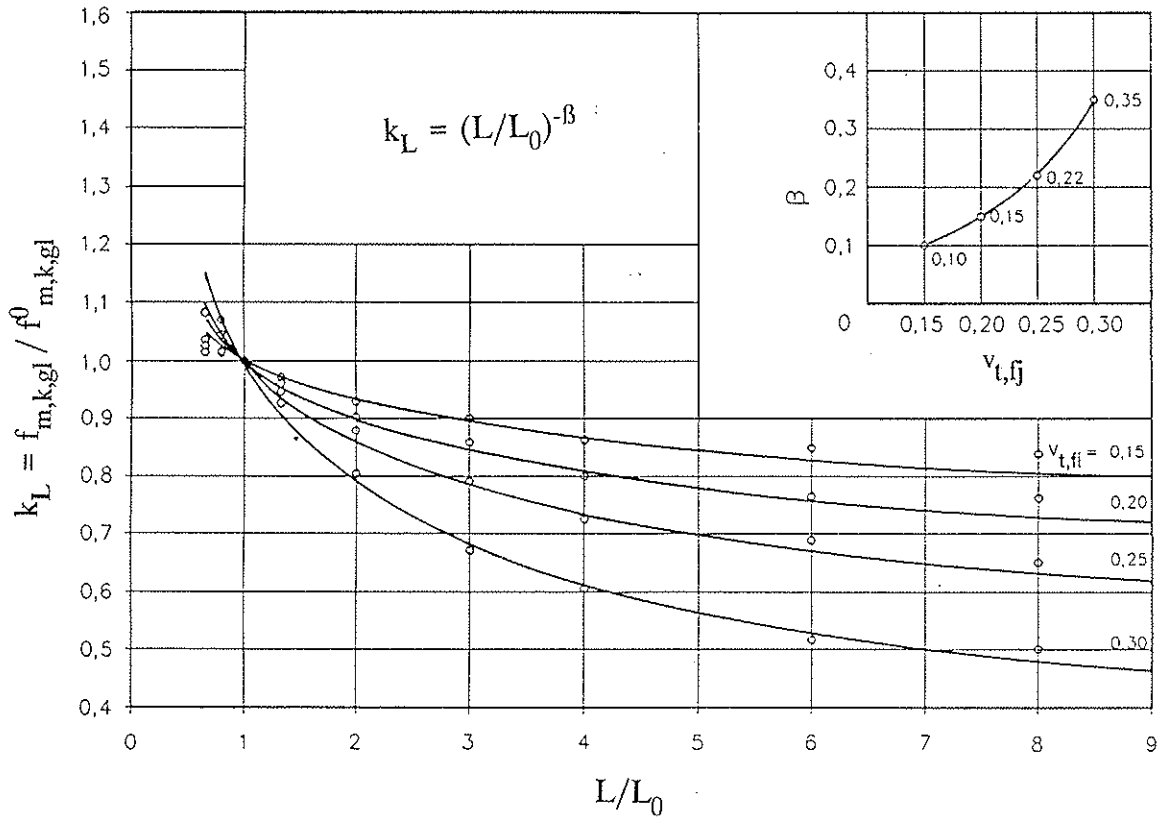


Figure 4: Length-effect for glulam beams with failure due to finger joints

The figure shows curves for different coefficients of variation  $v_{t,fj}$  of the finger-joint's tensile strength. It is obvious that the coefficient of variation is of evident importance:

- with increasing c.o.v. the influence of the volume effect is also increasing.

When there is only a visual grading used for the lamellations (i.e. when density and MOE are unknown), then the c.o.v. can be expected at a level of approximately 0,20. Then, the exponent to take into account the volume effect results in 0,15 (see also [7]).



The strength of finger-joints also depends significantly on production effects. Therefore, it should be possible to reduce the variability of the strength of finger-joints considerably by tightening up the production requirements (e.g. routine quality control). If the requirements recommended before (see clause 3.2) are fixed, it can be expected that the glulam producers will aim at a small variability of the finger-joints bending strength, because then the characteristic value will increase considerably.

In view of a machine grading based on density and/or MOE it is possible to reduce the c.o.v. of the strength values (see table 3 and 4). Therefore, it seems to be adequate to lower the exponent in the volume effect. It is proposed to use the following formula:

$$f_{m,k,gl} = \left( \frac{H}{300} \cdot \frac{L}{5400} \right)^{-0,10} \cdot f_{m,k,gl}^0 \quad (14)$$

with H and L in mm.

This equation is very close to that used for glulam beams with timber failure only (eq. 6).

#### 4 Conclusion

It can be summarized that for aiming at certain glulam strength classes the minimum requirements for the lamellations and the finger-joints, as given in Table 8, may be used.

Table 8: Requirements to comply with some glulam strength classes

glulam strength class	LH 25	LH 30	LH 35	LH 40
strength class of the laminations	C 18	C 24	C 30	C 37
requirements due to finger joints:				
$\rho >$	none	390	440	510
MOE >	none	9000	12000	15000

$\rho$  = mean density in kg/m<sup>3</sup> (moisture content  $u=12\%$ )

MOE = mean lengthwise MOE in N/mm<sup>2</sup>

The influence of the beam depth and the beam length can be taken into account by using the eq. (14).

**Literature cited**

- [1] Ehlbeck, J.; Colling, F. 1986: Strength of glued laminated timber. CIB-W18/19-12-1. Florence, Italy
- [2] Riberholt, H.; Ehlbeck, J.; Fewell, A. 1990: Glued laminated timber - strength classes and determination of characteristic properties. CIB-W18/23-12-2. Lisbon, Portugal
- [3] Görlacher, R. 1990: Klassifizierung von Brettschichtholzlamellen durch Messung von Longitudinalschwingungen. Dissertation, Universität Karlsruhe
- [4] Colling, F. 1988: Estimation of the effect of different grading criterions on the bending strength of glulam beams using the "Karlsruhe calculation model". IUFRO, Turku, Finland
- [5] Colling, F.; Görlacher, R. 1989: Eigenschaften des in Leimbau-betrieben verarbeiteten Schnittholzes. bauen mit holz 91(1989): 327-331
- [6] Colling, F. 1990: Tragfähigkeit von Biegeträgern aus Brettschicht-holz in Abhängigkeit von den festigkeitsrelevanten Einflußgrößen. Dissertation, Universität Karlsruhe
- [7] Ehlbeck, J.; Colling, F. 1990: Bending strength of glulam beams - a design proposal. CIB-W18/23-12-1. Lisbon, Portugal
- [8] Ehlbeck, J.; Colling, F. 1990: Bending strength of finger joints. IUFRO, St. John, Canada

<b>size effect</b>
--------------------

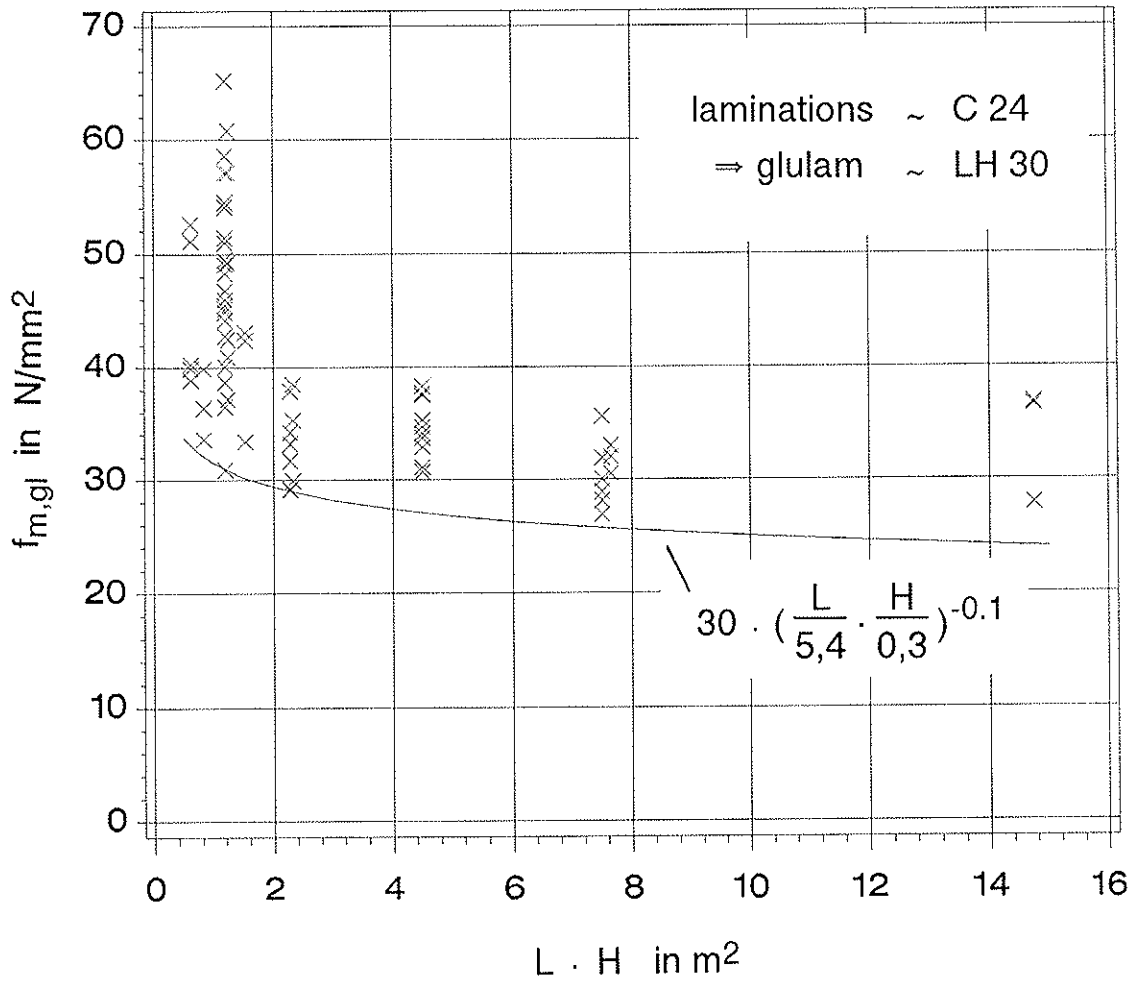


Figure 5: Test results; beams with timber failure and failure in finger joints

INTERNATIONAL COUNCIL FOR BUILDING RESEARCH STUDIES AND DOCUMENTATION  
WORKING COMMISSION W18 - TIMBER STRUCTURES

INFLUENCE OF PERPENDICULAR-TO-GRAIN STRESSED VOLUME ON THE LOAD-  
CARRYING CAPACITY OF CURVED AND TAPERED GLULAM BEAMS

by

J Ehlbeck  
J Kürth  
University of Karlsruhe  
Federal Republic of Germany

MEETING TWENTY - FOUR

OXFORD

UNITED KINGDOM

SEPTEMBER 1991



# Influence of perpendicular-to-grain stressed volume on the load-carrying capacity of curved and tapered glulam beams

by

Jürgen Ehlbeck and Jürgen Kürth

University of Karlsruhe, Germany

## 1 Introduction

According to EUROCODE 5 -Draft (1987) the design of curved beams with constant depth and of double tapered beams has to take into account a volume factor  $k_{vol}$  and a stress distribution factor  $k_{dis}$  to satisfy the design conditions covering the perpendicular-to-grain tensile stresses:

$$\sigma_{t,90,d} \leq k_{vol} \cdot k_{dis} \cdot f_{t,90,d} \quad (1)$$

In eq.(1) is:

$$k_{vol} = \left( \frac{V_0}{V} \right)^{\frac{1}{k_{wei}}} \quad (2)$$

assuming a 2-parameter Weibull distribution,

$$k_{dis} = \frac{\sigma_{max}}{\left( \frac{1}{V} \cdot \int_V \sigma(x, y, z)^{k_{wei}} dV \right)^{\frac{1}{k_{wei}}}} \quad (3)$$

taking into account the stress distribution, and

$$f_{t,90,d} = \frac{k_{mod}}{\gamma_M} \cdot f_{t,90,k} \quad (4)$$

This design method is based on the 2-parametric statistical distribution function for homogeneous and isotropic material with brittle fracture behaviour developed by WEIBULL 1939. It takes into account the influence on the perpendicular-to-grain tensile strength

- of the stressed volume by  $k_{vol}$ ,
- of the stress distribution by  $k_{dis}$ .

The design strength  $f_{t,90,d}$  is calculated with eq.(4) from the characteristic perpendicular-to-grain tensile strength of a uniformly stressed volume  $V_0$ . This volume  $V_0$  is a defined reference volume, which is given in the EC 5 - draft with  $0,02 \text{ m}^3$ .

For application of this design method it is necessary to know the following data:

- Weibull-factor,  $k_{wei}$
- characteristic perpendicular-to-grain tensile strength,  $f_{t,90,k}$
- stressed volume,  $V$
- stress distribution,  $\sigma(x,y,z)$ .

In this paper, the test results of tests with curved and tapered beams (EHLBECK, KÜRTH 1990) are evaluated to find values for  $k_{wei}$  and  $f_{t,90,k}$ . Using a finite-element programme, the values for  $k_{dis}$  and  $k_{vol}$  are found. All results are compared with the proposals given in the EUROCODE 5 - draft of 1987.

## 2 Tests and test results

### 2.1 Test performance

During the tests it was important to vary the dimensions and shapes of the beams as well as the type of loading in order to achieve different distributions and values of the perpendicular-to-grain tensile stresses.

The following beams were tested (see Fig. 1):

- curved beams of constant depth  
(defined as type **G**),
- double-tapered curved beams  
(defined as type **P**),
- double-tapered pitched and curved beams  
(defined as type **K**).

The following spans were used:

- 11,00 m (beam no. 1),
- 9,24 m (beam no. 2),
- 6,36 m (beam no. 3),
- 3,60 m (beam no. 4).



For each shape and span two matched beams were manufactured (No. A and B).

To be sure that perpendicular-to-grain tensile failures will occur, all beams were produced with a roof slope angle (upper chord angle) of  $\alpha_0 = 20^\circ$ . All detailed dimensions are given in **Table 1**.

In order to find the relationship between the perpendicular-to-grain tensile strength and the stressed volume, the test beams with different spans were geometrically similar, i.e. all dimensions - except the beam width - were changed in the same proportion. A direct comparison of the perpendicular-to-grain tensile strengths of the different shapes of the beams was possible because the basic beam shape was the curved beam with constant depth (type G), and the dimensions of the beams of type P were identical, except in the apex region. Beams of type P, on the other hand, were equal to those of type K, except the slope of the lower chord (angle  $\alpha_{\text{U}}$ ).

The production of all beams was made in one glulam factory using lamellations of 120 mm width with their thickness ranging from 10 to 25 mm with respect to the individual beam curvatures. The wood species was European white wood (*picea abies*) glued together with adhesives on resorcinol-formaldehyde basis (Adhesive type RF).

All test beams were tested as simply supported beams with one fixed support and one rolling support. Lateral bracing was ensured by beams of high bending stiffness in the plane perpendicular to the upper chord of the test beam. The loads were applied at a distance of  $L/4$  (quarter span) from the supports (see **Fig. 1**) to generate a constant moment in the apex zone of the beam (inner half span). In some cases a uniformly distributed load was simulated by eight single loads equally distributed over the total span.

The test results are listed in **Table 2**. The ultimate test load is given by the ultimate load at the support at time of failure. From these failure loads the maximum radial stresses (perpendicular-to-grain) were calculated by using a finite element programme as well as by using the design rules as given in the EC 5 - draft of 1987.

## 2.2 Evaluation of the test results

Based on Weibull, the survival probability  $P$  of a member can be described by using the cumulative distribution function  $S$  with:

$$P = 1 - S = \exp \left[ - \int_V \cdot \left( \frac{\sigma(x, y, z)}{\sigma'} \right)^{k_{wei}} dV \right] \quad (5)$$

In eq.(5) is:

$\sigma(x, y, z)$  = function of the stress distribution  
 $\sigma', k_{wei}$  = parameters of the Weibull-distribution  
 $V$  = volume stressed by  $\sigma(x, y, z)$

COLLING 1986a and b defined so-called "fullness-parameters",  $\lambda_L$  and  $\lambda_H$ , to describe the fullness of the stress distribution;  $\lambda = 1$  stands for constant stress distribution over the stressed volume. Then, eq.(5) can be written:

$$P = \exp \left[ -V \cdot \left( \lambda_L \cdot \lambda_H \cdot \frac{\max \sigma}{\sigma'} \right)^{k_{wei}} \right] \quad (6)$$

with

$\max \sigma$  = maximum stress within  $V$

The parameters  $\lambda_L$  and  $\lambda_H$  can be evaluated from the stress distribution as calculated by using a finite element method:

$$\lambda_L \cdot \lambda_H = \left[ \frac{\sum \left[ \left( \frac{\sigma_{t,90,i}}{\max \sigma_{t,90}} \right)^{k_{wei}} \cdot V_i \right]}{V_{tot}} \right]^{\frac{1}{k_{wei}}} \quad (7)$$

In eq.(7) is:

$V_i$	=	volume of a finite element with perpendicular-to-grain tensile stresses
$\sigma_{t,90,i}$	=	perpendicular-to-grain tensile stress of a finite element of volume $V_i$
$V_{tot}$	=	total stressed volume
$\max \sigma_{t,90}$	=	maximum perpendicular-to-grain tensile stress within $V_{tot}$

According to BARRETT, FOSCHI and FOX 1975 the relation between a perpendicular-to-grain tensile strength of a unity volume,  $f_{t,90,V=1}$ , and the perpendicular-to-grain tensile strength,  $f_{t,90}$ , of any volume  $V$  under uniform stress distribution can be described, in case of equal survival probability, as follows:

$$\log_{10} f_{t,90} = \log_{10} f_{t,90,V=1} - 1/k_{wei} \cdot \log_{10} V \quad (8)$$

The parameters  $\sigma'$  and  $k_{wei}$  in eq.(5) can be evaluated from test data by converting all failure stresses with uneven stress distribution into an even (uniform) stress distribution. This is possible under the assumption of the Weibull theory. By choosing a value for  $k_{wei}$ , the parameters  $\lambda_L$  and  $\lambda_H$  can be calculated. Then, a fictitious uniformly distributed perpendicular-to-grain tensile strength value,  $\sigma_{t,90,id}$ , can be determined from the calculated failure stress,  $\max \sigma_{t,90}$ :

$$\sigma_{t,90,id} = \max \sigma_{t,90} \cdot \lambda_L \cdot \lambda_H \quad (9)$$

A linear regression analysis between the logarithm of  $\sigma_{t,90,id}$  and the logarithm of the total stress volume,  $V_{tot}$ , of all test data results in:

$$\log_{10} \sigma_{t,90,id} = -0,390 - 0,191 \cdot \log_{10} V_{tot} \quad (10)$$

In eq.(10),  $\sigma_{t,90,id}$  is given in [N/mm<sup>2</sup>] or [MPa], whereas  $V_{tot}$  is given in [m<sup>3</sup>].

The parameters in eq.(10) correspond to the values of  $\log_{10} f_{t,90,V=1}$  and  $1/k_{wei}$  in eq.(8), respectively. If, during the evaluation of the test data, the value  $k_{wei}$  does not be in accordance with the originally estimated  $k_{wei}$ , the procedure can be repeated by choosing a better value for  $k_{wei}$ .

Eq.(10) gives the final version of this analysis and leads to

$$k_{wei} = 1 / 0,191 = 5,24$$

Fig. 2 demonstrates this analysis. The second parameter of the Weibull-distribution is then determined from eq.(6). Firstly, the strength value  $f_{t,90,V=1}$  is to be calculated for a unity volume of  $V_{tot} = 1 \text{ m}^3$ . From Fig. 2 can be seen, that  $f_{t,90,V=1} = 0,41 \text{ N/mm}^2$ . With  $f_{t,90,V=1} = \max \sigma$ ,  $V = V_{tot}$ ,  $\lambda_L \cdot \lambda_H = 1$  and a survival probability of  $P = 0,5$ , the parameter  $\sigma'$  is:

$$\sigma' = \frac{0,41}{(-\ln 0,5)^{0,191}} = 0,44 \left[ \frac{N}{mm^2} \right] \quad (11)$$

For any volume under uniformly distributed stresses perpendicular to grain ( $\lambda_L \cdot \lambda_H = 1$ ) and any survival probability, the perpendicular-to-grain tensile strength can be determined from eq.(6) with:

$$f_{t,90}(P) = \left( \frac{-\ln(P)}{V_{tot}} \right)^{0,191} \cdot 0,44 \quad (12)$$

When we evaluate for all beams tested

- the fictitious perpendicular-to-grain tensile strength  $f_{t,90,id}$  for a reference volume of  $0,02 \text{ m}^3$  - as e.g. proposed in EC 5 - draft 1987 -
- the distribution factor  $k_{dis}$  using the "fullness-parameters"  $\lambda_L \cdot \lambda_H$ , and
- the volume factor  $k_{vol}$  using  $V_{tot}$  and a constant value for  $k_{wei} = 5,24$ ,

then, theoretically all data should result in the same ideal perpendicular-to-grain tensile strength, as long as there is no effect of variability.

**Fig. 3** gives these data. It can be recognized that most values concentrate around  $0,9 \text{ N/mm}^2$ , approximately. This corresponds to a perpendicular-to-grain tensile strength for a survival probability of  $P = 0,5$ . For the characteristic strength value,  $f_{t,90,k}$ , we get the 5-percentile with

$$f_{t,90,k} = 0,53 \text{ N/mm}^2.$$

### 3 Calculation of $k_{\text{vol}}$ and $k_{\text{dis}}$ for other beams

In order to check how  $k_{\text{vol}}$  and  $k_{\text{dis}}$  depend on the beam geometry, eight more beams of each type (G, P and K) with a constant span of 9,24 m were investigated by calculation. For these beams the upper chord angle,  $\alpha_o$ , and the radius of curvature, R, were varied. The dimensions of these beams are given in **Table 3**. The notations of each individual beam are similar to those in **Table 1**, completed by values for  $\alpha_o$  and R.

For these beams stress calculations with a finite element method were made under two single loads, each acting at quarter-span from the supports, i.e. under constant moment in the curved zones of the beam. After that, the factors  $k_{\text{vol}}$  and  $k_{\text{dis}}$  were calculated assuming  $k_{\text{wei}} = 5,0$ . The results of this study are presented in **Fig. 4 to 9**. For comparison, also the values in line with the EUROCODE 5 - draft (1987) as well as new proposals are given in these figures.

As a result can be stated that the perpendicular-to-grain stressed volume increases with increasing angle  $\alpha_o$ , i.e. decreasing  $k_{\text{vol}}$  with increasing  $\alpha_o$ . The distribution factor  $k_{\text{dis}}$  is significantly dependent on  $\alpha_o$  and the radius of curvature, R. Consequently, the product of  $k_{\text{vol}}$  and  $k_{\text{dis}}$  is also dependent of  $\alpha_o$  as well as of R, but it can sufficiently good be approximated by a linear regression line.

#### 4 Comparison with EUROCODE 5 - draft (1987)

Comparing the results from the tests with the proposals given in the EC 5 - draft (1987), it can be stated that  $k_{wei} = 5,24$ , as derived from the tests, is in good accordance with  $k_{wei} = 5,0$ . A significant difference is, however, to realize as far as the characteristic perpendicular-to-grain tensile strength is concerned. It was found for the glued laminated timber tested, that  $f_{t,90,k} = 0,53 \text{ N/mm}^2$ . Following the proposed values in prEN 338 "Structural timber - strength classes" (August 1990), for tension perpendicular-to-grain a value of  $f_{t,90,k} = 0,40 \text{ N/mm}^2$  is proposed, i.e. only 75 % of those values derived from the tests.

As far as the factors  $k_{vol}$  and  $k_{dis}$  are concerned, EC 5 - draft (1987) proposed values in order to simplify design calculations; but in some cases these values deviate considerably from values according to the Weibull-theory. It was found, on the one hand, that the perpendicular-to-grain stressed volume in most cases is estimated too small leading to factors  $k_{vol}$  which are overestimated, especially for small slope angles  $\alpha_o$ . With increasing angle  $\alpha_o$  the  $k_{vol}$ -values as defined in the EC 5 - draft approximate more and more those values which are calculated by FE-methods. On the other hand, the distribution factors  $k_{dis}$  according to EC 5 - draft are in most cases too small and should be raised.

The product of  $k_{vol}$  and  $k_{dis}$  can be considered as an index how the beam geometry changes the strength or load-carrying capacity of curved and double-tapered glulam beams. Therefore, this product is a factor to modify the design strength,  $f_{t,90,d}$  (see eq.(1)). This product being in all cases higher than proposed in the EC 5 - draft (1987), it is recommended to increase the distribution factor  $k_{dis}$  accordingly.

#### 5 Proposals for design rules in EUROCODE 5

The method given in EUROCODE 5 - draft (1987) is principally appropriate to design curved and double-tapered glued laminated timber beams. The advantage of this method is its simple application:

- the maximum perpendicular-to-grain tensile stress is calculated according to the application rules given in EC 5 or other relevant literature,
- $k_{vol}$  is determined according to the application rules given in EUROCODE 5 - draft (1987),
- $k_{dis}$  is - for simplification - for all types of curved, double-tapered and cambered beams for actions giving a constant or nearly constant moment in the curved part of the beam taken as  $k_{dis} = 1,4$ .

Using these rules, the product of  $k_{vol} \cdot k_{dis}$  leads to a realistic modification of the characteristic design strength.

Furthermore, it should be discussed to modify or change the characteristic strength values for tension perpendicular-to-grain, given in prEN 338, e.g. from  $0,40 \text{ N/mm}^2$  to  $0,55 \text{ N/mm}^2$  when timber is used for glulam. In case of changing the reference volume  $V_0$  from  $0,02 \text{ m}^3$  to a smaller volume (under discussion with respect to adequate test methods), the characteristic strength values should be modified accordingly.

## 6 Literature

- BARRETT, J. D.; FOSCHI, R. O.; FOX, S. P. 1975: Perpendicular-to-grain strength of Douglas-fir. Canadian Journal of Civil Engineering 2(1): 50-57
- COLLING, F. 1986a: Einfluß des Volumens und der Spannungsverteilung auf die Festigkeit eines Rechteckträgers. Holz als Roh- und Werkstoff 44: 121-125, 179-183
- COLLING, F. 1986b: Influence of volume and stress distribution on the shear-strength and tensile-strength perpendicular to grain. CIB - W18 Paper 19-12-3, Florence, Italy
- EHLBECK, J.; KÜRTH, J. 1990: Einfluß des querzugbeanspruchten Volumens auf die Tragfähigkeit gekrümmter Träger konstanter Höhe und gekrümmter Satteldachträger aus Brettschichtholz, Forschungsbericht der Versuchsanstalt für Stahl, Holz und Steine, Abt. Ingenieurholzbau und Baukonstruktionen der Universität Fridericiana, Karlsruhe, Germany
- EUROCODE 5: see COMMISSION OF THE EUROPEAN COMMUNITIES 1987
- COMMISSION OF THE EUROPEAN COMMUNITIES 1987: Eurocode 5, Common unified rules for timber structures (1. draft), Report EUR 9887 EN
- WEIBULL, W. 1939: A statistical theory of the strength of materials. Proc. Roy. Swed. Inst. Eng., Res. 151



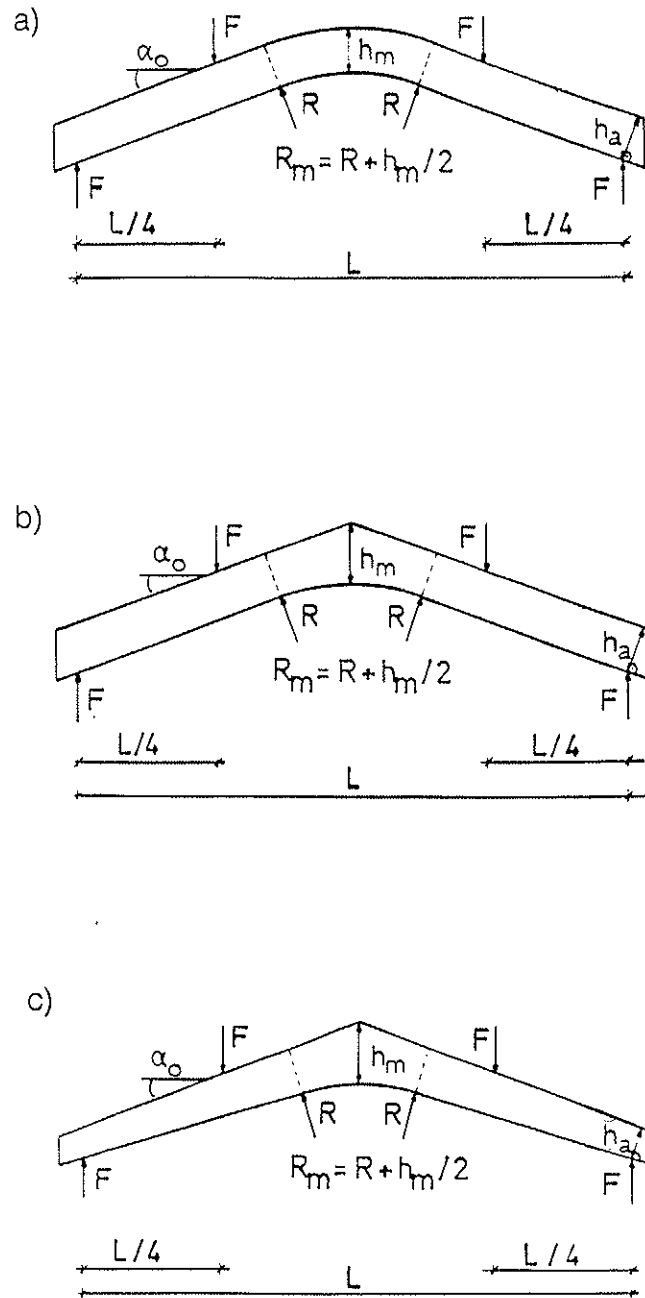


**Fig. 1:** Test specimens  
 a) Curved beam of constant depth (type G)  
 b) Double-tapered curved beam (type P)  
 c) Double-tapered pitched and curved beam (type K)

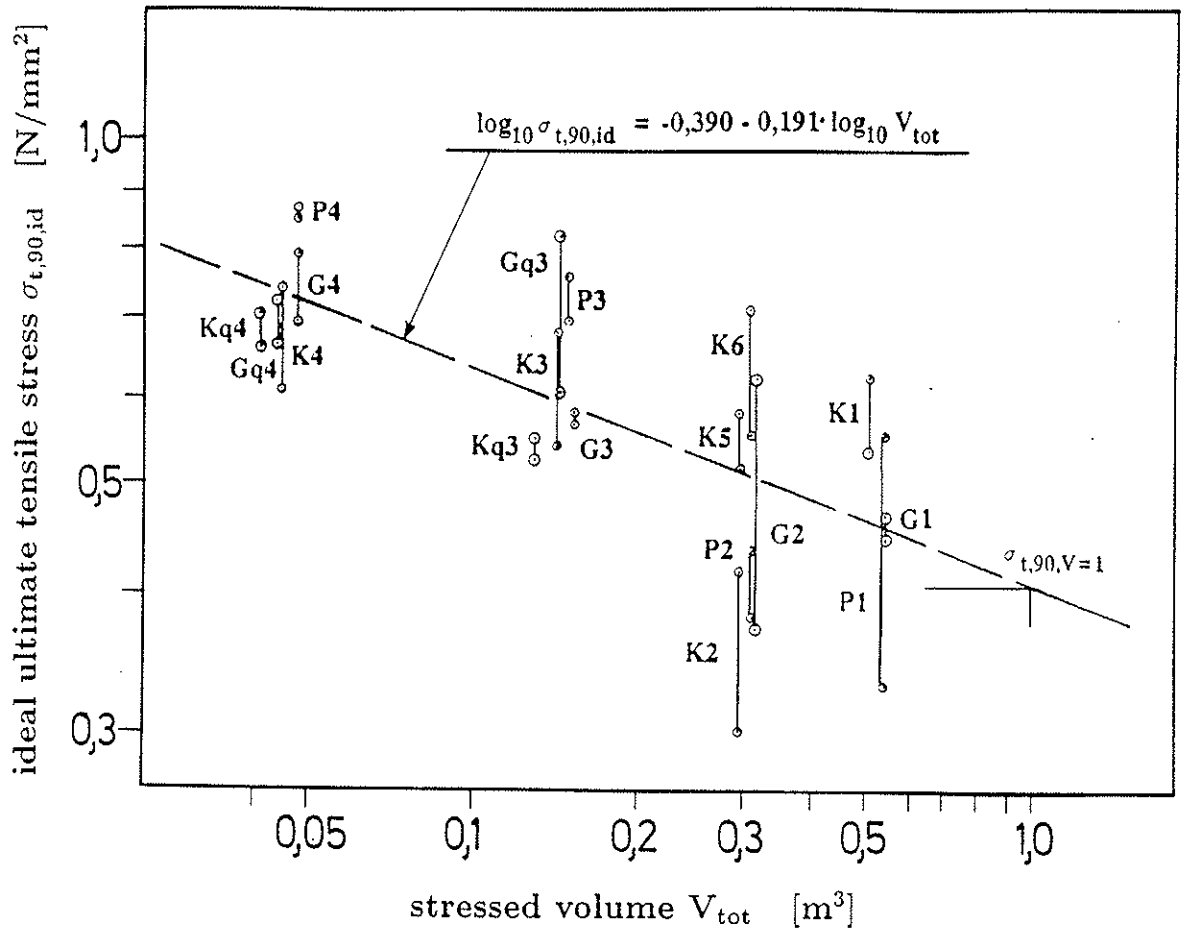


**Fig. 2:** Uniformly distributed ideal fictitious ultimate tensile stresses perpendicular to the grain in relation to the stressed volume

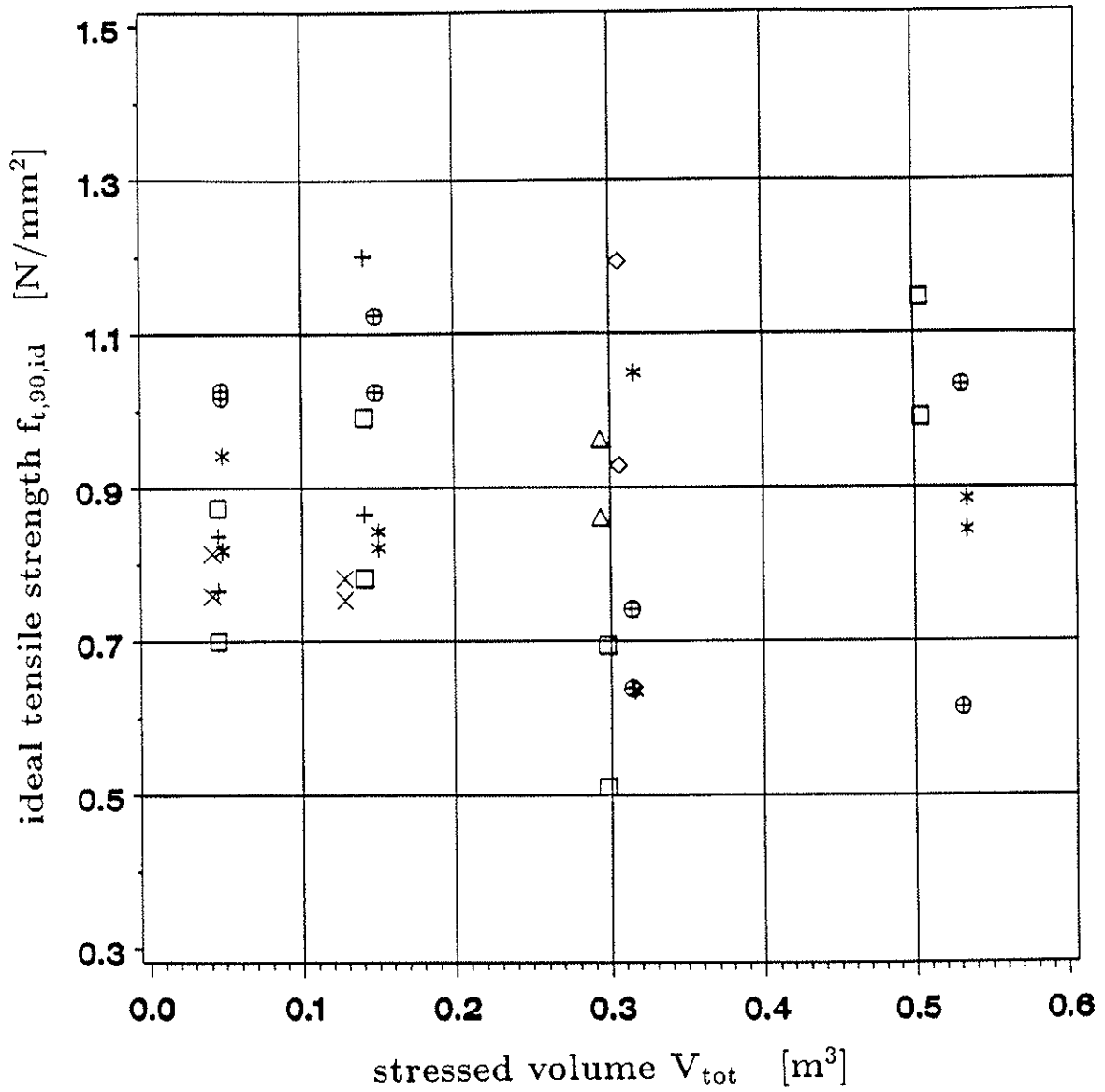


**Fig. 3:** Ideal tensile strength of the test specimens in relation to the stressed volume

( \* : G1-G4 / ⊕ : P1-P4 / □ : K1-K4 / △ : K5 /  
 ◇ : K6 / + : Gq3-Gq4 / × : Kq3-Kq4 )

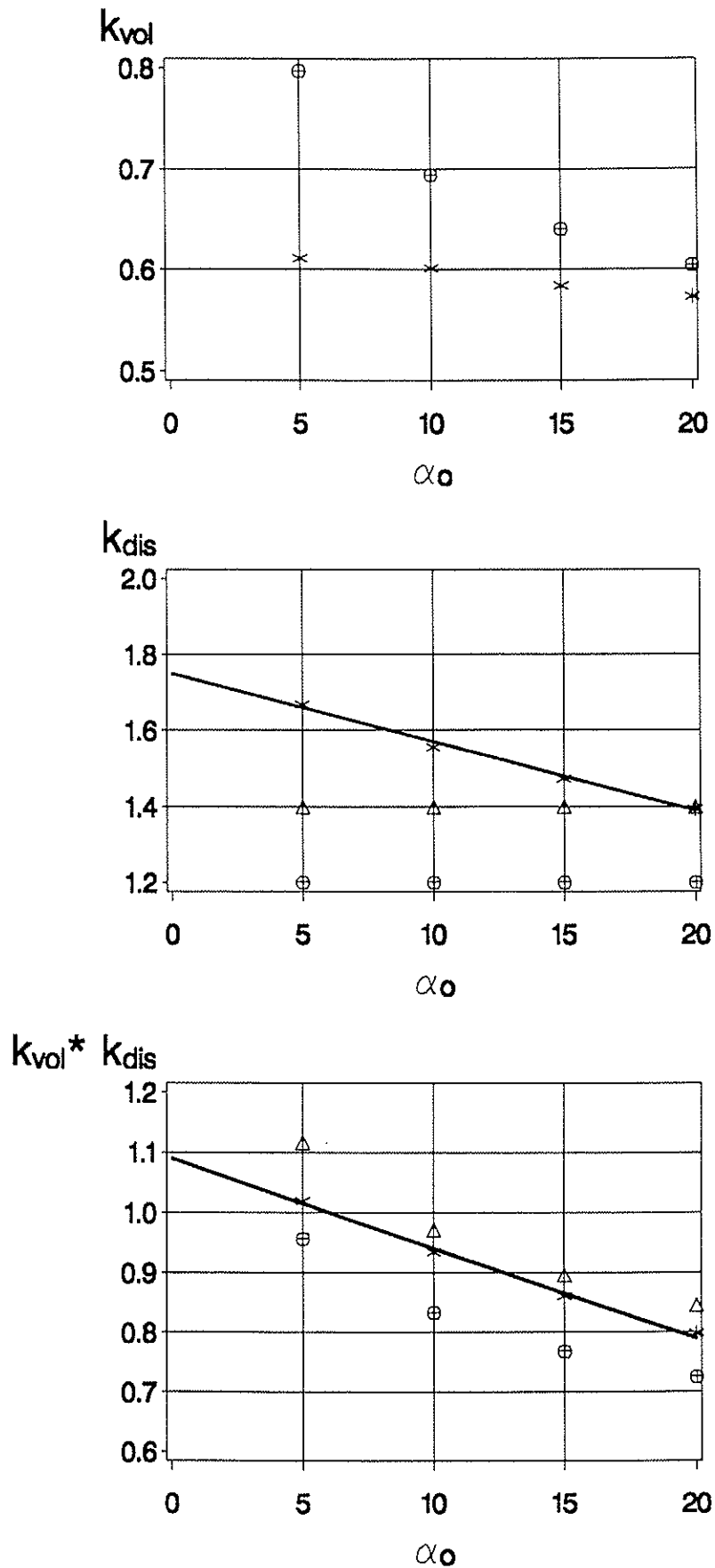


**Fig. 4:** Volume factor  $k_{vol}$ , distribution factor  $k_{dis}$  and product of  $k_{vol} \cdot k_{dis}$  over upper chord angle  $\alpha_0$  for beam type G205 to G220  
 (\* = FE, ⊕ = EC5, Δ = proposal)

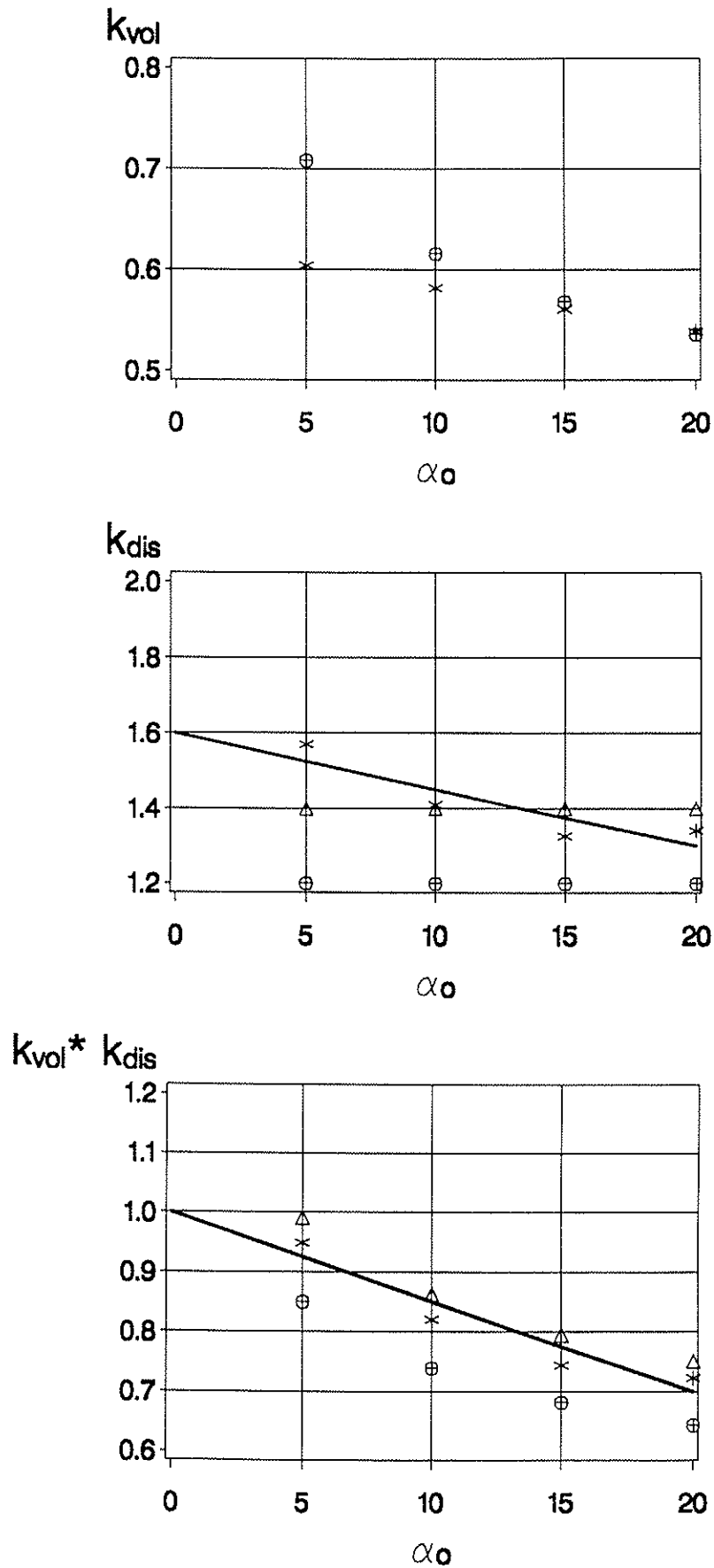


**Fig. 5:** Volume factor  $k_{vol}$ , distribution factor  $k_{dis}$  and product of  $k_{vol} \cdot k_{dis}$  over upper chord angle  $\alpha_0$  for beam type G205R to G220R  
 (\* = FE,  $\oplus$  = EC5,  $\Delta$  = proposal)

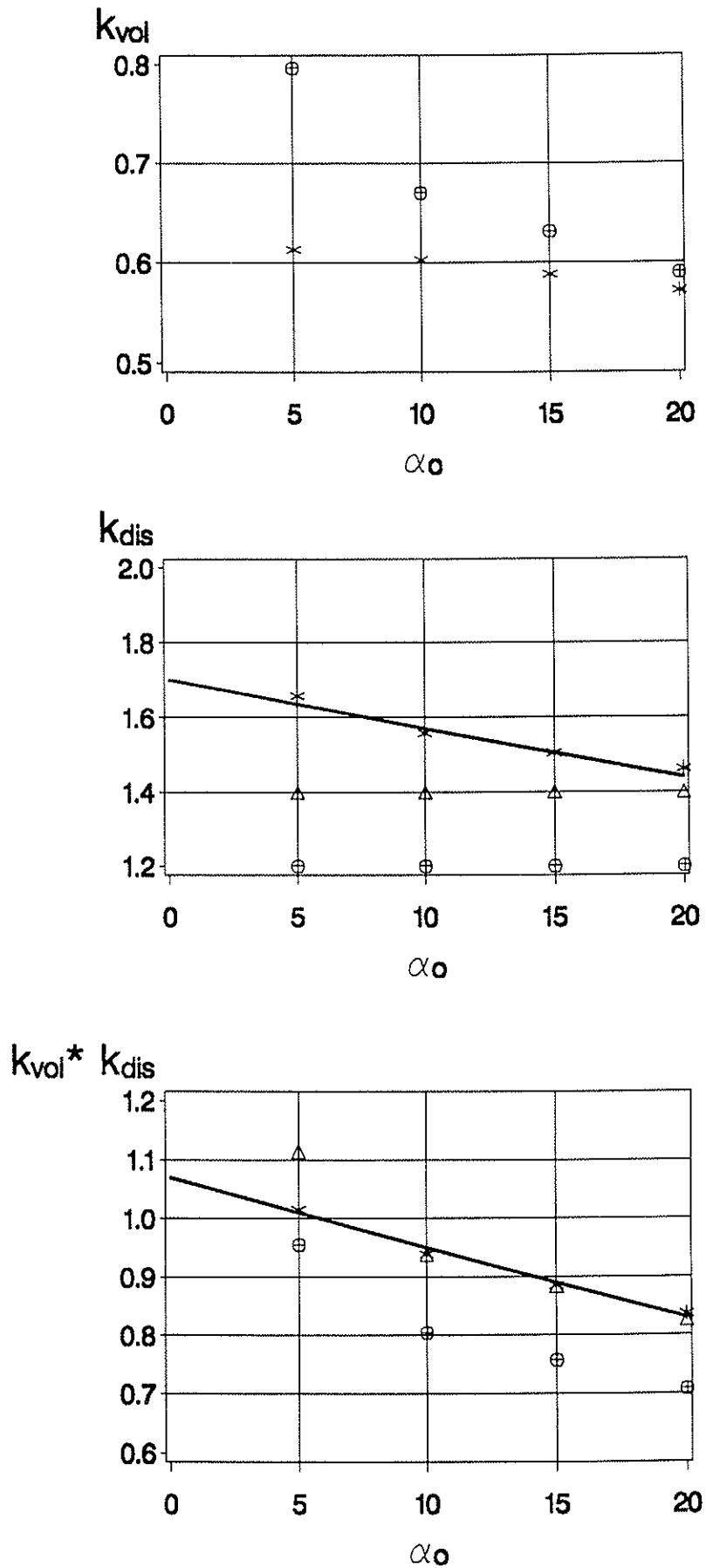


**Fig. 6:** Volume factor  $k_{vol}$ , distribution factor  $k_{dis}$  and product of  $k_{vol} \cdot k_{dis}$  over upper chord angle  $\alpha_0$  for beam type P205 to P220  
 (\* = FE,  $\oplus$  = EC5,  $\triangle$  = proposal)

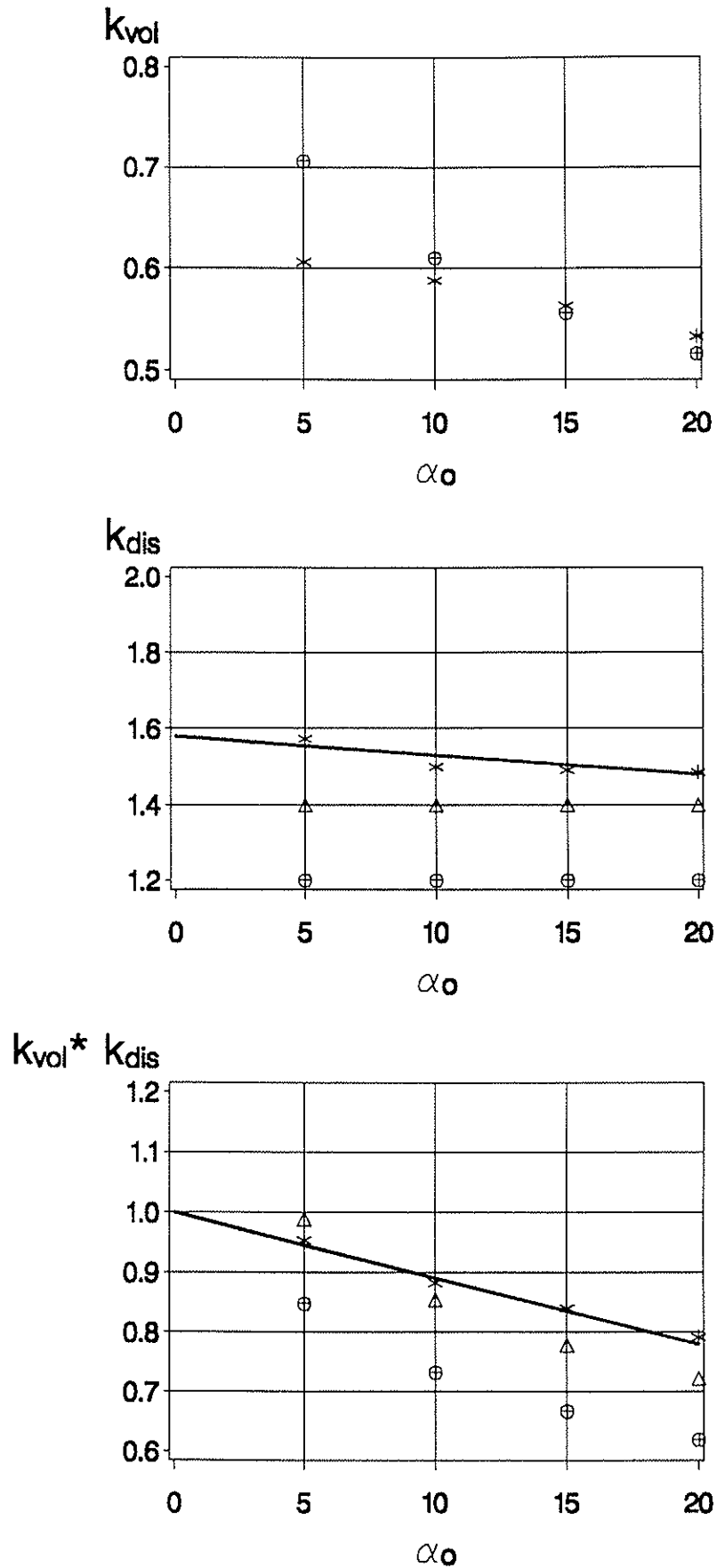


**Fig. 7:** Volume factor  $k_{vol}$ , distribution factor  $k_{dis}$  and product of  $k_{vol} \cdot k_{dis}$  over upper chord angle  $\alpha_0$  for beam type P205R to P220R  
 (\* = FE,  $\oplus$  = EC5,  $\triangle$  = proposal)

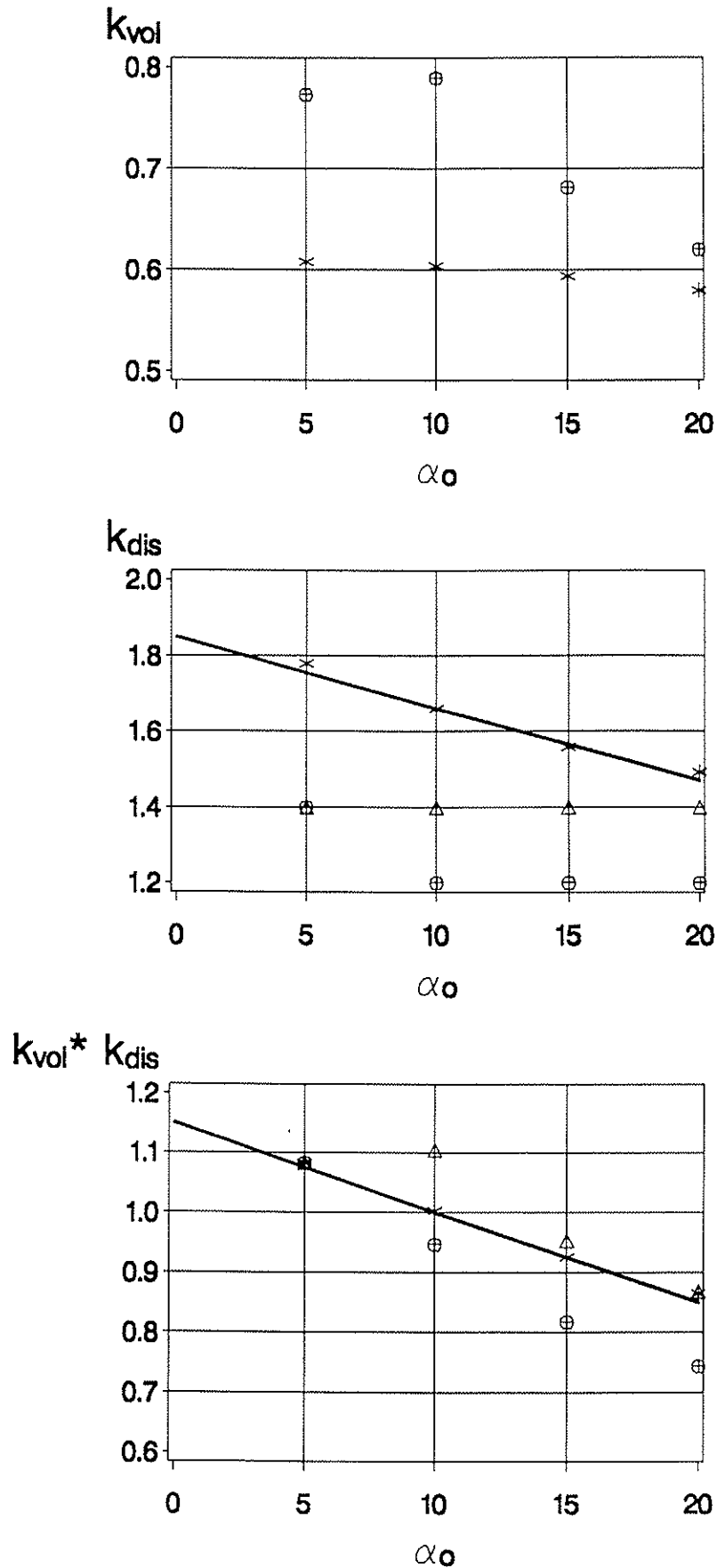


**Fig. 8:** Volume factor  $k_{vol}$ , distribution factor  $k_{dis}$  and product of  $k_{vol} \cdot k_{dis}$  over upper chord angle  $\alpha_0$  for beam type K205 to K220  
 (\* = FE, ⊕ = EC5, Δ = proposal)



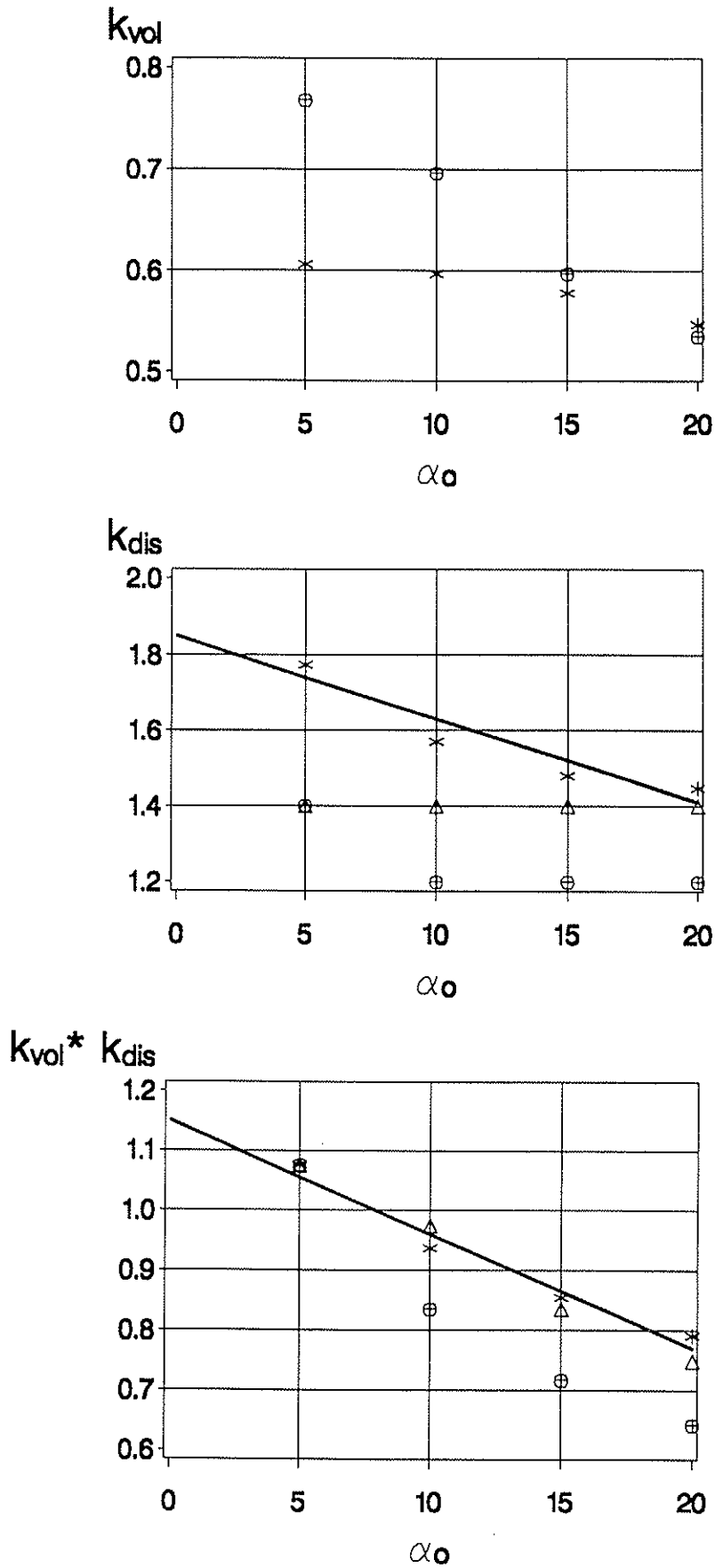


**Fig. 9:** Volume factor  $k_{vol}$ , distribution factor  $k_{dis}$  and product of  $k_{vol} \cdot k_{dis}$  over upper chord angle  $\alpha_0$  for beam type K205R to K220R  
 (\* = FE,  $\oplus$  = EC5,  $\Delta$  = proposal)

Beam no. (beam type)	Span L [ m ]	Depth at support $h_a$ [ cm ]	Depth at midspan $h_m$ [ cm ]	Upper chord angle $\alpha_o$ [ ° ]	Lower chord angle $\alpha_u$ [ ° ]	Radius to the innermost lamination R [ cm ]	$\frac{h_m}{R_m}$ [ ]
G1	11,00	100,0	100,0	20	20	450,0	0,20
G2	9,24	77,0	77,0	20	20	346,5	0,20
G3	6,36	53,0	53,0	20	20	238,5	0,20
G4	3,60	30,0	30,0	20	20	135,0	0,20
P1	11,00	100,0	135,3	20	20	450,0	0,26
P2	9,24	77,0	104,2	20	20	346,5	0,26
P3	6,36	53,0	71,7	20	20	238,5	0,26
P4	3,60	30,0	40,6	20	20	135,0	0,26
K1	11,00	70,4	135,3	20	16	450,0	0,26
K2	9,24	51,4	104,2	20	16	346,5	0,26
K3	6,36	35,4	71,7	20	16	238,5	0,26
K4	3,60	20,0	40,6	20	16	135,0	0,26
K5	9,24	38,4	104,2	20	14	346,5	0,26
K6	9,24	64,3	104,2	20	18	346,5	0,26

**Table 1:** Test beam dimensions

Loading and beam type	Beam number	Ultimate load at support F kN	Estimated radial stress at ultimate load		
			by FEM $\sigma_{t,90,ult}$ N/mm <sup>2</sup>	by EC 5 $\sigma_{t,90,ult}$ N/mm <sup>2</sup>	
Constant moment in curved part of the beam	Curved beam of constant depth (type G)	G1A	94,6	0,62	0,59
		G1B	99,0	0,64	0,62
		G2A	51,4	0,51	0,50
		G2B	84,9	0,84	0,83
		G3A	54,2	0,78	0,77
		G3B	52,8	0,76	0,75
		G4A	42,6	1,09	1,06
		G4B	37,0	0,94	0,92
	Double tapered curved beam (type P)	P1A	112,6	0,79	0,79
		P1B	67,0	0,47	0,47
		P2A	49,4	0,54	0,54
		P2B	57,3	0,63	0,62
		P3A	69,0	1,10	1,09
		P3B	62,9	1,00	0,99
		P4A	44,3	1,25	1,24
		P4B	43,9	1,24	1,22
	Double tapered pitched and curved beam (type K)	K1A	107,7	0,78	0,74
		K1B	124,6	0,90	0,85
		K2A	53,6	0,60	0,57
		K2B	39,4	0,44	0,42
		K3A	47,9	0,79	0,74
		K3B	60,7	1,00	0,94
		K4A	29,9	0,87	0,84
		K4B	37,3	1,09	1,05
		K5A	66,3	0,76	0,71
		K5B	74,2	0,85	0,80
		K6A	92,1	1,03	0,99
		K6B	71,6	0,80	0,77
Uniformly distributed load	Curved beam of constant depth (type G)	Gq3A	63,2	0,84	0,89
		Gq3B	87,8	1,17	1,24
		Gq4A	43,0	1,01	1,08
		Gq4B	39,4	0,93	0,99
	Double tapered pitched and curved beam (type K)	Kq3A	60,8	0,80	0,94
		Kq3B	58,6	0,77	0,91
		Kq4A	41,6	0,97	1,14
		Kq4B	44,6	1,04	1,22

**Table 2:** Test results: Ultimate loads and calculated ultimate radial stresses at failure

Beam no. (beam type)	Span L [ m ]	Depth at support $h_a$ [ cm ]	Depth at midspan $h_m$ [ cm ]	Upper chord angle $\alpha_o$ [ ° ]	Lower chord angle $\alpha_u$ [ ° ]	Radius to the innermost lamination R [ cm ]	$\frac{h_m}{R_m}$ [ ]
G205	9,24	77,0	77,0	5	5	346,5	0,20
G210	9,24	77,0	77,0	10	10	346,5	0,20
G215	9,24	77,0	77,0	15	15	346,5	0,20
G220	9,24	77,0	77,0	20	20	346,5	0,20
G205R	9,24	77,0	77,0	5	5	660,0	0,11
G210R	9,24	77,0	77,0	10	10	660,0	0,11
G215R	9,24	77,0	77,0	15	15	660,0	0,11
G220R	9,24	77,0	77,0	20	20	660,0	0,11
P205	9,24	77,0	78,6	5	5	346,5	0,20
P210	9,24	77,0	83,5	10	10	346,5	0,22
P215	9,24	77,0	92,0	15	15	346,5	0,23
P220	9,24	77,0	104,2	20	20	346,5	0,26
P205R	9,24	77,0	79,8	5	5	660,0	0,11
P210R	9,24	77,0	88,4	10	10	660,0	0,13
P215R	9,24	77,0	103,0	15	15	660,0	0,14
P220R	9,24	77,0	124,3	20	20	660,0	0,17
K205	9,24	38,2	78,6	5	0	346,5	0,20
K210	9,24	40,7	83,5	10	5	346,5	0,22
K215	9,24	42,9	92,0	15	10	346,5	0,23
K220	9,24	44,9	104,2	20	15	346,5	0,26
K205R	9,24	39,4	79,8	5	0	660,0	0,11
K210R	9,24	44,3	88,4	10	5	660,0	0,13
K215R	9,24	49,0	103,0	15	10	660,0	0,14
K220R	9,24	53,4	124,3	20	15	660,0	0,17

**Table 3:** Beam dimensions for calculation with finite element method